TECHNISCHE UNIVERSITÄT WIEN
Vienna University of Technology

Dissertation

TOWARDS SELECTIVE LIGANDS FOR THE $GABA_A$ RECEPTOR α+/β– INTERFACE

ausgeführt zum Zwecke der Erlangung des akademischen Grades eines Doktors der technischen Wissenschaften unter der Leitung von

Assoc. Prof. Dr. Michael Schnürch,

Prof. Dr. Marko D. Mihovilovic

Institut für Angewandte Synthesechemie, E163

Und unter Mitbetreuung im Rahmen des MolTag-Doktoratskollegs durch

Assoc. Prof. Dr. Margot Ernst

Zentrum für Hirnforschung, Medizinische Universität Wien

eingereicht an der Technischen Universität Wien

Fakultät für Technische Chemie

von

MSc. David Chan Bodin Siebert

Lindengasse 62/9, 1070 Wien

Vienna, Janurary 30, 2018

“THERE IS NOTHING NOBLE IN BEING SUPERIOR

TO YOUR FELLOW MAN;

TRUE NOBILITY IS BEING SUPERIOR

TO YOUR FORMER SELF.”

-ERNEST HEMINGWAY-

Declaration

This thesis entitled “Towards selective ligands for the $GABA_A$ receptor $\alpha+/\beta-$ interface” was conducted from March 1, 2015, until the February 28, 2018 in the group of Assoc. Prof. Michael Schnürch and Prof. Marko D. Mihovilovic at the Institute of Applied Synthetic Chemistry at the TU Wien.

I, David Chan Bodin Siebert, hereby declare that the thesis at hand submitted for obtaining the Doctor of Philosophy degree at the TU Wien has not been previously submitted by me at any other university for any degree.

I applied synthetic organic chemistry and *in silico* methods (homology modeling, docking and pharmacophore modeling) to study $GABA_A$ receptors during my time as PhD student. Experimentally, I focused on the synthesis of diverse pyrazoloquinolinones (see, C I.1, C II.2.2, C II.2.4 and C V.4) and triazoloquinazolinediones (see C I.2). Other compounds presented in this thesis were obtained by commercial suppliers, e.g. different benzodiazepines (see C III). Computationally, I generated various homology models based on the human $\beta3$-homopentameric $GABA_A$ receptor and used them in docking studies to study binding mode hypotheses of pyrazoloquinolinones (see C IV) and benzodiazepine like ligands (see C III.4). Moreover, I applied pharmacophore modeling (see C V.4.4) to identify new scaffolds as starting point for selective compounds for the $\alpha+/\beta-$ interface of $GABA_A$ receptors.

While the synthetic work of my PhD thesis (main part) was conducted at the Institute of Applied Synthetic Chemistry, TU Wien under the supervision of Assoc. Prof. Michael Schnürch and Prof. Marko D. Mihovilovic, the computational part was performed at the Center for Brain Research at the Medical University of Vienna under the supervision of Prof. Margot Ernst and at the Department of Pharmaceutical Chemistry at the University of Vienna under the supervision of Dr. Lars Richter and Prof. Gerhard Ecker.

I have two shared first authorship and one co-authorship publications in peer-reviewed journals. In both shared first authorship publications I contributed to the study design, writing, the synthesis of the investigated compounds, homology modeling and/or computational analysis of protein sequences, conformational analysis of ligands and with docking studies. In the co-authorship publication I synthesized and crystallized the reported compound. Moreover, I contributed to a patent by suggesting a new ligand design.

In addition, this thesis covers unpublished data which is mainly reported in chapters C III, C IV and C V (and certain subchapters). In chapter C III I contributed by conceiving the study, writing and performing the docking study. In chapter C IV I contributed in the study design, writing and conducting the docking part. Chapter C V deals with conclusions drawn

from the previous chapters and the synthesis of new compounds based on these conclusions which were all done by me.

Biological data obtained by colleagues are discussed within this thesis as well, since they are of crucial importance for further guidance of synthesis and computational analysis, and hence for presenting a clear and concise story in this thesis. The contributions to this work by others:

Michael Schnürch and Marko D. Mihovilovic supervised the synthetic part of my work and contributed to the writing of all papers and manuscripts mentioned in this thesis.

Margot Ernst supervised the study design, analyzed pharmacological results and contributed to the writing of all papers and manuscripts mentioned in this thesis.

Petra Scholze contributed to all papers and manuscripts by either performing binding assays or by writing.

Lars Richter supervised the study design of the manuscript in chapter C IV, contributed to the evaluation of the computational data and to the writing of the manuscript.

Marcus Wieder contributed to the manuscript in chapter C IV by performing the Molecular Dynamic simulations and by participating in the writing.

Thierry Langer and Gerhard Ecker contributed to the writing of the manuscript in chapter C IV.

Marco Treven contributed to the study design and the writing of the papers (C II.2.1 and C II.2.3) and by performing electrophysiological measurements.

Konstantina Bampali contributed to the study design and the writing of the manuscript in chapter C III and performed electrophysiological measurements for the papers (C II.2.1 and C II.2.3).

Xenia Simeone contributed to the study design of one paper (C II.2.1) and performed electrophysiological measurements.

Zdravko Varagic, Sabah Rehman, Jakob Pyszkowski and Raphael Holzinger performed electrophysiological measurements for the paper mentioned in chapter C II.2.1.

Raphael Holzinger, Fabjan Jure and Zdravko Varagic performed electrophysiological measurements for the paper mentioned in chapter C II.2.3.

Friederike Steudle performed binding assays for both papers in chapter C II.2.1 and C II.2.3.

Lydia Schlener contributed to the study design of the manuscript in chapter C IV.

Roshan Puthenkalam, Zdravko Varagic, Isabella Sarto-Jackson and Werner Sieghart contributed either by performing electrophysiological measurements or by writing to the manuscript in chapter C III.

Front Matter

Table of Contents

Declaration iii

Front Matter i

Table of Contents i
Acknowledgements vii
Abstract ix
Kurzfassung x

A Synthetic schemes 11
A I Pyrazoloquinolinones – precursors of R^6 series 12
A II Pyrazoloquinolinones – precursors of R^7 and R^8 series 13
A III Pyrazoloquinolinones –R^6 series 14
A IV Pyrazoloquinolinones – R^7 series 15
A V Pyrazoloquinolinones – alkyl series 16
A VI Pyrazoloquinolinones – R^8 fluoro series 17
A VII Pyrazoloquinolinones – R^8 chloro series 19
A VIII Pyrazoloquinolinones – R^8 bromo series 21
A IX Pyrazoloquinolinones – R^8 methoxy series 23
A X Pyrazoloquinolinones – mixed series 25
A XI Pyrazoloquinolinones – 2nd generation 26
A XII Pyrazoloquinolinones – $\alpha+/\gamma-$ vs. $\alpha+/\beta-$ 27
A XIII Triazoloquinazolinediones – chloro precursors 30
A XIV Triazoloquinazolinediones – ethyl 1-(aryl)hydrazine-1-carboxylates 31
A XV Triazoloquinazolinediones – R^8 chloro and methoxy series 32

B Introduction 33
B I Prelude 33
B II $GABA_A$ receptors 34
B III Ligands interacting with $GABA_A$ receptors 37
B III.1 Endogenous ligands 37
B III.2 Exogenous ligands 38
B III.2.1 Benzodiazepines 39
B III.2.2 Barbiturates 39
B III.2.3 General anesthetics 40
B III.2.4 Natural products 41
B III.2.4.1 Flavonoids 41
B III.2.4.2 Terpenoids 42
B III.2.4.3 Alkaloids 42
B III.2.4.4 Polyacetylenic alcohols 43
B IV Identification of binding sites and binding modes of ligands 44
B IV.1 Experimental localization of binding sites 44
B IV.2 Homology models and crystal structures 45
B IV.3 Determination and evaluation of the binding mode 47
B IV.3.1 Molecular docking 47

B IV.3.1.1 Ligand sampling 47
B IV.3.1.2 Protein flexibility 48
B IV.3.1.3 Scoring Functions 48
B IV.3.2 Site-directed irreversible photoaffinity labeling 49
B V Biological methods and subtype selectivity 50
B VI Pyrazoloquinolinones and the α+/β– interfaces 52
B VII Objective 54

C Results and Discussion 55
C I Synthesis of modulators for the α+/β– interface 55
C I.1 Pyrazoloquinolinones 55
C I.1.1 Pyrazoloquinolinones – Alkyl series 56
C I.1.2 Systematic library to explore SAR of positions R^8, R'^3 and R'^4 59
C I.2 Triazoloquinazolinediones 64
C I.2.1 Synthesis of Triazoloquinazolinediones 64
C II Subtype selectivity – where to start at? 68
C II.1 Pyrazoloquinolinones - Substitution of the ring D 72
C II.2 Towards subtype selective tool compounds 74
C II.2.1 α1+/β1– Selectivity – a proof of concept 74
C II.2.1.1 Mini library of compounds aimed at studying potency driving ligand features 74
C II.2.1.2 Compound [47] exerts very similar effects in α1β3, α1β3γ2 and α1β3δ receptors 74
C II.2.1.3 Potency selectivity for β1-containing receptors 75
C II.2.1.4 Mutational analysis supports the main site of action to be at the extracellular minus side of the β subunit 77
C II.2.1.5 The investigated compounds show limited α selectivity 80
C II.2.1.6 The δ or the γ1 subunits have no impact on compound [47] potency for the α1+/β1– site 81
C II.2.1.7 A derivative of compound [47] that lacks affinity for the benzodiazepine binding site also modulates α1β1 containing receptors 81
C II.2.1.8 Discussion 83
C II.2.2 Towards β1 efficacy selectivity 85
C II.2.3 Exploring α6β3γ2 subtype selectivity – Part I 90
C II.2.3.1 Impact of R^8 = chloro and of variations in the position of ring D methoxy substitution on GABAAR subtype modulatory profile 90
C II.2.3.2 Compound [148] does not bind at the α6+/β3– interface 91
C II.2.3.3 R8 = chloro compounds with varying *m*-substituents on ring D display distinct efficacy profiles 94
C II.2.3.4 Discussion 95
C II.2.4 Exploring α6β3γ2 subtype selectivity – Part II 98
C II.3 Triazoloquinazolinediones as modulators for the α+/β– interface 101
C II.4 Triazoloquinazolinediones as potential BZ antagonists 102
C III Similar BZ ligands possess different binding modes - comparing homologous binding sites 103
C III.1 Design and generation of the conversion mutants 103
C III.2 Mutations Q64A and D43Y increase the apperent affinity of CGS9895 [XXXVII] and CGS20625 [164] 107
C III.3 Ro 15-1788 [165] and Ro 15-8670 [166] act as positive allosteric modulators in α1β3(mut) receptors 108
C III.4 Computational docking suggests distinct binding modes for certain benzodiazepines 111
C III.5 Discussion 114
C IV Evaluation of PQ binding mode by SAR scoring function 116
C IV.1 Molecular docking of CGS8216 [XXXVI] 116
C IV.2 Structure Activity of PQs 117
C IV.3 SAR guided pose selection 119
C IV.4 SAR scoring identifies two candidate binding modes (BM) – BM I and BM II 121
C IV.5 Comparing SAR guided docking versus conventional molecular docking 122
C IV.6 Analysis of BM I and BM II in the light of SAR 123
C IV.7 Evaluating the stability of compound [170] and [175] in BM I and BM II by Molecular Dynamics simulations 125
C IV.7.1 Stability of compound [170] (R'^4 = COOH) during the simulations 126
C IV.7.2 Stability of compound [175] (R'^4 = NH_2) during the simulations 127
C IV.8 Prospective validation of BM I by γ2D56A mutant 128
C IV.9 Discussion 129

C V Combining the puzzle pieces 131
C V.1 Revisiting α6 selectivity 131
C V.2 Transferring PQ binding mode to the α+/β– interface 133
C V.3 Ligand features – what we learned so far 134
C V.4 Tackling α+/γ– vs α+/β– 135
C V.4.1 Empirical ligand-based approach 136
C V.4.2 Structure-based approach 139
C V.4.3 Preliminary pharmacological profiling of [251] 146
C V.4.4 Prospective scaffold hop, putatively new structures 147
C V.4.4.1 Strcture-based pharmacophore modeling and virtual screening 147
C V.4.4.2 Ligand-based pharmacophore modeling and virtual screening 148

D Conclusion and perspective 151

E Experimental part 154
E I Methods – computational part 154
E I.1 Homology modeling 154
E I.2 Molecular Docking 154
E I.3 Pharmacophore modeling 154
E II Materials and methods – chemical synthesis 155
E II.1 NMR spectroscopy 155
E II.2 Chromatographic methods 155
E II.3 Microwave 156
E II.4 Melting point 156
E II.5 HR-MS 156
E III General operating proceducer (E°°II) 157
E III.1 Condensation 157
E III.2 Cyclization 157
E III.3 Chlorination 157
E III.4 Formation of pyrazoloquinolinone 158
E III.5 Basic hydrolysis to the carboxylic acid 158
E III.6 Acidic hydrolysis to the benzamide 158
E III.7 Reduction to the amine 158
E IV Chemical synthesis 159
E IV.1 Pyrazoloquinoline precursors of R^6 series 159
E IV.1.1 N-(2-Ethylphenyl)acetamide [183] DCBSPU28 159
E IV.1.2 N-(2-Ethylphenyl)acetamide [184] DCBSPU29 160
E IV.1.3 N-(4-Chloro-2-ethylphenyl)acetamide [185] DCBSPU30 and 4-Chloro-2-ethylaniline [187] DCBSPU43 161
E IV.1.4 N-(4-Chloro-2-isopropylphenyl)acetamide [186] DCBSPU41 162
E IV.1.5 4-Chloro-2-isopropylaniline [188] DCBSPU44 163
E IV.1.6 Diethyl 2-(((4-chloro-2-fluorophenyl)amino)methylene)-malonate [194] DCBSPU7 164
E IV.1.7 Diethyl 2-(((2,4-dichlorophenyl)amino)methylene)-malonate [195] DCBSPU18 165
E IV.1.8 Diethyl 2-(((2-bromo-4-chlorophenyl)amino)methylene)-malonate [196] DCBSPU5 166
E IV.1.9 Diethyl 2-(((4-chloro-2-(trifluoromethyl)phenyl)amino)-methylene)malonate [197] DCBSPU6 167
E IV.1.10 Diethyl 2-(((4-chloro-2-methylphenyl)amino)methylene)-malonate [198] DCBSPU17 168
E IV.1.11 Diethyl 2-(((4-chloro-2-ethylphenyl)amino)methylene)-malonate [199] DCBSPU47 169
E IV.1.12 Diethyl 2-(((4-chloro-2-isopropylphenyl)amino)-methylene)malonate [200] DCBSPU46 170
E IV.1.13 Ethyl 6-chloro-8-fluoro-4-oxo-1,4-dihydroquinoline-3-carboxylate [201] DCBSPU13 171
E IV.1.14 Ethyl 6,8-dichloro-4-oxo-1,4-dihydroquinoline-3-carboxylate [202] DCBSPU23 172
E IV.1.15 Ethyl 8-bromo-6-chloro-4-oxo-1,4-dihydroquinoline-3-carboxylate [203] DCBSPU11 173
E IV.1.16 Ethyl 6-chloro-4-oxo-8-(trifluoromethyl)-1,4-dihydro-quinoline-3-carboxylate [204] DCBSPU12 174
E IV.1.17 Ethyl 6-chloro-8-methyl-4-oxo-1,4-dihydroquinoline-3-carboxylate [205] DCBSPU22 175
E IV.1.18 Ethyl 6-chloro-8-ethyl-4-oxo-1,4-dihydroquinoline-3-carboxylate [206] DCBSPU50 176
E IV.1.19 Ethyl 6-chloro-8-isopropyl-4-oxo-1,4-dihydroquinoline-3-carboxylate [207] DCBSPU48 177
E IV.1.20 Ethyl 4,6-dichloro-8-fluoroquinoline-3-carboxylate [208] DCBSPU16 178
E IV.1.21 Ethyl 4,6,8-trichloroquinoline-3-carboxylate [209] DCBSPU25 179
E IV.1.22 Ethyl 8-bromo-4,6-dichloroquinoline-3-carboxylate [210] DCBSPU14 180
E IV.1.23 Ethyl 4,6-dichloro-8-(trifluoromethyl)quinoline-3-carboxylate [211] DCBSPU15 181
E IV.1.24 Ethyl 4,6-dichloro-8-methylquinoline-3-carboxylate [212] DCBSPU24 182
E IV.1.25 Ethyl 4,6-dichloro-8-ethylquinoline-3-carboxylate [213] DCBSPU52 183

E IV.1.26 Ethyl 4,6-dichloro-8-isopropylquinoline-3-carboxylate [214] DCBSPU49 184
E IV.2 Pyrazoloquinoline precursors of R^7 and R^8 series 185
E IV.2.1 Diethyl 2-(((4-fluorophenyl)amino)methylene)malonate [23] DCBSLK001 185
E IV.2.2 Diethyl 2-(((4-chlorophenyl)amino)methylene)malonate [24] DCBS21 186
E IV.2.3 Diethyl 2-(((4-bromophenyl)amino)methylene)malonate [25] DCBS01 187
E IV.2.4 Diethyl 2-(((3-bromophenyl)amino)methylene)malonate [160] DCBSLG01 188
E IV.2.5 Diethyl 2-(([1,1'-biphenyl]-4-ylamino)methylene)-malonate [88b] DCBS02 189
E IV.2.6 Diethyl 2-(((4-methoxyphenyl)amino)methylene)-malonate [6] DCBS10 190
E IV.2.7 Diethyl 2-(((3-methoxyphenyl)amino)methylene)-malonate [177] DCBSLA8 191
E IV.2.8 Ethyl 6-fluoro-4-oxo-1,4-dihydroquinoline-3-carboxylate [26] DCBSLK005 192
E IV.2.9 Ethyl 6-chloro-4-oxo-1,4-dihydroquinoline-3-carboxylate [27] DCBS25 193
E IV.2.10 Ethyl 6-bromo-4-oxo-1,4-dihydroquinoline-3-carboxylate [28] DCBS08 194
E IV.2.11 Ethyl 7-bromo-4-oxo-1,4-dihydroquinoline-3-carboxylate [161] DCBSLG02 195
E IV.2.12 Ethyl 4-oxo-6-phenyl-1,4-dihydroquinoline-3-carboxylate [88c] DCBS07 196
E IV.2.13 Ethyl 6-methoxy-4-oxo-1,4-dihydroquinoline-3-carboxylate [7] DCBS50 197
E IV.2.14 Ethyl 7-methoxy-4-oxo-1,4-dihydroquinoline-3-carboxylate [178] DCBSLA11 198
E IV.2.15 Ethyl 4-chloro-6-fluoroquinoline-3-carboxylate [29] DCBSLK008 199
E IV.2.16 Ethyl 4,6-dichloroquinoline-3-carboxylate [30] DCBS30 200
E IV.2.17 Ethyl 6-bromo-4-chloroquinoline-3-carboxylate [31] DCBS16 201
E IV.2.18 Ethyl 7-bromo-4-chloroquinoline-3-carboxylate [162] DCBSLG03 202
E IV.2.19 Ethyl 4-chloro-6-phenylquinoline-3-carboxylate [88d] DCBS15 203
E IV.2.20 Ethyl 4-chloro-6-methoxyquinoline-3-carboxylate [8] DCBS19 204
E IV.2.21 Ethyl 4-chloro-7-methoxyquinoline-3-carboxylate [179] DCBSLA13 205
E IV.3 Pyrazoloquinolinones – R^6 series 206
E IV.3.1 8-Chloro-6-fluoro-2-(4-methoxyphenyl)-2,5-dihydro-3H-pyrazolo[4,3-c]quinolin-3-one [215] DCBSPU21 206
E IV.3.2 6,8-Dichloro-2-(4-methoxyphenyl)-2,5-dihydro-3H-pyrazolo[4,3-c]quinolin-3-one [216] DCBSPU27 207
E IV.3.3 6-Bromo-8-chloro-2-(4-methoxyphenyl)-2,5-dihydro-3H-pyrazolo[4,3-c]quinolin-3-one [217] DCBSPU19 208
E IV.3.4 8-Chloro-2-(4-methoxyphenyl)-6-(trifluoromethyl)-2,5-dihydro-3H-pyrazolo[4,3-c]quinolin-3-one [218] DCBSPU42 209
E IV.3.5 8-Chloro-2-(4-methoxyphenyl)-6-methyl-2,5-dihydro-3H-pyrazolo[4,3-c]quinolin-3-one [219] DCBSPU26 210
E IV.3.6 8-Chloro-6-ethyl-2-(4-methoxyphenyl)-2,5-dihydro-3H-pyrazolo[4,3-c]quinolin-3-one [220] DCBSPU53 211
E IV.3.7 8-Chloro-6-isopropyl-2-(4-methoxyphenyl)-2,5-dihydro-3H-pyrazolo[4,3-c]quinolin-3-one [221] DCBSPU51 212
E IV.4 Pyrazoloquinolinones – R^7 series 213
E IV.4.1 7-Methoxy-2-(3-methoxyphenyl)-2,5-dihydro-3H-pyrazolo[4,3-c]quinolin-3-one [180] DCBS165 213
E IV.4.2 7-Bromo-2-(4-methoxyphenyl)-2,5-dihydro-3H-pyrazolo[4,3-c]quinolin-3-one [163] DCBSLG04 214
E IV.4.3 2-(4-Methoxyphenyl)-7-((trimethylsilyl)ethynyl)-2,5-dihydro-3H-pyrazolo[4,3-c]quinolin-3-one [155] DCBS172 215
E IV.4.4 7-Ethynyl-2-(4-methoxyphenyl)-2,5-dihydro-3H-pyrazolo[4,3-c]quinolin-3-one [156] DCBS176 216
E IV.4.5 7-Ethyl-2-(4-methoxyphenyl)-2,5-dihydro-3H-pyrazolo[4,3-c]quinolin-3-one [157] DCBS177 217
E IV.4.6 7-Acetyl-2-(4-methoxyphenyl)-2,5-dihydro-3H-pyrazolo[4,3-c]quinolin-3-one [158] DCBS183 218
E IV.5 Pyrazoloquinolinones – alkyl series 219
E IV.5.1 1-Benzyl-8-methoxy-1,2-dihydro-3H-pyrazolo[4,3c]qui-nolin-3-one [10] DCBS45A and 2-Benzyl-8-methoxy-1,2-dihydro-3H-pyrazolo[4,3-c]quinolin-3-one [9] DCBS45B 219
E IV.5.2 1-Cyclohexyl-8-methoxy-1,2-dihydro-3H-pyrazolo[4,3-c]-quinolin-3-one [13] DCBS40A and 2-Cyclohexyl-8-methoxy-1,2-dihydro-3H-pyrazolo[4,3-c]quinolin-3-one [12] DCBS40B 221
E IV.5.3 1-Isopropyl-8-methoxy-1,2-dihydro-3H-pyrazolo[4,3-c]quinolin-3-one [16] DCBS63A and 2-Isopropyl-8-methoxy-1,2-dihydro-3H-pyrazolo[4,3-c]quinolin-3-one [15] DCBS63B 223
E IV.5.4 8-Methoxy-1-methyl-1,2-dihydro-3H-pyrazolo[4,3-c]quinolin-3-one [11] DCBSLS25 225
E IV.5.5 8-Methoxy-1,2-dimethyl-1,2-dihydro-3H-pyrazolo[4,3-c]quinolin-3-one [14] DCBS105 226
E IV.5.6 2-(t*ert*-Butyl)-8-methoxy-1,2-dihydro-3H-pyrazolo[4,3-c]quinolin-3-one [17] DCBS66B 227
E IV.5.7 8-Methoxy-2,5-dihydro-3H-pyrazolo[4,3-c]quinolin-3-one [18] DCBS53 228
E IV.5.8 2-Methoxy-10,11-dihydro-7H,9H-pyrazolo[1',2':1,2]-pyrazolo[4,3-c]quinolin-7-one [19] DCBS38 229
E IV.6 Pyrazoloquinolinones – R^8 fluoro series 230
E IV.6.1 8-Fluoro-2-(*p*-tolyl)-2,5-dihydro-3*H*-pyrazolo[4,3-*c*]quinolin-3-one [32] DCBSLK024 230
E IV.6.2 8-Fluoro-2-(*m*-tolyl)-2,5-dihydro-3*H*-pyrazolo[4,3-*c*]quinolin-3-one [39] DCBSLK017 231
E IV.6.3 8-Fluoro-2-(4-methoxyphenyl)-2,5-dihydro-3*H*-pyrazolo[4,3-*c*]quinolin-3-one [33] DCBSLK012 232
E IV.6.4 8-Fluoro-2-(3-methoxyphenyl)-2,5-dihydro-3*H*-pyrazolo[4,3-*c*]quinolin-3-one [40] DCBSLK029 233
E IV.6.5 8-Fluoro-2-(4-nitrophenyl)-2,5-dihydro-3*H*-pyrazolo[4,3-*c*]quinolin-3-one [34] DCBSLK059 234
E IV.6.6 8-Fluoro-2-(3-nitrophenyl)-2,5-dihydro-3*H*-pyrazolo[4,3-*c*]quinolin-3-one [41] DCBSLK023 235
E IV.6.7 4-(8-Fluoro-3-oxo-3,5-dihydro-2*H*-pyrazolo[4,3-*c*]quinolin-2-yl)benzonitrile [35] DCBSLK015 236
E IV.6.8 3-(8-Fluoro-3-oxo-3,5-dihydro-2*H*-pyrazolo[4,3-*c*]quinolin-2-yl)benzonitrile [42] DCBSLK040 237
E IV.6.9 2-(4-Aminophenyl)-8-fluoro-2,5-dihydro-3H-pyrazolo[4,3-c]quinolin-3-one [36] DCBS193 238
E IV.6.10 2-(3-Aminophenyl)-8-fluoro-2,5-dihydro-3*H*-pyrazolo[4,3-*c*]quinolin-3-one [43] DCBSLK055 239
E IV.6.11 4-(8-Fluoro-3-oxo-3,5-dihydro-2*H*-pyrazolo[4,3-*c*]quinolin-2-yl)benzoic acid [37] DCBSLK038 240

E IV.6.12 3-(8-Fluoro-3-oxo-3,5-dihydro-2*H*-pyrazolo[4,3-*c*]quinolin-2-yl)benzoic acid [44] DCBSLK039 241
E IV.6.13 4-(8-Fluoro-3-oxo-3,5-dihydro-2*H*-pyrazolo[4,3-*c*]quinolin-2-yl)benzamide [38] DCBSLK032 242
E IV.6.14 3-(8-Fluoro-3-oxo-3,5-dihydro-2*H*-pyrazolo[4,3-*c*]quinolin-2-yl)benzamide [45] DCBSLK033 243
E IV.7 Pyrazoloquinolinones – R^8 chloro series 244
E IV.7.1 8-Chloro-2-(p-tolyl)-1,2-dihydro-3H-pyrazolo[4,3-c]quinolin-3-one [46] DCBS54 244
E IV.7.2 8-Chloro-2-(*m*-tolyl)-2,5-dihydro-3H-pyrazolo[4,3-c]quinolin-3-one [52] DCBS142 245
E IV.7.3 8-Chloro-2-(4-methoxyphenyl)-2,5-dihydro-3H-pyrazolo[4,3-c]quinolin-3-one [47] DCBS138 246
E IV.7.4 8-Chloro-2-(3-methoxyphenyl)-2,5-dihydro-3H-pyrazolo[4,3-c]quinolin-3-one [53] DCBS137 247
E IV.7.5 8-Chloro-2-(4-nitrophenyl)-1,2-dihydro-3H-pyrazolo[4,3-c]quinolin-3-one [48] DCBSLS02 248
E IV.7.6 8-Chloro-2-(3-nitrophenyl)-2,5-dihydro-3H-pyrazolo[4,3-c]quinolin-3-one [54] DCBS119 249
E IV.7.7 4-(8-Chloro-3-oxo-3,5-dihydro-2H-pyrazolo[4,3-c]quinolin-2-yl)benzonitrile [49] DCBS139 250
E IV.7.8 3-(8-Chloro-3-oxo-3,5-dihydro-2H-pyrazolo[4,3-c]quinolin-2-yl)benzonitrile [55] DCBS146 251
E IV.7.9 2-(4-Aminophenyl)-8-chloro-1,2-dihydro-3H-pyrazolo[4,3-c]quinolin-3-one [50] DCBSLS17 252
E IV.7.10 2-(3-Aminophenyl)-8-chloro-2,5-dihydro-3H-pyrazolo[4,3-c]quinolin-3-one [56] DCBS120 253
E IV.7.11 4-(8-Chloro-3-oxo-3,5-dihydro-2H-pyrazolo[4,3-c]quinolin-2-yl)benzoic acid [51] DCBS128 254
E IV.7.12 3-(8-Chloro-3-oxo-3,5-dihydro-2H-pyrazolo[4,3-c]quinolin-2-yl)benzoic acid [57] DCBS152A 255
E IV.7.13 4-(8-Chloro-3-oxo-3,5-dihydro-2H-pyrazolo[4,3-c]quinolin-2-yl)benzamide [52] DCBSLK36 256
E IV.7.14 3-(8-Chloro-3-oxo-3,5-dihydro-2H-pyrazolo[4,3-c]quinolin-2-yl)benzamide [58] DCBS152B 257
E IV.8 Pyrazoloquinolinones – R^8 bromo series 258
E IV.8.1 8-Bromo-2-(p-tolyl)-2,5-dihydro-3H-pyrazolo[4,3-c]quinolin-3-one [60] DCBS148 258
E IV.8.2 8-Bromo-2-(*m*-tolyl)-2,5-dihydro-3H-pyrazolo[4,3-c]quinolin-3-one [67] DCBS155 259
E IV.8.3 8-Bromo-2-(4-methoxyphenyl)-2,5-dihydro-3H-pyrazolo[4,3-c]quinolin-3-one [61] DCBS149 260
E IV.8.4 8-Bromo-2-(3-methoxyphenyl)-2,5-dihydro-3H-pyrazolo[4,3-c]quinolin-3-one [68] DCBS156 261
E IV.8.5 8-Bromo-2-(4-nitrophenyl)-2,5-dihydro-3H-pyrazolo[4,3-c]quinolin-3-one [62] DCBS147 262
E IV.8.6 8-Bromo-2-(3-nitrophenyl)-2,5-dihydro-3H-pyrazolo[4,3-c]quinolin-3-one [69] DCBS154 263
E IV.8.7 4-(8-Bromo-3-oxo-3,5-dihydro-2H-pyrazolo[4,3-c]quinolin-2-yl)benzonitrile [63] DCBS150 264
E IV.8.8 3-(8-Bromo-3-oxo-3,5-dihydro-2H-pyrazolo[4,3-c]quinolin-2-yl)benzonitrile [70] DCBS157 265
E IV.8.9 2-(4-Aminophenyl)-8-bromo-1,2-dihydro-3H-pyrazolo[4,3-c]quinolin-3-one [64] DCBS164 266
E IV.8.10 2-(3-Aminophenyl)-8-chloro-2,5-dihydro-3H-pyrazolo[4,3-c]quinolin-3-one [71] DCBS163 267
E IV.8.11 4-(8-Bromo-3-oxo-3,5-dihydro-2H-pyrazolo[4,3-c]quinolin-2-yl)benzoic acid [65] DCBS153A 268
E IV.8.12 3-(8-Bromo-3-oxo-3,5-dihydro-2H-pyrazolo[4,3-c]quinolin-2-yl)benzoic acid [72] DCBS162 269
E IV.8.13 4-(8-Bromo-3-oxo-3,5-dihydro-2H-pyrazolo[4,3-c]quinolin-2-yl)benzamid [66] DCBS153B 270
E IV.8.14 3-(8-Bromo-3-oxo-3,5-dihydro-2H-pyrazolo[4,3-c]quinolin-2-yl)benzamide [73] DCBSLK58 271
E IV.9 Pyrazoloquinolinones – R^8 methoxy series 272
E IV.9.1 8-Methoxy-2-(p-tolyl)-2,5-dihydro-3H-pyrazolo[4,3-c]quinolin-3-one [74] DCBS76 272
E IV.9.2 8-Methoxy-2-(*m*-tolyl)-2,5-dihydro-3H-pyrazolo[4,3-c]quinolin-3-one [81] DCBS141 273
E IV.9.3 8-Methoxy-2-(3-methoxyphenyl)-2,5-dihydro-3H-pyrazolo[4,3-c]quinolin-3-one [82] DCBS135 274
E IV.9.4 8-Methoxy-2-(4-nitrophenyl)-2,5-dihydro-3H-pyrazolo[4,3-c]quinolin-3-one [76] DCBS93 275
E IV.9.5 8-Methoxy-2-(3-nitrophenyl)-1,2-dihydro-3H-pyrazolo[4,3-c]quinolin-3-one [83] DCBS52 276
E IV.9.6 4-(8-Methoxy-3-oxo-3,5-dihydro-2H-pyrazolo[4,3-c]quinolin-2-yl)benzonitrile [77] DCBS84 277
E IV.9.7 3-(8-Methoxy-3-oxo-3,5-dihydro-2H-pyrazolo[4,3-c]quinolin-2-yl)benzonitrile [84] DCBS145 278
E IV.9.8 2-(4-Aminophenyl)-8-methoxy-2,5-dihydro-3H-pyrazolo[4,3-c]quinolin-3-one [78] DCBS96 279
E IV.9.9 2-(3-Aminophenyl)-8-methoxy-2,5-dihydro-3H-pyrazolo[4,3-c]quinolin-3-one [85] DCBSLS24 280
E IV.9.10 4-(8-Methoxy-3-oxo-3,5-dihydro-2H-pyrazolo[4,3-c]quinolin-2-yl)benzoic acid [79] DCBS88 281
E IV.9.11 3-(8-Methoxy-3-oxo-3,5-dihydro-2H-pyrazolo[4,3-c]quinolin-2-yl)benzoic acid [86] DCBS151A 282
E IV.9.12 4-(8-Methoxy-3-oxo-3,5-dihydro-2H-pyrazolo[4,3-c]quinolin-2-yl)benzamide [80] DCBSLK60 283
E IV.9.13 3-(8-Methoxy-3-oxo-3,5-dihydro-2H-pyrazolo[4,3-c]quinolin-2-yl)benzamide [87] DCBS151B 284
E IV.10 Pyrazoloquinolinones – R^8 mixed series 285
E IV.10.1 8-Bromo-2-phenyl-2,5-dihydro-3H-pyrazolo[4,3-c]quinolin-3-one [91] DCBS20 285
E IV.10.2 2,8-Diphenyl-2,5-dihydro-3H-pyrazolo[4,3-c]quinolin-3-one [92] DCBS23 286
E IV.10.3 2-(3-Bromophenyl)-8-methoxy-2,5-dihydro-3H-pyrazolo[4,3-c]quinolin-3-one [90] DCBS24 287
E IV.10.4 2-(3-Bromophenyl)-8-chloro-2,5-dihydro-3H-pyrazolo[4,3-c]quinolin-3-one [89] DCBS32 288
E IV.11 Pyrazoloquinolinones – 2nd generation 289
E IV.11.1 2-(4-Bromophenyl)-8-chloro-2,5-dihydro-3H-pyrazolo[4,3-c]quinolin-3-one [141] DCBS192 289
E IV.11.2 8-Chloro-2-(4-hydroxyphenyl)-2,5-dihydro-3H-pyrazolo[4,3-c]quinolin-3-one [139] DCBS198 290
E IV.11.3 N-(4-(8-Chloro-3-oxo-3,5-dihydro-2H-pyrazolo[4,3-c]quinolin-2-yl)phenyl)acetamide [140] DCBS199 291
E IV.11.4 8-Chloro-2-(4-((trimethylsilyl)ethynyl)phenyl)-2,5-dihydro-3H-pyrazolo[4,3-c]quinolin-3-one [142] DCBS209 292
E IV.11.5 8-Chloro-2-(4-ethynylphenyl)-2,5-dihydro-3H-pyrazolo[4,3-c]quinolin-3-one [143] DCBS212 293
E IV.11.6 2-(4-Acetylphenyl)-8-chloro-2,5-dihydro-3H-pyrazolo[4,3-c]quinolin-3-one [144] DCBSBRP23 294
E IV.12 Pyrazoloquinolinones – $\alpha+/\gamma-$ vs. $\alpha+/\beta-$ 295
E IV.12.1 2-(4-Chlorophenyl)-8-methoxy-2,5-dihydro-3H-pyrazolo[4,3-c]quinolin-3-one [222] DCBS122 295
E IV.12.2 2-(5-Chloropyrazin-2-yl)-8-methoxy-2,5-dihydro-3H-pyrazolo[4,3-c]quinolin-3-one [223] DCBS133 296
E IV.12.3 8-Methoxy-2-(pyrazin-2-yl)-2,5-dihydro-3H-pyrazolo[4,3-c]quinolin-3-one [224] DCBS85 297

E IV.12.4 7-Methoxy-2-(pyrazin-2-yl)-2,5-dihydro-3H-pyrazolo[4,3-c]quinolin-3-one [225] DCBS126 298
E IV.12.5 *N,N'*-(Ethane-1,2-diyl)bis(4-methylbenzenesulfonamide) [236] DCBSBRP01 299
E IV.12.6 1,4-Ditosyl-1,4-diazepan-6-ol [237] DCBSBRP03 300
E IV.12.7 1,4-Ditosyl-1,4-diazepan-6-yl methanesulfonate [238] DCBSBRP06 301
E IV.12.8 1,4-Ditosyl-1,4-diazepan-6-one [241] DCBSJS08 302
E IV.12.9 *tert*-Butyl 2-(1,4-ditosyl-1,4-diazepan-6-ylidene)-hydrazine-1-carboxylate [243] DCBSJS11 303
E IV.12.10 2-(1,4-Ditosyl-1,4-diazepan-6-yl)-8-methoxy-2,5-dihydro-3H-pyrazolo[4,3-c]quinolin-3-one [244] DCBSJS14 304
E IV.12.11 *N,N'*-(Ethane-1,2-diyl)bis(4-nitrobenzenesulfonamide) [246] DCBS218 305
E IV.12.12 1,4-Bis((4-nitrophenyl)sulfonyl)-1,4-diazepan-6-ol [247] DCBS220 306
E IV.12.13 1,4-Bis((4-nitrophenyl)sulfonyl)-1,4-diazepan-6-one [248] DCBS225 307
E IV.12.14 *tert-Butyl* 2-(1,4-bis((4-nitrophenyl)sulfonyl)-1,4-diazepan-6-ylidene)hydrazine-1-carboxylate [249] DCBS227 308
E IV.12.15 2-(1,4-Bis((4-nitrophenyl)sulfonyl)-1,4-diazepan-6-yl)-8-chloro-2,5-dihydro-3H-pyrazolo[4,3-c]quinolin-3-one [250] DCBS229 309
E IV.12.16 6-(8-Chloro-3-oxo-3,5-dihydro-2H-pyrazolo[4,3-c]quinolin-2-yl)-1,4-diazepane-1,4-diium chloride [251] DCBS231 310
E IV.13 Triazoloquinazolinediones 311
E IV.13.1 5-Chloro-2-(3-(ethoxycarbonyl)thioureido)benzoic acid [103] DCBSBJ03 311
E IV.13.2 2-(3-(Ethoxycarbonyl)thioureido)-5-methoxybenzoic acid [104] DCBSBJ12 312
E IV.13.3 Ethyl 6-chloro-4-oxo-2-thioxo-1,4-dihydroquinazoline-3(2H)-carboxylate [105] DCBSBJ04 313
E IV.13.4 Ethyl 6-methoxy-4-oxo-2-thioxo-1,4-dihydroquinazoline-3(2H)-carboxylate [106] DCBSBJ15 314
E IV.13.5 6-Chloro-2-thioxo-2,3-dihydroquinazolin-4(1H)-one [107] DCBSBJ05 315
E IV.13.6 6-Methoxy-2-thioxo-2,3-dihydroquinazolin-4(1H)-one [108] DCBSBJ17 316
E IV.13.7 6-Chloro-2-(methylthio)quinazolin-4(3H)-one [109] DCBSBJ23 317
E IV.13.8 6-Methoxy-2-(methylthio)quinazolin-4(3H)-one [110] DCBSBJ22 318
E IV.13.9 4,6-Dichloro-2-(methylthio)quinazoline [111] DCBSBJ26 319
E IV.13.10 4-Chloro-6-methoxy-2-(methylthio)quinazoline [112] DCBSBJ25 320
E IV.13.11 Ethyl 1-(p-tolyl)hydrazine-1-carboxylate [118] DCBSBJ02 321
E IV.13.12 Ethyl 1-(4-methoxyphenyl)hydrazine-1-carboxylate [120] DCBSBJ13 322
E IV.13.13 Ethyl 1-(4-aminophenyl)hydrazine-1-carboxylate [119] DCBSLA1 323
E IV.13.14 Ethyl 1-(4-cyanophenyl)hydrazine-1-carboxylate [117] DCBSLA9 324
E IV.13.15 *tert*-Butyl (4-iodophenyl)carbamate [121] DCBS99 325
E IV.13.16 Ethyl 1-(4-((*tert*-butoxycarbonyl)amino)phenyl)hydrazine -1-carboxylate [122] DCBS100 326
E IV.13.17 9-Chloro-5-(methylthio)-2-(p-tolyl)-[1,2,4]triazolo[4,3-c]quinazolin-3(2H)-one [124] DCBSBJ27 327
E IV.13.18 9-Chloro-2-(4-methoxyphenyl)-5-(methylthio)-[1,2,4]triazolo-[4,3-c]quinazolin-3(2H)-one [125] DCBSBJ52 328
E IV.13.19 9-Methoxy-5-(methylthio)-2-(p-tolyl)-[1,2,4]triazolo[4,3-c]quinazolin-3(2H)-one [127] DCBSBJ43 329
E IV.13.20 9-Methoxy-2-(4-methoxyphenyl)-5-(methylthio)-[1,2,4]triazolo-[4,3-c]quinazolin-3(2H)-one [128] DCBSBJ34 330
E IV.13.21 4-(9-Chloro-5-(methylthio)-3-oxo-[1,2,4]triazolo[4,3-c]quinazolin-2(3H)-yl)benzonitrile [123] DCBSLA20 331
E IV.13.22 *tert*-Butyl (4-(9-chloro-5-(methylthio)-3-oxo-[1,2,4]tria-zolo[4,3-c]quinazolin-2(3H)-yl)phenyl)carbamate [126] DCBS101 332
E IV.13.23 9-Chloro-2-(p-tolyl)-2,6-dihydro-[1,2,4]triazolo[4,3-c]quinazoline-3,5-dione [130] DCBSBJ28 333
E IV.13.24 9-Chloro-2-(4-methoxyphenyl)-2,6-dihydro-[1,2,4]tria-zolo[4,3-c]quinazoline-3,5-dione [131] DCBSBJ55 334
E IV.13.25 9-Methoxy-2-(p-tolyl)-2,6-dihydro-[1,2,4]triazolo[4,3-c]quinazoline-3,5-dione [133] DCBSBJ48 335
E IV.13.26 9-Methoxy-2-(4-methoxyphenyl)-2,6-dihydro-[1,2,4]tria-zolo-[4,3-c]quinazoline-3,5-dione [134] DCBSBJ30 336
E IV.13.27 4-(9-Chloro-3,5-dioxo-5,6-dihydro-[1,2,4]triazolo[4,3-c]quinazolin-2(3H)-yl)benzonitrile [129] DCBS136 337
E IV.13.28 *tert*-Butyl (4-(9-chloro-3,5-dioxo-5,6-dihydro-[1,2,4]tria-zolo-[4,3-c]quinazolin-2(3H)-yl)phenyl)carbamate [132] DCBS104 338
E IV.13.29 2-(4-Aminophenyl)-9-chloro-2,6-dihydro-[1,2,4]tria-zolo[4,3-c]quinazoline-3,5-dione [135] DCBS117 339

F Appendix 340
F I Publications resulting from this thesis 341
F II Curriculum vitae 344
F III List of abbreviations 346
F IV List of laboratory journal codes 347
F V References 350

Acknowledgements

Mein Dank gilt unzähligen Freunden und Bekannten, die ich leider hier nicht alle anführen kann. Dennoch vorweg ein ehrliches Dankeschön an Alle, die mich in dieser intensiven und schönen Zeit unterstützt haben.

Ich hatte während meiner Zeit das Glück drei BetreuerInnen an meiner Seite zu haben, die mich, jeder auf Seine/Ihre eigene Weise, gefordert und unterstützt haben: Margot Ernst, Michael Schnürch und Marko D. Mihovilovic.

Lieber Michl, ich bedanke mich in erster Linie für das spannende und anspruchsvolle Projekt, das Du mir anvertraut hast. Ich bin Dir auch sehr dankbar für Deine „lange Leinen" Betreuung, da ich gerne auch mal selbst vor mich hinarbeite. Dein Vertrauen und Deine regelmäßigen Denkanstöße haben, meiner Meinung nach, einen Großteil zu meinem erfolgreichen Abschluss dieser Arbeit beigetragen. Danke!

Liebe Margot, ich möchte mich ganz herzlich für Deine sehr familiäre Betreuung bedanken! Ich habe sämtliche Besuche in Deinem Labor positiv in Erinnerung und das wird auch immer so bleiben. Vielen Dank auch für die unzähligen und ausführlichen „private lessons", die mein biologisches Verständnis der Thematik enorm verstärkt haben. Danke!

Lieber Marko, ich möchte mich bei Dir auch für die Überlassung des Themas und das angenehme Arbeiten in Deiner Arbeitsgruppe bedanken. Deine professionelle, aber auch freundschaftliche Betreuung habe ich sehr geschätzt. Des Weiteren auch vielen Dank für Deinen Einsatz und Deine Unterstützung in manch „MolTag politischen" Angelegenheiten. Vielen Dank!

Ebenso gilt mein aufrichtiger Dank einmal mehr Margot Ernst und Thierry Langer für das Begutachten dieser Arbeit.

Maria „vaffanculo" Teresa Iorio! "Voglio compiacerti senza pudore" probably says it all. I remember the first day we had lunch together back in 2015 and my first thoughts were just: "Damn, she talks way too much"! However, it turned out (to my surprise) we became like brother and sister. Thank you for the great time in Vienna and wherever we traveled around during our time together. All the best and do not lose your "sparkling personality" even when the pieces of your heart will miss me ;). Grazie, bacio!

Ahoi Captain! Dein Engagement Unseren nicht-enden-wollenden Durst nach bevorzugt ca. 95% wasserhältigen Getränken zu löschen hat mir ein unvergleichliches Heimatgefühl vermittelt. Ich freue mich jetzt schon auf zukünftige Segelirrfahrten à la Jack Sparrow, nur mit mehr Wein und Rum versteht sich;). Danke für die gute Zeit in Wien und im Labor! Signalflagge P.

Γειά σου μαλάκα! Yes I mean you Konsti ;). Thanks for being the great person you just are and my "+1" at some cultural events. I am a bit disappointed though that we did not manage to visit either Greece or Thailand together. But I am sure we will stay in contact and cross that from our lists :). Thanks for being a really good friend!

Lieber Heiko auch Dir danke für die gemeinsame Zeit in Konstanz und Wien. Deine überaus reizende Gesellschaft bei unzähligen, außeruniversitären, alkohol- und spaßreichen Aktivitäten hat mir sowohl die Zeit in Konstanz als auch in Wien sehr versüßt. Danke!

Danke auch an die ganze Arbeitsgruppe Mihovilovic/Schnürch: Danke Dominik („Hollywood“) für unvergessliche Zeiten beim Skifahren und in Kroatien, Danke Daniela („Cintulover“) für unsere tolle gemeinsame Zeit und unzählige Massagen, Danke „Herr Diplom Ingeneur Hecko“ für gemeinsamen Konsum und Spaß bei der Arbeit, Danke David für einen unvergesslichen Sieg beim Rodeln und Danke auch an Alle anderen: Florian, Christian, Laszlo, Spettel, Martin, Blanca, Rafaella, Hubert, Clemens, Marcello, Erna, Hamid und Yago für die tolle Zeit (ich hoffe, dass ich niemanden vergessen habe)!

An dieser Stelle auch vielen Dank an die ehemaligen Kollegen, die nun schon erfolgreich abgeschlossen haben: Danke Kollegin Schaaf für einen enorm spaßigen Einstand in Wien und das Ausleben Unserer musikalischen Highlights („Style und das Geld“, „Tearin‘ up my heart“, nur um zwei gennant zu haben ;)), Danke Donzi für eine unvergessliche vergessliche Nacht im Kamera Club und die viele Liebe, die Du am Arbeitsplatz verbreitet hast (#riceislife), Danke Wiesinger für das Verstreuen von Lockerheit bei der Arbeit und mehrfache Erinnerungen an meine Heimt („DEUTSCHER!“), Danke Kollegin Ressmann für eine sehr unterhaltsame und zweideutige Zeit zusammen :).

Ich möchte mich auch bei meinen Studenten der letzten Jahre, Marco Calio („Cazzino“), Bernhard Jandl („Mr. BJ“), Lukas Kalchgruber, Daniele Catorci, Lukas Gaggl, Lisa Sinawehl, Mahdieh Bagheri, Leila Ayatollahi, Benjamin Regen-Preziger, Josefine Sprachmann, Philipp Miksovsky, Patricia Ulrich, Marlon Millard und Alexander Krifda sehr bedanken. Jeder von Ihnen hat in Form einer Master-/Bachelorarbeit oder in Form eines Wahlpraktikums einen wesentlichen Teil beigetragen. Diese Arbeit wäre in diesem Umfang ohne Euch nicht zustande gekommen. Danke!

Vielen Dank geht auch an die Herrschaften aus dem Erdgeschoss (Max und Nici) und an das gesamte Institut für grandiose Weihnachtsfeiern und weitere Spaßveranstaltungen.

Vielen Dank auch an das ganze „Ernst Lab“ für das Messen meiner Substanzen und die freundlichen Aufenthalte in Eurem Labor: Danke Marco, Raphi, Xenia, Filip, Sabah und Philip.

Weiterer Dank auch an Lars und Marcus „the nerds“ von denen ich Vieles über *in silico* Arbeit lernen durfte.

Ich möchte hier auch noch meine Dankbarkeit ausprechen Teil von „MolTag“ gewesen zu sein. Wir hatten auch eine unvergessliche Zeit zusammen, danke an alle PI’s und alle Stundent. Besonderer Danke gebührt: Susanne, Marco, Eva, Jasmin, Stefanie, Alex, Catherine, Ximena, Stan, Harald, Marco and Felix.

Danke auch an alle Freunde von zuhause und von meiner Zeit in Konstanz und Saarbrücken: Thomas, Lynn, Moritz, Dominic, Benjamin, Markus, Stammtisch „In yer face“, Stammtisch Tübingen und selbstverständlich vielen, vielen mehr :).

Zu guter letzt möchte ich meiner Familie danken ohne die dies alles nicht möglich gewesen wäre! Danke Mama und danke Papa für Eure Unterstützung während meines Studiums in Konstanz, meiner Zeit in Saarbrücken und in Wien. Sarah, ohne Dich wäre Nichts auch annährend möglich gewesen. Ich wüsste nicht wo ich in meinem Leben stünde, wenn es Dich nicht geben würde. Vielen Dank, dass Du die beste Schwester bist, die man sich vorstellen kann!

Abstract

The neurotransmitter γ - aminobutyric acid (GABA) occurs ubiquitously in our central nervous system (CNS) and binds, *inter alia*, to a class of ligand-gated ion channels called $GABA_A$ receptors. These pentameric receptors are targets of many clinically relevant drugs (e.g. benzodiazepines). The family contains many different subunits which are further classified into isoforms (e.g. α1-6, β1-3, γ1-3, etc). Thus, there exists an enormous number of possible different subunit assemblies (receptor subtypes) which results in a very complex pharmacology of these receptors. Hence, the exploration of selective pharmacological tool compounds to study $GABA_A$ receptors is of great importance.

The compound class of pyrazoloquinolinones (PQs) is known to interact with the high affinity α+/γ2− interface (benzodiazepine binding site) and the low affinity modulatory site at the α+/β−interface. Therefore, PQs represent a suitable starting point to study the molecular determinants which influence the mechanism of allosteric modulation at the two homologous binding sites.

In this thesis we focused on the synthesis of a systematic library of differently substituted PQs to examine molecular determinants which trigger potency and efficacy at the α+/β− and the α+/γ2− sites. Based on this library we were able to identify two subtype selective prototypes which served as proof of concept in the development of urgently required subtype selective tool compounds. Furthermore, we identified one compound which represents a lead towards subtype selective ligands for the α+/β− interface exclusively.

Moreover, different homology models were generated to improve the understanding of the structural requirements of allosteric modulation. Experimentally, we studied a quadruple mutant to study different benzodiazepine ligands. Interestingly, we revealed that the allosteric modulation at both sites seemingly follows a quite conserved mechanism and that similar benzodiazepine ligands can have different binding poses.

Ultimately, we elucidated the binding mode of PQs at the α1+/γ2- site by establishing a novel docking protocol which assesses SAR data during the scoring process. The combination of these findings led to innovative ligand designs which should exclusively interact with the α+/β− interfaces and will be investigated in future studies.

Kurzfassung

Der Neurotransmitter γ-Aminobuttersäure (GABA) ist in unserem Zentralennervensystem (ZNS) weit verbreitet und bindet unter anderem an eine Klasse von ligandengesteuerten Ionenkanälen, die $GABA_A$-Rezeptoren genannt werden. Diese pentameren Rezeptoren sind Zieleobjekte vieler klinisch relevanter Arzneimittel (z. B. Benzodiazepine) und bestehen aus vielen verschiedenen Untereinheiten, die sich zusätzlich in Isoformen unterscheiden (z. B. α1-6, β1-3, γ1-3 usw.). Daher existiert eine enorme Anzahl an möglichen Anordnungen der unterschiedlichen Untereinheiten (Rezeptor-Subtypen), was zu einer sehr komplexen Pharmakologie dieser Rezeptoren führt. Die Forschung nach selektiven pharmakologischen Diagnoseverbindungen zur Untersuchung von $GABA_A$-Rezeptoren ist ergo von großer Bedeutung.

Es ist bekannt, dass die Verbindungsklasse von Pyrazolochinolinonen (PQs) mit hoher Affinität an die α+/γ2− Grenzfläche (Benzodiazepin-Bindungsstelle) und mit niedriger Affinität an die α+/β− Grenzfläche bindet. Somit stellen PQs einen geeigneten Ausgangspunkt dar, um die molekularen Determinanten zu untersuchen, die den Mechanismus der allosterischen Modulation zwischen den zwei homologen Bindungsstellen beeinflussen.

In dieser Arbeit haben wir uns auf die Synthese einer systematischen Bibliothek unterschiedlich substituierter PQs konzentriert, um molekulare Determinanten zu untersuchen, die an der α+/β− und der α+/γ2− Bindestellen Wirksamkeit auslösen. Basierend auf dieser Bibliothek konnten wir zwei subtyp-selektive Prototypen identifizieren, die als Beweis für die Entwicklung dringend benötigter subtyp-selektiver Diagnoseverbindungen dienten. Darüber hinaus identifizierten wir eine Verbindung, die als Voreiter für subtyp-selektive Liganden ausschließlich für die α+/β− Bindestelle dient.

Weiters wurden verschiedene Homologiemodelle generiert, um das Verständnis der strukturellen Anforderungen allosterischer Modulation zu verbessern. Experimentell untersuchten wir eine Vierfach-Mutante unter der Verwendung verschiedener Benzodiazepinliganden. Interessanterweise zeigten wir, dass die allosterische Modulation an beiden Stellen scheinbar einem recht konservierten Mechanismus folgt und dass ähnliche Benzodiazepin-Liganden unterschiedliche Bindungsorientierungen einnehmen können.

Abschließend haben wir die Bindungsorientierung von PQs an der α1+/γ2− Bindestelle aufgeklärt, indem wir ein neues Docking-Protokoll etabliert haben, das während des Bewertungsprozesses auf Struktur-Aktivität-Beziehungsdaten zurückgreift. Die Kombination dieser Ergebnisse führte zu innovativen Liganden-Designs, welche zu Verbindung führen sollten, die ausschließlich an die α+/β− Bindestelle binden. Die Evaluierung dieser Verbindungen wird in zukünftigen Studien untersucht werden.

A Synthetic schemes

All compounds prepared or used as starting materials in this thesis are numbered in bold Arabic numerals. Compounds unknown to the literature are additionally underlined. Compounds mentioned in the introduction are numbered in bold Roman numerals.

A I Pyrazoloquinolinones – precursors of R^6 series

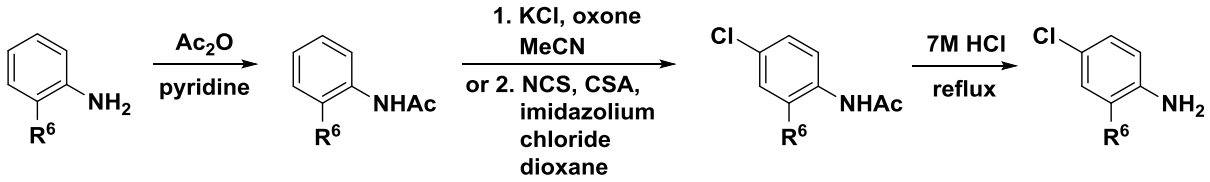

[181] R^6 = Et
[182] R^6 = *i*Pr

[183] R^6 = Et (58%)
[184] R^6 = *i*Pr (90%)

[185] R^6 = Et (crude)*
[186] R^6 = *i*Pr (50%)**

[187] R^6 = Et (28%)***
[188] R^6 = *i*Pr (85%)

*According to procedure 1; regioisomer mixture, separation after next step
**According to procedure 2
*** yield over 2 steps

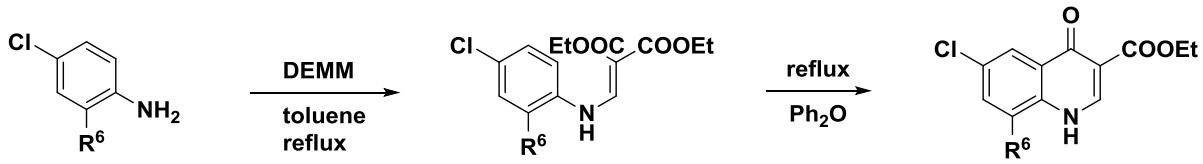

[189] R^6 = F
[190] R^6 = Cl
[191] R^6 = Br
[192] R^6 = CF_3
[193] R^6 = Me
[187] R^6 = Et
[188] R^6 = *i*Pr

[194] R^6 = F (87%)
[195] R^6 = Cl (89%)
[196] R^6 = Br (91%)
[197] R^6 = CF_3 (75%)
[198] R^6 = Me (77%)
[199] R^6 = Et (85%)
[200] R^6 = *i*Pr (53%)

[201] R^6 = F (75%)
[202] R^6 = Cl (79%)
[203] R^6 = Br (81%)
[204] R^6 = CF_3 (33%)
[205] R^6 = Me (77%)
[206] R^6 = Et (74%)
[207] R^6 = *i*Pr (36%)

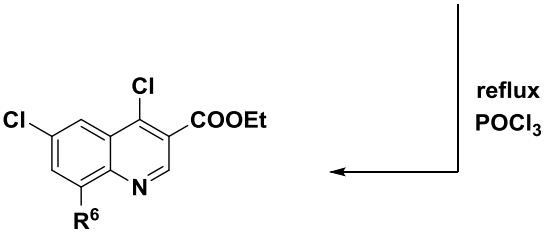

[208] R^6 = F (75%)
[209] R^6 = Cl (32%)
[210] R^6 = Br (72%)
[211] R^6 = CF_3 (69%)
[212] R^6 = Me (63%)
[213] R^6 = Et (55%)
[214] R^6 = *i*Pr (62%)

A II Pyrazoloquinolinones – precursors of R^7 and R^8 series

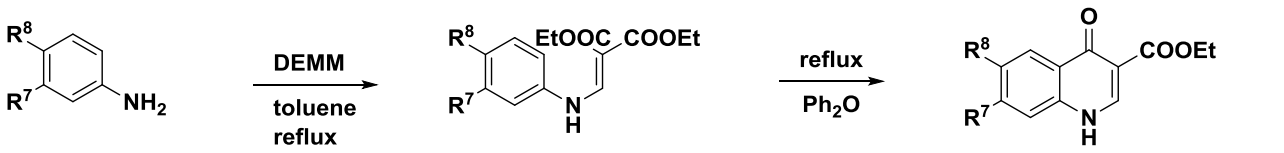

[20] R^7 = H, R^8 = F
[21] R^7 = H, R^8 = Cl
[22] R^7 = H, R^8 = Br
[88a] R^7 = H, R^8 = Ph
[5] R^7 = H, R^8 = OMe
[159] R^7 = Br, R^8 = H
[176] R^7 = OMe, R^8 = H

[23] R^7 = H, R^8 = F (quant.)
[24] R^7 = H, R^8 = Cl (quant.)
[25] R^7 = H, R^8 = Br (99%)
[88b] R^7 = H, R^8 = Ph (91%)
[6] R^7 = H, R^8 = OMe (73%)
[160] R^7 = Br, R^8 = H (quant.)
[177] R^7 = OMe, R^8 = H (quant.)

[26] R^7 = H, R^8 = F (41%)
[27] R^7 = H, R^8 = Cl (57%)
[28] R^7 = H, R^8 = Br (73%)
[88c] R^7 = H, R^8 = Ph (47%)
[7] R^7 = H, R^8 = OMe (54%)
[161] R^7 = Br, R^8 = H (66%)
[178] R^7 = OMe, R^8 = H (55%)

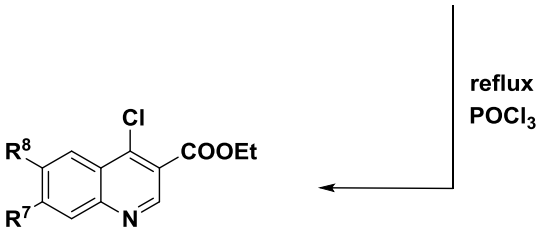

[29] R^7 = H, R^8 = F (63%)
[30] R^7 = H, R^8 = Cl (76%)
[31] R^7 = H, R^8 = Br (90%)
[88d] R^7 = H, R^8 = Ph (43%)
[8] R^7 = H, R^8 = OMe (66%)
[162] R^7 = Br, R^8 = H (82%)
[179] R^7 = OMe, R^8 = H (62%)

A III Pyrazoloquinolinones –R^6 series

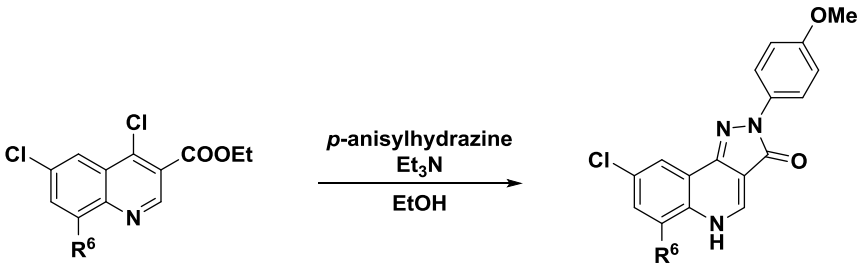

[208] R^6 = F
[209] R^6 = Cl
[210] R^6 = Br
[211] R^6 = CF_3
[212] R^6 = Me
[213] R^6 = Et
[214] R^6 = *i*Pr

[215] R^6 = F
[216] R^6 = Cl
[217] R^6 = Br
[218] R^6 = CF_3
[219] R^6 = Me
[220] R^6 = Et
[221] R^6 = *i*Pr

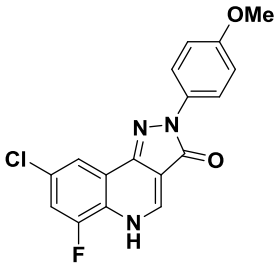

[215] (20%)

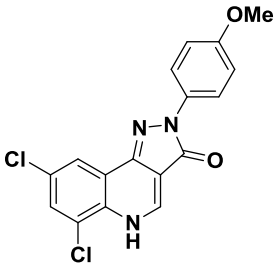

[216] (27%)

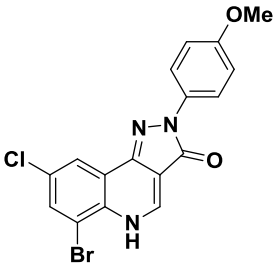

[217] (30%)

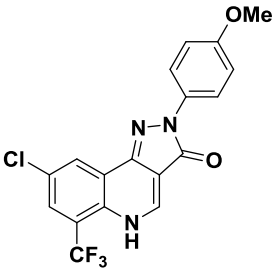

[218] (7%)

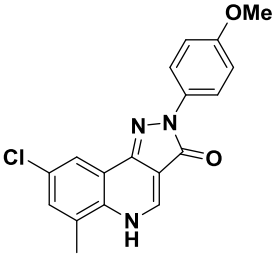

[219] (38%)

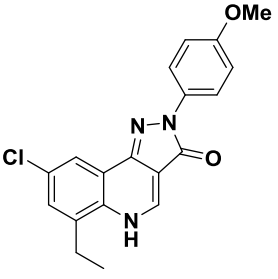

[220] (80%)

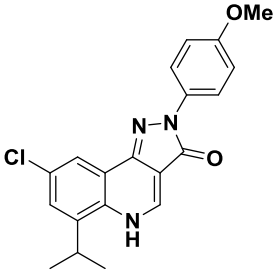

[221] (37%)

A IV Pyrazoloquinolinones – R^7 series

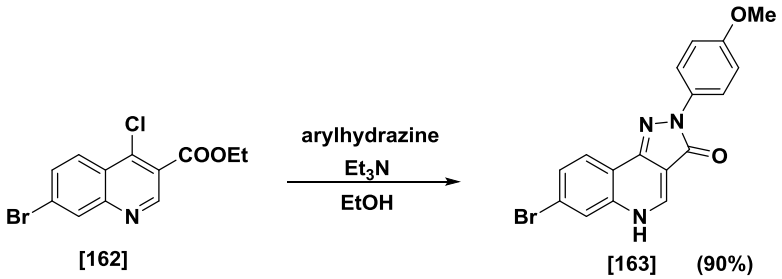

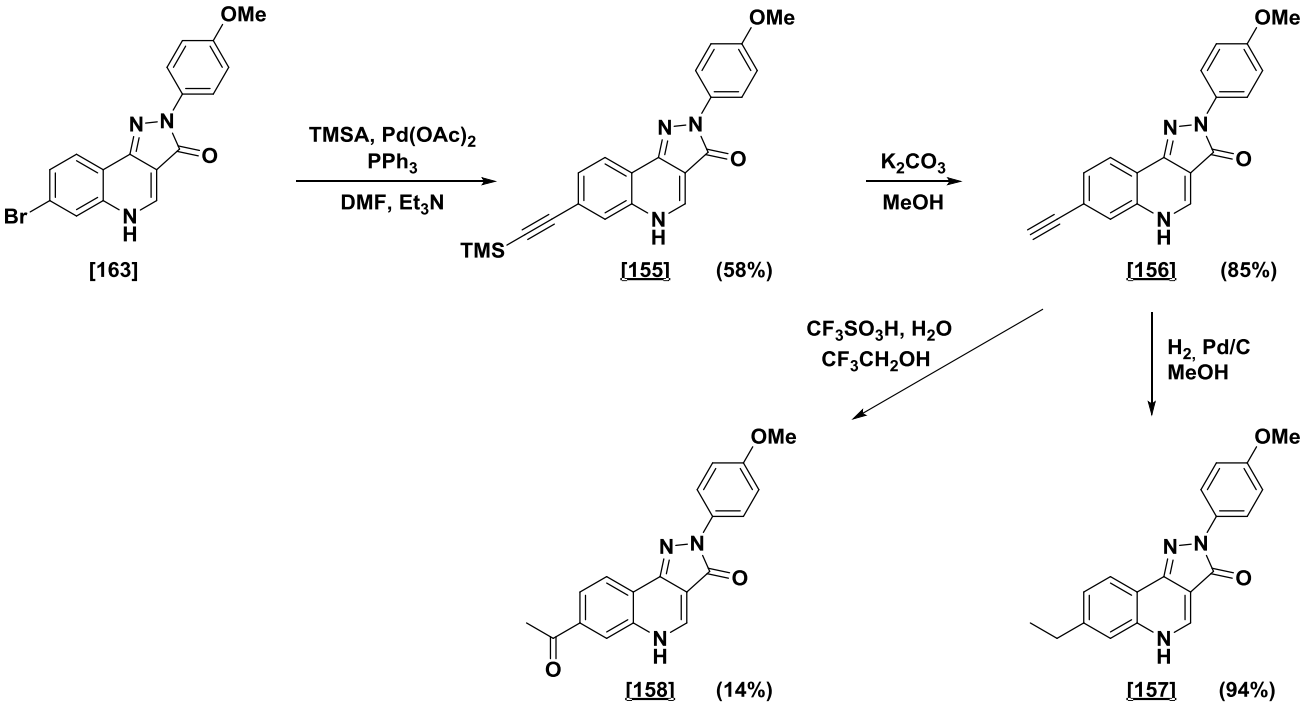

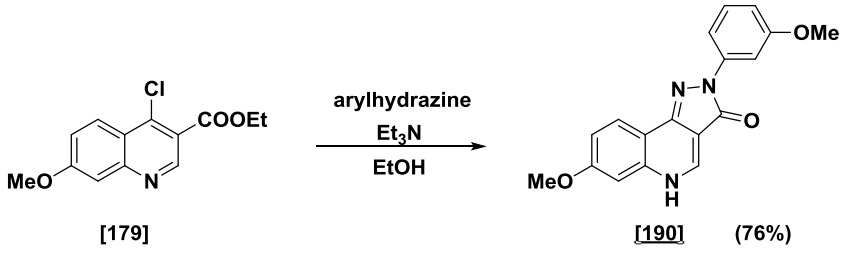

A V Pyrazoloquinolinones – alkyl series

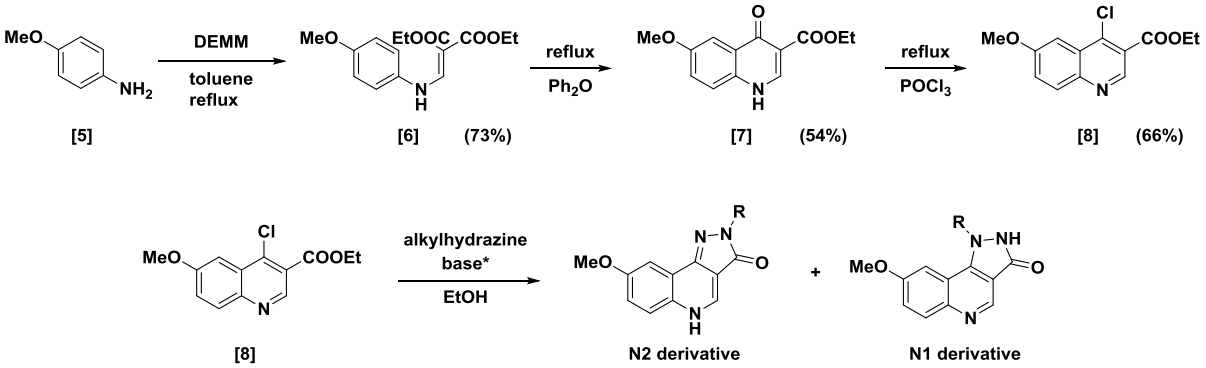

* a: Et_3N used as base
b: NaOMe used as base

R=

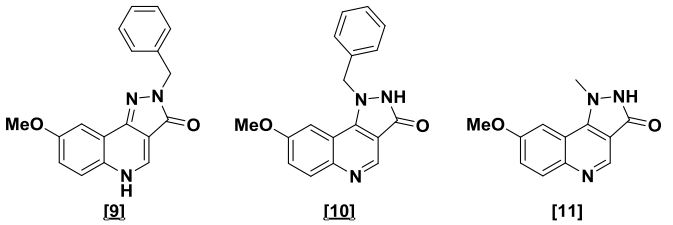

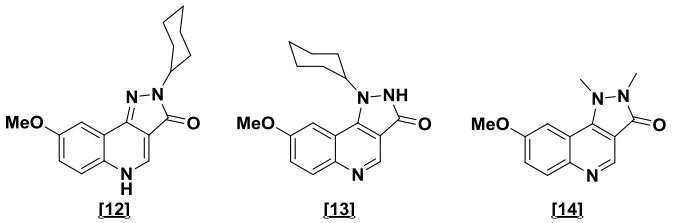

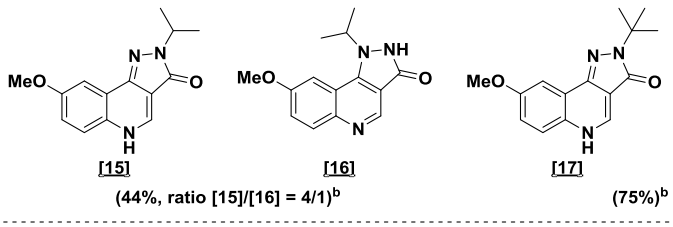

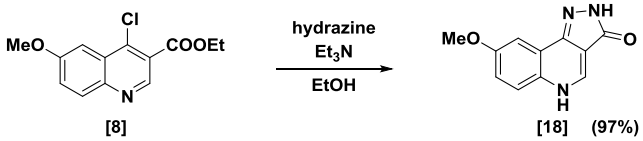

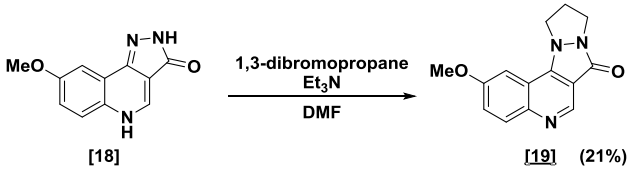

A VI Pyrazoloquinolinones – R^8 fluoro series

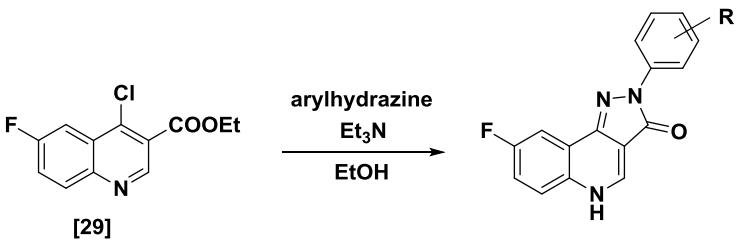

[29]

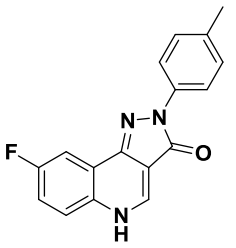

[32] (66%)

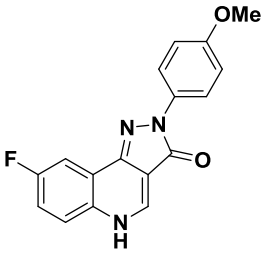

[33] (quant.)

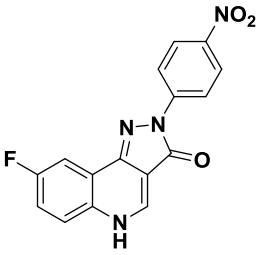

[34] (37%)

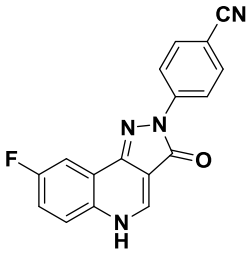

[35] (61%)

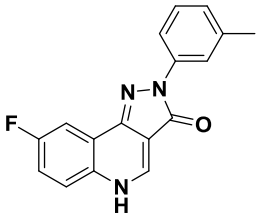

[39] (76%)

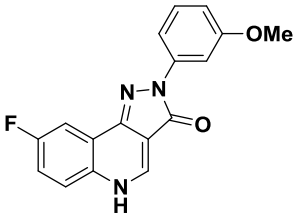

[40] (81%)

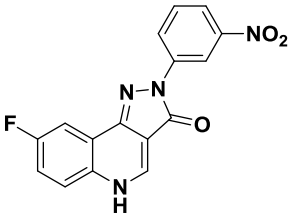

[41] (70%)

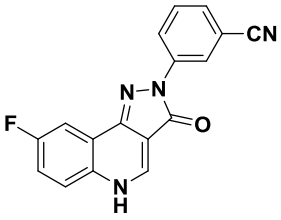

[42] (52%)

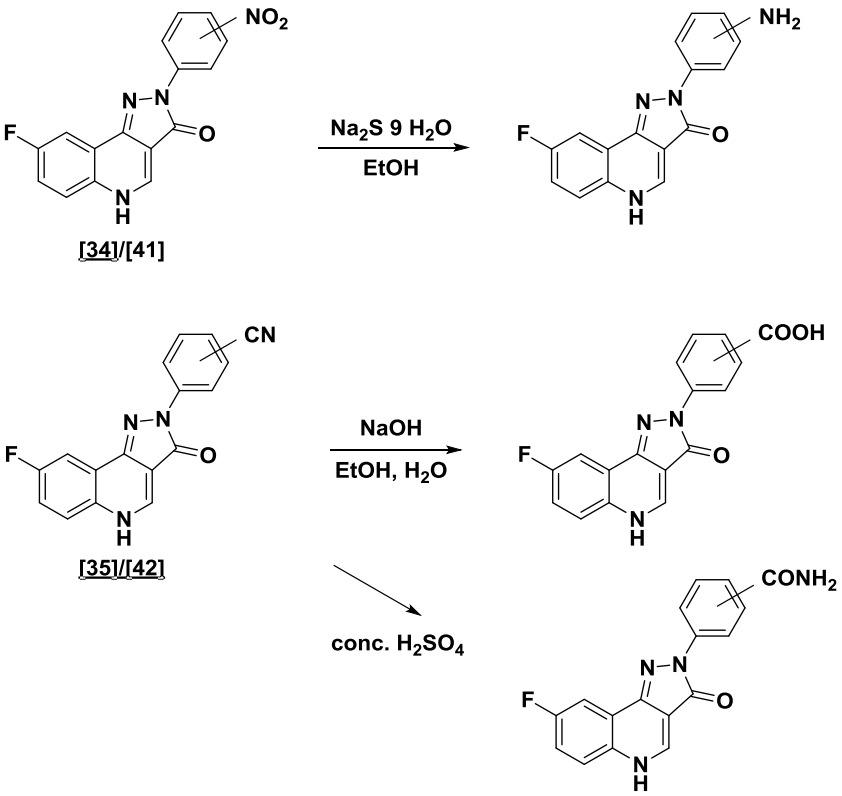

[34]/[41]

[35]/[42]

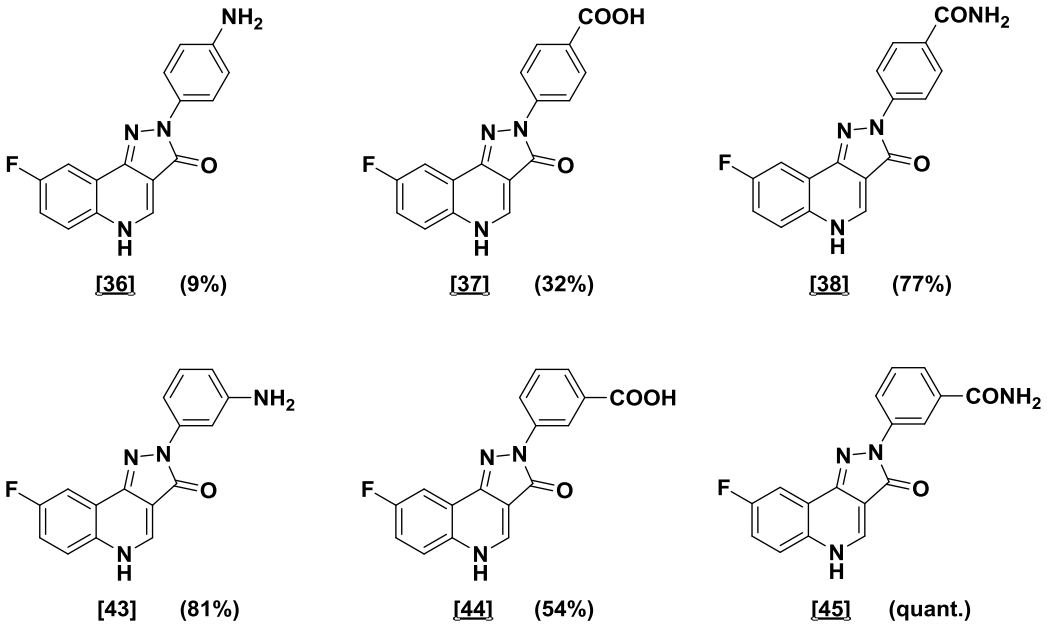

[36] (9%) [37] (32%) [38] (77%)

[43] (81%) [44] (54%) [45] (quant.)

A VII Pyrazoloquinolinones – R^8 chloro series

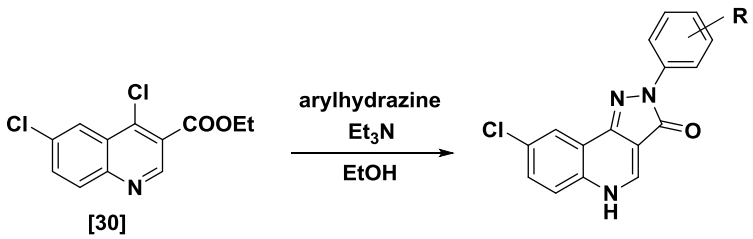

[30]

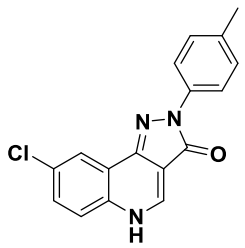

[46] (79%)

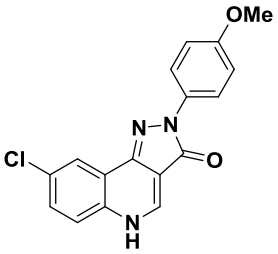

[47] (58%)

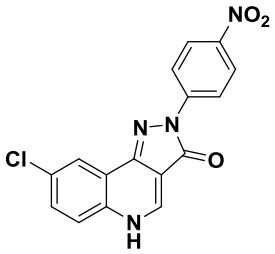

[48] (37%)

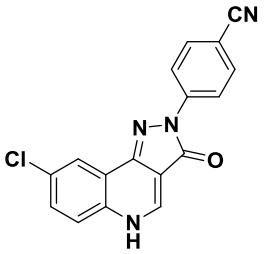

[49] (84%)

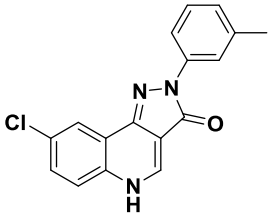

[52] (63%)

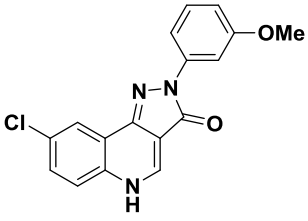

[53] (76%)

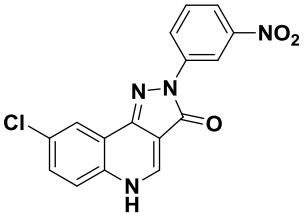

[54] (92%)

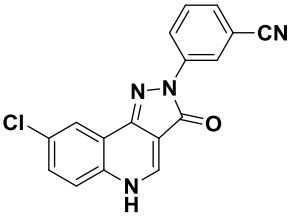

[55] (71%)

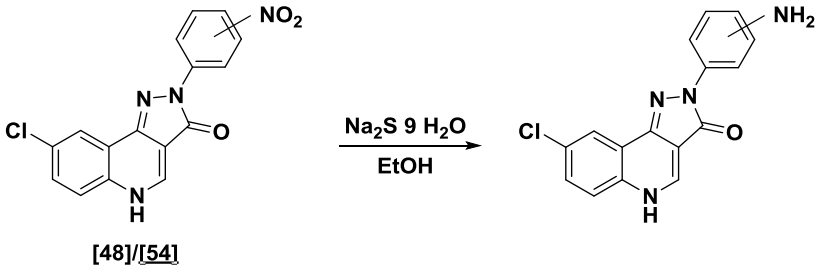

[48]/[54]

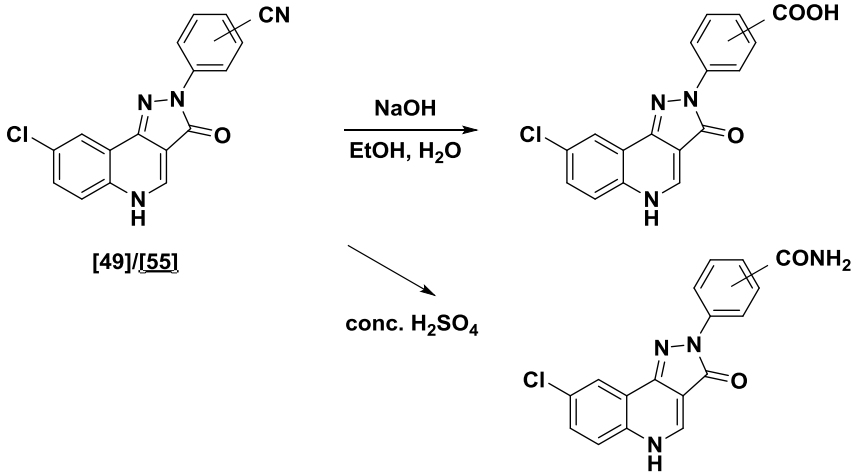

[49]/[55]

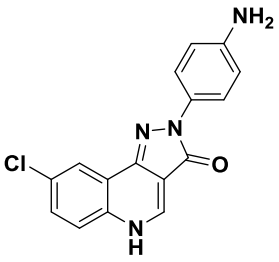

[50] (81%)

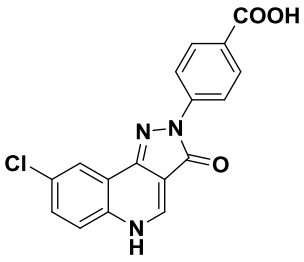

[51] (65%)

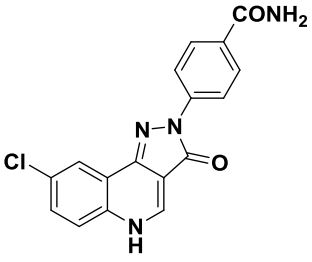

[52] (quant.)

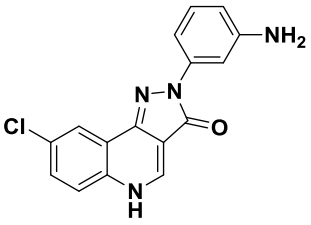

[56] (82%)

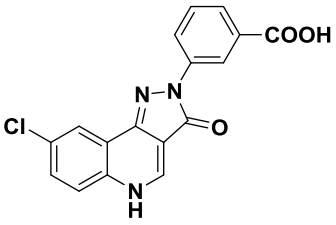

[57] (70%)

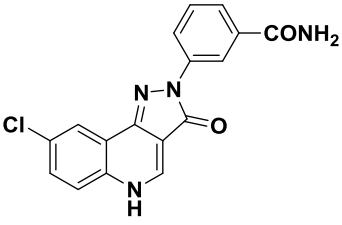

[58] (75%)

A VIII Pyrazoloquinolinones – R^8 bromo series

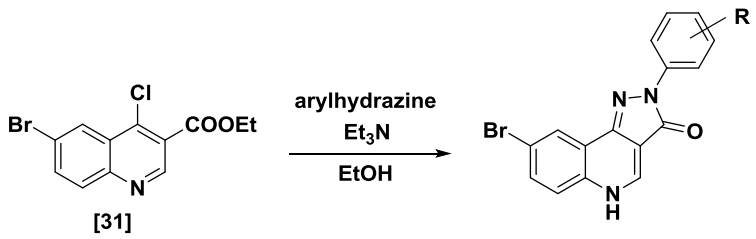

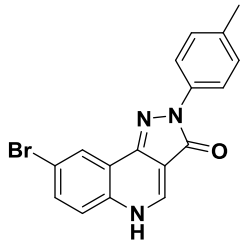

[60] (64%)

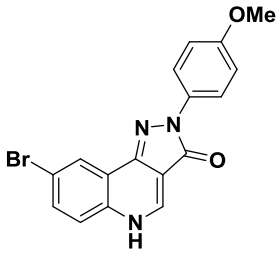

[61] (63%)

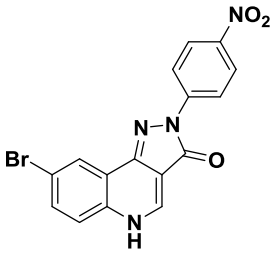

[62] (55%)

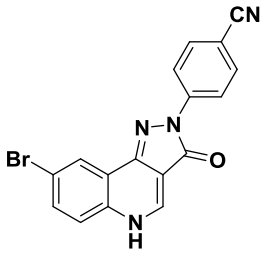

[63] (77%)

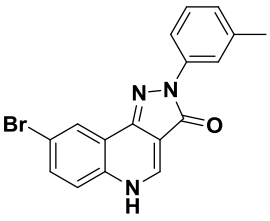

[67] (52%)

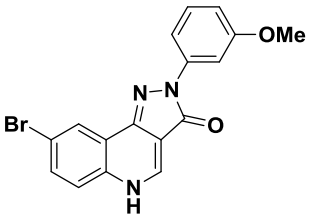

[68] (63%)

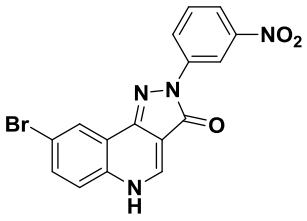

[69] (62%)

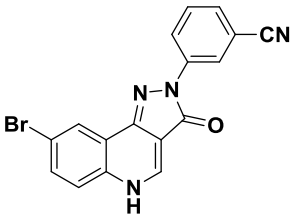

[70] (86%)

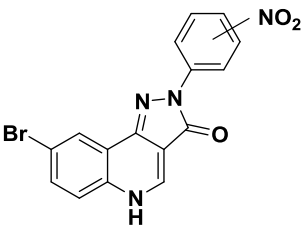

[62]/[69]

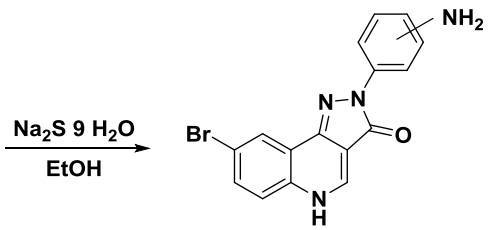

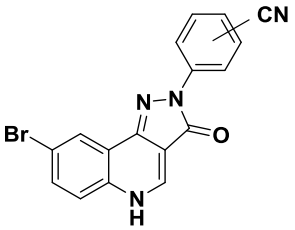

[63]/[70]

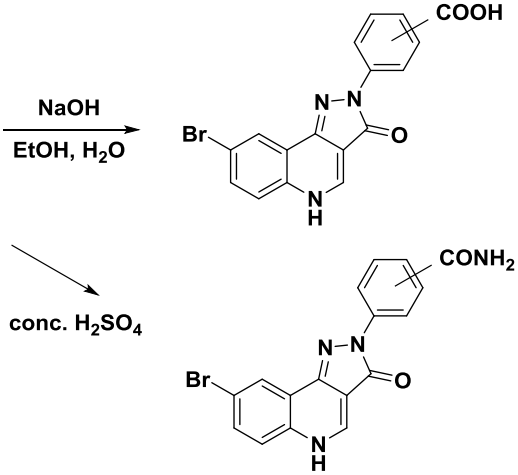

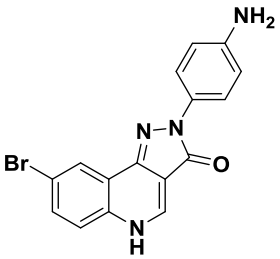

[64] (77%)

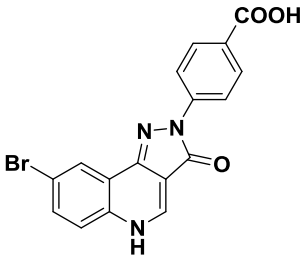

[65] (66%)

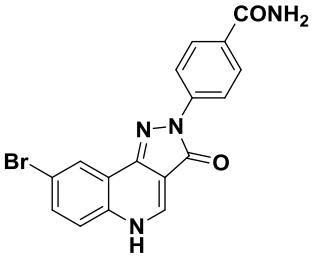

[66] (55%)

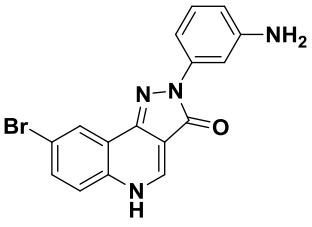

[71] (80%)

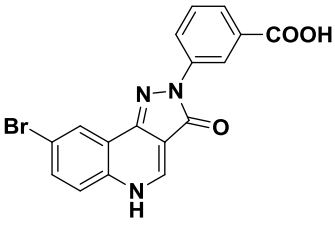

[72] (66%)

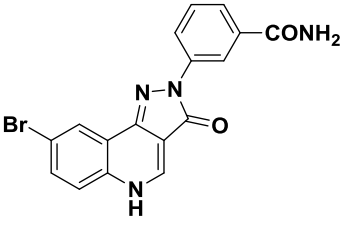

[73] (58%)

A IX Pyrazoloquinolinones – R^8 methoxy series

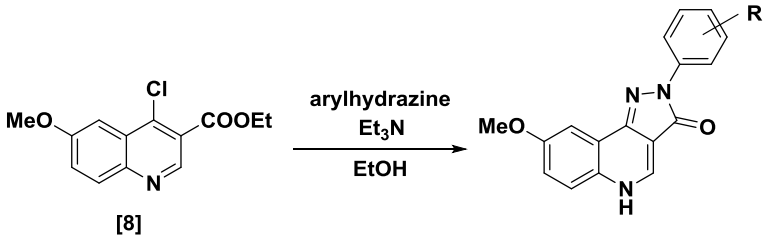

[8]

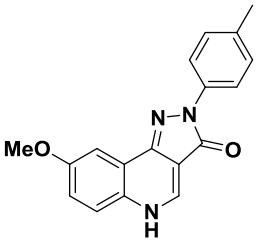

[74] (74%)

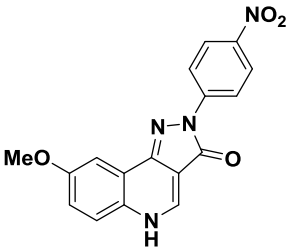

[76] (63%)

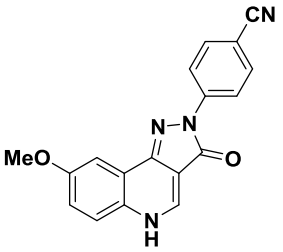

[77] (57%)

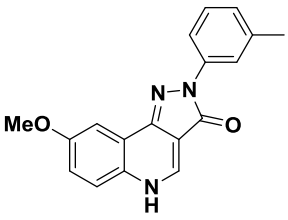

[81] (62%)

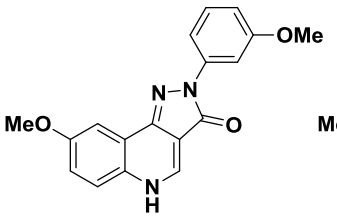

[82] (68%)

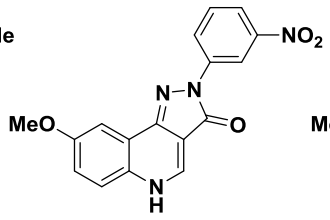

[83] (25%)

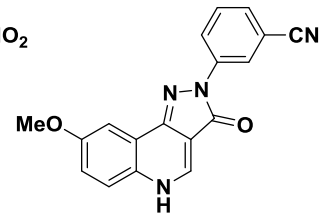

[84] (53%)

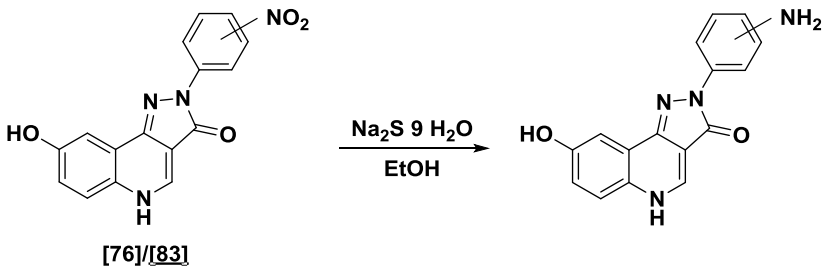

[76]/[83]

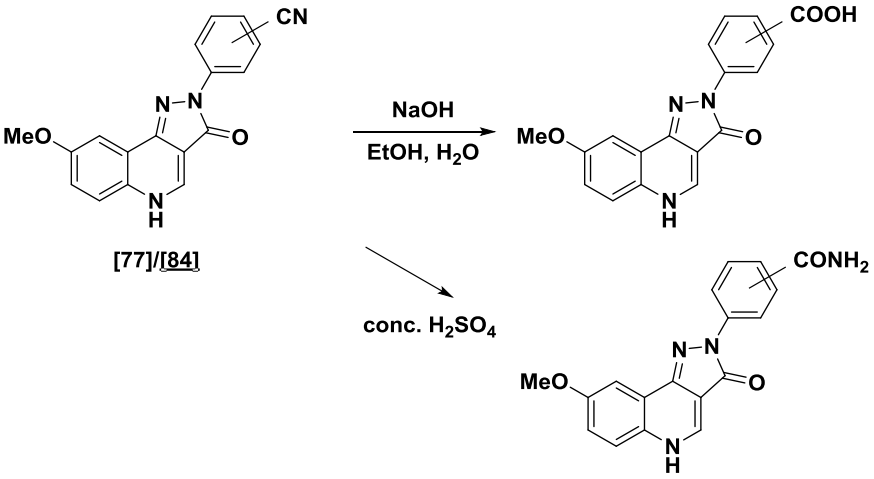

[77]/[84]

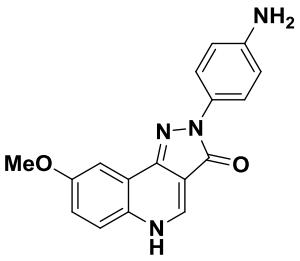

[78] (16%)

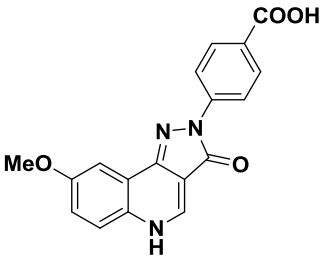

[79] (66%)

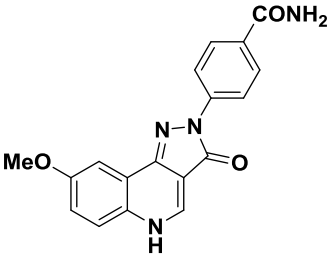

[80] (67%)

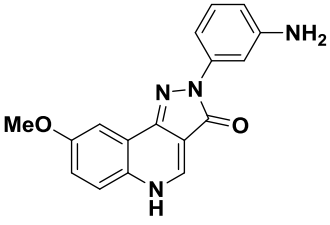

[85] (65%)

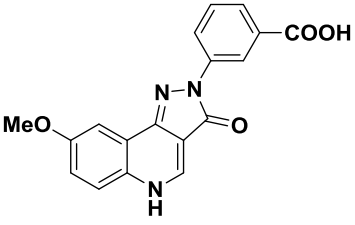

[86] (57%)

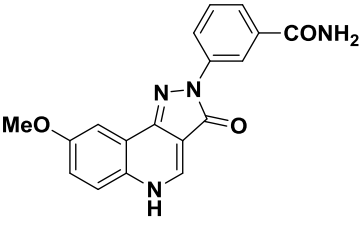

[87] (66%)

A X Pyrazoloquinolinones – mixed series

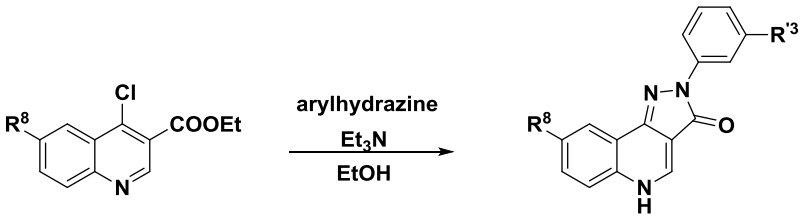

[30] R^8 = Cl
[31] R^8 = Br
[8] R^8 = OMe
[88d] R^8 = Ph

[89] R^8 = Cl R'^3 = Br
[90] R^8 = Br R'^3 = H
[91] R^8 = OMe R'^3 = Br
[92] R^8 = Ph R'^3 = H

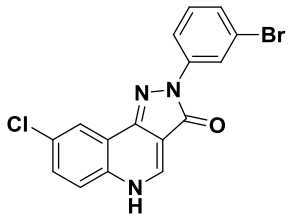

[89] (75%)

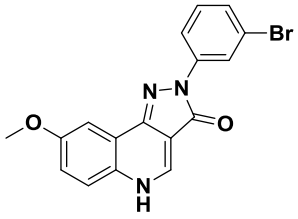

[90] (39%)

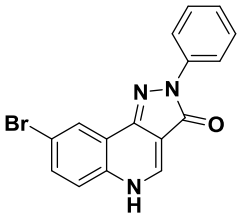

[91] (41%)

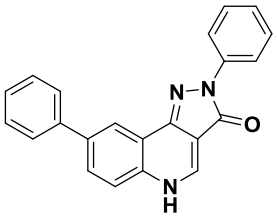

[92] (12%)

A XI Pyrazoloquinolinones – 2nd generation

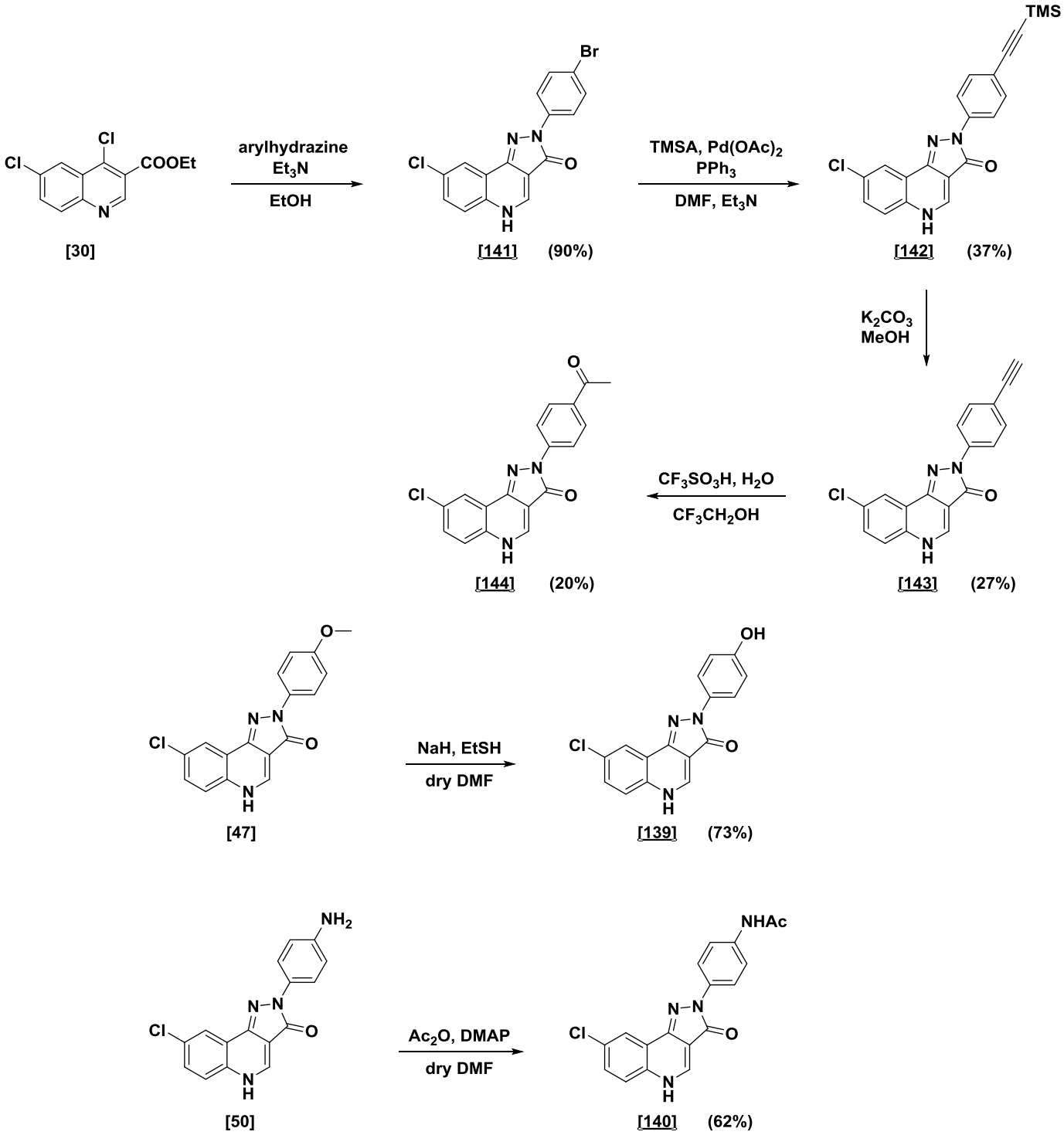

A XII Pyrazoloquinolinones – α+/γ– vs. α+/β–

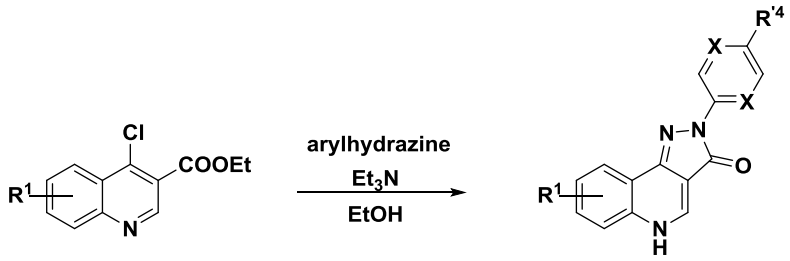

R^1: [8] R^8 = OMe
[179] R^7 = OMe

R^1: R^8 = OMe
R^7 = OMe

R'4 = H or Cl
X = C or N

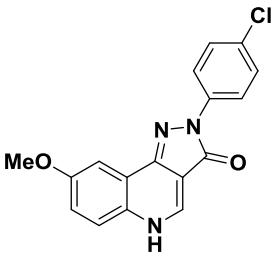

[222] (54%)

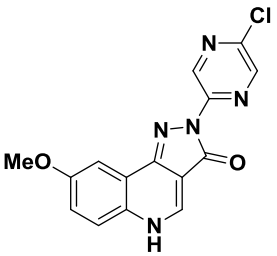

[223] (85%)

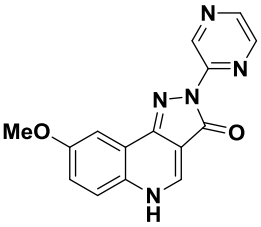

[224] (67%)

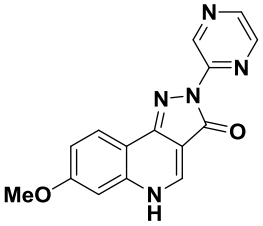

[225] (58%)

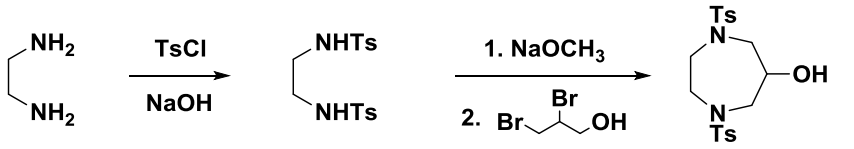

[235] [236] (85%) [237] (50%)

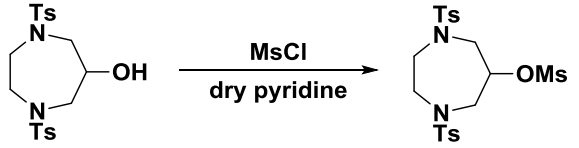

[237] [238] (72%)

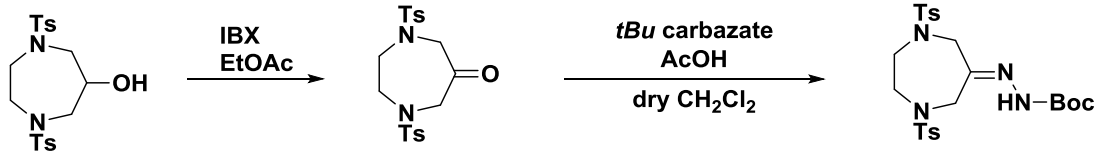

[237] [241] (67%) [243] (66%)

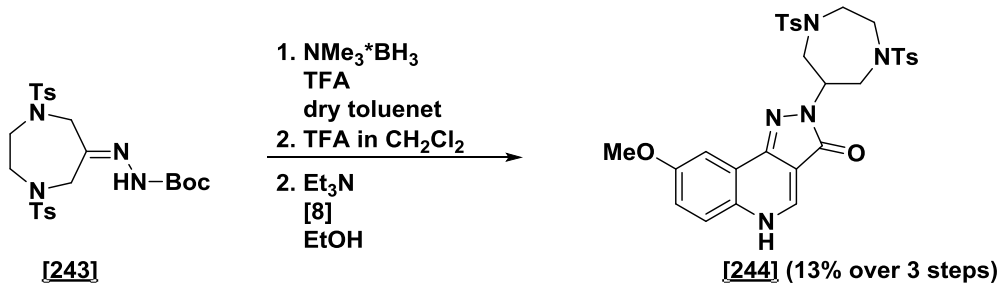

[243] [244] (13% over 3 steps)

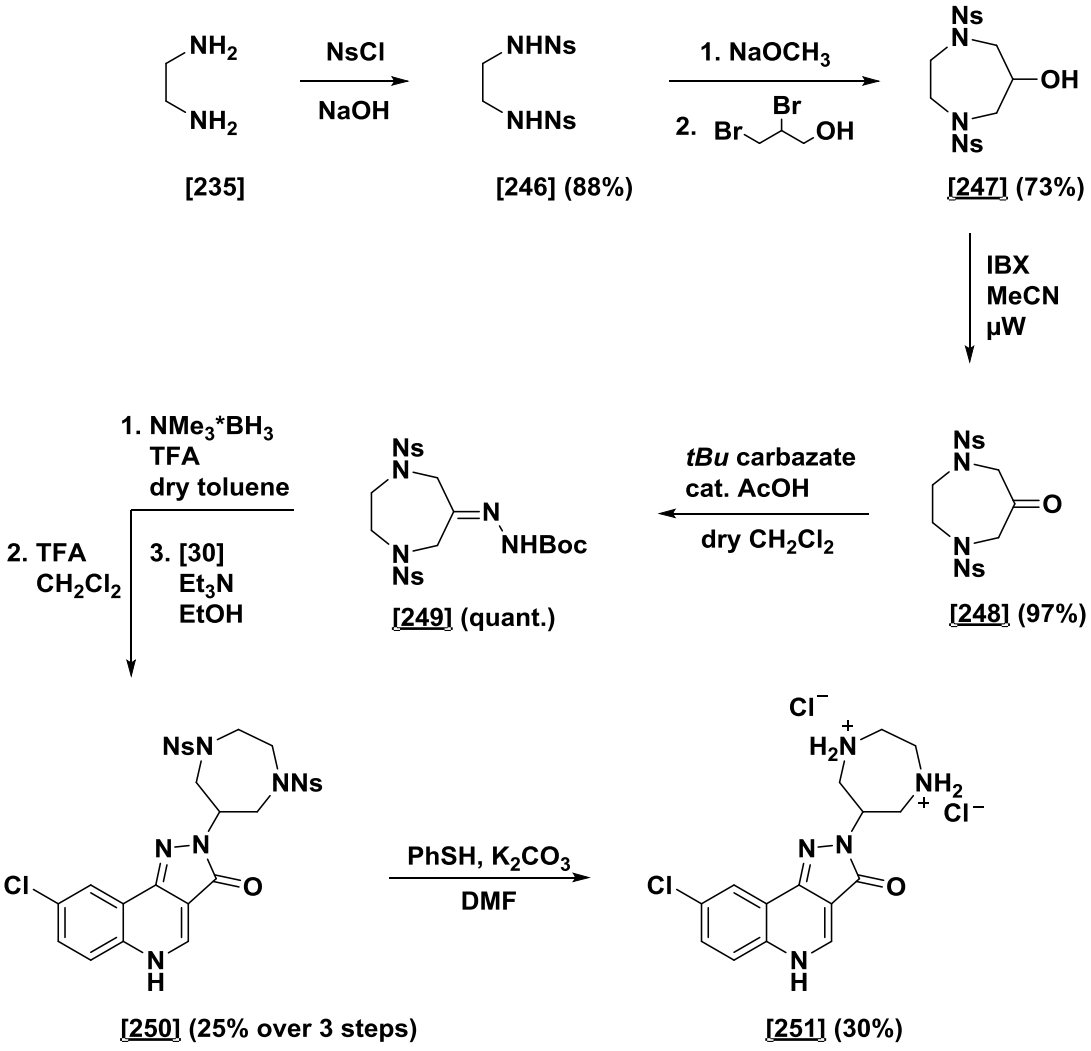
NH2
NH2
NsCl
NaOH
NHNs
NHNs
1. NaOCH3
2. Br
Br
OH
Ns
N
OH
N
Ns
[235]
[246] (88%)
[247] (73%)
IBX
MeCN
µW
1. NMe3*BH3
TFA
dry toluene
2. TFA
CH2Cl2
3. [30]
Et3N
EtOH
Ns
N
N
NHBoc
N
Ns
tBu carbazate
cat. AcOH
dry CH2Cl2
Ns
N
O
N
Ns
[249] (quant.)
[248] (97%)
NsN
NNs
N–N
Cl
O
N
H
PhSH, K2CO3
DMF
Cl−
H2N+
NH2
+ Cl−
N–N
Cl
O
N
H
[250] (25% over 3 steps)
[251] (30%)

A XIII Triazoloquinazolinediones – chloro precursors

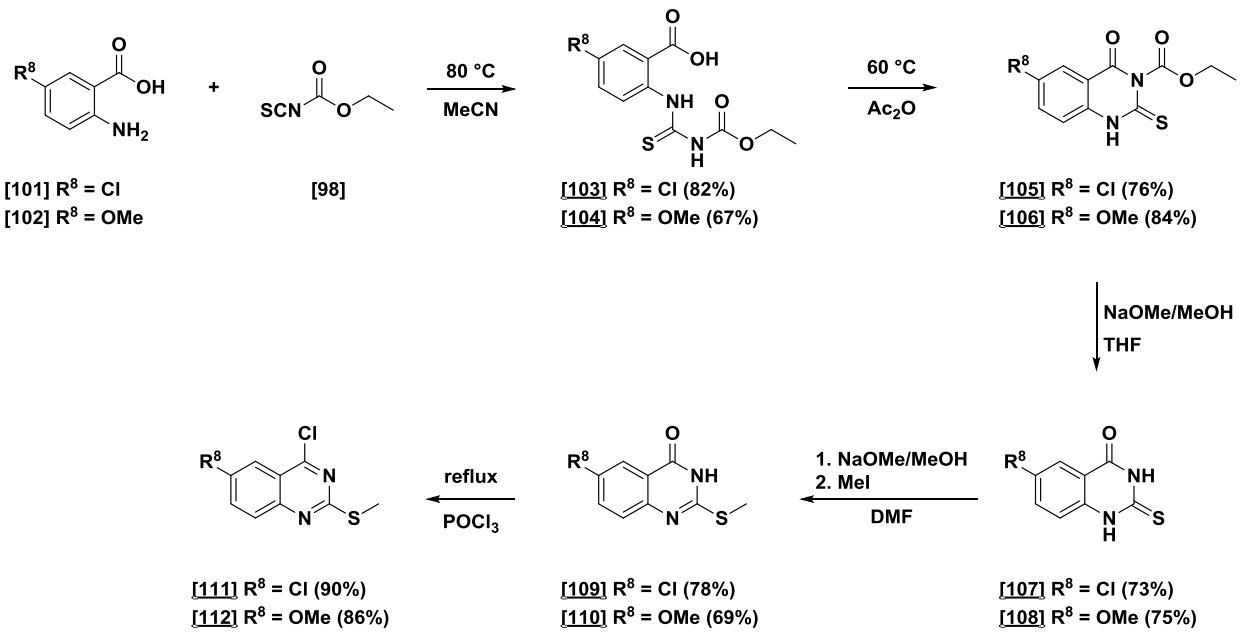

[101] R^8 = Cl
[102] R^8 = OMe

[98]

[103] R^8 = Cl (82%)
[104] R^8 = OMe (67%)

[105] R^8 = Cl (76%)
[106] R^8 = OMe (84%)

[107] R^8 = Cl (73%)
[108] R^8 = OMe (75%)

[109] R^8 = Cl (78%)
[110] R^8 = OMe (69%)

[111] R^8 = Cl (90%)
[112] R^8 = OMe (86%)

A XIV Triazoloquinazolinediones – ethyl 1-(aryl)hydrazine-1-carboxylates

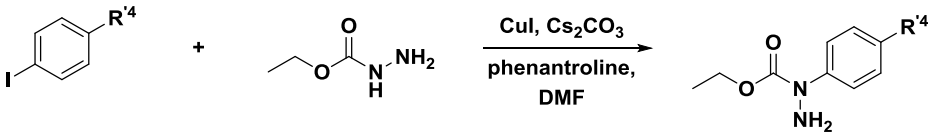

[113] R'^4 = CN
[114] R'^4 = Me
[115] R'^4 = NH_2
[116] R'^4 = OMe

[99]

[117] R'^4 = CN (72%)
[118] R'^4 = Me (58%)
[119] R'^4 = NH_2 (69%)
[120] R'^4 = OMe (65%)

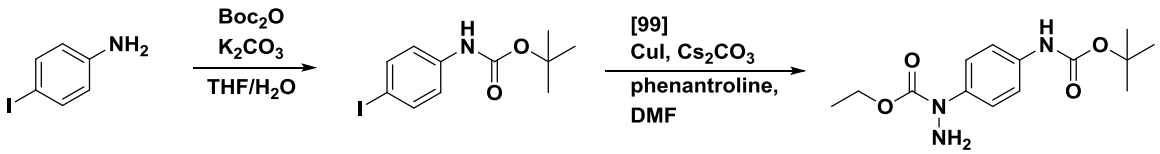

[115]

[121] (86%)

[122] (31%)

A XV Triazoloquinazolinediones – R^8 chloro and methoxy series

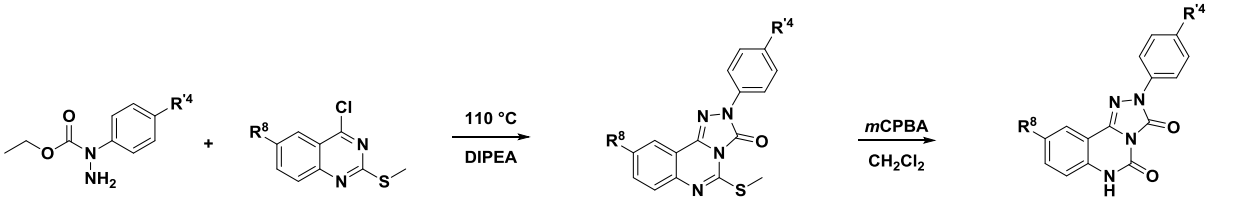

[117] R'^4 = CN
[118] R'^4 = Me
[120] R'^4 = OMe
[122] R'^4 = NHBoc

[111],[112] R^8 = Cl, OMe

[123] R^8 = Cl, R'^4 = CN (59%)
[124] R^8 = Cl, R'^4 = Me (70%)
[125] R^8 = Cl, R'^4 = OMe 59%)
[126] R^8 = Cl, R'^4 = NHBoc (32%)
[127] R^8 = OMe, R'^4 = Me (56%)
[128] R^8 = OMe, R'^4 = OMe (64%)

[129] R^8 = Cl, R'^4 = CN
[130] R^8 = Cl, R'^4 = Me
[131] R^8 = Cl, R'^4 = OMe
[132] R^8 = Cl, R'^4 = NHBoc
[133] R^8 = OMe, R'^4 = Me
[134] R^8 = OMe, R'^4 = OMe

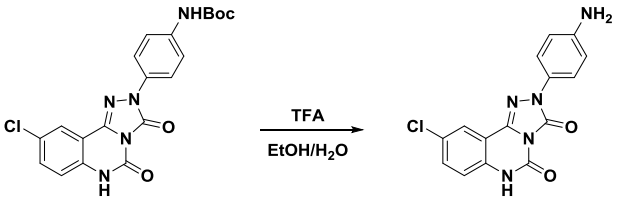

[132] (40%)

[135] (quant.)

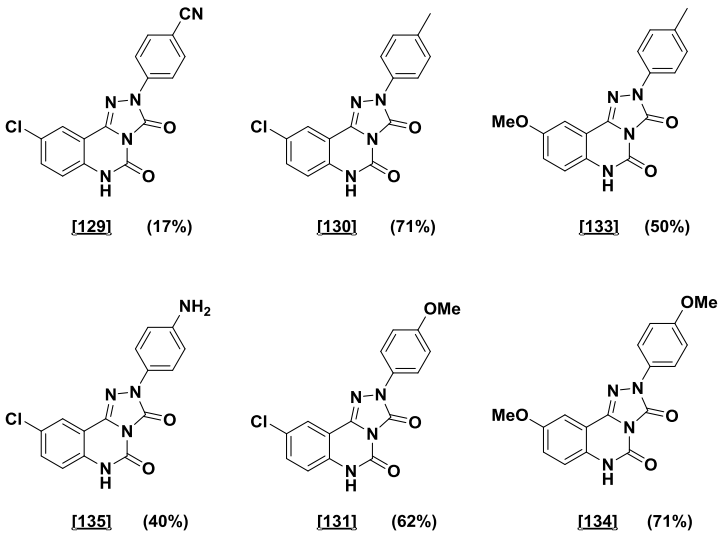

[129] (17%)

[130] (71%)

[133] (50%)

[135] (40%)

[131] (62%)

[134] (71%)

B Introduction

The present thesis deals with investigations towards an improved understanding of subtype selective allosteric modulation at the $\alpha+/\beta-$ and the $\alpha+/\gamma2-$ sites of the $GABA_A$ receptors. This aim was pursued by derivatization of the pyrazoloquinolinone scaffold upon assistance of *in silico* methods.

B I Prelude

Over the last decades an alteration of the expression “stress” emerged translating it into a synonym for expressions like “hurry”, “rush” or “being annoyed”. But what does “stress” really mean and how does it influence our psychological and physiological behavior? Among others, these questions were attempted to be answered in the “Stressstudie” of “Die Techniker Krankenkasse” in Germany.[4] To get a representative overview 1200 people were surveyed about their stress levels concerning their daily lives, spare times and professions (Figure 1).

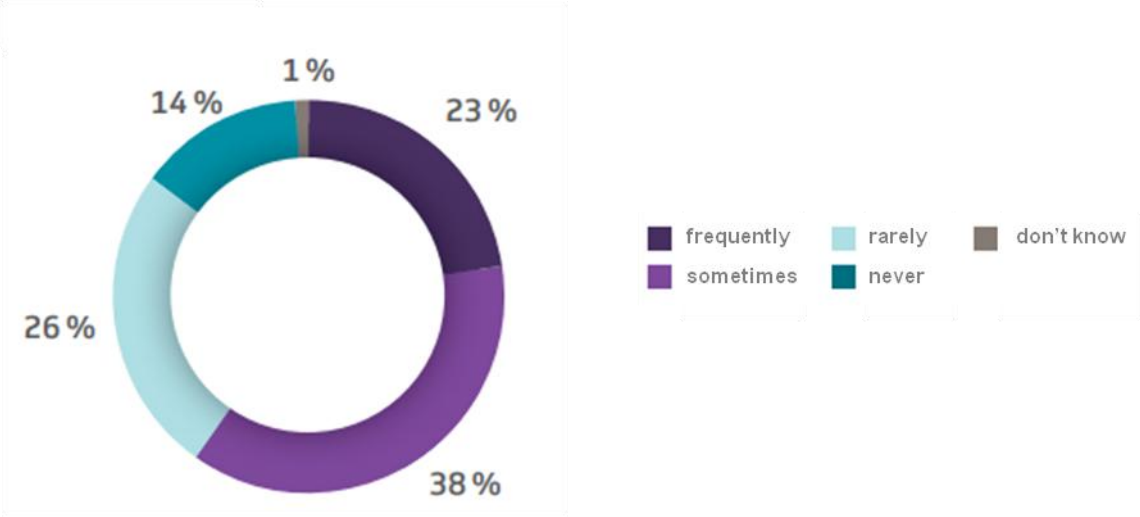

Figure 1: Percentage of the frequency of feeling stressed. 1200 people above the age of 18 were surveyed all over Germany.[4]

Surprisingly, according to these data a worrying amount of 60% feel generally stressed and even 23% feel stressed frequently. Besides the beneficial influence of stress on our body (termed eustress) which leads to an increased performance over a short time, a permanently stressed stage results in a very critical condition (termed distress) in which we become irritable, exhausted and overchallenged. In addition, this repetitive stress might even lead to severe disorders like depression and anxiety disorders.

Anxiety disorders can be grouped into panic disorders, social anxiety, generalized anxiety disorders (GAD) and several phobias.[7] In primary care, anxiety disorders have a high prevalence and are frequent causes of medical intervention. In the treatment of such

disorders antidepressants like escitalopram and paroxetine (selective serotonin reuptake inhibitors, "SSRIs")[8] or benzodiazepines like lorazepam are used. While many antidepressants target the monoamine transporters, benzodiazepines affect the γ-aminobutyric acid system (GABAergic system). Their anxiolytic effect is based on the enhancement of the GABAergic transmission whereas $GABA_A$ receptor blockers, e.g. pentylenetetrazole, are able to even induce extreme anxiety. However, side effects like sedation and addiction preclude benzodiazepines for long term use and are associated with an unselective interaction profile at $GABA_A$ receptors.[9]

The task to discover selective drugs lacking the undesired side effects requires a profound understanding of the distribution as well as of the mechanisms of $GABA_A$ receptors on the molecular level. In this thesis we are aiming for compounds which serve as tools to improve the overall understanding of $GABA_A$ receptors which constitutes the first milestone in drug discovery towards new therapeutics.

B II $GABA_A$ receptors

The class of GABA receptors responds to γ-aminobutyric acid (GABA) which is the major inhibitory neurotransmitter in the mammalian central nervous system (CNS).[10] These receptors are subdivided into two main classes: ligand-gated ion channels (GABA type A receptors) and G-protein coupled receptors (GABA type B receptors). The GABA type A receptors ($GABA_AR$) mediate neuronal transmission upon binding of their natural agonist GABA which causes the endogenous anion channel to open leading in adult neurons mainly to hyperpolarization. This process can be divided into three different main states: closed/resting state (unbound), open/activated state (agonist-bound) and closed/desensitized state (agonist-bound). In addition, several intermediate states are discussed in the literature.[11] Ultimately, this process results in an inhibition of the neuronal signal transmission of the respective neuron.[12]

$GABA_A$ receptors are pentameric ligand-gated chloride ion channels (pLGIC) that belong to the Cys-loop receptor superfamily in which also the anion-selective strychnine-sensitive glycine receptors (GlyRs), the cation-selective nicotinic acetylcholine receptors (nAChRs) and the serotonin (5-hydroxytryptamine) type 3 receptors ($5\text{-}HT_3Rs$) are part of.[13] Structurally these proteins share similar features, like an extracellular domain (ECD), a transmembrane domain (TMD) and an intracellular domain (ICD)(Figure 2c).[14] Nineteen genes encode subunits of $GABA_A$ receptors resulting in a repertoire of nineteen subunits and their further variants, such as splice isoforms e.g. $\alpha 1\text{–}6, \beta 1, \beta 2S, \beta 2L, \beta 3, \gamma 1\text{–}3, \delta, \varepsilon, \theta, \pi$ and $\rho 1\text{–}3$. The sequence similarity of these subunits is high, e.g. approx. 70% sequence identity within a subunit class and 20-40% sequence identity among the different classes. Further, the

pentameric assemblies result in defined receptor subtypes according to the composition and the arrangement of their assembly (homo- or heteropentameric). For example, ternary αβγ and binary αβ receptor subtypes exist (Figure 2a, b).[15] In a pentamer the subunits are arranged in a counter-clockwise fashion and by definition each subunit interface has a principal (plus) and a complementary (minus) side (Figure 2a, b).[16,17]

Generally, it is accepted that the majority of $GABA_A$ receptors in the adult brain are composed of two α1, two β2/β3 and one γ2 subunits. For the α1β3γ2 receptor subtype, for instance, an order of β3–α1–γ2–β3–α1 was shown.[15] However, for other receptor subtypes the exact compositions are still unknown. In addition, the formation of receptors consisting of four or even five different subunits might be possible as well as αβγ receptors consisting of two different α or β subunits,[18,19] e.g. α1α3βγ receptors[20] or α1α5-containing receptors.[21]

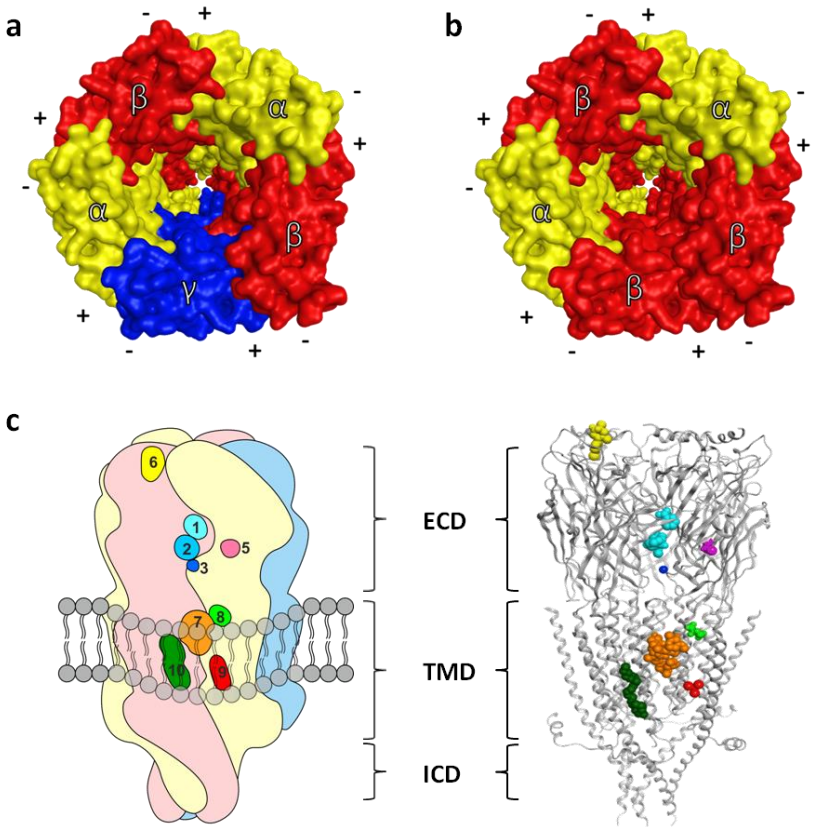

Figure 2: Strucutral overview of $GABA_A$ receptors. a: top view of a ternary αβγ heteropentamer (α subunit = yellow, β subunit = red, γ subunit = blue); **b:** top view of a binary αβ heteropentamer (α subunit = yellow, β subunit = red, γ subunit = blue); **c:** side view of a $GABA_A$ receptor as comic (bottom left) and as homology model (bottom right). Highlight are the extracellular domain (ECD), the trans-membrane domain (TMD), the intracellular domain (ICD) and several putative small molecule binding sites at the interface and the subunit itself (different color coding).[6]

The pharmacology of $GABA_A$ receptors is highly complex which is mainly based on the astounding variety of receptor subtypes and the large number of binding sites on each subtype.[10] *In silico* studies of the binding pockets revealed that there is a possible number of ten small molecule and cation binding sites per subunit.[6] As shown in Figure 2c there are

extracellular and transmembrane small molecule binding pockets, and even in the intracellular domain binding sites are under debate.[22] Six of the ten pockets are mostly formed by a single subunit whereas the other four pockets (1, 2, 3 and 7, Figure 2c) are formed by two subunits due to the localization at interfaces. While the binding pockets in the transmembrane domain are quite conserved we find highly variable binding sites on the extracellular domain, e.g. the high affinity benzodiazepine binding site (BZ-site, consisting of subsites 1 and 2) at the $\alpha+/\gamma-$ interfaces[23], the GABA sites at $\beta+/\alpha-$ interfaces[24] and the $\alpha+/\beta-$ interfaces (Figure 16).[25]

The pharmacology of ligands interacting with $GABA_A$ receptors can be classified according to their clinical effects or to their effects elicited at the target (e.g. a specific binding site at a particular receptor subtype). The focus here is set on the latter interaction profile, on the molecular level.

The binding site of the neurotransmitter GABA is termed orthosteric binding site whereas all other binding sites are referred to as allosteric binding sites. Ligands which bind to the orthosteric site are called agonist, inverse agonist or antagonist. While an agonist (e.g. GABA) activates the receptor, the inverse agonist possesses the opposite pharmacological effect. An antagonist is able to block the effects of the agonist and the inverse agonist by competing for the orthosteric binding site (e.g. bicuculline **[XXXI]**, see Figure 10). The compounds interacting with the allosteric binding sites can be grouped as follows: Positive allosteric modulators (PAM), negative allosteric modulators (NAM) and silent (or null) modulators (SAM).[26]

Such allosteric modulators are only able to modulate the receptor in the presence of GABA. Whereas PAMs lead to an enhancement of the GABA-induced chloride ion current NAMs have the inverse effect by reducing the GABA-induced current (Figure 3). SAMs for a specific binding site lack an intrinsic modulatory effect but they are able to displace PAMs and NAMs (Figure 3). An overview of different allosteric modulators interacting with $GABA_A$ receptors are given in the following chapter B III.

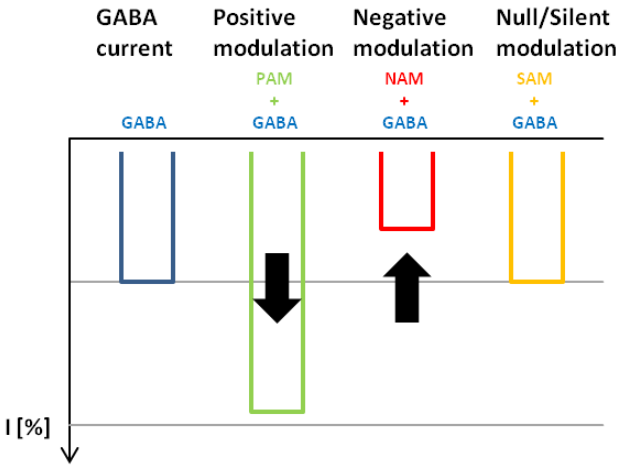

Figure 3: Schematic illustration of allosteric modulation of PAM, NAM and SAM.

B III Ligands interacting with $GABA_A$ receptors

$GABA_A$ receptors can be activated not only by their endogenous agonist GABA but also inhibited by various endogenous or exogenous ligands which can presumably be related to the high amount of cavities on the $GABA_A$ receptor surface.[27] Thus, $GABA_A$ receptors represent interesting targets for general anesthetics, antiepileptic medications and sleeping aids even though the binding sites of the drugs might be unknown.

A snapshot of the staggering variety of compounds and their binding sites which interact with the $GABA_A$ receptors is given in the following. Here a classification in two groups, endogenous and exogenous ligands, was made.

B III.1 Endogenous ligands

Neurosteroids[28], histamine[29], dopamine[30] and endocannabinoids[31] are among the most prominent endogenous ligands which allosterically modulate $GABA_A$ receptors. For example, allopregnanolone **[I]** and allotetrahydrodeoxycorticosterone (THDOC) **[II]** possess sedative, anxiolytic and anticonvulsant properties due to their strong positive allosteric modulation of $GABA_A$ receptors.[32] Contrary, pregnenolone sulfate (PS) **[III]** and dehydroepiandrosterone sulfate (DHEAS) **[IV]** possess anxiogenic and proconvulsant effects due to their negative modulatory effects of the GABA current.[32] Additionally, neurosteroids are even able to directly enable the gating of the channel at submicromolar to micromolar concentrations. Very recently crystallization of allotetrahydrodeoxycorticosterone **[II]** in an $\alpha 1$ GLIC-$GABA_AR$ chimera was successful and indicated the binding site to be at the $\alpha 1$ subunit transmembrane domain.[33,34] For histamine[29] **[V]** and dopamine[30] **[VI]** the binding sites are also still unknown whereas for the endocannabinoids 2-arachidonglycerol (2-AG) **[VII]** and anandamide **[VIII]** a binding site in a non-interface position is proposed.[31]

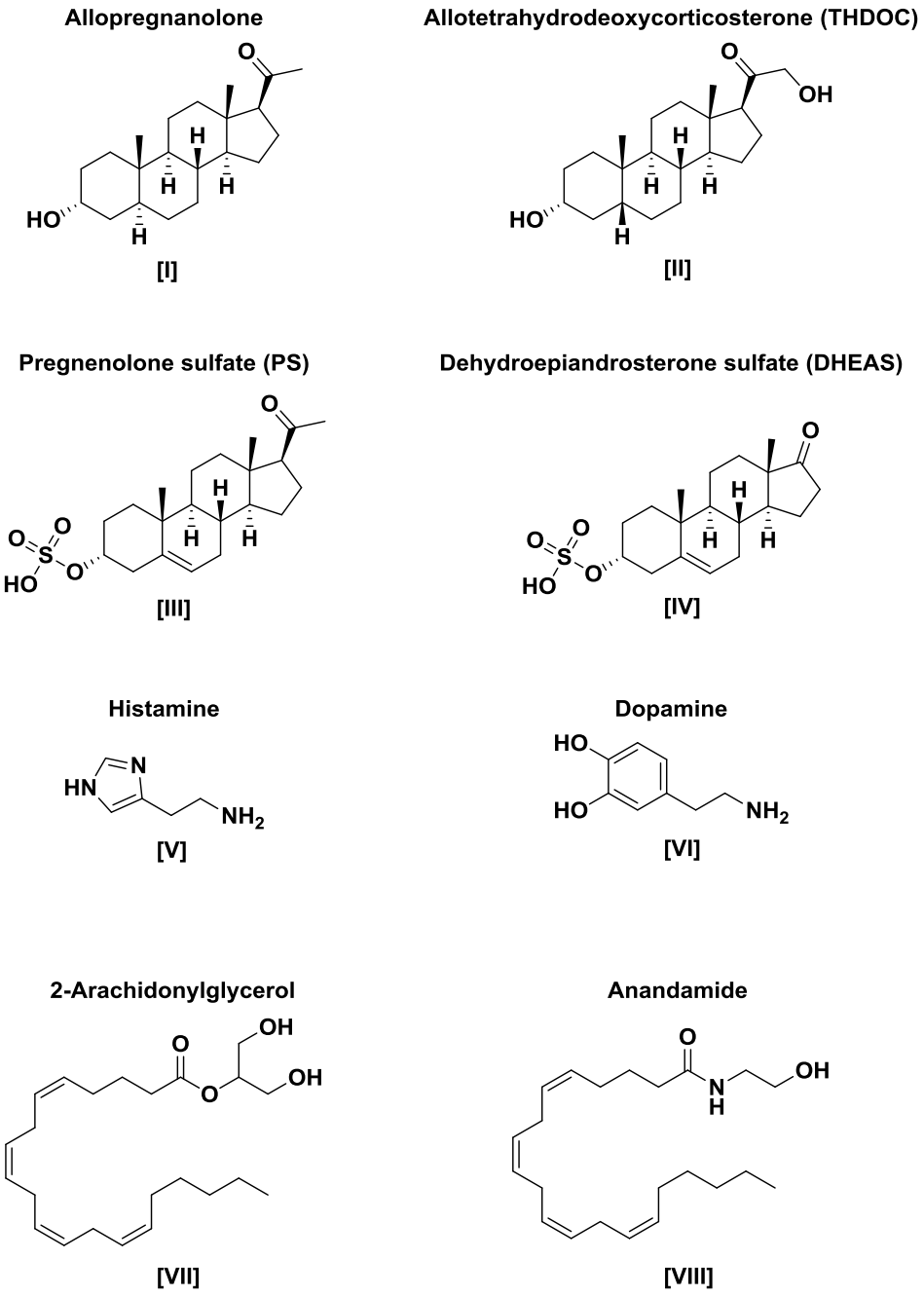

Figure 4: Endogenous ligands which are active at $GABA_A$ receptors.

B III.2 Exogenous ligands

The number of known exogenous ligands exceeds the number of known endogenous ligands, by far. A selection of benzodiazepines, barbiturates and other general anestethics is presented due to their application in various therapies. Additionally, some natural products which are used in traditional medicine are presented.

B III.2.1 Benzodiazepines

Chlordiazepoxide **[IX]** (Librium®) was the first benzodiazepine which was introduced to the market in 1960 by Hoffmann–La Roche. To date, benzodiazepines are among the most frequently prescribed drugs with over 20 distinct derivatives in use, including flunitrazepam **[X]** (Rohypnol®), alprazolam **[XI]** (Xanax®) and diazepam **[XII]** (Valium®).[35,36] Most benzodiazepines exert a positive allosteric modulation *via* the eponymous binding site at the $\alpha 1,2,3,5+/\gamma 2-$ interfaces (DS, diazepam-sensitive) resulting in anxiolytic, sedative and anticonvulsant effects.[37] Thus, one of their main applications (*inter alia* sleeping aids and antiepileptic medication) is in the treatment of anxiety even though they suffer from undesired side effects, e.g. ataxia, loss of coordination and impairment of cognition.[38]

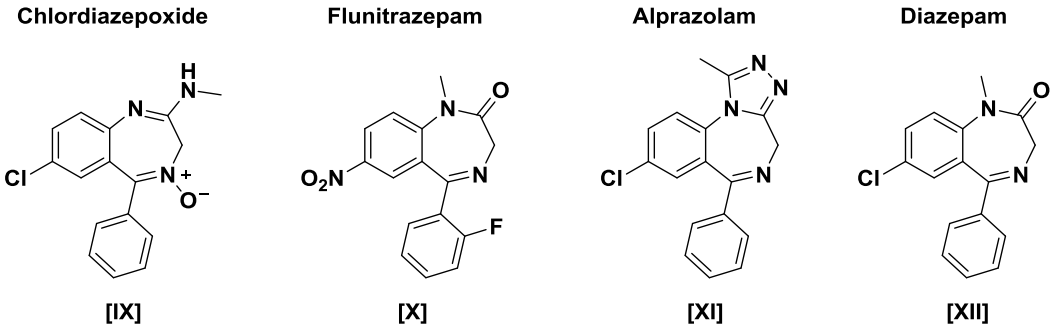

Figure 5: Exogenous ligands – selected benzodiazepines which are active at $GABA_A$ receptors.

B III.2.2 Barbiturates

The compound class of barbiturates was already discovered in 1904 by Farbwerke Fr Bayer and Co and is based on the barbituric acid as core scaffold.[39] The derivatization of barbituric acid **[XIII]** led to a large number of therapeutic agents (e.g. pentorbital **[XVI]**, barbital **[XIV]**, allobarbital **[XV]**) which have been used as anxiolytics, antiepileptics, sedatives and hypnotics by suppressing the CNS activity. The pharmacology of barbiturates is quite complex since they show a promiscuous behavior especially at higher concentrations. Apart from their activity at $GABA_A$ receptors they also show activity on excitatory amino acid-gated receptors[40] and voltage gated Ca^+ channels.[41] Additionally, they are able to activate $GABA_A$ receptors in the absence of GABA at high concentrations as well as to act as channel-blockers at very high concentrations.[42,43] Based on their effects the binding site of barbiturates is believed to be disparate from the GABA and BZ binding sites and presumably requires an α subunit to modulate $GABA_A$ receptors.[44] In 2014 and 2016 it was revealed that the binding sites of barbiturates seem to be located at the $\alpha+/\beta-$, $\gamma+/\beta-$ and $\beta+/\beta-$ interfaces.[45,46]

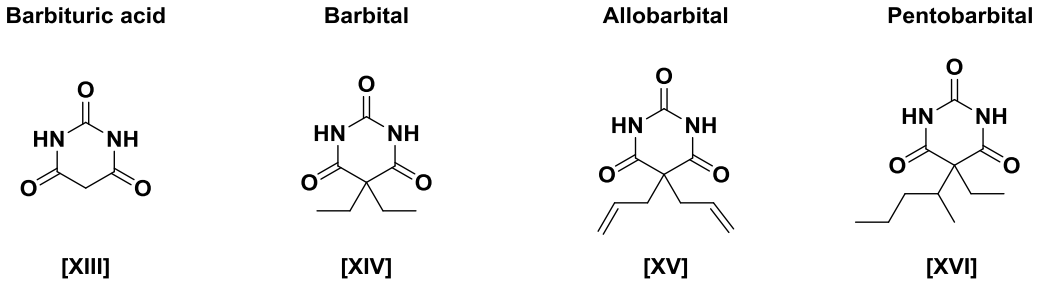

Figure 6 Exogenous ligands – selected barbiturates which are active at $GABA_A$ receptors.

B III.2.3 General anesthetics

In modern medicine the use of general anesthetics became a routine to render patients unconscious prior to their surgery. In this context $GABA_A$ receptors are one of the most important targets which are triggered by 7 of the 10 most frequently used anesthetics. These can be subdivided into two groups: Inhalational: Isoflurane **[XVII]**, Sevoflurane **[XIX]** and Desflurane **[XVIII]**; Intravenous: Propofol **[XX]**, Etomidate **[XXI]**, Methohexital **[XXII]** and Thiopental **[XXIII]**.[47] However, even these clinically used drugs possess a spectrum of modest to strong effects on other ion channels, including glycine receptors, glutamate receptors, 5-HT_3 receptors (serotonine receptors), neuronal nicotinic receptors and two pore potassium channels.[48,49] Additionally, compounds like isoflurane **[XVII]** or propofol **[XX]** are able to interact in distinct ways with the receptors depending on the concentration applied. A positive modulation is observed at low concentrations, moderate concentrations lead to direct gating and high concentrations result in a blocking of the channel.[50-52] Due to their promiscuous pharmacological profile it is obvious that their precise mode of action is still ambiguous.

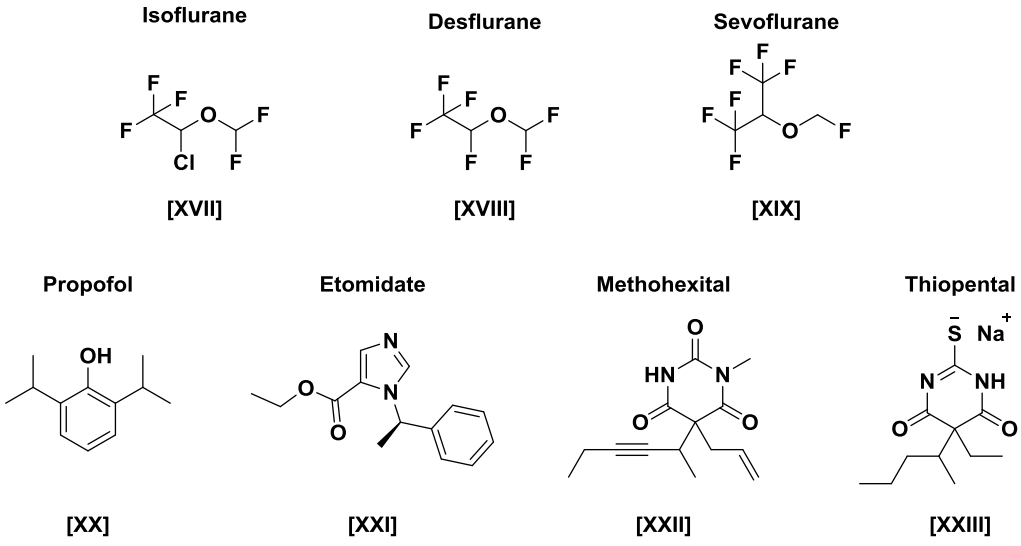

Figure 7: Exogenous ligands – 7 most frequently used general anesthetics which are active at $GABA_A$ receptors.

B III.2.4 Natural products

In traditional medicine plant derived natural products are frequently used in the treatment of various diseases. However, between 1981 and 2006 only 6 natural products derivatives and 1 natural product have been approved for the usage in CNS related disorders.[53-56] Among the most extensively studied plants which exert GABAergic activity are e.g. winter cherry (*Withania somnifera*)[57], passionflower (*Passiflora incarnate*)[58] and valerian roots (*Valeriana officinalis*).[59] A selection of natural product derived compounds exerting GABAergic activity is presented in the following.

B III.2.4.1 Flavonoids

Currently, the most intensively studied ligands on the $GABA_A$ receptors are the ubiquitously occurring flavonoids. For instance, the naturally occurring flavone hispidulin **[XXV]** was found to be a positive allosteric modulator in $\alpha 6\beta 2\gamma 2$S receptors (among others) and is thought to be the active ingredient of a plant compound that was reported to induce remission in a single patient suffering from intractable motor tic disorders.[60,61] The biflavonoids amentoflavone **[XXV]** and hesperidin **[XXIV]** possess both a modulatory activity at $GABA_A$ receptors. For amentoflavone **[XXV]** antidepressant and anxiolytic effects are reported[62] while hesperidin **[XXIV]** shows sedative and anticonvulsant activity.[63,64] However, the binding site of both natural products is not clarified, so far, and data suggest a rather complex interaction mechanism.[63,65] Due to their interesting pharmacological profiles a lot of effort has been expended to improve their effects by chemical diversification which led to a large number of new compounds. Two representatives of the synthetically generated flavonoids are 6,3'-dinitroflavone **[XXVIII]** and 6-bromoflavone **[XVII]** which both possess high affinities for the benzodiazepine binding site.[66,67]

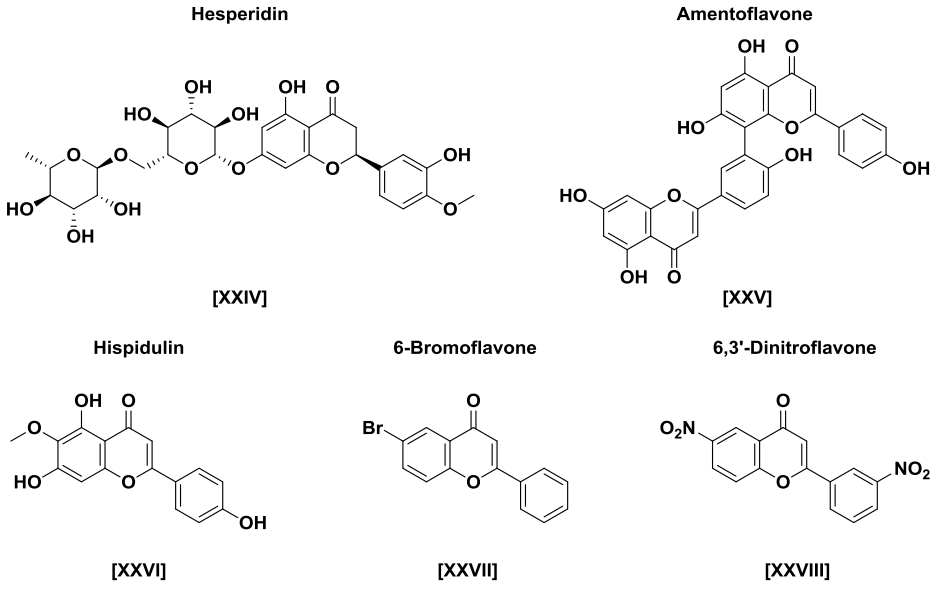

Figure 8: Exogenous ligands – naturally occurring and synthetic flavonoids which are active at $GABA_A$ receptors.

B III.2.4.2 Terpenoids

Terpenes are ubiquitously distributed in nature and possess various pharmacological properties. Chemically, they are composed of single isoprene units and their classification is derived from the number of single isoprene moieties which are required to construct the final carbon skeleton.[68] Accordingly, we distinguish between mono- (two isoprene units), sesqui- (three isoprene units), di- (four isoprene units) and triterpenoids (six isoprene units).

Thymol **[XXIX]**, a monoterpenoid, was first isolated from thyme essential oil and positively modulates $GABA_A$ receptors.[69] Additionally, thymol is even able to directly activate the ion channels in very high concentrations.[70]

The plant *Valeriana officinalis* served as mild sedative and anxiolytic agent in traditional medicine over a long time.[71] Later, valerenic acid **[XXX]** was identified as major constituent. Due to its very interesting pharmacological effects on the GABAergic system it turned into a highly diversified and studied compound class. For instance, valerenic acid exerts positive allosteric modulation with a pronounced functional selectivity for $GABA_A$ receptors containing the $\beta 2$ and $\beta 3$ isoforms. The binding site is believed to be in the transmembrane domain. [72,73]

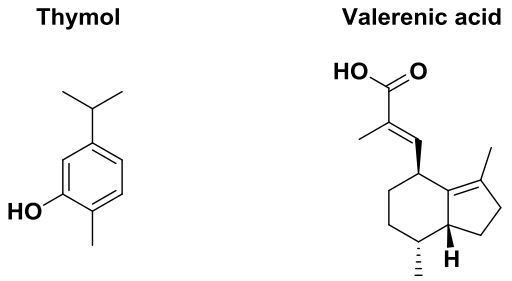

[XXIX] **[XXX]**

Figure 9: Exogenous ligands – selected terpenes which are active at $GABA_A$ receptors.

B III.2.4.3 Alkaloids

Alkaloids represent another class of compounds which possess GABAergic acitivity. The two most prominent ones are muscimol **[XXXII]** and bicuculline **[XXXI]**. Muscimol, a structural analog of GABA, was isolated from *Amanita muscaria* and shows competitive orthosteric agonistic behavior[74] while bicuculline acts as $GABA_A$-receptor antagonist with convulsant *in vivo* activity.[75,76]

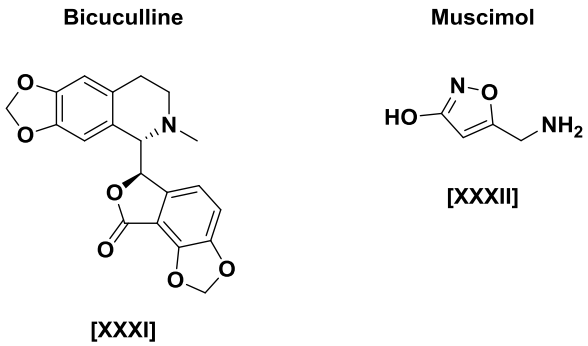

Figure 10: Exogenous ligands – selected alkaloids which are active at $GABA_A$ receptors.

B III.2.4.4 Polyacetylenic alcohols

Sometimes, also very toxic substances are found in plants like the compound class of polyacteylenic alcohols. While cunaniol **[XXXV]** is a highly potent convulsant which has antagonistic effects at $GABA_A$ receptors[77,78], cicutoxin **[XXXIV]** is the major toxic component isolated from *Cicuta virosa* (water hemlock) inducing clonic convulsion, paralysis and even death.[79] The second toxic component of *C. virosa* is virol A **[XXXIII]** which is believed to inhibit $GABA_A$ induced currents *via* the agonist site and the Cl^- channel.[80] However, the exact mechanism how and where these compounds interact with the $GABA_A$ receptors is still unknown.

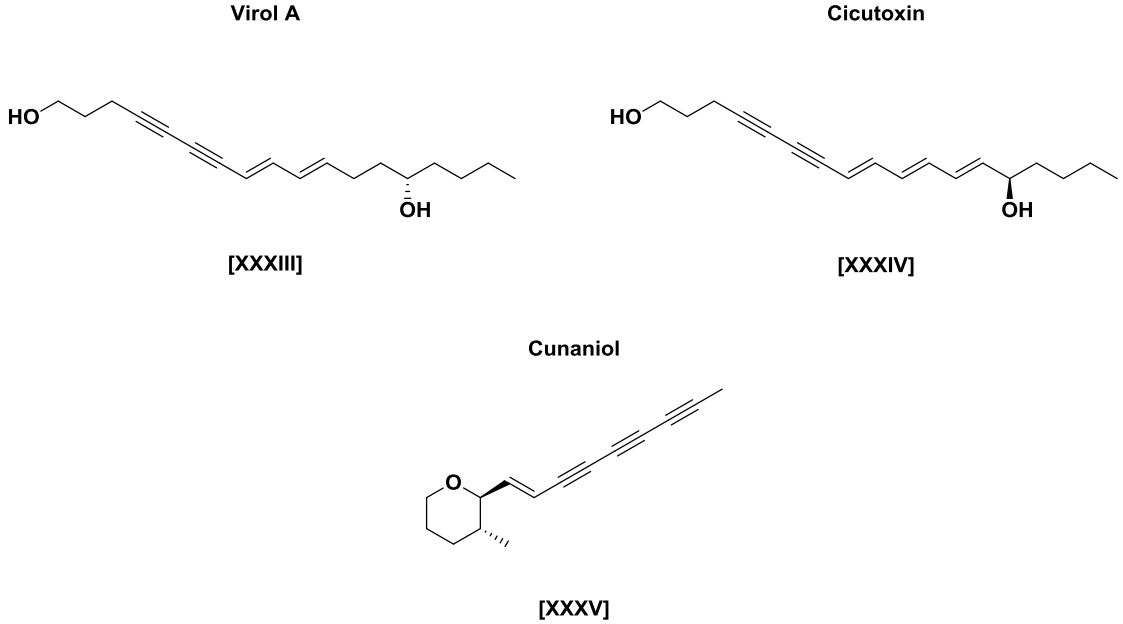

Figure 11: Exogenous ligands – selected polyacetylenic alcohols which are active at $GABA_A$ receptors.

B IV Identification of binding sites and binding modes of ligands

A preferred way to determine an unknown binding site and/or binding mode of a specific ligand in a protein is represented by crystallization of the protein in a ligated state. However, to apply this method pure and crystallisable proteins are required. Since these requirements do not comply with many proteins there are other methods how to tackle the identification of binding sites and/or binding modes. Some of these methods are outlined in the following.

B IV.1 Experimental localization of binding sites

Different approaches to identify binding sites have been introduced until today, among them saturation transfer difference (STD) NMR and photoaffinity labeling, which all possess their advantages and disadvantages.

In 1999 Mayer and Meyer reported about STD NMR spectroscopy which enables to selectively determine the binding affinity of a compound and molecular determinants of its binding site.[81] Here, a selective pulse saturates the whole protein resonance by spin diffusion (intramolecular saturation transfer) while the ligand remains mainly unsaturated except for the atoms interacting with the protein. Subsequently, the same sample is measured without the saturation pulse and a difference spectrum is calculated. This enables to identify the sections of the ligand that interact with the protein as well as the amino acids participating in this interaction, thus the binding site. On the one hand this method allows measurements directly from mixtures and it eliminates the risk of false positives in screenings, but on the other hand it also requires purified proteins representing a major challenge for membrane bound proteins like the $GABA_A$ receptor.

Photoaffinity labeling was first described by Ruoho *et al*. and relies on covalent binding of an active ligand to its binding site.[82] This can be achieved by introduction of a photoreactive group (e.g. azide and diazirine) in the ligand while not influencing its pharmacological features. Upon irradiation by light the photoreactive group is converted to a highly reactive carbene species which unspecifically reacts with the protein resulting in the formation of a covalent bond. The labeled residues are identified by either microsequencing or mass spectroscopy.

The importance of the amino acids putatively participating in the molecular ligand-protein-interactions is analyzed by mutagenesis studies. Thereby, commonly uncharged small amino acids are introduced, e.g. alanine or cysteine. The latter is additionally used to attach bulky molecules like MTSEA biotin to enforce the evidence for the binding site by abolishing effects of active ligands as shown by Ramerstorfer and coworkers.[83] Furthermore, so-called conversion mutants are used where homologous amino acids of different subunits are

mutated into each other. Thus, a differentiation of binding or functional molecular determinants can be identified. Baur *et al*. for example reported a loss of binding of diazepam by introducing α1H101R while the conversion mutant α6R100H enabled binding in the usually diazepam-insensitive α6 containing $GABA_A$ receptors.[84]

B IV.2 Homology models and crystal structures

As mentioned earlier a crystallized protein-ligand complex is highly desired to identify the binding site of a certain ligand. However, in terms of binding mode determination a crystal structure represents only a static "snapshot" of the protein structure which was determined under unnatural conditions. Thus, to improve the understanding of protein-ligand binding and, in particular, to assess conformational adaptations, it is prevalent to compare and use crystal structures of different conformational states, e.g. bound state and non-bound state structures, and also from closely related proteins. Additionally, the crystallization of especially membrane proteins (e.g. $GABA_A$ receptor) bears many obstacles since it is difficult to isolate as well as to stabilize them under crystallization conditions.[85] In such cases homology models are gathered which are three dimensional representations of target proteins based on a template protein of certain sequence homology. Thereby, the backbone of the amino acid sequence of the target protein is arranged according to the template backbone (Figure 12).[86-88] This leads to models with moderate accuracy for C_α-atoms in regions with high sequence identity and inaccuracy for sidechain positions and loop regions.

Homology modeling itself has various crucial steps which can dramatically influence the quality of the generated model, e.g. template selection, proper alignment and the used force field (Figure 12b). To reduce these difficulties a multi sequence alignment is advantageous to identify conservations within the family or superfamily of the proteins. Nevertheless, the modeling of more variable parts (e.g. flexible loops) still remains very challenging.

For the $GABA_A$ receptors the first homology models were generated based on the acetylcholine-binding protein (AChBP) which suffered from a low sequence identity of 15-30%.[17,89] However, the models delivered first important insights into the topology of the extracellular interface binding sites due to high structurally conserved areas. In 2014 the crystal structure of the human β3 homopentameric $GABA_A$ receptor was published which was a major step towards improved models in this research area, especially for models containing the three β subunit isoforms.[90] However, depending on the purpose the model is used for, it still could be more reasonable to chose a closely related crystal structure from the same protein family over the $GABA_A$ crystal structure (Figure 12a).

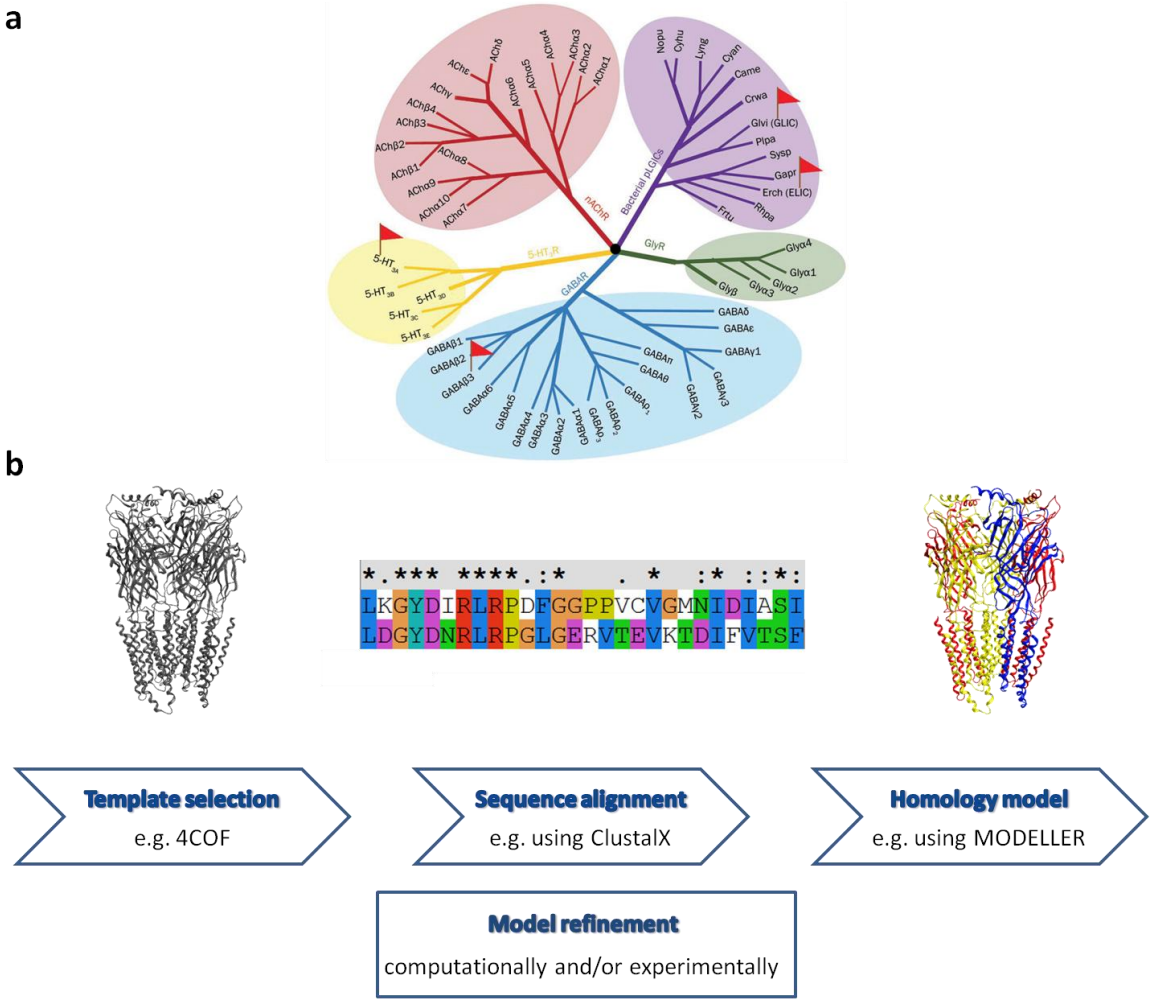

Figure 12: Phylogenetic treeof the pLGIC superfamily and overview of homology modeling workflow. a: Evolutionary relations within the pLGIC superfamily. Color coding: red: nAChR subunits, violet: bacterial homologues, blue: $GABA_A$ receptor subunits, green: GlyR subunits and yellow: 5-HT3 receptor subunits.[1] The invertebrate channels (GluCl, and the histamine and serotonin-gated channels) are not shown in this image. Since recently, the structures of GlyR $\alpha 1$ and GlyR $\alpha 3$ are available.[2,3] **b**: Main steps of homology modeling: template selection, template to sequence alignment, model generation and model refinement (computationally via energy minimization as well as based on experimental data).

B IV.3 Determination and evaluation of the binding mode

The determination of the ligand-bound state is crucial for the understanding of the molecular interaction mechanism between the ligand and the protein and thus essential for structure guided ligand design. There are different methods known to identify the binding orientation of a compound, among them molecular docking (*in silico* method) and site-directed irreversible photoaffinity labeling (experimental method).

B IV.3.1 Molecular docking

Molecular docking generates diverse ligand orientations at a protein site which are evaluated computationally in the next step. Considering that the first step consists of “ligand sampling” and “protein flexibility”, the docking process can be classified into three components: ligand sampling, protein flexibility and scoring. During the first two steps potential ligand binding orientations/conformations and protein “conformations” are generated at the putative binding site. The generated poses are then evaluated during the scoring which assesses the tightness of the individual ligand binding orientations/conformations and protein “conformations” *via* various physical or empirical energy functions. The ligand orientation with the lowest energy score is considered as the putative binding mode.[91] Note, that in a final step the putative binding mode should always be evaluated experimentally, if possible.

Each single step of molecular docking can be performed according to different algorithms. A small overview of the single steps and selected algorithms is given in the following.

B IV.3.1.1 Ligand sampling

Ligand sampling represents the most basic part in the docking process. There are many algorithms generating reasonable orientations and conformations of ligands on different ways. One of the simplest algorithms is shape matching which uses shape complementarity as criterion. Here, a large number of ligand-bound orientations is generated based on the six degrees of freedom (three translational and three rotational). The shape matching algorithm is included for example in docking program like DOCK[92], FRED[93], LigandFit[94] and MDock.[95,96] A more advanced method represents the stochastic algorithm which assesses the conformational and the translational/rotational space of the ligand by random changes. The resulting orientations are challenged by a probabilistic criterion which either leads to acceptance or rejection of the orientation. For instance, evolutionary algorithms (EAs)

evaluate the randomly generated binding poses including considerations inspired by biological evolution to find the correct binding orientation. EAs are used for example in GOLD[97,98], AutoDock[99], MolDock[100] and EADock.[101]

B IV.3.1.2 Protein flexibility

Two algorithms, among others, which take protein flexibility into account, are soft docking and side-chain flexibility. Whereas soft docking is a simple method which softens the interatomic van der Waals interactions between ligand and protein by tolerating a small degree of overlap,[102,103] side-chain flexibility is more complex. Here, usually the backbone of the protein is kept fixed while different conformations of side chains are sampled according to the ligand conformations.[104] Currently, even slight backbone changes can be considered through the usage of so called “soft potentials” like in the GOLD software.[97,98]

B IV.3.1.3 Scoring Functions

To determine the accuracy of the docking algorithm a scoring function is used which ideally works in a computationally efficient and reliable manner.[105-109] During recent years various scoring functions have been developed and based on their way of derivation they can be classified into three groups: force field, empirical, and knowledge-based scoring functions.

Scoring functions, which are based on individual interaction terms (e.g. electrostatic energies, bond stretching/bending/torsional energies, van der Waals energies, etc) to describe the ligand binding energy, use force field-field parameters like AMBER[110] or CHARMM[111,112] and belong to the group of force field (FF) scoring functions. [99,113,114] However, the inclusion of solvents effects still remains a major challenge in FF scoring functions. In contrast, an empirical scoring function uses individual energy terms which are additionally weighted by a coefficient. This coefficient reflects binding affinity data of a training set of protein-ligand complexes.[115-117] Overall, this scoring function benefits from its simple energy terms which makes it computationally more efficient, but suffers from restricted applicability due to the dependency on the training set. Representatives of this group are LigScore[118], GlideScore[119] and ChemScore. [115] More general scoring functions are knowledge-based scoring functions.[120-122] They represent a nice compromise between accuracy and speed compared to the earlier mentioned scoring functions. Here, the parameters are directly derived from data based on a large number of protein-ligand complexes which are determined experimentally.[123-126]

B IV.3.2 Site-directed irreversible photoaffinity labeling

One experimental approach to determine the binding site or even the binding mode of ligands is *via* site-directed irreversible photoaffinity labeling.[127,128] Thereby, if not already existing, a chemically reactive moiety has to be incorporated into a target binding site, e.g. a cysteine amino acid. Note, only cysteine mutations which ensure complete functionality of the protein are considered. In a next step these reactive groups are able to covalently bind to affinity markers which possess reactive counterparts, such as isothiocyanates. Compared to the classical photoaffinity labeling approach[129], this method has the advantage that the formation of the covalent bond only occurs if both moieties are in close contact with each other in the binding pocket.

For instance, Middendorp *et al*. investigated different benzodiazepine ligands at their high affinity binding site in $\alpha 1\beta 2\gamma 2$ $GABA_A$ receptors using the proximity accelerated chemical coupling reaction (PACCR).[130] They mutated several pocket forming amino acids into cysteins residues and applied a reactive diazepam derivative (chloro substituted with isothiocyanate) to further examine its binding mode. Using this PACCR they were able to demonstrate in combination with computational methods that diazepam rather uses a different binding mode compared to the one favored by Richter *et al*.[131]

B V Biological methods and subtype selectivity

$GABA_A$ receptors possess a high number of receptor subtypes which requires a very time consuming characterization of the ligands at the desired binding site in each subtype. However, in order to examine subtype selective behavior of the compounds this step is inevitable.

In this thesis the pharmacological profile of a compound was determined using electrophysiology. $GABA_A$ receptors were recombinantly expressed in oocytes (lat. *Xenopus leavis*) and investigated using the two-electrode voltage clamp method (TEV) to measure the compound induced change of the chloride ion current. Thereby, increasing compound concentrations are applied at a fixed GABA concentration which is usually given as EC_{3-5} (concentration which elicits 3-5% of the GABAmax (usually 1 mM GABA solution)). This fixed concentration can vary depending on the response of the receptor subtype and is normalized to the reference current (Figure 13).

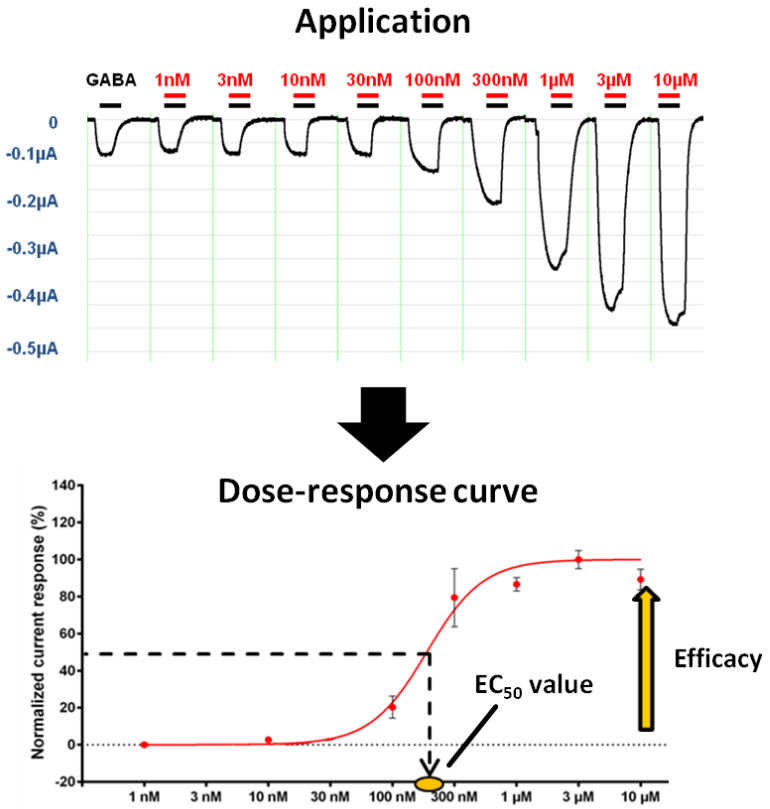

Figure 13: Illustration of the co-application of compound + GABA showing the measured current traces (top). Illustration of the resulting DR curve with indicated EC_{50} value (potency) and efficacy (bottom).

Since this functional assay is quite time consuming some compounds were first measured in a two-point screening (at 1 µM and 10 µM) to identify the more interesting compounds. For the interesting compounds dose-response (or concentration-response) curves (DR curves)

were determined which allows the assessment of their complete pharmacological profile (Figure 13). In the DR curves two measurement parameters are distinguished: potency and efficacy. The potency (apparent affinity) refers to the onset of compound effects (x-axis) and is reported as the half maximal concentration (EC_{50}). The efficacy describes the impact of the compound on the modulation itself and is reported in percent (y-axis) (Figure 13). This specification results in two different selectivity profiles: potency selectivity (binding selectivity) and efficacy selectivity (functional selectivity). A compound which displays a preferred onset of its effects in a certain receptor subtype is called potency- (or binding-) selective, respectively (Figure 14a). A compound which strongly modulates a specific receptor subtype over other subtypes is called efficacy- (or functionally-) selective respectively (Figure 14b).

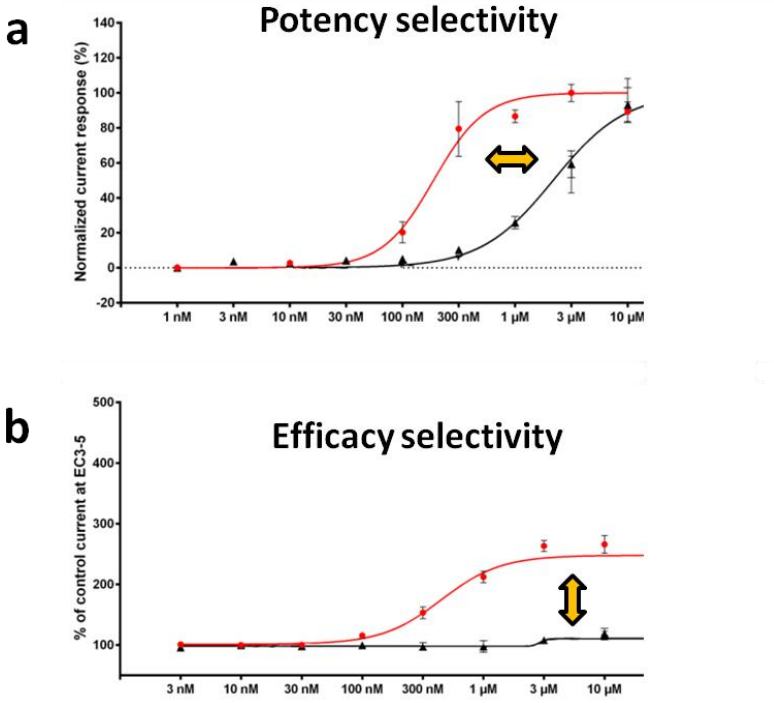

Figure 14: Illustration of potency and efficacy selectivity.

In addition, radioligand binding assays can be performed to determine direct binding affinities (IC_{50} value). However, this can only be applied for binding sites where a high affinity radioligand is available, e.g. the benzodiazepine binding sites at the $\alpha 1,2,3,5+/\gamma 2-$ interfaces. For the $\alpha+/\beta-$ sites such ligands are not available yet and thus the characterization can be conducted only *via* the functional assays.

B VI Pyrazoloquinolinones and the α+/β– interfaces

In the 1980s pyrazoloquinolinones (PQs) were synthesized first in the laboratories at Ciba-Geigy and were investigated further due to their promising non-sedative anxiolytic effects which were assumed to be mediated *via* the BZ site (α+/γ–) at $GABA_A$ receptors. However, the first *in vivo* results revealed rather ambiguous pharmacological profiles of benzodiazepine site agonism, partial agonism and antagonism.[132] As consequence Czernik *et al.* commenced to examine the ability of pyrazoloquinolinones as benzodiazepine antagonists.[133] After first successful results, e.g. CGS8216 **[XXXVI]** (Figure 15) antagonized the muscle relaxant effect of diazepam[134,135] or the sedative effect of the non-benzodiazepine hypnotic CL 218,872[136], also inconsistent results were obtained while studying their anxiolytic and anxiogenic effects.[137-139] In sum, these observations sufficed to terminate the development of pyrazoloquinolinones into useful pharmacological tools or therapeutics.

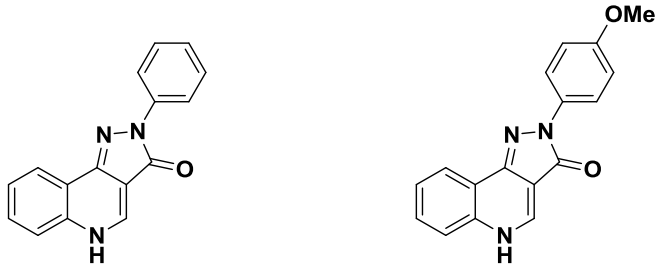

CGS8216
[XXXVI]

CGS9895
[XXXVII]

Figure 15: Chemical structures of pyrazoloquinolinones CGS8216 and CGS9895.

In 2011 our group started to revisit the modulatory effects pyrazoloquinolinones at the BZ-site and explored a second allosteric binding site at the α+/β– interfaces. For instance, the pyrazoloquinolinone CGS9895 **[XXXVII]** (Figure 15) showed a silent modulatory effect at the BZ-site while it exerted strong positive modulatory effects via the α+/β– interfaces.[83] Interestingly, these compounds possess a significantly higher potency for the BZ-sites compared to their homologous α+/β– interfaces (Figure 16). In addition, a transmembrane binding site of pyrazoloquinolinones was suggested by Maldifassi *et al*.[140]

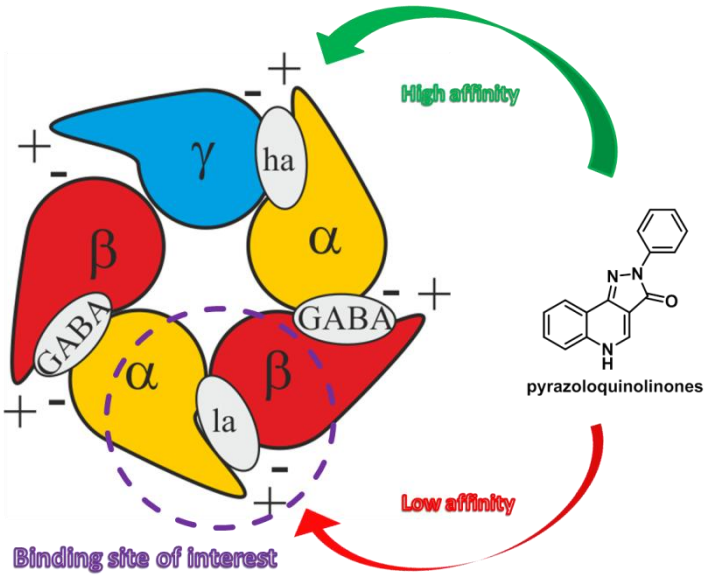

Figure 16: Schematic view of the extracellular domain of an αβγ $GABA_A$ receptor subtype with the plus and minus sides of the subunits indicated. The GABA binding site is labeled as "GABA", the high affinity benzodiazepine/ CGS site as "ha", and the low affinity CGS site as "la". The green arrow represents the high affinity of the PQs towards the α+/γ– site while the red arrow indicates their low affinity towards the α+/β– interface. The α+/β– interface, binding site of interest, is highlighted in purple.

However, the described binding sites at the α+/β– interfaces represent highly attractive targets for subtype selective chemical probes (tool compounds) to study the abundance and distribution of certain $GABA_A$ receptor subtypes in tissue and to detect them in living organisms. [141] The α+/β– binding sites are particularly suitable since the six α and the three β isoforms contribute unique amino acid residues to the extracellular binding site, which theoretically bears the opportunity to develop highly selective ligands for any αk+/βl– interface (k=1-6; l=1-3). A first milestone towards the subtype selective tool compounds would be the identification of a high affinity α+/β– selective compound.

Moreover, the α+/β– interfaces are highly interesting for compounds interacting with benzodiazepine-insensitive $GABA_A$ receptor isoforms (e.g. lacking the γ subunit).[83] While benzodiazepines mostly exert their effects on αkβlγ2/3 receptor subtypes (k=1,2,3,5; l=1-3), compounds using the α+/β– interfaces are expected to have a broader range of activity due to their high abundance in various subtypes (αβ, αβγ and αβδ).[6,25] In addition, it was hypothesized by Sieghart *et al.* that therapeutics targeting the α+/β– interface might be specifically suitable for the long-term treatment of epilepsy.[25] While benzodiazepines possess excellent anticonvulsant effects, they suffer from a loss of activity during repetitive applications. This tolerance phenomenon supposably might be explained by an uncoupling of BZ-site containing receptors (e.g. overexpression of benzodiazepine-insensitive receptor subtypes).[142] Thus, compounds interacting with the α+/β– interface should remain active since both subunits are required for the agonistic binding sites.

B VII Objective

The aim of this thesis was to improve the understanding of the molecular rules which underlie subtype selective allosteric modulation of $GABA_A$ receptors. This goal was pursued using synthetic chemistry to create various compound libraries for SAR studies. We focused on diverse modifications of the ring A and ring D of the pyrazoloquinolinone scaffold which is known to bind at the $\alpha+/\gamma2-$ and the $\alpha+/\beta-$ interfaces. Biological evaluation of these compounds was conducted from our collaboration partners who investigated the compounds using electrophysiology and binding assays. In addition, computational methods (homology modeling, molecular docking and pharmacophore modeling) were applied to obtain insights into ligand interactions with both the high affinity and the low affinity site, respectively. Ultimately, these models should provide a starting point towards new scaffolds which selectively interact with the $\alpha+/\beta-$ interfaces only.

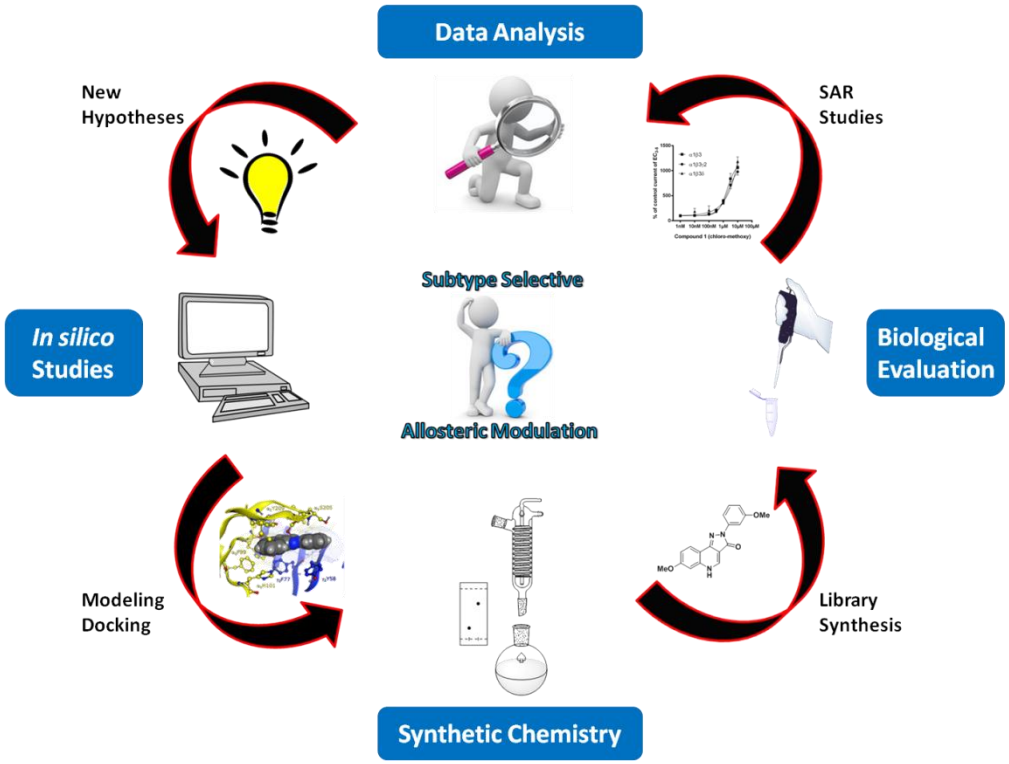

Figure 17: Schematic illustration of the workflow applied in the thesis at hand.

C Results and Discussion

C I Synthesis of modulators for the α+/β– interface

This chapter describes the synthesis of all new ligands which are reported in this thesis. In case of the pyrazoloquinolinones the focus was set on the examination of the necessity of ring D and additionally on the introduction of different substitution patterns on ring A and ring D.

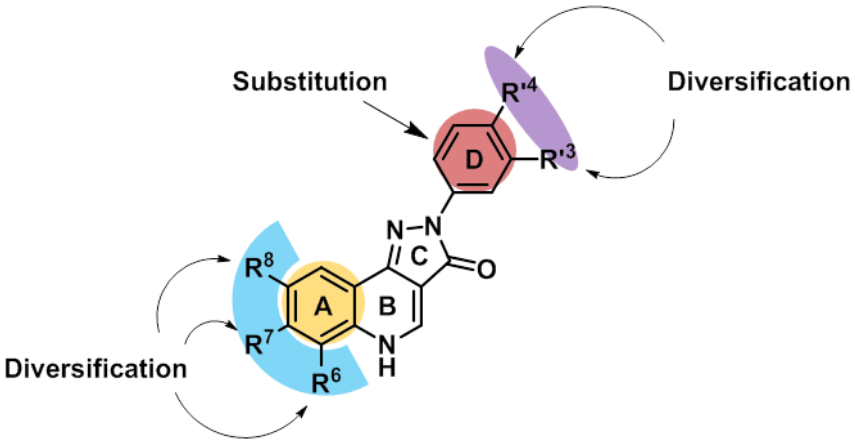

Figure 18: Pyrazoloquinolinone scaffold modifications.

C I.1 Pyrazoloquinolinones

The synthetic route of pyrazoloquinolinones **[1a,b]** is well established and was first described in the literature by Yokoyama *et al.* in 1982.[132] Retrosynthetically, the first cut results in the corresponding aryl/alkyl hydrazines and the chlorinated quinoline precursors **[2]**. Note, the use of alkyl hydrazines leads to two regioisomers due to the increased nucleophilicity of the nitrogen next to the alkyl moiety – in contrast to aryl hydrazines with distinctly different reactivity of the two N-atoms. Functional group interconversion of **[2]** suggests the desired quinoline precursors **[3]**. The 4-oxo-quinolines **[3]** are prepared by the Gould-Jacobs reaction. Thereby, a condensation reaction of substituted anilines **[4]** with diethyl methylenemalonate followed by thermal cyclization is conceived (Scheme 1).

Using this synthesis route a simple diversification of the substitution pattern can be achieved by utilization of different aniline ($R^{6,7,8}$), aryl hydrazine ($R^{'3,'4}$) and alkyl hydrazine derivatives respectively (Figure 18).

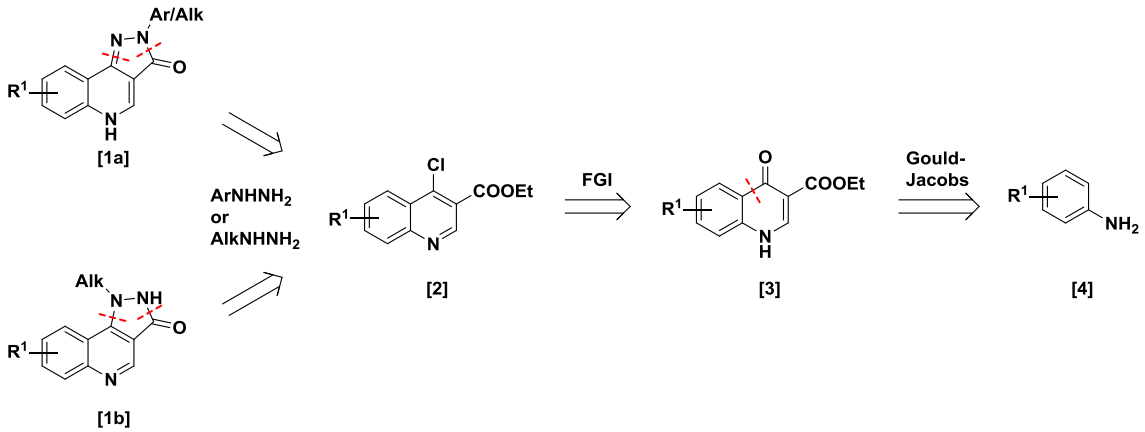

Scheme 1: Retrosynthetic analysis of pyrazoloquinolinones.

C I.1.1 Pyrazoloquinolinones – Alkyl series

In the years around 2000 the Carotti and the Cook group investigated the benzodiazepine binding site ($\alpha+/\gamma-$ interface) by extensive ligand-based approaches which resulted in a putative pharmacophore model (Figure 19).[143-145]

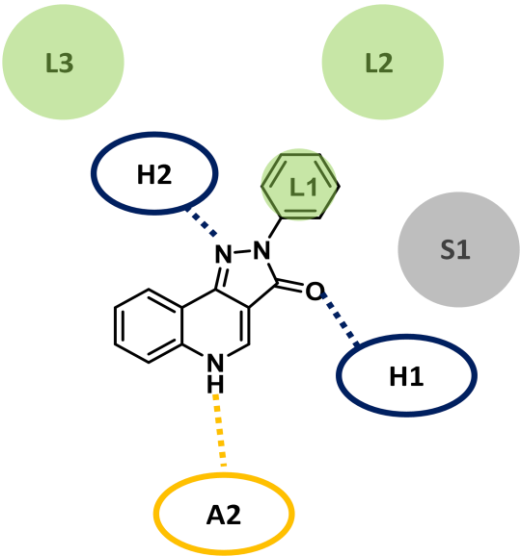

Figure 19: Illustration of pharmacophore model according to Savini *et al.* L1 and L2 are indicating hydrophobic sites, whereas L3 is a liphophilic region (green). H1 and H2 are showing hydrogen bond donor sites (blue), whereas A2 shows a hydrogen bond acceptor site (yellow). S1 represents a sterically unacessible region (grey).

Based on this model some key interactions were proposed, e.g. hydrogen bonding interactions of the NH of the quinoline system and the nitrogen of the pyrazolo-moiety. Furthermore, ring D is pointing in a hydrophic pocket (L1 and L2). These observations prompted us to investigate the role of ring D and the hydrogen bond interactions at the $\alpha+/\gamma-$ interface. Since the $\alpha+/\gamma-$ and the $\alpha+/\beta-$ interfaces are very homologous we were also curious how the new compounds interact with our target site of action, at the $\alpha+/\beta-$ interface.

Consequently, we synthesized a set of 11 PQs possesing small and large sterical bulk (**[11]** and **[15]** - **[17]**), cyclic aliphatic (**[12]** and **[13]**) and flexible aromatic (**[9]** and **[10]**) features. In addition, we removed ring D (**[18]**) and created a dimethylated (**[14]**) and cyclopentyl derivative (**[19]**) (Scheme 2).

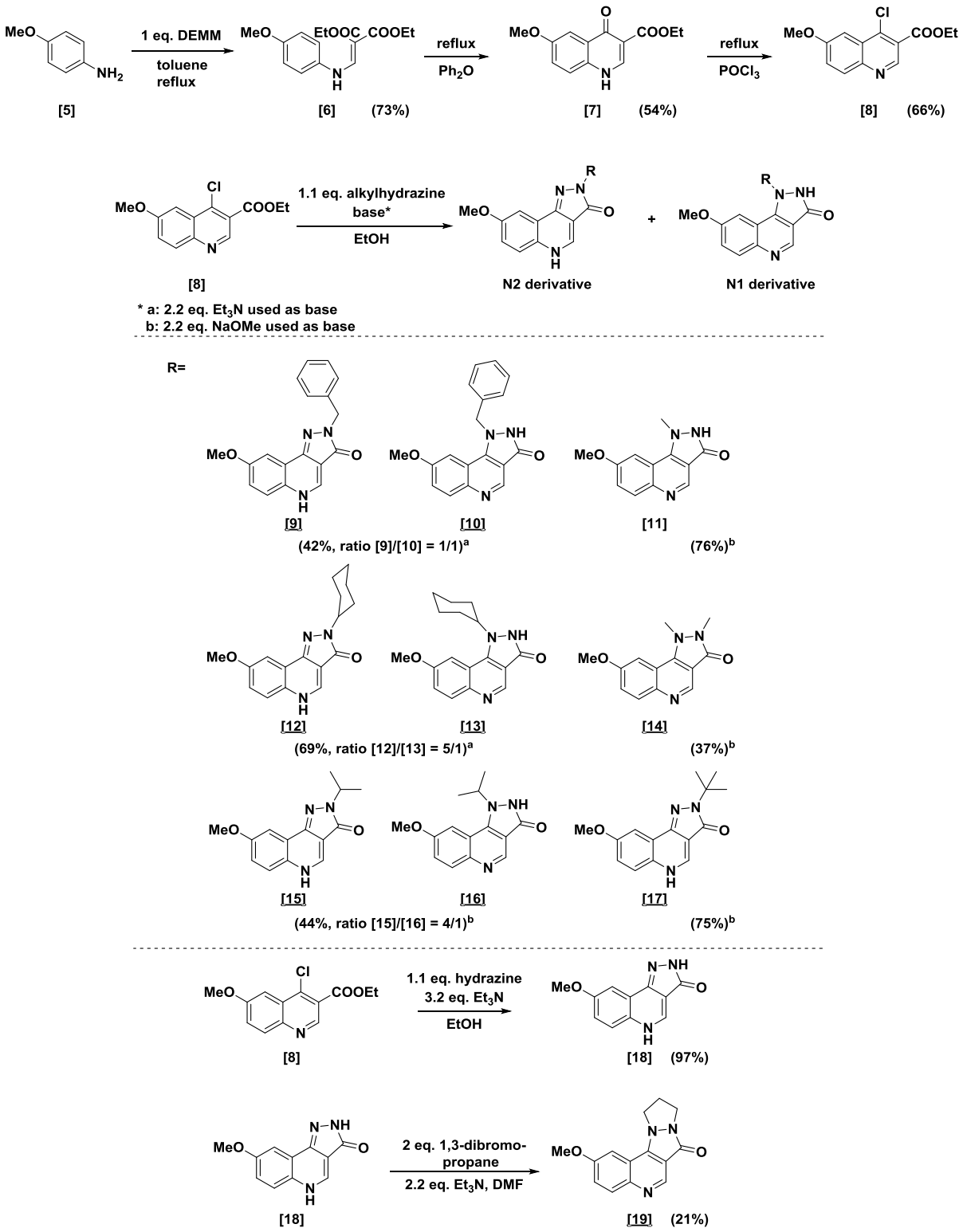

Scheme 2: Synthetic overview of the pyrazoloquinolinone alkyl series.

Varagic et *al*.[146] reported an overall high efficacy profile in $\alpha 1\beta 3$ receptor subtypes for PQ derivatives with a methoxy residue in position R^8. Thus, we chose *p*-anisidine as starting material which was converted via the Gould-Jacobs reaction to the corresponding quinoline derivative **[7]**. Upon chlorination with $POCl_3$ the precursor **[8]** for the pyrazoloquinolinone formation was obtained (Scheme 2). The use of aliphatic hydrazines resulted in the formation of two regioisomers (N1 and N2 derivatives) which could easily be separated by prep-HPLC. For the benzylic residues Rivilli *et al.* reported an influence of the ratio of the isomers using different bases.[147] The use of 2 eq. of NaOMe compared to 2 eq. triethylamine shifted the ratio of N2/N1 isomers from 1/2 (Et_3N) to 1/1 (NaOMe). Here, a ratio of 1/1 for the corresponding benzyl derivatives **[9]** and **[10]** was achieved by the use NaOMe. However, this was not possible for the other derivatives (see Scheme 2, ratio **[12]/[13]**). Thus, for the isopropyl analogs **[15]** and **[16]** we used triethylamine, again. In case of the *tert*-butyl hydrazine derivative only the formation of the N2 isomer was observed due to steric bulk which reduces the nucleophilicity of the N2 nitrogen. On the contrary, the mono methyl derivative **[11]** resulted in the N1 isomer, exclusively, suggesting a highly increased nucleophilicity of the N1 nitrogen due to the +I effect of the methyl group. Interestingly, all N1 derivatives appeared as a colorless solids whereas the N2 derivatives are yellow solids. In addition, for the N1 derivatives inferior solubility in common organic solvents (e.g. in DMSO-d_6 and MeOD during NMR analysis and in MeOH during HPLC purification) compared to their N2 analogues was observed. The low yields of compound **[14]** and **[19]** might be explained by the small scale of the conducted reactions (20 mg starting material).

C I.1.2 Systematic library to explore SAR of positions R^8, R'^3 and R'^4

As shown in our previous studies[146], we oberserved a rather large influence on activity of single substitutional changes on ring A and ring D. For example the exchange from R^8=OMe to R^8=Cl leads to an improved potency of our compounds whereas changes in position R'^3 and R'^4 differently impact on modulation in various receptor subtypes. Therefore, we aimed for a systematic library to investigate a) the impact of different halogens in position R^8 on potency and b) to understand selectivity profiles of different substituents on the ring D.

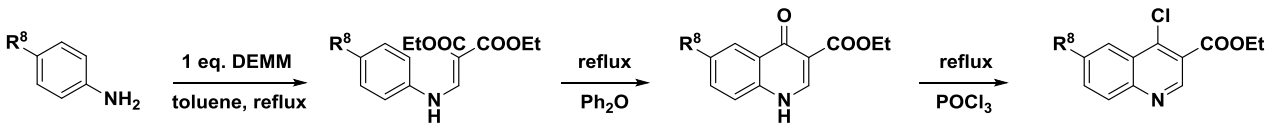

[20] R^8 = F
[21] R^8 = Cl
[22] R^8 = Br
[5] R^8 = OMe

[23] R^8 = F (quant.)
[24] R^8 = Cl (quant.)
[25] R^8 = Br (99%)
[6] R^8 = OMe (73%)

[26] R^8 = F (41%)
[27] R^8 = Cl (57%)
[28] R^8 = Br (73%)
[7] R^8 = OMe (54%)

[29] R^8 = F (63%)
[30] R^8 = Cl (76%)
[31] R^8 = Br (90%)
[8] R^8 = OMe (66%)

Scheme 3: Precursor synthesis of systematic library.

The precurosors with variation in position R^8 were synthesized in three steps according to the earlier mentioned synthetic route (Scheme 2). The reaction sequence proceeded in good yields except for the thermal cyclization step in which a yield of around 50% could be obtained, only. Here, the reaction mixture is poured into petroleum ether to precipitate the crude product of **[7]** and **[26]**-**[28]**. Next, the crude product is washed with a mixture of PE/EtOAc (1/1) which led to the pure products. However, incomplete precipitation and a slight solubility of the oxoquinolines might serve as explanation of the lower yields. The conversion of the oxoquinolines into chloro compounds was achieved in overall acceptable to good yields (Scheme 3).

The formation of the distinct pyrazoloquinolinones was performed using 8 different phenylhydrazines (*para*- and *meta*-substitution with: Me, OMe, CN, NO_2) to obtain the first 32 derivatives (Scheme 4). Further diversification was made by reducing the nitro compounds using either Na_2S in EtOH or by catalytic reduction using palladium on charcoal. The nitril compounds were either converted to the corresponding benzamides by acidic hydrolysis using conc. H_2SO_4 or to the corresponding carboxylic acids by basic hydrolysis with NaOH (Scheme 4). This led to a library of 56 pyrazoloquinolinones in total of which 8 were already known to the literature (indicated by non bold letters, Table 1).

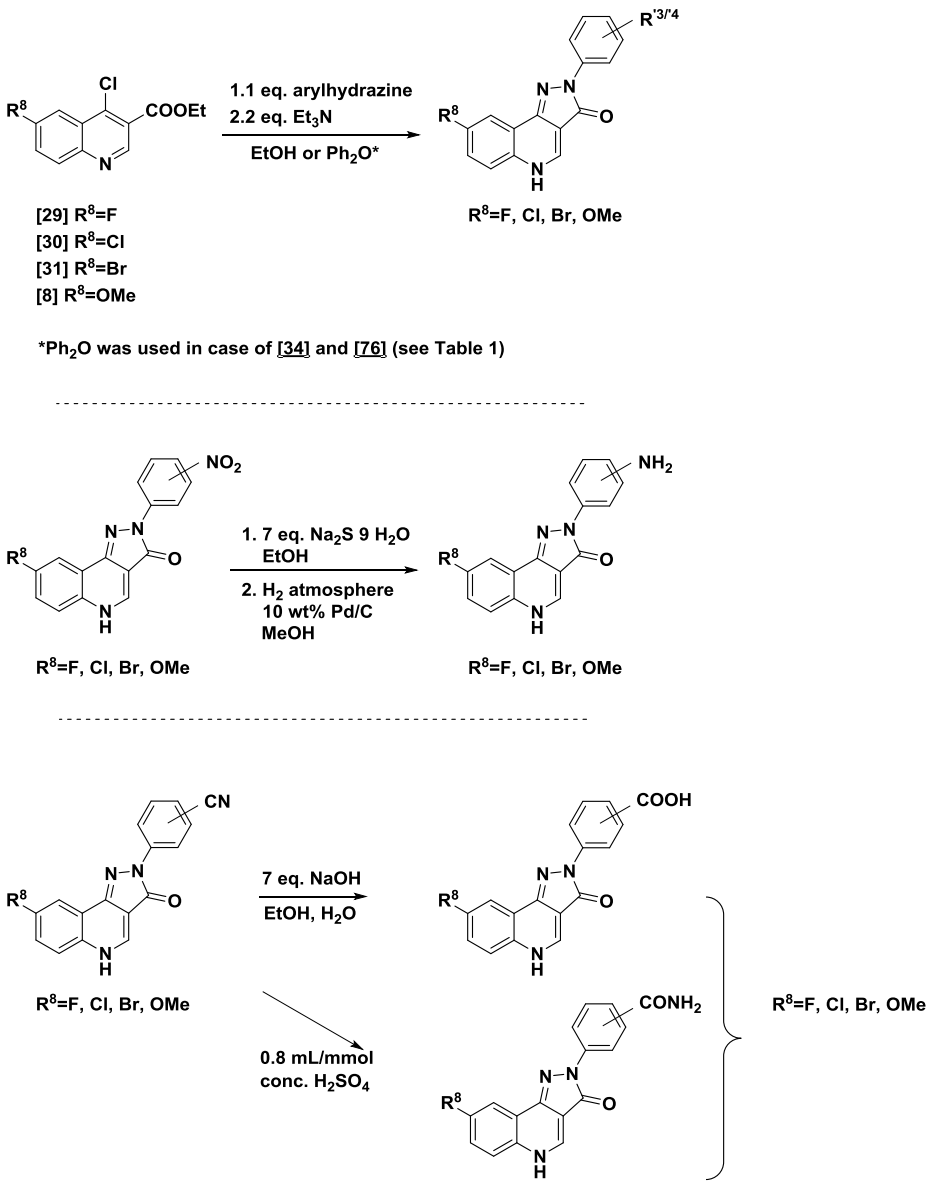

Scheme 4: Synthesis of the pyrazoloquinolinone library.

Table 1: Overview of the systematic library of pyrazoloquinolinones focusing on position R^8, R'^3 and R'^4.

Compound	Lab code	R^8	R'^3	R'^4	Isolated yield [%]
[32]	DCBSLK024	F	H	CH_3	66
[33]	DCBSLK012	F	H	OCH_3	quant.
[34]	DCBSLK014	F	H	NO_2	37
[35]	DCBSLK015	F	H	CN	61
[36]	DCBS193	F	H	NH_2	9
[37]	DCBSLK038	F	H	COOH	32
[38]	DCBSLK032	F	H	$CONH_2$	77
[39]	DCBSLK025	F	CH_3	H	76
[40]	DCBSLK029	F	OCH_3	H	81
[41]	DCBSLK023	F	NO_2	H	70
[42]	DCBSLK019	F	CN	H	52
[43]	DCBSLK057	F	NH_2	H	81
[44]	DCBSLK039	F	COOH	H	54
[45]	DCBSLK033	F	$CONH_2$	H	quant.
[46] (LAU156)	DCBS54	Cl	H	CH_3	79
[47] (PZ-II-028)	DCBS138	Cl	H	OCH_3	58
[48] (LAU157)	DCBS191	Cl	H	NO_2	37
[49] (LAU161)	DCBS139	Cl	H	CN	84
[50] (LAU206)	DCBSLS17	Cl	H	NH_2	81
[51]	DCBS128	Cl	H	COOH	65
[52]	DCBSLK36	Cl	H	$CONH_2$	quant.
[53]	DCBS142	Cl	CH_3	H	63
[54] (LAU159)	DCBS137	Cl	OCH_3	H	76
[55]	DCBS119	Cl	NO_2	H	92
[56]	DCBS146	Cl	CN	H	71
[57]	DCBS120	Cl	NH_2	H	82
[58]	DCBS152A	Cl	COOH	H	70
[59]	DCBS152B	Cl	$CONH_2$	H	75
[60]	DCBS148	Br	H	CH_3	64
[61]	DCBS149	Br	H	OCH_3	63
[62]	DCBS147	Br	H	NO_2	55
[63]	DCBS150	Br	H	CN	77
[64]	DCBS164	Br	H	NH_2	81
[65]	DCBS153A	Br	H	COOH	66
[66]	DCBS153B	Br	H	$CONH_2$	55
[67]	DCBS155	Br	CH_3	H	52
[68]	DCBS156	Br	OCH_3	H	63
[69]	DCBS154	Br	NO_2	H	62
[70]	DCBS157	Br	CN	H	86
[71]	DCBS163	Br	NH_2	H	80
[72]	DCBS162	Br	COOH	H	66
[73]	DCBSLK58	Br	$CONH_2$	H	58
[74]	DCBS76	OCH_3	H	CH_3	74
[75] (LAU176)	-*	OCH_3	H	OCH_3	-
[76]	DCBS93	OCH_3	H	NO_2	63
[77] (LAU177)	DCBS84	OCH_3	H	CN	57
[78]	DCBS96	OCH_3	H	NH_2	16
[79]	DCBS88	OCH_3	H	COOH	66
[80]	DCBSLK60	OCH_3	H	$CONH_2$	67
[81]	DCBS141	OCH_3	CH_3	H	62
[82]	DCBS135	OCH_3	OCH_3	H	68
[83]	DCBS52	OCH_3	NO_2	H	25
[84]	DCBS145	OCH_3	CN	H	53
[85]	DCBSLS24	OCH_3	NH_2	H	65
[86]	DCBS151A	OCH_3	COOH	H	57
[87]	DCBS151B	OCH_3	$CONH_2$	H	66

***compound not synthesized within this thesis but shown for the sake of completeness.

Overall, the synthesis of most final products worked well. However, we observed a trend towards lower yields for several nitro derivatives (see **[34]**, **[48]**, **[62]**, **[76]** and **[83]**). In fact, these are all *para* substituted compounds except for **[83]** which is a *meta* substituted compound. Thus, the –M effect of the *para* nitro substituent significantly lowers the nucleophilicity of the hydrazine resulting in a lower yield compared to the other phenylhydrazines and the *meta* substituted nitrophenyl hydrazines. The cyclization of the nitro phenylhydrazine derivatives **[34]** and **[76]** with their corresponding precursor resulted in very low yields (not shown in Table 1, **[34]** = ~10% yield; **[76]** = ~20% yield) under the established general reaction conditions using EtOH as solvent. Therefore, the solvent was changed to a higher boiling solvent (diphenyl ether at 150°C) which led to a small improvement of the yields in case of compound **[34]** (37% yield) and to a large improvement for compound **[76]** (63% yield) (Table 1, Scheme 4). In case of **[48]**, **[62]** and **[83]** this reaction step was not repeated in diphenyl ether since sufficient amounts of substance were isolated for the next reaction step. The low yield of the *meta* nitro derivative **[83]** leads to the assumption that the cyclization reaction also strongly depends on the chloro precursor (here **[8]**, Scheme 3). Hence, the cyclization of the precursors **[8]** and **[29]** with nitro phenylhydrazines seems not to be favored.

Surprisingly, the reduction of the two nitro compounds **[34]** and **[76]** was achieved in very poor yields compared to their analogous with different substituents in position R^8 (Scheme 4, Table 1).

Interestingly, fluorinated compounds **[32]**-**[45]** showed an improved solubility in organic solvents compared to their analogues with different substituents in position R^8. During the work up of the last step the reaction mixture was rinsed with water which led to a precipitation of the product in case of compounds with other substituents than fluorine in position R^8. However, for the fluorinated series we observed a rather poor precipitation which required an extraction of the aqueous phase with EtOAc to obtain the desired products. Additionally, we observed that we were able to dissolve larger amounts of compound for NMR analysis in DMSO-d_6 (usually max. 4 mg, here up to 8 mg). Thus, the introduction of fluorine in position R^8 might represent one reasonable strategy to generally improve the poor solubility of pyrazoloquinolinones.In addition to this systematic library we synthesized a small set of additional structures consisting of 4 compounds **[89]**-**[92]** (“mixed library”) to follow up on earlier SAR considerations (Scheme 5). Precursor **[88d]** was synthesized according to Scheme 3 in an overall yield of 19% over 3 steps. Surprisingly, the last step yielded compound **[92]** in 12%, only, whereas the other compound were obtained in good yields.

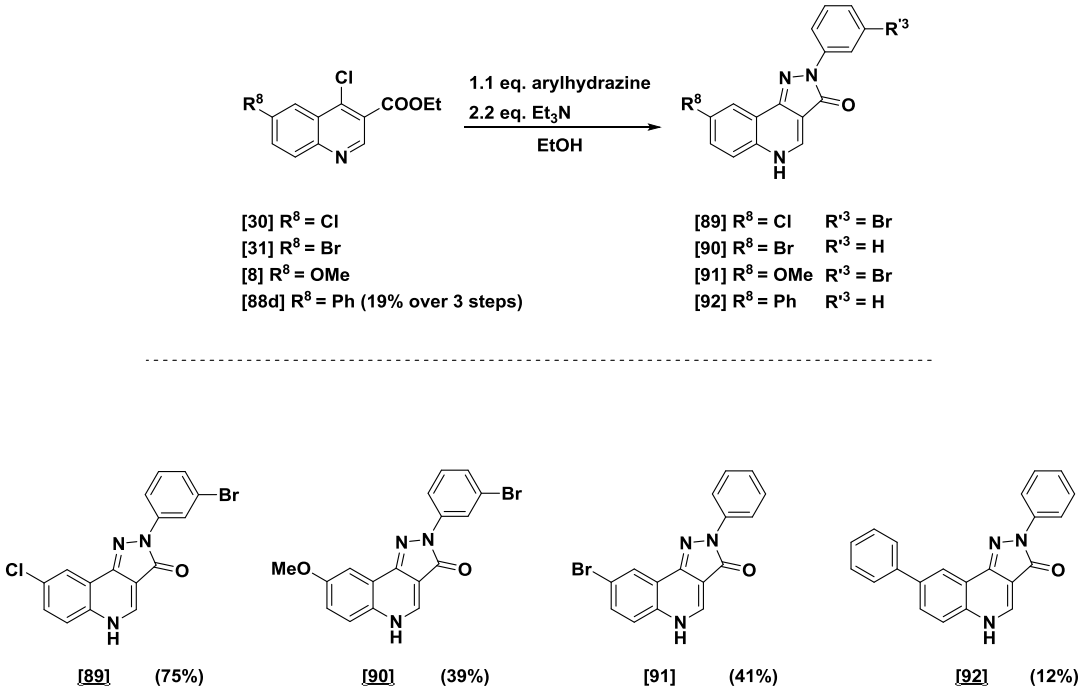

Scheme 5: Synthesis of the small mixed library.

Overall, the synthesis of pyrazoloquinolinones worked straight forward. However, for some compounds (e.g. **[34]**, **[36]**, **[76]**, **[78]** and **[83]**) unexpectedly low reactivities either in the last cyclization to the pyrazoloquinolinone core or in the reduction to the amine derivatives were observed, which could be partially improved. Thus, we synthesized a library of 52 new pyrazoloquinolinones to investigate the allosteric modulation at the homologous $\alpha+/\beta-$ and $\alpha+/\gamma-$ sites of certain $GABA_A$ receptors.

C I.2 Triazoloquinazolinediones

This chapter deals with the synthesis of triazoloquinazolinediones, which are reported as high affinity binders for the $\alpha1+/\gamma2-$ interface.[148] However, these compounds were not investiagate towards their modulatory effect at the $\alpha+/\beta-$ interface and thus we aimed for a small library to get first insights into their biological activity profile. In the synthesis we focused on substitution patterns of pyrazoloquinolinones which are well studied at the $\alpha+/\beta-$ interface. Therefore, we transferred the known substituent combinations of the positions R^8 and R'^4 to the other chemotype (Figure 20).

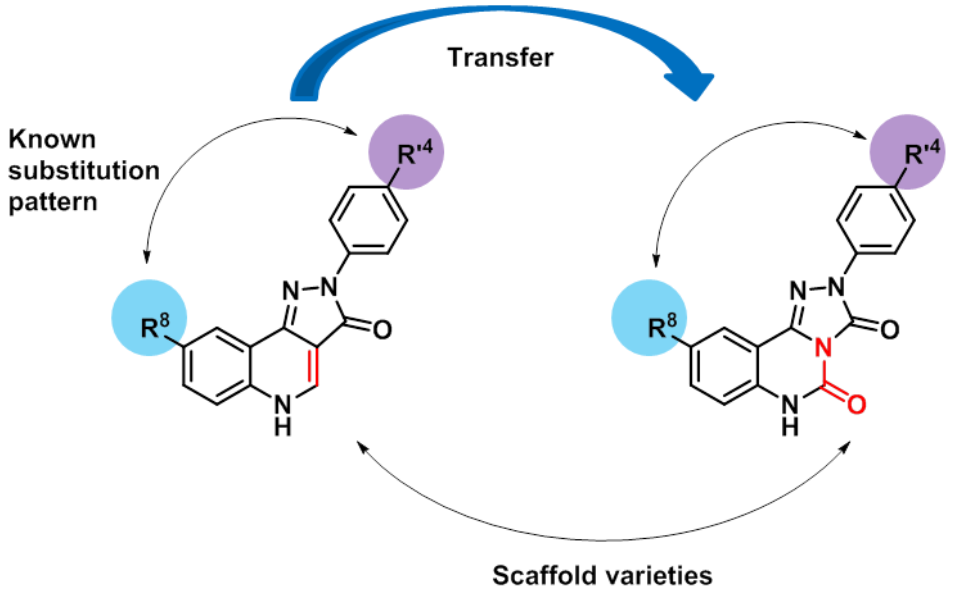

Figure 20: Comparison of the pyrazoloquinolinone scaffold with the triazoloquinazolinedione scaffold. Scaffold varieties are highlight in red, positions R^8 and R'^4 are highlight in light blue and light purple.

C I.2.1 Synthesis of Triazoloquinazolinediones

The synthetic route of triazoloquinazolinediones was first described by Nilsson *et al.*[148] A retrosynthetic analysis of this compound class is shown in Scheme 6. First, two cuts of the triazolo moiety **[93]** are made to give 1-phenylhydrazine-1-carboxylates **[94]** and chlorinated quinazolines **[95]**. The chlorinated quinazoline **[95]** is accessible by functional group interconversion of the quinazoline **[96]**. Two final cuts lead to anthranilic acid derviates **[97]** and ethoxycarbonyl isothiocyanat **[98]** as suitable starting materials. 1-Phenylhydrazine-1-carboxylates **[94]** can be synthesized by a regioselective amidation reaction starting with different substituted aryl iodides **[100]** and ethyl carbazate **[99]**.

This synthetic strategy should allow easy access to differently substituted derivatives of this compound class with respect to R^1 and R^2.

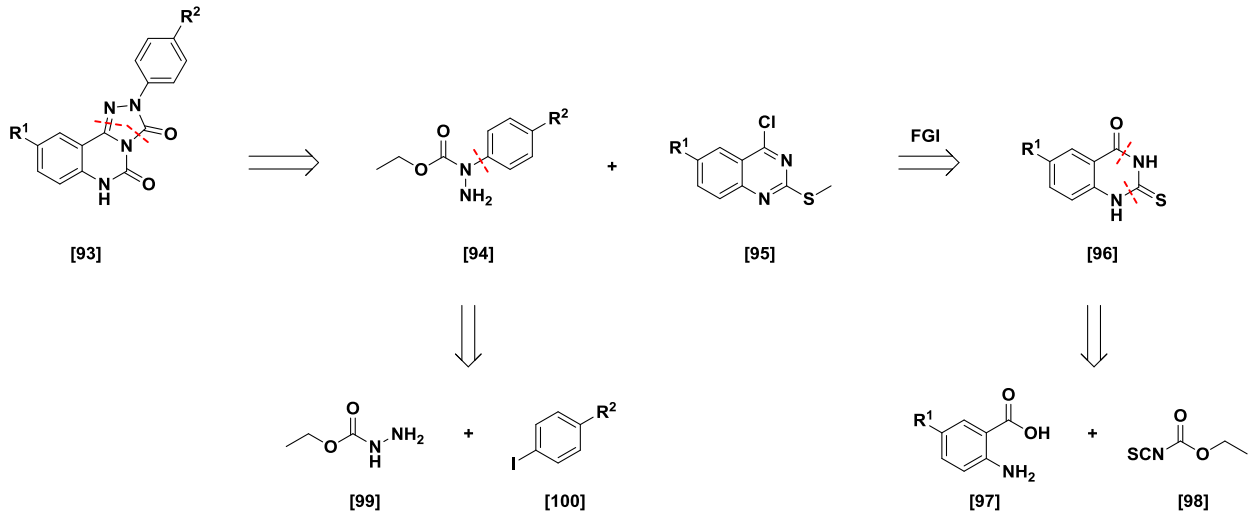

Scheme 6: Retrosynthetic analysis of triazoloquinazolinediones.

According to the considerations shown in Figure 20 we started the synthesis using two different anthranilic acid derivatives (**[101]** and **[102]**) and converted them with ethoxycarbonyl isothiocyanat **[98]**. The addition products **[103]** and **[104]** were cyclized intramolecularly using acetic anhydride. Next, the ester of **[105]** and **[106]** were cleaved under basic conditions and the quinazoline derivatives **[107]** and **[108]** were protected selectively at the sulfur atom. After activation *via* chlorination the first building blocks **[111]** and **[112]** were obtained in good yields (Scheme 7).

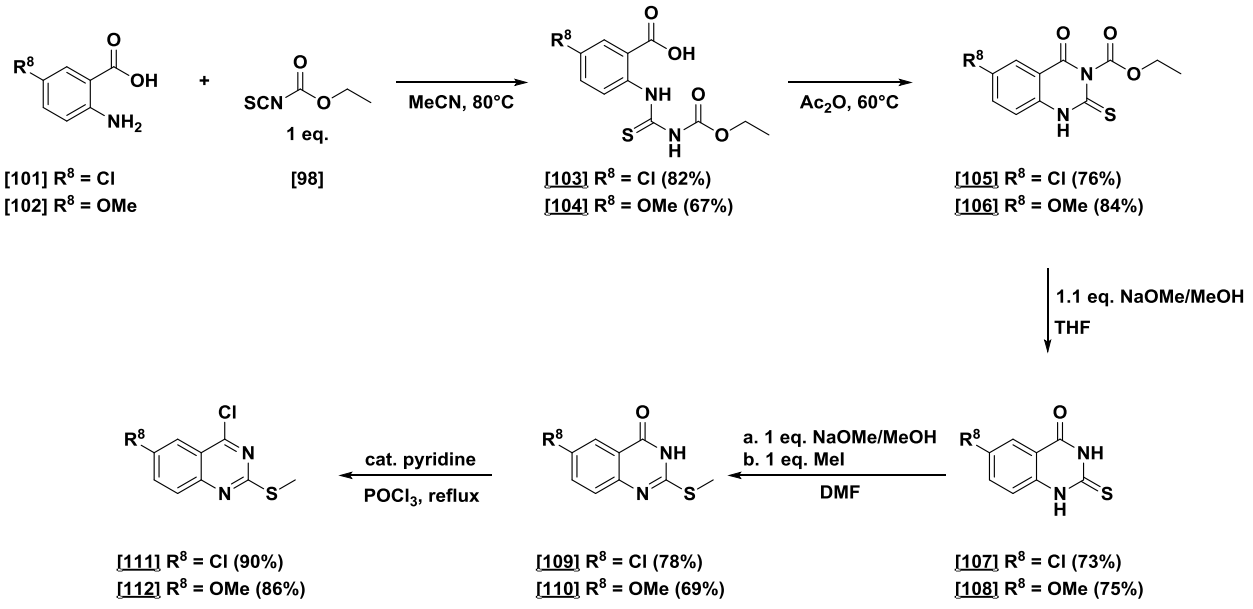

Scheme 7: Synthesis of the first building block.

The second building block was synthesized by a regioselective amidation using copper.[149] Here, four different substrates **[113]**-**[116]** were selected as starting materials based on their analogous PQ derivatives (**[46]**, **[47]**, **[49]**, **[50]**, **[74]**, **[75]**, **[77]** and **[78]**) leading to the corresponding triazoloquinazolinediones with same substituents in the position R'^4 (Figure 20, Scheme 8). While **[118]**-**[120]** were converted under the same reaction conditions, compound **[117]** required modified reaction conditions using higher catalyst (5 mol%) and ligand (20 mol%) loading and a decreased reaction time of 4 h as reported by Wolter *et al* (Scheme 8).[149]

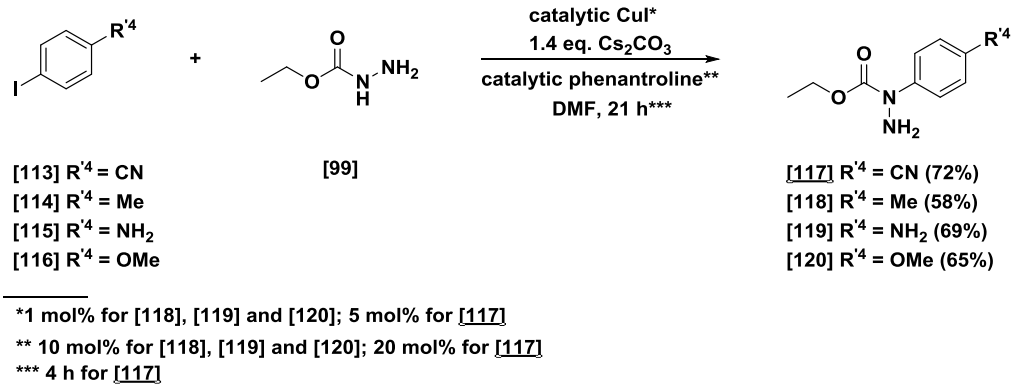

Scheme 8: Cooper catalyzed regionselective amidation.

The different building blocks **[111]**-**[112]** and **[117]**-**[120]** were further converted to the cyclized compounds **[123]**, **[124]**, **[125]**, **[127]** and **[128]** (Scheme 9, central line). The initial step is likely to be a S_NAr displacement of a chlorine followed by a base promoted cyclization in neat diisopropylethylamine. In this step the starting material with the free amine group **[119]** reacted intermolecularly to a byproduct **[136]** which presumably consists of two moieties of **[111]** according to ^1H NMR analysis (Scheme 9, bottom right line). Full characterization of the byproduct **[136]** could not be achieved due to its very poor solubility. However, the formation of the desired product was not observed. Thus, the competitive reactivity of the additional free amine group at the phenyl ring prompted us to introduce a Boc protecting group to prevent this unwanted side reaction (Scheme 9, top line). Consequently, 4-iodoaniline **[115]** was converted to the Boc protected compound **[121]** which was coupled by a copper catalyzed amidation reaction to the desired Boc protected building block **[122]** in acceptable yields. Next, cyclization in neat DIPEA was conducted providing **[126]** in 31% yield which is remarkably lower compared to the yields obtained for the other derivatives (average ~60%). This observation might be explained by thermal cleavage of the Boc protecting group under the reaction conditions at 110°C. Additionally, the introduction of the Boc protecting group leads to an increase of the steric bulk which could

interfere during the cyclization process. Hydrolysis of the methylthioquinazolines **[123]**-**[128]** was achieved by oxidation to the corresponding sulfoxides which represent a good leaving group. Nucleophilic substitution by water yielded the desired carbonyl derivatives **[129]**-**[134]**. In case of the Boc protected derivative **[132]** a subsequent deprotection using TFA yielded the final product **[135]** (Scheme 9).

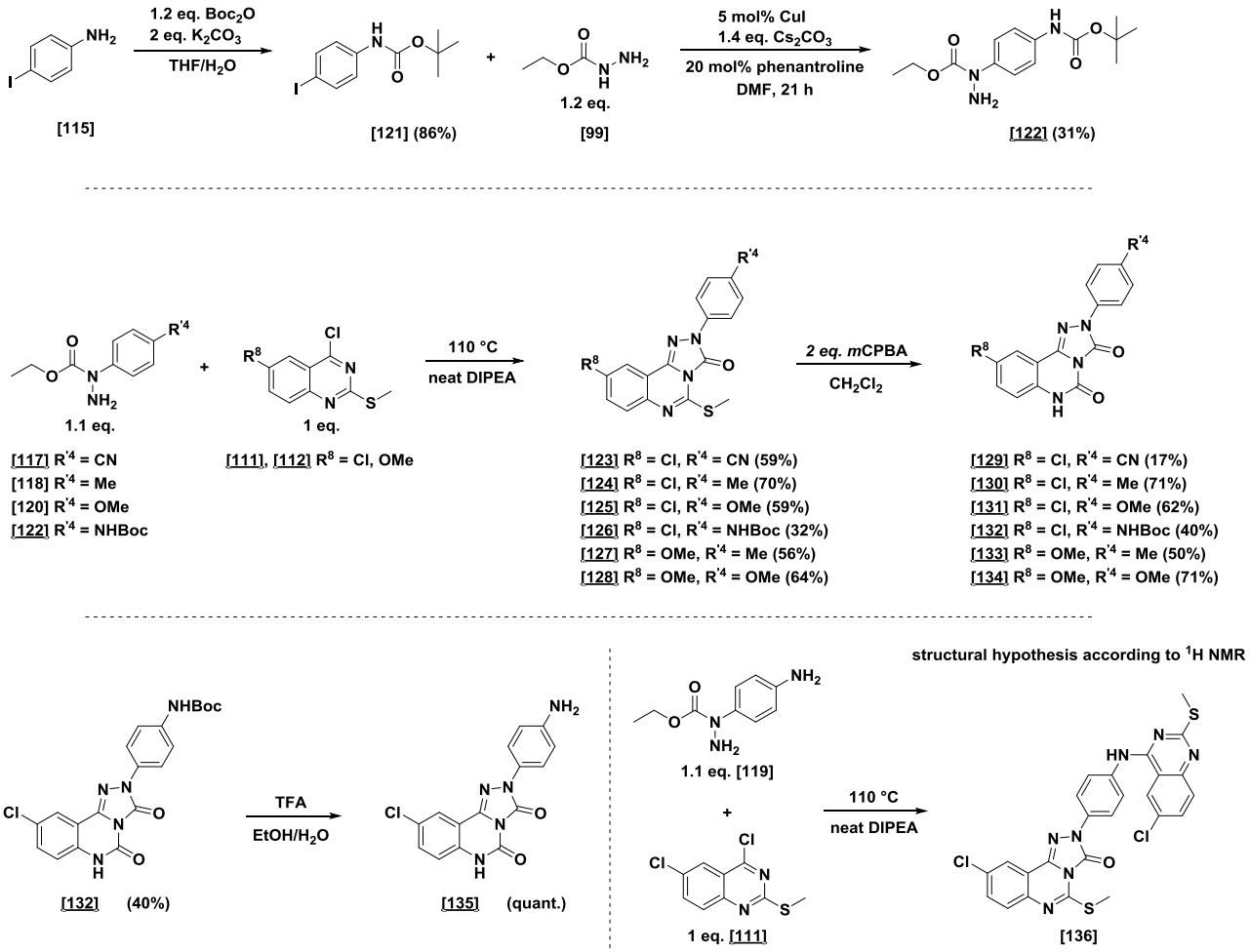

Scheme 9: Intermolecular cyclizaiton and Boc protection of the amino derivative.

In summary, we successfully synthesized a library of 6 new triazoloquinazolinediones **[129]**-**[134]** and **[135]**. The synthesis worked well and smaller obstacles, e.g. competitive reactivity of **[119]**, could be solved using protecting groups. The new set of compounds was investigated towards their modulatory activity at the $\alpha+/\beta-$ interfaces (C II.3). In addition, we aimed to compare their activity at the $\alpha1-/\gamma2-$ vs. $\alpha6+/\gamma2-$ sites (C II.4).

C II Subtype selectivity – where to start at?

In general, $GABA_A$ receptors' subunits possess a high sequence identity and a high sequence similarity which is probably reflected in their promiscuous pharmacological profiles. While there is a sequence identity of ~20% or ~50% between different subunit families, we find within in a subunit family a sequence identity up to ~70%.[150]

At the 18 extracellular α+/β− interfaces (six α and three β subunits) unique amino acid residues contribute to each of their binding pockets. However, also among them there exist subunits which are more alike and which differentiate a lot. Global similarities among subunits are represented in a phylogenetic tree which reveals a separation of the 6 α subunits into two groups, so called diazepam-sensitive (α1, 2, 3, 5) and diazepam-insensitive (α 4, 6). Furthermore, within the diazepam-sensitive group the following α subunit pairs are globally more similar: α1 with α2 and α3 with α5. For the three β subunits we expect the β1 subunit to be globally more different to the β2 and β3 (Figure 21).[12]

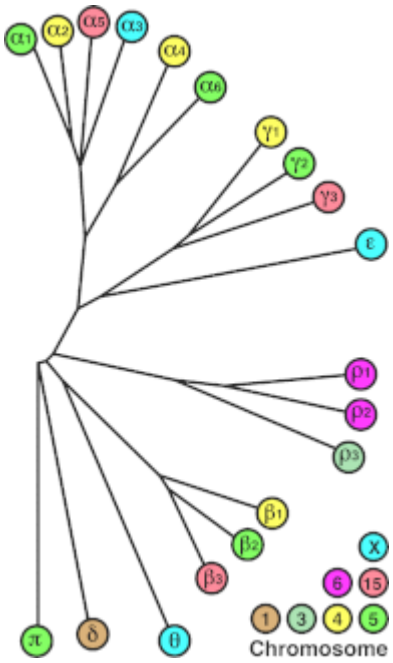

Figure 21: Phylogenetic tree representation of the 19 known genes coding for human $GABA_A$ receptor subunits.

To get an overview in how much the global similarity of the different subunits is reflected locally at the extracellular binding pocket at the α+/β− interfaces, we used homology modeling. Based on the human $GABA_A$ receptor amino acid sequences (uniprot[151]) we created 18 homology models using the crystal structure of the human β3 homopentameric $GABA_A$ receptor as template.[90] Next, we categorized the amino acid residues into amino acids which are variable among the isoforms and which are conserved. The C_α-atoms of

these amino acids were represented as spheres (for α: conserved amino acids: yellow spheres; variable amino acids: orange spheres). Moreover, amino acids which contribute to the extracellular binding pocket are highlighted with a green asterisk to assess which amino acids might be important to address for the design of subtype selective compounds (Figure 22).

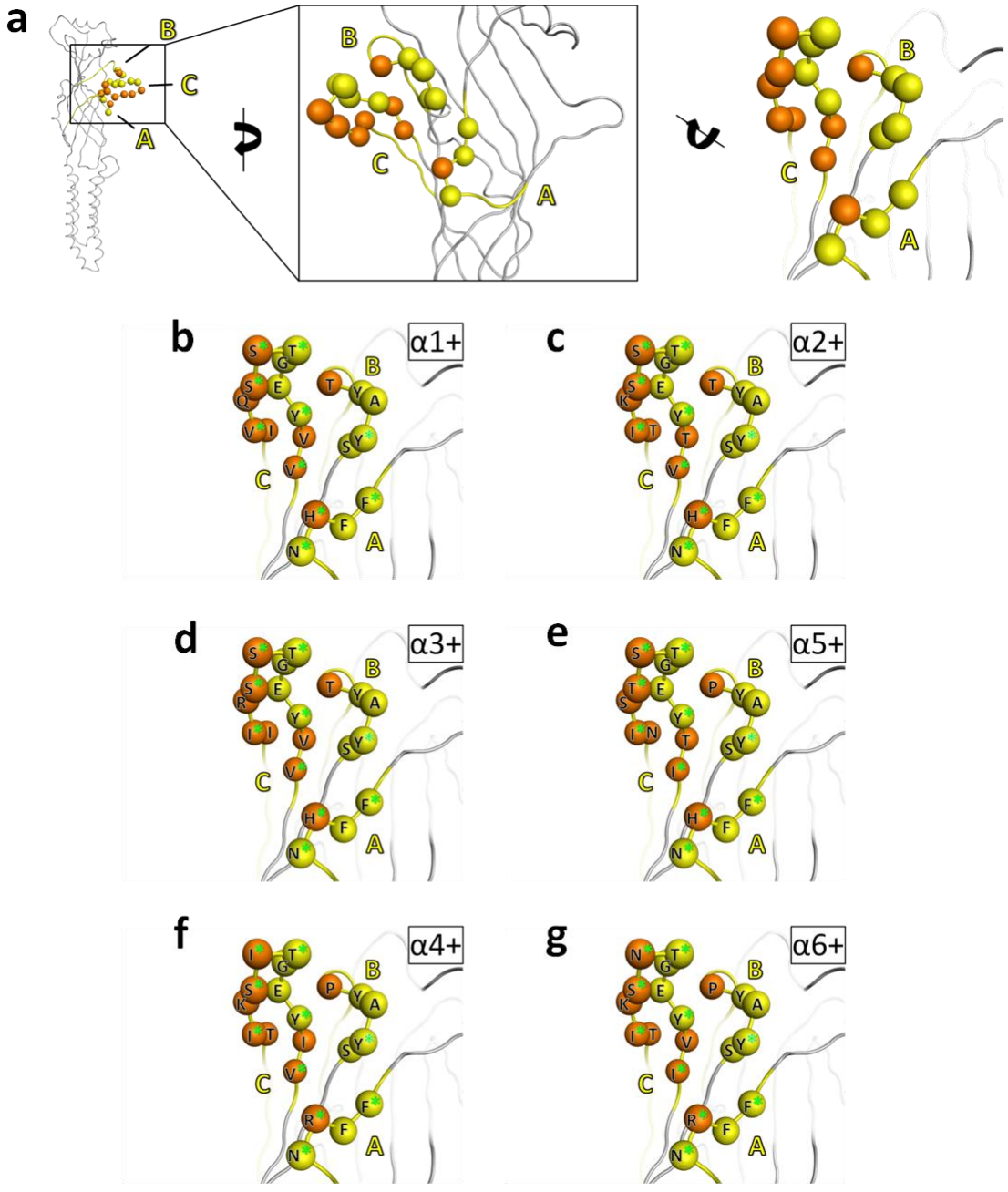

Figure 22: Differences between the six α isoforms at the extracellular α+/β– binding pocket. a:Perspective of the illustrated α subunit representations. **b-g**: The extracellular plus sides of α1–6 subunits are displayed from a perspective from below into the tilted pocket showing the loops A, B and C (highlighted with capital yellow letters). The C_α-atoms of conserved amino acids are displayed as yellow spheres whereas C_α-atoms of variable amino acids are displayed in orange. Amino acids contributing with their side chains to the binding pocket are labeled with a green asterisk.

The panels a-d in Figure 22 show the diazepam-sensitive (DS) α isoforms whereas the diazepam-insensitive (DI) are shown in panel e and f. Among others, the major local difference between these groups in a rigid protein area (not loop C) is the amino acid residue on loop A, for α1, 2, 3, 5 = histidine (H) and for α4, 6 = arginine (R) (Figure 22). This has already been demonstrated by mutagenesis experiments in which the α1H101R point mutant induced a loss of binding of diazepam in the diazepam-sensitive α1 containing receptors and *vice versa* the α6R100H mutant enabled a gain of binding for diazepam in the diazepam-insensitive α6 containing receptors.[84] While the local similarity of loop A is in accordance with its global similarity, in loop B this is not the case. Here, we observe locally a threonine (T) residue on loop B in α1, 2, 3 (Figure 22b, c, d) whereas in α4, 5, 6 (Figure 22e, f, g) there is a proline (P) which further splits the α subunits in so called zolpidem-sensitive (α1, 2, 3) and zolpidem-insensitive (α4, 5, 6) groups.

According to our structural considerations and in line with the phylogenetic tree it presumably is easier to address α subtype selectivity for one of the DI or DS groups, either α4, 6 or α1, 2, 3, 5 containing receptors. For the DI receptors it should even be possible to distinguish between α4 and α6 containing receptors due to the rather significant difference in the tip of the loop C (Figure 22, α4 = isoleucine (I) vs α6 = asparagines (N)) which has already been shown by Varagic *et al*. who reported an α6 preferring compound.[152]

Analogously, we analyzed the three β isoforms (Figure 23) and showed that there are huge differences of variable positions between the conserved beta strand area (segments E, D and G) and the flexible loop F. While most variable amino acid positions are located on loop F we avoided to analyze them in detail due to the difficulties in the modeling of flexible loop areas which often provide unreliable results.[153,154]

In the conserved area there are only two variable amino acid positions, one on segment D and one on segment G. While the amino acid residue on segment G seems to be more central and differs only between β1 (R41) vs β2/3 (N40/N41), the amino acid position on segment D is variable among all three β isoforms but presumably too distant from a putative binding cavity. Thus, a distinction between β1 and β2/3 at the extracellular α+/β− sites seems to be feasible. So far, known β subtype selective compounds are either believed to bind in the transmembrane domain or their binding site is still unknown.[72,73,155,156]

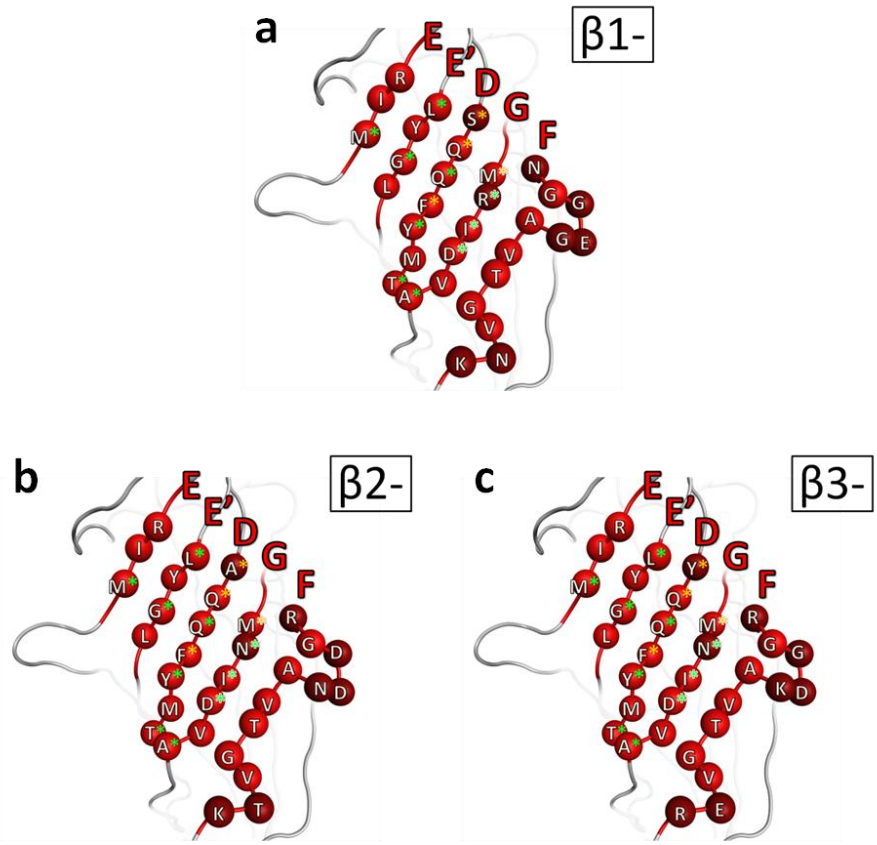

Figure 23: Differences between the three β isoforms at the extracellular α+/β– binding pocket. a-c: The extracellular minus sides of β1–3 subunits are displayed from a front perspective showing the segments E, E', D, G and loop F (highlighted with capital red letters). The C_α-atoms of conserved amino acids are displayed as red spheres whereas C_α-atoms of variable amino acids are displayed in dark red. Amino acids contributing with their side chains to the binding pocket are labeled with a green asterisk. Amino acids with ambiguous contributions are labeled with an orange asterisk.

C II.1 Pyrazoloquinolinones - Substitution of the ring D

According to the pharmacophore model of Savini *et al*. (Figure 19) the ring D of the pyrazoloquinolinone scaffold is believed to point into a hydrophobic pocket.[144,157] Thus, we omitted the ring D completely and replaced it with various alkyl substituents (C I.1.1) to assess its necessity for activity at the high affinity $\alpha+/\gamma2-$ and the low affinity modulatory $\alpha+/\beta-$ site. We screened for modulatory effects (see chapter B V) in binary $\alpha1\beta3$ $GABA_A$ receptors and determined IC_{50} values to get preliminary insights (Figure 24).

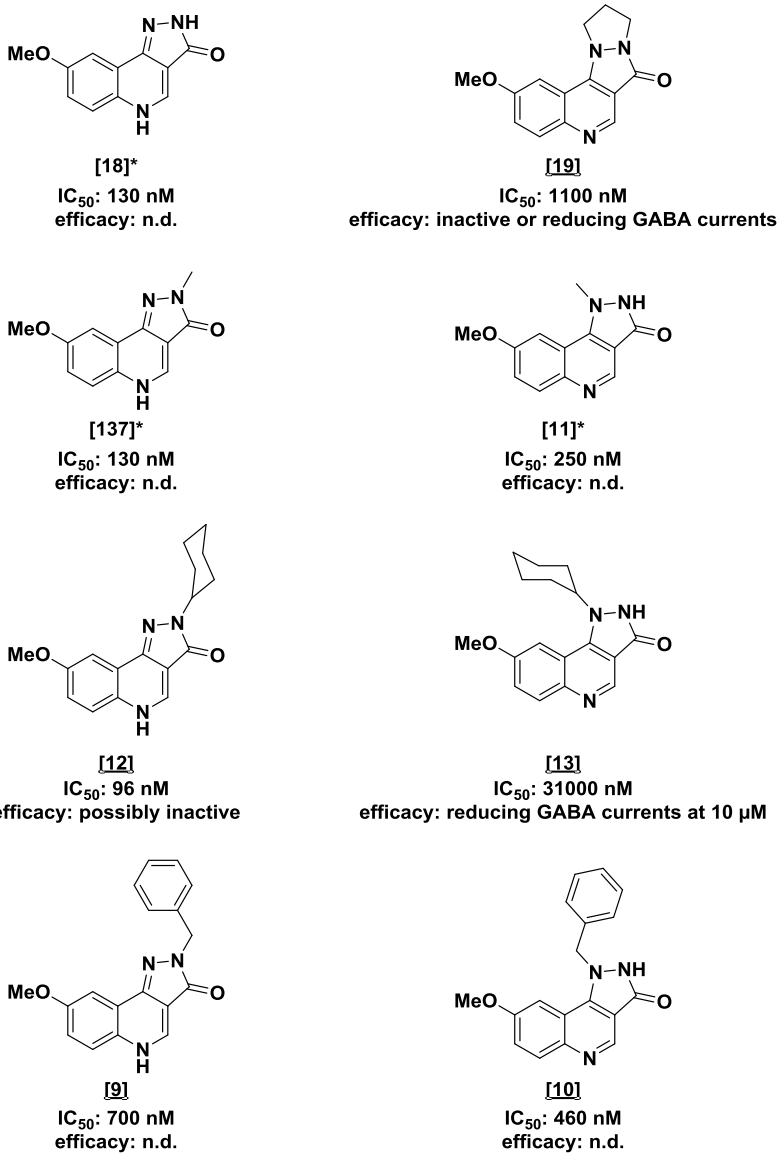

Figure 24: Prelimniary binding and efficacy data of a number of alkyl substituted pyrazoloquinolinone derivatives. Modulatory effects were measured in binary $\alpha1\beta3$ $GABA_A$ receptors at EC_3 and binding data were measured in cerebellar membranes. n.d. = not determined. *Compounds were first synthesized by Markus Draskovits.[5]

These very preliminary results showed quite inconclusive data sets. Six compounds possess sub micromolar affinities whereas two compounds can be considered as weak binder or non-binder. While we observed a decreased binding affinity for three N1 substituted derivatives (N1 = substituent at the left nitrogen), the N1 benzyl substituted compound possesses a higher affinity than its N2 substituted analog (N2 = right nitrogen substituted). The modulatory effects of the compounds, which were measured first, were very small or negative modulatory effects and were thus not determined for most of the compounds.

Since we were not able to identify any trends or promising effects of this preliminary series we discarded the approach to substitute the ring D of the pyrazoloquinolinone scaffold by simple alkyl substituents and went back to aromatic substituents.

C II.2 Towards subtype selective tool compounds

C II.2.1 $\alpha1+/\beta1-$ Selectivity – a proof of concept

C II.2.1.1 Mini library of compounds aimed at studying potency driving ligand features

In this study we started with a set of compounds based on our previous results where compounds **[47]**, **[46]** and **[50]** showed a modulation of higher than ~300% at the extracellular $\alpha1+/\beta3-$ interface.[146] In addition, we identified position R^8 to possess a strong impact on efficacy and thus we synthesized the corresponding three analogous **[75]**, **[74]** and **[78]**. Here, these six ligands were investigated for potential potency preferences for any subtype (Figure 25).

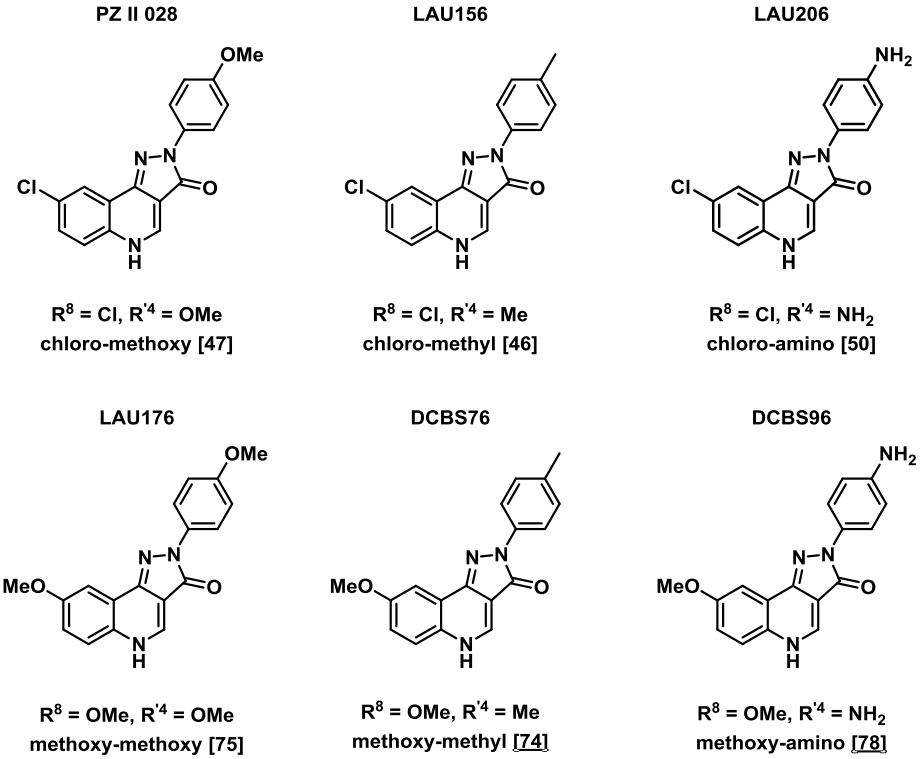

Figure 25: Chemical structures of the ligands **[47]**, **[46]**, **[50]**, **[75]**, **[74]** and **[78]** employed in this study.

C II.2.1.2 Compound [47] exerts very similar effects in $\alpha1\beta3$, $\alpha1\beta3\gamma2$ and $\alpha1\beta3\delta$ receptors

First, we examined the modulatory effects of compound **[47]** in $\alpha1\beta3$, $\alpha1\beta3\gamma2$ and $\alpha1\beta3\delta$ receptor subtypes to assess the influence of the third subunit. As shown in (Figure 26) the

modulatory effects exerted *via* the α+/β− interface are almost unaffected by the presence of a γ2 or a δ subunit. This observation pleased us to use binary receptors (α1βI (I = 1,2,3)) for our mini library screen since binary receptors possess the advantage to lack the high affinity benzodiazepine binding site (αk+/γ2− interface) and they express robustly in *oocytes*.

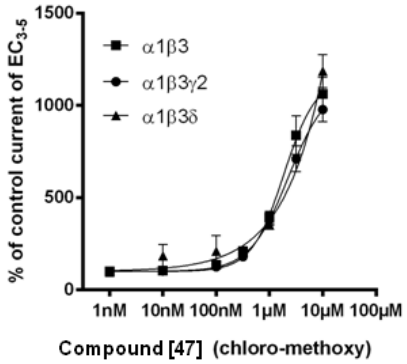

Figure 26: Compound [47] modulates GABA-evoked currents from α1β3, α1β3γ2 and α1β3δ similarly. Concentration-dependent modulation of GABA EC_{3-5} current at α1β3, α1β3γ2 and α1β3δ. Data represent means ± SEM (n=3-8). α1β3 and α1β3γ2 data are identical with those published previously

C II.2.1.3 Potency selectivity for β1-containing receptors

Next, we looked into a potential β selectivity of the compounds **[47]**, **[46]**, **[50]**, **[75]**, **[74]** and **[78]** using α1βI (I = 1,2,3) receptor subtypes. We observed that all compounds showed positive modulation in the investigated subtypes and additionally they displayed higher potencies in α1β1 receptors than in α1β2 or α1β3 receptors (Figure 27a-f). In α1β1 compounds **[47]**, **[50]** and **[75]** showed the highest potencies (130 nM, ~200 nM and ~200 nM). Furthermore, at GABA EC_{3-5} all compounds possess approximately the same efficacy in α1β1 (modulation of ~400%) whereas in α1β2 and α1β3 the efficacies vary widely. Interestingly, this variation in modulation corresponds to the chemical entity at ring D (position R'4): compounds **[47]** and **[75]** (R'4 = OCH_3) show a much higher efficacy in α1β2 and α1β3 compared to α1β1, compounds **[46]** and **[74]** (R'4 = CH_3) have a modulation of the same degree in all three receptors, while compounds **[50]** and **[78]** (R'4 = NH_2) display a diminished modulation in α1β2 and α1β3 compared to α1β1. It is noteworthy, that compound **[78]** seems to be an efficacy selective positive modulator for α1+/β1− interface (Figure 27f).

In addition, we observed an influence on the receptor kinetics of compounds **[47]**, **[50]**, **[75]** and **[78]** which accelerate the current decay at higher concentrations, while structures **[46]** and **[74]** do not display such an effect. For instances sample traces for compound **[47]** are shown in Figure 27g-i. This observation is reported for other modulators and might explain the apparent drop in efficacy at high concentrations of compounds **[47]** and **[50]**.[158]

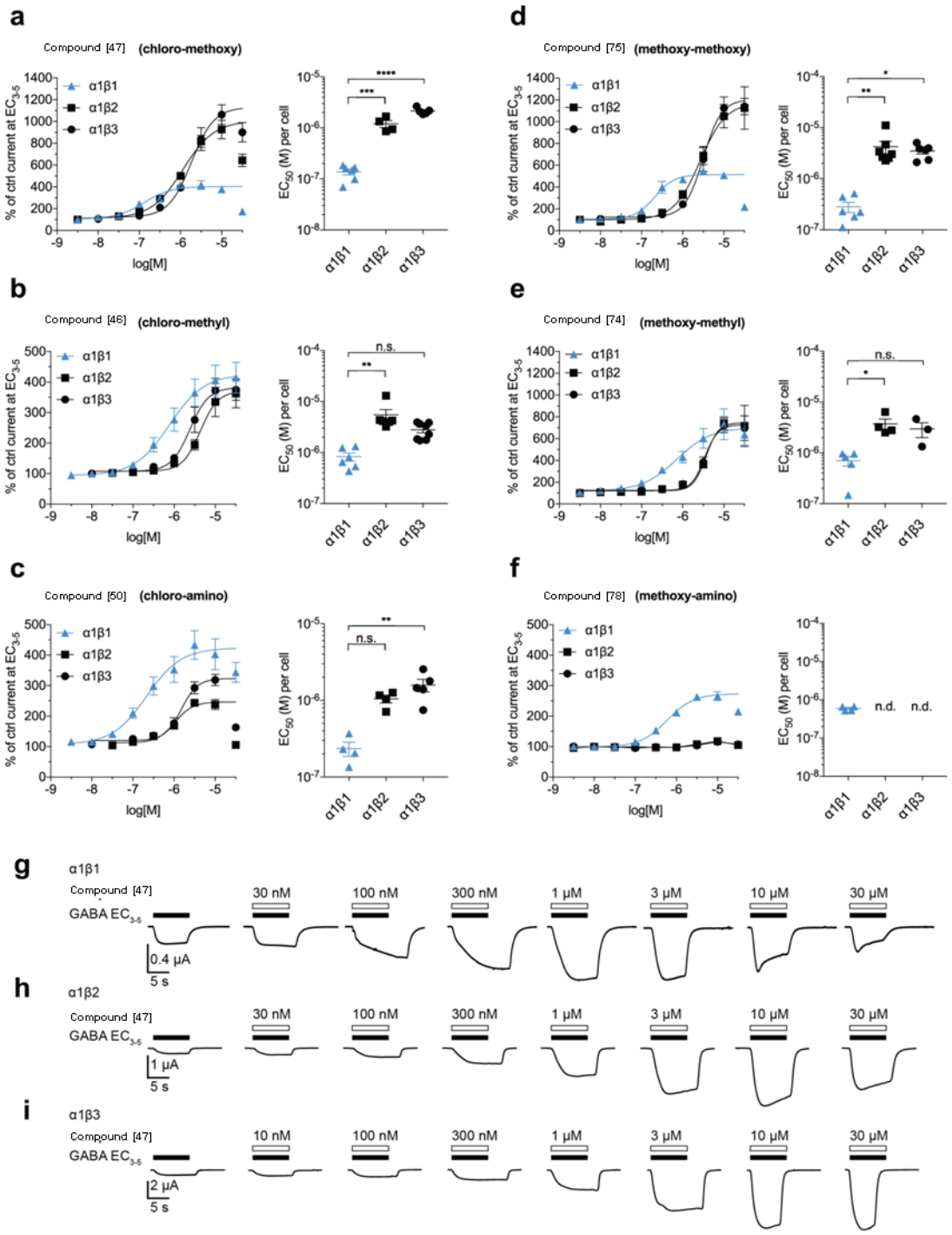

Figure 27: Compounds [47], [46], [50], [75], [74] and [78] show potency selectivity for β1-containing receptors. Dose response data of compounds **[47]**, **[46]**, **[50]**, **[75]**, **[74]** and **[78]** at α1β1, α1β2 and α1β3 subunit combinations; a-c: Left, aggregate dose-response curves of R^8 = chloro compounds **[47]**, **[46]** and **[50]** co-applied with GABA EC_{3-5}. Right, EC_{50} values obtained by fitting data of each cell individually; d-f: Left, aggregate dose-response curves of R^8 = methoxy compounds **[75]**, **[74]** and **[78]** co-applied with GABA EC_{3-5}. Right, EC_{50} values obtained by fitting data of each cell individually. Highest potency was consistently observed at α1β1 receptors. Compound **[78]** (f) lacked efficacy at α1β2 and α1β3, therefore EC_{50} values could not be obtained. In those instances where high compound concentrations elicited substantial desensitization (see panels a, c, d, f and sample traces in (g, h)), the highest compound concentration was excluded from the fit. Statistically significant differences were assessed by one-way ANOVA with Tukey's multiple comparison test; *=p<0.05, **=p<0.01, ***=p<0.001, ****=p<0.0001, n.s.=not significant, n.d.=not determined. n=3-8. g-i: Sample traces obtained with compound **[47]**. Note the desensitization in α1β1 (g) at 10 µM and 30 µM, increasingly limiting maximum current amplitudes.

C II.2.1.4 Mutational analysis supports the main site of action to be at the extracellular minus side of the β subunit

As Maldifassi *et al*.[140] proposed additional binding sites for pyrazoloquinolinones we were curious about the main site of action of our compounds. Therefore, we analyzed the three extracellular minus sides of the β isoforms using homology models based on the β3 homopentameric crystal structure (Figure 28).

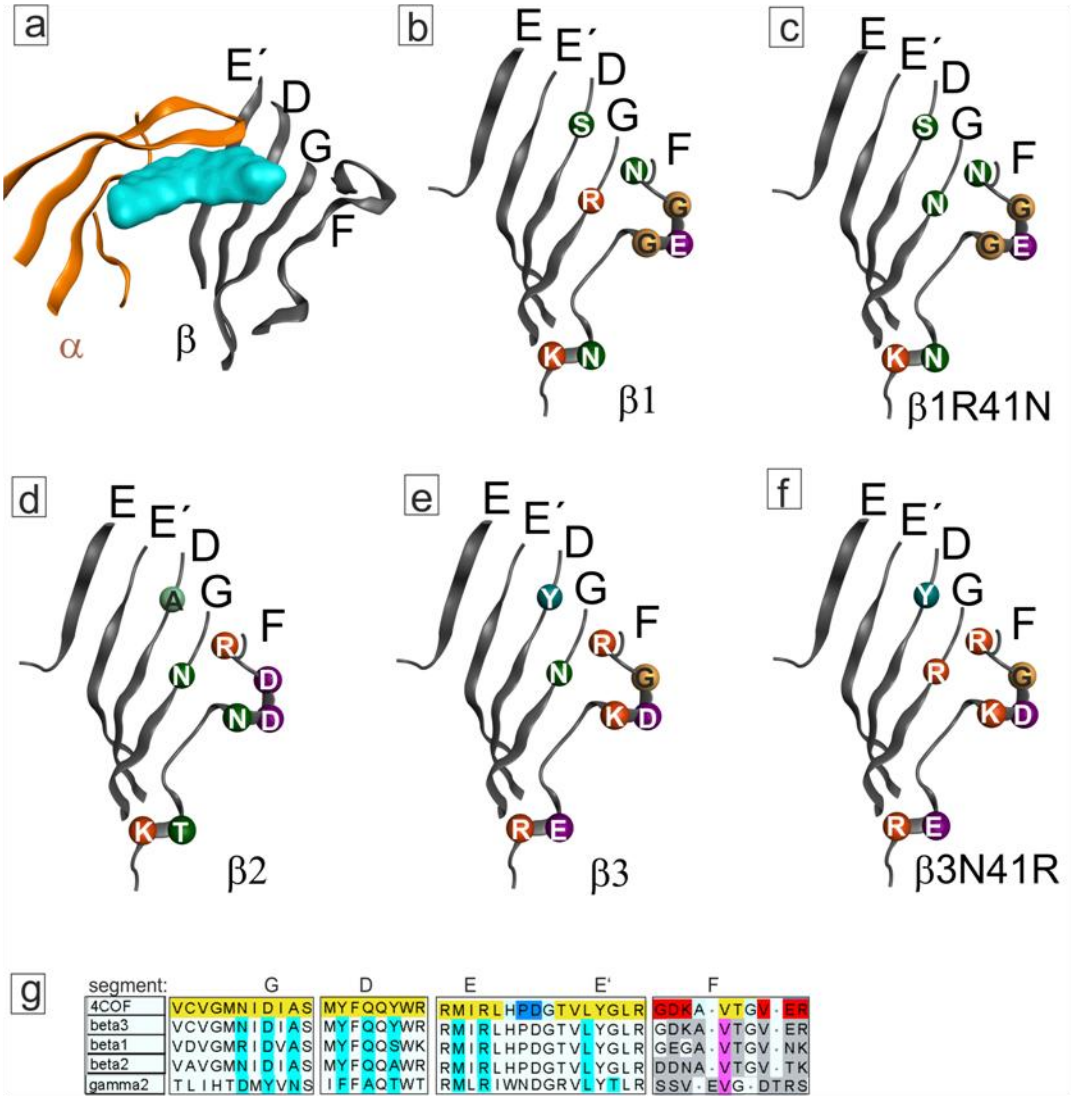

Figure 28: Homology models of the structural differences at the β- half pocket of the three β isoforms. a: View of the entire binding site at the extracellular α+ (light brown) β- (gray) with the predicted ligand occupied volume shown as cyan space filling surface. The amino acid at position 41 of loop G (β1, β3 counting of rat mature protein) is localized most central to the pocket among the variable amino acids. All other minus side amino acids are identical in all three isoforms. **b, d, e**: Minus sides of the three beta isoforms. Color coding of the amino acids is according to the ClustalX color scheme. **c, f**: Minus sides of the two mutants β1R41N and β3N41R. **g**: Alignment of segments ("loops") G, D, E and F of the three β- isoforms with the γ2 sequence and with the 4COF sequence to indicate homologous positions. Color code for 4COF: beta strands: yellow; helices: red; turns: blue. Color code for the subunit sequences: cyan indicates pocket forming positions, magenta indicates a structurally conserved position in "loop F", grey indicates structurally uncertain positions due to low homology.

According to these models the amino acids in position 41, namely β1R41 and β3N41, are most central in the pocket and close to the ligand occupied volume (Figure 28a, b and e). Thus, we decided to exchange these two amino acids which resulted in two engineered subunits possessing the point mutations β1R41N and β3N41R. These mutants should presumably show comparable properties from the parent subunit and additionally provide information about the main site of action.

Unfortunately, the binary α1β1R41N mutant displayed large holding currents suggesting spontaneous channel activity which is described for several point mutations in the literature[159,160] while the α1β3N41R mutant behaved similarly to the wild type α1βl (l=1,2,3) receptors.

We investigated all ligands in both mutant receptors. In α1β1R41N a complete loss of modulation for three ligands and for compounds **[47]** and **[75]** a severe reduction was observed (Table 2). Interestingly, compound **[46]** is reducing GABA induced currents. On the contrary, in α1β3N41R we observed modulatory effects for all six compounds. For compounds **[47]**, **[50]** and **[75]** a potency shift towards the parent wild type receptor α1β3 was noticed. Compounds **[46]** and **[74]** displayed a higher efficacy due to the introduced point mutation (Figure 29).

Table 2: EC_{50} and efficacy of compounds **[47]**, **[46]**, **[50]**, **[75]**, **[74]** and **[78]** at increasing concentrations in α1β1R41N receptors. Data are reported as mean ± SEM. Control current = 100% (GABA $EC_{3\text{-}5}$).

	[47]	**[46]**	**[50]**	**[75]**	**[74]**	**[78]**
EC_{50} [μM]	0.8	n.d.	n.d.	1.2	n.d.	n.d.
$LogEC_{50}$	-6.1±0.13	n.d.	n.d.	-5.9±0.23	n.d.	n.d.
% of control current at $EC_{3\text{-}5}$						
100 nM	80±10	70±5	70±1	80±10	95±20	75±10
300 nM	100±10	62±8	65±6	85±12	85±25	90±10
1 μM	140±16	62±8	85±7	110±20	100±30	90±15
3 μM	195±20	60±9	100±8	150±25	120±30	90±20
10 μM	205±20	60±10	125±5	180±45	155±40	70±10
30 μM	150±10	60±8	110±10	140±15	160±40	115±10
n	4	4	4	3	3	3

Interestingly, the interaction of the ligands with the α1β3N41R mutant receptor seems to be triggered by residue R'4. Compounds with the same R'4 substituent display similar trends, e.g. compounds **[47]** and **[75]** (R'4 = OCH_3) show a left potency shift towards the α1β1 wild type receptor, compounds **[46]** and **[74]** (R'4 = CH_3) show an increase in efficacy but no changes in potency, whereas compound **[50]** (R'4 = NH_2) showed an identical potency and compound **[78]** an identical efficacy like in the α1β1 receptor (Figure 29).

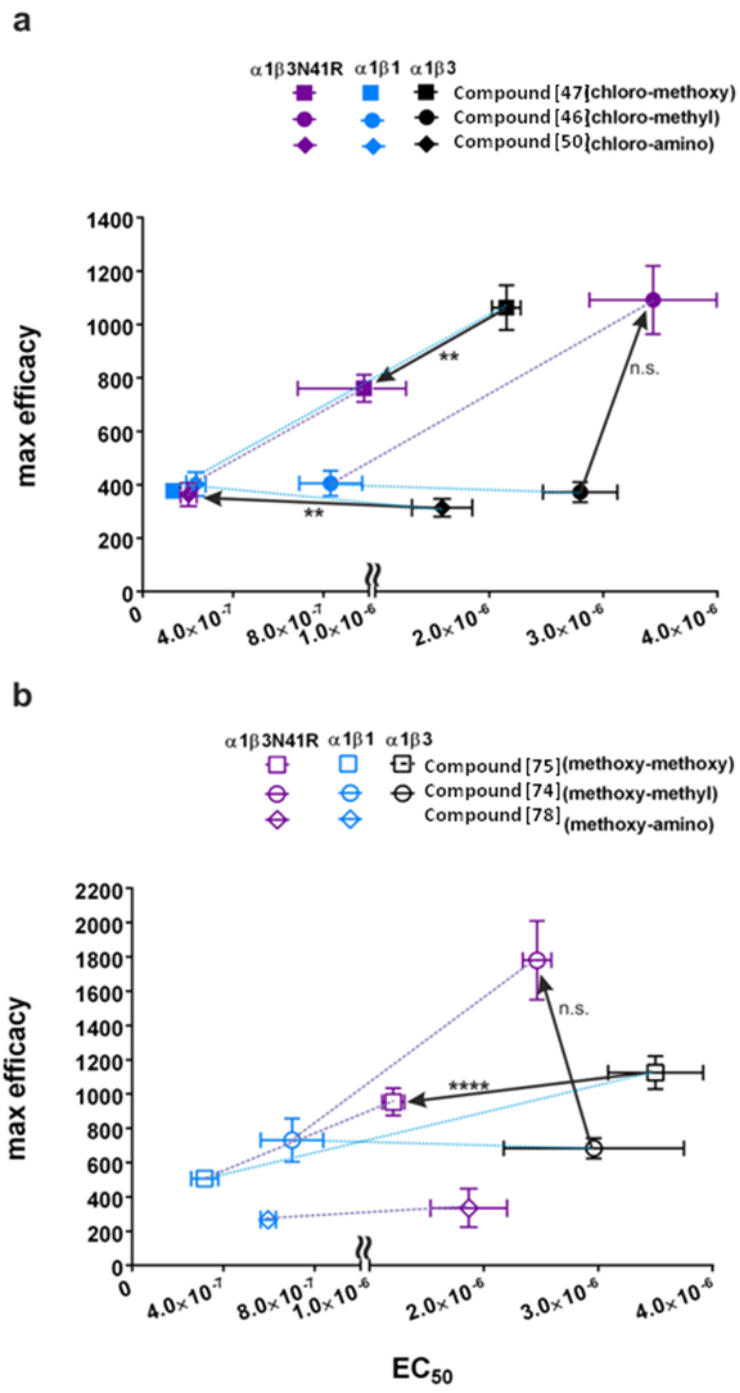

Figure 29: Comparison of EC_{50} and maximum efficacy among α1β1, α1β3 and α1β3N41R. a,b: The plots show the mean EC_{50} on the x-axis (note that the axis is broken to accommodate the range) and the mean maximum efficacy at 10 µM (% of control current at $EC_{3\text{-}5}$) on the y-axis (note the different scales on the two panels) of compounds **[47]**, **[46]**, **[50]**, **[75]**, **[74]** and **[78]**. The difference between wild type α1β3 and α1β3N41R is indicated with a black arrow, statistically significant EC_{50} differences are indicated. The potency differences between α1β3 and α1β3N41R for compounds **[47]**, **[50]** and **[75]** are statistically significant (**,**,****, respectively). Arrows pointing to the left show a decrease of the EC_{50} value between wild type and mutated receptors, which corresponds to an increase in potency. Simultaneously, changes in efficacy can be seen (arrows with upward or downward component indicating increase or decrease in maximum efficacy, respectively). The values obtained with wild type α1β3 and α1β1 receptors are connected with a blue dotted line. The dotted purple line visualizes the difference between α1β1 and α1β3N41R. EC_{50} values for the mutated receptors are 0.98 µM, 3.44 µM, 0.2 µM, 1.2 µM, 2.47 µM and 1.87 µM for compounds **[47]**, **[46]**, **[50]**, **[75]**, **[74]** and **[78]**, respectively. EC_{50} values were calculated for each individual experiment and are presented as mean ± SEM. Statistically significant differences were assessed by one-way ANOVA with Tukey's multiple comparison test. Note that the EC_{50} value of compound **[78]** in α1β3 receptors is not depicted, since this compound has nearly no efficacy in this receptor subtype. Bars indicate mean ± SEM, n=3-8.

In conclusion, these results demonstrate that position 41 of the minus side of segment G in $\alpha1\beta1$ and $\alpha1\beta3$ receptors strongly influences on potency and efficacy of our ligands, thus supporting the hypothesis of the main site of action to be at the extracellular $\alpha+/\beta-$ interface.

C II.2.1.5 The investigated compounds show limited α selectivity

After identifying the β selectivity profile and the main site of action of our compounds we were interested in the α selectivity profile. We investigated the three chloro substituted compounds **[47]**, **[46]** and **[50]** since all of them possess a higher potency compared to their methoxy analogous. To assess for the α selectivity profile we chose αkβ3γ2 (k = 1-6) subtypes due to a robust expression.

Table 3: Impact of α isoform on potency of compound [47], [46] and [50]. EC_{50} of R^8 = Cl compound **[47]** (PZ-II-028), **[46]** (LAU156) and **[50]** (LAU206) are shown. Compound **[47]** modulates all receptors in a range of 0.6 – 3.3 µM. Compound **[46]** modulates all receptors, EC_{50} ranges from 4 µM to 13 µM, where in α6β3γ2 the EC_{50} value could not be obtained as saturation was not reached. Compound **[50]** has moderate modulatory effects in α1- and α3β3γ2 receptors with an EC_{50} at ~ 1 µM and in α6β3γ2 with an EC_{50} of ~ 2 µM. Due to the extremely low efficacy in α2-, α4- and α5β3γ2, these EC_{50} values could not be obtained; (n.d.=not determined).

	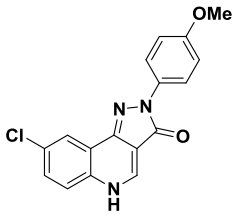 [47]	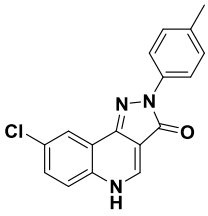 [46]	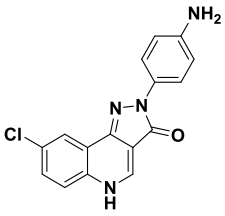 [50]
		EC_{50} [µM]	
α1β3γ2	1.8	4.4	1.2
α2β3γ2	2.2	5.5	n.d.
α3β3γ2	1.5	7.2	1.2
α4β3γ2	0.9	13.4	n.d.
α5β3γ2	0.6	6.4	n.d.
α6β3γ2	3.3	>5	2.3

EC_{50} values of compounds **[47]** and **[50]** are in a range of 0.6 to 3.3 µM whereas compound **[46]** shows potencies up to 13.4 µM. However, the influence of the α subunit seems to be rather limited. Combining these results with the outcome of the β selectivity profiling, compound **[47]** constitutes the most potent ligand at the α1+/β1− site.

C II.2.1.6 The δ or the γ1 subunits have no impact on compound [47] potency for the α1+/β1− site

Based on these results we were wondering how a third subunit influences the potency of compound **[47]**, since previously published data showed only little impact of a γ2 subunit. Thus, we examined compound **[47]** in α1β1γ1 and α1β1δ receptor subtypes (Figure 30). As shown in Figure 30 potency and efficacy of compound **[47]** are rather poorly influenced by either a γ1 or a δ subunit.

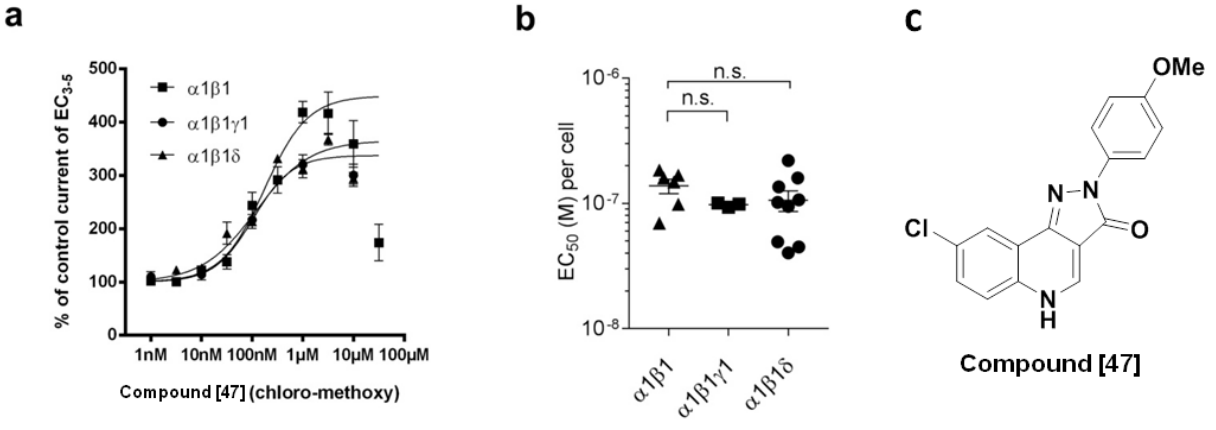

Figure 30: Compound [47] modulates GABA-evoked currents in α1β1, α1β1γ1 and α1β1δ receptors with similar potencies. a: Concentration-dependent modulation of GABA EC_{3-5} current at α1β1, α1β1γ1 and α1β1δ. Data represent means ± SEM (n=3-10). **b**: EC_{50} values were calculated for each individual experiment and are presented as mean ± SEM. One-Way ANOVA was used for multiple comparisons followed by a *Tukey post hoc* test and showed no significant differences between the mean EC_{50} values for each subtype. c: Chemical structure of compound **[47]**.

C II.2.1.7 A derivative of compound [47] that lacks affinity for the benzodiazepine binding site also modulates α1β1 containing receptors

Many R^8 and R'^4 substituted pyrazoloquinolinones are mostly silent high affinity binders for the benzodiazepine binding site at αk+/γ2− (k = 1,2,3 and 5) interfaces even though the main modulatory effect is elicited *via* the α+/β− interfaces. Therefore, we performed flunitrazepam displacement assays at the α1+/γ2− site using cerebellar membrane preparations from rat brains. Unfortunately, according to these results all six compounds are also high affinity binders at the major α1+/γ2− BZ site (Table 4). Nevertheless, we previously reported about a R^6 substituted pyrazoloquinolinone with decreased BZ site affinity and retained α+/β− modulatory effects.[146] Thus, we synthesized compound **[138]** which represents a merged version of compound **[47]** and the previously published compound (Figure 31).

LAU462

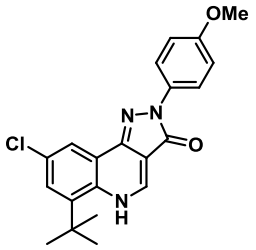

R^8 = Cl, R^6 = *t*Bu, R'^4 = OMe
chloro-*t*Bu-methoxy [138]

Figure 31: Chemical structure of **[138]**.

Table 4: K_i values of compounds **[47]**, **[46]**, **[50]**, **[75]**, **[74]**, **[78]** and **[138]** determined by displacement of [^{3}H]flunitrazepam binding to rat cerebellar membranes (mean ± SEM, n = 3-4).

R^6	R^4	R^8 = Cl			R^8 = OCH_3		
		cpd	K_i [nM]	(n)	cpd	K_i [nM]	(n)
H	OMe	**[47]**	0.06 ± 0.02	(3)	**[75]**	0.07 ± 0.007	(4)
H	Me	**[46]**	0.05 ± 0.001	(3)	**[74]**	0.05 ± 0.002	(3)
H	NH_2	**[50]**	0.12 ± 0.03	(3)	**[78]**	1.00 ± 0.08	(3)
*t*Bu	OMe	**[138]**	n.d.>100 **µM**	(3)	-	-	-

In fact, compound **[138]** showed a reduced affinity for the benzodiazepine binding site (Table 4). Therefore, we next examined the compound in $\alpha1\beta1$, $\alpha1\beta1\gamma1$ and $\alpha1\beta1\delta$ receptor subtypes.

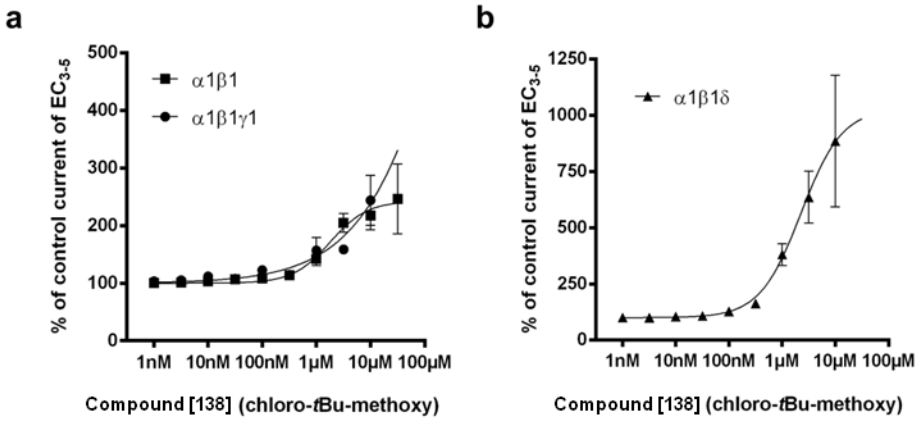

Figure 32: Compound [138] modulates GABA-evoked currents in α1β1, α1β1γ1 and α1β1δ receptors. a,**b**: Concentration-dependent modulation of GABA EC_{3-5} current at α1β1, α1β1γ1 and α1β1δ receptors. Data represent means ± SEM (n=4-17).

Remarkably, it displayed modulatory effects comparable to the parent compound **[47]** (efficacies at 10 µM in $\alpha1\beta1$ ~400% and in $\alpha1\beta1\gamma1$ ~300% at EC_{3-5}), but with an almost twenty-fold potency loss. On the other hand, it exerted a higher efficacy in $\alpha\beta1\beta\delta$ receptors compared to compound **[47]**. Considerably, there is a divergent impact of the *tert*-butyl residue in position R^6 concerning the binding at the $\alpha+/\gamma-$ vs the $\alpha+/\beta-$ interfaces. However, due to its exclusive selectivity and its useful potency, compound **[138]** represents the first proof of concept compound towards highly selective ligands for the $\alpha1+/\beta1-$.

C II.2.1.8 Discussion

In conclusion, we identified a set of six β1 preferring pyrazoloquinolnones which differ in positions R^8 and R'^4. Among them compound **[47]** possesses the highest potency for any α+/β− interface and thus represents an important starting point for the exploration of β1 specific high affinity ligands while showing a rather unselective behavior with respect to the principal α subunit.

As shown in Figure 28 all β isoforms contribute different amino acid residues to the putative pyrazoloquinolinone binding site at the extracellular α+/β− interface, which results in a theoretical opportunity to design selective ligands also for the β2 and β3 isoforms. In this context future libraries are needed to explore ligand features that are required for high potency with respect to the certain β isoform. This can be seen when we compare the potency rank orders between different receptor subtypes: The potency rank order for the α1+/β3− interface is depending on the polarity of the substituent in position R'^4 which results in a rank order of **[50]**>**[47]**>**[46]** as previously shown.[146] In this study the same rank order is observed in α1β2 receptors whereas in α1β1 receptors the rank order for the R^8 = Cl series is **[47]**>**[50]**>**[46]**.

Our six pyrazoloquinolinones are not the first known β1 preferring allosteric modulators. For instance, the partial negative modulator salicylidene salicylhydrazide (SCS) has been used successfully in various functional and biological assays for the detection of β1 containing receptors.[156] It possesses a very high potency but the binding site is still unknown even though it is assumed to be located in the transmembrane domain. Another class of compounds preferring β1 containing receptor subtypes are the fragrant dioxane derivatives (FDDs) which possess a quite low potency (most potent FDD EC_{50} = 2500 nM vs EC_{50} = 130 nM of compound **[47]**) and the binding site is also unknown.[155] Thus, pyrazoloquinolinones represent a more interesting lead towards β1 selective allosteric modulators due to their known binding site and their biologically useful potency.

Future improvements of pyrazoloquinolinones will focus particularly on the ligand features which drive the affinity towards α+/β1− while reducing the affinity for α+/γ2−. Additionally, a long term goal is to convert the pyrazoloquinolinones into radioligands which can be used for specific detection and quantification of β1-containing receptor subtypes. In this context four of the presented PQs (compounds **[47]**, **[75]**, **[74]**, **[78]** and **[138]**) enable an easy access for isotopic labeling due to their methoxy group where a [$^{11}CH_3$] could be introduced in the last stage of the synthesis using the correspondig phenols as starting material. Moreover, tritiation of nitrogen containing heterocycles was described by Gröll *et al*. which could be applied to all presented compounds in this study.[161]

The potential range of application for such selective tool compounds is huge. For instance, Sergeeva *et al*. reported that there is no evidence for the expression of $\beta 1$ subunits in cerebellar Purkinje cells whereas Kelley *et al*. presented evidence in favor.[155,162] Here, specific tool compounds interacting with $\alpha+/\beta 1-$ interfaces would represent another approach to investigate this controversially discussed topic further by e.g. radioligand assays or autoradiographic studies. In addition, pyrazoloquinolinones are particularly suitable for *in vivo* used tool compounds (e.g. PET ligands) due to their low level of toxicity and their decent bio-availability.[163]

C II.2.2 Towards β1 efficacy selectivity

By analyzing the dose-response curves in Figure 27 a trend towards β1 efficacy selectivity in binary αβ $GABA_A$ receptors was observed. This trend correlates with the chemical entity in position R'^4 and seems to be only weakly affected by the substituent in position R^8. Considering position R'^4, in α1β1 receptors the methoxy (H-bond acceptor) and the methyl (hydrophobic) substitutent displayed a weaker or equally strong modulation compared to the modulation in α1β2 and α1β3 receptors (Figure 27). Interestingly, the amino group (H-bond donor) exerted a stronger modulation in α1β1 receptors compared to the modulation in α1β2 and α1β3 receptors (Figure 27). Based on these considerations we aimed to examine two different approaches.

In the first approach we investigated the change of the substituents from the *para* (R'^4) to the *meta* position (R'^3). Here, we chose the substituent which showed the best efficacy selectivity effects of their analogues in the position R'^4, namely the amino substituent (Figure 27). Thus, we investigated compounds **[57]** and **[85]** in binary αβ receptors (for synthesis see chapter C I.1.2). Remarkably, we observed a pronounced efficacy (~400-600% at GABA EC_{3-5}) as well as potency selectivity for both compounds (Figure 33). Compound **[85]** even lacked any modulatory effects in α1β2/3 $GABA_A$ receptors (Figure 33b). This behavior we observed already for its para analogue but with half of the efficacy (~300%, see Figure 27f). Obviously, the methoxy substituent in position R^8 beneficially influences the selectivity for β1 containing α1β receptors by inducing silent modulation in α1β2/3 receptors. These are very promising results which should be further investigated.

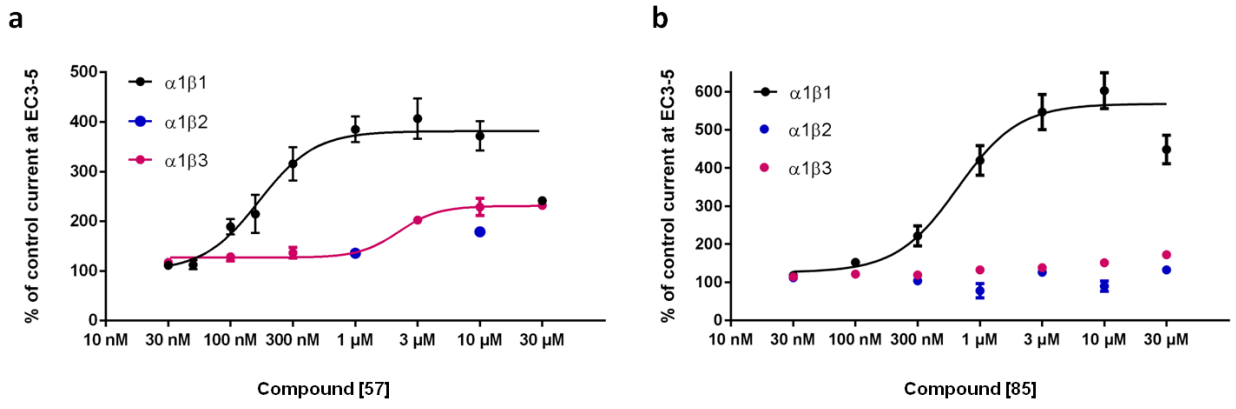

Figure 33: Preliminary dose-response curves of **[57]** and **[85]** in α1β1,2,3 $GABA_A$ receptors.

In the second approach we followed up on the observation that the efficacy is presumably triggered by the H-bond donor/acceptor functionality of the substituent in position R'[4]. Hence, we synthesized a "2nd generation" of pyrazoloquinolinones possessing different H-bond donor and acceptor groups in this position. We decided to introduce an acyl group as H-bond acceptor, a hydroxyl group as another H-bond donor and an amide group which possesses both functionalities. Synthetically, the hydroxyl derivative and the amide were easily accessible *via* compounds **[47]** and **[50]**. Demethylation of compound **[47]** using ethanthiol yielded compound **[139]** in 73% and acetylation of compound **[50]** using DMAP and acetic anhydride led to the desired compound **[140]** in 62% yield (Scheme 10).

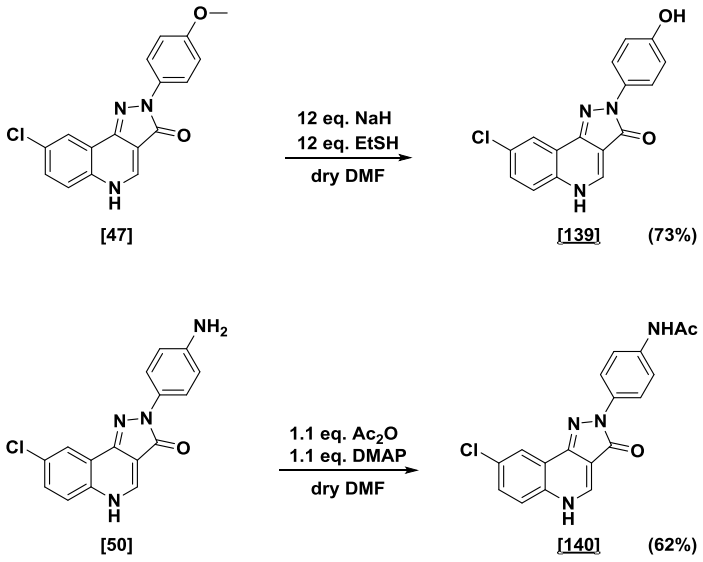

Scheme 10: Synthesis of compounds **[139]** and **[140]**.

Due to the poor solubility of the pyrazoloquinolinones we chose a rather long synthetic route to obtain the acyl compound. First, we synthesized the R'[4] = bromo derivative **[141]** according to the general synthetic route of PQs (C I.1.2). Next, the TMS protected acetylene was introduced by a copper free Sonogashira coupling reaction which gave product **[142]** in acceptable yields. Interestingly, under classical Sonogashira conditions using copper and palladium catalyst, no conversion was observed (Scheme 11). Deprotection with K_2CO_3 led to acetylene compound **[143]**. For the hydration of the alkyne we looked specifically for procedures including either DMSO, DMF or alcoholic solutions as reaction medium due to the poor solubility of our starting material **[143]**. First, we tried a gold catalyzed procedure using 5 mol % $AuCl_3$ with 4 eq. H_2O in methanol which was reported by Das *et al*.[164] However, we observed only a very low conversion of the starting material and no formation of the desired product **[144]**. Next, we used conditions reported by Liu and coworkers who established a mild protocol using CF_3SO_3H as catalyst for the Markovnikov-type addition of water to the terminal alkyne at room temperature.[165]

Further, they reported to heat the reaction to 70 °C for alkynes which are hard to hydrate. Thus, we converted starting material **[143]** under these conditions and were able to isolate the desired product **[144]** in at least 20% yield (Scheme 11).

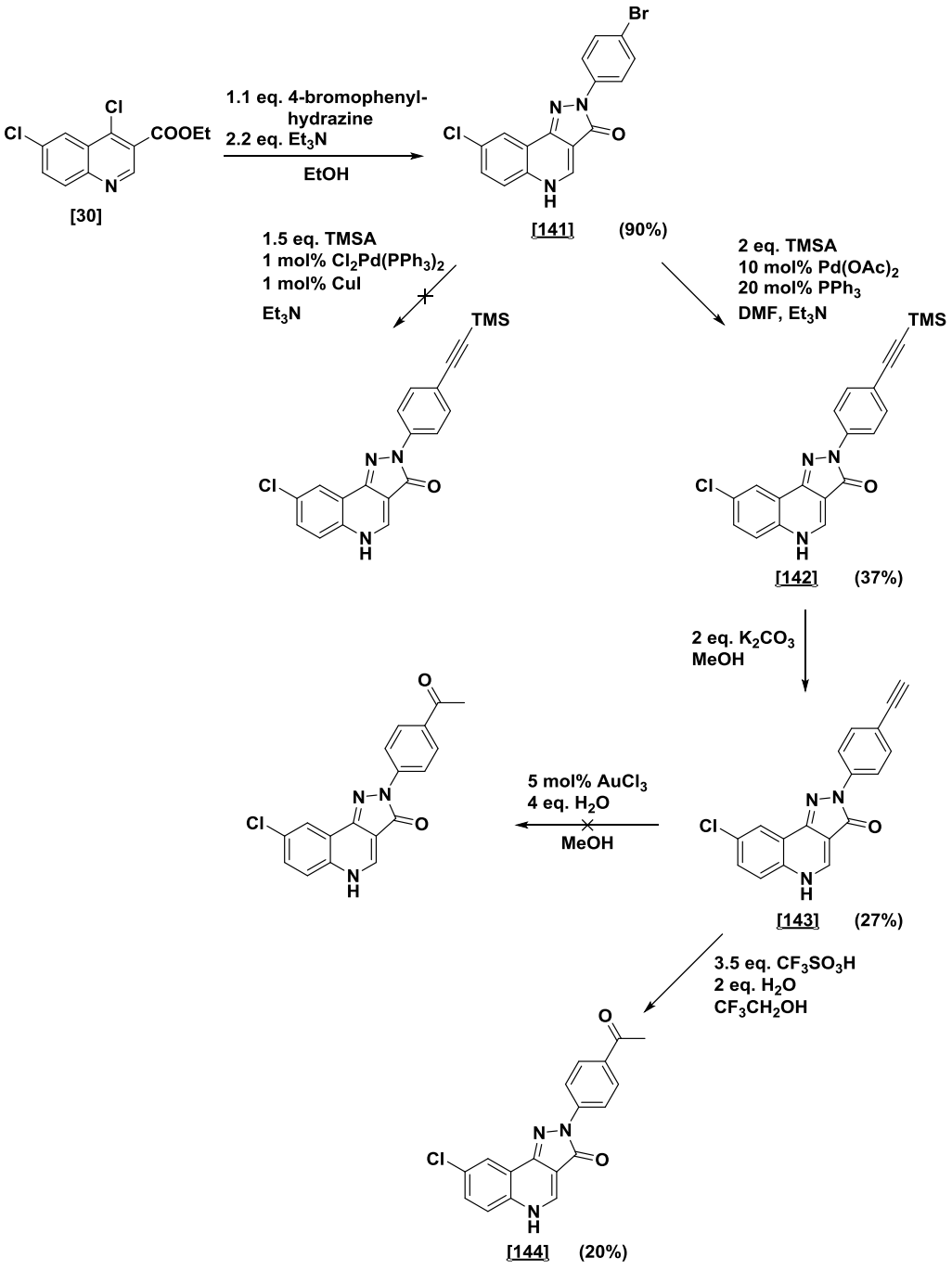

Scheme 11: Synthetic route to the acyl compound **[144]**.

The first preliminary data were measured in $\alpha1\beta1\gamma1$ $GABA_A$ receptors, since they express more robustly than the binary $\alpha1\beta1$ receptor subtypes. While the new compounds with the H-bond acceptor **[144]** and H-bond donor groups **[139]** are rather modulatory silent, compound **[140]** displayed a very strong positive modulatory effect of ~800% at $EC_{3\text{-}5}$ in $\alpha1\beta1\gamma1$ $GABA_A$ receptors (Figure 34a). Intrigued by this finding we measured **[140]** in $\alpha1\beta3\gamma1$ receptors to figure out if we see a comparable selectivity in ternary $\alpha\beta\gamma1$ receptors compared to binary $\alpha\beta$ receptors (Figure 34b). Regrettably, the obtained data so far is too ambiguous to draw significant conclusions and additional experiments and eventual further structure refinement is required. However, presumably there is a significantly weaker modulation in $\alpha1\beta3\gamma1$ receptors.

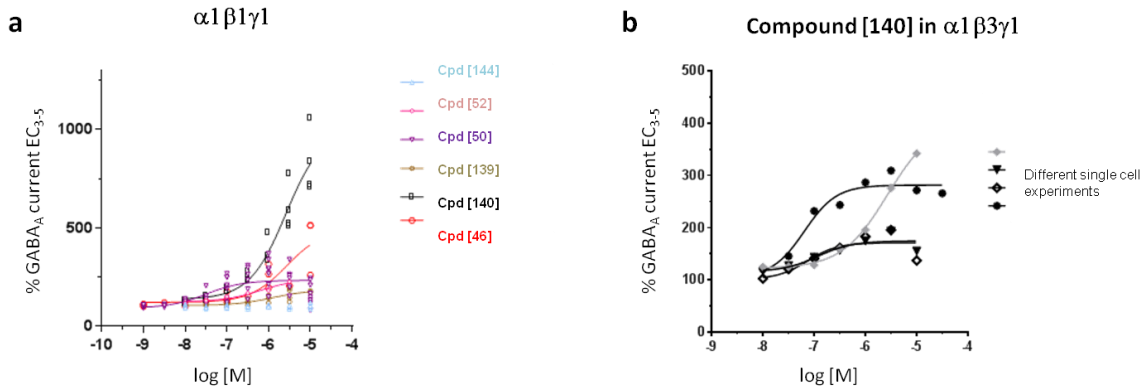

Figure 34: Modulation of GABA currents at $EC_{3\text{-}5}$ in ternary αβγ1 receptors. a: Dose-response curves of a variety of compounds with different substituent in position R'[4] in $\alpha1\beta1\gamma1$ $GABA_A$ receptors**. b:** Preliminary single cell experiments of **[140]** in $\alpha1\beta3\gamma1$ receptors.

In summary, even though we are looking at preliminary data, we observed compounds with promising efficacy selectivity profiles for $\beta1$ containing $GABA_A$ receptors. Based on these first data we are even able to extract information with respect to their structure-activity relationship (SAR). A comparison of the data between the R^8 = methoxy and the R^8 = chloro series of Figure 27 and Figure 33 indicates that the methoxy series, especially with amino substituents, shows an improved selectivity for $\alpha1\beta1$ receptors compared to the chloro series even independently of the substituent in positions R'[3] or R'[4]. While the compound with the amino group in position R'[4] possesses a rather low positive modulation (~300% at GABA $EC_{3\text{-}5}$) the compound with the amino group in position R'[3] displays double the efficacy (~600% at GABA $EC_{3\text{-}5}$). In addition, **[140]** showed strong positive modulatory effects in $\alpha1\beta1\gamma1$ receptors and seems to be a very weak positive modulator in $\alpha1\beta3\gamma1$ receptors. Thus, the acetylation of the amino group might induce desired properties as well. Combining these observations we suggest a ligand design of R^8 = methoxy and R'[3] = acetyl **[145]** to be very auspicious. Nevertheless, to get a broader understanding the synthesis of the analogues **[146]** and **[147]** seems to be reasonable (Figure 35).

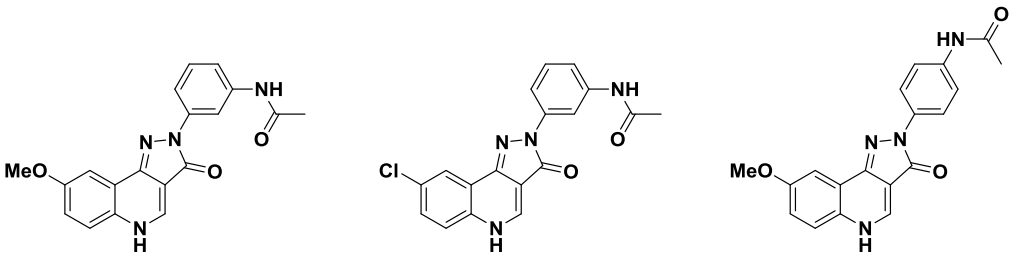

Figure 35: Putative efficacy selective compounds.

C II.2.3 Exploring α6β3γ2 subtype selectivity – Part I

C II.2.3.1 Impact of R^8 = chloro and of variations in the position of ring D methoxy substitution on $GABA_AR$ subtype modulatory profile

In previous studies we were able to identify CGS9895 **[XXXVII]** as α6 preferring compound by screening all αkβ3γ2 (k=1-6) subunit combinations.[83] Interestinlgy, the introduction of a chloro residue in position R^8 (**[47]**) resulted in a three-fold enhancement of modulation in all tested receptor subtypes by preserving the modulation differences among the different subunit combinations (Figure 37b). Based on these data we explored the *ortho*-, *meta*- and *para*-position of the ring D.

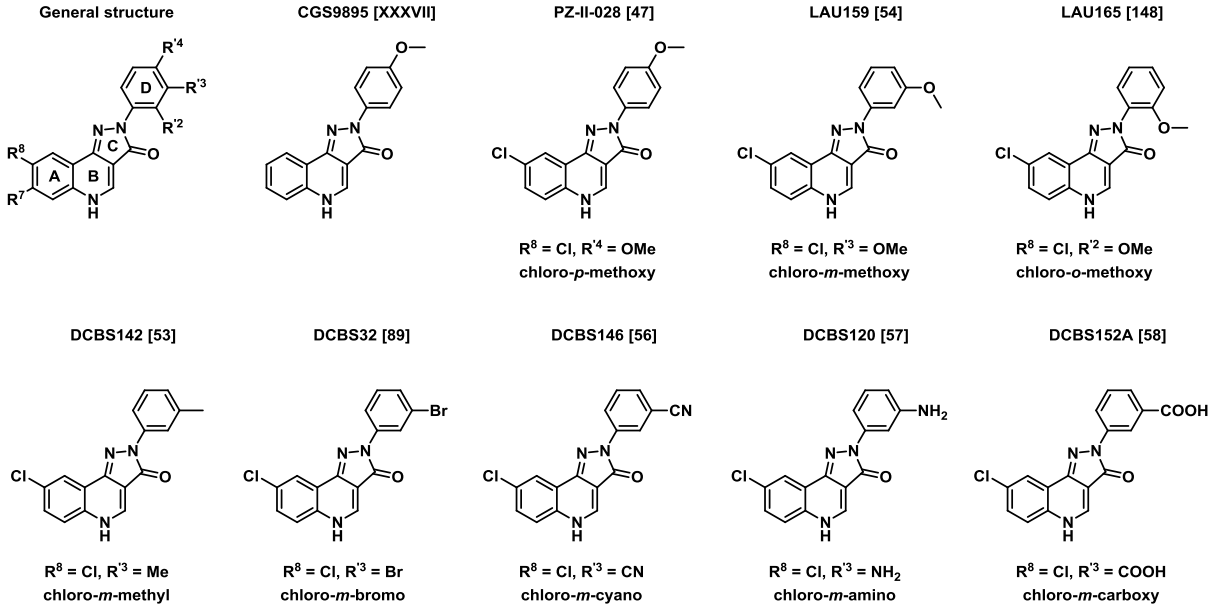

Figure 36: Pyrazoloquinolinone (PQ) structures. Top left: PQ scaffold with labels for rings A to D and residue numbering (R^7 and R^8 on ring A; R'^2 (*o*), R'^3 (*m*), R'^4 (*p*) on ring D). Top row: 1 is a *p*-methoxy compound with unsubstituted ring A. R^8 = chloro compounds are derived from varying the position of the methoxy group at ring D. Bottom row: Compound variants with different residues in R'^3 *m*-position. Thesis numbering: **[XXXVII]**, **[47]**, **[54]**, **[148]**, **[53]**, **[89]**, **[56]**, **[57]** and **[58]**.

Intriguingly, the change of the methoxy residue in the *meta*-position led to a highly efficacy selective α6β3γ2 compound **[54]** where the efficacies in αkβ3γ2 (k=1-5) are mostly abolished (Figure 37c). Even though compound **[54]** is not acting as positive modulator in α1β3γ2 subtypes, it still binds to the modulatory PQ site since we were able to reduce modulatory effects of **[47]** at 10 and 30 µM in this receptor subtype (Figure 37f). Thus, compound **[54]** is a null modulator in this subtype. The change of the methoxy group to the *ortho*-position **[148]** led to an abolishment of any PAM activity, while in α5β3γ2 a weak NAM activity could be observed (Figure 37d).

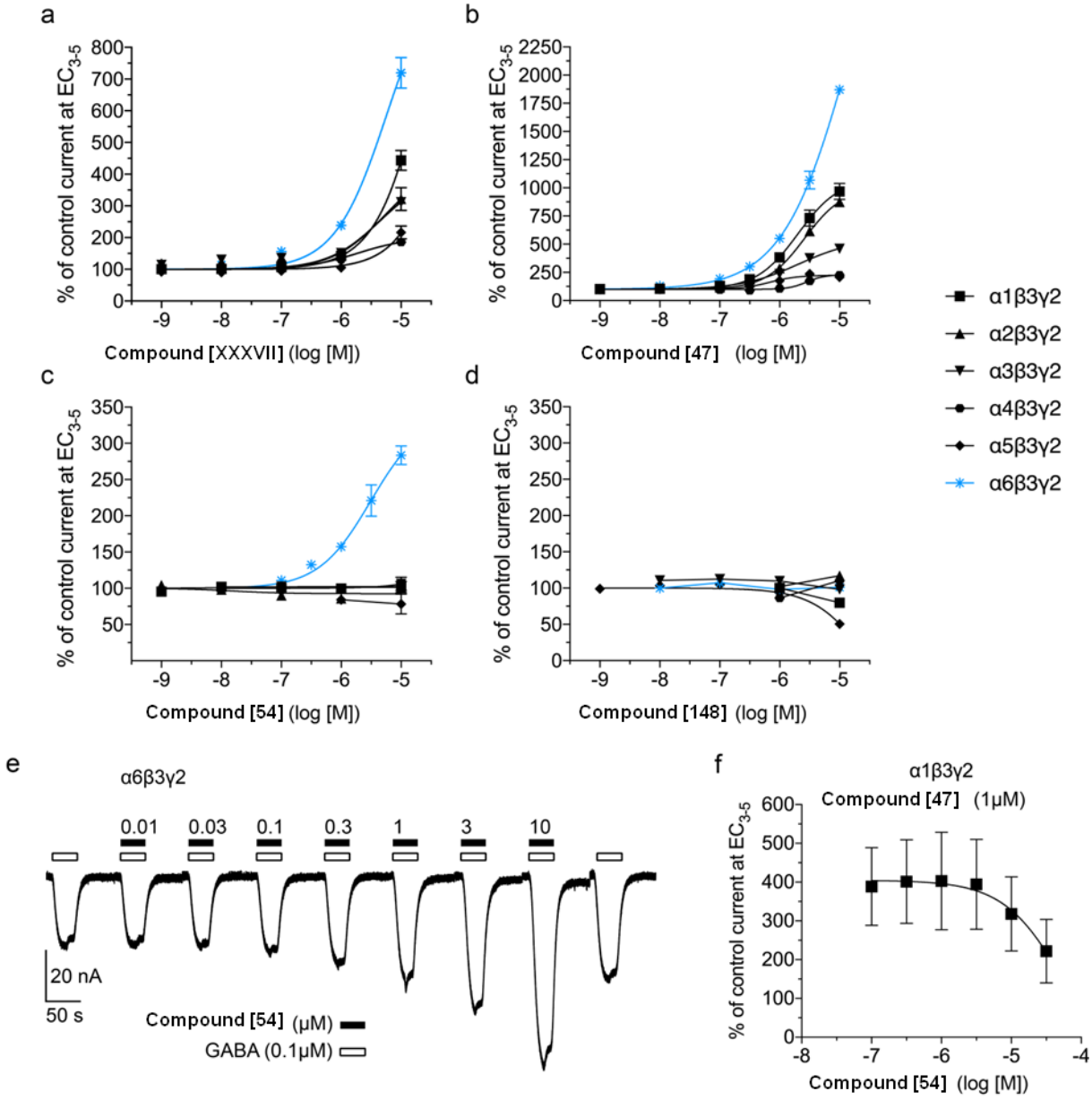

Figure 37: (a-d) $GABA_AR$ subtype activity profile of compounds with systematically varying position of the methoxy-group on ring D (compound [XXXVII], compound [47]: *p*-methoxy; compound [54]: *m*-methoxy; compound [148]: *o*-methoxy) at αxβ3γ2 (x=1-6) $GABA_A$ receptors. Y-axis shows % modulation of currents elicited by a GABA concentration amounting to 3-5% of maximum GABA currents per cell. For the purpose of structure-activity comparison, some datasets are reproduced: compound **[XXXVII]** at αxβ3γ2 (x=1,2,3 and 5) reproduced with permission (Ramerstorfer et al., 2011). Compound **[47]** at αxβ3γ2 (x=1-6) reproduced with permission (Varagic et al., 2013a). (e) Sample recording of GABA currents and co-application of increasing concentrations of compound **[54]**, from an oocyte injected with α6β3γ2 subunits. (f) Co-application of compound **[54]** (10 and 30 μM) can inhibit positive GABA current modulation by 1 μM of compound **[47]**.

C II.2.3.2 Compound [148] does not bind at the α6+/β3− interface

The lack of modulation of compound **[148]** in α6β3γ2 receptors (Figure 37d) could either be based on silent binding or non-binding of our compound to the α6+/β3− modulatory PQ site. Since binding assays cannot be made for the α+/β− site due to missing high affinity radioligands we thus tried to inhibit the modulatory effect of compound **[54]** by co-application

of compound **[148]**. As shown in Figure 38 the modulatory effects of compound **[54]** remained unaffected upon co-application of compound **[148]** and thus compound **[148]** seems to be a non-binder at the $\alpha 6+/\beta 3-$ interface (Figure 38).

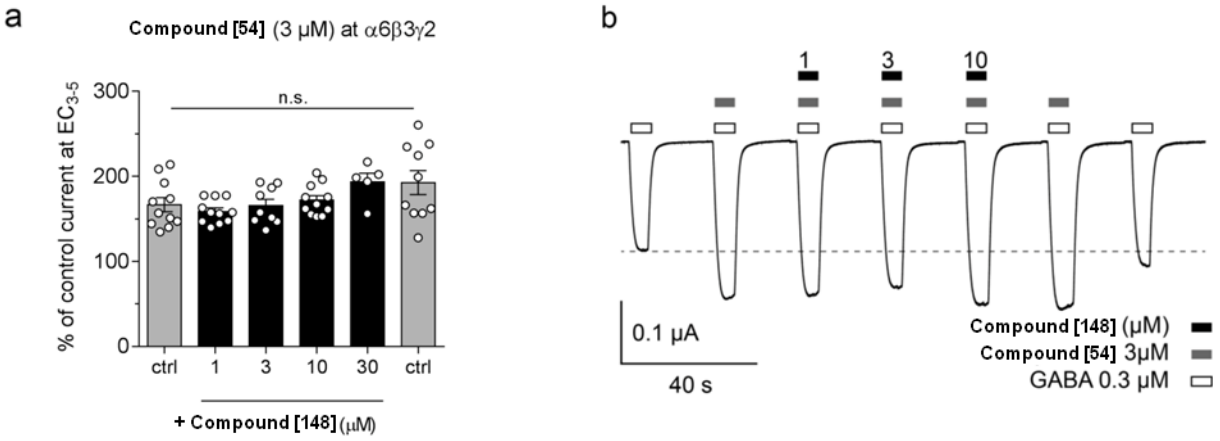

Figure 38: Compound [148] is unable to block modulatory effects of compound [54] at α6β3γ2. (a) Modulation by compound **[54]** (3 µM) is unaffected by co-application of compound **[148]** (n.s.=not significant; n=9; p>0.05 all groups vs. control before, one-way ANOVA with Dunnett's multiple comparison test). (b) Sample recording of one oocyte sequentially exposed to 3 µM of compound **[54]** + increasing concentrations of compound **[148]** (one experiment from data presented in a).

The biological inactivity of compound **[148]** prompted us to investigate the role of the methoxy residue in *ortho*-position and how this could interfere with the biological activity. Since the biological effect of a compound may not always arise from only one conformation (e.g. energetic global minimum) but rather from an ensemble of conformations we made a conformational analysis using MOE (Molecular Operating Environment). Due to the inflexibility of the pyrazoloquinolinones we set our focus on the dihedral angle (φ) between the two plane surfaces of the rings A-C and ring D (Figure 39).

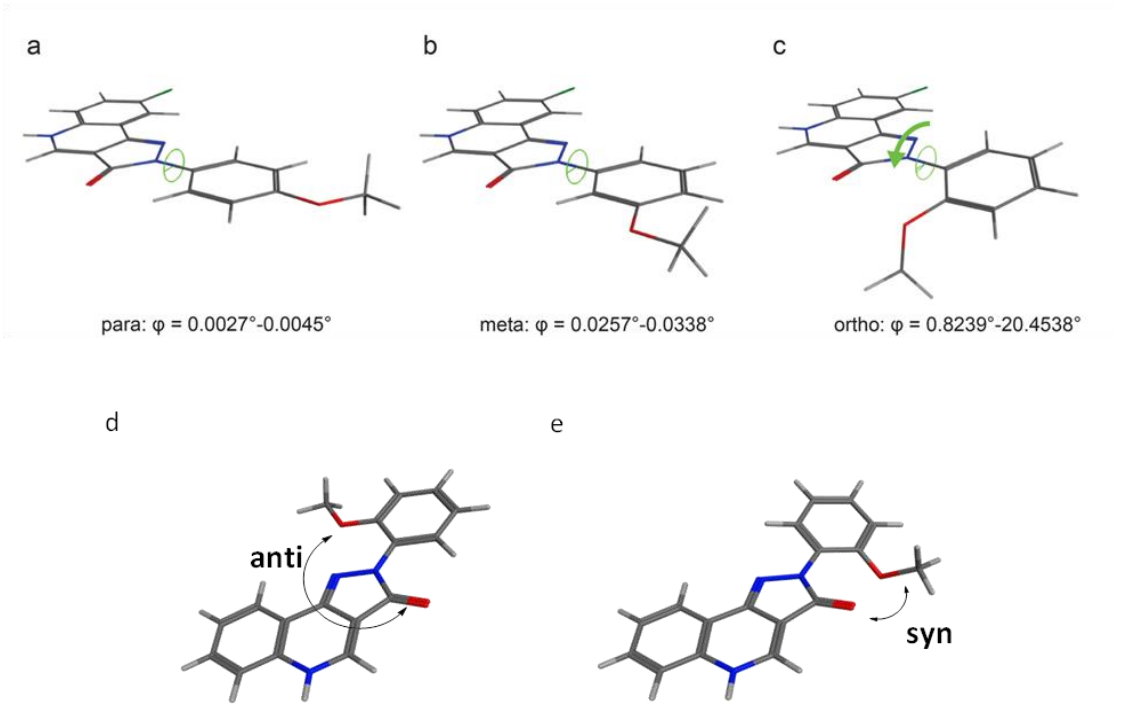

Figure 39: Conformational analysis of compounds [47] (a), [54] (b) and [148] (c). Position of the methoxy substituent on ring D influences the dihedral angle φ between the planes of rings A-C and ring D. Methoxy substitution in *o*-position rotates ring D by up to ~20° (green arrow); Anti (d) and syn (b) conformation of compound **[148]**. The steric hindrance in the syn conformation leads to a strong rotation of ring D up to φ=~20°. Furthermore, the anti conformation shows a 20 to 200 times stronger tilt (φ=~0.85°) compared to the *m*- and *p*-substituted compounds (φ=~0.003° and φ=~0.03°), namely compounds **[54]** and **[47]**.

Accodring to this analysis the *ortho* substituted compound **[148]** features two possible conformations (syn and anti, Figure 39d,e) while the *para*- and *meta*- substitution only lead to one main conformation which shows co-planarity between rings A-C and ring D (φ=~0.003° and φ=~0.03°, Figure 39a,b). In case of compound **[148]** the anti conformation displays a 20 to 200 times stronger rotation between the plane surfaces and the syn conformation even induces a severe rotation of the ring D up to a dihedral angle of 20° (Figure 39). Based on these results the rotation of the ring D might be a reasonable explanation of the inactivity of compound **[148]**.

Table 5: K_i values of compounds [47], [54] and [148]. The values were determined by displacement of [^{3}H]flunitrazepam (α1+/γ2-; K_D = 4.8 ± 0.3 nM (n=3)) and [^{3}H]Ro15-4513 in the presence of 50 mM diazepam (α6+/γ2-; K_D = 1.4 ± 0.1 nM (n=3)) binding to rat cerebellar membranes (mean ± SEM).

Compound	K_i [nM] α1+/γ2–	(n)	K_i [nM] α6+/γ2–	(n)
[47]	0.018 ± 0.004	3	0.55 ± 0.04	3
[54]	0.17 ± 0.007	4	15.4 ± 0.2	4
[148]	7.8 ± 0.6	4	329 ± 76	3

Since pyrazoloquinolinones are known to bind with high affinity to the benzodiazepine binding site[83] we were next interested how our compounds **[47]**, **[54]** and **[148]** interact with the BZ-site. Thus, we performed radioligand displacement assays in rat cerecellar membranes to determine their affinities in α1+/γ2– and α6+/γ2– sites (Table 5).

The results show that the tested compounds are high to very high affinity binders at the α1+/γ2– BZ-site and moderate to high affinity binders at the diazepam-insensitive α6+/γ2– BZ-site. Furthermore, we observed a decrease of affinity when changing the substituent from the *p*- to the *o*-position in α1+/γ2– as well as in α6+/γ2–. Interestingly, even though compound **[148]** possesses the lowest affinities in α1+/γ2– and in α6+/γ2–, the effect of the distorted ring D is not as significant as at the α+/β– site.

C II.2.3.3 R_8 = chloro compounds with varying *m*-substituents on ring D display distinct efficacy profiles

The interesting selectivity of the *meta* methoxy compound **[54]** for $\alpha6\beta3\gamma2$ receptor subtypes prompted us to synthesize compounds with different substituents at the position R'^3 and investigate their modulation at $\alpha6\beta3\gamma2$ receptors (Figure 36, bottom row). Compounds **[53]** and **[58]** showed comparable or higher modulation at 1 µM concentration in this receptor subtype compared to compound **[54]** (Figure 37c and Figure 40a). Thus, we screened for their α-selectivity profile (Figure 40b,c). However, both compounds did not show an improved selectivity profile compared to compound **[54]**. A quantification of the selectivity of $\alpha6\beta3\gamma2$ over $\alpha1\beta3\gamma2$ is shown in Figure 40d at 10 µM. While the subtype profile of compound **[53]** is comparable to compound **[XXXVII]**, the profile of compound **[58]** displayed bi-directional modulatory effects. In $\alpha6\beta3\gamma2$ subtypes it is a positive modulator whereas in $\alpha1\beta3\gamma2$ it possesses negative modulatory effects (Figure 40c). Furthermore, the modulatory effects of compound **[53]** and **[58]** are independent of the presence of a $\gamma2$ subunit as shown in Figure 40e.

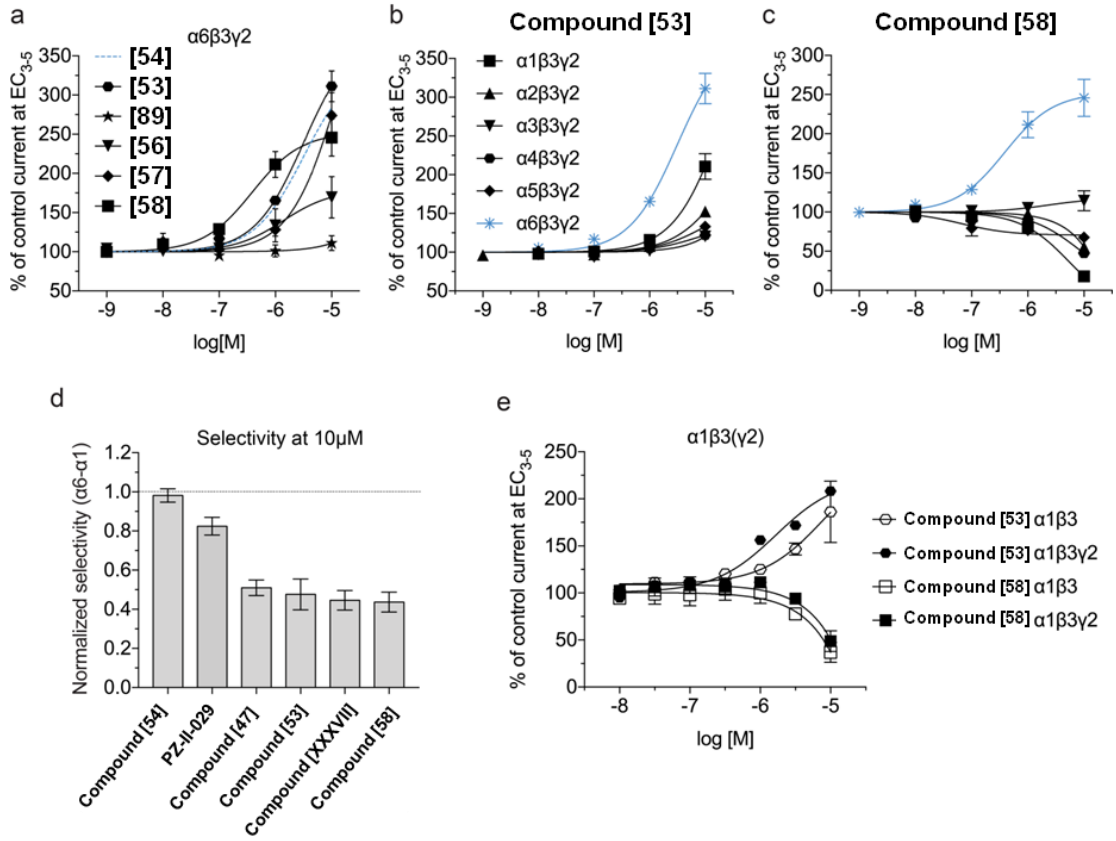

Figure 40: (a) Screening of a series of compounds **[53]**, **[89]**, **[56]**, **[57]** and **[58]** at α6β3γ2 $GABA_A$ receptors (see bottom row in Fig. 1). At 1 µM compound concentration, compounds **[54]** (dashed blue line representing the fitted curve of Fig. 2c), **[53]** and **[58]** show more than 150% modulation of GABA $EC_{3\text{-}5}$ currents. At 10 µM compound concentrations, compounds **[53]**, **[57]** and **[58]** show strongest modulation of GABA $EC_{3\text{-}5}$ currents, comparable to compound **[54]**. (b, c) Subunit profile of compounds **[53]** (b) and **[58]** (c) at αxβ3γ2 (x=1-6) $GABA_A$ subunit combinations. Note that some receptors, particularly α1β3γ2, are positively modulated by compound **[53]**, but negatively modulated by compound **[58]**. (d) Efficacy selectivity of 10 µM compound at α6β3γ2 over α1β3γ2. Modulation at α1β3γ2 was calculated as fraction of the modulation at α6β3γ2 (baseline (100 %) = 0, efficacy at α6β3γ2 = 1; all signs positive), and subtracted from 1. (e) Separate experiment comparing effects of compound **[53]** and compound **[58]** at α1β3 versus α1β3γ2 receptors, demonstrating independence from the γ subunit.

Based on the data of compounds **[53]** and **[58]** we were curious to investigate compound **[54]** regarding its functional selectivity profile with respect to another third subunit. As reported by Jechlinger *et al*. $\alpha6\beta\gamma2$ and $\alpha6\beta\delta$ receptor subtypes are populations of comparable size which prompted us to investigate our compounds in $\alpha1,4,6\beta3\delta$ receptor subtypes.[166] Interestingly, the current modulation of compound **[54]** was also not affected by the presence of a $\gamma2$ subunit which is in line with the data for compound **[53]** and **[58]**. Additionally, compound **[54]** showed a comparable functional selectivity for the $\alpha6$ subunit in the $\alpha\beta\delta$ receptors subtype (Table 6).

Table 6: Functional data in δ containing receptor subtypes. EC_{50} values and efficacy of compound **[54]** at increasing concentrations in α1β3δ, α4β3δ and α6β3δ receptors, given in % of control current (mean ± SEM). Due to low efficacy, the EC_{50} value in α1β3δ could not be obtained (n.d.=not determined). Control current = 100% (GABA $EC_{3\text{-}10}$).

[54]	**α1β3δ**	**α4β3δ**	**α6β3δ**
EC_{50} [μM]	n.d.	15.7	7.7
1 nM	99.5±0.4	100.0±0	102.8±4.7
10 nM	100.0±0	99.0±1.4	101.1±1.4
100 nM	100.0±0	102.1±1.7	102.1±3.8
300 nM	-	-	98.1±3.2
1 μM	100.0±0	109.0±3.3	118.4±14.3
3 μM	-	-	118.3±0.2
10 μM	108.9±0.2	121.4±4.5	158.9±13.4
30 μM	106.5±0.5	129.8±4.0	179.5±8.7
n	2	3-4	4

C II.2.3.4 Discussion

In summary, we were able to identify another substitution pattern (R^8 and R'^3 substituted compounds) of pyrazoloquinolinones which partially even displayed an improved modulatory preference for $\alpha6\beta3\gamma2$ receptor subtypes compared to the substitution pattern (R^7 and R'^4 substituted compounds) in earlier studies.[146] The introduction of a chloro residue in position R^8 greatly enhanced the efficacy while preserving the preferential modulatory effects for $\alpha6\beta3\gamma2$ over the other $\alpha k\beta3\gamma2$ (k=1-5) receptor subtypes. Furthermore, the systematic variation of the methoxy residue on ring D led to the conclusion that position R'^3 seems to trigger $\alpha6$ selectivity depending on the certain chemically diverse substituent. Thus, compound **[54]** (R^8 = Cl, R'^3 = OCH_3) shows the best $\alpha6/\alpha k$ (k=1-5) ratio in $\alpha k\beta3\gamma2$ (k=1-6) receptor subtypes known to date. It displayed a modulation of control GABA currents in $\alpha6\beta3\gamma2$ subtypes around 300% at 10 μM with an estimated EC_{50} of 3.1 μM.

Moreover, the introduction of the methoxy residue in position R'[2] (compound **[148]**) led to a complete loss of modulatory activity and binding at any receptors subtype as shown by co-application of compound **[54]**. According to a conformational analysis of the dihedral angles between the plane surfaces of the ring systems A-C and D of compound **[47]**, **[54]** and **[148]** the inactivity at the $\alpha+/\beta-$ sites might presumably be based on a distorted ring D. In contrast, compound **[148]** still showed a binding affinity at the benzodiazepine binding site in submicromolar range indicating a non-linear impact on the homologous binding sites.

The variation of different *m*-substituents did not lead to improved efficacy or potency selective compounds for $\alpha6\beta3\gamma2$ receptor subtypes. However, two compounds, namely compound **[53]** and compound **[58]**, displayed interesting modulatory profiles especially in the $\alpha1\beta3\gamma2$ receptor subtype. Compound **[53]** (R'[3] = CH_3) showed positive modulatory effects whereas compound **[58]** (R'[3] = COOH) exerted negative modulatory effects. Interestingly, it is the first time that a negative modulation mediated by the $\alpha+/\beta-$ site is observed since we showed that the modulation is exerted also in absence of a $\gamma2$ subunit. In addition, we demonstrated that compound **[54]** is still functionally $\alpha6$ selective in $\alpha\beta\delta$ receptor subtypes and thus does also not require a $\gamma2$ subunit for current modulation. The comparison of the three compounds **[54]**, **[53]** and **[58]** led to the conclusion that we are able to trigger a certain modulatory effect (**[54]** = null (silent) modulator or SAM, **[53]** = PAM and **[58]** = NAM) by changing the chemical properties of the substituents in the *m*-position only. Intriguingly, the null modulatory effect of compound **[54]** corresponds to an electron withdrawing hydrogen bond acceptor group (**[54]**, R'[3] = OCH_3), while positive allosteric modulation is observed for an electron donating hydrophobic substituent (**[53]**, R'[3] = CH_3) and negative modulation is exerted by an electron withdrawing negatively ionisable group (**[58]**, R'[3] = COOH). Based on these structure-activity findings a systematic expansion should provide more insights into the SAR of efficacy selectivity and thus may lead to compounds with desired subtype profiles.

The usefulness of $\alpha6$ selective compounds is expressed in their assumed involvement in various diseases, e.g. tic disorders[167], depressive behaviours[168] or inflammatory[169] and myofascial pain of the trigeminal innervations area.[170] Furthermore, they possess a very distinct expression pattern in the central and peripheral nervous system and are mostly found in CGCs, olfactory bulb, cochlear nucleus, hippocampus, trigeminal ganglion, sensory neurons and dorsal horn.[168,169,171,172] For instance, the $\alpha6$ preferring flavone hispidulin (PAM in $\alpha6\beta2\gamma2$S receptors) was extracted from a plant and applied successfully in the treatment of intractable motor tic disorders.[60,61] Furthermore, the administration of hispidulin led specifically to a reduction of metamphetamine-induced hyperlocomotion *via* cerebellar $\alpha6$ $GABA_A$ receptors.[167] Remarkably, an interference of the impact of hispidulin on spontaneous locomotor activity or motor coordination (rotarod performance) was not observed. Another

example deals with α6 expression in the trigeminal ganglion. Here, a knockdown of the α6 subunit expression led to an aggravation of the hypersensitivity related to inflammatory temporomandibular joint arthritis[169] and additionally increased myofascial nociception.[170] Hence, the inhibition of processing nociceptive signals in the trigeminal pathway might be associated with α6 containing $GABA_A$ receptors. This leads to the assumption that α6 selective positive modulators might be suitable for the alleviation of pain states of the trigeminal innervations area.

C II.2.4 Exploring α6β3γ2 subtype selectivity – Part II

The pyrazoloquinolinone called “compound 6” (in internal discussions, structure shown in Figure 41) possesses a methoxy substituent in position R^7 and in position R'^4 and displayed a pronounced α6β3γ2 subtype efficacy selectivity which prompted us to follow up on these observations.[152] Since the selectivity seems to derive from the position R^7 (as shown by Varagic *et al*.[152]) we aimed to modify this position with chemically diverse substituents to explore the requirements for the selectivity profile of “compound 6”. We decided to introduce different halogens as well as substituents with and without “functionality” (Figure 41).

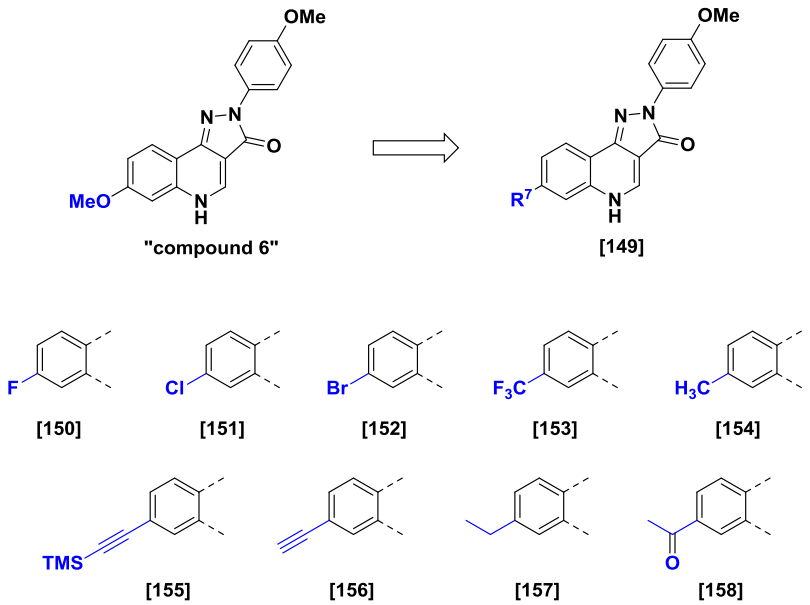

Figure 41: Overview of the planed chemical modifications of position R^7.

While the upper series **[150]**-**[154]** was synthesized by a colleague, we focused on the synthesis of the lower series **[155]**-**[158]** (Figure 41). Here, we decided to introduce a TMS protected acetylene which - after deprotection - serves as nice handle to obtain the ethylated and acylated derivatives. Thus, after synthesizing the brominated starting material **[163]** according to our general route (Scheme 2), we followed the synthetic route outlined in chapter C II.2.2 which led to the TMS protected acetylene derivative **[155]** in acceptable yields. Deprotection using 2 eq. K_2CO_3 gave the acetylene compound **[156]** in 85% yield (Scheme 12). From this stage the two other desired compounds **[157]** and **[158]** were accessible. The acyl compound **[158]** was synthesized as mentioned previously in chapter C II.2.2 using CF_3SO_3H as catalyst for the Markovnikov-type addition of water to the terminal alkyne at room temperature which gave **[158]** in 14% yield. Reduction of the acetylene compound **[156]** under hydrogen atmosphere led to the ethyl derivative **[157]** in almost quantitative yields (Scheme 12).

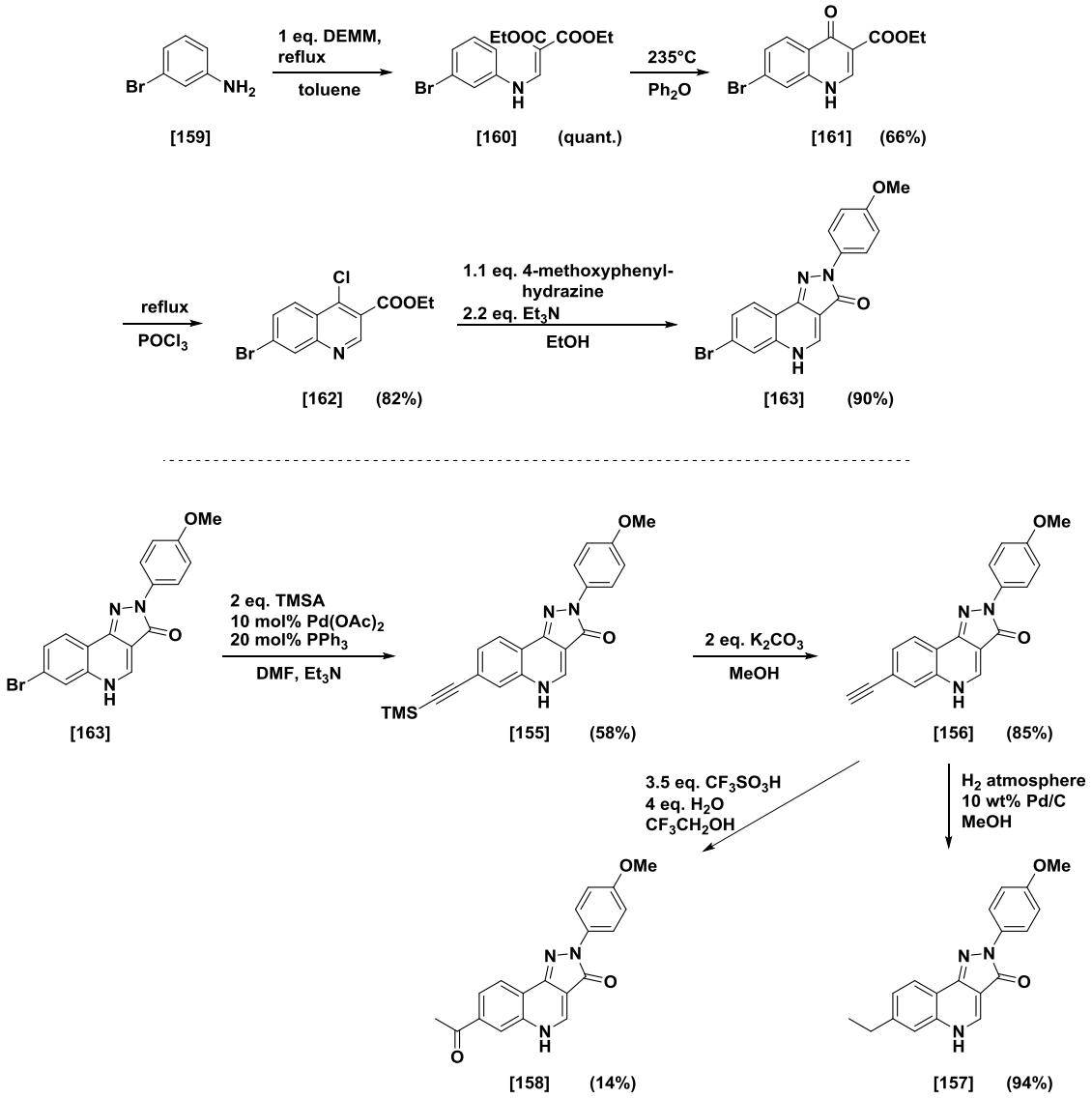

Scheme 12: Synthetic pathway of R^7 series.

First preliminary results of modulatory effects in $\alpha 6\beta 3\gamma 2$ receptor subtypes of the new compound series is shown in Figure 42.

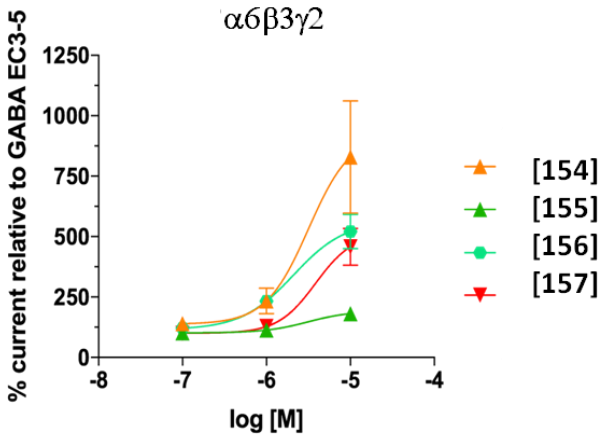

Figure 42: Preliminary results of the modulation of $EC_{3\text{-}5}$ elicited GABA currents by [154], [155], [156] and [157].

Among these four compounds **[154]** ($R^7 = CH_3$) displayed the highest modulatory effects which are in the same range as for “compound 6” (Figure 41).[152] **[156]** (R^7 = acetylene) and **[157]** (R^7 = Et) modulated the GABA elicited current to ~500% at an $EC_{3\text{-}5}$ while **[156]** seems to be slightly more potent than **[157]**. Interestingly, **[155]** (R^7 = TMS acetylene) did not modulate the GABA elicited current, at all. This observation might be based on a putative sterical clash of the very large substituent in the binding pocket.

However, these findings are very preliminary and further experiments have to be carried out to draw reasonable conclusions.

C II.3 Triazoloquinazolinediones as modulators for the α+/β– interface

We started to investigate a set of four triazoloquinazolinediones in recombinant binary $GABA_A$ receptors. To get a first idea how the compounds perform in binary αβ $GABA_A$ receptors we conducted a two point screening of the structures **[130]**-**[134]** (Figure 43). This screening revealed that the four compounds seem to be modulatory silent in α1β2 receptor subtypes. Two compounds, namely **[131]** and **[134]**, were also examined in α1β3 receptor subtypes where **[134]** acted as weak positive modulator (Figure 43b). However, the preliminary results were not promising and thus we stopped to further investigate this set of compounds in other receptor subtypes.

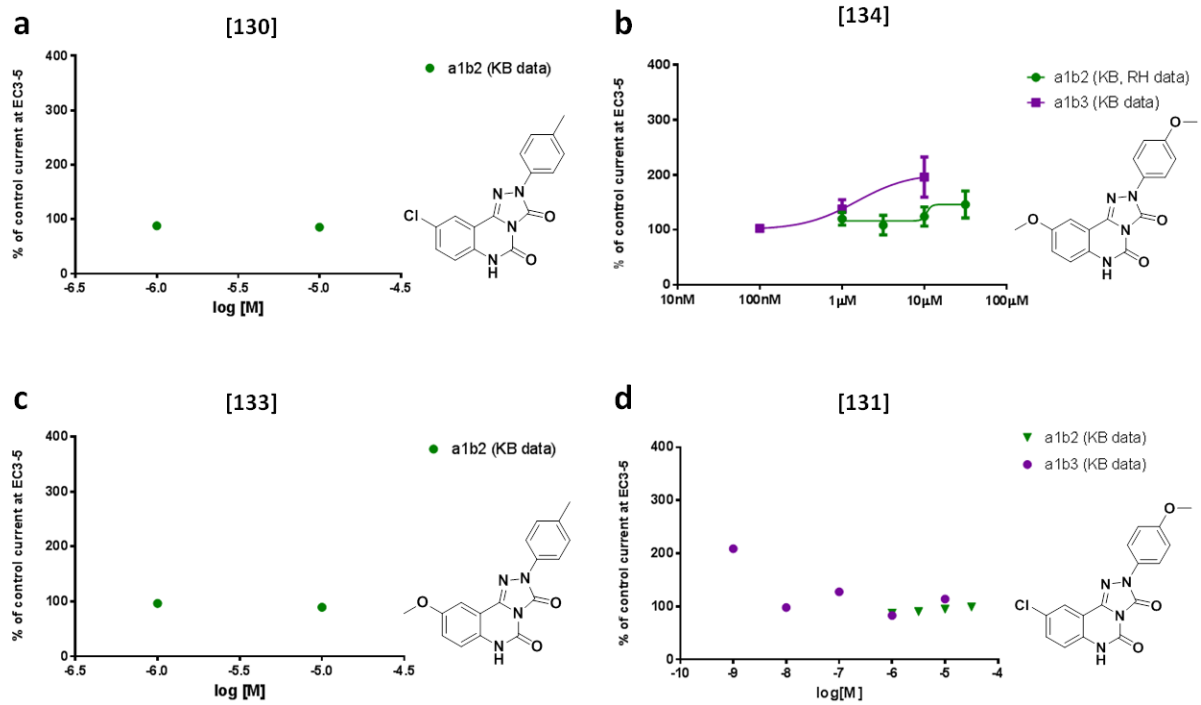

Figure 43: Modulatory effects of four triazoloquinazolinediones in α1β2 and α1β3 $GABA_A$ receptor subtypes.

Nevertheless, we were interested if these compounds are also high affinity binders for the benzodiazepine binding site like the compounds reported by Nilsson *et al*.[148] Therefore, we conducted displacement assays using [3H]-flunitrazepam at the α1+/γ2– interface in rat cerebellum membranes. The very preliminary results showed that the four investigated compounds bind in the sub nanomolar range to the BZ site. Note, **[131]** binds ten to fifteen times stronger at the BZ site compared to the other synthesized analogues. Additionally, it seems that the compounds with a chloro substituent in position R^8 bind stronger at the BZ site compared to their methoxy analogues.

Table 7: Preliminary IC_{50} values of four triazoloquinazolinediones determined by displacement assay using [3H]-flunitrazepam in rat cerebellum membranes.

Compounds	IC_{50} [nM]
[130]	0.48
[131]	0.06
[133]	0.78
[134]	0.69

C II.4 Triazoloquinazolinediones as potential BZ antagonists

Since the tested triazoloquinazolinediones showed a rather silent binding profile at the $\alpha+/\beta-$ interfaces but are generally high affinity binders for the diazepam-sensitive $\alpha x+/\gamma 2-$ interfaces (x = 1, 2, 3 and 5) (Table 7), we aimed to examine compounds **[130]**, **[131]**, **[133]** and **[134]** at the diazepam-insensitive sites (x = 4 and 6). Thus, we performed binding assays in $\alpha 1-$ and $\alpha 6-$containing $GABA_A$ receptors expressed in cerebellar membranes.

All compounds showed sub-nanomolar Ki values in the $\alpha 1-$containing receptors which confirmed the preliminary results of the previous chapter C II.3. For $\alpha 6-$containing receptors we observed a slightly more diverse profile. For compound **[133]** the Ki value could not be determined due to a very poor solubility. Compounds **[130]** and **[134]** showed Ki values in the nanomolar range. Remarkably compound **[131]** displayed a Ki value of 62 ± 9 nM.

Table 8: Binding data of compounds **[131]**, **[131]**, **[133]** and **[134]** in $\alpha 1-$ and $\alpha 6$-containing $GABA_A$ receptors expressed in rat cerebellar membranes.

Compounds	Ki values [nM]	
	$\alpha 1+/\gamma 2-$	$\alpha 6+/\gamma 2-$
[130]	0.99 ± 0.24 (n = 3)	294 ± 32 (n = 3)
[131]	0.28 ± 0.03 (n = 3)	62 ± 9 (n = 3)
[133]	0.44 ± 0.11 (n = 3)	> 0.5 µM (poor solubility)
[134]	0.21 ± 0.04 (n = 3)	164 ± 3 (n = 3)

The high affinity of compound **[131]** is quite unique and will thus be further investigated in future studies. Here, the antagonism of **[131]** against diazepam will be investigated in mice which will give also information about the toxicity of the triazoloquinazolindiones in general. Additionally, docking studies will be performed to elucidate a potential binding orientation or key interactions supporting the observed effects.

C III Similar BZ ligands possess different binding modes - comparing homologous binding sites

Benzodiazepine ligands and pyrazoloquinolinones possess a promiscuous binding profile and their molecular interactions are still not fully clarified. Therefore, we were aiming for a structural comparison of the two homologous binding sites, namely the high affinity α+/γ− site and the low affinity α+/β− site (Figure 44a), by a mutational approach in which we successively introduced key amino acids of the γ2− site into the β3− site. Investigations of our ligands in the mutant construct in comparison to the wild type receptors should provide highly interesting insights in benzodiazepine-ligand recognition properties and requirements.

C III.1 Design and generation of the conversion mutants

In line with these considerations we decided to transfer the high affinity binding features of the γ2− site into the β3− site. Thus, we examined the surfaces which interact with the ligand in our models (based on 4COF)[90] and analyzed the difference between the γ2− and the β3− sides. This analysis revealed that the conserved area of interest consists of eight amino acid residues on segments D, G, E and F (Figure 44b, highlighted as space filling C_α-atoms). A closer look showed that only four of those eight amino acid residues are different among the homolgous sides and additionally they are closest to the BZ ligand occupied space (compare Figure 44c, d and e). Thus, we aimed to mutate these four vicinal amino acids (one on segment E, two on segment D and one on segment G) in the β3− side (Figure 44d) leading to a consistent γ2− like contact area for interacting ligands (Figure 44e).

The introduction of the point mutations was made according to published data and geometric considerations. The first introduced point mutant was β3Q64A (termed D1) since Kucken *et al*. demonstrated that the space provided by γ2A79 (corresponding to β3Q64, Figure 44c, d) of loop D seemed to be required for high affinity binding of various imidazobenzodiazepines.[173] Therefore, we created this space by replacing the bulky glutamine (Q) residue by a small alanine residue. Based on this first mutation all other mutations were consecutively introduced to achieve a γ2-like environment on the β3− side. The second mutation resulted in a β3Q64A;Y62F construct (termed D2) due to the conversion of β3Y62 into the homologous phenylalanine (F). The reversed conversion of

γ2F77 into tyrosine (Y) has been studied intensively and showed both an increase and decrease of affinity depending on the ligands tested.[174]

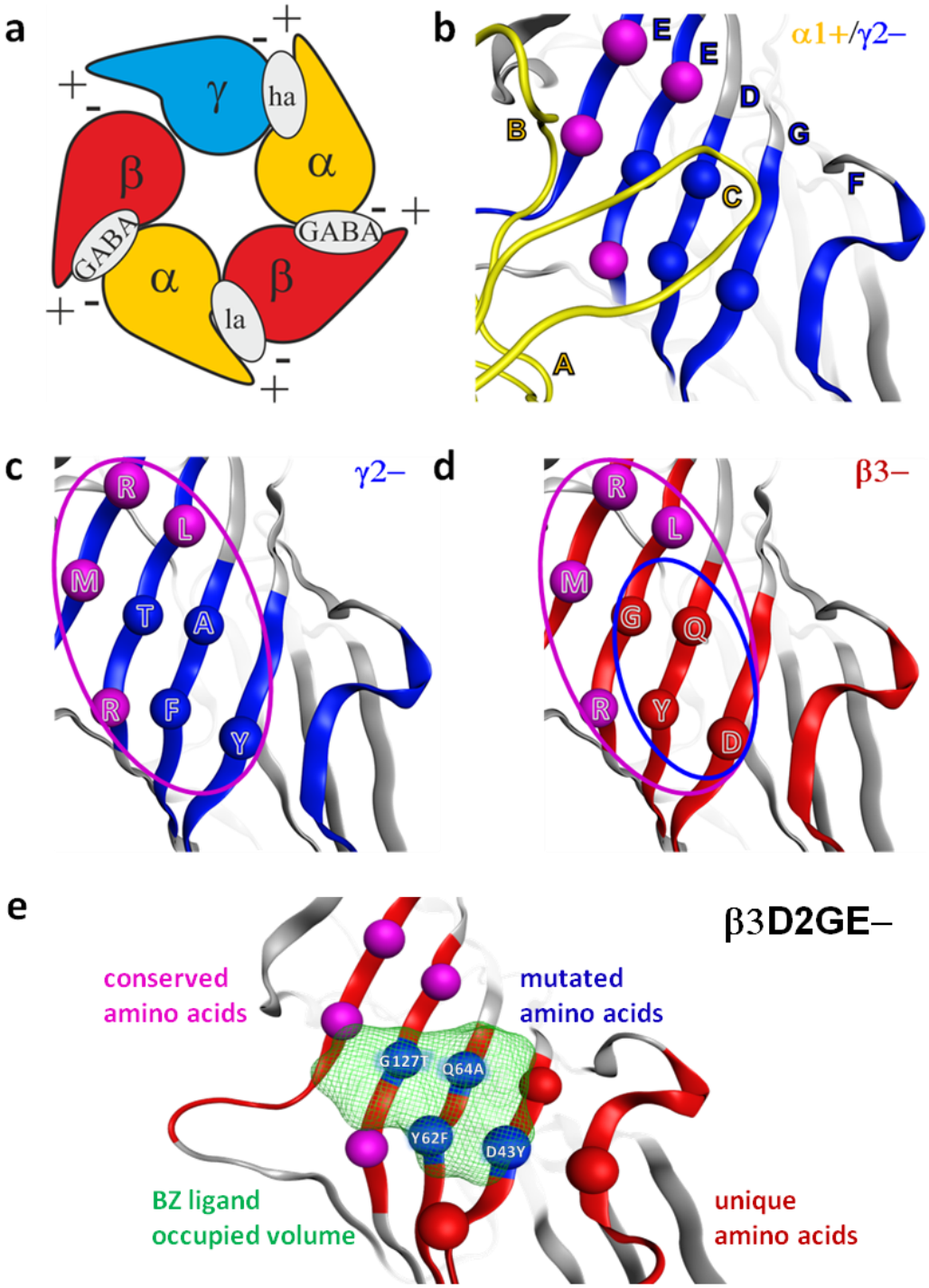

Figure 44: a: Schematic view of the extracellular domain of a $GABA_A$ receptor with the plus and minus sides of the subunits indicated. The GABA binding site is labeled as "GABA", the high affinity benzodiazepine/ CGS site as "ha", and the low affinity CGS site as "la". **b:** View of the binding site "through" the plus side (yellow thin tube) onto the minus side (blue). Binding site forming segments and loops are labeled by Arabic letters (D, E, F and G). Amino acids unique to the γ2 subunit are highlighted in blue whereas amino acids that are conserved between γ2 and β3 are highlighted in purple. **c, d:** Detail view of the γ2 **(c)** and β3 **(d)** minus sides. Conserved amino acids are highlighted in purple whereas unique amino acids are highlighted in either blue (γ2– side) or red (β3– side). The blue oval is highlighting the four amino acids selected for mutational analysis **(d)** and the purple oval is indicating the entire "identical surface" that results from the four conversion mutants. Note that segment (loop) F of the γ2 subunit may differ considerably due to low conservation, but the amino acid that is displayed is predicted to be structurally conserved.[6] **e:** Ligand occupied volume of benzodiazepine ligands (highlighted in green) in the engineered quadrauple mutant β3D2GE- (conserved amino acids = purple; mutated amino acids = blue; unique amino acids = red).

Next, we analyzed segment D in the area of interest and identified β3D43 (homologous to γ2Y58) as major difference. Thus, we converted β3D43 to a tyrosine which resulted in triple mutant β3Q64A;Y62F;D43Y (termed D2G) leading to a more lipophilic character in the area of segment G. After we confirmed that all three constructs (D, D2 and D2G) showed promising results (GABA dose response curves Figure 45a and modulation of compounds CGS9895 **[XXXVII]** and CGS20625 **[164]** in Figure 47) we continued with our transformation by introducing the β3G127T[175] mutation leading to the quadrauple mutant β3Q64A;Y62F;D43Y;G127T (termed D2GE) (Figure 45a).[83] Based on our model, there are further difference on loop F between the to homologous sides which have been shown to play an important role not only for affinity (zolpidem) and positive allosteric modulation (flunitrazepam)[176] of some ligands but also in the overall stabilization of the minus side' structure and conformation.[90] Thus, mutations on loop F might destabilize the whole protein. However, we attempted the introduction of mutations on loop F which led to a reduction of functional expression like hypothesized by Miller and Aricescu.[90] Furthermore, we tried to introduce two different chimeras on the loop F which also showed only reduced expression in oocytes as well as in HEK293 cells, and thus could not be characterized (Figure 45b). Hence, we discontinued the introduction of further mutants and used the four constructs which showed an adequate expression.

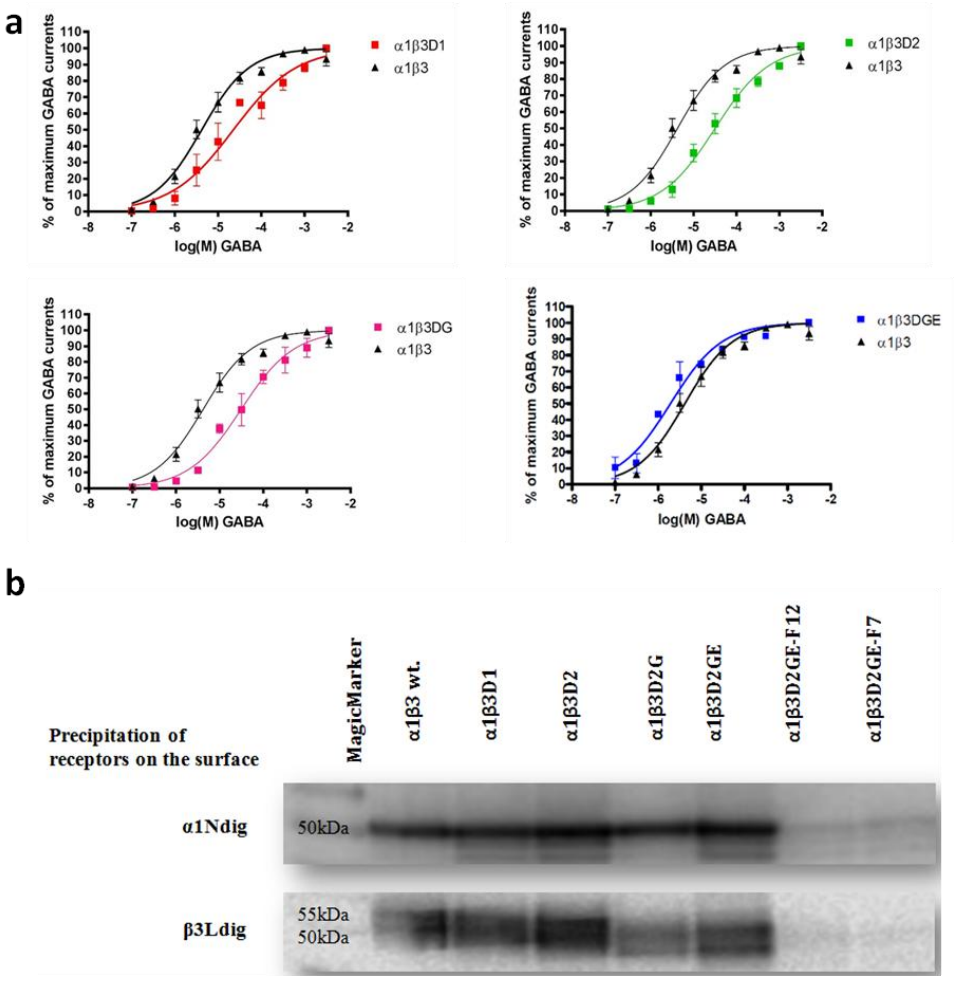

Figure 45: a: GABA dose-response curves in α1β3D1 (■),α1β3D2 (■),α1β3D2G (■) and α1β3D2GE (■) $GABA_A$ receptors compared to the GABA dose-response curve of α1β3 receptors (n=2). **b:** Cell surface expression of $GABA_A$ receptors containing wild-type α1 and β3 or mutated β3 subunits. HEK cells were co-transfected with α1 and β3, β3D1, β3D2, β3D2G, β3D2GE, β3D2GE-F12 or β3D2GE-F7 subunits. $GABA_A$ receptors expressed at the surface were immunolabeled by an incubation of intact cells with β3(1-13) antibody. Receptors were then extracted, precipitated by Immunoprecipitin, and subjected to SDS-PAGE and Western blot analysis using digoxigenin-labeled α1(1-9) or β3(345-408) antibodies. The complete experiment was performed once.

Based on the promising modulatory results of the two CGS compounds **[XXXVII]** and **[164]** (Figure 47) we aimed to investigate the quadrauple mutant for high affinity binding using radioligand displacement assays. Even though CGS20625 **[164]** showed auspicious results in the binding assay using labeled Ro15-1788 (flumazenil) as radioligand, we discontinued this approach since only very low Bmax values were obtained which represents the maximum amount of radioligand that can bind to the receptors. Consequently, this would require an uneconomic amount of cells for further experiments (Figure 46).

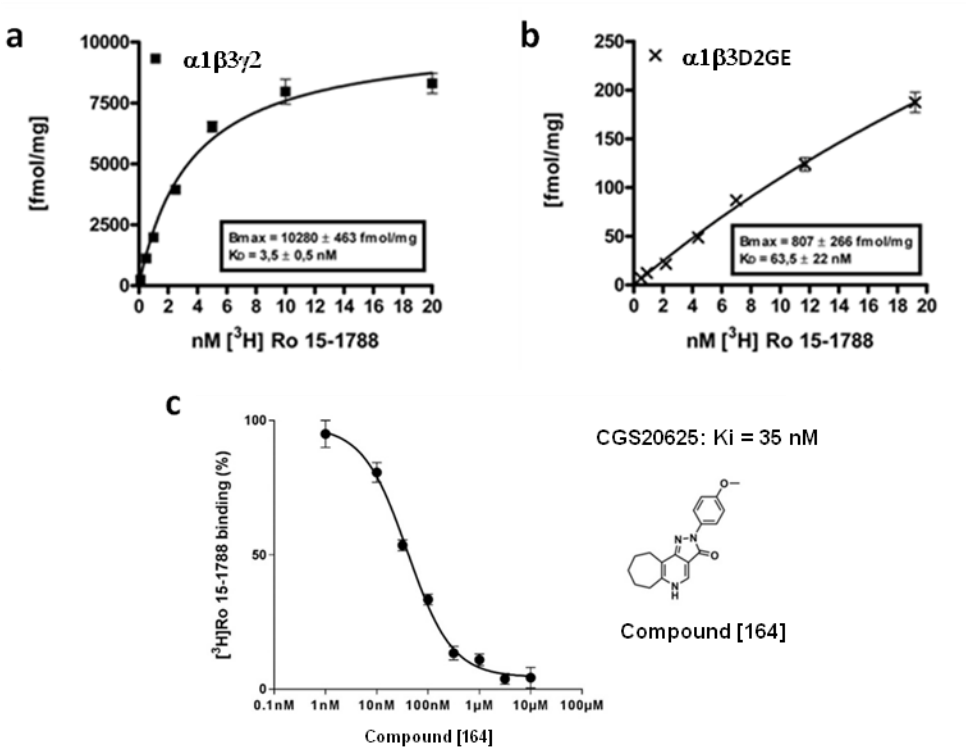

Figure 46: a,b: Saturation assay of [^{3}H]Ro15-1788 (flumazenil) binding in HEK cell membranes of (**a**) wild type α1β3γ2 (■) and (**b**) recombinant α1β3D2GE (×) receptors. Membranes were incubated with increasing concentrations of [^{3}H]Ro15-1788 (0,1-20 nM) in the absence or presence of 100 µM diazepam or Ro15-1788. Membranes were filtered through Whatman GF/B filters and specifically bound radioactivity was measured. Data are presented as mean ± S.D. of one experiment performed in triplicates. Experiments were performed once (**a**) or three times (**b**) with comparable results. B_{max} gives the maximal number of binding sites of the specific ligand per mg/protein. K_D gives the concentration at which 50% of the receptor is occupied by the ligand. **c:** Potency of **[164]** for inhibition of [^{3}H]Ro15-1788 binding in HEK cell membranes of recombinant α1β3DGE (●) receptors. Membranes were incubated with 30 nM [^{3}H]Ro15-1788 in the presence of 1 nM to 10 µM **[164]**. Membranes were filtered through Whatman GF/B filters and specifically bound radioactivity was measured. Data are presented as means ± S.D. of one experiment performed in triplicates and were fitted by GraphPad Prism using the equation for one site binding.

C III.2 Mutations Q64A and D43Y increase the apperent affinity of CGS9895 [XXXVII] and CGS20625 [164]

Since the binding assays turned out to be not suitable we returned to functional studies in the oocyte system. Here, a stepwise conversion of β3 into γ2 should be reflected in a receptor's response to pyrazolopyridinone derivatives in a successive manner. Thus, we investigated the modulation exerted by the pyrazoloquinolinone CGS9895 **[XXXVII]** and the pyrazolopyridinone CGS20625 **[164]** in α1β3 wild type and in the four α1β3(mut) receptors.

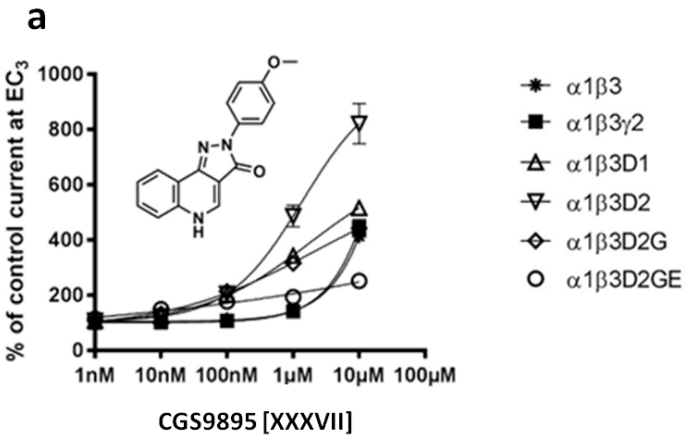

Figure 47: Concentration-response curves of modulation by CGS 9895 **[XXXVII]** (**a**) and CGS 20625 **[164]** (**b**) in wild type α1β3 (*) and α1β3γ2 (■) receptors and the mutated α1β3D1 (△), α1β3D2 (▽), α1β3D2G (◊) and α1β3D2GE (○) receptors at GABA EC_3. EC_{50} values: for CGS9895 **[XXXVII]** 23 µM (*), 38 µM (■), 0.6 µM (△), 1 µM (▽), 0.3 µM (◊), 0.03 µM (○) and for CGS20625 **[164]** 20 µM (*), 35 µM (■), 3 µM (△), 10 µM (▽), 2 µM (◊) and 0.3 µM (○), respectively. The EC_{50} values are estimated by fitting the data to a hill slope of 1, since in all but α1β3D2GE saturation was not reached. Data represent mean ± SEM (n=3-11).

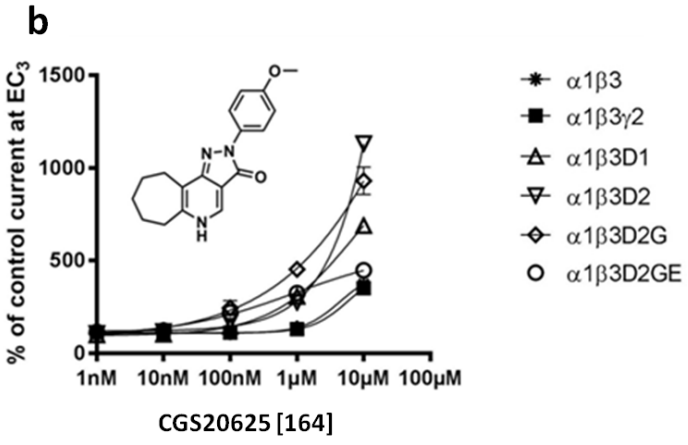

Comparing the low potency modulation of CGS9895 **[XXXVII]** and CGS20625 **[164]** in α1β3 and α1β3γ2 receptors, we can conclude that they are both silent or "null" modulators at the high affinity benzodiazepine binding site and exert their modulatory effects *via* the α1+/β3− site exclusively.[146] In α1β3D1 receptors we observed that the introduction of alanine (A) leads to shift of the modulatory effects to lower concentrations of both compounds compared to the wild type (Figure 47a, b). Thus, the increase of space in the pocket due to the replacement of a glutamine (Q) side chain seems to improve the shape complementarity between the ligands and the receptor. In the second mutant receptor α1β3D2 we observed slight differences in potency and higher efficacies of the two compounds compared to the effects observed in α1β3D1. This leads to the assumption that

the change from tyrosine (Y) to phenylalanine (F) seems to affect the efficacy. The introduction of the third mutation ($\alpha1\beta3$D2G) showed a slight left shift of the dose-response curve for CGS20625 **[164]** (Figure 47b) whereas the dose-response curve of CGS9895 **[XXXVII]** remained unaffected compared to the dose-response curves in $\alpha1\beta3$D2 (Figure 47a). The last mutation led to a decrease of the maximum modulatory effects of both compounds (Figure 47a, b). A further small increase of potency was indicated by a weak positive modulation of CGS 9895 **[XXXVII]** in α1β3D2GE receptors which could be seen at 100 nM compound concentration (Figure 47a). In summary, these results affirm the favoured interactions of both compounds with the $\gamma2-$ like site. Additionally, we observed that potency and efficacy are differentially influenced by the individual amino acids which contribute to the binding.

C III.3 Ro 15-1788 [165] and Ro 15-8670 [166] act as positive allosteric modulators in $\alpha1\beta3$(mut) receptors

Since pyrazolopyridinone CGS20625 **[164]** showed proper activities in our mutant receptors we were wondering if we could displace it with benzodiazepine antagonist Ro15-1788 **[165]** which shows high affinity null modulatory effects in most subtypes. Thus, if CGS20625 **[164]** uses the engineered binding site we should be able to antagonize its effect by **[165]**. Suprisingly, we observed a positive modulation of **[165]** in $\alpha1\beta3$D1, $\alpha1\beta3$D2, $\alpha1\beta3$D2G and $\alpha1\beta3$D2GE receptors at GABA EC_3 which was comparable to the positive modulation elicited by **[164]** (Figure 48a). A similar observation is reported in literature in which **[165]** displayed positive modulatory effect by the introduction of a single point mutation in $\alpha1\beta1\gamma2$L receptors.[175] As seen before for pyrazolopyridinone derivatives we observed a change of the modulation according to the order of the introduced mutations. Whereas **[165]** shows modulatory silent effect in $\alpha1\beta3$ receptor subtypes, the introduction of D1 ($\gamma2$Q64A) resulted in a low potency modulation. The second mutation D2 ($\gamma2$Y62F) showed no differences in modulation which is in accordance with the results of Sigel *et al*.[174] The introduction of D2G and D2GE led to further increases in potency and efficacy (Figure 48a).

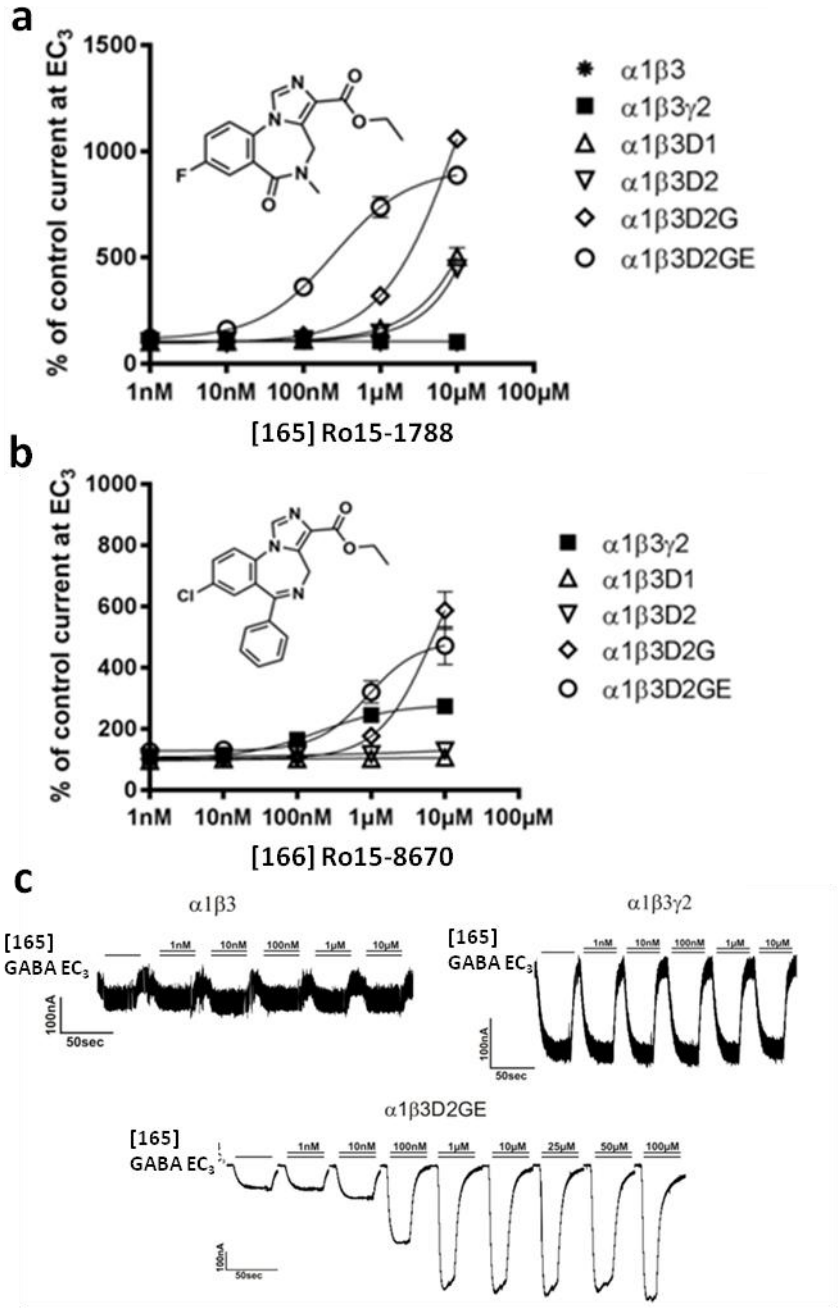

Figure 48: Dose response curves of GABA EC_3 modulation by Ro 15-1788 **[165]** (**a**) and Ro 15-8670 **[166]** (**b**) in wild type $\alpha1\beta3$(*) and $\alpha1\beta3\gamma2$ (■) receptors and the mutated $\alpha1\beta3$D1 (△), $\alpha1\beta3$D2 (▽), $\alpha1\beta3$D2G (◊) and $\alpha1\beta3$D2GE (○) receptors with EC_{50} values: for **[165]** 17 µM (△), 82 µM (▽), 6 µM (◊), 0.2 µM (○) and for **[166]** 0.2 µM (■), 16 µM (◊) and 1 µM (○). The EC_{50} values are estimated by fitting the data to a hill slope of 1, since in many cases saturation was not reached. The respective EC_{50} values where low or no efficacy was observed could not be obtained, namely for **[165]** in wild type receptors ($\alpha1\beta3$, $\alpha1\beta3\gamma2$) and for Ro **[166]**in the mutated receptors ($\alpha1\beta3$D1 and $\alpha1\beta3$D2). Data represent mean ± SEM (n=1-6). Sample traces of the measurements (**c**) in wild type $\alpha1\beta3$ (*) and $\alpha1\beta3\gamma2$ (■) receptors, as well as in the mutated $\alpha1\beta3$D2GE (○) receptors.

Intrigued by this finding, we were curious if structurally related compounds display similar effects. Thus, we investigated Ro15-8670 **[166]** and diazepam **[XII]** in our constructs. While the imidazobenzodiazepine **[166]** did not exert modulatory effects in $\alpha1\beta3$D1 and $\alpha1\beta3$D2 receptors, it acted as positive modulator in the $\alpha1\beta3$D2G and $\alpha1\beta3$D2GE receptors (Figure 48b). Hence, we concluded that the amino acid residue in loop G (γ2Y58) seems to play an important role for the activity of **[166]**. In contrast, the classic benzodiazepine diazepam **[XII]** remained inactive in all of our mutational constructs (Figure 49). This result was very unexpected since **[XII]** represents the smallest ligand of our tested series (total hydrophobic surface area: diazepam **[XII]** = 411.27, flumazenil **[165]** = 518.90, Ro15-8670 **[166]** = 618.24) and should thus perfectly overlap with our other BZ ligands which would be in accordance with the common binding mode hypothesis[131] and the accepted pharmacophore model considerations.[177]

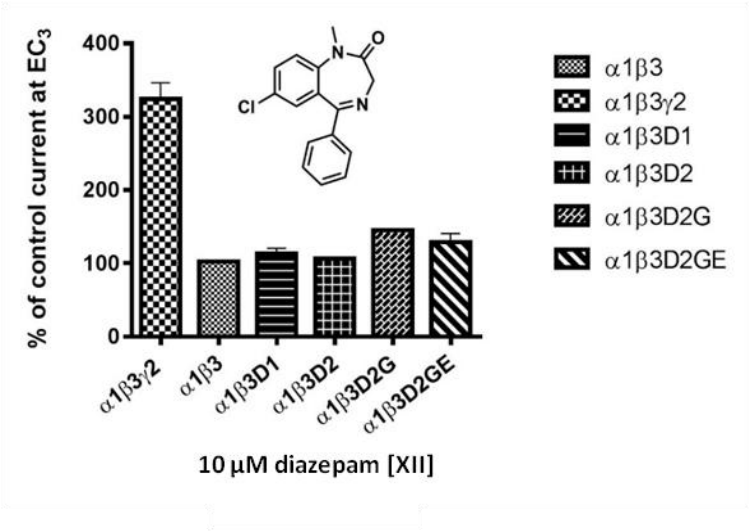

Figure 49: Effect of GABA EC_3 modulation by 10 µM **[XII]** in wild type $\alpha1\beta3$ and $\alpha1\beta3\gamma2$ receptors and the mutated $\alpha1\beta3$D1, $\alpha1\beta3$D2, $\alpha1\beta3$D2G and $\alpha1\beta3$D2GE receptors. Data represent mean ± SEM (n=2-4).

C III.4 Computational docking suggests distinct binding modes for certain benzodiazepines

The inactivity of diazepam triggered us to perform molecular docking in order to assess the binding modes of our tested ligands at the wild type high affinity site ($\alpha1+/\gamma2-$) and in the quadruple mutant ($\alpha1+/\beta3$D2GE–). In detail, we aimed to investigate: a) whether we are able to identify similar bound states of our tested ligands at the $\alpha1+/\gamma2-$ site and at the $\alpha1+/\beta3$D2GE– site, b) whether these bound states are in accordance with our experimental data, and c) whether a combination of our experimental and *in silico* results leads to an improved understanding of the current binding mode hypotheses.

The docking of **[166]** resulted into one consistently highly ranked ligand orientation at the $\alpha1+/\gamma2-$ site as well as in the $\alpha1+/\beta3$D2GE– mutant, which we termed BM I (Figure 51a).

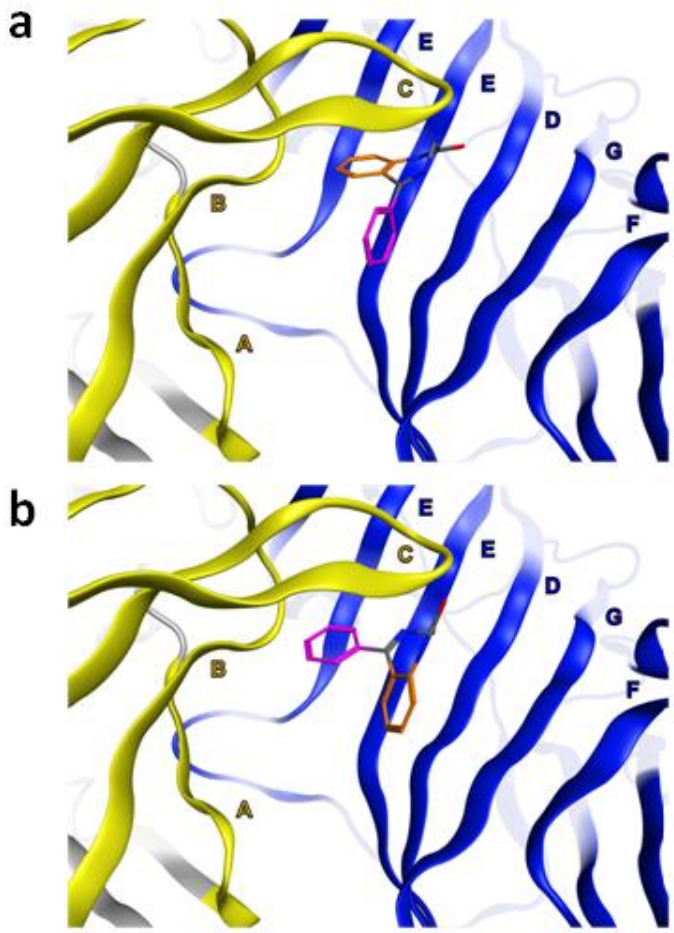

Figure 50: General orientation of BM I and BM II of the benzodiazepine core scaffold Color codes for the protein ribbon: $\alpha1$ subunit: yellow; $\gamma2$ subunit: blue. **a**: BM I of the benzodiazepine core scaffold at the $\alpha1+/\gamma2-$ interface. The fused phenyl ring (highlighted in orange) is directed towards the $\alpha1$ subunit while the pendant phenyl ring (highlighted in purple) is oriented towards the $\gamma2$ subunit. Binding site forming segments (Strands and loops A-F) are labeled by Arabic letters;

This pose is in accordance with the CBM I (common binding mode I) orientation which was reported by Richter *et al*. for high affinity BZ site (Figure 50a).[131] Contrary, we obtained two prominent binding poses for diazepam **[XII]** at the $\alpha1+/\gamma2-$ site. The first one is in accordance with our BM I while the second pose resembles CBM II (common binding mode II) as reported by Richter *et al*. [131] and thus was termed BM II (Figure 50a, b). According to the ChemScore fitness function (implemented in GOLD) BM II was ranked consistently higher for **[XII]**. Hence, our results rather support the work reported by Middendorp *et al*.,[130] which is also in favor of a BM II binding orientation at the $\alpha1+/\gamma2-$ binding site for **[XII]** than the common binding mode hypothesis claimed by Richter *et al*. [131]

Surprisingly, in the α1+/β3D2GE– mutant we did not observe any pronounced binding pose for **[XII]**. Thus, the findings of our docking study suggest that **[XII]** is lacking a preferred binding mode in the quadrauple mutant which is in line with our experimental results where we observed inactivity in the α1+/β3D2GE– mutant (Figure 49).

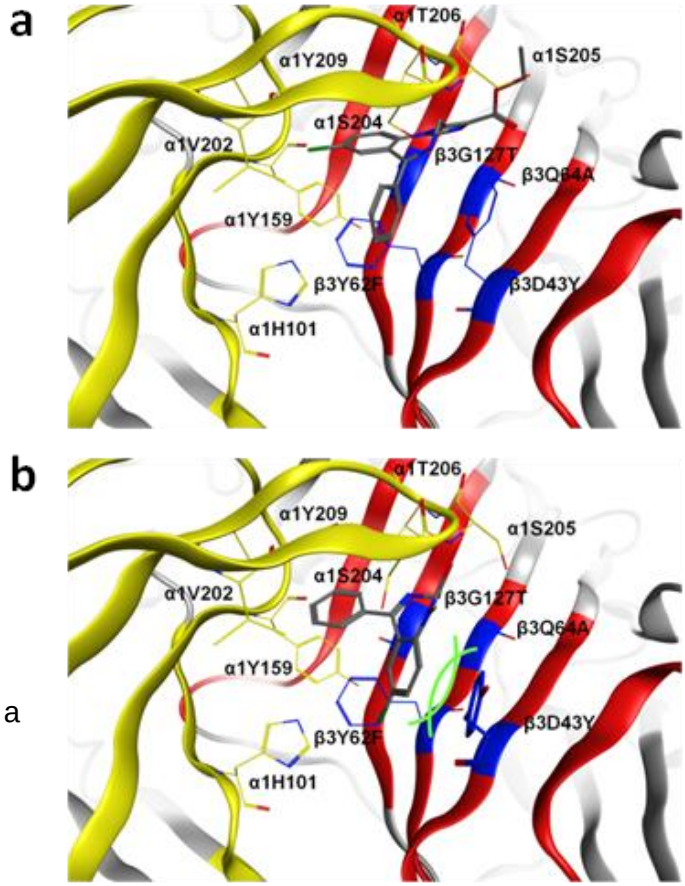

Figure 51: Distinct binding modes of Ro15-8670 [166] and diazepam [XII] in the α1β3D2GE mutant. Color cdes for the protein ribbon: α1 subunit: yellow; β3 subunit: red, conversion mutation sites: blue. **a**: BM I of **[166]** (α1 subunit, yellow; β3D2GE mutant, red); **b**: BM II of **[XII]** (α1 subunit, yellow; β3D2GE mutant, red) is sterically hindered by a severe clash between the annealed ligand fragment and β3D43Y, which is highlighted in blue. The steric clash is schematically shown in lime green.

a

Further analysis of our models revealed that the volume of the α1+/γ2– pocket is larger compared to the volume of the α1β3D2GE pocket (Figure 52a, b). The lack of activity of **[XII]** might be explained if we enforce BM II orientation in the mutant pocket which leads to severe clashes (Figure 50b). In contrast, BM I would be compatible with the mutant pocket. Thus, according to our experimental data **[XII]** and **[166]** seem to interact with the mutant pocket in significantly different ways. If we combine these observations with our docking study, we assume that the ligands use two distinct binding modes, BM I (**[166]**) and BM II (**[XII]**), which possess a sort of “pseudo symmetry” (Figure 52c).

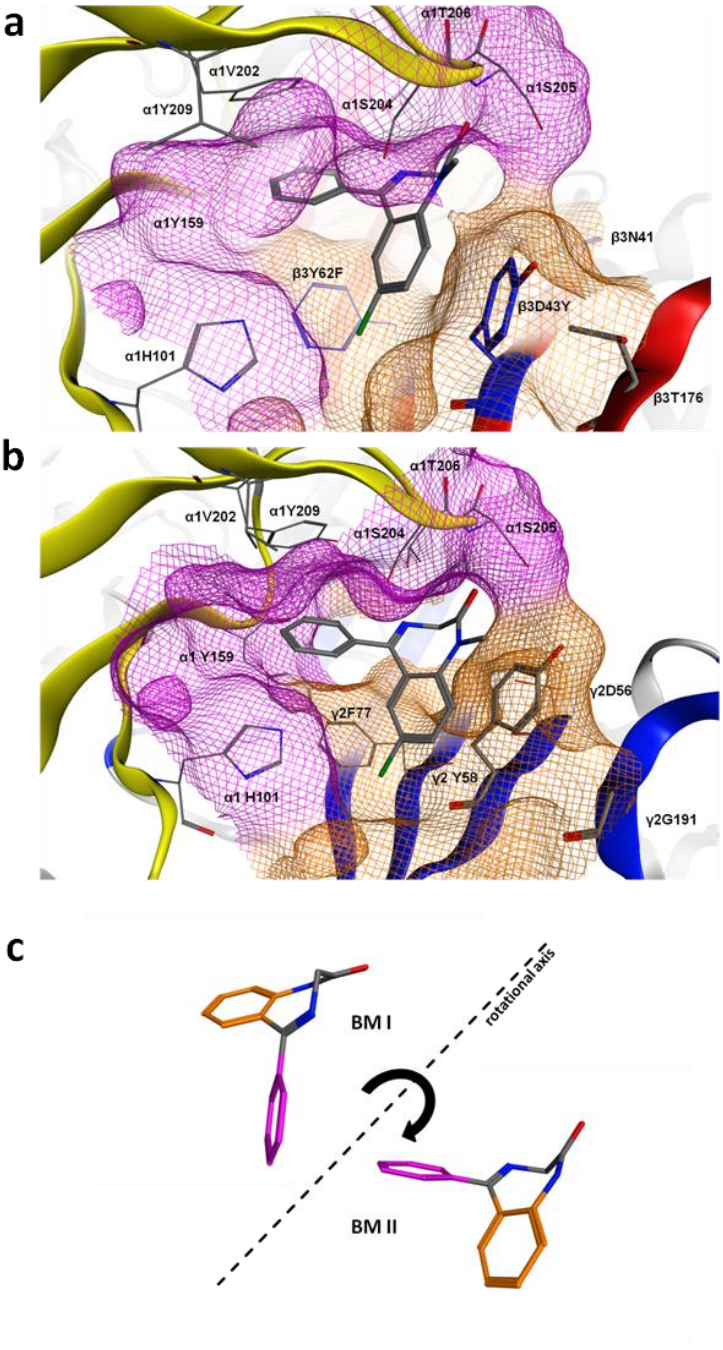

Figure 52: a,b: The panels show diazepam **[XII]** in the BM II at the α1β3D2GE and the α1γ2 interface. Additionally, the pocket surface is shown (α1 subunit, yellow; β3 mutant, red; γ2 subunit, blue; surface contributing from α1 subunit, purple lines; surface contributing from the β3D2GE or γ2 subunit, brown lines). Careful analysis of the minus side of the α1β3D2GE pocket identified residue β3D43Y to be the major determinant of the volume reduction compared to the wild type γ2- situation. Thus, we examined the rotational freedom of this residue at both minus sides using the Rotamer Explorer of MOE. In the γ2– wild type four rotamers were accessible whereas in the quadruple mutant β3 case only a single rotamer is available due to more sterically demanding sidechains in the vicinity of this residue. **c**: The pseudosymmtery is demonstrated by a rotation along the shown rotational axis after which the two aromatic phenyl rings (highlighted in pink and orange) change their place.

Moreover, compound **[165]** displayed a very ambiguous pose space at α1+/γ2– and at α1β3D2GE, whereby BM I was found as one possible orientation for both pockets. We believe that this inconclusive pose space is based on the small size of the ligand (lacking a phenyl ring) and might serve as explanation of the distinct modulatory effects of **[165]** vs **[166]** at the α1+/γ2– (null modulator) and the α1β3D2GE pocket (Figure 48a, b).

In summary, these findings comply with our experimental data and affirm our hypothesis that slightly different BZ ligands rather possess distinct binding modes than a common binding mode pattern.

C III.5 Discussion

Ligands like CGS20625 **[164]** and the pyrazoloquinolinones are able to interact with $GABA_A$ receptors *via* different binding sites which stirred us to examine their binding behavior at the $\alpha1+/\gamma2-$ interface in more detail. Here, we demonstrated a mutational approach in which we transformed the low affinity $\beta3-$ side step by step into a high affinity $\gamma2-$ side to study key determinants for high affinity binding. Interestingly, we observed a correlation between the gain of potency and two crucial amino acids in our mutant construct, namely $\beta3$D43Y and $\beta3$G127T. Inspired by this finding we sought to investigate other known BZ site ligands which should display comparable potencies in our quadruple mutant. Consequently, we chose three structurally related compounds for our further studies in our $\alpha1\beta3$(mut) receptors.

The imidazobenzodiazepine Ro15-1788 **[165]** is known to be a non-binder at the $\alpha1+/\beta3-$ interface. Surprisingly, **[165]** displayed a low potent positive allosteric modulation after the introduction of the first mutation $\alpha1\beta3$Q64A. This observation is in accordance with a proposed binding orientation of imidazobenzodiazepines requiring space in position $\gamma2$A79.[173] While the introduction of the second mutation ($\beta3$Y62F) did not show any changes, the triple and quadruple mutation led to an increase of potency and efficacy. Interestingly, its analogue **[166]** displayed modulatory effects only after the conversion of the third and the fourth amino acids suggesting that the $\gamma2$Y58 plays an important role in the overall interaction of this ligand with our mutant construct (Figure 48b). Thus, our engineered binding site apparently possesses the features which are required for four high affinity benzodiazepine site ligands to bind with high potency and to exert similar allosteric modulations on GABA currents. Counter-intuitively, the smallest ligand diazepam **[XII]** completely lacks activity at this engineered high affinity binding site.

The staggering activity differences between **[166]** and **[XII]** motivated us to re-evaluate the reported *in silico* benzodiazepine binding mode models. Our docking studies provide reasonable evidence for the contradictory experimental results by suggesting that BM I is used from larger ligands like imidazobenzodiazepines with an additional phenyl group (e.g. **[166]**). Here, the fused core moiety is presumably sandwiched between both subunits and the ester group is pointed in the direction of $\gamma2$A79 which complies with previous results (Figure 50a).[173] For **[XII]** we found BM II to be more feasible in which the fused ring system is more located towards the minus side of the pocket (Figure 50b). While BM I seemingly tolerates subtle differences between our mutant construct and the wild type $\gamma2-$ side, BM II does not.

The idea of benzodiazepine ligands utilizing distinct binding modes has been under debate in literature for a long time. In 1995 Zhang *et al*. explored the binding orientations of benzodiazepine ligands using the planar and rigid pyrazoloquinolinones as “ruler ligands” in a pharmacophore approach. This resulted in four equivalent alignments as putative orientations and based on a small experimental data set of imidazobenzodiazepines one orientation out of these four was considered as the correct one.[177] Subsequently, this led to a generalized assumption that this binding orientation is applicable for all benzodiazepine ligands and not only for structurally closely related compounds. Follow up work used these slightly misleading results to postulate a “common binding mode (CBM)” hypothesis in which the fused moiety of the scaffold is located at the same position, irrespective of the substitution pattern.[177] However, our results strongly support the binding hypothesis that **[166]** uses BM I while **[XII]** utilizes BM II at the $\alpha 1+/\gamma 2-$ site and thus we propose a rather limited common binding mode hypothesis depending on the nature of the ligands.

Moreover, we demonstrated by successively imparting $\gamma 2$-like features into a $\beta 3$ subunit that the allosteric modulation of known positive modulators, like imidazobenzodiazepines and pyrazolopyridinone chemotypes, apparently follows a highly conserved mechanism at the examined interfaces.

C IV Evaluation of PQ binding mode by SAR scoring function

The current binding hypothesis for pyrazoloquinolinones is derived from abstract ligand-based pharmacophore models which are not suitable for rational ligand design due to their low accuracy with respect to the detailed ligand-protein interactions.[143,144,157] However, a structure-based approach has not been made so far due to the lack of appropriate crystal structures. Fortunately, in 2014 the crystal structure of a human β3 homopentameric $GABA_A$ receptor was released, which serves as ideal starting point for improved $GABA_A$ receptor models.[90] In addition, huge structure-activity relationship (SAR) datasets for pyrazoloquinolinones exist which are very useful in the evaluation of binding modes.[143,144,157] Thus, we aimed to combine these features in our study and introduced a novel molecular binding protocol which utilizes SAR data in their evaluation step to tackle the elucidation of the pyrazoloquinolinone binding mode.

C IV.1 Molecular docking of CGS8216 [XXXVI]

We started our workflow with the docking of CGS8216 **[XXXVI]** into the benzodiazepine binding site of an α1β2γ2 $GABA_A$ receptor homology model. This homology model was created using the human β3 homopentameric $GABA_A$ receptor crystal structure as template.[90] Since the rotameric state of the amino acid residues in a homology model relies on the template, we performed flexible docking with GOLD considering flexible side chains as well as flexibility of the loop C by using soft potentials.[97] To avoid potential clashes we minimized the pose geometries using the software package MOE. While sampling algorithms of docking programs succeed in the exploration of the pose space to generate the correct binding mode of a ligand, there are still difficulties in the ranking process of ligand poses by scoring functions. Thus, we selected the 100 best scored poses of the CGS8216 **[XXXVI]** docking run for further evaluation.

C IV.2 Structure Activity of PQs

In the last three decades pyrazoloquinolinones were studied extensively for their promising effects at the BZ site of $GABA_A$ receptors resulting in an enormous amount of experimental as well as computational datasets.[143,144,157,178] The analysis of these data shows a quite diverse SAR landscape. On the one hand we observed strong activity cliffs in which the introduction of even small substituents led to large potency shift (positions R^5, R^6, R'^4), while on the other hand *vice versa* the introduction of large substituents led to an almost unchanged activity profile (position R^8, R^9; Figure 53 and Table 9).

In detail, an increase in Van-der-Waals volume in position R^6 by bulky substituents results in a significant loss in potency. For instance, the introduction of a CF_3 residue in position R^6 (compound **[167]**, Table 9) leads to a drop of potency by almost 4 log units compared to **[XXXVI]** (Table 9). Furthermore, methylation of position R^5 results in a considerable loss of potency (drop by 2 orders of magnitude) which could be either explained by also sterical clashes as well or by a possible prevention of a hydrogen bond formation.

Interestingly, compound **[170]** (R^8 = OCF_3, R'^4 = COOH) and compound **[175]** (R^8 = OCF_3, R'^4 = NH_2) which only differ in position R'^4, display another dramatic potency cliff (Table 9) by almost 4 orders of magnitude. For this case we are assuming a strong electrostatic repulsion in close proximity of position R'^4 by another electron rich counterpart, e.g. an aspartate.

In contrast, sterically demanding groups at positions R^8, R^9 and R'^4 are quite tolerated which results in a rather flat SAR landscape in this positions. In detail, the R^8 = *tert*butyl, $R^{8,9}$ = benzofused and $R^{7,8}$ = methylenedioxo derivatives remain highly potent (Table 9).

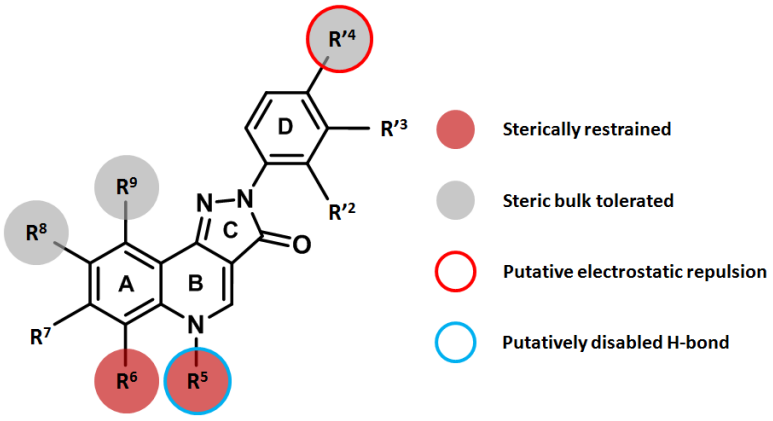

Figure 53: 2D representation of SAR landscape of pyrazoloquinolinones. The letters A, B, C and D refer to the different rings in the scaffold. The different positions and numbering of the different residues are shown by R^5-R^9 and R'^2-R'^4 respectively. Positions which tolerate steric bulk (R^8, R^9 and R'^4) are indicated by gray spheres, whereas positions which do not tolerate steric bulk (R^6) are indicated by red spheres. Electrostatic repulsion is indicated by a red frame and prevented H-bond formation by a light blue frame.

For pose evaluation we selected PQ analogous with mainly rigid substituents and which are in correspondence with the previously generated SAR landscape (compound **[167]**-**[175]**, Table 9). The correct PQ binding mode should be in accordance with the main characteristics (Figure 53): i) sterically restrained in position R^6 (compounds **[167]** and **[168]**), ii) sterically restrained and/or putatively disabled hydrogen bonding in position R^5 (compound **[169]**), iii) steric bulk tolerated in positions R^8, R^9 and R'^4 (compounds **[171]**, **[172]**, **[173]** and **[174]**) and iv) putative electrostatic repulsion at position R'^4 (compounds **[174]** and **[175]**).

Table 9: Chemical structures and binding affinities of pyrazolo[4,3-*c*]quinolin-3-ones **[XXXVI]**, **[167]**-**[175]**.

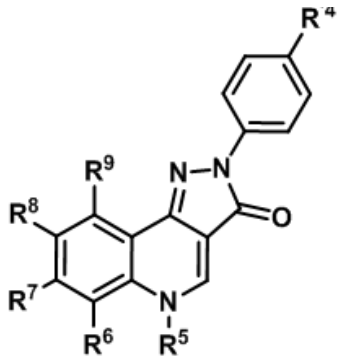

	cpd	R^5	R^6	R^7	R^8	R^9	R'^4	K_i [nM]
	[XXXVI]	H	H	H	H	H	H	0.3
Inactives	[167]	H	CF_3	H	H	H	H	2000
	[168]	H	6,7-benzofused		H	H	H	1000
	[169]	CH_3	H	H	H	H	H	1600
	[170]	H	H	H	OCF_3	H	COOH	3200
actives	[171]	H	H	H	*t*Bu	H	H	0.1
	[172]	H	H	H	8,9-benzofused		H	8.0
	[173]	H	H	7,8-OCH_2O		H	H	3.2
	[174]	H	H	H	H	H	$CCCH_3$	2.0
	[175]	H	H	H	OCF_3	H	NH_2	0.8

C IV.3 SAR guided pose selection

To evaluate our docking results we incorporated the extracted SAR landscape (Figure 53) in an automatized approach which allows a fast analysis of huge datasets of docking orientations within two steps. During the first step, called post-docking derivatization, ligand-receptor complexes of the pyrazoloquinolinones **[167]**-**[174]** were created. Thereby, the 3D coordinates of the original docking of CGS8216 **[XXXVI]** were used as template and subsequently the different substitution patterns of the other compounds were added. This resulted in a total number of 800 ligand-receptor complexes (100 orientations of **[XXXVI]** docking x 8 analogues per orientation). Based on this dataset all following analyses were made (Figure 54).

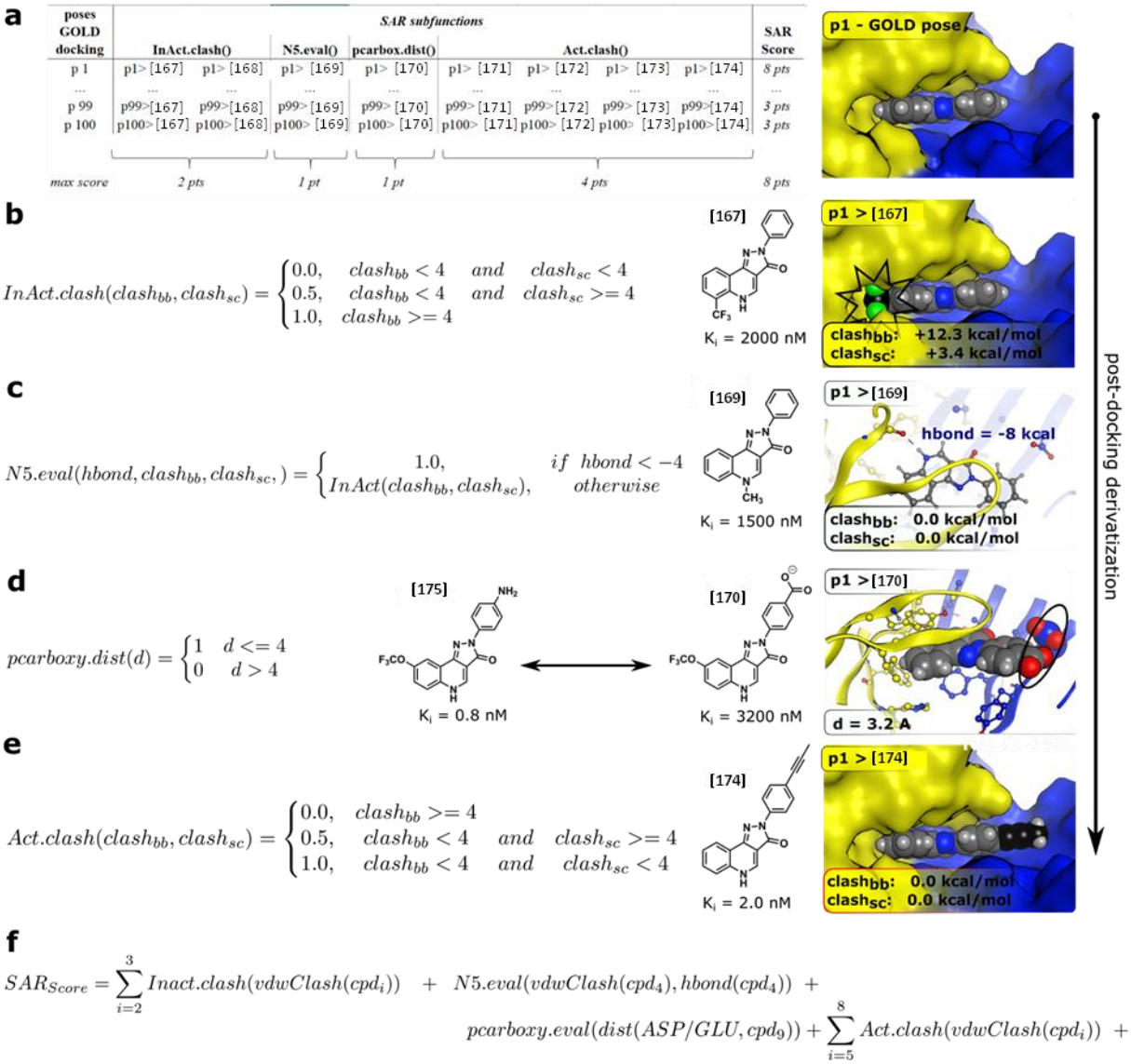

Figure 54: Illustration of SAR guided pose selection. On the left the subfuntion is given and on the right a picture of the corresondig interaction in $\alpha 1+/\gamma 2-$ ($\alpha 1$: yellow; $\gamma 2$: blue). **a:** table shows a representation of the docking poses. "P1>**[167]**" means that pose 1 is derivatized to compound **[167]** which is done for each pose and each compound. **b-e:** subfunction of the SAR scoring function with corresponding picture on the right. f: Complete SAR scoring function.

In the second step we implemented the extracted SAR data into a SAR scoring function to prioritize binding orientations which are in accordance with these data. In the evaluation process of this SAR scoring function the eight post-docking derivatized analogues served as input for each **[XXXVI]** pose (Figure 54).The congruency of the **[XXXVI]** pose with the SAR model is assessed by clash analysis, hydrogen bond interaction and distance calculations of the eight derivatized analogues. Our scoring function will add one point if the derivatized analogue aligns perfectly with the extracted SAR data resulting in a maximum SAR score of eight points.

In detail, the binary output of four subfunctions add up to the SAR scoring function: *inact.clash(), act.clash()*, *N5.eval()* and *pcarboxy.eval()*(Figure 54f). The steric hindrance information of compounds **[167]**-**[168]** (actives) and **[171]**-**[174]** (inactives) is utilized in form of calculated clash energies in the subfunctions *inact.clash()* and *act.clash()*. The clashes with rigid moieties such as backbones and C_β-atoms (clashbb) and sidechain atoms (clashsc) were evaluated differently since our process does not include an energy minimization step (Figure 54b, c and e). The huge loss of activity of compound **[169]** is considered in the subfunction *N5.eval()* which might result from a sterical clash or a disruption of a H-bond. Thus, this subfunction accounts for both, potential sterical hindrance or a loss of hydrogen bonding (Figure 54c). The last subfunction *pcarboxy.eval()* evaluates for an electronic repulsion (with either an aspartate or glutamate) which is not allowed to occur in close vicinity (< 5 Å) of the 4'-carboxylate group of compound **[170]** (Figure 54d).

C IV.4 SAR scoring identifies two candidate binding modes (BM) – BM I and BM II

Our two step approach resulted in two orientations out of 100 which had the maximum SAR score of 8 and in total 14 poses reached a score ≥ 6.

Next, we calculated the root-mean-square deviation (RMSD) distances of the ligand atoms between all orientations to visualize to whole pose space. This resulted in a 100 x 100 distance matrix which displayed a huge disparity among the derivatized poses (average RMSD = 5.5 Å, maximum RMSD = 12.7 Å). Since the similarity between the binding orientations is more important for our considerations we performed multidimensional scaling (MDS).[179] Thereby, a two dimensional grid is generated which reflects the computed three dimensional RMSD matrix as good as possible (see Methods). Consequently, we created a two dimensional representation in which similar docking poses are arranged closer to each other while dissimilar ones are distant to each other. The goodness of the MDS fit is expressed by the Kruskal-Stress value which is 0.19 for the shown MDS plot and thus in an acceptable range for the illustration of the whole pose space.[180]

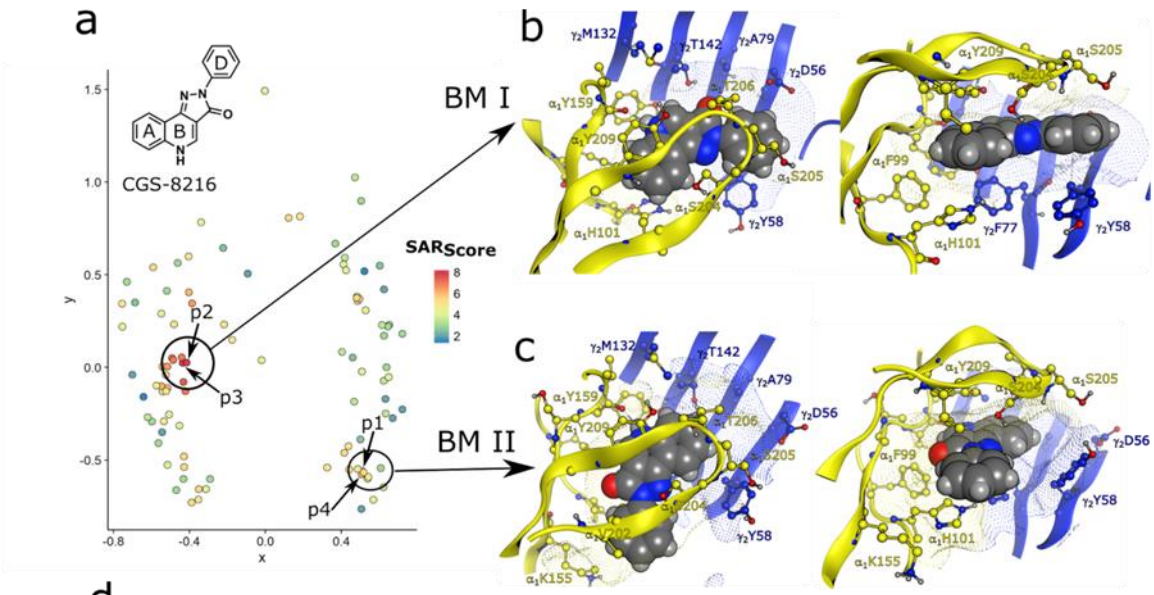

binding mode	docking pose id	[167] Inact.clash() $clash_{bb}$	[167] Inact.clash() $clash_{sc}$	[168] Inact.clash() $clash_{bb}$	[168] Inact.clash() $clash_{sc}$	[169] N5.eval() $clash_{bb}$	[169] N5.eval() $clash_{sc}$	[169] N5.eval() hbond	[170] pcarboxy.dist() d	[171] Act.clash() $clash_{bb}$	[171] Act.clash() $clash_{sc}$	[172] Act.clash() $clash_{bb}$	[172] Act.clash() $clash_{sc}$	[173] Act.clash() $clash_{bb}$	[173] Act.clash() $clash_{sc}$	[174] Act.clash() $clash_{bb}$	[174] Act.clash() $clash_{sc}$	SAR_{score}
BM I	2	12.3	3.4	4.9	2.8	0.0	0.0	-8.2	3.8	0.0	2.8	0.0	0.0	0.0	0.0	0.0	0.0	8.0
BM I	3	15.0	3.2	7.4	2.3	0.0	0.0	-8.0	4.3	0.0	2.8	0.0	0.2	0.0	0.0	0.0	0.0	8.0
BM II	1	0.2	4.8	0.0	4.1	0.0	0.0	-8.6	> 10	1.4	2.0	0.0	1.0	0.0	0.0	0.0	0.0	6.0
BM II	4	1.5	6.2	0.0	5.8	0.2	0.2	-8.0	> 10	1.4	0.0	0.0	0.0	0.0	0.0	0.0	0.0	6.0

1pt. 0.5 pt. 0 pt.

Figure 55: Identification of BM I and BM II. a: MDS plot showing similarities of different binding poses based on their RMSD. The size and the color of the dots reflect their compliance with the SAR scoring function from blue (low compliance) to red (high compliance); **b**: right BM I orientation displayed from a top and side view perspective; **c**: right BM II orientation displayed from a top and side view perspective; **d**: the four highest scored poses in an extract of scoring table are shown.

Based on this MDS plot we can group the top fourteen ranked poses with a SAR score ≥ 6 into two distinct binding modes (BM), BM I and BM II (Figure 55a-c). Geometrically, BM I and BM II differ mostly in the orientation of the rind D (Figure 53). In BM I the ring D is pointing in the direction of the $\gamma 2$ subunit while interacting with $\gamma 2$Y58 via hydrophobic and π–π interactions. Note, an aspartate ($\gamma 2$D56) is located in close proximity of $\gamma 2$Y58. In contrast, in BM II ring D is located towards the $\alpha 1$ subunit interacting with $\alpha 1$H101. Regarding the interaction profile of rings A and B we identified largely the same interactions: N5 forms a hydrogen bond with the backbone carbonyl oxygen of $\alpha 1$Y159, the quinoline core seems to be sandwiched by $\gamma 2$F77 and $\alpha 1$Y209 stabilized by hydrophobic and π–π interactions. The highest scored pose with an SAR score of 8 referred to BM I while the highest scored pose in BM II had a SAR score of 6.

C IV.5 Comparing SAR guided docking versus conventional molecular docking

After the identification of our two binding modes (BM I and BM II) using the SAR guided docking approach we were wondering if conventional docking protocols would lead to comparable results. Thus, we conducted flexible docking of **[XXXVI]** into the $\alpha 1\beta 2\gamma 2$ GABA receptor homology model using MOE 2016.08, GOLD 5.2, Schrödinger's Induced Fit and AutoDock Vina 1.1.220. The outcome of each run was ranked according to six different scoring functions: GBVI/WSA dG, London dG, ChemScore, GoldScore, Glide SP and AutoDock Vina. In the next step we compared the best orientation of the SAR guided approach (pose 2, BM I) to the best scored pose per scoring function. Interestingly, AutoDock Vina (RMSD=1.5 Å) and Induced Fit (RMSD = 2.8 Å) resulted in similar binding modes compared to our protocol while the other scoring function identified completely distinct orientations with RMSD distances greater than 6 Å.

C IV.6 Analysis of BM I and BM II in the light of SAR

Pose 2 from our previous docking showed the highest SAR score and thus was selected for the characterization of BM I. Consequently, we analyzed the 8 post-derivatized analogues **[167]**-**[174]** in this orientation. The 6-CF_3 substituted **[167]** and the 6,7-benzofused compound **[168]** displayed strong sterical clashes with the backbone of loop B (α1Y159 and α1S158) as well as with the side chain of α1F99 located on loop A. N5 methylated compound **[169]** did not show severe sterical clashes but the methylation resulted in a disruption of a strong hydrogen bond which was formed between the nitrogen of ring B and the carbonyl oxygen of α1Y159. We attribute the inactivity of compound **[170]** (8-OCF_3; '4-COOH) to its carboxylate group which is directed in the close proximity of an electronrich residue γ2D56 located in a stable beta-stranded sheet. While compound **[167]** and **[168]** are inactive due to severe sterical backbone clashes, structures **[171]**-**[174]** are active despite their bulky residues in the positions 8-*tert*buyl, 8,9-benzofused, 7,8-OCH_2O and 4'-$CCCH_3$. These compounds showed only minor to no clashes since the substituted position R^8, R^9 and R'^4 are pointing to the water exposed area outside of the binding pocket.

For BM II the highest SAR score was 7 and corresponds to pose 1 which was thus selected for characterization. Here, the substituent 6-CF_3 leads to severe clashes with the side chains of γ2M130 and γ2T142 which would explain inactivity of compound **[167]**. However, different rotameric states of the side chains could alleviate the clashes. The same rotameric adoption could relieve also the clashes for the inactive 6,7-benzofused compound **[168]** by switching the rotamers of γ2M130. Similarly to BM I, the loss of potency of the methylated compound **[169]** might be explained by the disruption of the hydrogen bond between the nitrogen of ring B and the carbonyl oxygen of α1Y159. In contrast to BM I, the inactivity of compound **[170]** lacks an explanation since the '4-COOH residue is pointed into an area of hydrophobic (α1V202) or basic amino acid residues (α1H101 and α1K155) which should result in a rather pronounced potency. Compounds **[171]**-**[174]** are again in accordance with the SAR data and perfectly fit into the binding pocket as also seen for BM I.

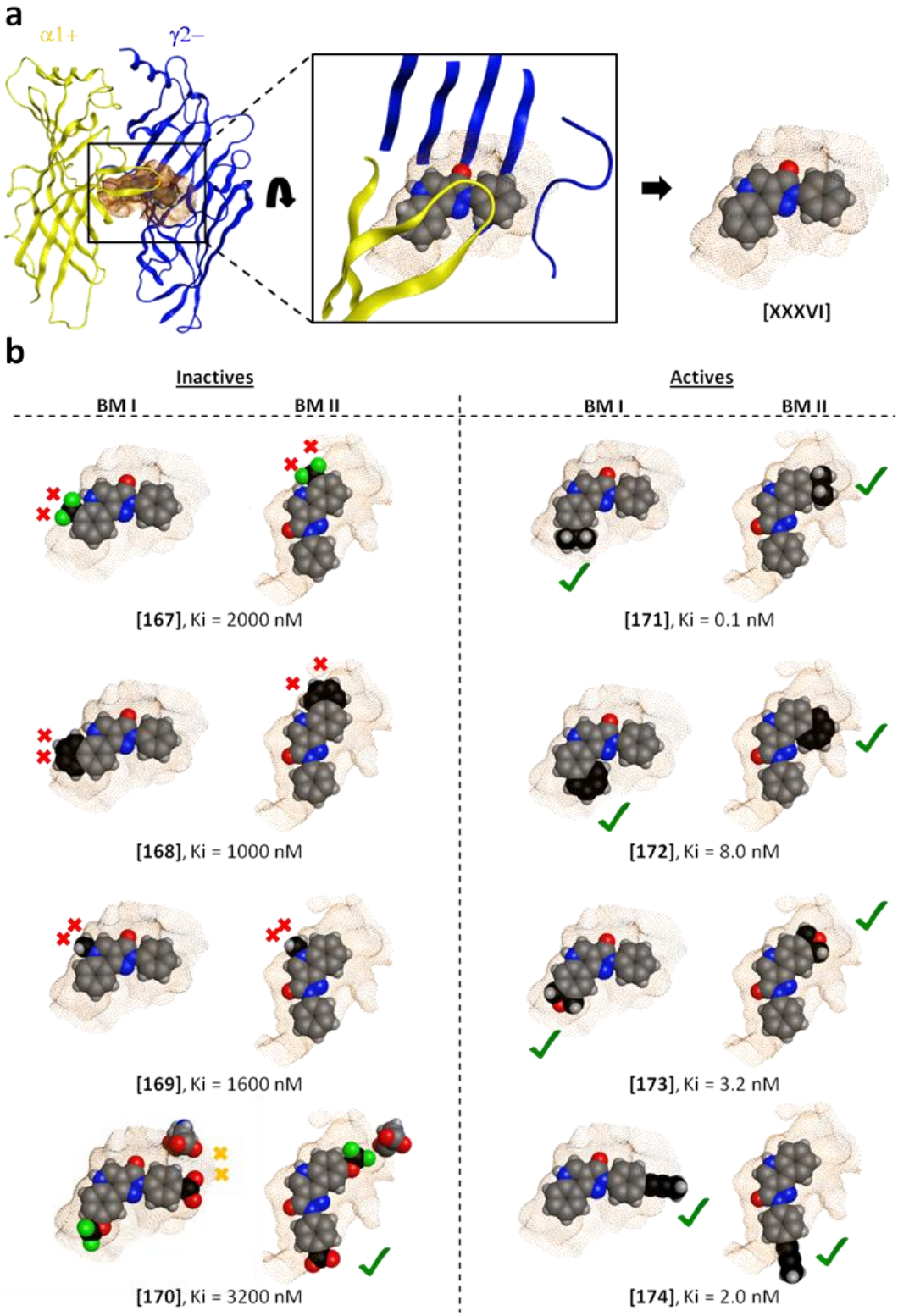

Figure 56: SAR comparison of BM I and BM II. a: Homology model of the high affinity binding site at the extracellular α1+/γ2– interface showing **[XXXVI]** in BM I orientation (α1+ = yellow, γ2– = blue, pocket surface = gold grid). Rotation to a top view and hiding of the subunits leads to a focused perspective of the ligand orientation in the pocket surface grid. **b**: Table of inactives and actives in orientations of BM I and BM II with their potencies in nM. Compliance with the pocket surface grid is displayed with green hooks and violation of the pocket surface grid is displayed with red crosses while chemical violations are indicated by orange crosses. This representation nicely demonstrates that the decisive difference between BM I and BM II is based on the interaction profile of compound **[170]**.

The evaluation of docking poses without using multiple protein structures results in an intrinsic failure of docking methods which might generate artifacts due to a bias in the scoring function.[181] In our case the algorithm disobeyed the electronic repulsion between two negatively charged residues and put the carboxylic group of compound **[170]** in close proximity of another carboxylic group in the protein. In fact, this observation represents the biggest difference between the compliances of BM I and BM II with the SAR data. To further validate this decisive point, we decided to investigate the two binding modes using molecular dynamics (MD) simulations. Recent studies just demonstrated the potential of MD simulations to adequately differentiate between correct and incorrect binding modes by assessing RMSD criteria only.[182]

C IV.7 Evaluating the stability of compound [170] and [175] in BM I and BM II by Molecular Dynamics simulations

For the MD simulations we selected two slightly distinct binding poses of BM I (pose 2 and 3) and BM II (pose 1 and 4) of compound **[170]** to have different starting coordinates. We would expect the ligand to form an instable complex in case of the correct binding mode resembling its low potency (Ki = 3160 nM). In addition, we performed MD simulations for a structural closely related compound (compound **[175]**), R^8 = OCF_3, R'^4 = NH_2) as control, which is highly potent (Ki = 0.8 nM) at the $\alpha+/\gamma 2-$ binding site. Thus, we would expect this ligand to form a stable complex during the MD simulation. The starting orientations for compound **[175]** were generated as described previously by the substituent placement from the scaffold coordinates of BM I (pose 2 and 3) and BM II (pose 1 and 4).

The stability of the poses was assessed by an adopted validation scheme as reported in literature.[182] In total we performed 80 independent MD simulations (same coordinates but different initial velocities), which means 10 MD simulations for each pose per ligand constituting a reasonable base for assumptions about ligand stability. To differentiate between stable and instable poses during either the full length or the last quarter of the MD simulation we utilized the mean L-RMSD and the number of MD simulations with a L-RMSD below a threshold of 2.0 Å. Note, with this method we cannot assess absolute binding affinities, only relative stabilities between distinct binding poses are accessible.

To describe the average of ten L-RMSD values of independent simulations we used <L-RMSD> throughout.

Table 10: Results for the MD-based stability analysis for compound **[170]** and **[175]** in BM I and BM II. The upper part of the table deals with the stability of the ligand during the MD simulations whereas the lower part describes the main interactions between the ligand and the binding site that occurred during the simulations in the different binding modes and pose. For the stability validation the average L-RMSD value (<L-RMSD>) for the 10 different simulations (sum over all L-RMSD values divided by the number) is shown as well as the number of MD simulations for which the L-RMSD value of the simulation was below 2.0 Å. The interaction analysis shows the main interaction partner for different parts of the ligand and indicates the type of interaction (hydrophobic and aromatic interaction, hydrogen bond interaction, ionic interaction).

	[170] (R'^4 = COOH)				**[175] (R'^4 = NH_2)**			
	BM I		**BM II**		**BM I**		**BM II**	
	Pose 2	**Pose 3**	**Pose 1**	**Pose 4**	**Pose 2**	**Pose 3**	**Pose 1**	**Pose 4**
<L-RMSD*>	2.3	2.6	1.7	1.9	1.5	1.7	2.4	2.6
<L-RMSD>**	2.2	2.7	1.8	2.2	1.4	1.8	2.6	2.7
< 2.0 Å§	7/10	2/10	8/10	7/10	10/10	8/10	3/10	2/10
< 2.0 Å§	6/10	2/10	7/10	4/10	9/10	9/10	1/10	2/10
AB- ring[a]	α1F99, α1H101, α1V202, α1Y209, γ2F77		γ2F77, α1Y209		α1F99, α1H101, α1V202, α1Y209, γ2F77		α1Y159, α1Y209, γ2F77	
N5-nitrogen[b]	-		-		α1Y159		-	
C-ring[b]	α1S204, γ2T142		-		α1S204, γ2T142		-	
D-ring[a]	γ2Y58		α1V202, γ2Y58, α1H101		γ2Y58		α1V202, γ2Y58, α1H101, α1F99	
Position R'^4: COOH/NH_2	γ2K184, γ2R194		α1K155, γ2R194, γ2R197		γ2D56		-	

* Full MD simulation considered
** Hast quarter of MD simulation considered
§ L-RMSD < 2.0 Å
[a] Hydrophobic and aromatic interactions
[b] Hydrogen bond interactions
[c] Ionic interactions

C IV.7.1 Stability of compound [170] (R'^4 = COOH) during the simulations

Regarding BM I, compound **[170]** appeared to be instable. When starting the MD simulations from pose 2 we observed a <L-RMSD> of 2.3 Å over 50 ns and 2.2 Å for the last 12.5 ns. Interestingly, only 3 MD simulations showed L-RMSD values above 2.0 Å but in 2 simulations we observed a high instability with L-RMSD values of 5.6 Å and 4.3 Å. In pose 3 we also observed a large movement of the ligand suggesting a rather weak stability which is resembled in L-RMSD values under 2.0 Å in only 2 out of 10 MD simulations. Compound **[170]** seems to be stable in BM II. For pose 1 the <L-RMSD> was below 2.0 Å during almost all MD simulations and for pose 4 we observed a comparable stability with a <L-RSMD> if 1.9 Å over the full length.

All in all, these data suggest that compound **[170]** is instable in BM I which is in accordance with our binding hypotheses and the biological data.

C IV.7.2 Stability of compound [175] ($R'^4 = NH_2$) during the simulations

Compound **[175]** seems to be instable in BM II. Starting from pose 1 led to a high overall <L-RMSD> value of 2.4 Å with an increasing instability towards the end of the simulation (<L-RMSD> during the last quarter of 2.6 Å). For pose 4 we observed the same trend with even higher <L-RMSD> values (overall length <L-RMSD> 2.6 Å and during the last quarter even 2.7 Å). In contrast, pose 2 and 3 showed very low <L-RMSD> values of 1.4 Å and 1.7 Å which strongly indicates a great stability of compound **[175]** in the BM I configuration. Even if we solely consider the last quarter of the MD simulation we observed low <L-RMSD> values of 1.4 Å and 1.8 Å.

Overall, BM I can be considered as stable for compound **[175]** compared to BM II which is in line with our binding hypothesis and the biological data.

C IV.8 Prospective validation of BM I by γ2D56A mutant

Next, we aimed for an experimental approach to further support our binding hypothesis and our very conclusive results of the *in silico* studies. Thus, we decided to mutate amino acid residue γ2D56 of which we suspected to have an impact on the low stability of compound **[170]** due to an electronic repulsion of the two carboxy groups in close proximity. Consequently, the mutant γ2D56A should lead to an increased potency of compounds with an electronrich carboxy group in the *para* position of ring D. Therefore, we investigated two new compounds, namely **[78]** and **[79]**, in analogy to compounds **[170]** and **[175]** which only differ in the substituent in position R^8 (Figure 57a, b) and performed binding studies.

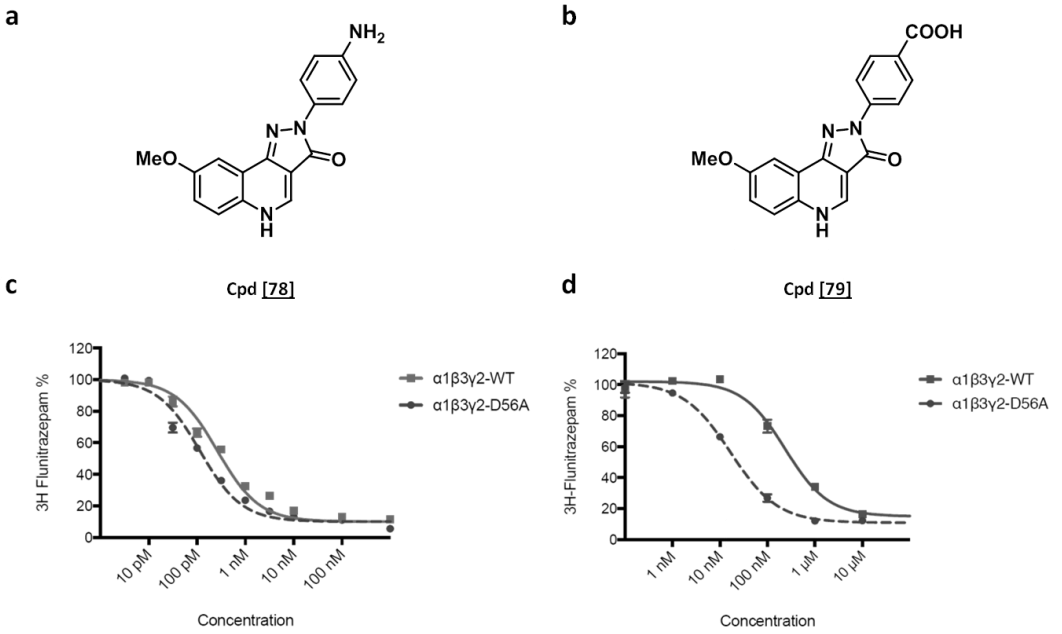

Figure 57: a,b: Chemical structures of **[78]** and **[79]**. **c**: [3H]-Flunitrazepam displacement assay of **[78]** in α1β3γ2S-WT receptors (■, K_i = 212 ± 26 pM) and α1β3γ2S-D56A mutants (●, K_i = 94 ± 5 pM) (mean ± SEM, n = 3-4). **d**: [3H]-Flunitrazepam displacement assay of **[79]** in α1β3γ2S-WT receptors (■, K_i = 126 ± 27 nM) and α1β3γ2S-D56A mutants (●, K_i = 15 ± 2 nM) (mean ± SEM, n = 3-4). Drug concentrations resulting in half maximal inhibition of specific 3H-Flunitrazepam binding (IC_{50}) were converted to Ki values by using the Cheng-Prusoff relationship.

First, we investigated our new ligands in $\alpha1\beta3\gamma2$ wild type receptors to confirm the hypothesis that compounds with a carboxylic group (here **[79]**) display a weaker binding compared to its amino analogue (**[78]**). As expected, the carboxylic analogue **[79]** showed binding affinities in the submicromolar rang (K_i = 126 ± 27 nM) whereas the amino analogue **[78]** displayed a three order of magnitude higher potency in the subnanomolar rang (Ki = 212 ± 26 pM) (Figure 57c, d). Thus, we continued to examine our compounds in the $\alpha1\beta3\gamma2$-D56A mutant.

Remarkably, the replacement of the carboxylic acid with an alanine led to an increase of potency by a factor of 8 of the carboxylic acid derivative (**[79]**, K_i = 15 ± 2 nM) whereas the

amino derivative showed only a small increase by a factor of 2 (**[78]**, K_i = 94 ± 5 pM) (Figure 57c, d). Hence, these findings further support our binding hypothesis that pyrazoloquinolinones favor BM I.

C IV.9 Discussion

Due to their promising properties as non-sedative anxiolytics and benzodiazepine-site antagonists, pyrazoloquinolinones have been extensively investigated at the $GABA_A$ receptor α+/γ- interface in the early 1980s. However, inconclusive pharmacological profiles and a rather poor solubility resulted in a lack of interest for this class of compounds.[132,133] Nevertheless, this chase led to huge SAR datasets which were utilized to generate computational models for the improvement of these interesting ligands.[143,144,157,178,183] After all, the ligand-based models were not able to conclusively explain the observed experimental data and structure-guided approaches were not available. Thus, the exploration of the PQ binding mode was left to be elucidated.

In this study, we revealed the binding mode of the former drug candidate chemotype at the $\alpha 1+/\gamma 2-$ benzodiazepine binding site of the $GABA_A$ receptor by establishing a novel docking protocol which utilizes the concordance with experimental data as criterion during the scoring process. The protocol starts with flexible sidechain docking of CGS8216 **[XXXVI]** where the 100 top ranked poses were selected for further evaluation steps. For the evaluation we extracted a SAR landscape of the PQs which reflected the most characteristic information of the enormous amount of experimental data. Based on these extracted data our scoring function was set up. Next, we examined a set of 8 compounds **[167]**-**[174]** with this protocol which led to two reasonable binding modes, BM I and BM II. While BM II failed to provide an explanation for the inactive compound **[170]**, BM I displayed compliance with the whole test set. For further evaluation we conducted MD simulations using the highly active compound **[175]** as benchmark for compound **[170]**. This experiment revealed that compound **[170]** negatively interacts with D56 (D = aspartate) of the $\gamma 2-$ side and thus showed a high instability during the MD simulations. This result additionally supported the outcome of our docking study favoring BM I over BM II. To strengthen the evidence for BM I even more we introduced a single point mutation $\gamma 2$D56A and synthesized two analogs of compound **[170]** and **[175]**, namely compound **[78]** and compound **[79]**. Remarkably, we observed for the carboxy derivative **[79]** an increase of affinity (by a factor of 8) while compound **[78]** was affected only marginally.

Overall, the conclusive *in silico* (MD simulations and docking) results in combination with the consistent experimental data (mutagenesis) strongly suggest BM I to be a reasonable binding mode for PQs at the benzodiazepine $\alpha 1/\gamma 2-$ site.

Interestingly, the former binding hypothesis from Savini *et al*.[144] (Figure 19) described the ring D of the PQ scaffold to be in a hydrophobic and rather sterically restricted area whereas our new binding hypothesis revealed a partially hydrophobic environment with additional contact to the water exposed area. This information might be of great importance for the improvement of the water solubility of pyrazoloquinolinones. For instance, the substitution of ring D with heteroaromatic rings (e.g. piperidine or morpholine) might increase the overall developability of pyrazoloquinolinones towards potential chemical probes with an increased solubility.[184]

In addition, recent studies disclosed that modulatory effects of many PQs in most $\alpha\beta\gamma$ receptors are predominantly exerted via another allosteric binding site at the $\alpha+/\beta-$ interface.[83] Functional profiling in recombinant $\alpha\beta\gamma$ $GABA_A$ receptors demonstrated that some PQs are effectively both silent and antagonistic ligands of the BZ site.[146,152] Thus, revisiting the pyrazoloquinolinones by using a structure-guided approach for the improvement towards benzodiazepine antagonists due to their sub-nanomolar affinity towards the α+/γ- interface appears to be promising. Interestingly, they lack a tendency to stronger modulate $\alpha 4$- and $\alpha 6$-containing subtypes via the $\alpha+/\gamma-$ site[178] compared to the diazepam-sensitive subtypes. Hence, they may also be suitable as antagonists for $\alpha 4,6+/\gamma-$ positive modulators such as flumazenil or bretazenil.

Ultimately, the binding pose at the $\alpha 1+/\gamma 2-$ site might provide valuable information about the binding mode of PQs at the $\alpha+/\beta-$ interfaces since the allosteric modulation at both sites seems to follow a quite conserved mechanism (see chapter C III) and the binding pockets itself are very homologous. The application of these considerations can be found in the follow up chapter C V.

C V Combining the puzzle pieces

C V.1 Revisiting α6 selectivity

The elucidation of the PQ binding mode prompted us to revisit the structure-activity relationship of our subtype selective compounds. We observed a pronounced α6β3γ2 selectivity for two different substitution patterns, R^8 + R'^3 and R^7 + R'^4, and thus wanted to know if we find a structural explanation in our models. Interestingly, we figured out that for both substitution patterns there are indeed unique structural differences (R^7: loop A = arginine (ARG), R'^3: loop C = asparagine (ASN)) in the binding pocket which are addressed by our modified ligands (Figure 58a, b). The position R^7 seems to be in close proximity of an amino acid residue located on the loop A which is different in the diazepam-sensitive α1,2,3,5 subunits (histidine = H) compared to the diazepam-insensitive α4,6 subunits (arginine = R, Figure 22). The position R'^3 seems to be directed in the vicinity of an α6 unique amino acid residue (asparagine = N, Figure 22) on the tip of the loop C.

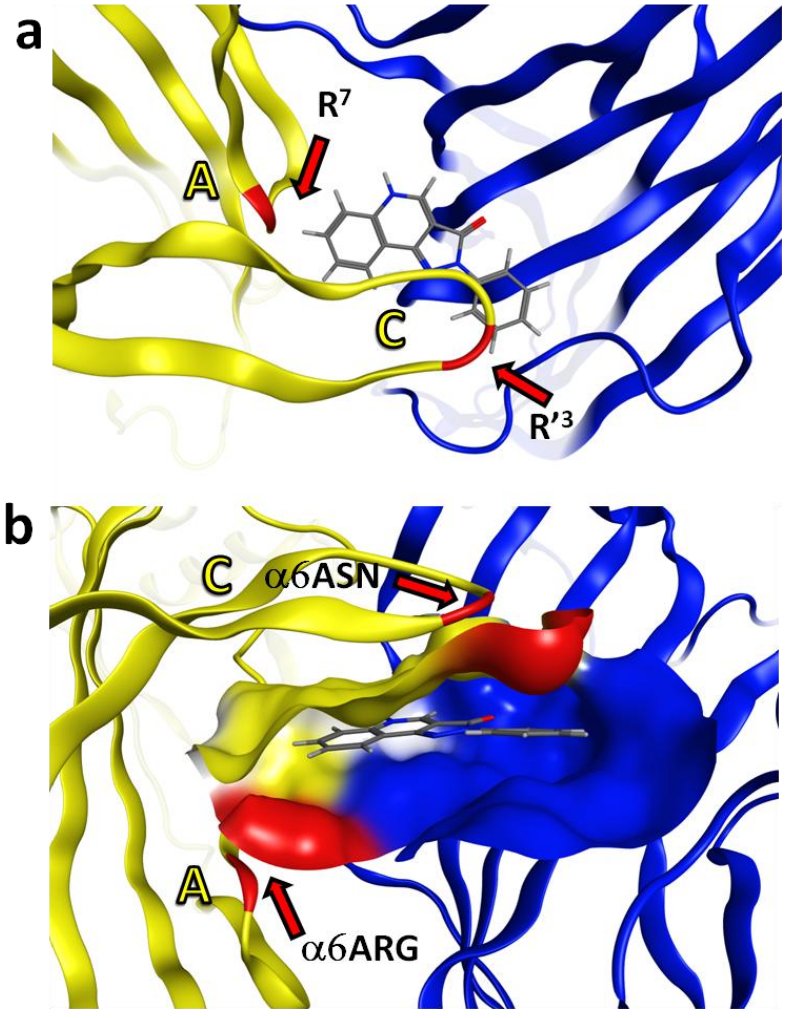

Figure 58: Pyrazoloquinolinone scaffold in BM I at the α6+/γ2– site (α6+: yellow; γ2–: blue). a: Top view of PQ in BM I showing that the positions R^7 and R'^3 are pointing in the directions of the unique amino acid residues (highlighted as red ribbon) on loop A and loop C in the binding site**. b:** Front view of the binding pocket highlighting the surface contributions of the unique amino acids of the α6 subunit (surface color code: red = unique amino acids, yellow = other α6 subunit contributions, blue = γ2 subunit contribution).

Hence, we assumed that the positions R^7 and R'^3 are the key parameters on the ligand which trigger the observed α6β3γ2 selectivity. However, due to intrinsic model inaccuracies (e.g. conformational state of the $GABA_A$ receptor in the template crystal structure) the interpretation of specific interactions with these amino acid residues should be done very carefully.

Based on these findings we synthesized a merged compound with a substitution pattern combining positions R^7 and R'^3 (**[180]** (DCBS165)). As substituents we selected the ones which displayed the highest selectivities ($R^7 = OCH_3$ and $R'^3 = OCH_3$).

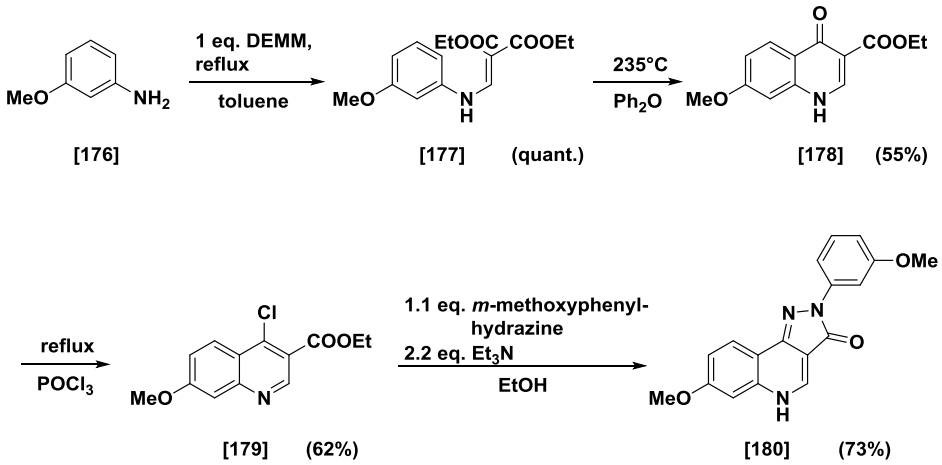

Scheme 13: Synthetic pathway of **[180]**.

The preliminary results of **[180]** in $\alpha1\beta3$ and $\alpha6\beta3\delta$ receptor subtypes revealed that there is a slight trend towards an efficacy preference for the $\alpha6$ containing receptor subtype (modulation ~240% at GABAmax) compared to the $\alpha1\beta3$ receptors (modulation ~180% at $EC_{1\text{-}3}$) (Figure 59). Compound **[54]**, which to the best of our knowledge is the best $\alpha6\beta3\gamma2$ efficacy selective compound, shows a modulation of ~300% at an $EC_{3\text{-}5}$ (Figure 37). However, to draw profound conclusions compound **[180]** has to be profiled in the same receptor subtypes like **[54]**, namely $\alpha1\text{–}6\beta3\gamma2$. This will show if this substitution pattern results in a synergistic selectivity effect or not. Nevertheless, different substituents in the positions R^7 and R'^3 might lead to an even improved selectivity.

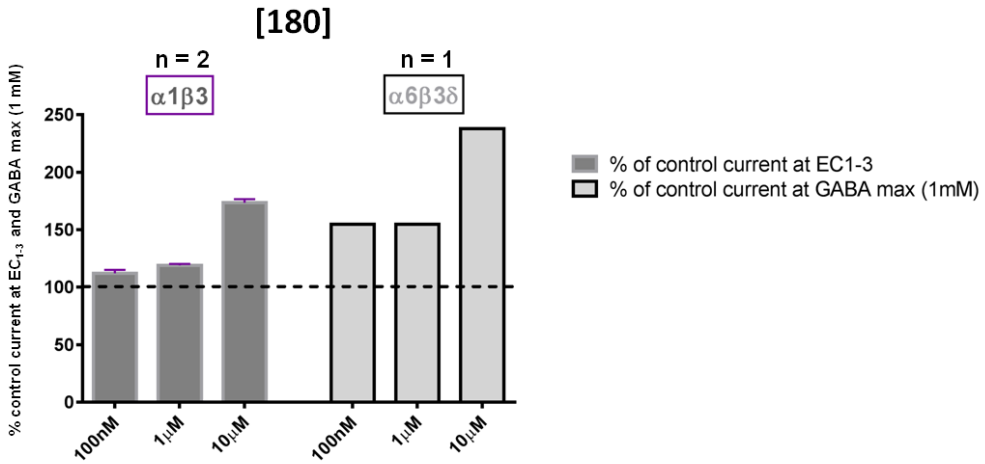

Figure 59: Preliminary biological results of compound **[180]** in $\alpha1\beta3$ and $\alpha6\beta3\delta$ receptor subtypes.

C V.2 Transferring PQ binding mode to the α+/β– interface

Since the high affinity α+/γ– and the low affinity α+/β– interfaces are very homologous we were wondering if the pyrazoloquinolinones feature a similar binding mode at these binding sites. Thus, we docked the CGS8216 **[XXXVI]** into an α1β3 binding pocket and were able to identify BM I like poses also at the low affinity binding site. Comparing the two poses in their distinct environments served as an explanation for the increased affinity at the α+/γ– interface. As shown in Figure 60a and b the main difference between the environments is below the ring D which is a rather lipophilic area at the α+/γ– site and a highly hydrophilic area at the α+/β– site. This observation originates from the amino acid residue βD43 which has presumably a major impact on the binding (Figure 60c, d). As we showed in chapter C III.2 the introduction of the β3D43Y mutant is able to induce a left shift of the apparent affinity. However, this does not represent direct evidence since the β3D43Y mutation was part of a triple mutant construct and not a single point mutation.

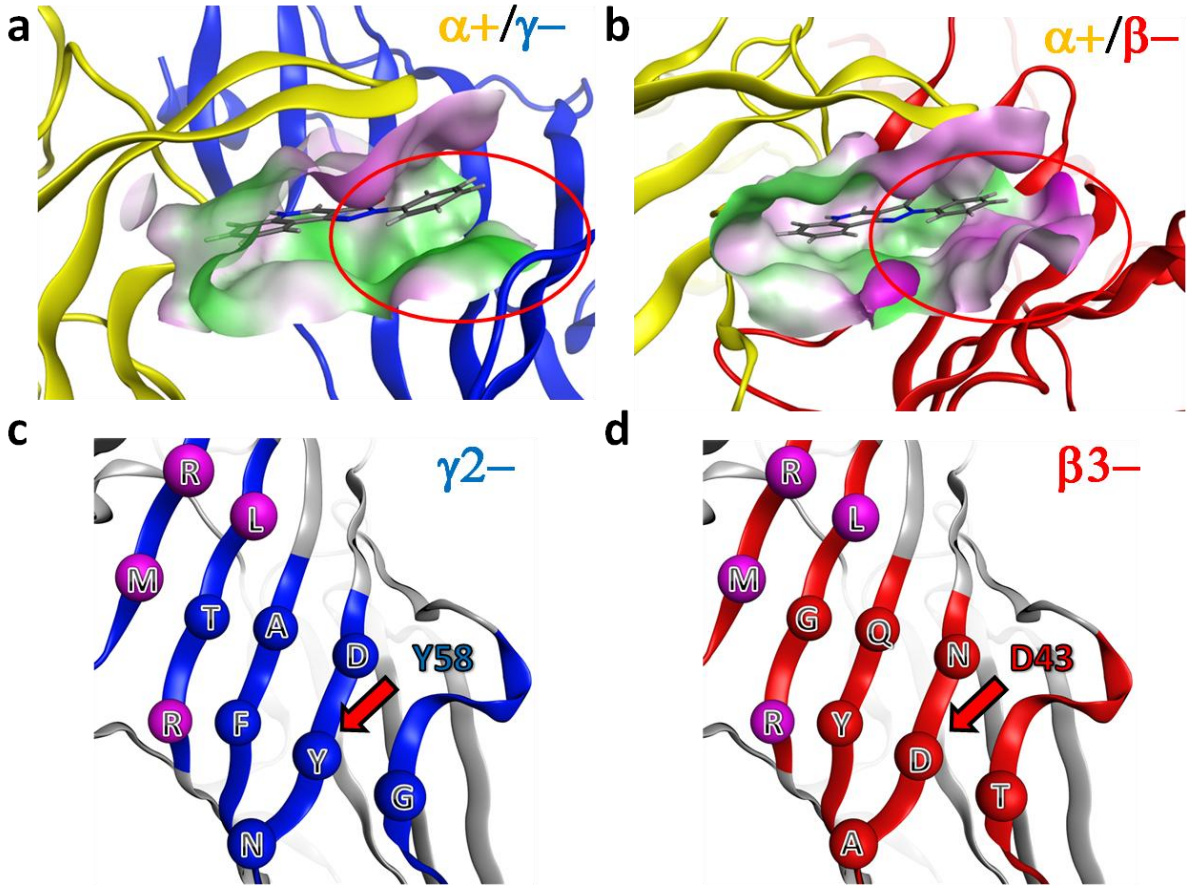

Figure 60: a: α1+/γ2- interface region (α subunit: yellow; γ subunit: blue). Ligand CGS8216 **[XXXVI]**. Surface map indicating lipophilic and hydrophilic areas (lipophilic: green; hydrophilic: purple). **b:** α1+/β3- interface region (α subunit: yellow; β subunit: red). Ligand CGS8216 **[XXXVI]**. Surface map indicating lipophilic and hydrophilic areas (lipophilic: green; hydrophilic: purple). Red oval highlights the main difference between α1+/γ2 and α1+/β3- concerning their surface area. **c, d:** Detail view of the γ2 **(c)** and β3 **(d)** minus sides. Conserved amino acids are highlighted in purple whereas unique amino acids are highlighted in either blue (γ2– side) or red (β3– side). Note that segment (loop) F of the γ2 subunit may differ considerably due to low conservation, but the amino acid that is displayed is predicted to be structurally conserved.

The rather inconclusive biological data we observed for different variations of the ring D might be explained by a tilting of the ring D due to electronic repulsion with βD43. Moreover, we demonstrated in chapter C III.2 that the mutation β3Q64A also leads to a left shift of the apparent affinity. Hence, the low affinity α+/β– binding pocket presumably might be smaller than the high affinity binding site at the α+/γ– interface. In addition, the flexibility of loop F largely differs between the β and γ subunits and will probably play a role in the ligand-binding process. However, refinement of homology models and especially of flexible loop regions remains a major issue in computational chemistry and might be resolved in future studies.[153,154]

Taking these considerations into account we propose a ligand improvement based on the knowledge about the conserved area in the β– side which will be illustrated in the next chapters.

C V.3 Ligand features – what we learned so far

Apart from our structural models we gained additional information from the ligand perspective. The current structure-activity relationship of the pyrazoloquinolinone scaffold for the α+/β– sites is outlined in Figure 61.

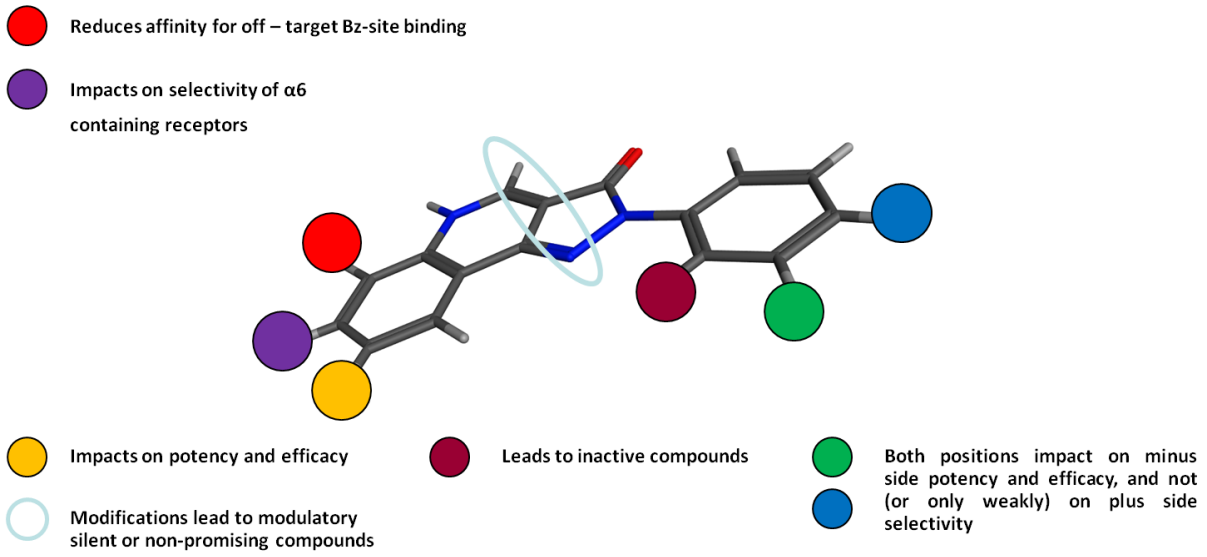

Figure 61: General representation of pyrazoloquinolinone interactions at the α+/β– interface based on our studies. Position R'^4 and R'^3 impact on potency and efficacy. Introduction of substitutes in position R'^2 leads to inactive compounds. Modifying the middle part of the core leads to non-promising compounds. Positions R^8 and R^7 impact on potency and efficacy while R^7 additionally contributes to α6 selectivity. Position R^6 reduces affinity for Bz-site.

Regarding ring D, positions R'^{3} and R'^{4} are both able to impact on efficacy and potency, whereas larger substituents in position R'^{2} lead to inactive compounds due to a putative twist of the ring D. Variations of positions R^7 and R^8 on ring A affect both potency and efficacy. In addition, certain combinations of these substituents are able to trigger potency and efficacy subtype selective behavior, e.g. $\alpha 6$ efficacy selectivity by R^7 + R'^{4} and R^8 + R'^{3}, $\beta 1$ potency selectivity by R^8 + R'^{4}. However, the variation by only small substituents does not seem to be promising for an improvement towards $\alpha+/\beta-$ selective ligands. Interestingly, the introduction of a *tert*-butyl residue in position R^6 led to a reduced affinity for the benzodiazepine binding site which is highly desired.

The triazoloquinazolindiones may be considered as further modified PQs at ring B and C (Figure 61). However, they still possess very high affinities for the BZ-site and showed very weak modulatory effects at the $\alpha+/\beta-$ site. Thus, we discontinued to investigate them as potential $\alpha+/\beta-$ selective compounds.

C V.4 Tackling $\alpha+/\gamma-$ vs $\alpha+/\beta-$

Based on our studies and the considerations mentioned above we approached the design of our ligands *via* two different strategies: 1) empirically ligand-based and 2) structure-based. Interestingly, the two strategies rest on contradictory evidence regarding their binding hypotheses. In the empirical ligand-based approach we are following a trend which showed a reduction of the off-target affinity while violating our current structure-based binding hypothesis. The introduction of especially large substituents should result in severe backbone clashes and thus lead to inactive compounds. However, as demonstrated in chapter C II.2.1 we were able to identify "compound 7" which still showed a decent modulatory activity via the $\alpha+/\beta-$ interface while lacking $\alpha+/\gamma 2-$ affinity. Combining these observations with the findings of chapter C III, where we demonstrated that similar benzodiazepine ligands feature different binding modes, we rather propose a distinct binding mode of "compound 7". Nevertheless, "compound 7" possesses the desired activity profile and thus we decided to modify the position R^6 with a variety of substituents to improve our knowledge of the observed activity profile.

C V.4.1 Empirical ligand-based approach

To explore the impact of position R^6 we introduced different halogens and alkyl residues. Since the desired properties of "compound 7" (**[138]**) are based on the very bulky *tert*-butyl residue we decided to decrease the size of this alkyl moiety from isopropyl to methyl. In addition, the introduction of halogens will shed light on the required chemical properties.

We synthesized the precursors for the halogen series and the R^6 = Me compound *via* the previously described procedures in chapter C I.1.2 (Scheme 3). Thereby, compound **[204]** could be obtained only crude eventhough it was purified by column chromatography twice. However, chlorination of the crude **[204]** yielded the pure precursor **[211]**.

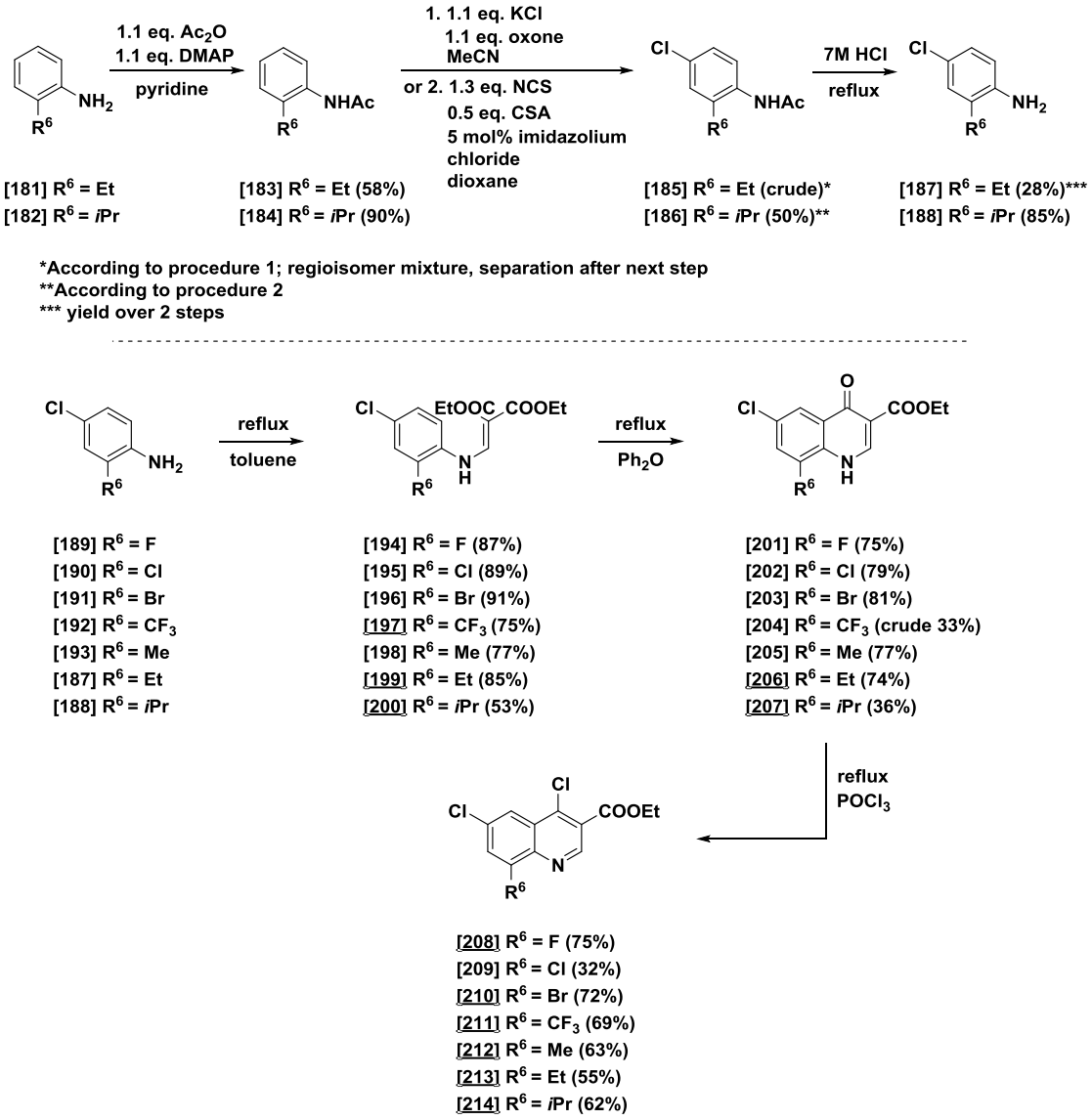

Scheme 14: Synthesis of precursors for R^6 series.

For the ethyl and isopropyl derivatives a synthetic pathway starting from the corresponding anilines **[181]** and **[182]** had to be carried out. The anilines **[181]** and **[182]** were protected by acetylation which worked almost quantitatively for **[182]** while for **[181]** a yield of 58% was obtained. Next, we aimed for a regioselective oxychlorination and tried first a procedure reported by Narender *et al*. who used potassium chloride and oxone (potassium peroxymonosulfate) as reagents.[185] We converted **[183]** using this procedure and observed the formation of one new spot after 18 h but no full consumption of the starting material according to TLC. However, we isolated the new spot by column chromatography and obtained a mixture of two compounds according to NMR and HPLC-MS analysis. We assumed the mixture to consist of the desired compound **[185]** and the *ortho* chlorinated isomer. Since the two compounds could not be separated by column chromatography we deprotected the crude mixture using 7M HCl and were able to isolate the pure para-chlorinated compound **[187]** in 28% yield over 2 steps. Based on these results, we tried a different procedure reported by Chen *et al*. to obtain **[186]**.[186] Here, 1,3-bis(1-isopropyl)imidazolium tetrafluoroborate was used in combination with *N*-chloro-succinimide (NCS) to selectively chlorinate different acetylated aniline derivatives. Thus, we converted **[184]** under the reported conditions and were able to isolate the desired compound **[186]** in 50% yield. After deprotection of **[186]** in 7M HCl the required R^6 substituted *para* chloroaniline **[188]** was obtained for the conversion to the corresponding chlorinated precursors.

In the last step the chlorinated precursors **[208]**-**[214]** were converted to the final R^6 substituted pyrazoloquinolinones in generally moderate yields (Scheme 15). The usual work up was applicable for six of the final compounds using water to precipitate the product and subsequent collection by filtration. However, compound **[218]** could not be isolated *via* this procedure due to an increased solubility in water. Thus, we tried to purify **[218]** by column chromatography even though we knew from former trials that PQs tend to stick to silica. Nevertheless, we were always able to isolate sufficient amounts of PQs after column chromatography. Here, we started with a mixture of 5% MeOH in CH_2Cl_2 as eluents and increased it to 30% MeOH in CH_2Cl_2. However, we were not able to flush **[218]** from the column. Consequently, we opened the column and tried to extract **[218]** directly from the silica by using different solvents (MeOH, EtOAc, CH_2Cl_2, Et_2O and DMSO). The highest amounts of **[218]** were obtained using MeOH and DMSO which could easily be detected by intensity of the coloring of the organic solvent (dissolved **[218]** possesses yellow color). NMR analysis revealed that the extraction with DMSO led to a purer mixture of **[218]** and unknown impurities while extraction with MeOH led to a very impure mixture of **[218]** and unknown impurities. After extraction of 10 mg crude **[218]** it was further purified by HPLC. Unfortunately, we were not able to isolate the pure compound **[218]** *via* this route and thus it needs to be resynthesized with an improved workup protocol.

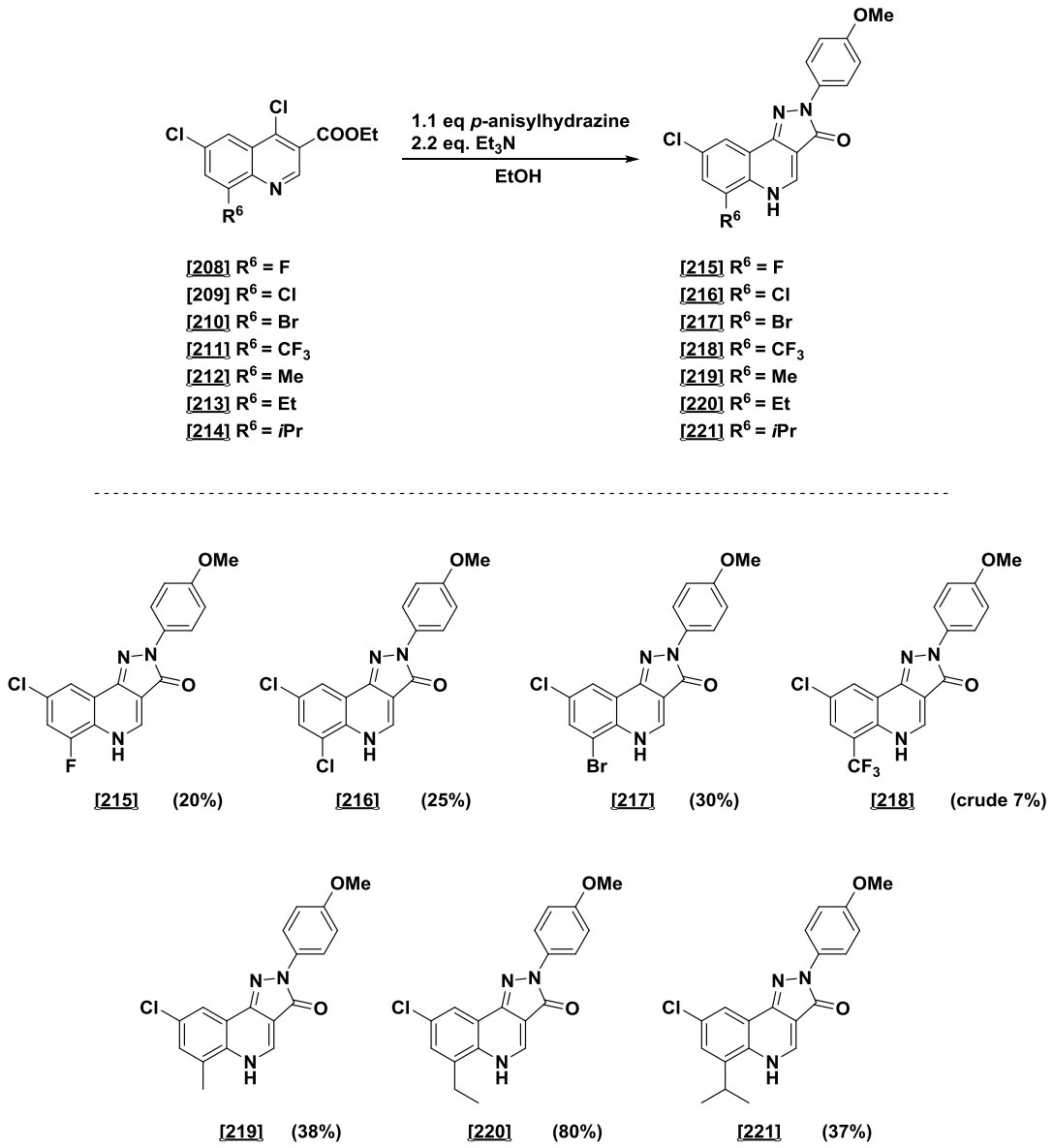

Scheme 15: R^6 substituted series of PQs to explore off-target affinity.

Overall, we were able to synthesize a set of R^6 substituated chloro-methoxy PQs which are about to be investigated for their affinities at the $\alpha+/\gamma 2-$ site as well as for their modulatory effects at the $\alpha+/\beta-$ sites.

C V.4.2 Structure-based approach

Based on our binding hypothesis for the α+/β− and α+/γ2− interfaces, ring D of the pyrazoloquinolinone scaffold should point in the direction of the β subunit while rings A and B of the scaffold are directed towards the α subunit. In detail, ring D is presumably in close contact with γ2Y58 which corresponds to the βD43 constituting the main difference between the β and γ2 subunits in close proximity of the ligand. In addition, further evidence was already reported by the study in chapter C II.2.1[141] in which we observed that the effects of our ligands, which differ only at position R'[4], are strongly influenced by the mutant α1β3N41R compared to the α1β3 wild type. Thus, exchanging the ring D with another moiety which either reduces the interaction with γ2Y58 or exclusively interacts with βD43 might result in highly selective α+/β− ligands.

First, we tried to reduce the π–π stacking interactions of the ring D with γ2Y58 by introducing electron deficient aromatic ring systems. Here, we synthesized (see synthetic route C I.1) three different compounds possessing a pyrazine moiety instead of a phenyl ring. Additionally, their corresponding reference substances were synthesized (reference substances of **[224]** and **[225]** existed) to compare the effects of the modified ring D (Scheme 16).

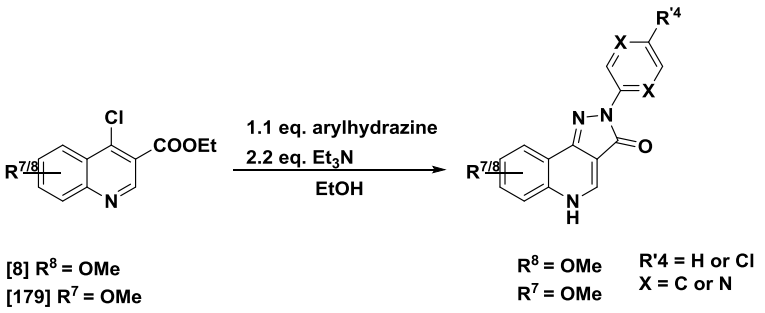

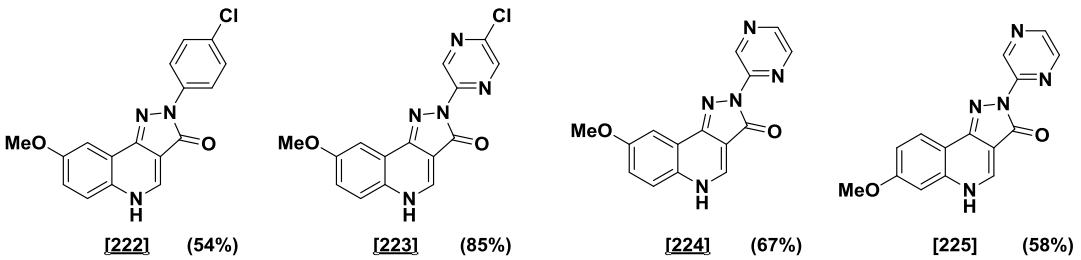

Scheme 16: Synthesis of electronpoor pyrazoloquinolinones **[223]**, **[224]**, **[225**] and the reference compound **[222]**.

In a second approach we aimed to replace ring D with a non-aromatic ring system possessing more basic nitrogens to directly address the acidic βD43 amino acid. We thought of introducing either a piperazine or diazepine ring for this purpose. Due to the asymmetry of a putative piperazine hydrazine derivative which will require a more complex asymmetric synthesis strategy we decided to aim for the 7 membered diazepine ring system. Before planning the synthesis we performed a docking of the desired ligand into the α1+/β1− site and identified very promising BM I like poses (H-bond of N5 with α1Y159) which even showed a salt bridge interaction of the diazepine ring with β1D43 (Figure 62).

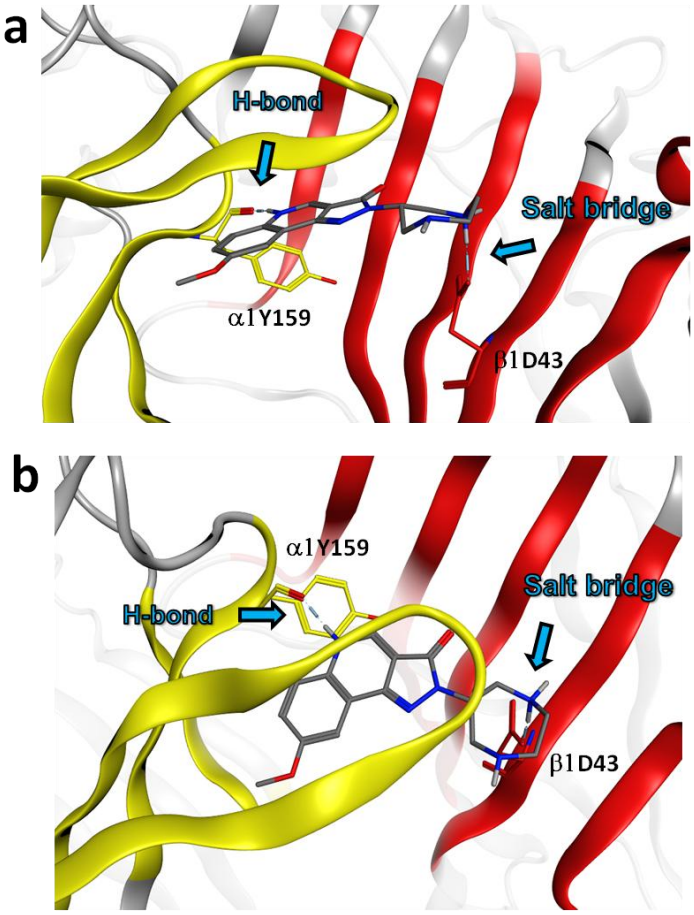

Figure 62: Docking pose of 7 membered diazepine compound into the α1+/β1− site. The α1 subunit is shown in yellow and the β1 subunit in red. Orientation of the desired ligand corresponds to BM I pose and shows very promising interactions with α1Y159 and β1D43 (highlighted in cyano).

Based on this docking pose we performed a retrosynthetic analysis of the desired compound **[226]** to plan the synthesis accordingly. The first cut was made according to the classical pyrazoloquinolione synthesis which splits the compound **[226]** into a chlorinated precursor **[227]** and a hydrazine derivative **[228]**. The chlorinated precursor **[227]** can easily be synthesized analogously to the route in chapter C I.1.2 while the hydrazine **[228]** should be accessible *via* two different ways. One possibility is using a functional group interconversion to the corresponding hydrazone derivative **[229]**. The hydrazone is accessible from the ketone **[230]** which can be synthesized by oxidation of the alcohol **[232]**. The second possibility is *via* classic nucleophilic substitution of the leaving group "X" in compound **[231]** which is as well accessible from the alcohol **[232]**. The ring formation to the diazepine alcohol **[232]** can be carried out using a protected diamine **[234]** which is converted with an *in situ* generated epoxide. This leads to ethylenediamine **[235]** and 2,3-dibromo-1-propanol **[233]** as commercially available starting materials (Scheme 17).

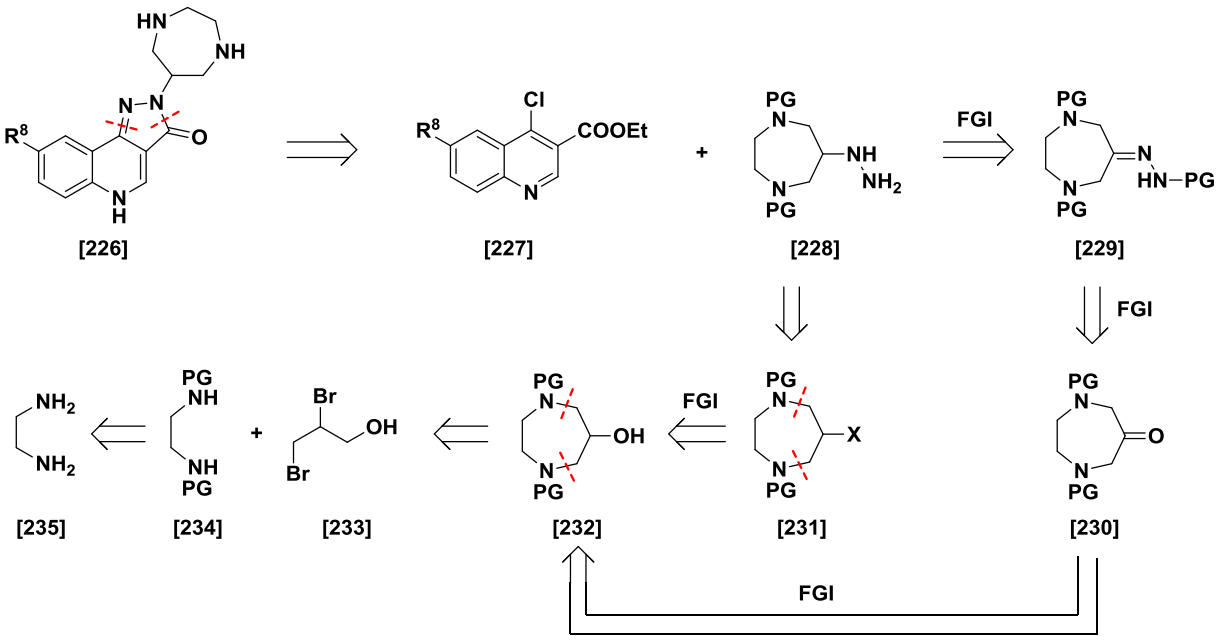

Scheme 17: Retrosynthetic analysis of the desired 7 membered ring derivative.

For the forward synthesis we found a synthetic route to the tosyl protected compound **[232]** and thus started according to this procedure.[187] First, we protected ethylenediamine **[235]** using tosyl chloride to obtain compound **[236]**. After this double protection step we regenerated the nucleophilicity of the amide-nitrogens in **[236]** by deprotonation employing sodium methoxide. Then an epoxide was generated *in situ* by addition of **[233]** to an ethanolic potassium hydroxide solution. After addition of the sodium salt a selective epoxide opening occured which led to the desired compound **[237]** in 50% yield (Scheme 18).

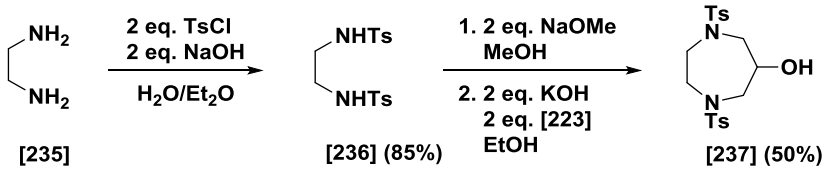

Scheme 18: Synthesis of compound **[236]**.

Next, we transformed the hydroxyl group of **[237]** into a leaving group by converting the alcohol with mesyl chloride yielding compound **[238]** in 72%. First, we tried to convert **[238]** using 3 eq. *tert*-butyl carbazate in DMF to the desired product **[239]**. However, after 72 h no conversion was observed. Consequently, we tried to favor the nucleophilic substitution reaction by changing to a polar protic solvent (EtOH) and using slight basic conditions by adding Et_3N. After 72 h again no conversion was observed. In the last attempt we used the free hydrazine which is more nucleophilic than the *tert*-butyl carbazate in EtOH to obtain compound **[240]**. However, after 48 h at room temperature and additional 24 h at 100 °C we did not observe any conversion and thus discontinued this approach.

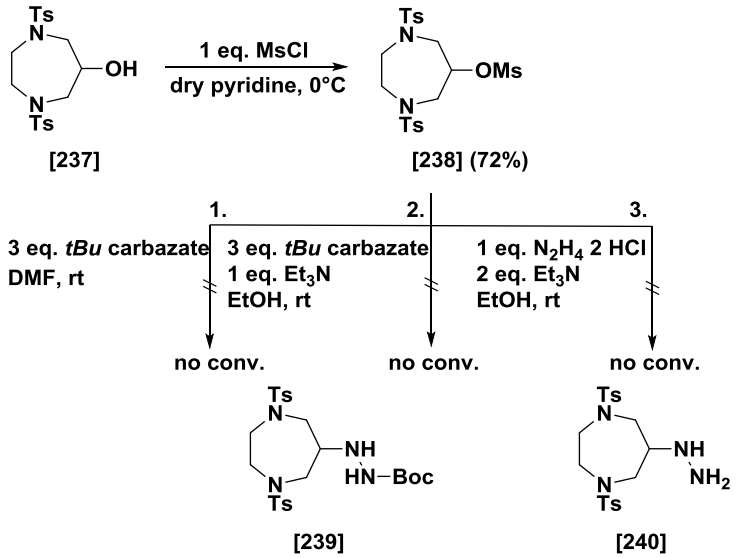

Scheme 19: Nucleophilic substitution of **[238]**, no conv. = no conversion.

The second synthetic route *via* oxidation and a reductive amination like reaction should yield the desired hydrazine building block **[228]** for the formation of the pyrazoloquinolinones **[226]** (Scheme 17). To obtain keton **[241]** different oxidation reagents were investigated: Dess-Martin periodinane (DMP), 2-iodobenzoic acid (IBX) and TEMPO in combination with sodium hypochlorite (Scheme 20).

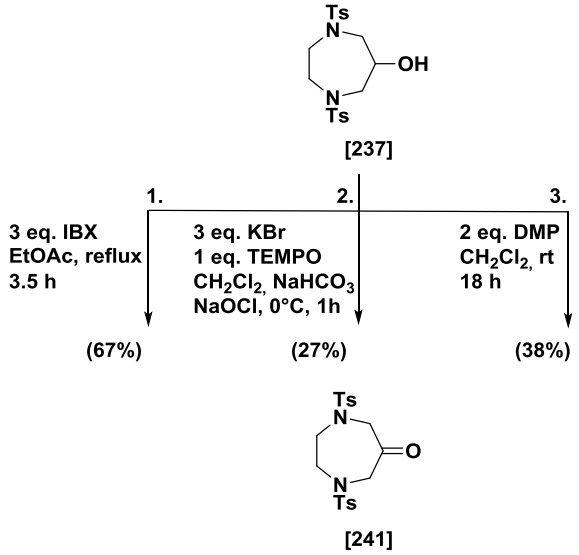

Scheme 20: Oxidation of **[237]** to the desired keton **[241]**.

While entries 2 and 3 resulted in low yields entry 1 gave the desired product **[241]** in moderate yields of 67%. The low yield of entry 2 might be explained by its biphasic reaction mixture which seems to be unfavorable for compound **[237]**. The reaction using DMP as oxidation reagent worked spot to spot on TLC. However, the separation of the desired product **[241]** by column chromatography and the formed iodinane led to a large mixed fraction which explains the low yield of 38%.

Next, we attempted to conduct a reductive amination like reaction with keton **[241]** using sodium triacetoxyborohydride and catalytical amounts of acetic acid in CH_2Cl_2 (Scheme 21). However, under these conditions we only obtained the hydrazone derivative **[243]** in low yields which seemed to be unreactive. Hence, we synthesized separately hydrazone **[243]** under slightly acidic conditions in moderate yields and investigated the reduction step to the hydrazine derivative **[242]** (Scheme 21).

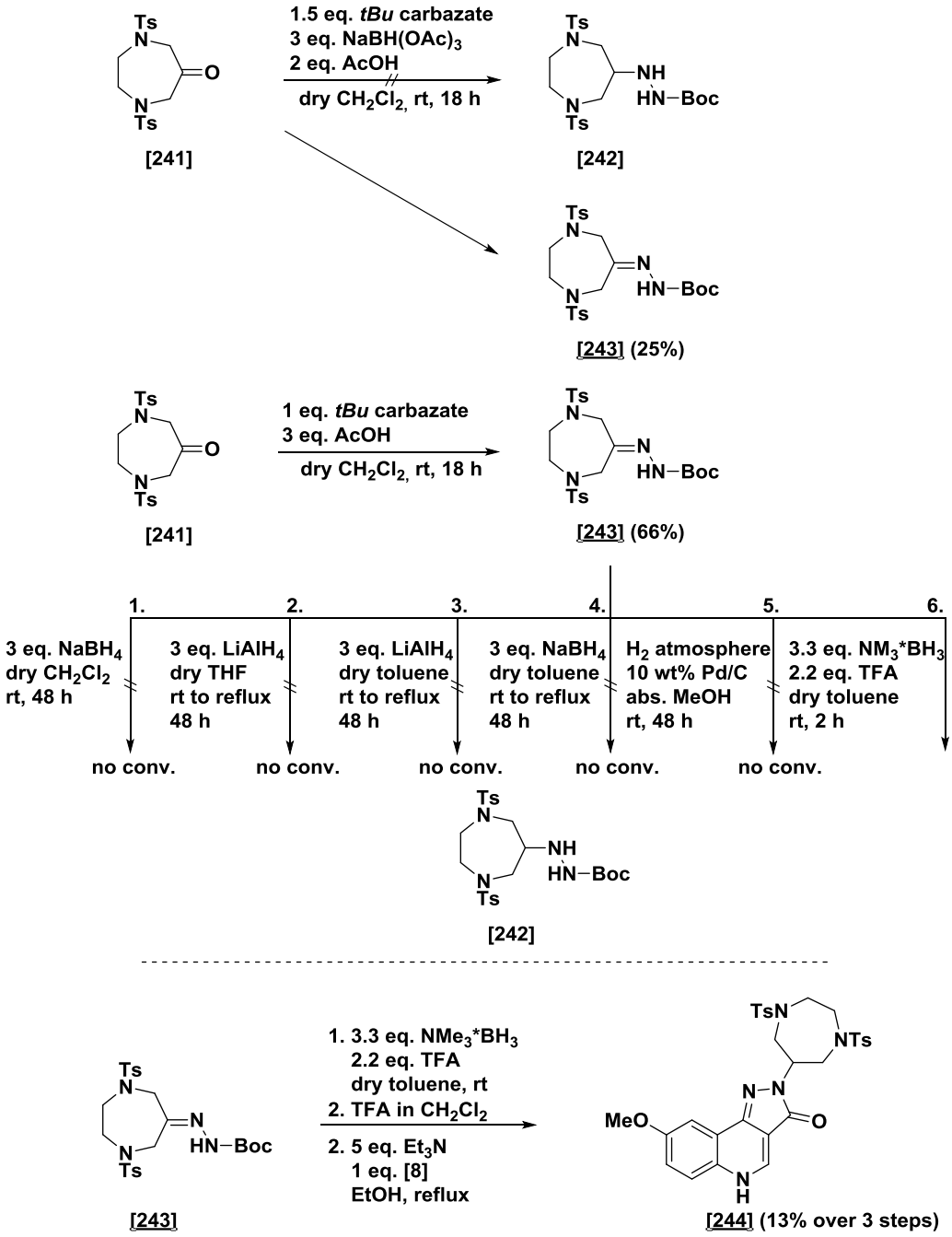

Scheme 21: Optimization of the synthesis of compound **[244]**, no conv.= no conversion.

For the reduction we examined 6 different reaction conditions varying from soft reducing reagents ($NaBH_4$) and low temperatures to strong reducing reagents ($LiAlH_4$) and high temperatures (entries 1-4, Scheme 21). However, the variation of these parameters failed to

yield the desired compound. Next, we tried to use palladium on charcoal to reduce the double bond which showed no conversion according to TLC as well (entry 5, Scheme 21). Since the first 5 entries are basically heterogeneous systems we tried a homogeneous reducing system as described by Perdicchia *et al*.[188] They reported a procedure using an amine-borane complexe, which is stable under acidic conditions, and gaseous HCl in toluene. Thus, we tried to convert our hydrazone **[243]** under these conditions using TFA as strong acid instead of gaseous HCl. This approach led to full conversion of the starting material **[243]** which could be monitored by TLC using toluene/EtOAc = 2/1 as eluents (note: using PE/EtOAc the starting material **[243]** and the hydrazine **[242]** have the same R_f value). Due to TFA we observed partial deprotection of the Boc group which prompted us to *in situ* cleave the Boc group completely. Thus, we evaporated the reaction mixture, added a mixture of TFA/CH_2Cl_2 =1/4 to the residue and stirred the solution for 45 min. After completion the solvents were evaporated and the crude product was directly converted with **[8]** using 5 eq. Et_3N in EtOH. After purification by HPLC the desired compound **[244]** was obtained in a yield of 13% over three steps (Scheme 21).

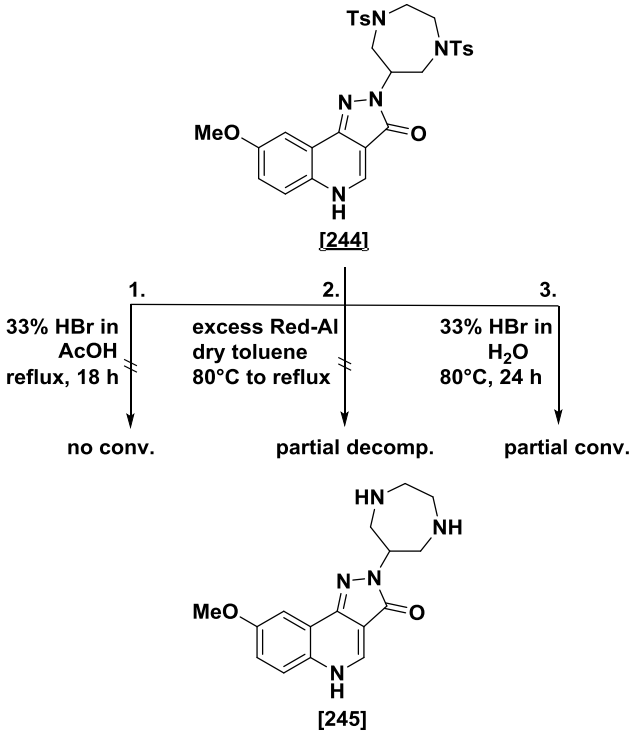

Scheme 22: Cleavage of the tosyl group, no conv. = no conversion, partial decomp. = partial decomposition, partial conv. = partial conversion.

The final step was to cleave to tosyl group which is usually conducted under harsh conditions (Scheme 22). The first attempt was made using 33% HBr in acetic acid which after 18 h at reflux did not show any conversion according to TLC and HPLC. The next attempt was made using Red-Al (sodium bis(2-methoxyethoxy)aluminum hydride) which led to partial decomposition of the starting material **[244]**. Possibly, the Red-Al reduced the carbonyl

moiety which induced the decomposition of the starting material. Interestingly, by using 33% HBr in H_2O we observed conversion of the starting material **[244]** to the mono deprotected compound (according to HPLC-MS) and the desired compound **[245]**. However, we were not able to push the reaction to full conversion. Since, we ran out of material and the cleavage of the tosyl group turned out to be difficult, we decided to resynthesize the compound while using a protecting group which is easier to cleave and possessing comparable stability with respect to the established synthetic route. Thus, we chose the nosyl protecting group and started to protect the diamine **[235]** under the same conditions as reported for the tosyl group to obtain **[246]** in 88% yield. Next, we formed the sodium salt and converted it subsequently to the 7 membered alcohol **[247]** in good yields (Scheme 23).

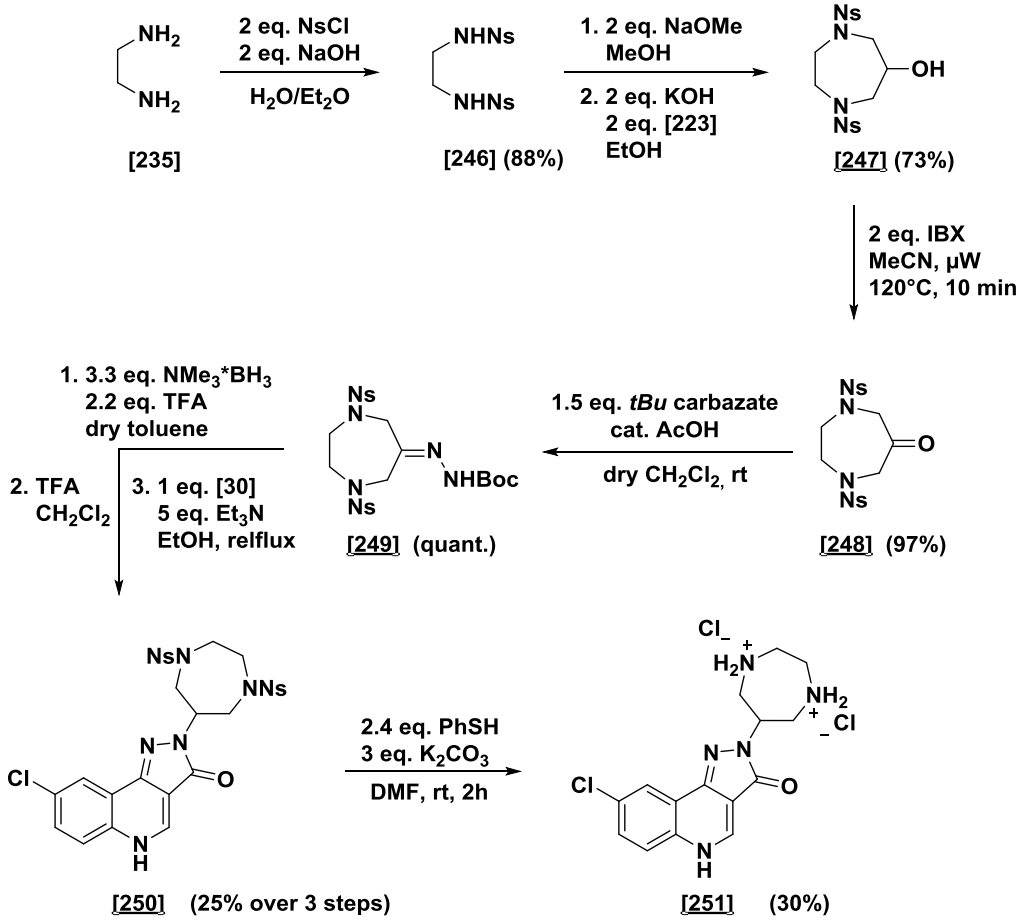

Scheme 23: Synthesis of the 7 membered ring derivative **[251]**.

The oxidation step was further optimized by using acetonitrile as solvent. Here, after 10 min at microwave irradiation the desired compound **[248]** was obtained in quantitative yields after simple filtration over silica using acetonitrile as eluent. The subsequent formation of the hydrazone **[249]** was achieved in quantitative yields, as well. To form the pyrazoloquinolinones core we used the procedure already reported in Scheme 21 (entry 6) which, after subsequent deprotection and conversion with **[30]** led to the desired product

[250] in acceptable yields of 25% over 3 steps. The deprotection of the nosyl group was carried out under mild conditions using thiophenol under slight basic conditions at room temperature (Scheme 23). According to TLC the reaction was finished fast and we observed full conversion of the starting material **[250]** after 2 h. The reaction mixture was rinsed with 20 mL H_2O and neutralized to extract the desired compound. However, after the aqueous layer was extracted three times with EtOAc a yellow precipitate was formed in the aqueous layer. HPLC-MS analysis revealed that the precipitate possessed only the mass of the desired compound **[251]** while in the organic layer a lot of impurities and desired compound were detected. Thus, the precipitate was collected by centrifugation and analyzed by powder diffraction which indicated contamination of NaCl within the precipitate. Hence, the solid was dissolved in MeOH and the residual solid was removed by centrifugation. The methanolic solution was treated with 2 M HCl in ether which led to precipitation of the desired compound **[251]** as HCl salt in 30% yield. Since the organic layer was not further purified we ended up with a moderate yield which is acceptable until we have first results of the biological evaluation.

All in all we were able to establish a synthetic route to synthesize the 7 membered ring derivative **[251]** in an over all acceptable yield.

C V.4.3 Preliminary pharmacological profiling of [251]

The first preliminary results of the promising compound **[251]** in $\alpha1\beta3$ receptor subtypes showed a modulatory silent behavior. Since the elicited modulation (efficacy) and the affinity (potency) of a compound are two different measures, this does not exclude **[251]** from being a high affinity binder at the $\alpha+/\beta-$ interfaces. Thus, co-application experiments with a compound binding to the $\alpha+/\beta-$ interfaces (e.g. PZ II 028) are required to confirm if **[251]** is a binder or a non-binder for these interfaces.

In addition, the pharmacophore of **[251]** differs from the classical benzodiazepine site pharmacophores which might enable to explore new structures representing highly potential binders for the $\alpha+/\beta-$ interfaces with novel pharmacological properties (see chapter C V.4.4).

C V.4.4 Prospective scaffold hop, putatively new structures

Although, the preliminary biological results of compound **[251]** were not promising, we performed pharmacophore modeling and virtual screening to explore new scaffolds which might be active at the α+/β– interface using LigandScout since the computational effort was reasonable.[189] Here, we used the structure of compound **[245]** which differs from **[251]** only in position R^8 (OMe vs. Cl) since the original docking was performed with **[245]**. We created two different pharmacophore models following on the one hand a structure-based approach (based on the binding pose of **[245]** shown in Figure 62) and on the other hand a ligand-based approach (starting from the structure of **[245]** only). For the virtual screening we used the Sigma Aldrich Database (7.4 million compounds) since the compounds should be commercially available.

C V.4.4.1 Strcture-based pharmacophore modeling and virtual screening

First, we tried to use the pharmacophore model which was created from the docking pose of **[245]** (Figure 63a) without any modification which resulted in no hits after the screening. Thus, we set one of the positively ionisable groups on the ring D as well as the aromatic interaction of the ring A optional (Figure 63b).

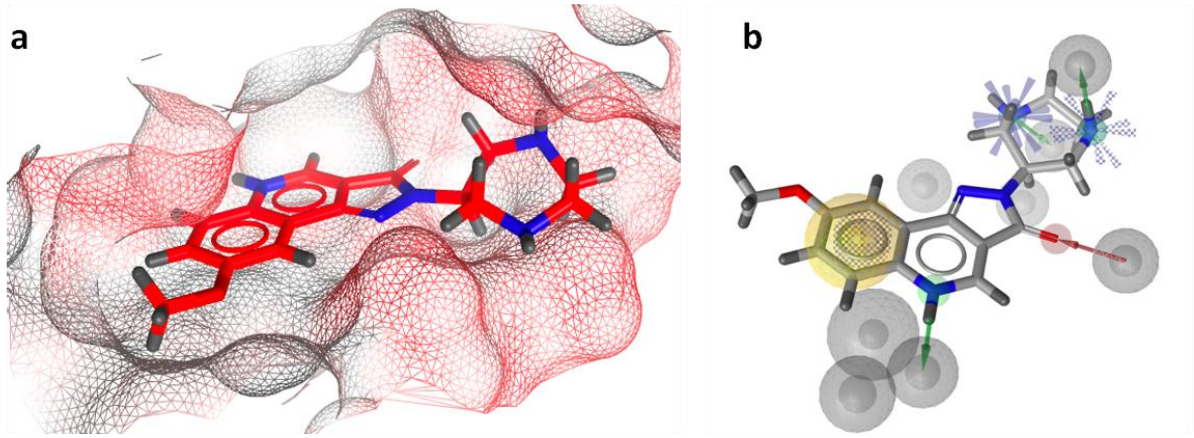

Figure 63: Structure-based pharmacophore modeling of compound [245]. a: Docking pose of **[245]** at the α+/β– interface (compare Figure 62). The polar surface is highlighted in red whereas the apolar surface is highlighted in grey. **b:** Structure-based pharmacophore model of **[245]** with two features being set optional. Shown features: yellow sphere: hydrophobic interaction, green arrow: hydrogen bond donor (vector), red arrow: hydrogen bond acceptor (vector), blue asterisk: positively ionisable group, blue ring (ring A): aromatic interaction, grey spheres: steric bulk, optional features: indicated with transparency.

This led to a variety of hits which were filtered using the following selection criteria: excluding “rule of five”[190] outliers, excluding sterically too demanding compounds based on empirical reasoning, focusing on hits with positively ionisable groups due to putative interaction with βD43, preferably scaffolds with fused ring systems. This led to a final selection of four compounds **[252]**-**[255]** which were redocked at the α+/β– interface using Autodock Vina 4.2 (implemented in LigandScout) (Figure 64).

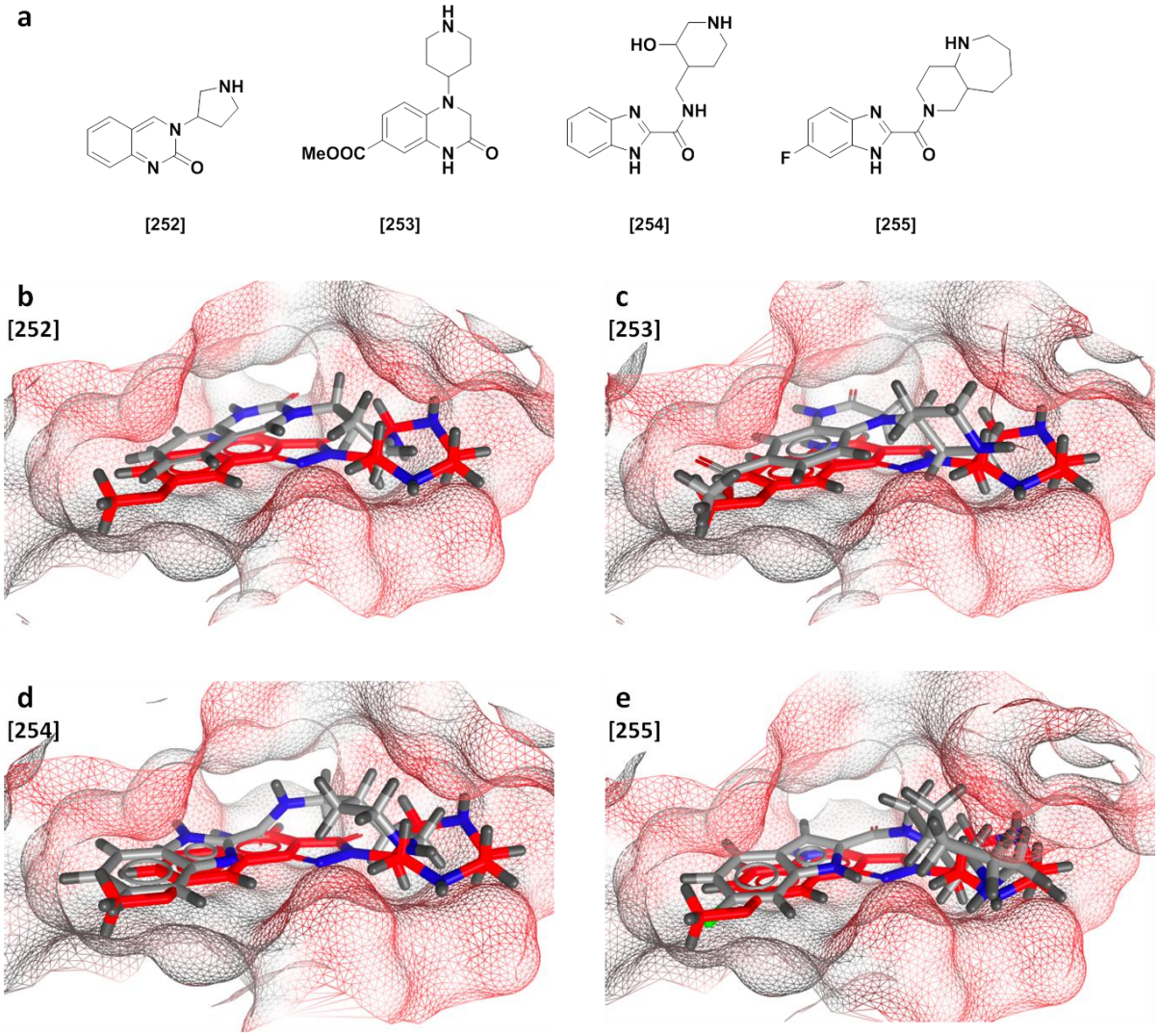

Figure 64: Virtual screening results of the structure-based approach. a: New putatively active structures **[252]-[255]** for the α+/β– interfaces. **b-e:** Superposed binding poses of **[252]-[255]** (grey) with **[245]** (red) after redocking with Autodock Vina 4.2. Polar surface areas are highlighted in red whereas apolar surface areas are highlighted in grey.

C V.4.4.2 Ligand-based pharmacophore modeling and virtual screening

In the ligand-based approach we first screened the library using the unmodified pharmacophore model of compound **[245]**. However, this again resulted in obtaining no hits. Thus, we set three features optional: one positively ionisable group at ring D, the aromatic interaction of ring B and the hydrogen bond acceptor interaction of the methoxy residue in position R^8 (Figure 65).

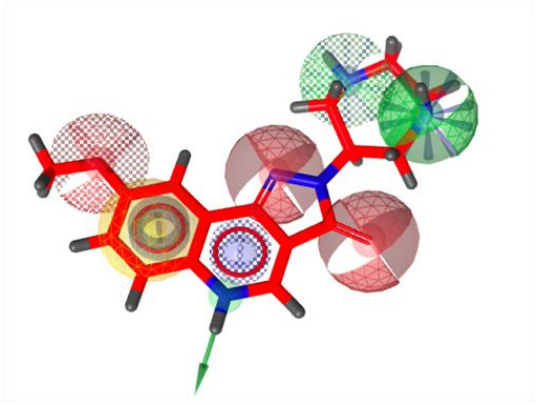

Figure 65: Ligand-based pharmacophore modeling of [245]. Ligand-based pharmacophore model of **[245]** with three features being set optional. Shown features: yellow sphere: hydrophobic interaction, green arrow: hydrogen bond donor (vector), green sphere: hydrogen bond donor without direction, red sphere: hydrogen bond acceptor without direction, blue asterisk: positively ionisable group, blue ring (ring B): aromatic interaction, optional features: indicated with transparency.

Following the procedure mentioned in chapter C V.4.4.1 we identified four compounds **[256]**-**[259]** as new putative ligands for the α+/β– interface (Figure 66).

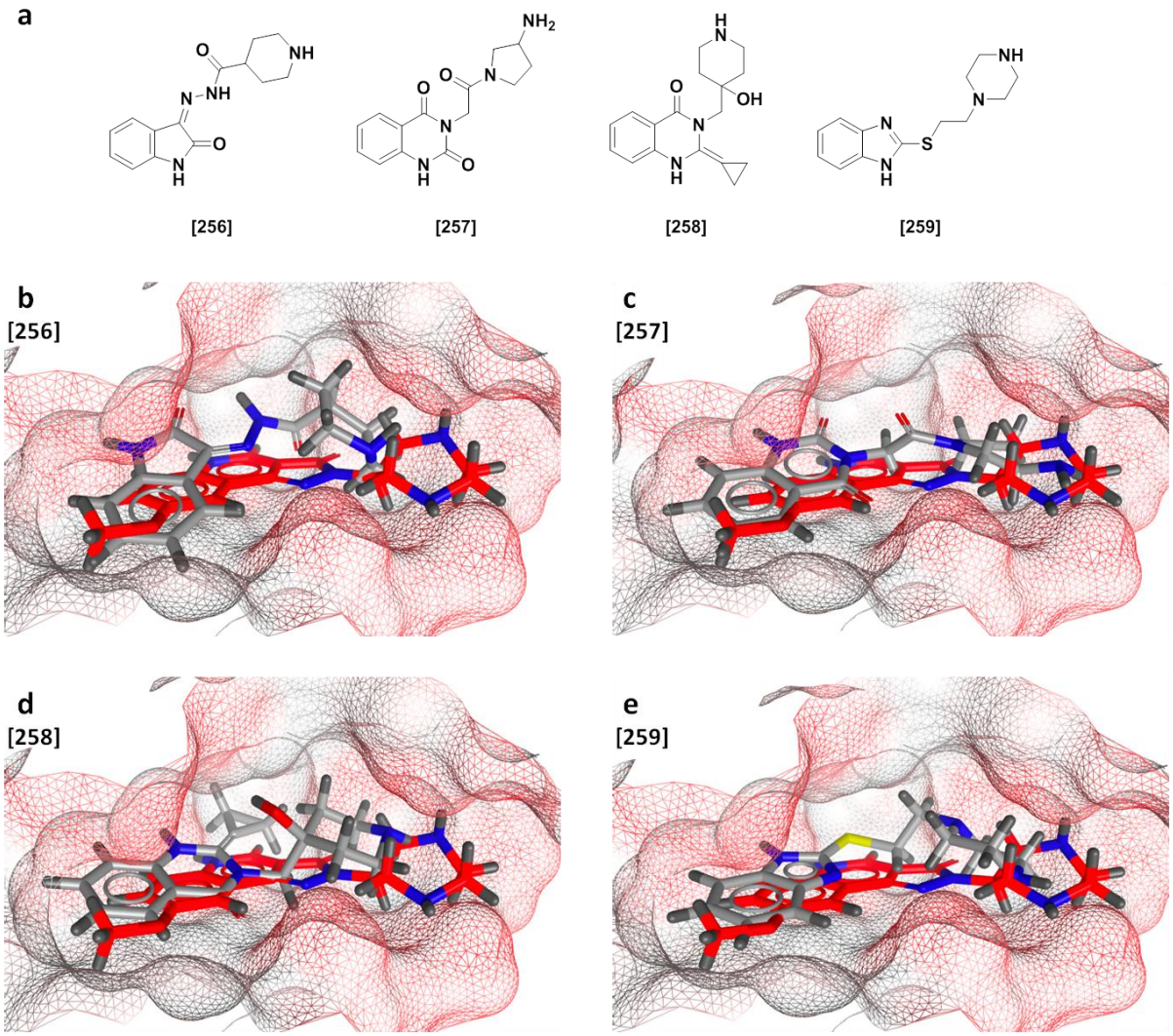

Figure 66: Virtual screening results of the ligand-based approach. a: New putatively active structures **[256]-[259]** for the α+/β– interfaces. **b-e:** Superposed binding poses of **[256]-[259]** (grey) with **[245]** (red) after redocking with Autodock Vina 4.2. Polar surface areas are highlighted in red whereas apolar surface areas are highlighted in grey.

Overall, we were able to identify 8 new putative scaffolds which might be active at the $\alpha+/\beta-$ interface using a pharmacophore modeling approach in combination with a virtual screening based on the compound **[245]** (parent compound of **[251]**). The compounds should be commcercially available which allows a rather fast pharmacological profiling. Future studies will reveal if the compounds turn out to be suitable as new scaffolds with promising properties at the $\alpha+/\beta-$ interface exclusively.

D Conclusion and perspective

$GABA_A$ receptors are ligand-gated ion channels which play an important role in neurotransmission. *Inter alia*, they are associated with many CNS functions such as sleep and wakefulness or learning and memory. Dysfunctions may lead to diseases like epilepsy or anxiety disorders.[18] These pentameric assemblies are composed of different subunits (six α, three β, three γ, three ρ, one δ, one ε, one π and one θ) which results into a wide range of diverse pharmacological properties.[191] In spite of years of research, the precise mechanism of the allosteric modulation (e.g. *via* the $\alpha+/\gamma-$ and $\alpha+/\beta-$ interfaces) remained still obscure.

In this thesis we focused on an improvement of the understanding of the molecular rules which underlie subtype selective allosteric modulation at the $\alpha+/\gamma-$ and $\alpha+/\beta-$ interfaces of $GABA_A$ receptors by applying synthetic chemistry, computational chemistry and electrophysiology.

Based on previous studies[146,152] we synthesized a systematic library of ring A and ring D modified pyrazoloquinolinones which are known to bind at both the $\alpha+/\gamma-$ (high affinity) and the $\alpha+/\beta-$ (low affinity) interface to study their pharmacological profiles.

In chapter C II we identified two subtype selective compounds, namely compound **[138]** and compound **[54]**. While compound **[138]** represents a proof of concept in the development of compounds preferentially interacting (potency selectivity) with the $\alpha1+/\beta1-$ site[141], compound **[54]** constitutes an improved prototype towards $\alpha6\beta3\gamma2$ efficacy selective ligands.[192] Furthermore, a mutational study strengthened the main site of modulatory action of PQs to be at the extracellular $\alpha+/\beta-$ site after Maldifassi *et al*.[140] reported evidence in favor of a transmembrane binding site of PQs. In addition, a substitution at the *ortho* position of ring D led to inactive compounds while the introduction of a *tert*-butyl residue in position R^6 of ring A resulted in a significant loss of off-target binding site activity ($\alpha+/\gamma-$ site).

The synthesis of a small set of triazoloquinazolinediones was described in chapter C I.2 and their preliminary biological effects were examined in chapter C II.3 and C II.4. While the whole set showed a rather modulatory silent profile at the $\alpha+/\beta-$ sites, they displayed very high affinities at the $\alpha1+/\gamma2-$ sites as reported by Nilsson *et al*.[148] Interestingly, we identified compound **[131]** as high affinity binder for $\alpha6$-containing $GABA_A$ receptors and thus representing a potential lead candidate for the development of novel benzodiazepine site antagonists.

Chapter C III outlined a comparison of the homologous extracellular high affinity ($\alpha1+/\gamma2-$ site) and low affinity ($\alpha+/\beta-$ site) binding sites. Here, a successive mutational approach was applied to reveal that the allosteric modulation of known positive allosteric modulators (e.g. imidazobenzodiazepines and pyrazolopyridinone chemotypes) presumably follows a highly

conserved mechanism. Furthermore, we found evidence that some benzodiazepine site ligands possess rather different binding modes than a common binding mode as proposed by Richter *et al*.[131]

The elucidation of the pyrazoloquinolinone binding mode at the $\alpha1+/\gamma2-$ binding site in chapter C IV represented a crucial step in this project. By establishing a new protocol called "post docking derivatization" which evaluates docking poses based on their concordance with experimental data and using MD simulations we were able to identify one reasonable binding pose, namely BM I. Further evidence for BM I was found by the introduction of the point mutation $\gamma2$D56A which led to an 8 fold increased affinity of the rather inactive compound **[79]**. This binding mode objects the ligand-based binding hypothesis of PQs by Savini *et al*.[144] and may thus represent an interesting starting point for a potential comeback of PQs as chemical probes *via* a structure-guided approach.

In the last chapter C V we combined the results of the previous chapters and demonstrated the consistency of the PQ binding mode at the $\alpha1+/\gamma2-$ site with current functional data of PQ derivatives. Furthermore, due to the high local homology of the two binding sites we transferred the binding hypothesis of the high affinity $\alpha1+/\gamma2-$ site to the low affinity $\alpha1+/\beta-$ site to design compounds exclusively interacting with the $\alpha+/\beta-$ sites. Here, we followed on the hand a hypothesis derived in chapter C II (modification of position R^6 of ring A) and on the other hand a hypothesis based on our structural approach. The structural approach resulted in compound **[251]** for which we successfully established a synthetic pathway. First preliminary results of **[251]** revealed a modulatory silent behavior in $\alpha1\beta3$ receptor subtypes which does not exclude the binding of the compound to the $\alpha+/\beta-$ interfaces. In future studies the binding or non-binding of **[251]** to the $\alpha+/\beta-$ interfaces will be elucidated.

Ultimately, based on the structural features of compound **[251]** we performed pharmacophore modeling and virtual screening to explore new active scaffolds for the $\alpha+/\beta-$ interfaces. In total we were able to identify 8 promising scaffolds which can be considered as potential candidates for the $\alpha+/\beta-$ interfaces.

Overall, the identification of two new subtype selective ligands (chapter C II) in combination with improved computational models led to a more structure-based understanding of subtype selective allosteric modulation. However, since only the $\beta3-$homopentameric $GABA_A$ receptor crystal structure[90] is resolved the accuracy of the models does not suffice to work in a predictive manner.

Besides the already mentioned findings in the main chapters, we should focus on the development of $\beta1$ efficacy selective compounds which is outlined in chapter C II.2.2. Here, compounds **[57]** and **[85]** showed very promising results. In addition, we investigated a set of triazoloquinazolinediones as putative $\alpha+/\beta-$ ligands which showed only a very low

modulatory activity in the investigated receptor subtypes. However, due to their enormously high affinity to the BZ site they might be interesting as potential BZ site antagonists for $\alpha 4,6$ containing receptors. The improved understanding of the binding of benzodiazepine ligands at the $\alpha+/\gamma 2-$ interface turned out to be additionally of great importance for the understanding of the binding of pyrazoloquinolinones at the homologous $\alpha+/\beta-$ interface. Future studies will reveal if the current binding hypothesis of compound **[251]** holds true or if the modifications of R^6 might turn out to be more promising in the design of $\alpha+/\beta-$ selective ligands.

E Experimental part

E I Methods – computational part

E I.1 Homology modeling

Homology models were generated using the software MODELLER 9v9 (http://salilab.org/modeller/).[193] The following input files are required: PDB file of the crystal structure (4COF) or a homologous template protein, an alignment file of the template and the trimmed $GABA_A$ receptor sequences (www.uniprot.org) and a python script to run the process. For the alignment the signal peptides of the sequences were removed and the ICD was replaced by a small linker. The sequence alignment was performed using ClustalX (http://www.clustal.org/).[194]

E I.2 Molecular Docking

Molecular Docking was performed using GOLD.[98] The putative binding sites at the $\alpha1+/\gamma2-$ and the $\alpha1+/\beta y-$ (y=1-3) interfaces were defined by a cut-off distance of 11.5 Å around the residue $\alpha1$S204 of the C-loop of the $\alpha1$ subunit. Further, we selected ten amino acids with flexible side chains (for $\alpha1+/\gamma2-$: $\gamma2$Y58, $\gamma2$F77, $\gamma2$T142, $\alpha1$H101, $\alpha1$Y159, $\alpha1$V202, $\alpha1$S204, $\alpha1$S205, $\alpha1$T206 and $\alpha1$Y209; for $\alpha1+/\beta y-$ (y=1-3): βyD43, βyY62, $\beta1$R41/$\beta2$N40/$\beta3$N41 , $\alpha1$H101, $\alpha1$Y159, $\alpha1$V202, $\alpha1$S204, $\alpha1$S205, $\alpha1$T206 and $\alpha1$Y209) and set a soft potential to increase to backbone flexibility of the C-loop ($\alpha1$S204, $\alpha1$S205, $\alpha1$T206 and $\alpha1$G207). To ensure convergence of the sampling, 100 genetic algorithm runs were performed using different ligands. The ligands were built in MOE (for benzodiazepine ligands the M conformation of the seven-membered ring that is supported by experimental studies was used) and energetically minimized using the MMFF94 force field before the docking run.

E I.3 Pharmacophore modeling

Pharmacophore modeling was performed using the software LigandScout.[189]

E II Materials and methods – chemical synthesis

Unless otherwise noted, chemicals were purchased from commercial suppliers and used without further purification. The purity of the compounds reported is > 95% according to NMR.

E II.1 NMR spectroscopy

NMR spectra were recorded on a Bruker *AC 200* (^{1}H: 200MHz, ^{13}C: 50 MHz), Bruker *Avance Ultrashield 400* (^{1}H: 400 MHz, ^{13}C: 101 MHz) and Bruker *Avance IIIHD 600* spectrometer equipped with a Prodigy BBO cryo probe (^{1}H: 600 MHz, ^{13}C: 151MHz). Chemical shifts are given in parts per million (ppm) and were calibrated with internal standards of deuterium labeled solvents $CHCl_3$-*d* (^{1}H 7.26 ppm, ^{13}C 77.16 ppm), MeOH-d_4 (^{1}H 3.31 ppm, ^{13}C 49.00 ppm) and DMSO-d_6 (^{1}H 2.50 ppm, ^{13}C 39.52 ppm). NMR assignments of unknown compounds were confirmed by ^{1}H - ^{1}H COSY, ^{1}H - ^{1}H, NOESY, ^{1}H - ^{13}C, HSQC and ^{1}H - ^{13}C, HMBC and by comparison to predicted spectra. Proton multiplicities are denoted by the following abbreviations: s (singlet), br s (broad singlet), d (doublet), br d (broad doublet), dd (doublet of a doublet), ddd (doublet of a doublet of a doublet), t (triplet), dt (doublet of a triplet), q (quartet), dq (doublet of a quartet), p (quintet), hep (septet), m (multiplet). Coupling constants (*J*) are presented in Hz (Hertz). Carbon multiplicities (suppressed CH coupling) are denoted by the following abbreviations: s (singlet), d (doublet), t (triplet) and q (quartet). In case of flouro structures the coupling constant is denoted generally as " xy, $^{z}J_{C,F}$ = …Hz " whereby x represents the multiplicity of the CH coupling, y the multiplicity of the CF coupling and z the order of spin-spin coupling.

E II.2 Chromatographic methods

TLC was performed using silica gel 60 aluminum plates containing fluorescent indicator from Merck and detected either with UV light at 254 nm or by charring in ninhydrin solution (300 mg ninhydrin, 3 mL acetic acid, 100 mL butanol) or potassium permanganate (1 g $KMnO_4$, 6.6 g K_2CO_3, 100 mg NaOH, 100 mL H_2O in 1M NaOH) with heating.

HPLC chromatography was carried out with an Autopurification system of Waters using an ACQUITY QDa Detector in combination with a 2998 Photodiode Array Detector. Analytical separation was conducted using XSELECT CSH Fluoro-Phenyl 5 µm 4.6 x 150 mm and XSELECT CSH C18 5 µm 4.6 x 150 mm columns. Preparative separation was performed using XSELECT CSH Prep Fluoro-Phenyl 5 µm 30 x 150 mm and XSELECT CSH Prep C18 5 µm OBD 30 x 150 mm columns. As solvents HPLC grade methanol and HPLC grade water were used containing 0.1 % formic acid.

Flash column chromatography (FC) was carried out at Büchi Sepacore™ MPLC system using silica gel 60 M (particle size 40-63 µm, 230-400 mesh ASTM, Macherey Nagel, Düren). Unless otherwise noted all compounds were purified with a ratio of 1/80 (weight (compound)/ weight (silica)).

E II.3 Microwave

Microwave reactions were performed on a Biotage Initiator Sixty™ microwave unit.

E II.4 Melting point

Melting points were determined by a Leica Galen III Kofler and a Büchi Melting Point B-545. Structures denoted with literature references and the comment “not reported” lack melting point information in the reference whereas structures denoted without literature references and the comment “no reference and not reported” were found in Scifinder or Reaxys (and thus considered as known) but lack a reference.

E II.5 HR-MS

An Agilent 6230 LC TOFMS mass spectrometer equipped with an Agilent Dual AJS ESI-Source was used for the analysis. The mass spectrometer was connected to a liquid chromatography system of the 1100/1200 series from Agilent Technologies, Palo Alto, CA, USA. The system consisted of a 1200SL binary gradient pump, a degasser, column thermostat, and an HTC PAL autosampler (CTC Analytics AG, Zwingen, Switzerland). A silica-based Phenomenex C-18 Security Guard Cartridge was used as stationary phase.

Data evaluation was performed using Agilent MassHunter Qulitative Analysis B.07.00. Identification was based on peaks obtained from extracted ion chromatograms (extraction width ± 20 ppm).

E III General operating proceducer (E°°II)

E III.1 Condensation

The substituted aniline (1 eq.) and diethyl(ethoxymethylene)malonate (1 eq.) were dissolved in toluene (1.25 mL/mmol) and the reaction mixture was heated to reflux. After 22 h the solvent was removed under reduced pressure and the residue was recrystallized in 2,2,3-trimethylpentane or purified by FC (gradient of 10%-30% EtOAc in PE and with a ratio of 1/80 (weight (compound)/ weight (silica)) if not otherwise noticed) to give the desired product.

E III.2 Cyclization

The condensed substituted aniline derivate (max. 2.5 g in 20 mL vial) was dispersed in diphenylether (1.7 mL/mmol), flushed with argon for 5 min and heated to 235 °C for 1 h by either normal heating or microwave irradiation. The reaction mixture was poured into PE, the formed precipitate was collected by filtration and washed with PE/EtOAc (1/1, 3 x 45 mL) to yield the desired product.

E III.3 Chlorination

The quinoline derivate/nitro quinolone was dispersed in $POCl_3$ (1 mL/mmol) and heated to reflux. After 2 h the reaction mixture was poured onto ice, neutralized with satd. $NaHCO_3$, extracted with CH_2Cl_2 (3 x 12 mL/mmol), washed with brine (1 x 12 mL/mmol), dried over Na_2SO_4, filtered and evaporated. The residue was purified by FC (gradient of 5%-15% EtOAc in PE and with a ratio of 1/80 (weight (compound)/ weight (silica)) if not otherwise noticed) to give the desired product.

E III.4 Formation of pyrazoloquinolinone

The chloro quinoline (1 eq.) and the substituted phenyl hydrazine/alkyl hydrazine hydrochloride (1.1 eq.) were dispersed in EtOH (4 mL/mmol), Et_3N (2.2 eq.) was added and the reaction mixture was heated to reflux under argon atmosphere. After 20 h the reaction mixture was rinsed with water (2 mL/mmol), filtered and the precipitate was washed with EtOAc/PE (1/1) (20 mL/mmol). The residue was dried under reduced pressure to give the desired product. Purification by HPLC was applied if specified.

E III.5 Basic hydrolysis to the carboxylic acid

PQ-benzonitrile (1 eq.) and NaOH (7 eq.) were dissolved in EtOH/H_2O (mixture 1/1; 23 mL/mmol) and the reaction mixture was heated to reflux. After 24 h the mixture was acidified with 2 M HCl and the precipitate was collected by filtration, washed with water (50 mL/mmol), PE (150 mL/mmol), EtOAc (150 mL/mmol) and dried under reduced pressure to give the desired carboxylic acid.

E III.6 Acidic hydrolysis to the benzamide

PQ-benzonitrile (1 eq.) and conc. sulfuric acid (0.8 mL/mmol) were heated to 90°C. After 1 h the reaction was allowed to cool to room temperature and ice water was added. After neutralization with satd. $NaHCO_3$ solution the precipitate was separated by centrifugation (10 min, 7000 RCF). The solid was washed with water (3 x 50 mL/mmol) and dried in vacuo to give the desired benzamide.

E III.7 Reduction to the amine

Nitro-PQ (1 eq.) was dissolved in EtOH (35 mL/mmol), $Na_2S \cdot 9H_2O$ (7 eq.) was added and the reaction mixture was heated to reflux. After 3 h water (50 mL/mmol) and 2 N HCl were added to adjust pH to 5-6. The precipitate was collected by filtration, washed with satd. $NaHCO_3$, water (2 x 30 mL/mmol) and was dried under reduced pressure to give the desired amine-PQ.

E IV Chemical synthesis

E IV.1 Pyrazoloquinoline precursors of R^6 series

E IV.1.1 N-(2-Ethylphenyl)acetamide [183] DCBSPU28

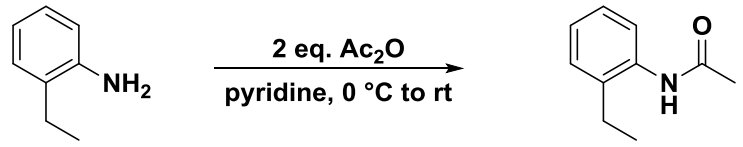

[181]

Chemical Formula: $C_8H_{11}N$
Molecular Weight: 121.18

[183] (58%)

Chemical Formula: $C_{10}H_{13}NO$
Molecular Weight: 163.22

The substrate 2-ethylaniline **[181]** (2 g, 16.5 mmol) was dissolved in anhydrous pyridine (40 mL) and cooled to 0 °C. Acetic anhydride (3.4 mL) was added dropwise and the reaction was allowed to warm to rt. After 18 h the solvent was evaporated and the residue was purified by FC (20-70% EtOAc in PE) to give the desired product **[183]** (1.56 g, 9.57 mmol, 58%).

^{1}H NMR (400 MHz, $CDCl_3$) δ 1.22 (t, *J* = 7.5 Hz, 3H, CH_3), 2.19 (s, 3H, $COCH_3$), 2.59 (q, *J* = 7.6 Hz, 2H, CH_2), 7.09 – 7.24 (m, 3H, H-Ar), 7.59 – 7.76 (m, 1H, H-Ar).

^{13}C NMR (101 MHz, $CDCl_3$) δ 14.0 (q, CH_3), 24.2 (t, CH_2), 24.3 (q, $CO\underline{C}H_3$), 124.4 (d, C-Ar), 125.8 (d, C-Ar), 126.6 (d, C-Ar), 128.5 (d, C-Ar), 134.8 (s, C1), 135.6 (s, C2), 168.7 (s, CO).

Appearance: Colorless crystals

Mp: 109-111 °C (Lit.[195]: 115-116 °C)

TLC: R_f = 0.36 (PE/EtOAc = 5/1)

E IV.1.2 N-(2-Ethylphenyl)acetamide [184] DCBSPU29

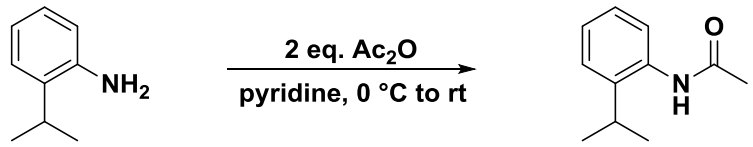

[182]

Chemical Formula: $C_9H_{13}N$
Molecular Weight: 135.21

[184] (90%)

Chemical Formula: $C_{11}H_{15}NO$
Molecular Weight: 177.25

The substrate 2-*iso*-propylaniline **[182]** (2 g, 14.8 mmol) was dissolved in anhydrous pyridine (40 mL) and cooled to 0 °C. Acetic anhydride (2.8 mL) was added dropwise and the reaction was allowed to warm to rt. After 18 h the solvent was evaporated and the residue was purified by FC (20-70% EtOAc in PE) to give the desired product **[184]** (2.36 g, 13.3 mmol, 90%).

^{1}H NMR (400 MHz, $CDCl_3$) δ 1.24 (d, *J* = 6.9 Hz, 6H, 2 CHC$\underline{H}_3$), 2.19 (s, 3H, $COCH_3$), 3.04 (hept, *J* = 6.9 Hz, 1H, CH), 7.08 – 7.22 (m, 2H, H-Ar), 7.27 – 7.35 (m, 1H, H-Ar), 7.54 – 7.63 (m, 1H, H-Ar).

^{13}C NMR (101 MHz, $CDCl_3$) δ 23.2 (q, 2 CH_3), 24.3 (d, CH), 28.1 (q, CO$\underline{C}H_3$), 125.5 (d, C-Ar), 125.8 (d, C-Ar), 126.4 (d, C-Ar), 126.5 (d, C-Ar), 134.1 (s, C1), 141.1 (s, C2), 168.9 (CO).

Appearance: Colorless crystals

Mp: 110-112 °C (Lit.[196]: 78-80 °C)

TLC: R_f = 0.90 (PE/EtOAc = 1/1)

E IV.1.3 N-(4-Chloro-2-ethylphenyl)acetamide [185] DCBSPU30 and 4-Chloro-2-ethylaniline [187] DCBSPU43

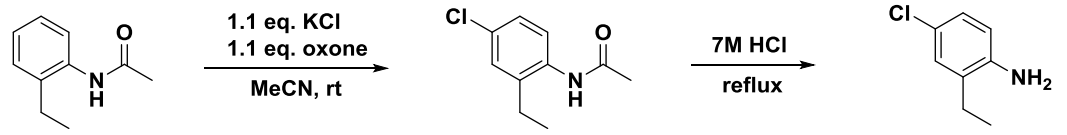

[183]

Chemical Formula: $C_{10}H_{13}NO$
Molecular Weight: 163.22

[185] (crude mixture)

[187] (28% over 2 steps)

Chemical Formula: $C_8H_{10}ClN$
Molecular Weight: 155.63

N-(2-Ethylphenyl)acetamide **[183]** (1.3 g, 7.97 mmol) and potassium chloride (890 mg) were suspended in acetonitrile (30 mL). Oxone (1.82 g) was added in small portions and the reaction mixture was stirred at rt. After 24 h the reaction mixture was filtered, evaporated and the residue was purified by FC (40% EtOAc in PE) to give 1.3 g (6.58 mmol) of a regioisomer mixture. Due to identical R_f values of the regioisomers the crude mixture was converted without further purification. The crude mixture was heated to reflux in 7M HCl for 18 h. The reaction was basified with 2M aq. NaOH and extracted with Et_2O (3 x mL). The combined organic layers were washed with brine (1 x mL), dried over Na_2SO_4 and evaporated. The residue was purified by FC (5-15% EtOAc in PE) to give the desired compound **[187]**[197] (497 mg, 3.19 mmol, 28% over 2 steps).

^{1}H NMR (400 MHz, DMSO-d_6) δ 1.10 (t, J = 7.5 Hz, 3H, CH_3), 2.41 (q, J = 7.5 Hz, 2H, CH_2), 4.98 (br s, 2H, NH_2), 6.59 (d, J = 8.2 Hz, 1H, H-Ar), 6.86 – 6.93 (m, 2H, H-Ar).

^{13}C NMR (101 MHz, DMSO-d_6) δ 12.9 (q, CH_3), 23.2 (t, CH_2), 115.5 (d, C-Ar), 119.1 (s, C2), 125.8 (d, C-Ar), 127.3 (d, C-Ar), 128.7 (s, C4), 145.0 (s, C1).

Appearance: Brown oil

TLC: R_f = 0.42 (PE/EtOAc = 5/1)

E IV.1.4 N-(4-Chloro-2-isopropylphenyl)acetamide [186] DCBSPU41

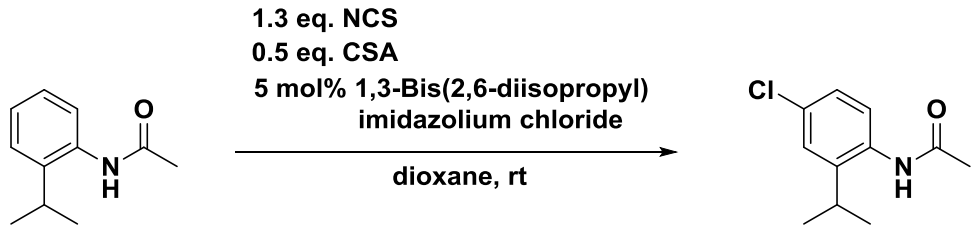

[184]

Chemical Formula: $C_{11}H_{15}NO$
Molecular Weight: 177.25

[186] (50%)

Chemical Formula: $C_{11}H_{14}ClNO$
Molecular Weight: 211.69

A mixture of **[184]** (2.19 g, 12.3 mmol), NCS (2.13g, 16 mmol), CSA (1.43 g, 6.2 mmol) and 1,3-bis(2,6-diisopropyl)imidazolium chloride (26 mg, 0.06 mmol) was stirred at room temperature under air. After 24 h the reaction mixture was quenched with satd. aq. $NaHCO_3$. The resulting mixture was extracted with EtOAc (3 x 30 mL) and the combined organic layers were washed with water (2 x 15 mL), dried over Na_2SO_4 and filtered. The solvent was removed under reduced pressure and the residue was purified by FC (20-50% EtOAc in PE) to give the desired product **[186]** (1.31 g, 6.17 mmol, 50%).

^{1}H NMR (400 MHz, DMSO-d_6) δ 1.13 (d, J = 6.8 Hz, 6H, 2 CHC$\underline{H}_3$), 2.04 (s, 3H, $COCH_3$), 3.14 (hept, J = 6.9 Hz, 1H, CH), 7.20 (dd, J = 8.5, 2.4 Hz, 1H, H-Ar), 7.26 – 7.33 (m, 2H, H-Ar), 9.38 (br s, 1H, NH).

^{13}C NMR (101 MHz, DMSO-d_6) δ 22.9 (q, 2 CH_3), 23.1 (d, CH), 27.2 (q, CO$\underline{C}H_3$), 125.5 (d, C-Ar), 125.6 (d, C-Ar), 128.5 (d, C-Ar), 130.1 (s, C4), 133.9 (s, C1), 145.3 (s, C2), 168.8 (s, CO).

Appearance: Colorless solid

Mp: 123-125 °C (Lit.: no reference and not reported)

TLC: R_f = 0.40 (PE/EtOAc = 1/2)

E IV.1.5 4-Chloro-2-isopropylaniline [188] DCBSPU44

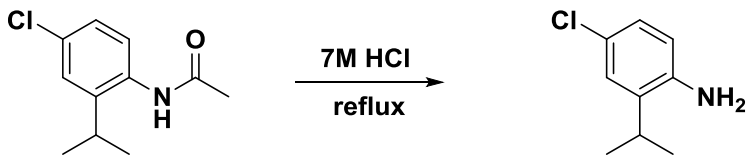

[186] **[188] (85%)**

Chemical Formula: $C_{11}H_{14}ClNO$
Molecular Weight: 211.69

Chemical Formula: $C_9H_{12}ClN$
Molecular Weight: 169.65

N-(4-Chloro-2-isopropylphenyl)acetamide **[186]** (1.3 g, 7.37) was heated to reflux in 7M HCl for 18 h. The reaction was basified with 2M aq. NaOH and extracted with Et_2O (3 x mL). The combined organic layers were washed with brine (1 x mL), dried over Na_2SO_4 and evaporated to give the desired compound **[188]** (1.06 g, 6.26 mmol, 85%).

^{1}H NMR (400 MHz, $CDCl_3$) δ 1.25 (d, *J* = 6.8 Hz, 6H, 2 CHC$\underline{H}_3$), 2.86 (hept, *J* = 6.8 Hz, 1H, CH), 4.16 (br s, 2H, NH_2), 6.60 (d, *J* = 8.5 Hz, 1H, H-Ar), 6.94 – 7.00 (dd, *J* = 8.5, 2.4 Hz, 1H, H-Ar), 7.09 (d, *J* = 2.4 Hz, 1H, H-Ar).

^{13}C NMR (101 MHz, $CDCl_3$) δ 22.2 (q, 2 CH_3), 28.0 (d, CH), 117.0 (d, C-Ar), 123.9 (s, C4), 125.7 (d, C-Ar), 126.4 (d, C-Ar), 134.6 (s, C2), 141.9 (s, C1).

Appearance: Brown oil

TLC: R_f = 0.47 (PE/EtOAc = 5/1)

E IV.1.6 Diethyl 2-(((4-chloro-2-fluorophenyl)amino)methylene)-malonate [194] DCBSPU7

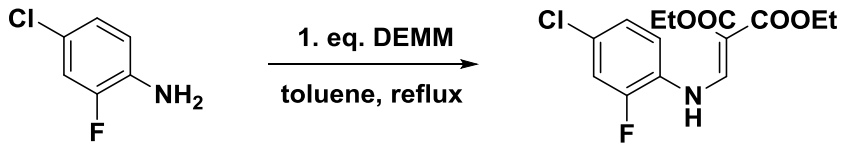

[189] **[194] (87%)**

Chemical Formula: C_6H_5ClFN
Molecular Weight: 145.56

Chemical Formula: $C_{14}H_{15}ClFNO_4$
Molecular Weight: 315.73

The compound was synthesized according to general procedure E III.1 using:

4-Chloro-2-fluoroaniline	510 mg	3.50 mmol	1 eq.
DEMM	707 µL	3.50 mmol	1 eq

After purification by FC (15-25% EtOAc in PE) diethyl 2-(((4-chloro-2-fluorophenyl)amino)methylene)malonate **[194]** was obtained (961 mg, 3.05 mmol, 87%).

^{1}H NMR (400 MHz, DMSO-d_6) δ 1.21 – 1.28 (m, 6H, 2 CH_3), 4.13 (q, J = 7.1 Hz, 2H. CH_2), 4.21 (q, J = 7.1 Hz, 2H, CH_2), 7.32 (ddd, J = 8.7, 2.3, 1.3 Hz, 1H, H5), 7.58 (dd, J = 11.0, 2.3 Hz, 1H, H3), 7.68 (t, J = 8.9 Hz, 1H, H6), 8.43 (d, J = 13.2 Hz, 1H, NHC<u>H</u>), 10.85 (br d, J = 12.9 Hz, 1H, NH).

^{13}C NMR (101 MHz, DMSO-d_6) δ 14.1 (q, CH_3), 14.2 (q, CH_3), 59.7 (t, CH_2), 60.0 (t, CH_2), 95.0 (s, C_{quart}), 116.6 (dd, $^{2}J_{C,F}$ = 22.6 Hz, C3), 118.9 (dd, $^{3}J_{C,F}$ = 1.8 Hz, C6), 125.5 (dd, $^{4}J_{C,F}$ = 3.5 Hz, C5), 126.8 (sd, $^{2}J_{C,F}$ = 10.0 Hz, C1), 128.3 (sd, $^{3}J_{C,F}$ = 10.3 Hz, C4), 150.9 (d, NHCH), 151.7 (sd, $^{1}J_{C,F}$ = 247.5 Hz, C2), 164.5 (s, CO), 167.6 (s, CO).

Appearance: Colorless solid

Mp: 92-94 °C (Lit.[198]: 93-94 °C)

TLC: R_f = 0.77 (PE/EtOAc = 3/1)

E IV.1.7 Diethyl 2-(((2,4-dichlorophenyl)amino)methylene)-malonate [195] DCBSPU18

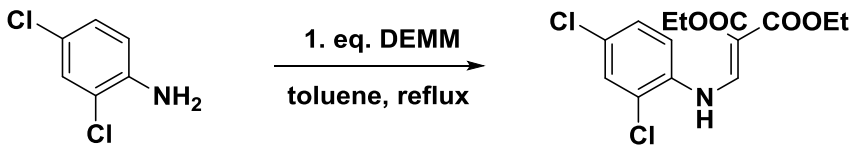

[190] **[195] (89%)**

Chemical Formula: $C_6H_5Cl_2N$
Molecular Weight: 162.01

Chemical Formula: $C_{14}H_{15}Cl_2NO_4$
Molecular Weight: 332.18

The compound was synthesized according to general procedure E III.1 using:

2,4-Dichloroaniline	495 mg	3.06 mmol	1 eq.
DEMM	618 µL	3.06 mmol	1 eq

After purification by FC (15-25% EtOAc in PE) diethyl diethyl 2-(((2,4-dichlorophenyl)amino)methylene)malonate **[195]** was obtained (904 mg, 2.72 mmol, 89%).

^{1}H NMR (400 MHz, $CDCl_3$) δ 1.33 (t, *J* = 7.1 Hz, 3H, CH_3), 1.38 (t, *J* = 7.1 Hz, 3H, CH_3), 4.26 (q, *J* = 7.1 Hz, 2H, CH_2), 4.34 (q, *J* = 7.1 Hz, 2H, CH_2), 7.23 (d, *J* = 8.8 Hz, 1H, H6), 7.28 (dd, *J* = 8.8, 2.3 Hz, 1H, H5), 7.43 (d, *J* = 2.2 Hz, 1H, H3), 8.44 (d, *J* = 13.2 Hz, 1H, NHC<u>H</u>), 11.29 (br d, *J* = 13.2 Hz, 1H, NH).

^{13}C NMR (101 MHz, $CDCl_3$) δ 14.4 (q, CH_3), 14.5 (q, CH_3), 60.6 (t, CH_2), 60.9 (t, CH_2), 96.3 (s, C_{quart}), 116.4 (d, C6), 124.3 (s, C2), 128.4 (d, C5), 129.7 (s, C4), 130.1 (d, C3), 135.4 (s, C1), 150.1 (d, NHCH), 165.6 (s, CO), 168.5 (s, CO).

Appearance: Colorless solid

Mp: 108-110 °C (Lit.[199]: 107-109 °C)

TLC: R_f = 0.77 (PE/EtOAc = 3/1)

E IV.1.8 Diethyl 2-(((2-bromo-4-chlorophenyl)amino)methylene)-malonate [196] DCBSPU5

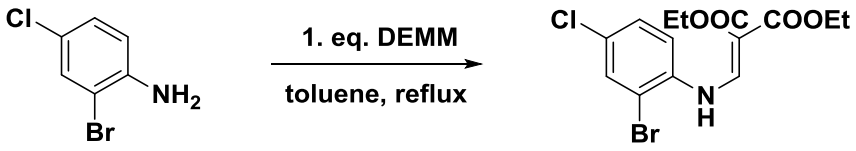

[191] **[196] (91%)**

Chemical Formula: C_6H_5BrClN
Molecular Weight: 206,47

Chemical Formula: $C_{14}H_{15}BrClNO_4$
Molecular Weight: 376.63

The compound was synthesized according to general procedure E III.1 using:

2-Bromo-4-chloroaniline	512 mg	2.48 mmol	1 eq.
DEMM	501 µL	2.48 mmol	1 eq

After purification by FC (15-25% EtOAc in PE) diethyl 2-(((2-bromo-4-chlorophenyl)amino)methylene)malonate **[196]** was obtained (850 mg, 2.26 mmol, 91%).

^{1}H NMR (400 MHz, $CDCl_3$) δ 1.33 (t, *J* = 7.1 Hz, 3H, CH_3), 1.38 (t, *J* = 7.1 Hz, 3H, CH_3), 4.26 (q, *J* = 7.1 Hz, 2H, CH_2), 4.34 (q, *J* = 7.1 Hz, 2H, CH_2), 7.21 (d, *J* = 8.8 Hz, 1H, H6), 7.33 (dd, *J* = 8.8, 2.3 Hz, 1H, H5), 7.60 (d, *J* = 2.3 Hz, 1H, H3), 8.42 (d, *J* = 13.3 Hz, 1H, NHC<u>H</u>), 11.25 (br d, *J* = 13.2 Hz, 1H, NH).

^{13}C NMR (101 MHz, $CDCl_3$) δ 14.4 (q, CH_3), 14.5 (q, CH_3), 60.6 (t, CH_2), 60.9 (t, CH_2), 96.3 (s, C_{quart}), 114.0 (s, C2), 116.6 (d, C6), 129.0 (d, C5), 130.0 (s, C4), 133.1 (d, C3), 136.8 (s, C1), 150.3 (d, NHCH), 165.6 (s, CO), 168.5 (s, CO).

Appearance: Colorless solid

Mp: 99-101 °C (Lit.: no reference and not reported)

TLC: R_f = 0.74 (PE/EtOAc = 3/1)

E IV.1.9 Diethyl 2-(((4-chloro-2-(trifluoromethyl)phenyl)amino)-methylene)malonate [197] DCBSPU6

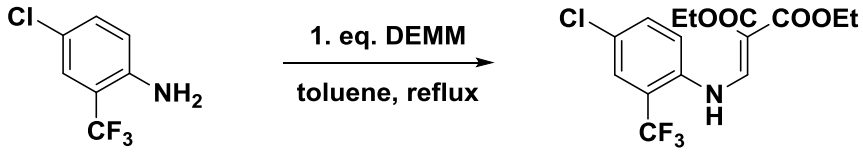

[192] **[197] (75%)**

Chemical Formula: $C_7H_5ClF_3N$
Molecular Weight: 195.57

Chemical Formula: $C_{15}H_{15}ClF_3NO_4$
Molecular Weight: 365.73

The compound was synthesized according to general procedure E III.1 using:

4-Chloro-2-(trifluoromethyl)aniline	1.00 g	5.11 mmol	1 eq.
DEMM	1.03 mL	5.11 mmol	1 eq

After purification by FC (15-25% EtOAc in PE) diethyl 2-(((4-chloro-2-(trifluoromethyl)phenyl)amino)methylene)malonate **[197]** was obtained (1.41 g, 3.83 mmol, 75%).

^{1}H NMR (400 MHz, $CDCl_3$) δ 1.33 (t, *J* = 7.1 Hz, 3H, CH_3), 1.37 (t, *J* = 7.1 Hz, 3H, CH_3), 4.26 (q, *J* = 7.1 Hz, 2H, CH_2), 4.33 (q, *J* = 7.1 Hz, 2H, CH_2), 7.31 (d, *J* = 8.8 Hz, 1H, H6), 7.53 – 7.58 (m, 1H, H5), 7.63 (d, *J* = 2.4 Hz, 1H, H3), 8.38 (d, *J* = 12.7 Hz, 1H, NHC<u>H</u>), 11.35 (br d, *J* = 12.7 Hz, 1H, NH).

^{13}C NMR (151 MHz, $CDCl_3$) δ 14.4 (q, CH_3), 14.5 (q, CH_3), 60.6 (t, CH_2), 61.0 (t, CH_2), 97.1 (s, C_{quart}), 119.5 (d, C6), 121.2 (qs, $^{2}J_{C,F}$ = 31.4 Hz, C2), 123.0 (qs, $^{1}J_{C,F}$ = 272.3 Hz, CF_3), 127.3 (qd, $^{3}J_{C,F}$ = 5.4 Hz, C3), 130.0 (s, C4) 133.6 (d, C5), 136.5 (s, C1), 151.4 (d, NHCH), 165.5 (s, CO), 168.3 (s, CO).

HR-MS: Calc.[M+Na]: 388.0534

Found [M+Na]: 388.0554 (Diff.: -5.08 ppm)

Appearance: Colorless solid

Mp: 92-94 °C

TLC: R_f = 0.78 (PE/EtOAc = 3/1)

E IV.1.10 Diethyl 2-(((4-chloro-2-methylphenyl)amino)methylene)-malonate [198] DCBSPU17

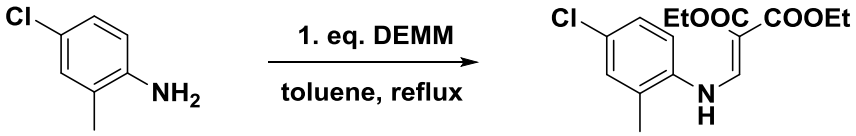

[193]

Chemical Formula: C_7H_8ClN
Molecular Weight: 141.60

[198] (77%)

Chemical Formula: $C_{15}H_{18}ClNO_4$
Molecular Weight: 311.76

The compound was synthesized according to general procedure E III.1 using:

4-Chloro-2-methylaniline	508 mg	3.59 mmol	1 eq.
DEMM	725 µL	3.59 mmol	1 eq

After purification by FC (15-25% EtOAc in PE) diethyl 2-(((4-chloro-2-methylphenyl)amino)methylene)malonate **[198]** was obtained (862 mg, 2.76 mmol, 77%).

^{1}H NMR (400 MHz, $CDCl_3$) δ 1.32 (t, *J* = 7.1 Hz, 3H, $CH_2C\underline{H}_3$), 1.38 (t, *J* = 7.1 Hz, 3H, $CH_2C\underline{H}_3$), 2.34 (s, 3H, CH_3), 4.25 (q, *J* = 7.1 Hz, 2H, CH_2), 4.32 (q, *J* = 7.1 Hz, 2H, CH_2), 7.14 (d, *J* = 8.3 Hz, 1H, H6), 7.18 – 7.28 (m, 2H, H3 and H5), 8.46 (d, *J* = 13.3 Hz, 1H, NHC<u>H</u>), 11.09 (br d, *J* = 13.3 Hz, 1H, NH).

^{13}C NMR (101 MHz, $CDCl_3$) δ 14.5(q, $CH_2\underline{C}H_3$), 14.6 (q, $CH_2\underline{C}H_3$), 17.6 (q, CH_3), 60.3 (t, CH_2), 60.7 (t, CH_2), 94.4 (s, C_{quart}), 116.7 (d, C6), 127.5 (d, C5), 129.1 (s, C2), 129.9 (s, C4), 131.1 (d, C3), 136.8 (s, C1), 152.1 (d, NHCH), 165.8 (s, CO), 169.3 (s, CO).

Appearance: Colorless solid

Mp: 56-58 °C (Lit.: no reference and not reported)

TLC: R_f = 0.67 (PE/EtOAc = 3/1)

E IV.1.11 Diethyl 2-(((4-chloro-2-ethylphenyl)amino)methylene)-malonate [199] DCBSPU47

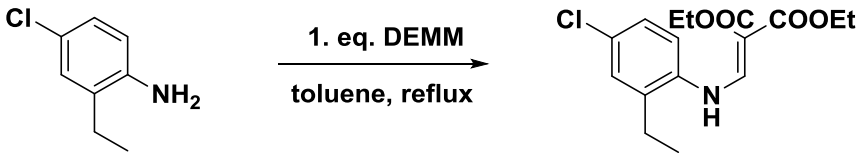

[187] **[199] (85%)**

Chemical Formula: $C_8H_{10}ClN$
Molecular Weight: 155.63

Chemical Formula: $C_{16}H_{20}ClNO_4$
Molecular Weight: 325.79

The compound was synthesized according to general procedure E III.1 using:

4-Chloro-2-ethylaniline	487 mg	2.87 mmol	1 eq.
DEMM	580 µL	2.87 mmol	1 eq

After purification by FC (15-25% EtOAc in PE) diethyl 2-(((4-chloro-2-ethylphenyl)amino)methylene)malonate **[199]** was obtained (793 mg, 2.44 mmol, 85%).

^{1}H NMR (400 MHz, $CDCl_3$) δ 1.29 (t, *J* = 7.7 Hz, 3H, CH_2CH_3), 1.33 (t, *J* = 7.1 Hz, 3H, OCH_2CH_3), 1.38 (t, *J* = 7.1 Hz, 3H, OCH_2CH_3), 2.68 (q, *J* = 7.5 Hz, 2H, CH_2CH_3), 4.25 (q, *J* = 7.2 Hz, 2H, OCH_2), 4.32 (q, *J* = 7.1 Hz, 2H, OCH_2), 7.11 – 7.18 (m, 1H, H-Ar), 7.20 – 7.29 (m, 2H, H-Ar), 8.46 (d, *J* = 13.3 Hz, 1H, NHCH), 11.17 (br d, *J* = 13.3 Hz, 1H, NH).

^{13}C NMR (101 MHz, $CDCl_3$) δ 13.5 (q, CH_2CH_3), 14.5 (q, OCH_2CH_3), 14.6 (q, OCH_2CH_3), 24.3 (t, CH_2CH_3), 60.3 (t, OCH_2CH_3), 60.6 (t, OCH_2CH_3), 94.3 (s, C_{quart}), 117.4 (d, C-Ar), 127.4 (d, C-Ar), 129.4 (d, C-Ar), 130.4 (s, C-Ar), 135.2 (s, C-Ar), 136.3 (s, C-Ar), 152.5 (d, NHCH), 165.8 (s, CO), 169.3 (s, CO).

HR-MS: Calc.[M+H]: 326.1154

Found [M+H]: 326.1173 (Diff.: -6.05 ppm)

Appearance: Colorless crystals

Mp: 77-79 °C

TLC: R_f = 0.77 (PE/EtOAc = 3/1)

E IV.1.12 Diethyl 2-(((4-chloro-2-isopropylphenyl)amino)-methylene)malonate [200] DCBSPU46

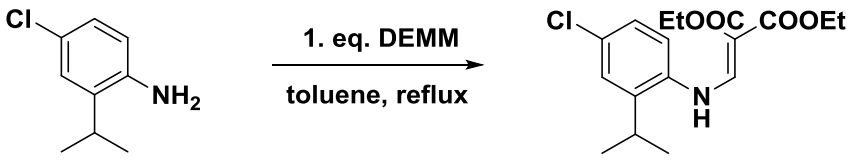

[188] **[200] (53%)**

Chemical Formula: $C_9H_{12}ClN$
Molecular Weight: 169.65

Chemical Formula: $C_{17}H_{22}ClNO_4$
Molecular Weight: 339.82

The compound was synthesized according to general procedure E III.1 using:

4-Chloro-2-isopropylaniline	1.06 g	6.24 mmol	1 eq.
DEMM	1.26 mL	6.24 mmol	1 eq

After purification by FC (15-25% EtOAc in PE) diethyl 2-(((4-chloro-2-isopropylphenyl)amino)methylene)malonate **[200]** was obtained (1.08 g, 3.31 mmol, 53%).

^{1}H NMR (400 MHz, $CDCl_3$) δ 1.22 (d, *J* = 6.8 Hz, 6H, 2 CHC$\underline{H}_3$), 1.25 (t, *J* = 7.2 Hz, 3H, $CH_2C\underline{H}_3$), 1.31 (t, *J* = 7.1 Hz, 3H, $CH_2C\underline{H}_3$), 3.05 (hept, *J* = 6.8 Hz, 1H, CH), 4.18 (q, *J* = 7.1 Hz, 2H, CH_2), 4.25 (q, *J* = 7.1 Hz, 2H, CH_2), 7.07 (d, *J* = 8.6 Hz, 1H, H-Ar), 7.15 (dd, *J* = 8.6, 2.4 Hz, 1H, H-Ar), 7.18 – 7.21 (m, 1H, H-Ar), 8.36 (d, *J* = 13.3 Hz, 1H, NHC$\underline{H}$), 11.16 (br d, *J* = 13.3 Hz, 1H, NH).

^{13}C NMR (101 MHz, $CDCl_3$) δ 14.5 (q, $CH_2\underline{C}H_3$), 14.6 (q, $CH_2\underline{C}H_3$), 22.6 (q, 2 CH$\underline{C}H_3$), 28.3 (d, $\underline{C}HCH_3$), 60.3 (t, CH_2), 60.6 (t, CH_2), 94.3 (s, C_{quart}), 118.4 (d, C-Ar), 126.7 (d, C-Ar), 127.3 (d, C-Ar), 131.0 (s, C-Ar), 135.8 (s, C-Ar), 140.1 (s, C-Ar), 153.1 (d, NHCH), 165.8 (s, CO), 169.4 (s, CO).

HR-MS: Calc.[M+H]: 340.1310

Found [M+H]: 340.1326 (Diff.: -4.74 ppm)

Appearance: Colorless crystals

Mp: 93-95 °C

TLC: R_f = 0.88 (PE/EtOAc = 3/1)

E IV.1.13 Ethyl 6-chloro-8-fluoro-4-oxo-1,4-dihydroquinoline-3-carboxylate [201] DCBSPU13

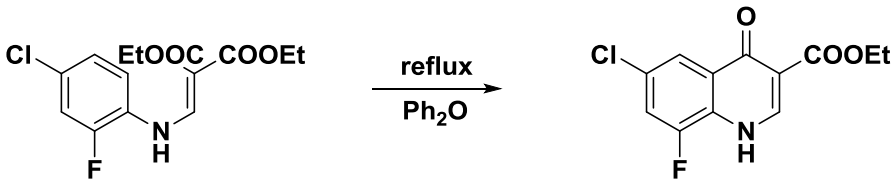

[194] **[201] (75%)**

Chemical Formula: $C_{14}H_{15}ClFNO_4$
Molecular Weight: 315.73

Chemical Formula: $C_{12}H_9ClFNO_3$
Molecular Weight: 269.66

Ethyl 6-chloro-8-fluoro-4-oxo-1,4-dihydroquinoline-3-carboxylate **[201]** was synthesized according to general procedure E III.2 using 965 mg (3.06 mmol) of diethyl 2-(((4-chloro-2-fluorophenyl)amino)methylene)malonate **[194]** (619 mg, 2.29 mmol, 75%).

^{1}H NMR (400 MHz, DMSO-d_6) δ 1.28 (t, J = 7.1 Hz, 3H, CH_3), 4.23 (q, J = 7.1 Hz, 2H, CH_2), 7.88 – 7.93 (m, 2H, H5 and H7), 8.39 (s, 1H, NHC<u>H</u>), 12.64 (br s, 1H, NH).

^{13}C NMR (151 MHz, DMSO-d_6) δ 14.3 (q, CH_3), 60.0 (t, CH_2), 110.8 (s, C3), 118.2 (dd, $^{2}J_{C,F}$ = 20.7 Hz, C7), 120.6 (dd, $^{4}J_{C,F}$ = 3.5 Hz, C5), 127.5 (sd, $^{2}J_{C,F}$ = 13.3 Hz, C6/C8a), 128.6 (sd, $^{3}J_{C,F}$ = 9.4 Hz, C6/C8a), 129.5 (s, C4a), 144.9 (d, C2), 152.1 (sd, $^{1}J_{C,F}$ = 253.95 Hz, C8), 164.2 (s, CO), 171.3 (s, CO).

Appearance: Colorless solid

Mp: Decomposes > 300 °C (Lit.[200]: 284 °C in EtOH)

TLC: R_f = 0.75 (2% MeOH in CH_2Cl_2)

E IV.1.14 Ethyl 6,8-dichloro-4-oxo-1,4-dihydroquinoline-3-carboxylate [202] DCBSPU23

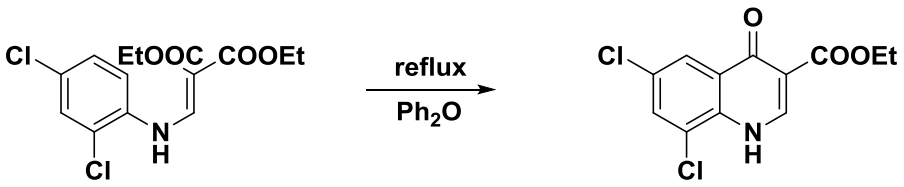

[195] **[202] (79%)**

Chemical Formula: $C_{14}H_{15}Cl_2NO_4$
Molecular Weight: 332.18

Chemical Formula: $C_{12}H_9Cl_2NO_3$
Molecular Weight: 286.11

Ethyl 6,8-dichloro-4-oxo-1,4-dihydroquinoline-3-carboxylate **[202]** was synthesized according to general procedure E III.2 using 813 mg (2.44 mmol) of diethyl 2-(((2,4-dichlorophenyl)amino)methylene)malonate **[195]** (552 mg, 1.93 mmol, 79%).

^{1}H NMR (400 MHz, DMSO-d_6) δ 1.28 (t, *J* = 7.1 Hz, 3H, CH_3), 4.23 (q, *J* = 7.1 Hz, 2H, CH_2), 8.05 (d, *J* = 2.4 Hz, 1H, H5), 8.10 (d, *J* = 2.3 Hz, 1H, H7), 8.41 (s, 1H, H2), 12.07 (s, 1H, NH).

^{13}C NMR (151 MHz, DMSO-d_6) δ 14.3 (q, CH_3), 60.0 (t, CH_2), 110.7 (s, C3), 123.8 (s, C8), 124.2 (d, C5), 129.1 (s, C4a/C8a), 129.3 (s, C4a/C8a), 132.1 (d, C7), 134.7 (s, C6), 145.5 (d, C2), 164.1 (s, CO), 171.7 (s, CO).

Appearance: Colorless solid

Mp: 306-308 °C (Lit.[201]: 305-308 °C)

TLC: R_f = 0.61 (2% MeOH in CH_2Cl_2)

E IV.1.15 Ethyl 8-bromo-6-chloro-4-oxo-1,4-dihydroquinoline-3-carboxylate [203] DCBSPU11

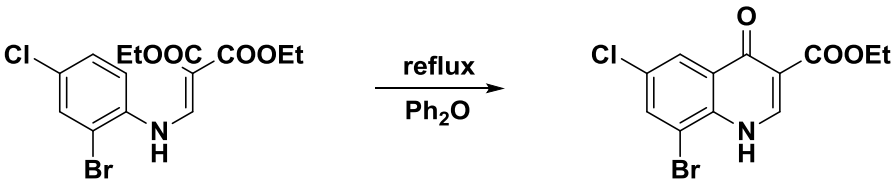

[196] **[203] (81%)**

Chemical Formula: $C_{14}H_{15}BrClNO_4$
Molecular Weight: 376.63

Chemical Formula: $C_{12}H_9BrClNO_3$
Molecular Weight: 330.56

Ethyl 8-bromo-6-chloro-4-oxo-1,4-dihydroquinoline-3-carboxylate **[203]** was synthesized according to general procedure E III.2 using 850 mg (2.26 mmol) of diethyl 2-(((2-bromo-4-chlorophenyl)amino)methylene)malonate **[196]** (605 mg, 1.83 mmol, 81%).

^{1}H NMR (400 MHz, DMSO-d_6) δ 1.27 (t, *J* = 7.1 Hz, 3H, CH_3), 4.23 (q, *J* = 7.1 Hz, 2H, CH_2), 8.09 (d, *J* = 2.4 Hz, 1H, H5), 8.20 (d, *J* = 2.4 Hz, 1H, H7), 8.45 (s, 1H, H2), 11.82 (br s, 1H, NH).

^{13}C NMR (151 MHz, DMSO-d_6) δ 14.4 (q, CH_3), 60.2 (t, CH_2), 110.5 (s, C3), 113.5 (s, C8), 124.8 (d, C5), 129.3 (s, C4a/C8a), 129.7 (s, C4a/C8a), 135.4 (d, C7), 135.9 (s, C6), 146.0 (d, C2), 164.2 (s, CO), 171.9 (s, CO).

Appearance: Colorless solid

Mp: 305-307 °C (Lit.: no reference and not reported)

TLC: R_f = 0.80 (2% MeOH in CH_2Cl_2)

E IV.1.16 Ethyl 6-chloro-4-oxo-8-(trifluoromethyl)-1,4-dihydro-quinoline-3-carboxylate [204] DCBSPU12

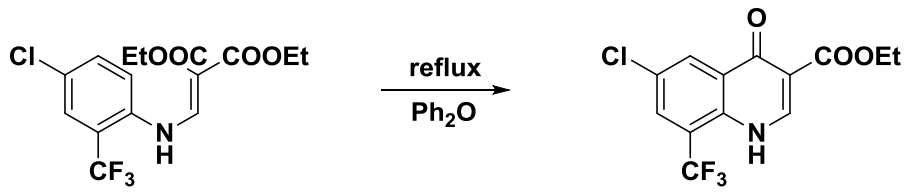

[197] **[204] (crude 33%)**

Chemical Formula: $C_{15}H_{15}ClF_3NO_4$
Molecular Weight: 365.73

Chemical Formula: $C_{13}H_9ClF_3NO_3$
Molecular Weight: 319.66

The conversion of diethyl 2-(((4-chloro-2-(trifluoromethyl)phenyl)amino)methylene)-malonate **[197]** 1.41 g (3.75 mmol) according to general procedure E III.2 yielded only the crude ethyl 6-chloro-4-oxo-8-(trifluoromethyl)-1,4-dihydroquinoline-3-carboxylate **[204]**. Thus, the crude **[204]** was purified by FC (1% MeOH in CH_2Cl_2) twice which only led to a slight increase of puritiy. Therefore, we decided to convert the crude mixture since the next step was easier to purify (crude: 396 mg, 1.24 mmol, 33%).

^{1}H NMR (400 MHz, DMSO-d_6) δ 1.29 (t, J = 7.1 Hz, 3H, $CH_2C\underline{H}_3$), 4.25 (q, J = 7.1 Hz, 2H, $C\underline{H}_2CH_3$), 8.08 – 8.13 (m, 1H, H5), 8.37 – 8.41 (m, 1H, H7), 8.55 (s, 1H, H2), 11.84 (br s, 1H, NH). Selected signlas were listed to confirm the formation of compound **[204]**.

^{13}C NMR not determined due to crude mixture.

Appearance: Colorless solid

TLC: R_f = 0.91 (2% MeOH in CH_2Cl_2)

E IV.1.17 Ethyl 6-chloro-8-methyl-4-oxo-1,4-dihydroquinoline-3-carboxylate [205] DCBSPU22

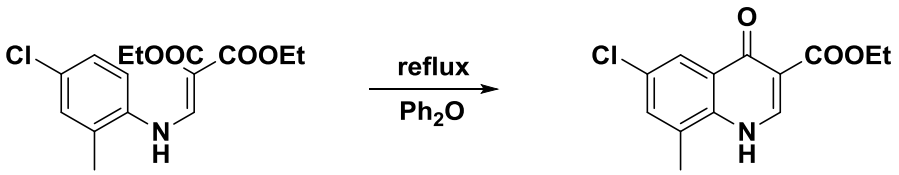

[198] **[205] (77%)**

Chemical Formula: $C_{15}H_{18}ClNO_4$
Molecular Weight: 311.76

Chemical Formula: $C_{13}H_{12}ClNO_3$
Molecular Weight: 265.69

Ethyl 6-chloro-8-methyl-4-oxo-1,4-dihydroquinoline-3-carboxylate **[205]** was synthesized according to general procedure E III.2 using 775 mg (2.49 mmol) of diethyl 2-(((4-chloro-2-methylphenyl)amino)methylene)-malonate **[198]** (779 mg, 2.93 mmol, 77%).

^{1}H NMR (400 MHz, DMSO-d_6) δ 1.28 (t, J = 7.1 Hz, 3H, $CH_2C\underline{H}_3$), 2.51 (s, 3H, CH_3), 4.22 (q, J = 7.1 Hz, 2H, $C\underline{H}_2CH_3$), 7.67 (d, J = 2.5 Hz, 1H, H7), 7.95 (d, J = 2.5 Hz, 1H, H5), 8.39 (d, J = 5.1 Hz, 1H, H2), 11.80 (br s, 1H, NH).

^{13}C NMR (151 MHz, DMSO-d_6) δ 14.3 (q, $CH_2\underline{C}H_3$), 16.8 (q, CH_3), 59.8 (t, $\underline{C}H_2CH_3$), 110.0 (s, C3), 122.4 (d, C5), 128.5 (s, C4a/C8a), 129.0 (s, C4a/C8a), 130.4 (s, C8), 132.9 (d, C7), 136.4 (s, C6), 144.8 (d, C2), 164.5 (s, CO), 172.4 (s, CO).

Appearance: Colorless solid

Mp: 301-303 °C (Lit.: no reference and not reported)

TLC: R_f = 0.80 (2% MeOH in CH_2Cl_2)

E IV.1.18 Ethyl 6-chloro-8-ethyl-4-oxo-1,4-dihydroquinoline-3-carboxylate [206] DCBSPU50

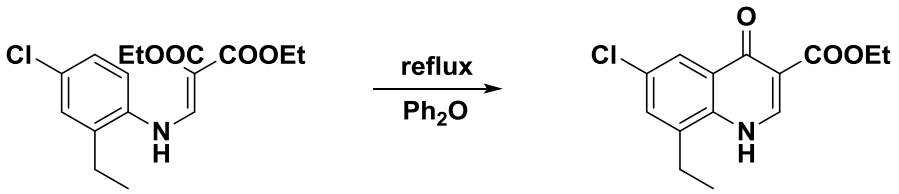

[199] **[206] (74%)**

Chemical Formula: $C_{16}H_{20}ClNO_4$
Molecular Weight: 325.79

Chemical Formula: $C_{14}H_{14}ClNO_3$
Molecular Weight: 279.72

Ethyl 6-chloro-8-ethyl-4-oxo-1,4-dihydroquinoline-3-carboxylate **[206]** was synthesized according to general procedure E III.2 using 827 mg (2.43 mmol) of diethyl 2-(((4-chloro-2-ethylphenyl)amino)methylene)-malonate **[199]** (503 mg, 1.80 mmol, 74%).

^{1}H NMR (400 MHz, DMSO-d_6) δ 1.20 – 1.31 (m, 6H, 2 CH_3), 2.90 (q, J = 7.5 Hz, 2H, CH_2CH_3), 4.22 (q, J = 7.1 Hz, 2H, OCH_2CH_3), 7.62 (d, J = 2.5 Hz, 1H, H7), 7.97 (d, J = 2.5 Hz, 1H, H5), 8.39 (s, 1H, H2), 11.79 (br s, 1H, NH).

^{13}C NMR (151 MHz, DMSO-d_6) δ 14.0 (q, CH_2CH_3), 14.3 (q, OCH_2CH_3), 22.9 (t, CH_2CH_3), 59.8 (t, OCH_2CH_3), 109.9 (s, C3), 122.5 (d, C5), 128.8 (s, C4a/C8a), 129.3 (s, C4a/C8a), 131.4 (d, C7), 135.6 (s, C8), 136.0 (s, C6), 144.9 (d, C2), 164.5 (s, CO), 172.4 (s, CO).

HR-MS: Calc.[M+Na]: 302.0554

Found [M+Na]: 302.0570 (Diff.: -5.17 ppm)

Appearance: Light brown powder

Mp: Decomposes > 250 °C

TLC: R_f = 0.11 (PE/EtOAc = 5/1)

E IV.1.19 Ethyl 6-chloro-8-isopropyl-4-oxo-1,4-dihydroquinoline-3-carboxylate [207] DCBSPU48

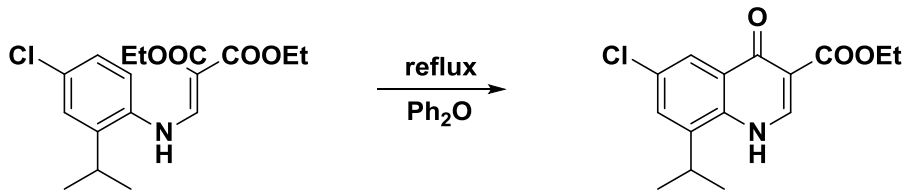

[200] **[207] (36%)**

Chemical Formula: $C_{17}H_{22}ClNO_4$
Molecular Weight: 339.82

Chemical Formula: $C_{15}H_{16}ClNO_3$
Molecular Weight: 293.75

Ethyl 6-chloro-8-isopropyl-4-oxo-1,4-dihydroquinoline-3-carboxylate **[207]** was synthesized according to general procedure E III.2 using 340 mg (1.16 mmol) of diethyl 2-(((4-chloro-2-isopropylphenyl)amino)methylene)-malonate **[200]** (123 mg, 0.42 mmol, 36%).

^{1}H NMR (400 MHz, DMSO-d_6) δ 1.29 (d, J = 7.0 Hz, 9H, 3 CH_3), 3.40 – 3.50 (m, 1H, C<u>H</u>CH_3), 4.22 (q, J = 7.1 Hz, 2H, CH_2), 7.60 – 7.73 (m, 1H, H7), 7.94 – 8.05 (m, 1H, H5), 8.39 (d, J = 6.9 Hz, 1H, H2), 11.80 (br d, J = 6.9 Hz, 1H, NH).

^{13}C NMR (101 MHz, DMSO-d_6) δ 14.3 (q, CH_2<u>C</u>H_3), 22.6 (q, 2 CH<u>C</u>H_3), 26.7 (d, <u>C</u>HCH_3), 59.8 (t, <u>C</u>H_2CH_3), 109.5 (s, C3), 122.5 (d, C5), 128.7 (d, C7), 128.9 (s, C4a/C8a), 129.7 (s, C4a/C8a), 135.1 (s, C6), 140.5 (s, C8), 145.0 (d, C2), 164.5 (s, CO), 170.3 (s, CO).

HR-MS: Calc.[M+H]: 294.0891

Found [M+H]: 294.0904 (Diff.: -4.39 ppm)

Appearance: Light brown powder

Mp: 239-241 °C

TLC: R_f = 0.78 (PE/EtOAc = 3/1)

E IV.1.20 Ethyl 4,6-dichloro-8-fluoroquinoline-3-carboxylate [208] DCBSPU16

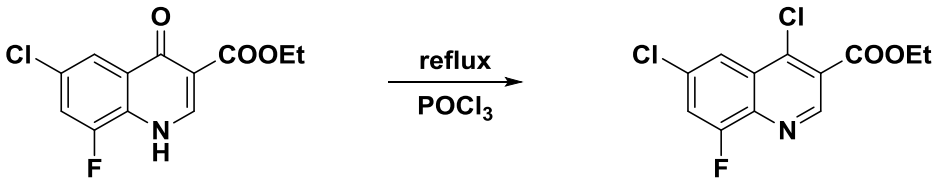

[201] **[208] (75%)**

Chemical Formula: $C_{12}H_9ClFNO_3$
Molecular Weight: 269.66

Chemical Formula: $C_{12}H_8Cl_2FNO_2$
Molecular Weight: 288.10

622 mg (2.31 mmol) of ethyl 6-chloro-8-fluoro-4-oxo-1,4-dihydroquinoline-3-carboxylate **[201]** were converted according to general procedure E III.3 to give ethyl 4,6-dichloro-8-fluoroquinoline-3-carboxylate **[208]** (500 mg, 1.73 mmol, 75%).

^{1}H NMR (400 MHz, $CDCl_3$) δ 1.47 (t, *J* = 7.1 Hz, 3H, CH_3), 4.51 (q, *J* = 7.2 Hz, 2H, CH_2), 7.55 (dd, *J* = 9.4, 2.2 Hz, 1H, H7), 8.19 (dd, *J* = 2.2, 1.5 Hz, 1H, H5), 9.19 (d, *J* = 0.6 Hz, 1H, H2).

^{13}C NMR (101 MHz, $CDCl_3$) δ 14.3 (q, CH_3), 62.7 (t, CH_2), 117.8 (dd, $^{2}J_{C,F}$ = 22.2 Hz, C7), 120.5 (dd, $^{4}J_{C,F}$ = 4.9 Hz, C5), 125.1 (s, C3), 128.3 (sd, $^{4}J_{C,F}$ = 2.2 Hz, C4), 134.2 (sd, $^{3}J_{C,F}$ = 10.1 Hz, C6), 138.6 (sd, $^{2}J_{C,F}$ = 12.6 Hz, C8a), 142.5 (sd, $^{3}J_{C,F}$ = 4.2 Hz, C4a), 150.4 (dd, $^{4}J_{C,F}$ = 1.5 Hz, C2), 158.0 (sd, $^{1}J_{C,F}$ = 262.9 Hz, C8), 164.0 (s, CO).

HR-MS: Calc.[M+H]: 294.0891

Found [M+H]: n.det.

Appearance: Colorless crystals

Mp: 81-83 °C (Lit.: no reference and not reported)

TLC: R_f = 0.83 (PE/EtOAc = 3/1)

E IV.1.21 Ethyl 4,6,8-trichloroquinoline-3-carboxylate [209] DCBSPU25

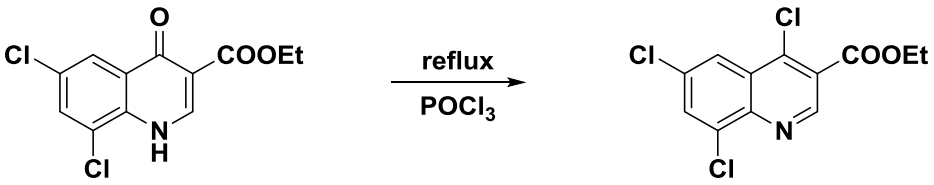

[202] **[209] (32%)**

Chemical Formula: $C_{12}H_9Cl_2NO_3$
Molecular Weight: 286.11

Chemical Formula: $C_{12}H_8Cl_3NO_2$
Molecular Weight: 304.55

207 mg (0.72 mmol) of ethyl 6,8-dichloro-4-oxo-1,4-dihydroquinoline-3-carboxylate **[202]** were converted according to general procedure E III.3 to give ethyl 4,6,8-trichloroquinoline-3-carboxylate **[209]** (70 mg, 0.23 mmol, 32%).

^{1}H NMR (400 MHz, $CDCl_3$) δ 1.46 (t, *J* = 7.1 Hz, 3H, CH_3), 4.51 (q, *J* = 7.1 Hz, 2H, CH_2), 7.94 (d, *J* = 2.2 Hz, 1H, H7), 8.33 (d, *J* = 2.2 Hz, 1H, H5), 9.27 (s, 1H, H2).

^{13}C NMR (101 MHz, $CDCl_3$) δ 14.3 (q, CH_3), 62.7 (t, CH_2), 123.7 (d, C5), 124.8 (s, C3), 128.1 (s, C4), 132.7 (d, C7), 134.2 (s, C6), 135.6 (s, C8), 142.9 (s, C8a), 144.5 (s, C4a), 150.7 (d, C2), 163.9 (s, CO).

Appearance: Colorless crystals

Mp: 108-110 °C (Lit.[201]: 109-110 °C)

TLC: R_f = 0.51 (PE/EtOAc = 3/1)

E IV.1.22 Ethyl 8-bromo-4,6-dichloroquinoline-3-carboxylate [210] DCBSPU14

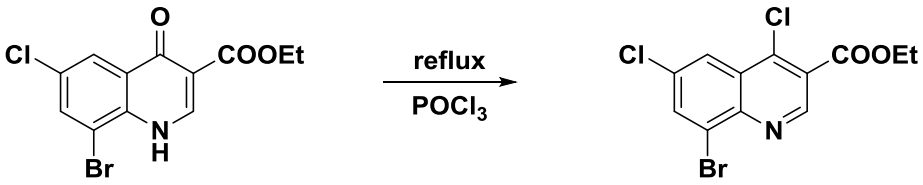

[203] **[210] (72%)**

Chemical Formula: $C_{12}H_9BrClNO_3$
Molecular Weight: 330.56

Chemical Formula: $C_{12}H_8BrCl_2NO_2$
Molecular Weight: 349.01

605 mg (1.83 mmol) of ethyl 8-bromo-6-chloro-4-oxo-1,4-dihydroquinoline-3-carboxylate **[203]** were converted according to general procedure E III.3 to give ethyl 8-bromo-4,6-dichloroquinoline-3-carboxylate **[210]** (460 mg, 1.32 mmol, 72%).

^{1}H NMR (400 MHz, DMSO-d_6) δ 1.39 (t, J = 7.1 Hz, 3H, CH_3), 4.45 (q, J = 7.1 Hz, 2H, CH_2), 8.38 (d, J = 2.3 Hz, 1H, H5), 8.48 (d, J = 2.2 Hz, 1H, H7), 9.24 (s, 1H, H2).

^{13}C NMR (101 MHz, DMSO-d_6) δ 14.0 (q, CH_3), 62.3 (t, CH_2), 123.9 (d, C5), 124.8 (s, C3), 126.2 (s, C8), 127.0 (s, C4), 133.6 (s, C6), 135.6 (d, C7), 141.1 (s, C8a), 144.4 (s, C4a), 150.7 (d, C2), 163.4 (s, CO).

HR-MS: Calc.[M+H]: 347.9188

Found [M+H]: n.det.

Appearance: Yellow solid

Mp: 125-127 °C

TLC: R_f = 0.76 (PE/EtOAc = 3/1)

E IV.1.23 Ethyl 4,6-dichloro-8-(trifluoromethyl)quinoline-3-carboxylate [211] DCBSPU15

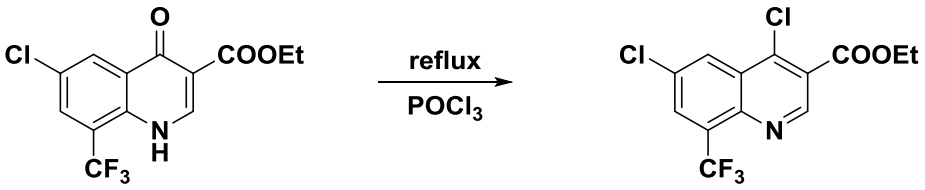

[204] **[211] (69%)**

Chemical Formula: $C_{13}H_9ClF_3NO_3$
Molecular Weight: 319.66

Chemical Formula: $C_{13}H_8Cl_2F_3NO_2$
Molecular Weight: 338.11

380 mg (1.19 mmol) of ethyl 6-chloro-4-oxo-8-(trifluoromethyl)-1,4-dihydroquinoline-3-carboxylate **[204]** were converted according to general procedure E III.3 to ethyl 4,6-dichloro-8-(trifluoromethyl)quinoline-3-carboxylate **[211]** (277 mg, 0.82 mmol, 69%).

^{1}H NMR (^{1}H NMR (400 MHz, $CDCl_3$) δ 1.46 (t, *J* = 7.1 Hz, 3H, CH_3), 4.52 (q, *J* = 7.1 Hz, 2H, CH_2), 8.15 (d, *J* = 2.1 Hz, 1H, H5), 8.61 (d, *J* = 2.1 Hz, 1H, H7), 9.32 (s, 1H, H2).

^{13}C NMR (101 MHz, $CDCl_3$) δ 14.3 (q, CH_3), 62.7 (t, CH_2), 122.9 (qs, $^{1}J_{C,F}$ = 274.9 Hz, CF_3), 124.7 (s, C3), 128.0 (s, C4), 128.7 (d, C5), 130.2 (qs, $^{2}J_{C,F}$ = 31.4 Hz, C8), 131.5 (qd, $^{3}J_{C,F}$ = 5.4 Hz, C7), 133.7 (s, C6), 142.6 (s, C8a), 144.6 (s, C4a), 151.2 (s, C2), 163.8 (s, CO).

HR-MS: Calc.[M+H]: 337.9957

Found [M+H]: n.det.

Appearance: Colorless crystals

Mp: 52-54 °C

TLC: R_f = 0.83 (PE/EtOAc = 3/1)

E IV.1.24 Ethyl 4,6-dichloro-8-methylquinoline-3-carboxylate [212] DCBSPU24

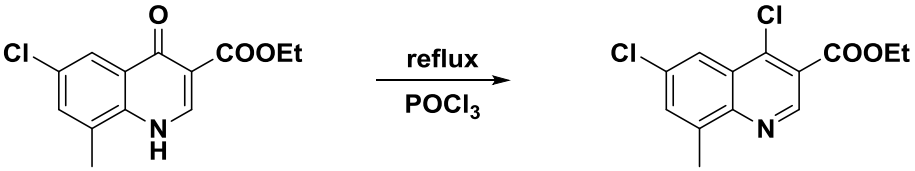

[205] **[212] (63%)**

Chemical Formula: $C_{13}H_{12}ClNO_3$
Molecular Weight: 265.69

Chemical Formula: $C_{13}H_{11}Cl_2NO_2$
Molecular Weight: 284.14

212 mg (0.80 mmol) of ethyl 6-chloro-8-methyl-4-oxo-1,4-dihydroquinoline-3-carboxylate **[205]** were converted according to general procedure E III.3 to give ethyl 4,6-dichloro-8-methylquinoline-3-carboxylate **[212]** (143 mg, 0.50 mmol, 63%).

^{1}H NMR (400 MHz, $CDCl_3$) δ 1.46 (t, *J* = 7.1 Hz, 3H, $CH_2C\underline{H}_3$), 2.79 (s, 3H, CH_3), 4.50 (q, *J* = 7.1 Hz, 2H, $C\underline{H}_2CH_3$), 7.62 – 7.65 (m, 1H, H7), 8.21 – 8.25 (m, 1H, H5), 9.17 (s, 1H, H2).

^{13}C NMR (101 MHz, $CDCl_3$) δ 14.4 (q, $CH_2\underline{C}H_3$), 18.3 (q, CH_3), 62.3 (t, CH_2), 122.3 (d, C5), 123.7 (s, C3), 127.2 (s, C4), 132.8 (d, C7), 134.3 (s, C6), 140.3 (s, C8), 142.5 (s, C8a), 147.2 (s, C4a), 149.0 (d, C2), 164.5 (s, CO).

HR-MS: Calc.[M+H]: 284.0240

Found [M+H]: n.det.

Appearance: Colorless crystals

Mp: 86-88 °C (Lit.[202]: not reported)

TLC: R_f = 0.70 (PE/EtOAc = 3/1)

E IV.1.25 Ethyl 4,6-dichloro-8-ethylquinoline-3-carboxylate [213] DCBSPU52

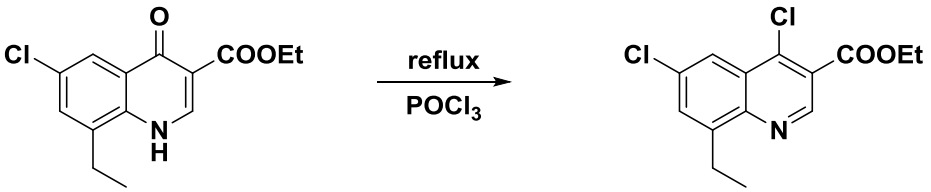

[206] **[213] (55%)**

Chemical Formula: $C_{14}H_{14}ClNO_3$
Molecular Weight: 279.72

Chemical Formula: $C_{14}H_{13}Cl_2NO_2$
Molecular Weight: 298.16

521 mg (1.77 mmol) of ethyl 6-chloro-8-ethyl-4-oxo-1,4-dihydroquinoline-3-carboxylate **[206]** were converted according to general procedure E III.3 to give ethyl 4,6-dichloro-8-ethylquinoline-3-carboxylate **[213]** (290 mg, 0.97 mmol, 55%).

^{1}H NMR (400 MHz, DMSO-d_6) δ 1.28 (t, *J* = 7.5 Hz, 3H, $CH_2C\underline{H}_3$), 1.38 (t, *J* = 7.1 Hz, 3H, $OCH_2C\underline{H}_3$), 3.21 (q, *J* = 7.5 Hz, 2H, $C\underline{H}_2CH_3$), 4.44 (q, *J* = 7.1 Hz, 2H, $OC\underline{H}_2CH_3$), 7.85 (d, *J* = 2.3 Hz, 1H, H7), 8.17 (d, *J* = 2.3 Hz, 1H, H5), 9.15 (s, 1H, H4).

^{13}C NMR (101 MHz, DMSO-d_6) δ 14.0 (q, $OCH_2\underline{C}H_3$), 14.9 (q, $CH_2\underline{C}H_3$), 24.0 (t, $\underline{C}H_2CH_3$), 62.1 (t, $O\underline{C}H_2CH_3$), 121.3 (d, C5), 123.9 (s, C3), 126.2 (s, C4), 131.1 (d, C7), 133.7 (s, C6), 140.7 (s, C8a), 145.7 (s, C4a/C8), 146.0 (s, C4a/C8), 148.9 (d, C2), 163.7 (s, CO).

HR-MS: Calc.[M+H]: 298.0396

Found [M+H]: n.det.

Appearance: Colorless crystals

Mp: 52-54 °C

TLC: R_f = 0.61 (PE/EtOAc = 10/1)

E IV.1.26 Ethyl 4,6-dichloro-8-isopropylquinoline-3-carboxylate [214] DCBSPU49

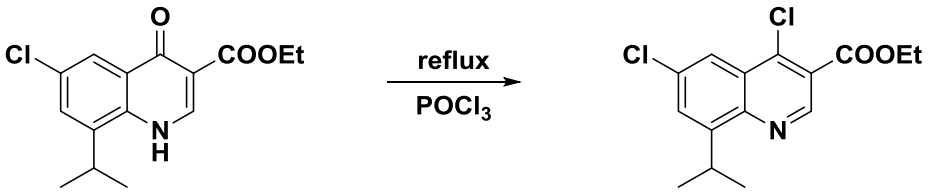

[207] **[214] (62%)**

Chemical Formula: $C_{15}H_{16}ClNO_3$
Molecular Weight: 293.75

Chemical Formula: $C_{15}H_{15}Cl_2NO_2$
Molecular Weight: 312.19

340 mg (1.16 mmol) of ethyl 6-chloro-8-isopropyl-4-oxo-1,4-dihydroquinoline-3-carboxylate **[207]** were converted according to general procedure E III.3 to give ethyl 4,6-dichloro-8-isopropylquinoline-3-carboxylate **[214]** (224 mg, 0.72 mmol, 62%).

^{1}H NMR (400 MHz, CDCl3) δ 1.37 (d, *J* = 6.9 Hz, 6H, 2 CHC$\underline{H}_3$), 1.46 (t, *J* = 7.1 Hz, 3H, CH_2CH_3), 4.29 (hept, *J* = 6.8 Hz, 1H, C$\underline{H}CH_3$), 4.50 (q, *J* = 7.1 Hz, 2H, CH2), 7.65 (d, *J* = 2.3 Hz, 1H, H5), 8.25 (d, *J* = 2.3 Hz, 1H, H7), 9.18 (s, 1H, H2).

^{13}C NMR (101 MHz, $CDCl_3$) δ 14.4 (q, $CH_2\underline{C}H_3$), 23.4 (q, 2 CH$\underline{C}H_3$), 28.0 (d, $\underline{C}HCH_3$), 62.3 (t, $\underline{C}H_2CH_3$), 122.0 (d, C5), 123.6 (s, C3), 127.4 (s, C4), 129.0 (d, C7), 134.9 (s, C6), 142.5 (s, C8a), 146.1 (d, C8), 148.9 (s, C2), 150.5 (s, C4a), 164.6 (s, CO).

HR-MS: Calc.[M+H]: 312.0553

Found [M+H]: n.det.

Appearance: Colorless crystals

Mp: 66-68 °C

TLC: R_f = 0.65 (PE/EtOAc = 10/1)

E IV.2 Pyrazoloquinoline precursors of R^7 and R^8 series

E IV.2.1 Diethyl 2-(((4-fluorophenyl)amino)methylene)malonate [23] DCBSLK001

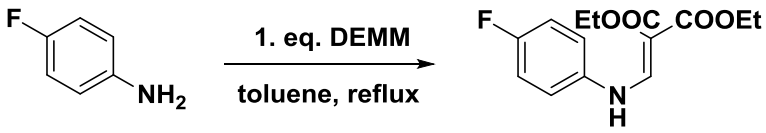

[20] **[23] (quant.)**

Chemical Formula: C_6H_6FN
Molecular Weight: 111.12

Chemical Formula: $C_{14}H_{16}FNO_4$
Molecular Weight: 281.28

The compound was synthesized according to general procedure E III.1 using:

4-Fluoroaniline	5.00 g	45.2 mmol	1 eq.
DEMM	7.39 mL	45.2 mmol	1 eq.

After evaporation diethyl 2-(((4-fluorophenyl)amino)methylene)malonate **[23]** was obtained without further purification (12.5 g, 45.0 mmol, quant.).

^{1}H NMR (400 MHz, $CDCl_3$) δ 1.32 (t, *J* = 7.1 Hz, 3H, CH_3), 1.37 (t, *J* = 7.1 Hz, 3H, CH_3), 4.24 (q, *J* = 7.1 Hz, 2H, CH_2), 4.30 (q, *J* = 7.1 Hz, 2H, CH_2), 7.01 – 7.17 (m, 4H, H2 and H3 and H5 and H6), 8.43 (d, *J* = 13.6 Hz, 1H, NHCH), 11.00 (br d, *J* = 13.6 Hz, 1H, NH).

^{13}C NMR (101 MHz, $CDCl_3$) δ 14.3 (q, CH_3), 14.4 (q, CH_3), 60.1 (t, CH_2), 60.5 (t, CH_2), 93.5 (s, C_{quart}), 116.7 (dd, $^2J_{C,F}$ = 23.1 Hz, C3 und C5),118.9 (dd, $^3J_{C,F}$ = 8.2 Hz, C2 und C6),135.6 (sd, $^4J_{C,F}$ = 2.8 Hz, C1), 152.4 (d, NHCH), 160.0 (sd, $^1J_{C,F}$ = 244.7 Hz, C4), 165.7 (s, CO), 169.1 (s, CO).

Appearance: Colorless solid

Mp: 69-71 °C (Lit.[203]: 74-76 °C)

TLC: R_f = 0.65 (PE/EtOAc = 3/1)

E IV.2.2 Diethyl 2-(((4-chlorophenyl)amino)methylene)malonate [24] DCBS21

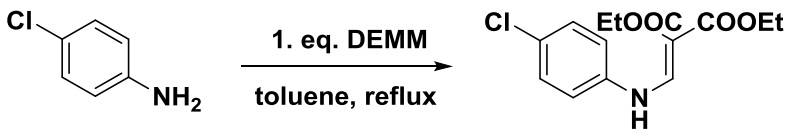

[21] **[24] (quant.)**

Chemical Formula: C_6H_6ClN
Molecular Weight: 127.57

Chemical Formula: $C_{14}H_{16}ClNO_4$
Molecular Weight: 297.74

The compound was synthesized according to general procedure E III.1 using:

4-Chloroaniline	8 g	57.0 mmol	1 eq.
DEMM	11.5 mL	57.0 mmol	1 eq.

After recrystallization diethyl 2-(((4-chlorophenyl)amino)methylene)malonate **[24]** was obtained (17.0 g, 57 mmol, quant.).

^{1}H NMR (400 MHz, $CDCl_3$) δ 1.33 (t, *J* = 7.1 Hz, 3H, CH_3), 1.38 (t, *J* = 7.1 Hz, 3H, CH_3), 4.25 (q, *J* = 7.2 Hz, 2H, CH_2), 4.30 (q, *J* = 7.2 Hz, 2H, CH_2), 7.07 (d, *J* = 8.8 Hz, 2H, H2 and H6), 7.33 (d, *J* = 8.8 Hz, 2H, H3 and H5), 8.45 (d, *J* = 13.6 Hz, 1H, NHC<u>H</u>), 11.00 (br d, *J* = 13.5 Hz, 1H, NH).

^{13}C NMR (101 MHz, $CDCl_3$) δ 14.4 (q, CH_3), 14.6 (q, CH_3), 60.4 (t, CH_2), 60.7 (t, CH_2), 94.4 (s, $C_{quart.}$), 118.5 (d, C2 and C6), 130.0 (d, C3 and C5), 130.2 (s, C4), 138.1 (s, C1), 151.7 (d, NHCH), 165.7 (s, CO), 169.1 (s, CO).

Appearance: Yellow crystals

Mp: 79-81 °C (Lit.[200]: 80-81 °C)

TLC: R_f = 0.85 (PE/EtOAc = 3/1)

E IV.2.3 Diethyl 2-(((4-bromophenyl)amino)methylene)malonate [25] DCBS01

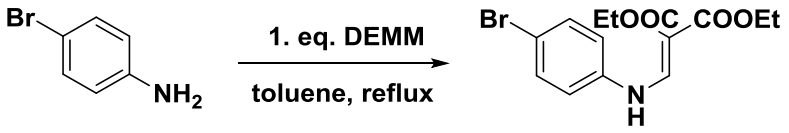

[22] **[25] (99%)**

Chemical Formula: C_6H_6BrN
Molecular Weight: 172.03

Chemical Formula: $C_{14}H_{16}BrNO_4$
Molecular Weight: 342.19

The compound was synthesized according to general procedure E III.1 using:

4-Bromoaniline	6.91 g	36.5 mmol	1 eq.
DEMM	7.39 mL	36.5 mmol	1 eq.

After recrystallization diethyl 2-(((4-bromophenyl)amino)methylene)malonate **[25]** was obtained (12.9 g, 36.2 mmol, 99%).

^{1}H NMR (400 MHz, $CDCl_3$) δ 1.32 (t, *J* = 7.1 Hz, 3H, CH_3), 1.37 (t, *J* = 7.1 Hz, 3H, CH_3), 4.24 (q, *J* = 7.1 Hz, 2H, CH_2), 4.30 (q, *J* = 7.1 Hz, 2H, CH_2), 6.98 – 7.05 (m, 2H, H2 and H6), 7.44 – 7.52 (m, 2H, H3 and H5), 8.45 (d, *J* = 13.6 Hz, 1H, NHCH), 10.99 (br d, *J* = 13.5 Hz, 1H, NH).

^{13}C NMR (101 MHz, $CDCl_3$) δ 14.4 (q, CH_3), 14.6 (q, CH_3), 60.4 (t, CH_2), 60.7 (t, CH_2), 94.5 (s, $C_{quart.}$), 117.7 (s, C4), 118.8 (d, C2 and C6), 133.0 (d, C3 and C5), 138.6 (d, C1), 151.5 (NHCH), 165.7 (s, CO), 169.1 (s, CO).

Appearance: Yellow crystals

Mp: 95-97 °C (Lit.[204]: 100-102 °C)

TLC: R_f = 0.74 (PE/EtOAc = 3/1)

E IV.2.4 Diethyl 2-(((3-bromophenyl)amino)methylene)malonate [160] DCBSLG01

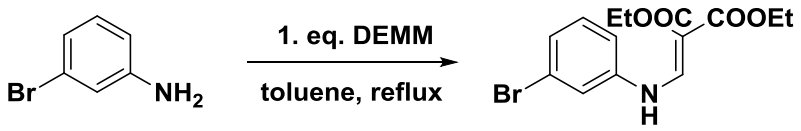

[159] **[160] (quant.)**

Chemical Formula: C_6H_6BrN
Molecular Weight: 172.03

Chemical Formula: $C_{14}H_{16}BrNO_4$
Molecular Weight: 342.19

The compound was synthesized according to general procedure E III.1 using:

3-Bromoaniline	5.03 g	29 mmol	1 eq.
DEMM	5.89 mL	29 mmol	1 eq

After purification by FC diethyl 2-(((3-bromophenyl)amino)methylene)malonate **[160]** was obtained (9.92 g, 29 mmol, quant.).

^{1}H NMR (400 MHz, $CDCl_3$) δ 1.33 (t, *J* = 7.1 Hz, 3H, CH_3), 1.37 (t, *J* = 7.1 Hz, 3H, CH_3), 4.25 (q, *J* = 7.1 Hz, 2H, CH_2), 4.30 (q, *J* = 7.1 Hz, 2H, CH_2), 7.02 – 7.06 (m, 1H, H2), 7.19 – 7.30 (m, 3H, H4/H5/H6), 8.44 (d, *J* = 13.4 Hz, 1H, NHC<u>H</u>), 10.98 (br d, *J* = 13.5 Hz, 1H, NH).

^{13}C NMR (101 MHz, $CDCl_3$) δ 14.4 (q, CH_3), 14.5 (q, CH_3), 60.4 (t, CH_2), 60.7 (t, CH_2), 94.8 (s, $C_{quart.}$), 115.9 (d, C2), 120.2 (d, C4/C6), 123.7 (s, C3), 127.8 (d, C4/C6), 131.2 (d, C5), 140.7 (s, C1), 151.3 (d, NHCH), 165.6 (s, CO), 169.0 (s, CO).

Appearance: Colorless crystals

Mp: 71-73 °C (Lit.[205]: 61-62 °C)

TLC: R_f = 0.86 (PE/EtOAc = 8/1)

E IV.2.5 Diethyl 2-(([1,1'-biphenyl]-4-ylamino)methylene)-malonate [88b] DCBS02

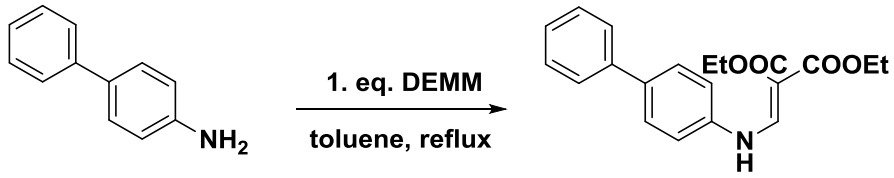

[88a]

Chemical Formula: $C_{12}H_{11}N$
Molecular Weight: 169.23

[88b] (91%)

Chemical Formula: $C_{20}H_{21}NO_4$
Molecular Weight: 339.39

The compound was synthesized according to general procedure E III.1 using:

4-Biphenylaniline	3 g	16.1 mmol	1 eq.
DEMM	3.25 mL	16.1 mmol	1 eq.

After purification by FC diethyl 2-(([1,1'-biphenyl]-4-ylamino)methylene)malonate **[88b]** was obtained (4.99 g, 14.7 mmol, 91%).

^{1}H NMR (400 MHz, $CDCl_3$) δ 1.34 (t, *J* = 7.1 Hz, 3H, CH_3), 1.40 (t, *J* = 7.1 Hz, 3H, CH_3), 4.27 (q, *J* = 7.1 Hz, 2H, CH_2), 4.33 (q, *J* = 7.1 Hz, 2H, CH_2), 7.19 – 7.24 (m, 2H, H3 and H5), 7.32 – 7.40 (m, 1H, H-Ar), 7.41 – 7.51 (m, 2H, 2 H-Ar), 7.54 – 7.63 (m, 4H, 2 H-Ar and H2 and H6), 8.57 (d, *J* = 13.7 Hz, 1H, NHC<u>H</u>), 11.08 (br d, *J* = 13.7 Hz, 1H, NH).

^{13}C NMR (101 MHz, $CDCl_3$) δ 14.5 (q, CH_3), 14.6 (q, CH_3), 60.3 (t, CH_2), 60.6 (t, CH_2), 93.9 (s, $C_{quart.}$), 117.6 (d, 2 C-Ar), 126.9 (d, 2 C-Ar), 127.5 (d, C-Ar), 128.6 (d, 2 C-Ar), 129.0 (d, 2 C-Ar), 138.0 (s, C1'/C4), 138.6 (s, C1), 140.1 (s, C1'/C4), 151.8 (d, NHCH), 165.9 (s, CO), 169.2 (s, CO).

Appearance: Yellow crystals

Mp: 82-84 °C (Lit.[206]: 88-89 °C)

TLC: R_f = 0.68 (PE/EtOAc = 3/1)

E IV.2.6 Diethyl 2-(((4-methoxyphenyl)amino)methylene)-malonate [6] DCBS10

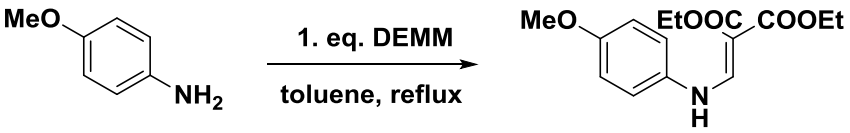

[5]

Chemical Formula: C_7H_9NO
Molecular Weight: 123.16

[6] (73%)

Chemical Formula: $C_{15}H_{19}NO_5$
Molecular Weight: 293.32

The compound was synthesized according to general procedure E III.1 using:

4-Methoxylaniline	5 g	36.9 mmol	1 eq.
DEMM	7.46 mL	36.9 mmol	1 eq.

After purification by FC diethyl 2-(((4-methoxyphenyl)amino)methylene)malonate **[6]** was obtained (7.90 g, 26.9 mmol, 73%).

^{1}H NMR (400 MHz, $CDCl_3$) δ 1.31 (t, *J* = 7.1 Hz, 3H, CH_3), 1.37 (t, *J* = 7.1 Hz, 3H, CH_3), 3.80 (s, 3H, OCH_3), 4.23 (q, *J* = 7.1 Hz, 2H, CH_2), 4.29 (q, *J* = 7.1 Hz, 2H, CH_2), 6.86 – 6.94 (m, 2H, H3 and H5), 7.05 – 7.10 (m, 2H, H2 and H6), 8.43 (d, *J* = 13.9 Hz, 1H, NHC<u>H</u>), 10.98 (br d, *J* = 13.8 Hz, 1H, NH).

^{13}C NMR (101 MHz, $CDCl_3$) δ 14.5 (q, CH_3), 14.6 (q, CH_3), 55.7 (q, OCH_3), 60.1 (t, CH_2), 60.4 (t, CH_2), 92.6 (s, $C_{quart.}$), 115.1 (d, C3 and C5), 119.0 (d, C2 and C6), 132.9 (s, C1), 152.8 (d, NHCH), 157.3 (s, C4), 166.0 (s, CO), 169.4 (s, CO).

Appearance: Yellow crystals

Mp: 32-34 °C (Lit.[203]: 38-39 °C)

TLC: R_f = 0.63 (PE/EtOAc = 3/1)

E IV.2.7 Diethyl 2-(((3-methoxyphenyl)amino)methylene)-malonate [177] DCBSLA8

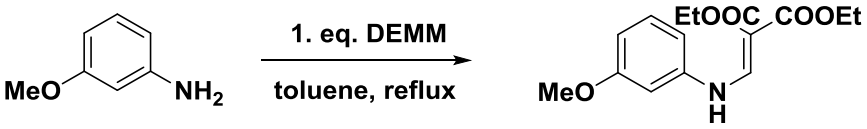

[176]

Chemical Formula: C_7H_9NO
Molecular Weight: 123.16

[177] (quant.)

Chemical Formula: $C_{15}H_{19}NO_5$
Molecular Weight: 293.32

The compound was synthesized according to general procedure E III.1 using:

3-Methoxylaniline	1.52 g	12.3 mmol	1 eq.
DEMM	2.49 mL	12.3 mmol	1 eq.

After purification by FC diethyl 2-(((3-methoxyphenyl)amino)methylene)malonate **[177]** was obtained (3.61 g, 12.3 mmol, quant.).

^{1}H NMR (200 MHz, $CDCl_3$) δ 1.35 (dt, *J* = 11.0, 7.1 Hz, 6H, 2 CH_3), 3.82 (s, 3H, OCH_3), 4.24 (q, *J* = 7.1 Hz, 2H, CH_2), 4.32 (q, *J* = 7.1 Hz, 2H, CH_2), 6.61 – 6.81 (m, 3H, H2 and H4 and H6), 7.18 – 7.36 (m, 1H, H5), 8.51 (d, *J* = 13.7 Hz, 1H, NHC<u>H</u>), 10.98 (br d, *J* = 13.6 Hz, 1H, NH).

^{13}C NMR (101 MHz, $CDCl_3$) δ 14.5 (q, CH_3), 14.6 (q, CH_3), 55.6 (q, OCH_3), 60.3 (t, CH_2), 60.6 (t, CH_2), 93.8 (s, $C_{quart.}$), 103.5 (d, C2), 109.6 (d, C4/C6), 110.4 (d, C4/C6), 130.8 (d, C5), 140.6 (s, C1), 152.0 (d, NHCH), 161.0 (s, C3), 165.8 (s, CO), 169.2 (s, CO).

Appearance: Yellow crystals

Mp: 39-41 °C (Lit.[207]: 40-41 °C)

TLC: R_f = 0.71 (PE/EtOAc = 3/1)

E IV.2.8 Ethyl 6-fluoro-4-oxo-1,4-dihydroquinoline-3-carboxylate [26] DCBSLK005

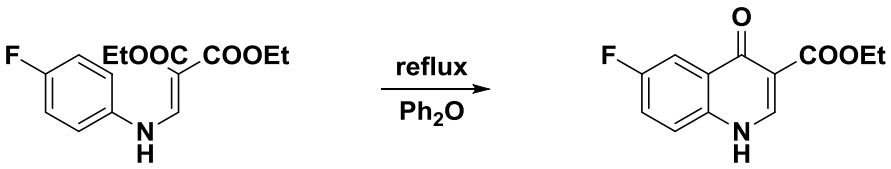

[23] **[24] (41%)**

Chemical Formula: $C_{14}H_{16}FNO_4$
Molecular Weight: 281.28

Chemical Formula: $C_{12}H_{10}FNO_3$
Molecular Weight: 235.21

Ethyl 6-fluoro-4-oxo-1,4-dihydroquinoline-3-carboxylate **[26]** was synthesized according to general procedure E III.2 using 5.1 g (45.2 mmol) of diethyl 2-(((4-chlorophenyl)amino)methylene)malonate **[23]** (4.1 g, 18.1 mmol, 41%).

^{1}H NMR (600 MHz, DMSO-d_6) δ 1.28 (t, J = 7.1 Hz, 3H, CH_3), 4.21 (q, J = 7.1 Hz, 2H, CH_2), 7.63 (td, J = 8.6, 3.0 Hz, 1H, H7), 7.71 (dd, J = 9.0, 4.6 Hz, 1H, H8), 7.80 (dd, J = 9.3, 3.0 Hz, 1H, H5), 8.58 (s, 1H, H2), 12.48 (br s, 1H, NH).

^{13}C NMR (151 MHz, DMSO-d_6) δ 14.4 (q, CH_3), 59.7 (t, CH_2), 109.0 (s, C3), 110.2 (dd, $^{2}J_{C,F}$ = 22.7 Hz, C5), 121.1 (dd, $^{2}J_{C,F}$ = 25.1 Hz, C7), 121.8 (dd, $^{3}J_{C,F}$ = 8.0 Hz, C8), 128.8 (sd, $^{3}J_{C,F}$ = 6.6 Hz, C4a), 135.8 (s, C8a), 145.1 (d, C2), 159.1 (sd, $^{1}J_{C,F}$ = 243.5 Hz, C6), 164.8 (s, CO), 172.6 (s, CO).

Appearance: Colorless powder

Mp: 280 - 281 °C (Lit.[208]: 296 - 298°C)

TLC: R_f = 0.35 (2% MeOH in CH_2Cl_2)

E IV.2.9 Ethyl 6-chloro-4-oxo-1,4-dihydroquinoline-3-carboxylate [27] DCBS25

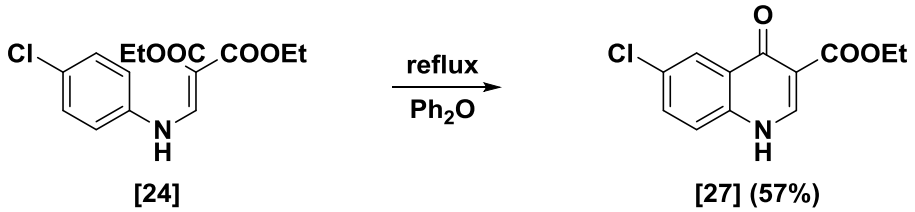

[24] **[27] (57%)**

Chemical Formula: $C_{14}H_{16}ClNO_4$
Molecular Weight: 297.74

Chemical Formula: $C_{12}H_{10}ClNO_3$
Molecular Weight: 251.67

Ethyl 6-chloro-4-oxo-1,4-dihydroquinoline-3-carboxylate **[27]** was synthesized according to general procedure E III.2 using 2 g (7.95 mmol) of diethyl 2-(((4-chlorophenyl)amino)methylene)malonate **[24]** (960 mg, 3.81 mmol, 57%).

^{1}H NMR (200 MHz, DMSO-d_6) δ 1.28 (t, *J* = 7.0 Hz, 3H, CH_3), 4.22 (q, *J* = 7.1 Hz, 2H, CH_2), 7.62 – 7.82 (m, 2H, H7 and H8), 8.02 – 8.12 (m, 1H, H5), 8.59 (d, *J* = 6.6 Hz, 1H, H2), 12.48 (br s, 1H, NH).

^{13}C NMR (151 MHz, DMSO-d_6) δ 14.4 (q, CH_3), 59.8 (t, CH_2), 110.1 (s, C3), 121.3 (d, C5/C7), 124.7 (d, C5/C7), 128.4 (s, C4a), 129.4 (s, C6), 132.6 (d, C8), 137.7 (s, C8a), 145.3 (d, C2), 164.6 (s, CO), 172.3 (s, CO).

Appearance: Light brown powder

Mp: Decomposes > 300 °C (Lit.[200]: 295-296 °C)

TLC: R_f = 0.30 (2% MeOH in CH_2Cl_2)

E IV.2.10 Ethyl 6-bromo-4-oxo-1,4-dihydroquinoline-3-carboxylate [28] DCBS08

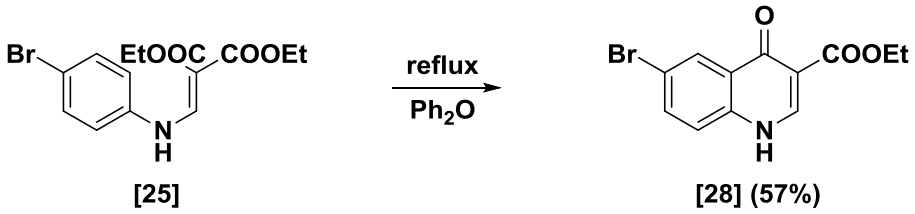

[25] **[28] (57%)**

Chemical Formula: $C_{14}H_{16}BrNO_4$
Molecular Weight: 342.19

Chemical Formula: $C_{12}H_{10}BrNO_3$
Molecular Weight: 296.12

Ethyl 6-bromo-4-oxo-1,4-dihydroquinoline-3-carboxylate **[28]** was synthesized according to general procedure E III.2 using 2 g (5.85 mmol) of diethyl 2-(((4-bromophenyl)amino)methylene)malonate **[25]** (1.26 g, 4.26 mmol, 73%).

^{1}H NMR (400 MHz, DMSO-d_6) δ 1.28 (t, *J* = 7.1 Hz, 3H, CH_3), 4.22 (q, *J* = 7.1 Hz, 2H, CH_2), 7.60 (d, *J* = 8.8 Hz, 1H, H8), 7.87 (dd, *J* = 8.8, 2.4 Hz, 1H, H7), 8.22 (d, *J* = 2.3 Hz, 1H, H5), 8.59 (s, 1H, H2), 12.46 (br s, 1H, NH).

^{13}C NMR (101 MHz, DMSO-d_6) δ 14.3 (q, CH_3), 59.7 (t, CH_2), 110.2 (s, C3), 117.4 (s, C6), 121.4 (d, C5/C7), 127.8 (d, C5/C7), 128.7 (s, C4a), 135.1 (d, C8), 138.0 (s, C8a), 145.2 (d, C2), 164.5 (s, CO), 172.1 (s, CO).

Appearance: Light brown powder

Mp: Decomposes > 300 °C (Lit.[209]: 320-322 °C)

TLC: R_f = 0.37 (2% MeOH in CH_2Cl_2)

E IV.2.11 Ethyl 7-bromo-4-oxo-1,4-dihydroquinoline-3-carboxylate [161] DCBSLG02

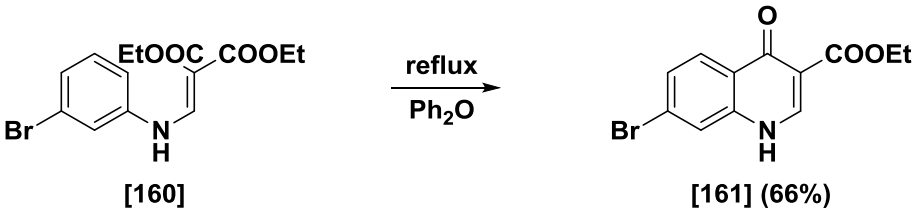

[160] **[161] (66%)**

Chemical Formula: $C_{14}H_{16}BrNO_4$
Molecular Weight: 342.19

Chemical Formula: $C_{12}H_{10}BrNO_3$
Molecular Weight: 296.12

Ethyl 7-bromo-4-oxo-1,4-dihydroquinoline-3-carboxylate **[161]** was synthesized according to general procedure E III.2 using 5 g (14.6 mmol) of diethyl 2-(((3-bromophenyl)amino)methylene)malonate **[160]** (2.86 g, 9.64 mmol, 66%).

^{1}H NMR (400 MHz, DMSO-d_6) δ 1.28 (t, *J* = 7.1 Hz, 3H, CH_3), 4.21 (q, *J* = 7.1 Hz, 2H, CH_2), 7.57 (dd, *J* = 8.6, 1.9 Hz, 1H, H6), 7.82 (d, *J* = 1.9 Hz, 1H, H8), 8.06 (d, *J* = 8.6 Hz, 1H, H5), 8.58 (d, *J* = 6.5 Hz, 1H, H2), 12.31 (br d, *J* = 6.4 Hz, 1H, NH).

13C NMR (101 MHz, DMSO-d_6) δ 14.3 (q, CH_3), 59.7 (t, CH_2), 110.5 (s, C3), 121.1 (d, C8), 125.8 (s, C4a/C7), 126.2 (s, C4a/C7), 127.7 (d, C6), 128.0 (d, C5), 140.0 (s, C8a), 145.5 (d, C2), 164.6 (s, CO), 172.9 (s, CO).

Appearance: Colorless solid

Mp: Decomposes > 300 °C (Lit.[205]: Decomposes at 334-335 °C)

TLC: R_f = 0.75 (5% MeOH in CH_2Cl_2)

E IV.2.12 Ethyl 4-oxo-6-phenyl-1,4-dihydroquinoline-3-carboxylate [88c] DCBS07

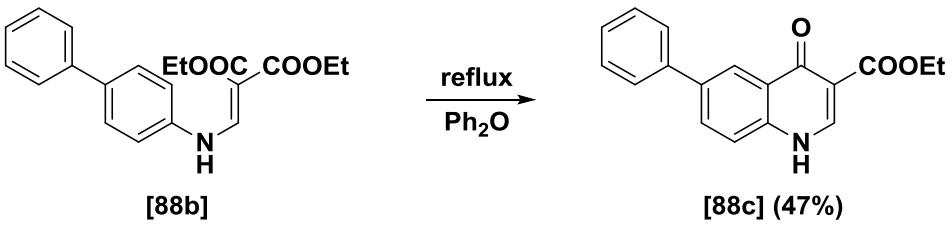

[88b]

Chemical Formula: $C_{20}H_{21}NO_4$
Molecular Weight: 339.39

[88c] (47%)

Chemical Formula: $C_{18}H_{15}NO_3$
Molecular Weight: 293.32

Ethyl 4-oxo-6-phenyl-1,4-dihydroquinoline-3-carboxylate **[88c]** was synthesized according to general procedure E III.2 using 0.5 g (1.47 mmol) of diethyl 2-(([1,1'-biphenyl]-4-ylamino)methylene)malonate **[88b]** (203 mg, 0.69 mmol, 47%).

^{1}H NMR (400 MHz, DMSO-d_6) δ 1.29 (t, *J* = 7.1 Hz, 3H, CH_3), 4.23 (q, *J* = 7.1 Hz, 2H, CH_2), 7.39 – 7.45 (m, 1H, H-Ar), 7.49 – 7.55 (m, 2H, H-Ar and H8), 7.70 – 7.76 (m, 3H, H-Ar), 8.04 (dd, *J* = 8.6, 2.2 Hz, 1H, H7), 8.38 (d, *J* = 2.2 Hz, 1H, H5), 8.57 (d, *J* = 6.4 Hz, 1H, H2), 12.40 (br d, *J* = 6.2 Hz, 1H, NH).

^{13}C NMR (101 MHz, DMSO-d_6) δ 14.8 (q, CH_3), 60.1 (t, CH_2), 110.4 (s, C3), 120.1 (d, C5/C7), 123.5 (d, C4'), 127.1 (d, C2'/C6'), 127.2 (d, C2'/C6'), 128.0 (s, C4a), 128.2 (d, C5/C7), 129.55 (d, C3'/C5'), 129.63 (d, C3'/C5'), 131.5 (d, C8), 137.0 (s, C6/C8a/C1'), 138.8 (s, C6/C8a/C1'), 139.6 (s, C6/C8a/C1'), 145.2 (d, C2), 165.3 (s, CO), 173.9 (s, CO).

Appearance: Yellow powder

Mp: Decomposes > 300 °C (Lit.[210]: 294-296 °C)

TLC: R_f = 0.28 (2% MeOH in CH_2Cl_2)

E IV.2.13 Ethyl 6-methoxy-4-oxo-1,4-dihydroquinoline-3-carboxylate [7] DCBS50

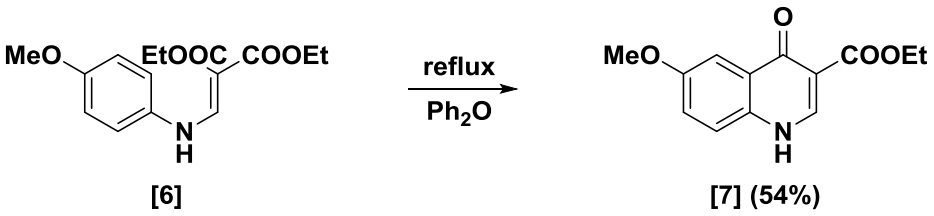

[6] **[7] (54%)**

Chemical Formula: $C_{15}H_{19}NO_5$
Molecular Weight: 293.32

Chemical Formula: $C_{13}H_{13}NO_4$
Molecular Weight: 247.25

Ethyl 6-methoxy-4-oxo-1,4-dihydroquinoline-3-carboxylate **[7]** was synthesized according to general procedure E III.2 using 2.5 g (8.52 mmol) of diethyl 2-(((4-methoxyphenyl)amino)methylene)malonate **[6]** (1.14 g, 4.62 mmol, 54%).

^{1}H NMR (600 MHz, DMSO-d_6) δ 1.27 (t, *J* = 7.1 Hz, 3H, CH_3), 3.84 (s, 3H, OCH_3), 4.20 (q, *J* = 7.1 Hz, 2H, CH_2), 7.34 (dd, *J* = 8.9, 3.0 Hz, 1H, H7), 7.56 (d, *J* = 3.0 Hz, 1H, H5), 7.58 (d, *J* = 9.0 Hz, 1H, H8), 8.49 (d, *J* = 6.7 Hz, 1H, H2), 12.30 (br d, *J* = 6.7 Hz, 1H, NH).

^{13}C NMR (151 MHz, DMSO-d_6) δ 14.4 (q, CH_3), 55.5 (q, OCH_3), 59.5 (t, CH_2), 105.5 (d, C5), 108.7 (s, C3), 120.6 (d, C7/C8), 122.2 (d, C7/C8), 128.5 (s, C4a), 133.4 (s, C8a), 143.7 (d, C2), 156.6 (s, C6), 165.0 (s, CO), 172.9 (s, CO).

Appearance: Brown powder

Mp: 265-267 °C (Lit.[211]: 273-276 °C)

TLC: R_f = 0.33 (2% MeOH in CH_2Cl_2)

E IV.2.14 Ethyl 7-methoxy-4-oxo-1,4-dihydroquinoline-3-carboxylate [178] DCBSLA11

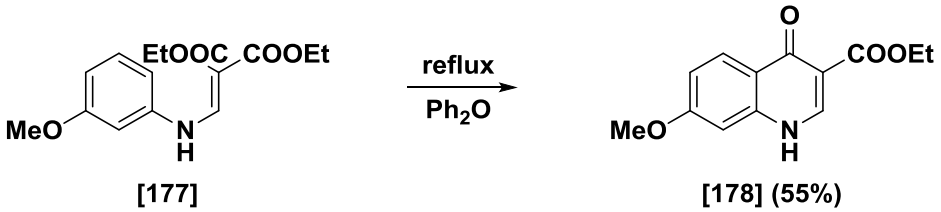

[177] **[178] (55%)**

Chemical Formula: $C_{15}H_{19}NO_5$
Molecular Weight: 293.32

Chemical Formula: $C_{13}H_{13}NO_4$
Molecular Weight: 247.25

Ethyl 7-methoxy-4-oxo-1,4-dihydroquinoline-3-carboxylate **[178]** was synthesized according to general procedure E III.2 using 1.66 g (5.64 mmol) of diethyl 2-(((3-methoxyphenyl)amino)methylene)malonate **[177]** (0.76 g, 3.09 mmol, 55%).

^{1}H NMR (400 MHz, DMSO-d_6) δ 1.27 (t, J = 7.1 Hz, 3H, CH_3), 3.86 (s, 3H, OCH_3), 4.20 (q, J = 7.1 Hz, 2H, CH_2), 6.97 – 7.03 (m, 2H, H6 and H8), 8.03 – 8.07 (m, 1H, H5), 8.48 (s, 1H, H2), 12.09 (br s, 1H, NH).

^{13}C NMR (101 MHz, DMSO-d_6) δ 14.3 (q, CH_3), 55.6 (q, OCH_3), 59.5 (t, CH_2), 100.1 (d, C5), 109.8 (s, C3), 114.1 (d, C6/C8), 121.3 (s, C4a), 127.5 (d, C6/C8), 140.7 (s, C8a), 144.8 (d, C2), 162.2 (s, C7), 164.8 (s, CO), 172.9 (s, CO).

Appearance: Light brown powder

Mp: Decomposes > 300 °C (Lit.[212]: not reported)

TLC: R_f = 0.48 (5% MeOH in CH_2Cl_2)

E IV.2.15 Ethyl 4-chloro-6-fluoroquinoline-3-carboxylate [29] DCBSLK008

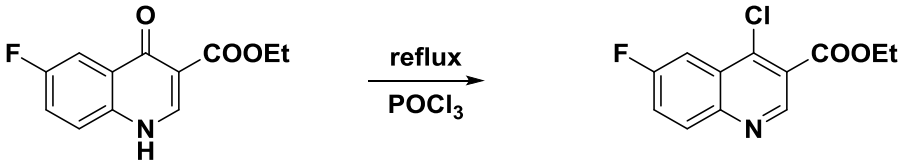

[26] **[29] (63%)**

Chemical Formula: $C_{12}H_{10}FNO_3$
Molecular Weight: 235.21

Chemical Formula: $C_{12}H_9ClFNO_2$
Molecular Weight: 253.66

4.13 g (17.5 mmol) of ethyl 6-fluoro-4-oxo-1,4-dihydroquinoline-3-carboxylate **[26]** were converted according to general procedure E III.3 to give ethyl 4-chloro-6-fluoroquinoline-3-carboxylate **[29]** (2.79 g, 11.0 mmol, 63%).

^{1}H NMR (400 MHz, $CDCl_3$) δ 1.46 (t, *J* = 7.1 Hz, 3H, CH_3), 4.50 (q, *J* = 7.1 Hz, 2H, CH_2), 7.61 (td, *J* = 8.4, 2.8 Hz, 1H, H7), 8.02 (dd, *J* = 9.5, 2.7 Hz, 1H; H5), 8.16 (dd, *J* = 9.3, 5.4 Hz, 1H, H8), 9.15 (s, 1H, H2).

^{13}C NMR (101 MHz, $CDCl_3$) δ 14.3 (q, CH_3), 62.4 (t, CH_2), 109.4 (dd, $^2J_{C,F}$ = 24.8 Hz, C5), 122.3 (dd, $^2J_{C,F}$ = 25.8 Hz, C7), 123.7 (s, C3),127.5 (sd, $^3J_{C,F}$ = 10.5 Hz, C4a), 132.7 (dd, $^3J_{C,F}$ = 9.2 Hz, C8), 142.6 (sd, $^3J_{C,F}$ = 5.7 Hz, C4/C8a), 146.7 (s, C4/C8a), 149.5 (dd, $^4J_{C,F}$ = 2.9 Hz, C2), 161.8 (sd, $^1J_{C,F}$ = 251.1 Hz, C6), 164.4 (s, CO).

Appearance: Colorless crystals

Mp: 60-62 °C (Lit.[213]: 62-63 °C)

TLC: R_f = 0.70 (PE/EtOAc = 3/1)

E IV.2.16 Ethyl 4,6-dichloroquinoline-3-carboxylate [30] DCBS30

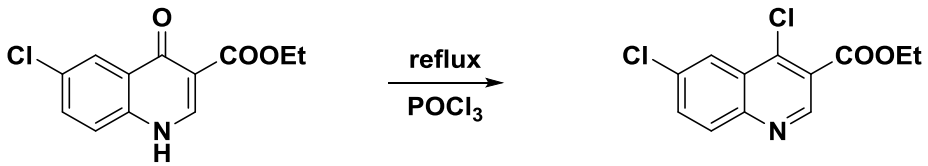

[27] **[30] (76%)**

Chemical Formula: $C_{12}H_{10}ClNO_3$
Molecular Weight: 251.67

Chemical Formula: $C_{12}H_9Cl_2NO_2$
Molecular Weight: 270.11

500 mg (1.99 mmol) of ethyl 6-chloro-4-oxo-1,4-dihydroquinoline-3-carboxylate **[27]** were converted according to general procedure E III.3 to give ethyl 4,6-dichloroquinoline-3-carboxylate **[30]** (406 mg, 1.50 mmol, 76%).

^{1}H NMR (200 MHz, $CDCl_3$) δ 1.46 (t, *J* = 7.1 Hz, 3H, CH_3), 4.50 (q, *J* = 7.1 Hz, 2H, CH_2), 7.77 (dd, *J* = 8.9, 2.2 Hz, 1H, H7), 8.08 (d, *J* = 9.0 Hz, 1H, H8), 8.38 (d, *J* = 2.2 Hz, 1H, H5), 9.18 (s, 1H, H2).

^{13}C NMR (50 MHz, $CDCl_3$) δ 14.4 (q, CH_3), 62.4 (t, CH_2), 123.9 (s, C3), 124.5 (d, C5), 127.1 (s, C4a), 131.6 (d, C7/C8), 133.0 (d, C7/C8), 134.9 (s, C6), 142.5 (s, C4/C8a), 148.0 (s, C4/C8a), 150.4 (d, C2), 164.3 (s, CO).

Appearance: Colorless crystals

Mp: 94-96 °C (Lit.[214]: 90-91 °C)

TLC: R_f = 0.51 (PE/EtOAc = 3/1)

E IV.2.17 Ethyl 6-bromo-4-chloroquinoline-3-carboxylate [31] DCBS16

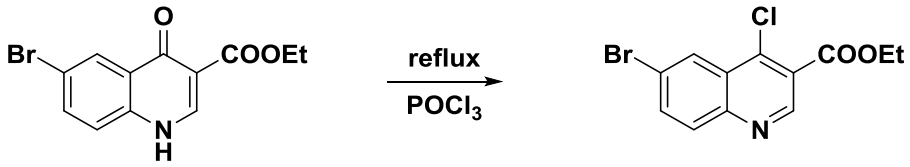

[28]

Chemical Formula: $C_{12}H_{10}BrNO_3$
Molecular Weight: 296.12

[31] (90%)

Chemical Formula: $C_{12}H_9BrClNO_2$
Molecular Weight: 314.56

1.35 g (3.95 mmol) of ethyl 6-bromo-4-oxo-1,4-dihydroquinoline-3-carboxylate **[28]** were converted according to general procedure E III.3 to give ethyl 6-bromo-4-chloroquinoline-3-carboxylate **[31]** (1.28 g, 4.08 mmol, 90%).

^{1}H NMR (200 MHz, $CDCl_3$) δ 1.46 (t, *J* = 7.1 Hz, 3H, CH_3), 4.50 (q, *J* = 7.1 Hz, 2H, CH_2), 7.90 (dd, *J* = 8.9, 2.0 Hz, 1H, H7), 8.01 (d, *J* = 8.9 Hz, 1H, H8), 8.56 (d, *J* = 1.9 Hz, 1H, H5), 9.19 (s, 1H, H2).

^{13}C NMR (50 MHz, $CDCl_3$) δ 14.4 (q, CH_3), 62.5 (t, CH_2), 123.0 (s, C3/C6), 123.9 (s, C3/C6), 127.5 (s, C4a), 127.8 (d, C5), 131.6 (d, C7/C8), 135.6 (d, C7/C8), 142.4 (s, C4/C8a), 148.2 (s, C4/C8a), 150.5 (d, C2), 164.3 (s, CO).

Appearance: Colorless crystals

Mp: 118-120 °C (Lit.[204]: 121-123 °C)

TLC: R_f = 0.90 (2% MeOH in CH_2Cl_2)

E IV.2.18 Ethyl 7-bromo-4-chloroquinoline-3-carboxylate [162] DCBSLG03

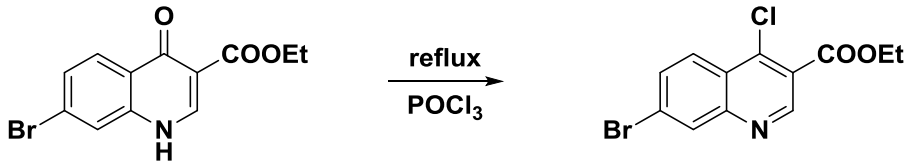

[161] **[162] (82%)**

Chemical Formula: $C_{12}H_{10}BrNO_3$
Molecular Weight: 296.12

Chemical Formula: $C_{12}H_9BrClNO_2$
Molecular Weight: 314.56

3.0 g (10.0 mmol) of ethyl 7-bromo-4-oxo-1,4-dihydroquinoline-3-carboxylate **[161]** were converted according to general procedure E III.3 to give ethyl 7-bromo-4-chloroquinoline-3-carboxylate **[162]** (2.46 g, 7.83 mmol, 82%).

^{1}H NMR (400 MHz, DMSO-d_6) δ 1.38 (t, *J* = 7.1 Hz, 3H, CH_3), 4.43 (q, *J* = 7.1 Hz, 2H, CH_2), 8.00 (dd, *J* = 9.0, 2.0 Hz, 1H, H6), 8.30 (d, *J* = 9.0 Hz, 1H, H5), 8.39 (d, *J* = 1.9 Hz, 1H, H8), 9.17 (s, 1H, H2).

^{13}C NMR ^{13}C NMR (101 MHz, DMSO-d_6) δ 14.0 (q, CH_3), 62.1 (t, CH_2), 123.6 (s, C3), 124.3 (s, C4a), 126.2 (s, C7), 127.1 (d, C5), 131.4 (d, C6/C8), 132.2 (d, C6/C8), 141.9 (s, C8a), 149.3 (s, C4), 150.9 (d, C2), 163.6 (s, CO).

Appearance: Colorless crystals

Mp: 88-90 °C (Lit.[215]: not reported)

TLC: R_f = 0.49 (PE/EtOAc = 6/1)

E IV.2.19 Ethyl 4-chloro-6-phenylquinoline-3-carboxylate [88d] DCBS15

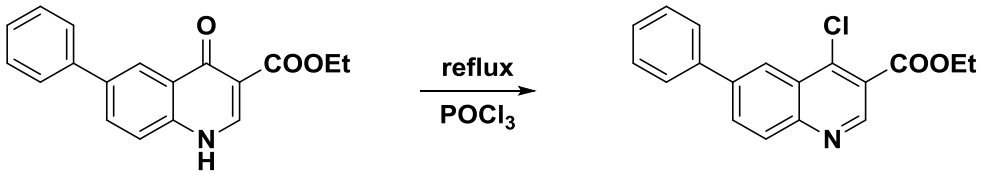

[88c] **[88d] (43%)**

Chemical Formula: $C_{18}H_{15}NO_3$
Molecular Weight: 293.32

Chemical Formula: $C_{18}H_{14}ClNO_2$
Molecular Weight: 311.77

227 mg (0.77 mmol) of ethyl 6 ethyl 4-oxo-6-phenyl-1,4-dihydroquinoline-3-carboxylate **[88c]** were converted according to general procedure E III.3 to give ethyl 4-chloro-6-phenylquinoline-3-carboxylate **[88d]** (103 mg, 0.33 mmol, 43%).

^{1}H NMR (200 MHz, $CDCl_3$) δ 1.48 (t, *J* = 7.1 Hz, 3H, CH_3), 4.52 (q, *J* = 7.1 Hz, 2H, CH_2), 7.32 – 7.64 (m, 3H, H-Ar), 7.67 – 7.84 (m, 2H, H-Ar), 8.10 (dd, *J* = 8.8, 1.9 Hz, 1H, H7), 8.22 (d, *J* = 8.7 Hz, 1H, H8), 8.58 (d, *J* = 1.6 Hz, 1H, H5), 9.20 (s, 1H, H2).

^{13}C NMR (50 MHz, $CDCl_3$) δ 14.4 (q, CH_3), 62.3 (t, CH_2), 110.2 (s, C3), 123.2 (d, C4'), 126.5 (s, C4a), 127.8 (d, C2' and C6'), 128.4 (d, C7), 129.3 (d, C3' and C5'), 130.5 (d, C5), 131.8 (d, C8), 139.8 (s), 141.4 (s), 143.6 (s), 149.0 (s), 150.1 (d, C2), 164.7 (s, CO).

HR-MS: Calc.[M+H]: 312.0786

Found [M+H]: n.det.

Appearance: Colorless crystals

Mp: 118-120 °C

TLC: R_f = 0.64 (PE/EtOAc = 3/1)

E IV.2.20 Ethyl 4-chloro-6-methoxyquinoline-3-carboxylate [8] DCBS19

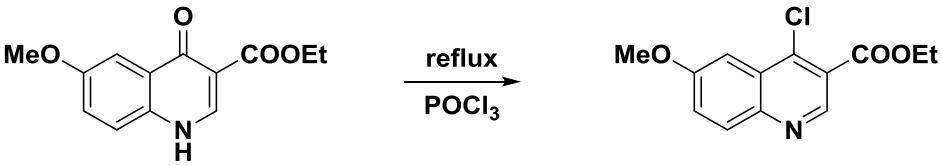

[7] **[8] (66%)**

Chemical Formula: $C_{13}H_{13}NO_4$
Molecular Weight: 247.25

Chemical Formula: $C_{13}H_{12}ClNO_3$
Molecular Weight: 265.69

200 mg (0.81 mmol) of ethyl 6-methoxy-4-oxo-1,4-dihydroquinoline-3-carboxylate **[7]** were converted according to general procedure E III.3 to give ethyl 4-chloro-6-methoxyquinoline-3-carboxylate **[8]** (142 mg, 0.54 mmol, 66%).

^{1}H NMR (200 MHz, $CDCl_3$) δ 1.30 – 1.56 (m, 3H, CH_3), 3.92 (s, 3H, OCH_3), 4.43 (q, *J* = 7.1 Hz, 2H, CH_2), 7.40 (dd, *J* = 9.2, 2.5 Hz, 1H, H7), 7.53 (d, *J* = 2.5 Hz, 1H, H5), 7.96 (d, *J* = 9.2 Hz, 1H, H8), 8.98 (s, 1H, H2).

^{13}C NMR (50 MHz, $CDCl_3$) δ 14.4 (q, CH_3), 55.9 (q, OCH_3), 62.2 (t, CH_2), 103.1 (d, C5), 123.7 (s, C3), 125.1 (d, C7), 127.6 (s, C4a), 131.7 (d, C8), 141.4 (s, C4/C8a), 145.9 (s, C4/C8a), 147.6 (d, C2), 159.5 (s, C6), 164.9 (s, CO).

Appearance: Colorless crystals

Mp: 88-90 °C (Lit.[216]: 93-95 °C)

TLC: R_f = 0.84 (2% MeOH in CH_2Cl_2)

E IV.2.21 Ethyl 4-chloro-7-methoxyquinoline-3-carboxylate [179] DCBSLA13

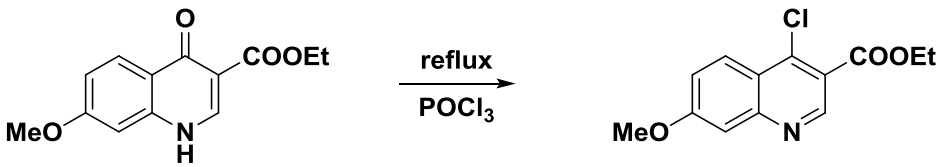

[178] **[179] (62%)**

Chemical Formula: $C_{13}H_{13}NO_4$
Molecular Weight: 247.25

Chemical Formula: $C_{13}H_{12}ClNO_3$
Molecular Weight: 265.69

353 mg (1.43 mmol) of ethyl 7-methoxy-4-oxo-1,4-dihydroquinoline-3-carboxylate **[178]** were converted according to general procedure E III.3 to give ethyl 4-chloro-7-methoxyquinoline-3-carboxylate **[179]** (234 mg, 0.88 mmol, 62%).

^{1}H NMR (400 MHz, $CDCl_3$) δ 1.46 (t, *J* = 7.1 Hz, 3H, CH_3), 3.98 (s, 3H, OCH_3), 4.48 (q, *J* = 7.1 Hz, 2H, CH_2), 7.32 (dd, *J* = 9.3, 2.6 Hz, 1H. H6), 7.43 (d, *J* = 2.5 Hz, 1H, H8), 8.29 (d, *J* = 9.3 Hz, 1H, H5), 9.16 (s, 1H, H2).

^{13}C NMR (101 MHz, $CDCl_3$) δ 14.3 (q, CH_3), 55.8 (q, OCH_3), 61.9 (t, CH_2), 107.7 (d, C5), 120.7 (s, C3/C4a), 121.3 (s, C3/C4a), 121.5 (d, C6/C8), 126.8 (d, C6/C8), 143.4 (s, C4/C8a), 150.9 (d, C2), 151.8 (s, C4/C8a), 162.7 (s, C7), 164.6 (s, CO).

Appearance: Colorless crystals

Mp: 128-130 °C (Lit.[217]: 130-132 °C)

TLC: R_f = 0.78 (5% MeOH in CH_2Cl_2)

E IV.3 Pyrazoloquinolinones – R^6 series

E IV.3.1 8-Chloro-6-fluoro-2-(4-methoxyphenyl)-2,5-dihydro-3H-pyrazolo[4,3-c]quinolin-3-one [215] DCBSPU21

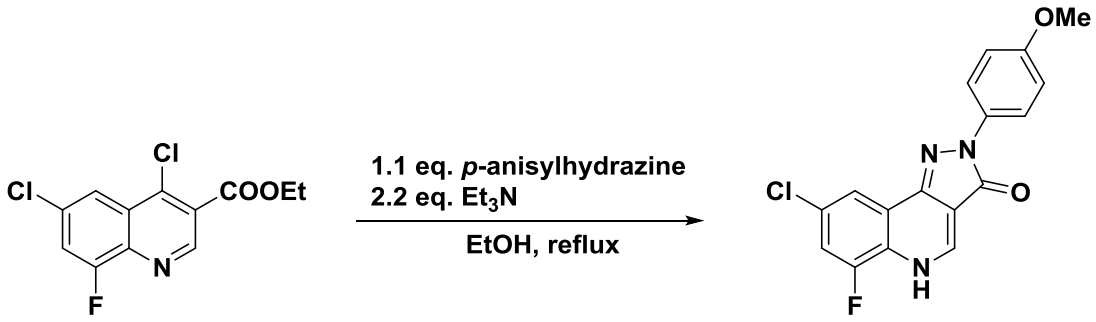

[208]

Chemical Formula: $C_{12}H_8Cl_2FNO_2$
Molecular Weight: 288.10

[215] (20%)

Chemical Formula: $C_{17}H_{11}ClFN_3O_2$
Molecular Weight: 343.74

The desired compound was synthesized according to general procedure E III.4 using:

Chlorinated quinoline	473 mg	1.63 mmol	1 eq.
Arylhydrazine HCl	305 mg	1.80 mmol	1.1 eq.

After purification by HPLC 8-chloro-6-fluoro-2-(4-methoxyphenyl)-2,5-dihydro-3H-pyrazolo[4,3-c]quinolin-3-one **[215]** was obtained (177 mg, 0.34 mmol, 20%).

^{1}H NMR (400 MHz, DMSO-d_6) δ 3.79 (s, 3H, OCH_3), 6.98 – 7.06 (m, 2H, H'3 and H'5), 7.79 (dd, J = 10.9, 2.2 Hz, 1H, H7), 7.98 (dd, J = 2.2, 1.2 Hz, 1H, H9), 8.03 – 8.11 (m, 2H, H'2 and H'6), 8.53 (s, 1H, H4).

^{13}C NMR (151 MHz, DMSO-d_6) δ 55.3 (q, OCH_3), 107.3 (s, C3a), 113.9 (d, C3' and C5'), 116.0 (dd, $^2J_{C,F}$ = 21.3 Hz, C7), 117.2 (dd, $^4J_{C,F}$ = 3.7 Hz, C9), 120.6 (d, C2' and C6'), 121.3 (sd, $^3J_{C,F}$ = 3.5 Hz, C9a), 123.9 (sd, $^3J_{C,F}$ = 12.9 Hz, C8), 130.2 (sd, $^2J_{C,F}$ = 10.0 Hz, C5a), 133.2 (s, C'1), 139.4 (d, C4), 140.8 (sd, $^1J_{C,F}$ = 3.5 Hz, C9b), 152.6 (sd, $^1J_{C,F}$ = 253.6 Hz, C6), 156.2 (s, C'4), 160.7 (s, CO).

HR-MS: Calc.[M+H]: 344.0597

Found [M+H]: 344.0590 (Diff.: +1.89 ppm)

Appearance: Yellow solid

Mp: Decomposes > 300 °C

TLC: R_f = 0.88 (2% MeOH in CH_2Cl_2)

E IV.3.2 6,8-Dichloro-2-(4-methoxyphenyl)-2,5-dihydro-3H-pyrazolo[4,3-c]quinolin-3-one [216] DCBSPU27

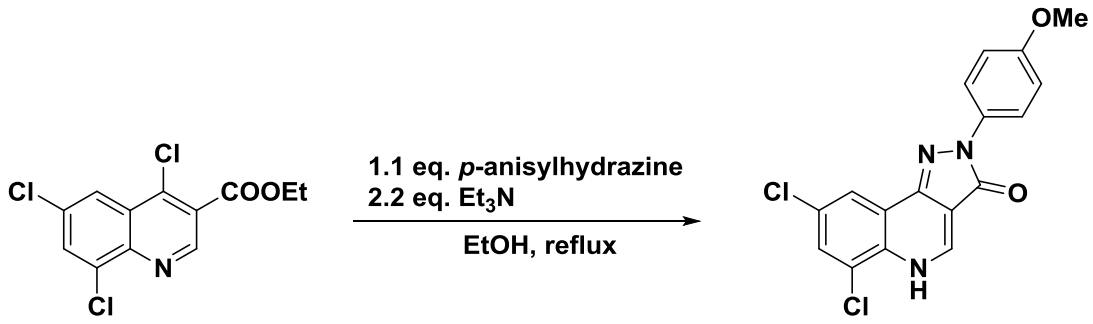

[209]

Chemical Formula: $C_{12}H_8Cl_3NO_2$
Molecular Weight: 304.55

[216] (25%)

Chemical Formula: $C_{17}H_{11}Cl_2N_3O_2$
Molecular Weight: 360.19

The desired compound was synthesized according to general procedure E III.4 using:

Chlorinated quinoline	113 mg	0.39 mmol	1 eq.
Arylhydrazine HCl	74 mg	0.42 mmol	1.1 eq.

After filtration 6,8-dichloro-2-(4-methoxyphenyl)-2,5-dihydro-3H-pyrazolo[4,3-c]quinolin-3-one **[216]** was obtained (35 mg, 0.098 mmol, 25%).

^{1}H NMR (400 MHz, DMSO-d_6) δ 3.79 (s, 3H, OCH_3), 6.97 – 7.06 (m, 2H, H'3 and H'5), 8.01 (d, *J* = 2.3 Hz, 1H, H7), 8.03 – 8.08 (m, 2H, H'2 and H'6), 8.14 (d, *J* = 2.3 Hz, 1H, H9), 8.41 (s, 1H, H4), 12.31 (br s, 1H, NH).

^{13}C NMR (151 MHz, DMSO-d_6) δ 55.3 (q, OCH_3), 107.5 (s, C3a), 113.9 (d, C3' and C5'), 120.3 (d, C9), 120.5 (d, C2' and C6'), 121.1 (s, C9a), 124.5 (s, C6), 129.8 (d, C7), 130.4 (s, C5a), 131.2 (s, C1'), 133.1 (s, C8), 139.4 (d, C4), 141.1 (s, C9b), 156.2 (s, C'4), 160.6 (s, CO).

HR-MS: Calc.[M+H]: 360.0301

Found [M+H]: 360.0305 (Diff.: -1.09 ppm)

Appearance: Yellow solid

Mp: Decomposes > 300 °C

TLC: R_f = 0.80 (1% MeOH in CH_2Cl_2)

E IV.3.3 6-Bromo-8-chloro-2-(4-methoxyphenyl)-2,5-dihydro-3H-pyrazolo[4,3-c]quinolin-3-one [217] DCBSPU19

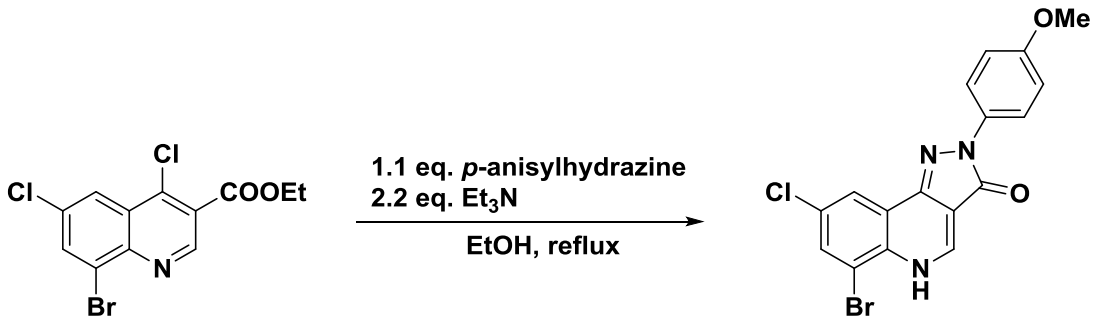

[210]

Chemical Formula: $C_{12}H_8BrCl_2NO_2$
Molecular Weight: 349.01

[217] (30%)

Chemical Formula: $C_{17}H_{11}BrClN_3O_2$
Molecular Weight: 404.65

The desired compound was synthesized according to general procedure E III.4 using:

Chlorinated quinoline	70 mg	0.26 mmol	1 eq.
Arylhydrazine HCl	32 mg	0.29 mmol	1.1 eq.

After filtration 6-bromo-8-chloro-2-(4-methoxyphenyl)-2,5-dihydro-3H-pyrazolo[4,3-c]quinolin-3-one **[217]** was obtained (32 mg, 0.078 mmol, 30%).

^{1}H NMR (400 MHz, DMSO-d_6) δ 3.79 (s, 3H, OCH_3), 6.98 – 7.06 (m, 2H, H'3 and H'5), 8.01 – 8.07 (m, 2H, H'2 and H'6), 8.12 (d, *J* = 2.3 Hz, 1H, H7/H9), 8.17 (d, *J* = 2.2 Hz, 1H, H7/H9), 8.36 (s, 1H, H4), 11.99 (br s, 1H, NH).

^{13}C NMR (151 MHz, DMSO-d_6) δ 55.3 (q, OCH_3), 107.5 (s, C3a), 113.9 (d, C3' and C5'), 114.1 (s, C6), 120.5 (d, C2' and C6'), 120.8 (d, C9), 121.1 (s, C9a), 130.7 (s, C5a), 132.3 (s, C1'), 133.0 (d, C7), 133.1 (s, C8), 139.6 (d, C4), 141.2 (s, C9b), 156.2 (s, C'4), 160.6 (s, CO).

HR-MS: Calc.[M+H]: 403.9796

Found [M+H]: 403.9830 (Diff.: -8.31 ppm)

Appearance: Yellow solid

Mp: Decomposes > 300 °C

TLC: R_f = 0.97 (2% MeOH in CH_2Cl_2)

E IV.3.4 8-Chloro-2-(4-methoxyphenyl)-6-(trifluoromethyl)-2,5-dihydro-3H-pyrazolo[4,3-c]quinolin-3-one [218] DCBSPU42

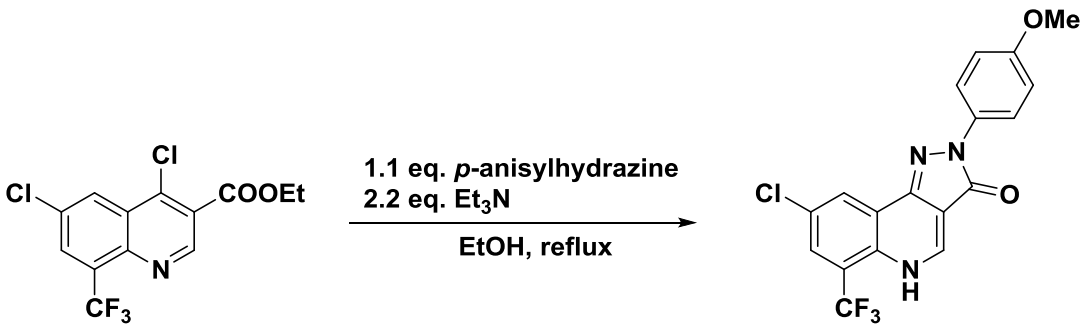

[211]

Chemical Formula: $C_{13}H_8Cl_2F_3NO_2$
Molecular Weight: 338.11

[218] (7%)

Chemical Formula: $C_{18}H_{11}ClF_3N_3O_2$
Molecular Weight: 393.75

The desired compound was synthesized according to general procedure E III.4 using:

Chlorinated quinoline	151 mg	0.44 mmol	1 eq.
Arylhydrazine HCl	85 mg	0.49 mmol	1.1 eq.

After 18 h the crude reaction mixture was evaporated and the residue was purified by FC (2 – 5% MeOH in CH_2Cl_2). However, the desired product sticked to the silica. Thus, the column was opened and the silica was extracted with DMSO which gave a crude mixture of **[218]**. Further purification by HPLC did unfortunately not yield the pure 8-chloro-2-(4-methoxyphenyl)-6-(trifluoromethyl)-2,5-dihydro-3H-pyrazolo[4,3-c]quinolin-3-one **[218]** (crude: 10 mg, 0.03 mmol, 7%).

^{1}H NMR (400 MHz, DMSO-d_6) δ 3.77 (s, 3H, OCH_3), 6.97 (d, *J* = 9.1 Hz, 2H, H'3 and H'5), 7.80 (d, *J* = 2.5 Hz, 1H, H7/H9), 8.19 (d, *J* = 8.6 Hz, 2H, H'2 and H'6), 8.32 (d, *J* = 2.5 Hz, 1H, H7/H9), 8.51 (s, 1H, H4). Selected signals were listed to confirm to formation of **[218]**.

^{13}C NMR not determined due to crude mixture.

HR-MS: Calc.[M+H]: 394.0565

Found [M+H]: 394.0572 (Diff.: -1.74 ppm)

Appearance: Yellow solid

TLC: R_f = 0.23 (2% MeOH in CH_2Cl_2)

E IV.3.5 8-Chloro-2-(4-methoxyphenyl)-6-methyl-2,5-dihydro-3H-pyrazolo[4,3-c]quinolin-3-one [219] DCBSPU26

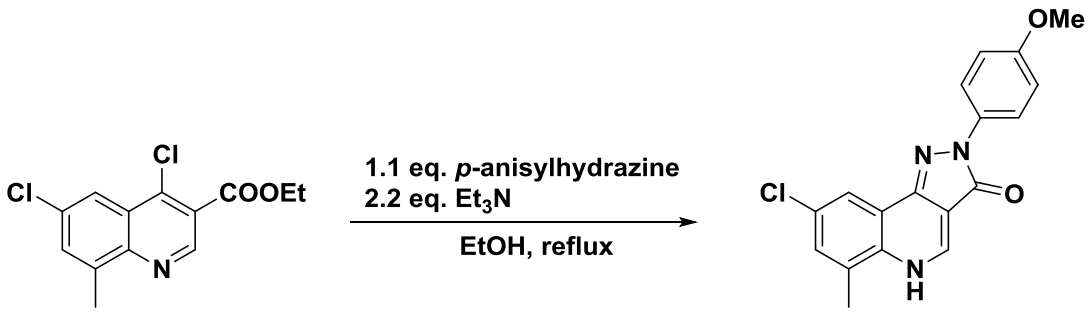

[212]

Chemical Formula: $C_{13}H_{11}Cl_2NO_2$
Molecular Weight: 284.14

[219] (38%)

Chemical Formula: $C_{18}H_{14}ClN_3O_2$
Molecular Weight: 339.78

The desired compound was synthesized according to general procedure E III.4 using:

Chlorinated quinoline	113 mg	0.39 mmol	1 eq.
Arylhydrazine HCl	74 mg	0.42 mmol	1.1 eq.

After filtration 8-chloro-2-(4-methoxyphenyl)-6-methyl-2,5-dihydro-3H-pyrazolo[4,3-c]quinolin-3-one **[219]** was obtained (50 mg, 0.15 mmol, 38%).

^{1}H NMR (400 MHz, DMSO-d_6) δ 2.56 (s, 3H, CH_3), 3.79 (s, 3H, OCH_3), 6.98 – 7.05 (m, 2H, H'3 and H'5), 7.60 (d, *J* = 2.4 Hz, 1H, H7), 8.01 (d, *J* = 2.4 Hz, 1H, H9), 8.05 – 8.11 (m, 2H, H'2 and H'6), 8.46 (s, 1H, H4), 12.09 (br s, 1H, NH).

^{13}C NMR (151 MHz, DMSO-d_6) δ 17.5 (q, CH_3), 55.3 (q, OCH_3), 106.7 (s, C3a), 113.9 (d, C3' and C5'), 118.7 (d, C9), 119.9 (s, C9a), 120.4 (d, C2' and C6'), 130.2 (s, C6), 130.8 (d, C7), 130.9 (s, C5a), 132.8 (s, C1'), 133.4 (s, C8), 138.9 (d, C4), 141.9 (s, C9b), 156.0 (s, C4'), 160.8 (s, CO).

HR-MS: Calc.[M+H]: 340.0847

Found [M+H]: 340.0864 (Diff.: -5.02 ppm)

Appearance: Yellow solid

Mp: Decomposes > 300 °C

TLC: R_f = 0.89 (2% MeOH in CH_2Cl_2)

E IV.3.6 8-Chloro-6-ethyl-2-(4-methoxyphenyl)-2,5-dihydro-3H-pyrazolo[4,3-c]quinolin-3-one [220] DCBSPU53

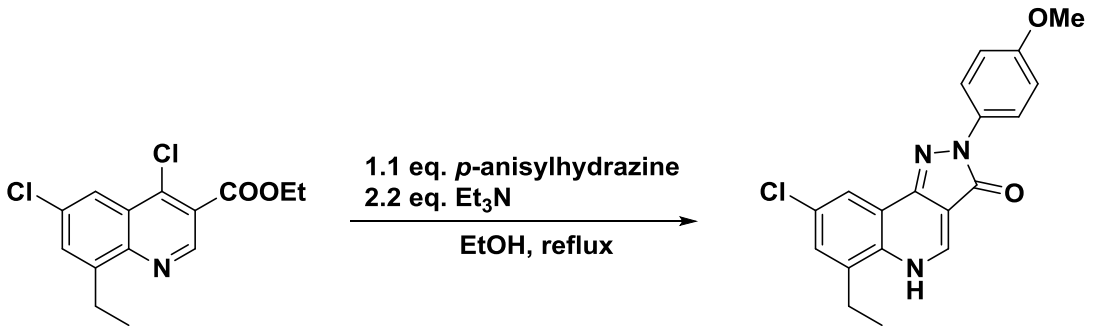

[213]

Chemical Formula: $C_{14}H_{13}Cl_2NO_2$
Molecular Weight: 298.16

[220] (80%)

Chemical Formula: $C_{19}H_{16}ClN_3O_2$
Molecular Weight: 353.81

The desired compound was synthesized according to general procedure E III.4 using:

Chlorinated quinoline	260 mg	0.89 mmol	1 eq.
Arylhydrazine HCl	172 mg	0.95 mmol	1.1 eq.

After filtration 8-chloro-6-ethyl-2-(4-methoxyphenyl)-2,5-dihydro-3H-pyrazolo[4,3-c]quinolin-3-one **[220]** was obtained (247 mg, 0.70 mmol, 80%).

^{1}H NMR (400 MHz, DMSO-d_6) δ 1.18 (t, *J* = 7.3 Hz, 3H, $CH_2C\underline{H}_3$), 2.96 (q, *J* = 7.5 Hz, 2H, $C\underline{H}_2CH_3$), 3.79 (s, 3H, OCH_3), 7.02 (d, *J* = 9.1 Hz, 2H, H'3 and H'5), 7.57 (d, *J* = 2.4 Hz, 1H, H7), 8.02 (d, *J* = 2.4 Hz, 1H, H9), 8.08 (d, *J* = 9.1 Hz, 2H, H'2 and H'6), 8.44 (s, 1H, H4), 12.14 (br s, 1H, NH).

^{13}C NMR (101 MHz, DMSO-d_6) δ 14.2 (q, $CH_2\underline{C}H_3$), 23.5 (t, $\underline{C}H_2CH_3$), 55.2 (q, OCH_3), 106.5 (s, C3a), 113.8 (d, C3' and C5'), 118.8 (d, C9), 120.1 (s, C9a), 120.4 (d, C2' and C6'), 129.3 (d, C7), 130.4 (s, C5a), 132.0 (s, C1'), 133.4 (s, C8), 136.5 (s, C6), 138.9 (d, C4), 142.0 (s, C9b), 156.0 (s, C4'), 160.7 (s, CO).

HR-MS: Calc.[M+H]: 354.1004

Found [M+H]: 354.1008 (Diff.: -1.24 ppm)

Appearance: Yellow solid

Mp: Decomposes > 300 °C

TLC: R_f = 0.51 (2% MeOH in CH_2Cl_2)

E IV.3.7 8-Chloro-6-isopropyl-2-(4-methoxyphenyl)-2,5-dihydro-3H-pyrazolo[4,3-c]quinolin-3-one [221] DCBSPU51

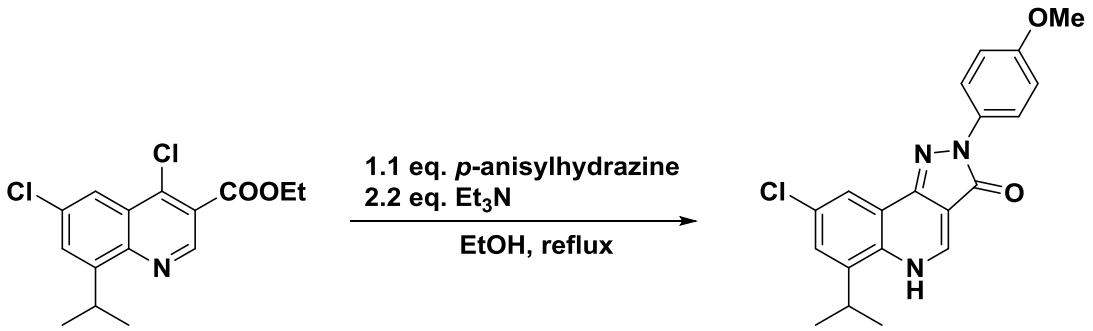

[214]

Chemical Formula: $C_{15}H_{15}Cl_2NO_2$
Molecular Weight: 312.19

[221] (37%)

Chemical Formula: $C_{20}H_{18}ClN_3O_2$
Molecular Weight: 367.83

The desired compound was synthesized according to general procedure E III.4 using:

Chlorinated quinoline	210 mg	0.67 mmol	1 eq.
Arylhydrazine HCl	128 mg	0.73 mmol	1.1 eq.

After filtration 8-chloro-6-isopropyl-2-(4-methoxyphenyl)-2,5-dihydro-3H-pyrazolo[4,3-c]quinolin-3-one **[221]** was obtained (87 mg, 0.25 mmol, 37%).

^{1}H NMR (400 MHz, DMSO-d_6) δ 1.31 (d, *J* = 6.6 Hz, 6H, 2 CHC$\underline{H}_3$), 3.57 (hept, *J* = 6.6 Hz, 1H, CH), 3.78 (s, 3H, OCH_3), 7.02 (d, *J* = 8.6 Hz, 2H, H'3 and H'5), 7.59 (d, *J* = 2.5 Hz, 1H, H7), 8.04 (d, *J* = 2.5 Hz, 1H, H9), 8.08 (d, *J* = 8.7 Hz, 2H, H'2 and H'6), 8.45 (s, 1H, H4), 12.12 (br s, 1H, NH).

^{13}C NMR (151 MHz, DMSO-d_6) δδ 22.7 (q, CH($\underline{C}H_3$)$_2$), 27.0 (d, $\underline{C}$H(CH_3)$_2$), 55.3 (q, OCH_3), 106.4 (s, C3a), 113.9 (d, C3' and C5'), 118.8 (d, C9), 120.3 (s, C9a), 120.4 (d, C2' and C6'), 126.5 (d, C7), 130.9 (s, C5a), 131.3 (s, C1'), 133.4 (s, C8), 138.9 (d, C4), 141.0 (s, C6), 142.1 (s, C9b), 156.0 (s, C4'), 160.8 (s, CO).

HR-MS: Calc.[M+H]: 368.1160

Found [M+H]: 368.1145 (Diff.: +4.07 ppm)

Appearance: Yellow solid

Mp: Decomposes > 300 °C

TLC: R_f = 0.64 (10% MeOH in CH_2Cl_2)

E IV.4 Pyrazoloquinolinones – R^7 series

E IV.4.1 7-Methoxy-2-(3-methoxyphenyl)-2,5-dihydro-3H-pyrazolo[4,3-c]quinolin-3-one [180] DCBS165

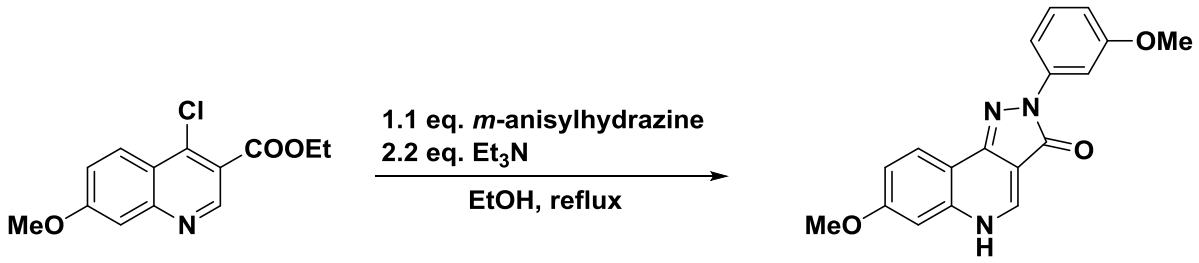

[179]

Chemical Formula: $C_{13}H_{12}ClNO_3$
Molecular Weight: 265.69

[180] (76%)

Chemical Formula: $C_{18}H_{15}N_3O_3$
Molecular Weight: 321.34

The desired compound was synthesized according to general procedure E III.4 using:

Chlorinated quinoline	50 mg	0.19 mmol	1 eq.
Arylhydrazine HCl	36 mg	0.21 mmol	1.1 eq.

After filtration 7-methoxy-2-(3-methoxyphenyl)-2,5-dihydro-3H-pyrazolo[4,3-c]quinolin-3-one **[180]** was obtained (46 mg, 0.14 mmol, 76%).

^{1}H NMR (400 MHz, DMSO-d_6) δ 3.80 (s, 3H, OCH_3), 3.88 (s, 3H, OCH_3), 6.74 (dd, *J* = 8.3, 2.5 Hz, 1H, H6'), 7.16 – 7.22 (m, 2H, H6 and H9), 7.33 (t, *J* = 8.2 Hz, 1H, H5'), 7.82 (d, *J* = 8.1 Hz, 1H, H2'), 7.84 – 7.88 (m, 1H, H4'), 8.13 (d, *J* = 9.4 Hz, 1H, H8), 8.67 (s, 1H, H4), 12.64 (br s, 1H, NH).

^{13}C NMR (101 MHz, DMSO-d_6) δ 55.1 (q, OCH_3), 55.6 (q, OCH_3), 101.9 (d, C6/C9), 104.3 (d, C4'), 106.4 (s, C3a), 109.2 (d, C6'), 110.8 (d, C2'), 112.1 (s, C9a), 115.4 (d, C6/C9), 123.7 (d, C8), 129.5 (d, C5'), 137.1 (s, C9b), 139.2 (d, C4), 141.3 (s, C5a/C1'), 143.1 (s, C5a/C1'), 159.5 (s, C7/C3'), 160.6 (s, C7/C3'), 161.7 (s, CO).

HR-MS: Calc.[M+H]: 322.1186

Found [M+H]: 322.1208 (Diff.: -6.91 ppm)

Appearance: Yellow solid

Mp: Decomposes > 300 °C

TLC: R_f = 0.33 (2% MeOH in CH_2Cl_2)

E IV.4.2 7-Bromo-2-(4-methoxyphenyl)-2,5-dihydro-3H-pyrazolo[4,3-c]quinolin-3-one [163] DCBSLG04

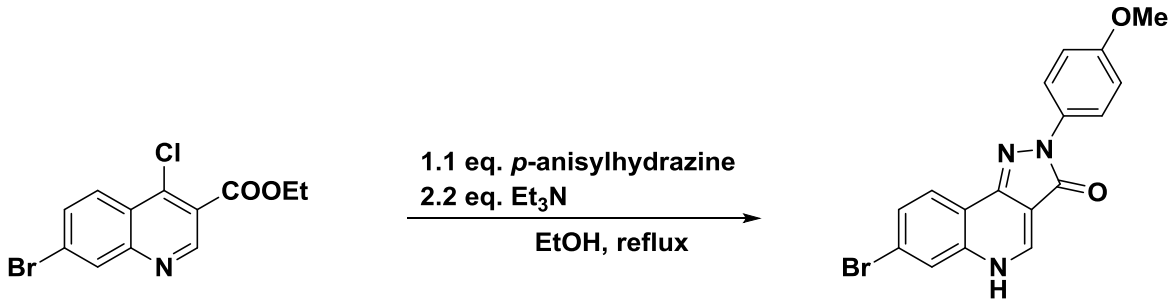

[162]

Chemical Formula: $C_{12}H_9BrClNO_2$
Molecular Weight: 314.56

[163] (90%)

Chemical Formula: $C_{17}H_{12}BrN_3O_2$
Molecular Weight: 370.21

The desired compound was synthesized according to general procedure E III.4 using:

Chlorinated quinoline	2.40 g	7.62 mmol	1 eq.
Arylhydrazine HCl	1.16 g	8.40 mmol	1.1 eq.

After filtration 7-bromo-2-(4-methoxyphenyl)-2,5-dihydro-3H-pyrazolo[4,3-c]quinolin-3-one **[163]** was obtained (2.54 g, 6.86 mmol, 90%).

^{1}H NMR (400 MHz, DMSO-d_6) δ 3.78 (s, 3H, OCH_3), 7.01 (d, *J* = 9.2 Hz, 2H, H3' and H5'), 7.69 (dd, *J* = 10.1, 2.0 Hz, 1H, H8), 7.88 (d, *J* = 1.9 Hz, 1H, H6), 8.06 (d, *J* = 9.2 Hz, 2H, H2' and H6'), 8.13 (d, *J* = 8.6 Hz, 1H, H9), 8.74 (s, 1H, H4), 12.80 (br s, 1H, NH).

^{13}C NMR (101 MHz, DMSO-d_6) δ 55.3 (q, OCH_3), 106.7 (s, C3a), 113.9 (d, C3' and C5'), 117.8 (s, C9a), 120.4 (d, C2' and C6'), 121.8 (d, C6), 122.5 (d, C7), 124.1 (d, C9), 129.2 (d, C8), 133.4 (s, C5a/C9b/C1'), 136.5 (s, C5a/C9b/C1'), 139.6 (d, C4), 141.9 (s, C5a/C9b/C1'), 156.0 (s, C4'), 160.9 (s, CO).

Appearance: Yellow solid

Mp: Decomposes > 300 °C (Lit.[218]: Decomposes > 330 °C)

TLC: R_f = 0.47 (5% MeOH in CH_2Cl_2)

E IV.4.3 2-(4-Methoxyphenyl)-7-((trimethylsilyl)ethynyl)-2,5-dihydro-3H-pyrazolo[4,3-c]quinolin-3-one [155] DCBS172

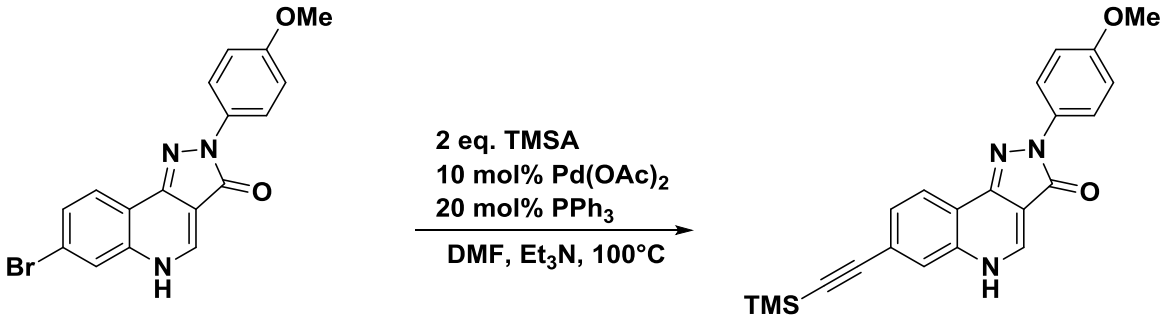

[163]

Chemical Formula: $C_{17}H_{12}BrN_3O_2$
Molecular Weight: 370.21

[155] (58%)

Chemical Formula: $C_{22}H_{21}N_3O_2Si$
Molecular Weight: 387.51

7-Bromo-2-(4-methoxyphenyl)-2,5-dihydro-3H-pyrazolo[4,3-c]quinolin-3-one **[163]** (265 mg, 0.72 mmol), $Pd(OAc)_2$ (16 mg, 10 mol%) and PPh_3 (38 mg, 20 mol%) were dissolved in Et_3N (4 mL) and DMF (8 mL). After the reaction apparatus was set under argon TMSAc (204 µL, 1.43 mmol) was added and the mixture was heated to 100 °C. After 17 h the reaction mixture was filtered through a syringe (5 mL) filled with cotton and silica (0.5 cm) using MeOH (50 mL) as eluent. The filtrate was concentrated, the residue was redissolved in DMSO and purified by HPLC to give 2-(4-methoxyphenyl)-7-((trimethylsilyl)ethynyl)-2,5-dihydro-3H-pyrazolo[4,3-c]quinolin-3-one **[155]** (160 mg, 0.41 mmol, 58%).

^{1}H NMR (400 MHz, DMSO-d_6) δ 0.27 (s, 9H, TMS), 3.78 (s, 3H, OCH_3), 7.01 (d, *J* = 9.2 Hz, 2H, H3' and H5'), 7.55 (dd, *J* = 8.2, 1.6 Hz, 1H, H8), 7.72 (d, *J* = 1.6 Hz, 1H, H6), 8.06 – 8.10 (m, 2H, H2' and H6'), 8.16 (d, *J* = 8.3 Hz, 1H, H9), 8.75 (s, 1H, H4), 12.70 (br s, 1H, NH).

^{13}C NMR (151 MHz, DMSO-d_6) δ -0.2 (q, TMS), 55.3 (q, OCH_3), 96.6 (s, $C_{acetylene}$), 104.1 (s, $C_{acetylene}$), 106.4 (s, C3a), 113.8 (d, C3' and C5'), 119.1 (s, C9a), 120.4 (d, C2' and C6'), 122.5 (d, C9), 122.7 (s, C7), 123.0 (d, C6), 129.1 (d, C8), 133.5 (s, C5a/C9b/C1'), 135.9 (s, C5a/C9b/C1'), 140.3 (d, C4), 142.0 (s, C5a/C9b/C1'), 156.0 (s, C4'), 161.0 (s, CO).

HPLC-MS: Calc.[M+H]: 388.15
Found [M+H]: 388.11

HR-MS: Calc.[M+H]: 388.1476
Found [M+H]: 388.1479
(Diff.: -0.77 ppm)

Appearance: Yellow solid

Mp: Decomposes > 300 °C

TLC: R_f = 0.71 (10% MeOH in CH_2Cl_2)

E IV.4.4 7-Ethynyl-2-(4-methoxyphenyl)-2,5-dihydro-3H-pyrazolo[4,3-c]quinolin-3-one [156] DCBS176

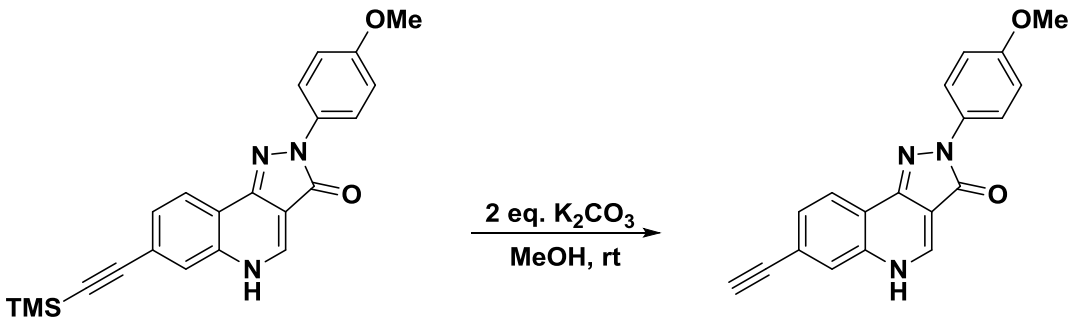

[155] **[156] (85%)**

Chemical Formula: $C_{22}H_{21}N_3O_2Si$
Molecular Weight: 387.51

Chemical Formula: $C_{19}H_{13}N_3O_2$
Molecular Weight: 315.33

2-(4-Methoxyphenyl)-7-((trimethylsilyl)ethynyl)-2,5-dihydro-3H-pyrazolo[4,3-c]quinolin-3-one **[155]** (150 mg, 0.39 mmol) was dissolved in 15 mL MeOH and K_2CO_3 (107 mg, 0.77 mmol) was added. After stirring for 2.5 h at rt the solvent was removed under reduced pressure. The residue was dissolved in DMSO, filtered through a syringe filter (0.2 µm) and purified by HPLC to give 7-ethynyl-2-(4-methoxyphenyl)-2,5-dihydro-3H-pyrazolo[4,3-c]quinolin-3-one **[156]** (104 mg, 0.33 mmol, 85%).

^{1}H NMR (400 MHz, DMSO-d_6) δ 3.78 (s, 3H,OCH_3), 4.47 (s, 1H, $H_{acetylene}$), 6.97 – 7.06 (m, 2H, H3' and H5'), 7.58 (dd, *J* = 8.3, 1.6 Hz, 1H, H8), 7.77 (d, *J* = 1.5 Hz, 1H, H6), 8.04 – 8.10 (m, 2H, H2' and H6'), 8.18 (d, *J* = 8.2 Hz, 1H, H9), 8.76 (s, 1H, H4), 12.82 (br s, 1H, NH).

^{13}C NMR (151 MHz, DMSO-d_6) δ 55.3 (q, OCH_3), 82.6 (s, $C_{acetylene}$), 83.0 (d, $C_{acetylene}$), 106.5 (s, C3a), 113.9 (d, C3' and C5'), 119.0 (s, C9a), 120.4 (d, C2' and C6'), 122.6 (s, C7), 122.7 (d, C9), 122.8 (d, C6), 129.1 (d, C8), 133.5 (s, C5a/C9b/C1'), 135.7 (s, C5a/C9b/C1'), 140.1 (d, C4), 142.0 (s, C5a/C9b/C1'), 156.0 (s, C4'), 161.0 (s, CO).

HPLC-MS: Calc.[M+H]: 316.11
Found [M+H]: 316.15

HR-MS: Calc.[M+H]: 316.1081
Found [M+H]: 316.1090
(Diff.: -2.88 pm)

Appearance: Yellow solid

Mp: Decomposes > 300 °C

TLC: R_f = 0.67 (10% MeOH in CH_2Cl_2)

E IV.4.5 7-Ethyl-2-(4-methoxyphenyl)-2,5-dihydro-3H-pyrazolo[4,3-c]quinolin-3-one [157] DCBS177

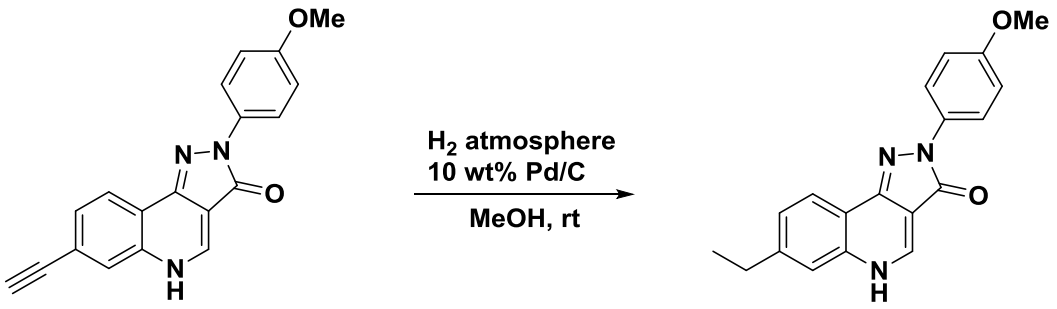

[156] **[157] (94%)**

Chemical Formula: $C_{19}H_{13}N_3O_2$
Molecular Weight: 315.33

Chemical Formula: $C_{19}H_{17}N_3O_2$
Molecular Weight: 319.36

7-Ethynyl-2-(4-methoxyphenyl)-2,5-dihydro-3H-pyrazolo[4,3-c]quinolin-3-one **[156]** (20 mg, 0.063 mmol) was dissolved in 3 mL MeOH and Pd/C (2 mg, 10 wt%) was added. The reaction mixture was stirred at room temperature under hydrogen atmosphere. After 3.5 h the solvent was removed under reduced pressure. The resiude was dissolved in DMSO, filtered through a syringe filter (0.2 µm) and purified by HPLC to give 7-ethyl-2-(4-methoxyphenyl)-2,5-dihydro-3H-pyrazolo[4,3-c]quinolin-3-one **[157]** (19 mg, 0.60 mmol, 94%).

^{1}H NMR (600 MHz, DMSO-d_6) δ 1.26 (t, *J* = 7.6 Hz, 3H, CH_3), 2.77 (q, *J* = 7.6 Hz, 2H, CH_2), 3.79 (s, 3H, OCH_3), 6.98 – 7.04 (m, 2H, H3' and H5'), 7.42 (dd, *J* = 8.2, 1.6 Hz, 1H, H8), 7.50 – 7.53 (m, 1H, H6), 8.10 (d, *J* = 9.1 Hz, 2H, H2' and H6'), 8.13 (d, *J* = 8.2 Hz, 1H, H9), 8.67 (s, 1H, H4), 12.70 (br s, 1H, NH).

^{13}C NMR (151 MHz, DMSO-d_6) δ 15.3 (q, CH_3), 28.2 (t, CH_2), 55.2 (q, OCH_3), 106.1 (s, C3a), 113.8 (d, C3' and C5'), 116.7 (s, C9a), 118.2 (d, C6), 120.3 (d, C2' and C6'), 122.1 (d, C9), 126.6 (d, C8), 133.7 (s, C5a/C9b/C1'), 136.1 (s, C5a/C9b/C1'), 139.4 (d, C4), 142.8 (s, C5a/C9b/C1'), 146.0 (s, C7), 155.8 (s, C4'), 161.1 (s, CO).

HPLC-MS: Calc.[M+H]: 320.14
Found [M+H]: 320.15

HR-MS: Calc.[M+H]: 320.1394
Found [M+H]: 320.1407
(Diff.: -4.23 ppm)

Appearance: Yellow solid

Mp: Decomposes > 300 °C

TLC: R_f = 0.67 (10% MeOH in CH_2Cl_2)

E IV.4.6 7-Acetyl-2-(4-methoxyphenyl)-2,5-dihydro-3H-pyrazolo[4,3-c]quinolin-3-one [158] DCBS183

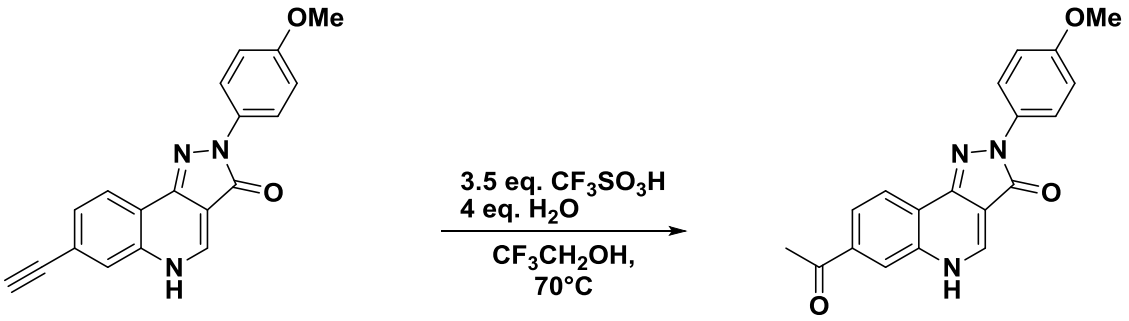

[156]

Chemical Formula: $C_{19}H_{13}N_3O_2$
Molecular Weight: 315.33

[158] (14%)

Chemical Formula: $C_{19}H_{15}N_3O_3$
Molecular Weight: 333.35

7-Ethynyl-2-(4-methoxyphenyl)-2,5-dihydro-3H-pyrazolo[4,3-c]quinolin-3-one **[156]** (64 mg, 0.2 mmol) was dissolved in 1 mL CF_3CH_2OH. Then H_2O (7.2 γL, 0.4 mmol) and CF_3SO_3H (62 γL, 0.7 mmol) were added and the reaction mixture was heated to 70 °C. After 3 days the solvent was removed under reduced pressure and the resiude was dissolved in DMSO, filtered through a syringe filter (0.2 µm) and purified by HPLC to give 7-acetyl-2-(4-methoxyphenyl)-2,5-dihydro-3H-pyrazolo[4,3-c]quinolin-3-one **[158]** (9 mg, 0.027 mmol, 14%).

^{1}H NMR (400 MHz, DMSO-d_6) δ 2.67 (s, 3H, $COCH_3$), 3.79 (s, 3H, OCH_3), 7.02 (d, *J* = 9.1 Hz, 2H, H3' and H5'), 8.05 (dd, *J* = 8.3, 1.3 Hz, 1H, H8), 8.10 (d, *J* = 9.1 Hz, 2H, H2' and H6'), 8.26 – 8.33 (m, 2H, H6 and H9), 8.77 (s, 1H, H4), 12.80 (br s, 1H, NH).

^{13}C NMR (151 MHz, DMSO-d_6) δ 26.9 (q, $CO\underline{C}H_3$), 55.3 (q, OCH_3), 106.4 (s, C3a), 113.9 (d, C3' and C5'), 120.5 (d, C2' and C6' and C9), 122.4 (d, C6), 125.2 (d, C8), 133.5 (s, C5a/C9b/C1'), 137.1 (s, C5a/C9b/C1'), 141.1 (d, C4), 142.1 (s, C5a/C9b/C1'), 156.0 (s, C4'), 161.0 (s, CO), 197.0 (s, $\underline{C}OCH_3$). Signals of C7 and C9a are either overlaid with other signals or not detectable.

HPLC-MS: Calc.[M+H]: 334.12
Found [M+H]: 334.15

HR-MS: Calc.[M+H]: 334.1186
Found [M+H]: 334.1194
(Diff.: -2.39 ppm)

Appearance: Yellow solid

Mp: Decomposes > 300 °C

TLC: R_f = 0.48 (10% MeOH in CH_2Cl_2)

E IV.5 Pyrazoloquinolinones – alkyl series

E IV.5.1 1-Benzyl-8-methoxy-1,2-dihydro-3H-pyrazolo[4,3c]quinolin-3-one [10] DCBS45A and 2-Benzyl-8-methoxy-1,2-dihydro-3H-pyrazolo[4,3-c]quinolin-3-one [9] DCBS45B

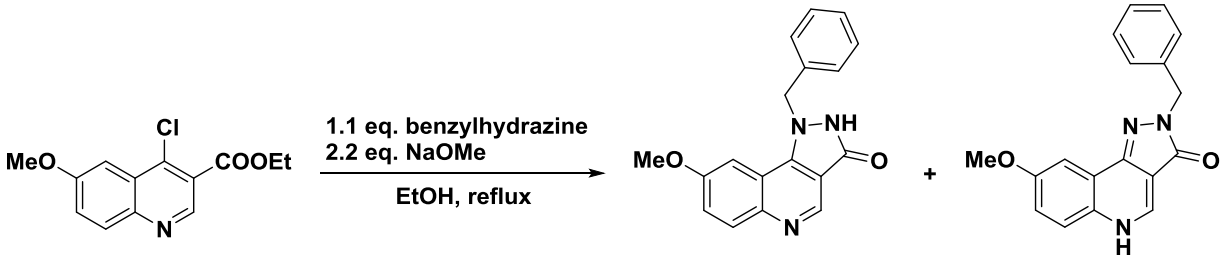

[8] [10] [9]

Chemical Formula: $C_{13}H_{12}ClNO_3$
Molecular Weight: 265.69

Chemical Formula: $C_{18}H_{15}N_3O_2$
Molecular Weight: 305.34

Ethyl 4-chloro-6-methoxyquinoline-3-carboxylate **[8]** (100 mg, 0.38 mmol) and benzylhydrazine dihydrochloride (81 mg, 0.41 mmol) were dispersed in 2 mL EtOH, NaOMe (45 mg, 0.83 mmol) was added and the reaction mixture was heated to reflux under argon atmosphere. After 20 h the reaction mixture was rinsed with water (2 mL), filtered and the precipitate was dried under reduced pressure. Purification by HPLC yielded separately 1-benzyl-8-methoxy-1,2-dihydro-3H-pyrazolo[4,3-c]quinolin-3-one **[10]** and 2-benzyl-8-methoxy-1,2-dihydro-3H-pyrazolo[4,3-c]quinolin-3-one **[9]** in a ratio of **[9]**/**[10]** = 1/1 (**[9]**: 24 mg, 0.08 mmol, 21%)/(**[10]**: 24 mg, 0.08 mmol, 21%).

[10] DCBS 45A

^{1}H NMR (400 MHz, DMSO-d_6) δ 3.74 (s, 3H, OCH_3), 5.89 (s, 2H, CH_2), 7.13 – 7.19 (m, 2H, H-Ar and H7), 7.21 – 7.36 (m, 4H, H-Ar), 7.41 (d, *J* = 2.8 Hz, 1H, H9), 7.96 (d, *J* = 9.1 Hz, 1H, H6), 8.94 (s, 1H, H4).

^{13}C NMR (101 MHz, DMSO-d_6) δ 54.2 (t, CH_2), 55.4 (q, OCH_3), 102.8 (d, C9), 106.8 (s, C3a), 116.4 (s, C9a), 118.8 (d, C7), 126.0 (d, C2' and C6'), 127.4 (d, C4'), 128.8 (d, C3' and C5'), 131.2 (d, C6), 137.8 (s, C5a/C9b/C1'), 138.5 (s, C5a/C9b/C1'), 140.9 (s, C5a/C9b/C1'), 142.5(d, C4), 155.2 (s, CO), 157.0 (s, C8).

HPLC-MS: Calc.[M+H]: 306.12
Found [M+H]: 306.04

HR-MS: Calc.[M+H]: 306.1237
Found [M+H]: 306.1256
(Diff.: -6.31 ppm)

Appearance: Colorless solid

Mp: Decomposes at 297 °C

TLC: R_f = 0.43 (10% MeOH in CH_2Cl_2)

[9] DCBS 45B

^{1}H NMR (400 MHz, DMSO-d_6) δ 3.86 (s, 3H, CH_3), 5.09 (s, 2H, CH_2), 7.15 – 7.27 (m, 4H, 3 H-Ar and H7), 7.27 – 7.36 (m, 2H, H-Ar), 7.42 (d, *J* = 2.8 Hz, 1H, H9), 7.64 (d, *J* = 9.1 Hz, 1H, H6), 8.59 (s, 1H, H4).

^{13}C NMR (101 MHz, DMSO-d_6) δ 47.5 (t, CH_2), 55.6 (q, OCH_3), 102.2 (d, C9), 104.2 (s, C3a), 109.5 (s, C9a), 119.0 (d, C7), 121.4 (d, C6), 126.9 (d, C4'), 127.3 (d, C2' and C6'), 128.3 (d, C3' and C5'), 129.8 (s, C1'), 137.7 (s, C5a/C9b), 138.9 (d, C4), 141.8 (s, C5a/C9b), 157.3 (s, C8), 161.8 (s, CO).

HPLC-MS: Calc.[M+H]: 306.12
Found [M+H]: 306.03

HR-MS: Calc.[M+H]: 306.1237
Found [M+H]: 306.1233
(Diff.: +1.22 ppm)

Appearance: Yellow solid

Mp: Decomposes > 300 °C

TLC: R_f = 0.42 (10% MeOH in CH_2Cl_2)

E IV.5.2 1-Cyclohexyl-8-methoxy-1,2-dihydro-3H-pyrazolo[4,3-c]-quinolin-3-one [13] DCBS40A and 2-Cyclohexyl-8-methoxy-1,2-dihydro-3H-pyrazolo[4,3-c]quinolin-3-one [12] DCBS40B

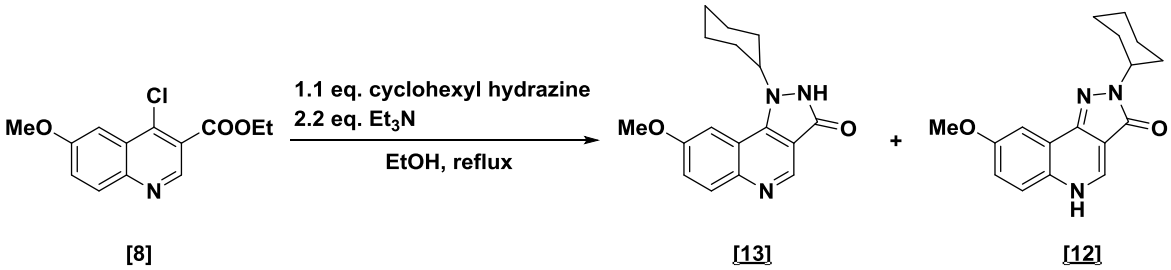

[8] [13] [12]

Chemical Formula: $C_{13}H_{12}ClNO_3$
Molecular Weight: 265.69

Chemical Formula: $C_{17}H_{19}N_3O_2$
Molecular Weight: 297.36

The desired compound was synthesized according to general procedure E III.4 using:

Chlorinated quinoline	150 mg	0.56 mmol	1 eq.
Cyclohexyl hydrazine HCl	93.5 mg	0.62 mmol	1.1 eq.

After purification by HPLC 1-cyclohexyl-8-methoxy-1,2-dihydro-3H-pyrazolo[4,3-c]quinolin-3-one **[13]** and 2-cyclohexyl-8-methoxy-1,2-dihydro-3H-pyrazolo[4,3-c]quinolin-3-one **[12]** were obtained separately in a ratio of **[13]**/**[12]** = 1/5 (**[13]**: 17 mg, 0.056 mmol, 12 %)/(**[12]**: 83 mg, 0.28 mmol, 57%).

[13] DCBS 40A

^{1}H NMR (400 MHz, DMSO-d_6) δ 1.26 – 1.38 (m, 1H, H_{cyc}), 1.50 – 1.68 (m, 2H, H_{cyc}), 1.74 (d, *J* = 13.2 Hz, 1H, H_{cyc}), 1.81 – 1.97 (m, 4H, H_{cyc}), 2.12 (d, *J* = 10.3 Hz, 2H, H_{cyc}), 3.97 (s, 3H, OCH_3), 4.89 (td, *J* = 11.0, 9.2, 5.7 Hz, 1H, NH_{cyc}), 7.40 (dd, *J* = 9.1, 2.7 Hz, 1H, H7), 7.63 (d, *J* = 2.7 Hz, 1H, H9), 8.02 (d, *J* = 9.1 Hz, 1H, H6), 8.86 (s, 1H, H4).

^{13}C NMR (101 MHz, DMSO) δ 25.0 (t, 2 C_{cyc}), 25.1 (t, C_{cyc}), 32.6 (t, 2 C_{cyc}), 55.4 (q, OCH_3), 59.1 (d, NC_{cyc}), 103.0 (d, C9), 105.8 (s, C3a), 116.7 (s, C9a), 118.2 (d, C7), 131.5 (d, C6), 137.5 (s, C5a/C9b), 140.9 (s, C5a/C9b), 142.4 (d, C4), 154.3 (s, CO), 157.2 (s, C8).

HPLC-MS: Calc.[M+H]: 298.16
Found [M+H]: 298.07

HR-MS: Calc.[M+H]: 298.1550
Found [M+H]: 298.1562
(Diff.: -3.88 ppm)

Appearance: Colorless solid

Mp: Decomposes at 277 °C

TLC: R_f = 0.41 (10% MeOH in CH_2Cl_2)

[13] DCBS 40B

^{1}H NMR (600 MHz, DMSO-d_6) δ 1.18 – 1.29 (m, 2H, H_{cyc}), 1.32 – 1.44 (m, 2H, H_{cyc}), 1.62 – 1.77 (m, 3H, H_{cyc}), 1.77 – 1.86 (m, 3H, H_{cyc}), 3.89 (s, 3H, OCH_3), 4.22 (ddd, *J* = 11.5, 7.5, 4.1 Hz, 1H, NCH_{cyc}), 7.21 (dd, *J* = 9.0, 2.8 Hz, 1H, H7), 7.44 (d, *J* = 2.9 Hz, 1H, H9), 7.61 (d, *J* = 9.0 Hz, 1H, H6), 8.52 (s, 1H, H4), 12.43 (br s, 1H, NH).

^{13}C NMR (151 MHz, DMSO-d_6) δ 25.6 (t, C_{cyc}), 25.9 (t, 2 C_{cyc}), 32.3 (t, 2 C_{cyc}), 52.3 (d, NC_{cyc}), 56.1 (q, OCH_3), 102.5 (d, C9), 105.5 (s, C3a), 119.4 (d, C7), 120.9 (s, C9a), 121.5 (d, C6), 129.7 (s, C5a), 137.5 (d, C4), 141.4 (s, C9b), 157.8 (s, C8), 161.3 (s, CO).

HPLC-MS: Calc.[M+H]: 298.16
Found [M+H]: 298.11

HR-MS: Calc.[M+H]: 298.1550
Found [M+H]: 298.1552
(Diff.: -0.59 ppm)

Appearance: Yellow solid

Mp: Decomposes > 300 °C

TLC: R_f = 0.42 (10% MeOH in CH_2Cl_2)

E IV.5.3 1-Isopropyl-8-methoxy-1,2-dihydro-3H-pyrazolo[4,3-c]quinolin-3-one [16] DCBS63A and 2-Isopropyl-8-methoxy-1,2-dihydro-3H-pyrazolo[4,3-c]quinolin-3-one [15] DCBS63B

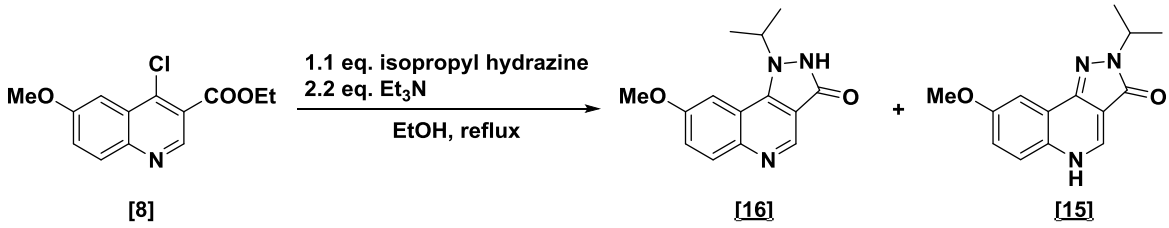

[8] [16] [15]

Chemical Formula: $C_{13}H_{12}ClNO_3$
Molecular Weight: 265.69

Chemical Formula: $C_{14}H_{15}N_3O_2$
Molecular Weight: 257.29

The desired compound was synthesized according to general procedure E III.4 using:

Chlorinated quinolinone	80 mg	0.30 mmol	1 eq.
Alkylhydrazine HCl	37 mg	0.33 mmol	1.1 eq.

After purification by HPLC 1-Isopropyl-8-methoxy-1,2-dihydro-3H-pyrazolo[4,3-c]quinolin-3-one **[16]** and 2-Isopropyl-8-methoxy-1,2-dihydro-3H-pyrazolo[4,3-c]quinolin-3-one **[15]** were obtained separately in a ratio of **[15]**/**[16]** = 1/4 (**[15]**: 7 mg, 0.026 mmol, 9%)/(**[16]**: 27 mg, 0.10 mmol, 35%).

[16] DCBS 63A

^{1}H NMR (400 MHz, DMSO-d_6) δ 1.54 (d, J = 6.4 Hz, 6H, CH_3), 3.97 (s, 3H, OCH_3), 5.34 (hept, J = 6.5 Hz, 1H, CH), 7.41 (dd, J = 9.1, 2.7 Hz, 1H, H7), 7.69 (d, J = 2.7 Hz, 1H, H9), 8.03 (d, J = 9.1 Hz, 1H, H6), 8.86 (s, 1H, H4), 11.17 (br s, 1H, NH).

^{13}C NMR (151 MHz, DMSO-d_6) δ 22.4 (q, 2 CH_3), 51.7 (d, CH), 55.6 (q, OCH_3), 103.3 (d, C9), 106.0 (s, C3a), 116.8 (s, C9a), 118.1 (d, C7), 131.6 (d, C6), 137.6 (s, C5a/C9b), 141.0 (s, C5a/C9b), 142.5 (d, C4), 154.6 (s, CO), 157.3 (s, C8).

HPLC-MS: Calc.[M+H]: 258.12
Found [M+H]: 258.06

HR-MS: Calc.[M+H]: 258.1237
Found [M+H]: 258.1257
(Diff.: -7.60 ppm)

Appearance: Colorless solid

Mp: Decomposes at 290 °C

TLC: R_f = 0.32 (10% MeOH in CH_2Cl_2)

[15] DCBS 63B

^{1}H NMR (600 MHz, DMSO-d_6) δ 1.33 (d, *J* = 6.7 Hz, 6H, CH_3), 3.90 (s, 3H, OCH_3), 4.64 (hept, *J* = 6.7 Hz, 1H, CH), 7.22 (dd, *J* = 9.0, 2.8 Hz, 1H, H7), 7.46 (d, *J* = 2.8 Hz, 1H, H9), 7.61 (d, *J* = 9.0 Hz, 1H, H6), 8.51 (s, 1H, H4), 12.55 (br s, 1H, NH).

^{13}C NMR (151 MHz, DMSO-d_6) δ 21.8 (q, 2 CH_3), 44.2 (d, CH), 55.7 (q, OCH_3), 102.1 (d, C9), 105.1 (s, C3a), 118.9 (d, C7), 120.5 (s, C9a), 121.0 (d, C6), 129.2 (s, C5a), 137.0 (d, C4), 141.0 (s, C9b), 157.3 (s, C8), 160.8 (s, CO).

HPLC-MS: Calc.[M+H]: 258.12
Found [M+H]: 258.06

HR-MS: Calc.[M+H]: 258.1237
Found [M+H]: 258.1254
(Diff.: -6.92 ppm)

Appearance: Yellow solid

Mp: Decomposes at 297 °C

TLC: R_f = 0.33 (10% MeOH in CH_2Cl_2)

E IV.5.4 8-Methoxy-1-methyl-1,2-dihydro-3H-pyrazolo[4,3-c]quinolin-3-one [11] DCBSLS25

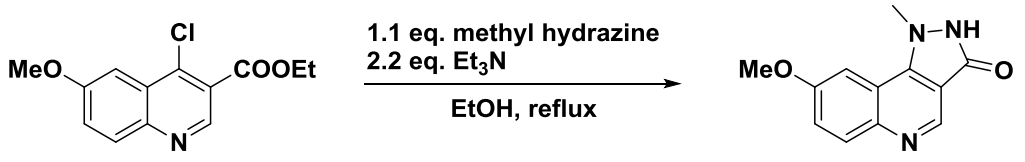

[8]

Chemical Formula: $C_{13}H_{12}ClNO_3$
Molecular Weight: 265.69

[11] (76%)

Chemical Formula: $C_{12}H_{11}N_3O_2$
Molecular Weight: 229.24

The desired compound was synthesized according to general procedure E III.4 using:

Chlorinated quinoline	150 mg	0.56 mmol	1 eq.
Alkylhydrazine HCl	29 mg	0.62 mmol	1.1 eq.

After filtration 8-methoxy-1-methyl-1,2-dihydro-3H-pyrazolo[4,3-c]quinolin-3-one **[11]** was obtained (98 mg, 0.43 mmol, 76%).

^{1}H NMR (400 MHz, DMSO-d_6) δ 3.97 (s, 3H, OCH_3), 4.28 (s, 3H, NCH_3), 7.39 (dd, *J* = 9.1, 2.8 Hz, 1H, H7), 7.76 (d, *J* = 2.8 Hz, 1H, H9), 8.00 (d, *J* = 9.1 Hz, 1H, H6), 8.86 (s, 1H, H4), 11.15 (br s, 1H, NH).

^{13}C NMR (151 MHz, DMSO-d_6) δ 30.7 (q, NCH_3), 55.6 (q, OCH_3), 103.1 (d, C9), 105.9 (s, C3a), 117.0 (s, C9a), 118.6 (d, C7), 131.0 (d, C6), 138.6 (s, C5a/C9b), 140.4 (s, C5a/C9b), 142.2 (d, C4), 154.2 (s, CO), 157.2 (s, C8).

HPLC-MS: Calc.[M+H]: 230.09

Found [M+H]: 230.11

Appearance: Colorless solid

Mp: Decomposes > 300 °C (Lit.[219]:Decomposes at 324 °C)

TLC: R_f = 0.67 (30% MeOH in CH_2Cl_2)

E IV.5.5 8-Methoxy-1,2-dimethyl-1,2-dihydro-3H-pyrazolo[4,3-c]quinolin-3-one [14] DCBS105

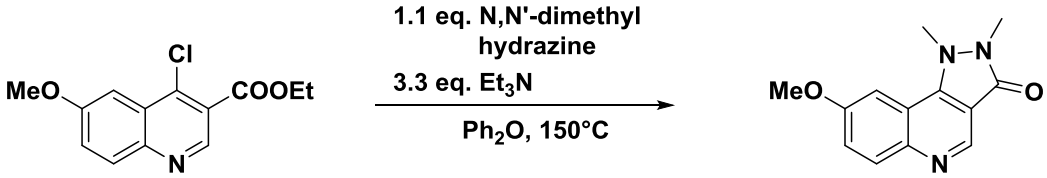

[8]

Chemical Formula: $C_{13}H_{12}ClNO_3$
Molecular Weight: 265.69

[14] (37%)

Chemical Formula: $C_{13}H_{13}N_3O_2$
Molecular Weight: 243.27

The chlorinated quinolinone **[8]** (60 mg, 0.23 mmol, 1 eq.) and the alkylhydrazine dihydrochloride (33 mg, 0.25, 1.1 eq.) were dispersed in 1.5 mL diphenylether, Et_3N (3.3 eq.) was added and the reaction mixture was heated to 150 °C under argon atmosphere. After 20 h the reaction mixture was allowed to cool to room temperature and was poured into PE (15 mL). The precipitate was collected by filtration, washed with water (2 x 3 mL) and dried under reduced pressure to give 8-methoxy-1,2-dimethyl-1,2-dihydro-3H-pyrazolo[4,3-c]quinolin-3-one **[14]** (20 mg, 0.08 mmol, 37%).

^{1}H NMR (400 MHz, DMSO-d_6) δ 3.49 (s, 3H, OCH_3), 3.83 (s, 3H, NCH_3), 3.99 (s, 3H, NCH_3), 7.53 (dd, *J* = 9.2, 2.8 Hz, 1H, H7), 7.62 (d, *J* = 2.8 Hz, 1H, H9), 8.04 (d, *J* = 9.2 Hz, 1H, H6), 8.86 (s, 1H, H4).

^{13}C NMR (101 MHz, DMSO-d_6) δ 28.5 (q, NCH_3), 37.8 (q, NCH_3), 55.8 (q, OCH_3), 102.7 (d, C9), 109.4 (s, C3a), 116.6 (s, C9a), 121.6 (d, C7), 131.4 (d, C6), 142.7 (d, C4), 143.6 (s, C5a/C9b), 148.6 (s, C5a/C9b), 157.4 (s, C8), 159.8 (s, CO).

HPLC-MS: Calc.[M+H]: 244.11
Found [M+H]: 244.21

HR-MS: Calc.[M+H]: 244.1081
Found [M+H]: 244.1091
(Diff.: -4.44 ppm)

Appearance: Colorless solid

Mp: Decomposes > 300 °C

TLC: R_f = 0.39 (5% MeOH in CH_2Cl_2)

E IV.5.6 2-(t*ert*-Butyl)-8-methoxy-1,2-dihydro-3H-pyrazolo[4,3-c]quinolin-3-one [17] DCBS66B

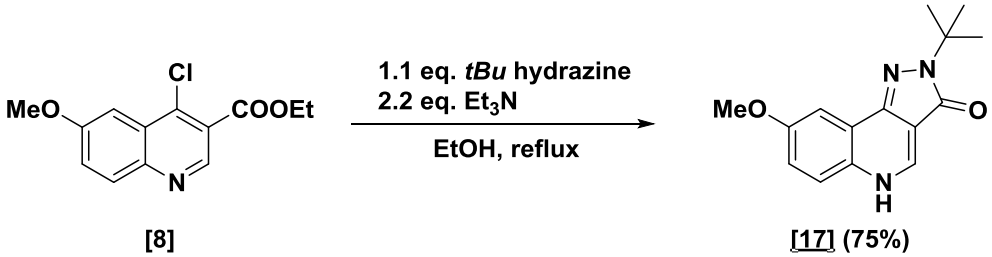

[8]

Chemical Formula: $C_{13}H_{12}ClNO_3$
Molecular Weight: 265.69

[17] (75%)

Chemical Formula: $C_{15}H_{17}N_3O_2$
Molecular Weight: 271.32

The desired compound was synthesized according to general procedure E III.4 using:

Chlorinated quinoline	100 mg	0.38 mmol	1 eq.
Alkylhydrazine HCl	61 mg	0.49 mmol	1.1 eq.

After purification by HPLC 2-(t*ert*-butyl)-8-methoxy-1,2-dihydro-3H-pyrazolo[4,3-c]quinolin-3-one **[17]** was obtained (76 mg, 0.28 mmol, 75%).

^{1}H NMR (400 MHz, DMSO-d_6) δ 1.59 (s, 9H, C(CH_3)$_3$), 3.88 (s, 3H, OCH_3), 7.20 (dd, *J* = 9.0, 2.9 Hz, 1H, H7), 7.42 (d, *J* = 2.8 Hz, 1H, H9), 7.60 (d, *J* = 9.0 Hz, 1H, H6), 8.39 (s, 1H, H4).

^{13}C NMR (151 MHz, DMSO-d_6) δ 28.4 (q, C($\underline{C}H_3$)$_3$), 55.6 (q, OCH_3), 56.7 (s, $\underline{C}(CH_3)_3$), 102.1 (d, C9), 106.4 (s, C3a), 118.6 (d, C7), 120.6 (s, C9a), 121.2 (d, C6), 129.6 (s, C5a/C9b), 136.9 (d, C4), 139.7 (s, C5a/C9b), 157.2 (s, C8), 162.1 (s, CO).

HPLC-MS: Calc.[M+H]: 272.14
Found [M+H]: 272.07

HR-MS: Calc.[M+H]: 272.1394
Found [M+H]: 272.1390
(Diff.: +1.17 ppm)

Appearance: Yellow solid

Mp: Decomposes > 300 °C

TLC: R_f = 0.37 (10% MeOH in CH_2Cl_2)

E IV.5.7 8-Methoxy-2,5-dihydro-3H-pyrazolo[4,3-c]quinolin-3-one [18] DCBS53

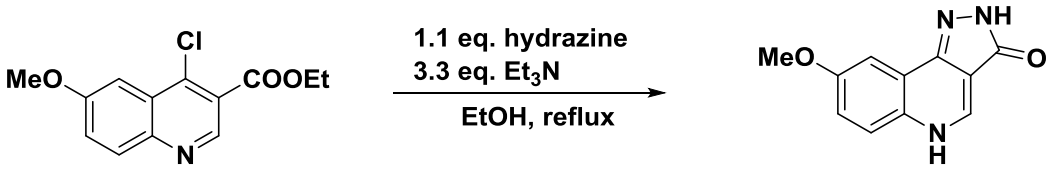

[8]

Chemical Formula: $C_{13}H_{12}ClNO_3$
Molecular Weight: 265.69

[18] (97%)

Chemical Formula: $C_{11}H_9N_3O_2$
Molecular Weight: 215.21

The desired compound was synthesized according to general procedure E III.4 using:

Chlorinated quinoline	179 mg	0.67 mmol	1 eq.
Hydrazine 2 HCl	185 mg	0.83 mmol	1.1 eq.

After filtration 8-methoxy-2,5-dihydro-3H-pyrazolo[4,3-c]quinolin-3-one **[18]** was obtained (140 mg, 0.65 mmol, 97%).

^{1}H NMR (600 MHz, DMSO-d_6) δ 3.87 (s, 3H, OCH_3), 7.21 (dd, *J* = 9.0, 2.9 Hz, 1H, H7), 7.46 (d, *J* = 2.9 Hz, 1H, H9), 7.60 (d, *J* = 9.1 Hz, 1H, H6), 8.46 (s, 1H, H4), 11.38 (br s, 1H, NH), 12.45 (br s, 1H, NH).

^{13}C NMR (151 MHz, DMSO-d_6) δ 55.6 (q, OCH_3), 102.5 (d, C9), 104.7 (s, C3a), 118.6 (d, C7), 120.9 (d, C6), 121.0 (s, C9a), 129.3 (s, C5a), 137.2 (d, C4), 142.7 (s, C9b), 157.2 (s, C8), 164.5 (s, CO).

HPLC-MS: Calc.[M+H]: 216.22

Found [M+H]: 216.11

Appearance: Yellow solid

Mp: Decomposes > 300 °C (Lit.[219]: decomposes at 325°C)

TLC: R_f = 0.34 (30% MeOH in EtOAc)

E IV.5.8 2-Methoxy-10,11-dihydro-7H,9H-pyrazolo[1',2':1,2]-pyrazolo[4,3-c]quinolin-7-one [19] DCBS38

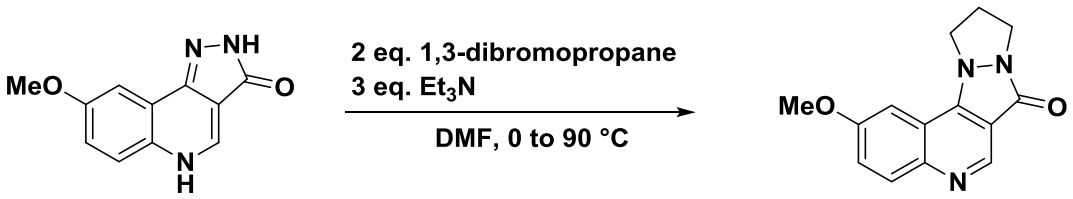

[18]

Chemical Formula: $C_{11}H_9N_3O_2$
Molecular Weight: 215.21

[19] (21%)

Chemical Formula: $C_{14}H_{13}N_3O_2$
Molecular Weight: 255.28

8-Methoxy-2,5-dihydro-3H-pyrazolo[4,3-c]quinolin-3-one **[18]** (20 mg, 0.09 mmol) was dispersed in DMF (1 mL) and Et_3N (26 µL, 0.19 mmol) was added at 0 °C. Dibromopropane (10 µL, 0.09 mmol) was added dropwise and the reaction mixture was stirred at 0 °C under argon atmosphere. After 10 h 1 eq. Et_3N and 1 eq. 1,3-dibromopropane were added and the suspension was stirred at 90 °C. After 18 h the solvent was removed under reduced pressure and the residue was purified by FC (gradient of 5%-50% MeOH in EtOAc) and HPLC to give 2-methoxy-10,11-dihydro-7H,9H-pyrazolo[1',2':1,2]pyrazolo[4,3-c]quinolin-7-one **[19]** (5 mg, 0.02 mmol, 21%).

^{1}H NMR (400 MHz, DMSO-d_6) δ 2.85 (p, J = 7.1 Hz, 2H, CH_2-C$\underline{H}_2$-CH_2), 4.03 (s, 3H, OCH_3), 4.04 – 4.08 (m, 2H, NCH_2), 4.80 (t, J = 7.2 Hz, 2H, NCH_2), 7.63 (d, J = 2.7 Hz, 1H, H9), 7.72 (dd, J = 9.3, 2.7 Hz, 1H, H7), 8.08 (d, J = 9.3 Hz, 1H, H6), 9.35 (s, 1H, H4).

^{13}C NMR (101 MHz, DMSO-d_6) δ 27.9 (t, CH_2), 41.2 (t, CH_2), 47.1 (t, CH_2), 56.3 (q, OCH_3), 104.3 (d, C9), 109.1 (s, C3a), 115.3 (s, C9a), 122.8 (d, C6/C7), 123.7 (d, C6/C7), 131.4 (s, C5a/C9b), 138.2 (s, C5a/C9b), 139.8 (d, C4), 155.4 (s, CO), 158.8 (s, C8).

HPLC-MS: Calc.[M+H]: 256.11
Found [M+H]: 256.10

HR-MS: Calc.[M+H]: 256.1081
Found [M+H]: 256.1095
(Diff.: -5.82 ppm)

Appearance: Colorless solid

Mp: Decomposes > 300 °C

TLC: R_f = 0.76 (15% MeOH in EtOAc)

E IV.6 Pyrazoloquinolinones – R^8 fluoro series

E IV.6.1 8-Fluoro-2-(*p*-tolyl)-2,5-dihydro-3*H*-pyrazolo[4,3-*c*]quinolin-3-one [32] DCBSLK024

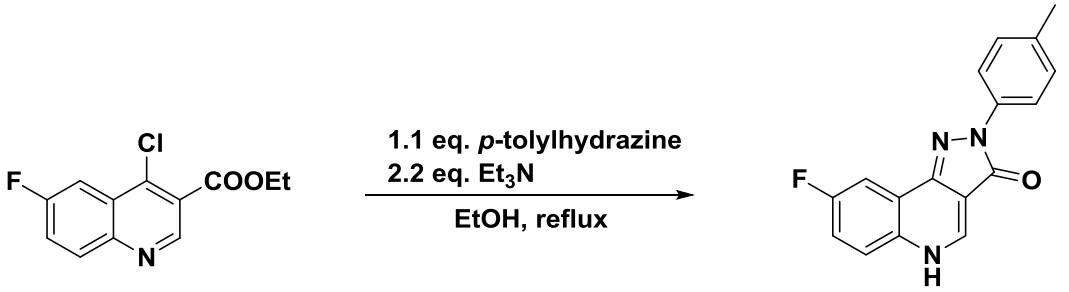

[29]

Chemical Formula: $C_{12}H_9ClFNO_2$
Molecular Weight: 253.66

[32] (66%)

Chemical Formula: $C_{17}H_{12}FN_3O$
Molecular Weight: 293.30

The desired compound was synthesized according to general procedure E III.4 using:

Chlorinated quinoline	80 mg	0.32 mmol	1 eq.
Arylhydrazine HCl	55 mg	0.35 mmol	1.1 eq.

The desired product **[32]** was obtained without further purification (62 mg, 0.21 mmol, 66%).

^{1}H NMR (600 MHz, DMSO-d_6) δ 2.32 (s, 3H, CH_3), 7.25 (d, J = 8.2 Hz, 2H, H3´ and H5´), 7.57 (td, J = 8.7, 2.9 Hz, 1H, H7), 7.78 (dd, J = 9.1, 4.8 Hz, 1H, H6), 7.90 (dd, J = 8.8, 2.9 Hz, 1H, H9), 8,09 (d, J = 8,41 Hz, 2H, H2´ and H6´), 8.75 (s, 1H, H4), 12.91 (br s, 1H, NH).

^{13}C NMR (151 MHz, DMSO-d_6) δ 21.0 (q, CH_3), 106.0 (s, C3a), 107.6 (dd, $^2J_{C,F}$ = 23.0 Hz, C9), 118.9 (dd, $^2J_{C,F}$ = 25.3 Hz, C7), 119.2 (d, C2´and C6´), 120.7 (sd, $^3J_{C,F}$ = 9.6 Hz, C9a), 122.7 (dd, $^3J_{C,F}$ = 9.4 Hz, C6), 129.6 (d, C3´and C5´), 132.8 (s, C1´/C4´), 133.6 (s, C1´/C4´), 138.2(s, C5a/C9b), 139.7 (d, C4), 142.9 (s, C5a/C9b), 160.2 (sd, $^1J_{C,F}$ = 245.4 Hz, C8), 161.8 (s, CO).

HR-MS: Calc.[M+H]: 294.1037

Found [M+H]: 294.1047 (Diff.: -3.30 ppm)

Appearance: Yellow solid

Mp: Decomposes > 300 °C

TLC: R_f = 0.41 (10% MeOH in CH_2Cl_2)

E IV.6.2 8-Fluoro-2-(*m*-tolyl)-2,5-dihydro-3*H*-pyrazolo[4,3-*c*]quinolin-3-one [39] DCBSLK017

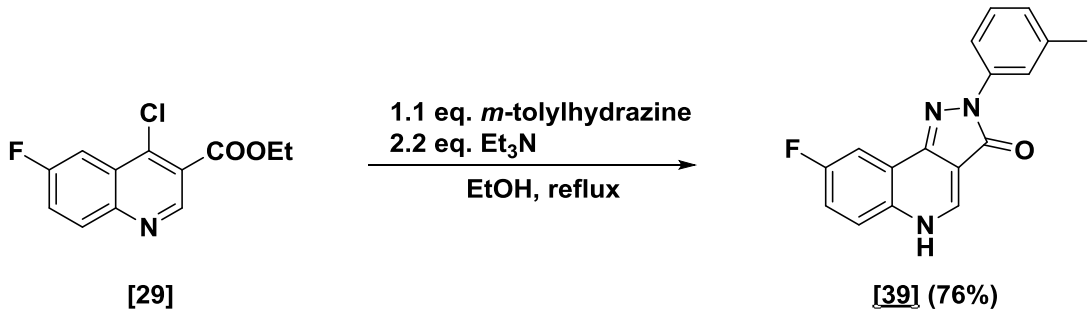

[29]

Chemical Formula: $C_{12}H_9ClFNO_2$
Molecular Weight: 253.66

[39] (76%)

Chemical Formula: $C_{17}H_{12}FN_3O$
Molecular Weight: 293.30

The desired compound was synthesized according to general procedure E III.4 using:

Chlorinated quinoline	80 mg	0.32 mmol	1 eq.
Arylhydrazine HCl	55 mg	0.35 mmol	1.1 eq.

The desired product **[39]** was obtained without further purification (70 mg, 0.24 mmol, 76%).

^{1}H NMR (600 MHz, DMSO-d_6) δ 2.37 (s, 3H, CH_3), 7.00 (dd, *J* = 7.5, 0.52 Hz, 1H, H6´), 7.32 (td, *J* = 7.5, 1.3 Hz, 1H, H5´), 7.57 (td, *J* = 8.7, 2.9 Hz, 1H, H7), 7.78 (dd, *J* = 9.1, 4.8 Hz, 1H, H6), 7.91 (dd, *J* = 8.9, 2.9 Hz, 1H, H9), 8.03 (d, *J* = 7.0 Hz, 2H, H2´ and H4`), 8.76 (s, 1H, H4), 12.92 (br s, 1H, NH).

^{13}C NMR (151 MHz, DMSO-d_6) δ 21.4 (q, CH_3), 105.5 (s, C3a), 107.2 (dd, $^2J_{C,F}$ = 23.4 Hz, C9), 116.0 (d, C2´/C4`), 118.5 (dd, $^2J_{C,F}$ = 24.8 Hz, C7), 119.2 (s, C1´/C3´), 120.3 (sd, $^3J_{C,F}$ = 9.1 Hz, C9a), 122.3 (dd, $^3J_{C,F}$ = 9.0 Hz, C6), 124.9 (d, C6´), 128.5 (d, C5´), 132.3 (s, C1´/C3´), 137.9 (d, C2´/C4`), 139.3 (d, C4), 140.0 (s, C5a/C9b), 142.5 (sd, $^4J_{C,F}$ = 3.2 Hz, C5a/C9b), 159.8 (sd, $^1J_{C,F}$ = 245.3 Hz, C8), 161.5 (s, CO).

HR-MS: Calc.[M+H]: 294.1037

Found [M+H]: 294.1035 (Diff.: +0.72 ppm)

Appearance: Yellow solid

Mp: Decomposes > 300 °C

TLC: R_f = 0.35 (10% MeOH in CH_2Cl_2)

E IV.6.3 8-Fluoro-2-(4-methoxyphenyl)-2,5-dihydro-3*H*-pyrazolo[4,3-*c*]quinolin-3-one [33] DCBSLK012

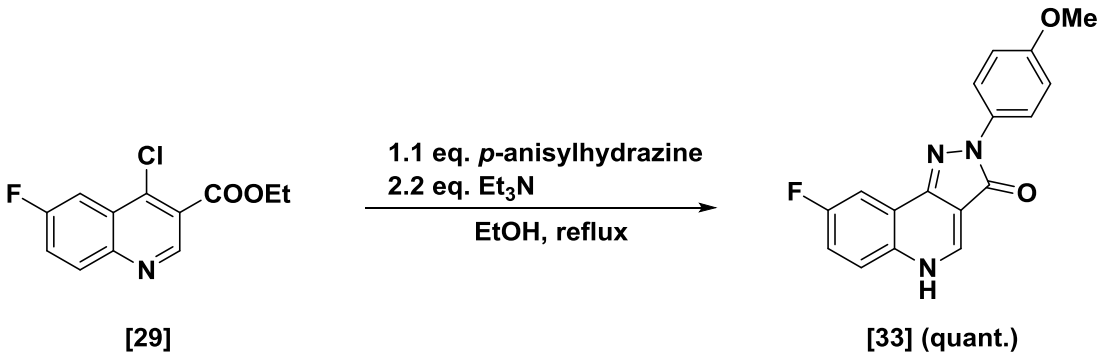

[29]

Chemical Formula: $C_{12}H_9ClFNO_2$
Molecular Weight: 253.66

[33] (quant.)

Chemical Formula: $C_{17}H_{12}FN_3O_2$
Molecular Weight: 309.30

The desired compound was synthesized according to general procedure E III.4 using:

Chlorinated quinoline	80 mg	0.32 mmol	1 eq.
Arylhydrazine HCl	61 mg	0.35 mmol	1.1 eq.

The desired product **[33]** was obtained without further purification (100 mg, 0.32 mmol, quant.).

^{1}H NMR (400 MHz, DMSO-d_6) δ 3.78 (s, 3H, OCH_3), 6.97 – 7.08 (m, 2H, H3´ and H5´), 7.57 (td, J = 8.7, 2.9 Hz, 1H, H7), 7.78 (dd, J = 9.1, 4.9 Hz, 1H, H6), 7.90 (dd, J = 9.0, 2.9 Hz, 1H, H9), 8.00 – 8.16 (m, 2H, H2´ and H6´), 8.74 (s, 1H, H4), 12.90 (br s, 1H, NH).

^{13}C NMR (151 MHz, DMSO-d_6) δ 55.3 (q, CH_3), 105.5 (s, C3a), 107.1 (dd, $^{2}J_{C,F}$ = 23.2 Hz, C9), 113.9 (d, C3´and C5), 118.4 (dd, $^{2}J_{C,F}$ = 24.59 Hz, C7), 120.3 (sd, $^{3}J_{C,F}$ = 9.3 Hz, C9a), 120.6 (d, C2 and C6), 122.3 (dd, $^{3}J_{C,F}$ = 9.1 Hz, C6), 132.2 (s, C1´/C4´), 133.5 (s, C1´/C4´), 139.2 (d, C4), 142.2 (s, C5a/C9b), 156.0 (s, C5a/C9b), 159.8 (sd, $^{1}J_{C,F}$ = 245.3 Hz, C8), 161.0 (s, CO).

Appearance: Yellow solid

Mp: Decomposes > 300 °C (Lit.[143]: Decomposition > 290 °C)

TLC: R_f = 0.49 (10% MeOH in CH_2Cl_2)

E IV.6.4 8-Fluoro-2-(3-methoxyphenyl)-2,5-dihydro-3*H*-pyrazolo[4,3-*c*]quinolin-3-one [40] DCBSLK029

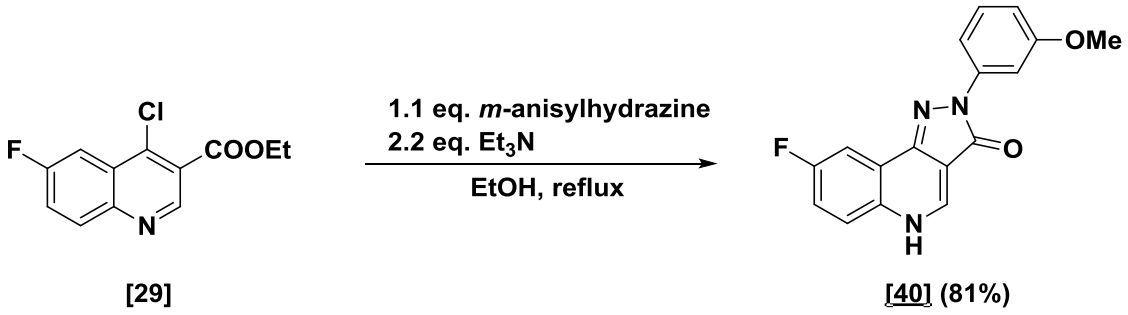

[29]

Chemical Formula: $C_{12}H_9ClFNO_2$
Molecular Weight: 253.66

[40] (81%)

Chemical Formula: $C_{17}H_{12}FN_3O_2$
Molecular Weight: 309.30

The desired compound was synthesized according to general procedure E III.4 using:

Chlorinated quinoline	139 mg	0.55 mmol	1 eq.
Arylhydrazine HCl	105 mg	0.60 mmol	1.1 eq.

The desired product **[40]** was obtained without further purification (107 mg, 0.35 mmol, 81%).

^{1}H NMR (600 MHz, DMSO-d_6) δ 3.81 (s, 3H, OCH_3), 6.77 (dd, *J* = 8.2, 2.6 Hz, 1H, H6´), 7.35 (t, *J* = 8.2 Hz, 1H, H5´), 7.58 (td, *J* = 8.7, 2.9 Hz, 1H, H7), 7.79 (dd, *J* = 9.1, 4.8 Hz, 1H, H6), 7.83 (dd, *J* = 8.1, 1.9 Hz, 1H, H4´), 7.86 (t, *J* = 2.3 Hz, 1H, H2´), 7.92 (dd, *J* = 8.9, 2.9 Hz, 1H, H9), 8.75 (s, 1H, H4), 12.94 (br s, 1H, NH).

^{13}C NMR (151 MHz, DMSO-d_6) δ 55.6 (q, CH_3), 105.0 (d, C2´), 106.0 (s, C3a), 107.7 (dd, $^{2}J_{C,F}$ = 23.4 Hz, C9), 109.9 (d, C6´), 111.5 (d, C4´), 119.0 (dd, $^{2}J_{C,F}$ = 24.6 Hz, C7), 120.7 (sd, $^{3}J_{C,F}$ = 9.2 Hz, C9a), 122.8 (dd, $^{3}J_{C,F}$ = 9.6 Hz, C6), 130.0 (d, C5´), 132.8 (s, C1´/C3´), 139.9 (d, C4), 141.6 (s, C5a/C9b), 143.1 (s, C5a/C9b), 160.0 (s, C1´/C3´), 160.1 (sd, $^{1}J_{C,F}$ = 245.4 Hz, C8), 162.1 (s, CO).

HR-MS: Calc.[M+H]: 310.0986

Found [M+H]: 310.0992 (Diff.: -1.71 ppm)

Appearance: Yellow solid

Mp: Decomposes > 300 °C

TLC: R_f = 0.40 (10% MeOH in CH_2Cl_2)

E IV.6.5 8-Fluoro-2-(4-nitrophenyl)-2,5-dihydro-3*H*-pyrazolo[4,3-*c*]quinolin-3-one [34] DCBSLK059

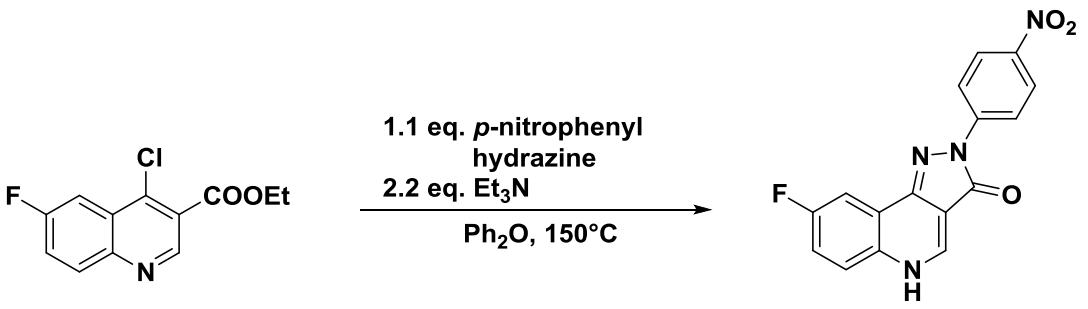

[29]

Chemical Formula: $C_{12}H_9ClFNO_2$
Molecular Weight: 253.66

[34] (37%)

Chemical Formula: $C_{16}H_9FN_4O_3$
Molecular Weight: 324.27

The chlorinated quinolinone **[29]** (80 mg, 0.32 mmol, 1 eq.) and the arylhydrazine hydrochloride (55 mg, 0.35 mmol, 1.1 eq.) were dispersed in 3 mL diphenylehter, Et_3N (2.2 eq.) was added and the reaction mixture was heated to 150 °C under argon atmosphere. After 20 h the reaction mixture was allowed to cool to room temperature and was rinsed with 3 mL EtOH/EtOAc. The precipitate was collected by filtration and the filtrate was concentrated. After the second filtration 8-fluoro-2-(4-nitrophenyl)-2,5-dihydro-3H-pyrazolo[4,3-c]quinolin-3-one **[34]** was obtained (38 mg, 0.12 mmol, 37%).

^{1}H NMR (600 MHz, DMSO-d_6) δ 7.59 (td, *J* = 8.7, 3.0 Hz, 1H, H7), 7.80 (dd, J = 9.1, 4.8 Hz, 1H, H6), 7.92 (dd, *J* = 8.8, 2.9 Hz, 1H, H9), 8.34 (d, *J* = 9.4 Hz, 2H, H3' and H5'), 8.53 (d, *J* = 9.5 Hz, 2H, H2' and H6'), 8.81 (s, 1H, H4).

^{13}C NMR (151 MHz, DMSO-d_6) δ 104.6 (s, C3a), 107.3 (dd, $^2J_{C,F}$ = 23.0 Hz, C9), 117.9 (d, C2´ and C6´), 118.9 (dd, $^2J_{C,F}$ = 24.5 Hz, C7), 120.3 (sd, $^3J_{C,F}$ = 8.8 Hz, C9a), 123.6 (dd, $^3J_{C,F}$ = 10.7 Hz, C6), 125.0 (d, C3´and C5), 141.2 (s, C1´and C4'), 142.6 (s, C5a/C9b), 144.9 (d, C4), 145.3 (s, C5a/C9b), 159.8 (sd, $^1J_{C,F}$ = 245.5 Hz, C8), 162.7 (s, CO).

Appearance: Yellow solid

Mp: Decomposes > 300 °C

TLC: R_f = 0.48 (10% MeOH in CH_2Cl_2)

E IV.6.6 8-Fluoro-2-(3-nitrophenyl)-2,5-dihydro-3*H*-pyrazolo[4,3-*c*]quinolin-3-one [41] DCBSLK023

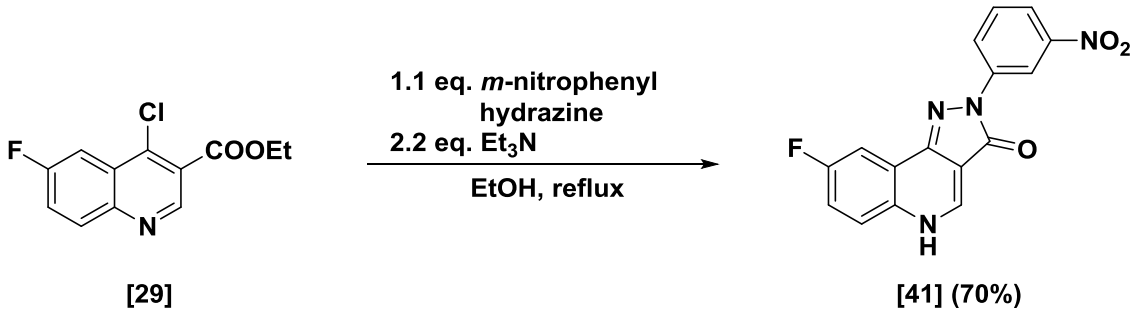

[29]

Chemical Formula: $C_{12}H_9ClFNO_2$
Molecular Weight: 253.66

[41] (70%)

Chemical Formula: $C_{16}H_9FN_4O_3$
Molecular Weight: 324.27

The desired compound was synthesized according to general procedure E III.4 using:

Chlorinated quinoline	100 mg	0.39 mmol	1 eq.
Arylhydrazine HCl	75 mg	0.49 mmol	1.1 eq.

The desired product **[41]** was obtained without further purification (89 mg, 0.27 mmol, 70%).

^{1}H NMR (400 MHz, DMSO-d_6) δ 7.57 (td, *J* = 8.7, 2.9 Hz, 1H, H7), 7.74 (t, *J* = 8.2 Hz, 1H, H5'), 7.79 (dd, *J* = 9.1, 4.9 Hz, 1H, H6), 7.93 (dd, *J* = 8.9, 2.9 Hz, 1H, H9), 8.01 (dd, *J* = 8.1, 2.4 Hz, 1H, H4'), 8.67 (dd, *J* = 8.5, 2.1 Hz, 1H, H6'), 8.80 (s, 1H, H4), 9.13 (t, *J* = 2.2 Hz, 1H, H2').

^{13}C NMR (151 MHz, DMSO-d_6) δ 104.8 (s, C3a), 107.3 (dd, $^{2}J_{C,F}$ = 23.3 Hz, C9), 112.2 (d, C2´), 118.2 (d, C4`), 118.7 (dd, $^{2}J_{C,F}$ = 24.7 Hz, C7), 120.2 (sd, $^{3}J_{C,F}$ = 9.0 Hz, C9a), 123.2 (dd, $^{3}J_{C,F}$ = 9.5 Hz, C6), 124.0 (d, C6´), 130.3 (d, C5´), 133.6 (s, C1´/C3´), 140.7 (s, C5a/C9b), 140.9 (d, C4), 143.95 (sd, $^{4}J_{C,F}$ = 3.3 Hz, C5a/C9b), 148.1 (s, C1´/C3´), 159.75 (sd, $^{1}J_{C,F}$ = 245.4 Hz, C8), 162.1 (s, CO).

Appearance: Yellow solid

Mp: Decomposes > 300 °C

TLC: R_f = 0.43 (10% MeOH in CH_2Cl_2)

E IV.6.7 4-(8-Fluoro-3-oxo-3,5-dihydro-2*H*-pyrazolo[4,3-*c*]quinolin-2-yl)benzonitrile [35] DCBSLK015

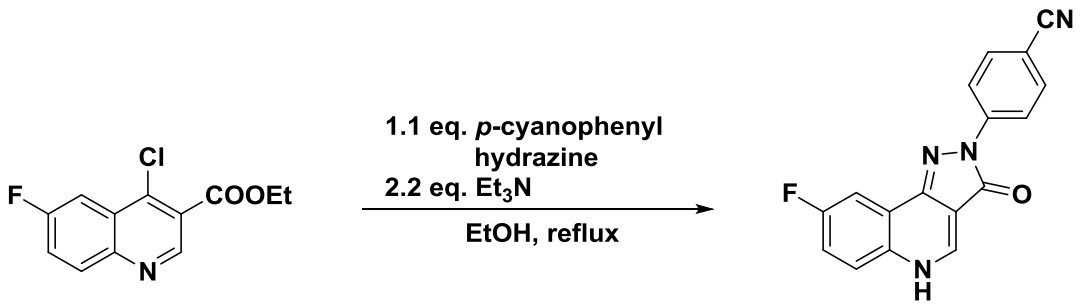

[29]

Chemical Formula: $C_{12}H_9ClFNO_2$
Molecular Weight: 253.66

[35] (61%)

Chemical Formula: $C_{17}H_9FN_4O$
Molecular Weight: 304.28

The desired compound was synthesized according to general procedure E III.4 using:

Chlorinated quinoline	1.00 g	3.94 mmol	1 eq.
Arylhydrazine HCl	0.74 g	4.33 mmol	1.1 eq.

The desired product **[35]** was obtained without further purification (0.73 g, 2.41 mmol, 61%).

^{1}H NMR (600 MHz, DMSO-d_6) δ 7.60 (td, J = 8.7, 2.9 Hz, 1H, H7), 7.79 (dd, J = 9.1, 4.8 Hz, 1H, H6), 7.89 – 7.93 (m, 3H, H2´and H6´and H9), 8.41 – 8.46 (m, 2H, H3 and H5), 8.83 (s, 1H, H4), 13.08 (br s, 1H, NH).

^{13}C NMR (151 MHz, DMSO-d_6) δ 104.9 (s, CN), 105.6 (s, C3a), 107.4 (dd, $^{2}J_{C,F}$ = 23.0 Hz, C9), 118.2 (d, C3 and C5), 119.0 (dd, $^{2}J_{C,F}$ = 24.7 Hz, C7), 119.2 (s, C1´/C4), 120.0 (sd, $^{3}J_{C,F}$ = 9.2 Hz, C9a), 122.5 (dd, $^{3}J_{C,F}$ = 9.0 Hz, C6), 132.5 (s, C1´/C4´), 133.3 (d, C2 and C6), 140.1 (d, C4), 143.4 (s, C5a/C9b), 144.0 (sd, $^{4}J_{C,F}$ = 3.1 Hz, C5a/C9b), 159.9 (sd, $^{1}J_{C,F}$ = 245.9 Hz, C8), 162.3 (s, CO).

HR-MS: Calc.[M+H]: 305.0833

Found [M+H]: 305.0829 (Diff.: +1.35 ppm)

Appearance: Yellow solid

Mp: Decomposes > 300 °C

TLC: R_f = 0.51 (10% MeOH in CH_2Cl_2)

E IV.6.8 3-(8-Fluoro-3-oxo-3,5-dihydro-2*H*-pyrazolo[4,3-*c*]quinolin-2-yl)benzonitrile [42] DCBSLK040

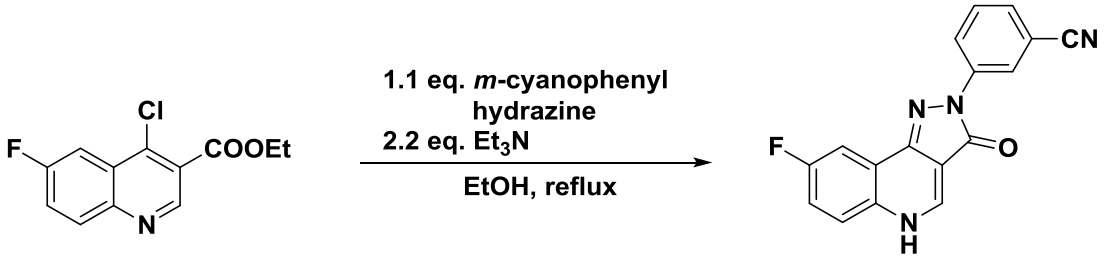

[29]

Chemical Formula: $C_{12}H_9ClFNO_2$
Molecular Weight: 253.66

[42] (52%)

Chemical Formula: $C_{17}H_9FN_4O$
Molecular Weight: 304.28

The desired compound was synthesized according to general procedure E III.4 using:

Chlorinated quinoline	100 mg	0.39 mmol	1 eq.
Arylhydrazine HCl	74 mg	0.43 mmol	1.1 eq.

The desired product **[42]** was obtained without further purification (75 mg, 0.25 mmol, 52%).

^{1}H NMR (600 MHz, DMSO-d_6) δ 7.60 (td, *J* = 8.7, 2.9 Hz, 1H, H7), 7.63 (dt, *J* = 7.6, 1.4 Hz, 1H, H4´), 7.67 (t, *J* = 7.9 Hz, 1H, H5´), 7.79 (dd, *J* = 9.1, 4.8 Hz, 1H, H6), 7.95 (dd, *J* = 8.8, 2.9 Hz, 1H, H9), 8.56 (ddd, *J* = 8.3, 2.2, 1.2 Hz, 1H, H6´), 8.63 (t, *J* = 1.9 Hz, 1H, H2´), 8.83 (s, 1H, H4), 13.07 (br s, 1H, NH).

^{13}C NMR (151 MHz, DMSO-d_6) δ 105.4 (s, C3a), 107.9 (dd, $^2J_{C,F}$ = 23.5 Hz, C9), 112.1 (s, CN), 119.2 (s, C1´/C3´), 119.4 (dd, $^2J_{C,F}$ = 24.7 Hz, C7), 120.6 (sd, $^3J_{C,F}$ = 9.2 Hz, C9a), 121.3 (d, C2´), 122.9 (dd, $^3J_{C,F}$ = 9.0 Hz, C6), 123.0 (d, C6´), 127.8 (d, C4`), 130.8 (d, C5´), 132.9 (s, C1´/C3´), 140.41 (d, C4), 140.43 (s, C5a/C9b), 144.0 (sd, $^4J_{C,F}$ = 3.3 Hz, C5a/C9b), 160.3 (sd, $^1J_{C,F}$ = 245.7 Hz, C8), 162.4 (s, CO).

HR-MS: Calc.[M+H]: 305.0833

Found [M+H]: 305.0833 (Diff.: +0.20 ppm)

Appearance: Yellow solid

Mp: Decomposes > 300 °C

TLC: R_f = 0.50 (10% MeOH in CH_2Cl_2)

E IV.6.9 2-(4-Aminophenyl)-8-fluoro-2,5-dihydro-3H-pyrazolo[4,3-c]quinolin-3-one [36] DCBS193

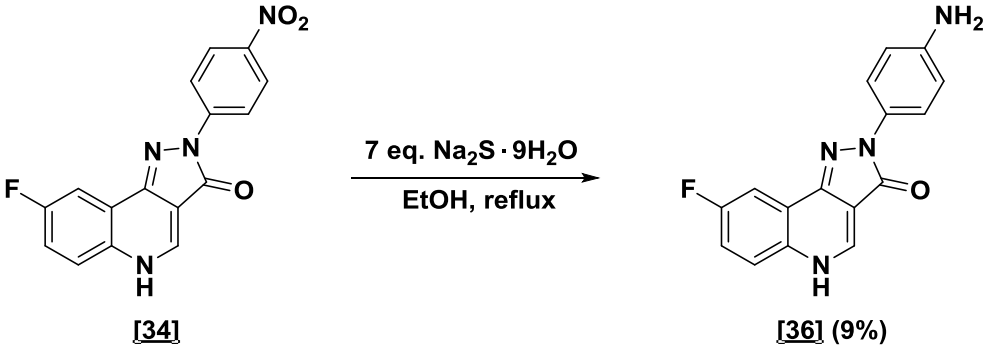

[34] **[36] (9%)**

Chemical Formula: $C_{16}H_9FN_4O_3$
Molecular Weight: 324.27

Chemical Formula: $C_{16}H_{11}FN_4O$
Molecular Weight: 294.29

The desired compound was synthesized according to general procedure E III.7 using:

Nitro PQ	45 mg	0.18 mmol	1 eq.
$Na_2S{\cdot}9H_2O$	303 mg	1.26 mmol	7 eq.

2-(4-Aminophenyl)-8-fluoro-2,5-dihydro-3*H*-pyrazolo[4,3-*c*]quinolin-3-one **[36]** was obtained after purification by HPLC (5 mg, 0.017 mmol, 9%).

^{1}H NMR (400 MHz, DMSO-d_6) δ 5.06 (br s, 2H, NH_2), 6.59 – 6.66 (m, 2H, H3 and H5), 7.54 (td, *J* = 8.8, 2.9 Hz, 1H, H7), 7.73 – 7.76 (m, 2H, H2´and H6), 7.76 – 7.79 (m, 1H, H6), 7.85 (dd, *J* = 9.0, 2.9 Hz, 1H, H9), 8.68 (s, 1H, H4), 12.81 (br s, 1H, NH).

^{13}C NMR (101 MHz, DMSO-d_6) δ 105.7 (s, C3a), 106.9 (dd, $^2J_{C,F}$ = 23.6 Hz, C9), 113.6 (d, C3 and C5), 118.0 (dd, $^2J_{C,F}$ = 24.9 Hz, C7), 120.3 (s, C9a), 121.0 (d, C2 and C6), 122.1 (dd, $^3J_{C,F}$ = 9.3 Hz, C6), 129.6 (s, C1´/C4´), 132.0 (s, C5a/C9b), 138.7 (d, C4), 141.5 (sd, $^4J_{C,F}$ = 2.8 Hz, C5a/C9b), 145.8 (s, C1´/C4´), 159.7 (sd, $^1J_{C,F}$ = 245.4 Hz, C8), 160.5(s, CO).

HR-MS: Calc.[M+H]: 295.0990

Found [M+H]: 295.0994 (Diff.: -1.36 ppm)

Appearance: Orange solid

Mp: Decomposes > 300 °C

TLC: R_f = 0.55 (10% MeOH in CH_2Cl_2)

E IV.6.10 2-(3-Aminophenyl)-8-fluoro-2,5-dihydro-3*H*-pyrazolo[4,3-*c*]quinolin-3-one [43] DCBSLK055

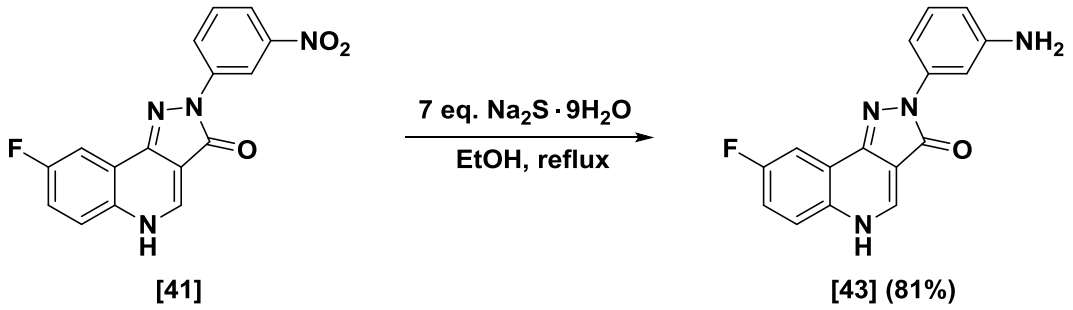

[41]

Chemical Formula: $C_{16}H_9FN_4O_3$
Molecular Weight: 324.27

[43] (81%)

Chemical Formula: $C_{16}H_{11}FN_4O$
Molecular Weight: 294.29

The desired compound was synthesized according to general procedure E III.7 using:

Nitro PQ	40 mg	0.12 mmol	1 eq.
$Na_2S{\cdot}9H_2O$	200 mg	0.84 mmol	7 eq.

2-(3-Aminophenyl)-8-fluoro-2,5-dihydro-3*H*-pyrazolo[4,3-*c*]quinolin-3-one **[43]** was obtained without further purification (29 mg, 0.10 mmol, 81%).

^{1}H NMR (600 MHz, DMSO-*d_6*) δ 5.19 (br s, 2H, NH_2), 6.39 (ddd, *J* = 7.9, 2.3, 1.0 Hz, 1H, H6'), 7.05 (t, *J* = 8.0 Hz, 1H, H5'), 7.37 (ddd, *J* = 8.0, 2.0, 1.0 Hz, 1H, H4`), 7.45 (t, *J* = 2.1 Hz, 1H, H2'), 7.57 (td, *J* = 8.7, 3.0 Hz, 1H, H7), 7.77 (dd, *J* = 9.1, 4.8 Hz, 1H, H6), 7.85 (dd, *J* = 8.9, 2.9 Hz, 1H, H9), 8.72 (s, 1H, H4), 12.86 (s, 1H, NH).

^{13}C NMR (151 MHz, DMSO-*d6*) δ 105.1 (d, C2´), 106.2 (s, C3a), 107.4 (dd, $^{2}J_{C,F}$ = 22.4 Hz, C9 and C4`), 110.7 (d, C6´), 118.8 (dd, $^{2}J_{C,F}$ = 24.7 Hz, C7), 120.7 (ds, $^{3}J_{C,F}$ = 9.2 Hz, C9a), 122.7 (dd, $^{3}J_{C,F}$ = 9.1 Hz, C6), 129.3 (d, C5´), 132.7 (s, C1´/C3´), 139.5 (d, C4), 141.2 (s, C5a/C9b), 142.5 (sd, $^{4}J_{C,F}$ = 3.2 Hz, C5a/C9b), 149.5 (s, C1´/C3-), 160.1 (sd, $^{1}J_{C,F}$ = 245.1 Hz, C8), 161.8 (s, CO).

Appearance: Yellow solid

Mp: Decomposes > 300 °C

TLC: R_f = 0.76 (10% MeOH in CH_2Cl_2)

E IV.6.11 4-(8-Fluoro-3-oxo-3,5-dihydro-2*H*-pyrazolo[4,3-*c*]quinolin-2-yl)benzoic acid [37] DCBSLK038

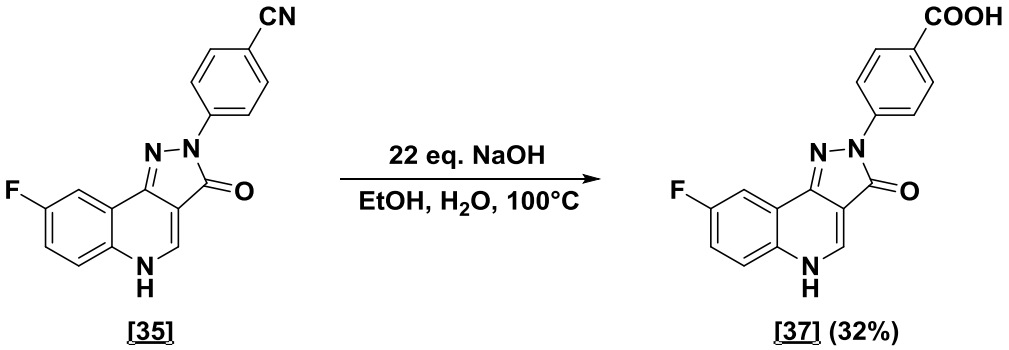

[35] **[37] (32%)**

Chemical Formula: $C_{17}H_9FN_4O$
Molecular Weight: 304.28

Chemical Formula: $C_{17}H_{10}FN_3O_3$
Molecular Weight: 323.28

The desired compound was synthesized according to an adapted procedure E III.5 using:

PQ benzonitrile	50 mg	0.16 mmol	1 eq.
NaOH	146 mg	3.65 mmol	22 eq.

After lyophilisation 4-(8-fluoro-3-oxo-3,5-dihydro-2H-pyrazolo[4,3-c]quinolin-2-yl)benzoic acid **[37]** was obtained (17 mg, 0.05 mmol, 32%).

^{1}H NMR (600 MHz, DMSO-d_6) δ 7.60 (td, J = 8.6, 2.9 Hz, 1H, H7), 7.81 (dd, J = 9.0, 4.9 Hz, 1H, H6), 7.93 (dd, J = 8.8, 2.9 Hz, 1H, H9), 8.03 (d, J = 8.8 Hz, 2H, H3´ and H5´), 8.38 (d, J = 8.9 Hz, 2H, H2´ and H6´), 8.82 (d, J = 6.4 Hz, 1H, H4), 13.07 (br s, 1H, NH/COOH).

^{13}C NMR (151 MHz, DMSO-d_6) δ 105.2 (s, C3a), 107.3 (dd, $^{2}J_{C,F}$ = 23.5 Hz, C9), 117.7 (d, C2´ and C6´), 118.9 (dd, $^{2}J_{C,F}$ = 24.9 Hz, C7), 120.2 (sd, $^{3}J_{C,F}$ = 9.0 Hz, C9a), 122.4 (dd, $^{3}J_{C,F}$ = 8.9 Hz, C6), 125.8 (s, C1´/C4´), 130.4 (d, C3´and C5´), 132.5 (s, C5a/C9b), 139.8 (d, C4), 143.5 (s, C1´/C4´), 143.6 (sd, $^{4}J_{C,F}$ = 3.1 Hz, C5a/C9b), 159.8 (sd, $^{1}J_{C,F}$ = 245.3 Hz, C8), 162.1 (s, CO), 167.0 (s, COOH).

HR-MS: Calc.[M+H]: 324.0779

Found [M+H]: 324.0801 (Diff.: -6.88 ppm)

Appearance: Yellow solid

Mp: Decomposes > 300 °C

TLC: R_f = 0.11 (10% MeOH in CH_2Cl_2)

E IV.6.12 3-(8-Fluoro-3-oxo-3,5-dihydro-2*H*-pyrazolo[4,3-*c*]quinolin-2-yl)benzoic acid [44] DCBSLK039

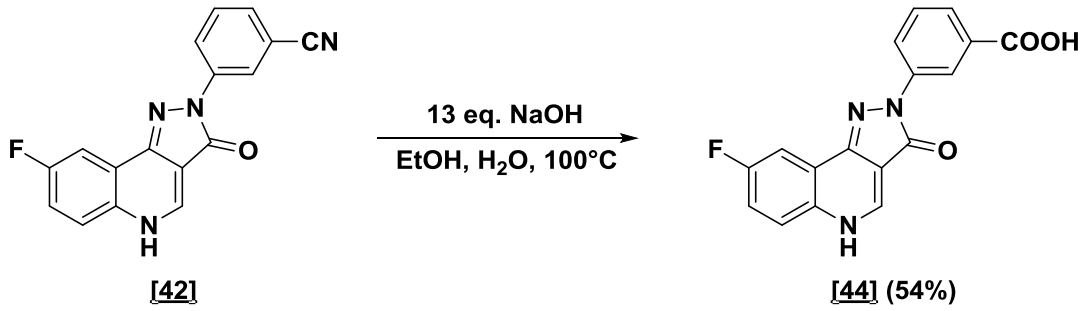

[42] **[44] (54%)**

Chemical Formula: $C_{17}H_9FN_4O$
Molecular Weight: 304.28

Chemical Formula: $C_{17}H_{10}FN_3O_3$
Molecular Weight: 323.28

The desired compound was synthesized according to general procedure E III.5 using:

PQ benzonitrile	57 mg	0.19 mmol	1 eq.
NaOH	100 mg	2.50 mmol	13 eq.

After lyophilisation 3-(8-fluoro-3-oxo-3,5-dihydro-2H-pyrazolo[4,3-c]quinolin-2-yl)benzoic acid **[44]** was obtained (33 mg, 0.10 mmol, 54%).

^{1}H NMR (600 MHz, DMSO-d_6) δ 7.53 – 7.63 (m, 2H, H7 and H5´), 7.75 (dt, *J* = 7.6, 1.4 Hz, 1H, H4´), 7.81 (dd, *J* = 9.1, 4.8 Hz, 1H, H6), 7.95 (dd, *J* = 8.8, 2.9 Hz, 1H, H9), 8.48 (ddd, *J* = 8.2, 2.3, 1.1 Hz, 1H, H6´), 8.77 – 8.84 (m, 2H, H2´ and H4), 13.06 (br d, *J* = 6.5 Hz, 1H, NH/COOH).

^{13}C NMR (151 MHz, DMSO-d_6) δ 105.3 (s, C3a), 107.3 (dd, $^2J_{C,F}$ = 23.4 Hz, C9), 118.7 (dd, $^2J_{C,F}$ = 24.7 Hz, C7), 119.3 (s, C2´), 120.2 (sd, $^3J_{C,F}$ = 9.2 Hz, C9a), 122.4 (dd, $^3J_{C,F}$ = 9.1 Hz, C6), 122.6 (d, C6´), 124.9 (d, C4´), 129.1 (d, C5`), 131.4 (d, C1´/C3´), 132.4 (s, C1´/C3´), 140.1 (s, C5a/C9b), 143.1 (sd, $^4J_{C,F}$ = 3.1 Hz, C5a/C9b), 149.6 (d, C4), 159.8 (sd, $^1J_{C,F}$ = 245.7 Hz, C8), 161.8 (s, CO), 167.3 (s, COOH).

HR-MS: Calc.[M+H]: 324.0779

Found [M+H]: 324.0779 (Diff.: +0.07 ppm)

Appearance: Yellow solid

Mp: Decomposes > 300 °C

TLC: R_f = 0.06 (10% MeOH in CH_2Cl_2)

E IV.6.13 4-(8-Fluoro-3-oxo-3,5-dihydro-2*H*-pyrazolo[4,3-*c*]quinolin-2-yl)benzamide [38] DCBSLK032

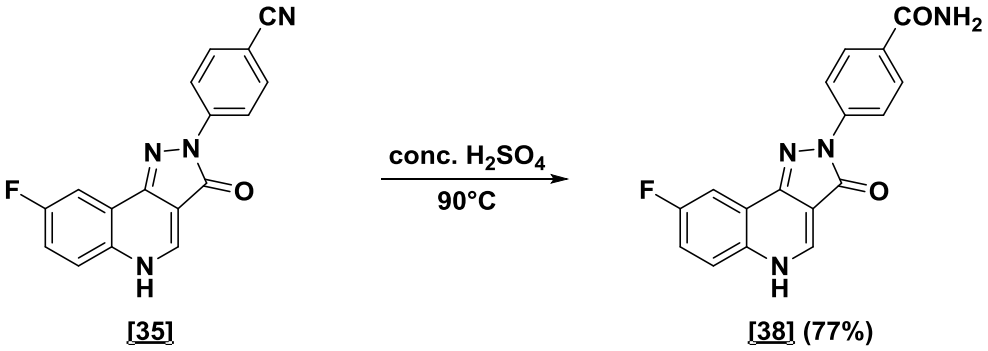

[35] [38] (77%)

Chemical Formula: $C_{17}H_9FN_4O$
Molecular Weight: 304.28

Chemical Formula: $C_{17}H_{11}FN_4O_2$
Molecular Weight: 322.30

The desired compound was synthesized according to general procedure E III.6 using:

PQ benzonitrile	80 mg	0.26 mmol	1 eq.
Conc. H_2SO_4	0.2 mL	0.8 mL/mmol	

After lyophilisation 4-(8-fluoro-3-oxo-3,5-dihydro-2*H*-pyrazolo[4,3-*c*]quinolin-2-yl)benzamide **[38]** was obtained (65 mg, 0.20 mmol, 77%).

^{1}H NMR (600 MHz, DMSO-d_6) δ 7.29 (s, 1H, NH_2), 7.53 (td, *J* = 8.7, 2.9 Hz, 1H, H7), 7.77 (dd, *J* = 9.1, 5.0 Hz, 1H, H6), 7.90 (dd, *J* = 8.9, 2.9 Hz, 1H, H9), 7.93 – 7.98 (m, 3H, H3´ and H5´ and NH_2), 8.32 – 8.35 (m, 2H, H2´ and H6´), 8.71 (br s, 1H, H4).

^{13}C NMR (151 MHz, DMSO-d_6) δ 104.9 (s, C3a), 106.9 (dd, $^2J_{C,F}$ = 22.9 Hz, C9), 117.5 (d, C2´and C6´), 118.1 (dd, $^2J_{C,F}$ = 24.5 Hz, C7), 120.6 (sd, $^3J_{C,F}$ = 9.5 Hz, C9a), 124.3 (d, C6), 128.3 (s, C1´/C4´), 129.0 (s, C3´and C5), 135.1 (s, C1´/C4´), 141.5 (d, C4), 142.6 (s, C5a/C9b), 144.0 (s, C5a/C9b) 158.7 (s, $CONH_2$), 161.2 (sd, $^1J_{C,F}$ = 246.2 Hz, C8), 167.6 (s, CO).

HR-MS: Calc.[M+H]: 323.0939

Found [M+H]: 323.0953 (Diff.: -4.33 ppm)

Appearance: Yellow solid

Mp: Decomposes > 300 °C

TLC: R_f = 0.50 (20% MeOH in CH_2Cl_2)

E IV.6.14 3-(8-Fluoro-3-oxo-3,5-dihydro-2*H*-pyrazolo[4,3-*c*]quinolin-2-yl)benzamide [45] DCBSLK033

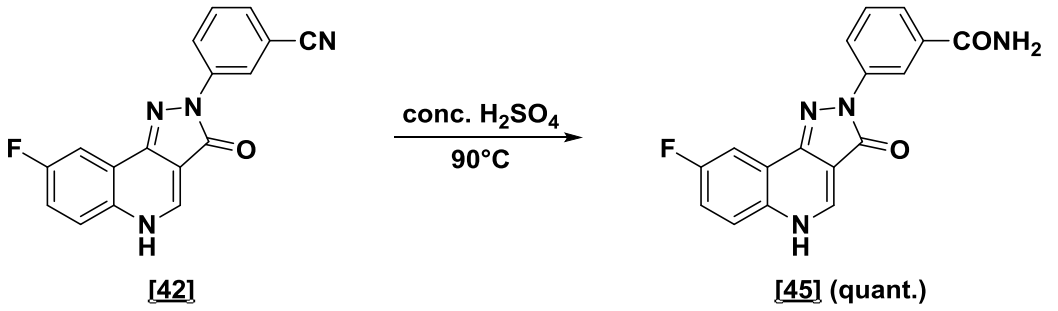

[42] [45] (quant.)

Chemical Formula: $C_{17}H_9FN_4O$
Molecular Weight: 304.28

Chemical Formula: $C_{17}H_{11}FN_4O_2$
Molecular Weight: 322.30

The desired compound was synthesized according to general procedure E III.6 using:

PQ benzonitrile	100 mg	0.33 mmol	1 eq.
Conc. H_2SO_4	0.3 mL	0.8 mL/mmol	

After lyophilisation 3-(8-fluoro-3-oxo-3,5-dihydro-2*H*-pyrazolo[4,3-*c*]quinolin-2-yl)benzamide **[45]** was obtained (106 mg, 0.33 mmol, quant.).

^{1}H NMR (600 MHz, DMSO-d_6) δ 7.28 (td, *J* = 8.7, 3.0 Hz, 1H, H7), 7.33 (s, 1H, NH_2), 7.42 (t, *J* = 7.9 Hz, 1H, H5´), 7.52 (dt, *J* = 7.7, 1.4 Hz, 1H, H4´), 7.68 (dd, *J* = 9.0, 5.6 Hz, 1H, H6), 7.76 (dd, *J* = 9.5, 3.0 Hz, 1H, H9), 7.97 (s, 1H, NH_2), 8.44 (s, 1H, H4), 8.57 (ddd, *J* = 8.1, 2.2, 1.0 Hz, 1H, H6´), 8.70 (t, *J* = 2.0 Hz, 1H, H2´).

^{13}C NMR (151 MHz, DMSO-d_6) δ 103.5 (s, C3a), 105.6 (dd, $^2J_{C,F}$ = 21.7 Hz, C9), 115.4 (dd, $^2J_{C,F}$ = 23.5 Hz, C7), 118.0 (s, C2´), 121.0 (d, C6´), 121.4 (d, C4´), 122.1 (sd, $^3J_{C,F}$ = 8.7 Hz, C9a), 128.1 (d, C5`), 130.4 (dd, $^3J_{C,F}$ = 8.7 Hz, C6), 134.8 (d, C1´/C3´), 141.7 (d, C1´/C3´), 143.7 (s, C5a/C9b), 145.7 (sd, $^4J_{C,F}$ = 3.1 Hz, C5a/C9b), 147.2 (d, C4), 158.6 (sd, $^1J_{C,F}$ = 240.9 Hz, C8), 161.6 (s, CO), 168.5 (s, $CONH_2$).

HR-MS: Calc.[M+H]: 323.0939

Found [M+H]: 323.0945 (Diff.: -1.95 ppm)

Appearance: Yellow solid

Mp: Decomposes > 300 °C

TLC: R_f = 0.36 (15% MeOH in CH_2Cl_2)

E IV.7 Pyrazoloquinolinones – R^8 chloro series

E IV.7.1 8-Chloro-2-(p-tolyl)-1,2-dihydro-3H-pyrazolo[4,3-c]quinolin-3-one [46] DCBS54

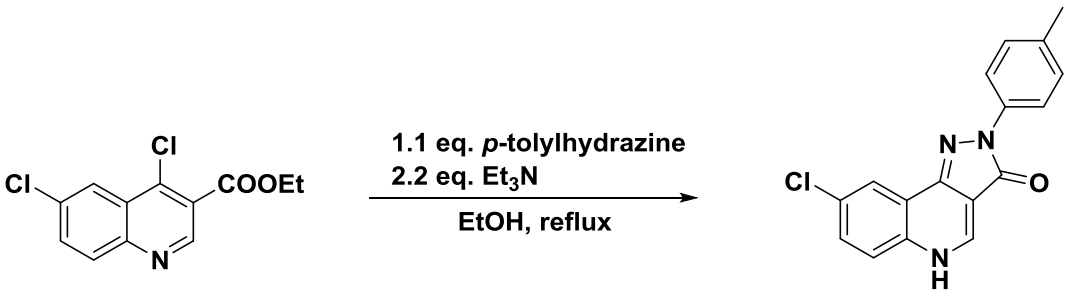

[30]

Chemical Formula: $C_{12}H_9Cl_2NO_2$
Molecular Weight: 270.11

[46] (79%)

Chemical Formula: $C_{17}H_{12}ClN_3O$
Molecular Weight: 309.75

The compound was synthesized according to general procedure E III.4 using:

Chlorinated quinoline	166 mg	0.61 mmol	1 eq.
Arylhydrazine HCl	107 mg	0.68 mmol	1.1 eq.

After purification by HPLC 8-chloro-2-(p-tolyl)-1,2-dihydro-3H-pyrazolo[4,3-c]quinolin-3-one **[46]** was obtained (150 mg, 0.48 mmol, 79%).

^{1}H NMR (400 MHz, DMSO-d_6) δ 2.32 (s, 3H, CH_3), 7.25 (d, J = 8.5 Hz, 2H, H3' and H5'), 7.70 – 7.73 (m, 2H, H6 and H7), 8.09 (d, J = 8.5 Hz, 2H, H2' and H6'), 8.16 (d, J = 2.0 Hz, 1H, H9), 8.75 (s, 1H, H4), 12.89 (br s, 1H, NH).

^{13}C NMR (151 MHz, DMSO-d_6) δ 20.6 (q, CH_3), 106.4 (s, C3a), 118.7 (d, C3' and C5'), 120.1 (s, C9a), 121.1 (d, C9), 121.8 (s, C8), 129.1 (d, C2' and C6'), 130.1 (s, C1'), 130.6 (d, C6/C7), 133.2 (d, C6/C7), 134.4 (s, C4'), 137.7 (d, C4), 139.7 (s, C5a/C9b), 141.8 (s, C5a/C9b), 161.3 (s, CO).

HPLC-MS: Calc.[M+H]: 310.07

Found [M+H]: 310.03

Appearance: Yellow solid

Mp: Decomposes > 300 °C (Lit.[146]: 323 °C)

TLC: R_f = 0.48 (10% MeOH in CH_2Cl_2)

E IV.7.2 8-Chloro-2-(*m*-tolyl)-2,5-dihydro-3H-pyrazolo[4,3-c]quinolin-3-one [52] DCBS142

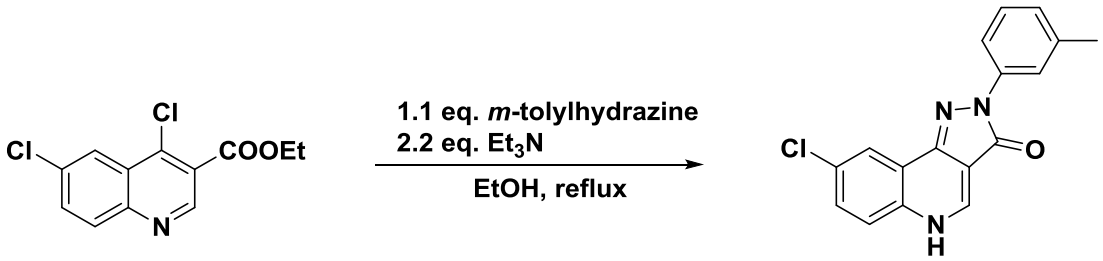

[30]

Chemical Formula: $C_{12}H_9Cl_2NO_2$
Molecular Weight: 270.11

[52] (63%)

Chemical Formula: $C_{17}H_{12}ClN_3O$
Molecular Weight: 309.75

The desired compound was synthesized according to general procedure E III.4 using:

Chlorinated quinoline	50 mg	0.19 mmol	1 eq.
Arylhydrazine HCl	32 mg	0.20 mmol	1.1 eq.

After filtration 8-chloro-2-(*m*-tolyl)-2,5-dihydro-3H-pyrazolo[4,3-c]quinolin-3-one **[52]** was obtained (36 mg, 0.12 mmol, 63%).

^{1}H NMR (400 MHz, DMSO-d_6) δ 2.37 (s, 3H, CH_3), 7.00 (d, *J* = 7.5 Hz, 1H, H6'), 7.32 (t, *J* = 7.7 Hz, 1H, H5'), 7.68 – 7.77 (m, 2H, H6 and H7), 7.99 – 8.07 (m, 2H, H2' and H4'), 8.14 – 8.22 (m, 1H, H9), 8.76 (s, 1H, H4), 12.91 (br s, 1H, NH).

^{13}C NMR (101 MHz, DMSO-d_6) δ 21.4 (q, CH_3), 106.4 (s, C3a), 115.9 (d, C9), 119.2 (d, C6'), 120.0 (s, C9a), 121.2 (d, C2'), 121.7 (d, C6), 124.9 (d, C7), 128.5 (d, C5'), 130.2 (d, C4'), 130.7 (s, C8/C1'), 134.3 (s, C8/C1'), 138.0 (s, C3'), 139.7 (d, C4), 139.9 (s, C5a/C9b), 141.9 (s, C5a/C9b), 161.4 (s, CO).

HR-MS: Calc.[M+H]: 310.0742

Found [M+H]: 310.0756 (Diff.: -4.77 ppm)

Appearance: Yellow solid

Mp: Decomposes > 300 °C

TLC: R_f = 0.24 (5% MeOH in CH_2Cl_2)

E IV.7.3 8-Chloro-2-(4-methoxyphenyl)-2,5-dihydro-3H-pyrazolo[4,3-c]quinolin-3-one [47] DCBS138

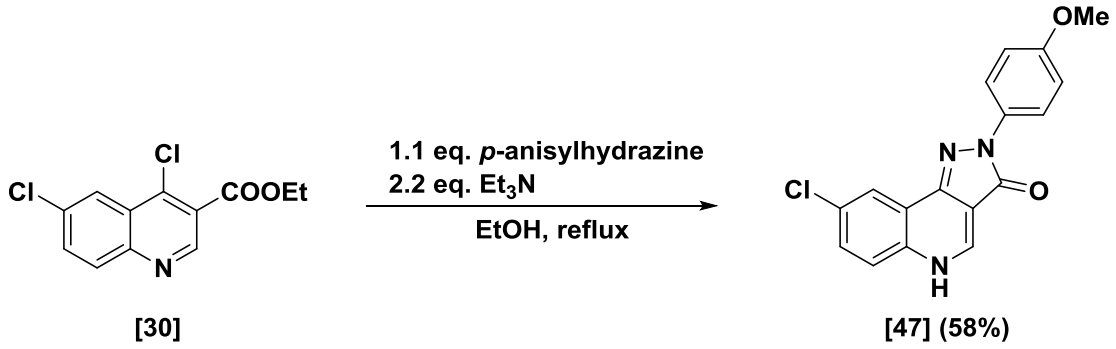

[30]

Chemical Formula: $C_{12}H_9Cl_2NO_2$
Molecular Weight: 270.11

[47] (58%)

Chemical Formula: $C_{17}H_{12}ClN_3O_2$
Molecular Weight: 325.75

The desired compound was synthesized according to general procedure E III.4 using:

Chlorinated quinoline	80 mg	0.30 mmol	1 eq.
Arylhydrazine HCl	57 mg	0.33 mmol	1.1 eq.

After filtration 8-chloro-2-(4-methoxyphenyl)-2,5-dihydro-3H-pyrazolo[4,3-c]quinolin-3-one **[47]** was obtained (56 mg, 0.17 mmol, 58%).

^{1}H NMR (400 MHz, DMSO-d_6) δ 3.79 (s, 3H, OCH_3), 7.02 (d, *J* = 9.2 Hz, 2H, H2' and H6'), 7.67 – 7.78 (m, 2H, H6 and H7), 8.08 (d, *J* = 9.1 Hz, 2H, H3' and H5'), 8.15 (d, *J* = 2.0 Hz, 1H, H9), 8.74 (s, 1H, H4), 12.89 (br s, 1H, NH).

^{13}C NMR (101 MHz, DMSO-d_6) δ 55.3 (q, OCH_3), 106.4 (s, C3a), 113.8 (d, C3' and C5'), 120.0 (s, C9a), 120.4 (d, C2' and C6'), 121.1 (d, C6/C7), 121.7 (d, C6/C7), 130.0 (d, C9), 130.6 (s, C8/C1'), 133.4 (s, C8/C1'), 134.2 (s, C5a/C9b), 139.5 (d, C4), 141.5 (s, C5a/C9b), 156.0 (s, C4'), 160.9 (s, CO).

HPLC-MS: Calc.[M+H]: 326.07

Found [M+H]: 326.02

Appearance: Yellow solid

Mp: Decomposes > 300 °C (Lit.[177]: 326 - 328 °C)

TLC: R_f = 0.63 (10% MeOH in CH_2Cl_2)

E IV.7.4 8-Chloro-2-(3-methoxyphenyl)-2,5-dihydro-3H-pyrazolo[4,3-c]quinolin-3-one [53] DCBS137

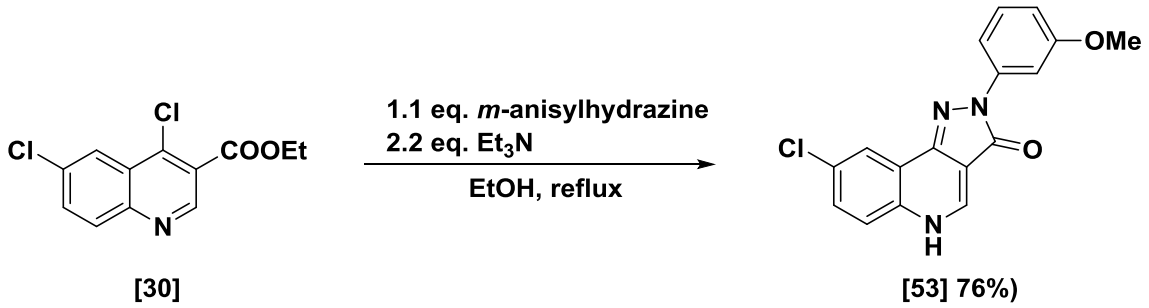

[30] **[53] 76%)**

Chemical Formula: $C_{12}H_9Cl_2NO_2$
Molecular Weight: 270.11

Chemical Formula: $C_{17}H_{12}ClN_3O_2$
Molecular Weight: 325.75

The desired compound was synthesized according to general procedure E III.4 using:

Chlorinated quinoline	50 mg	0.19 mmol	1 eq.
Arylhydrazine HCl	36 mg	0.20 mmol	1.1 eq.

After filtration 8-chloro-2-(3-methoxyphenyl)-2,5-dihydro-3H-pyrazolo[4,3-c]quinolin-3-one **[53]** was obtained (46 mg, 0.14 mmol, 76%).

^{1}H NMR (400 MHz, DMSO-d_6) δ 3.81 (s, 3H, OCH_3), 6.73 – 6.80 (m, 1H, H4'), 7.35 (t, *J* = 8.1 Hz, 1H, H5'), 7.73 (d, *J* = 2.2 Hz, 2H, H-Ar), 7.81 – 7.87 (m, 2H, H-Ar), 8.18 (d, *J* = 2.3 Hz, 1H, H9), 8.75 (s, 1H, H4), 12.92 (br s, 1H, NH).

^{13}C NMR (101 MHz, DMSO-d_6) δ 55.1 (q, OCH_3), 104.5 (d, C3'/C9), 106.4 (s, C3a), 109.6 (d, C3'/C9), 111.0 (d, C4'/C6'), 120.0 (s, C9a), 121.2 (d, C4'/C6'), 121.7 (d, C6/C7), 129.5 (d, C6/C7), 130.3 (d, C5'), 130.7 (s, C8/C1'), 134.3 (s, C8/C1'), 139.7 (d, C4), 141.1 (s, C5a/C9b), 142.0 (s, C5a/C9b), 159.5 (s, C3'), 161.5 (s, CO).

HR-MS: Calc.[M+H]: 326.0691

Found [M+H]: 326.0701 (Diff.: -3.01 ppm)

Appearance: Yellow solid

Mp: Decomposes > 300 °C

TLC: R_f = 0.66 (10% MeOH in CH_2Cl_2)

E IV.7.5 8-Chloro-2-(4-nitrophenyl)-1,2-dihydro-3H-pyrazolo[4,3-c]quinolin-3-one [48] DCBSLS02

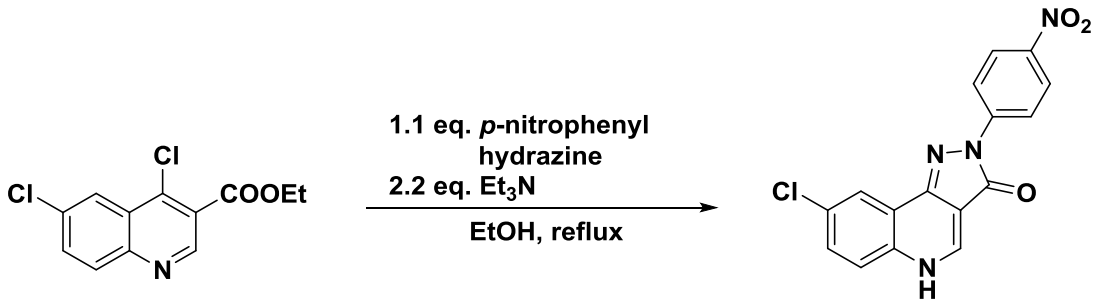

[30]

Chemical Formula: $C_{12}H_9Cl_2NO_2$
Molecular Weight: 270.11

[48] (37%)

Chemical Formula: $C_{16}H_9ClN_4O_3$
Molecular Weight: 340.72

The desired compound was synthesized according to general procedure E III.4 using:

Chlorinated quinoline	300 mg	1.23 mmol	1 eq.
Arylhydrazine HCl	350 mg	1.84 mmol	1.1 eq.

After purification by HPLC 8-chloro-2-(4-nitrophenyl)-1,2-dihydro-3H-pyrazolo[4,3-c]quinolin-3-one **[48]** was obtained (155 mg, 0.45 mmol, 37%).

^{1}H NMR (400 MHz, DMSO-d_6) δ 7.63 – 7.78 (m, 2H, H6 and H7), 8.15 (d, *J* = 2.3 Hz, 1H, H9), 8.32 (d, *J* = 9.4 Hz, 2H, H2 and H6), 8.54 (d, *J* = 9.4 Hz, 2H, H3 and H5), 8.74 (s, 1H, H4).

^{13}C NMR (151 MHz, DMSO-d_6) δ 105.1 (s, C3a), 115.3 (s, C8/C1'), 118.1 (d, C3' and C5'), 119.8 (s, C9a), 121.4 (d, C9), 125.3 (d, C2' and C6'), 126.4 (s, C8/C1'), 130.0 (d, C6/C7), 130.1 (d, C6/C7), 142.5 (d, C4), 144.7 (s, C5a/C9b), 145.8 (s, C5a/C9b), 146.3 (s, C4'), 163.1 (s, CO).

HPLC-MS: Calc.[M+H]: 341.04

Found [M+H]: 341.05

Appearance: Red-orange solid

Mp: Decomposes > 300 °C (Lit.[146]: 293-298 °C)

TLC: R_f = 0.60 (10% MeOH in CH_2Cl_2)

E IV.7.6 8-Chloro-2-(3-nitrophenyl)-2,5-dihydro-3H-pyrazolo[4,3-c]quinolin-3-one [54] DCBS119

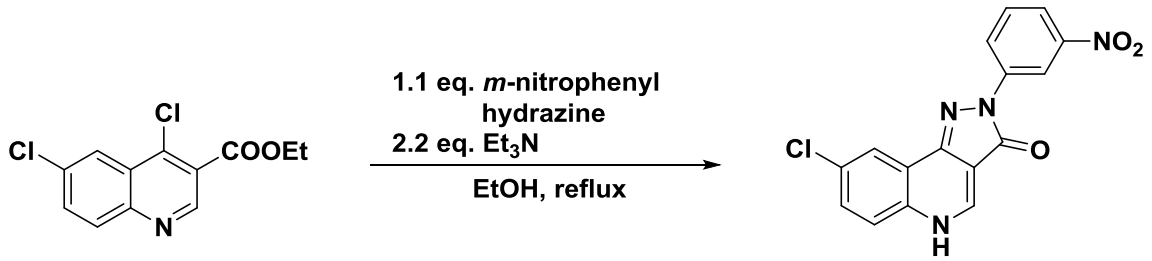

[30]

Chemical Formula: $C_{12}H_9Cl_2NO_2$
Molecular Weight: 270.11

[54] (92%)

Chemical Formula: $C_{16}H_9ClN_4O_3$
Molecular Weight: 340.72

The desired compound was synthesized according to general procedure E III.4 using:

Chlorinated quinoline	96 mg	0.36 mmol	1 eq.
Arylhydrazine HCl	102 mg	0.54 mmol	1.5 eq.

After filtration 8-chloro-2-(3-nitrophenyl)-2,5-dihydro-3H-pyrazolo[4,3-c]quinolin-3-one **[54]** was obtained (112 mg, 0.33 mmol, 92%).

^{1}H NMR (600 MHz, DMSO-d_6) δ 7.72 – 7.78 (m, 3H, H6 and H7 and H5'), 8.02 (ddd, *J* = 8.1, 2.3, 1.0 Hz, 1H, H6'), 8.16 – 8.22 (m, 1H, H9), 8.65 (ddd, *J* = 8.3, 2.1, 1.0 Hz, 1H, H4'), 8.85 (s, 1H, H4), 9.11 (t, *J* = 2.2 Hz, 1H, H2'), 13.12 (br s, 1H, NH).

^{13}C NMR (151 MHz, DMSO-d_6) δ 105.8 (s, C3a), 112.2 (d, C9), 118.4 (d, C2'), 119.8 (s, C9a), 121.4 (d, C4'/C6), 121.8 (d, C4'/C6), 124.0 (d, C6'), 130.4 (d, C5'), 130.7 (d, C7), 131.0 (s, C8), 134.4 (s, C5a/C9b/C1'), 140.4 (d, C4), 140.6 (s, C5a/C9b/C1'), 143.0 (s, C5a/C9b/C1'), 148.1 (s, C3'), 162.0 (s, CO).

HR-MS: Calc.[M+H]: 341.0436

Found [M+H]: 341.0433 (Diff.: +0.84 ppm)

Appearance: Yellow solid

Mp: Decomposes > 300 °C

TLC: R_f = 0.25 (2% MeOH in CH_2Cl_2)

E IV.7.7 4-(8-Chloro-3-oxo-3,5-dihydro-2H-pyrazolo[4,3-c]quinolin-2-yl)benzonitrile [49] DCBS139

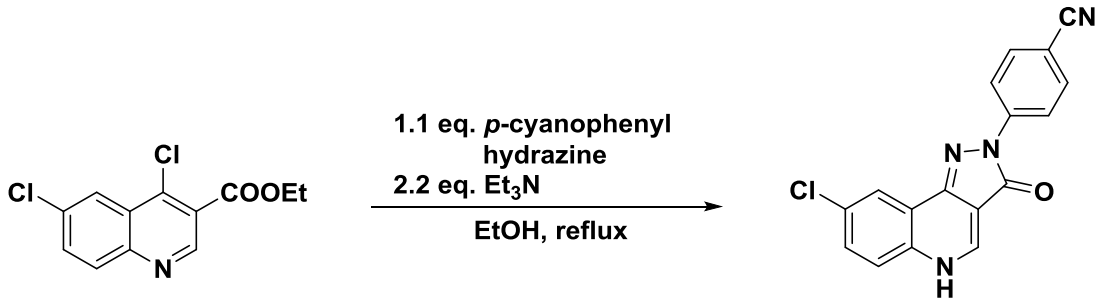

[30]

Chemical Formula: $C_{12}H_9Cl_2NO_2$
Molecular Weight: 270.11

[49] (84%)

Chemical Formula: $C_{17}H_9ClN_4O$
Molecular Weight: 320.74

The desired compound was synthesized according to general procedure E III.4 using:

Chlorinated quinoline	80 mg	0.30 mmol	1 eq.
Arylhydrazine HCl	55 mg	0.33 mmol	1.1 eq.

After filtration 4-(8-chloro-3-oxo-3,5-dihydro-2H-pyrazolo[4,3-c]quinolin-2-yl)benzonitrile **[49]** was obtained (80 mg, 0.25 mmol, 84%).

^{1}H NMR (400 MHz, DMSO-d_6) δ 7.65 – 7.82 (m, 2H, H6 and H7), 7.91 (d, *J* = 8.9 Hz, 2H, H2' and H6'), 8.17 – 8.23 (m, 1H, H9), 8.44 (d, *J* = 8.9 Hz, 2H, H3' and H5'), 8.84 (s, 1H, H4), 13.08 (br s, 1H, NH).

^{13}C NMR (101 MHz, DMSO-d_6) δ 105.6 (s, C3a/C4'), 105.8 (s, C3a/C4'), 118.2 (d, C3' and C5'), 119.1 (s, C9a/CN), 119.8 (s, C9a/CN), 121.3 (d, C6/C7), 121.8 (d, C6/C7), 130.7 (d, C9), 130.9 (s, C8), 133.2 (d, C2' and C6'), 134.5 (s, C1'), 140.3 (d, C4), 143.28 (s, C5a/C9b), 143.33 (s, C5a/C9b), 162.2 (s, CO).

HPLC-MS: Calc.[M+H]: 321.05

Found [M+H]: 321.03

Appearance: Yellow solid

Mp: Decomposes > 300 °C (Lit.[146]: Decomposition > 368 °C)

TLC: R_f = 0.70 (10% MeOH in CH_2Cl_2)

E IV.7.8 3-(8-Chloro-3-oxo-3,5-dihydro-2H-pyrazolo[4,3-c]quinolin-2-yl)benzonitrile [55] DCBS146

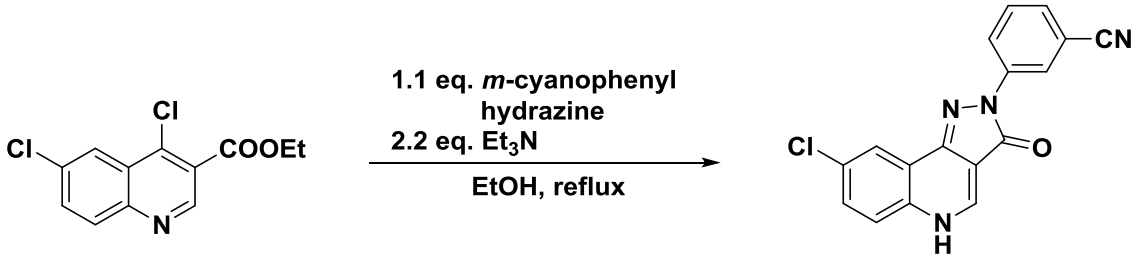

[30]

Chemical Formula: $C_{12}H_9Cl_2NO_2$
Molecular Weight: 270.11

[55] (71%)

Chemical Formula: $C_{17}H_9ClN_4O$
Molecular Weight: 320.74

The desired compound was synthesized according to general procedure E III.4 using:

Chlorinated quinoline	80 mg	0.30 mmol	1 eq.
Arylhydrazine HCl	55 mg	0.33 mmol	1.1 eq.

After filtration 3-(8-chloro-3-oxo-3,5-dihydro-2H-pyrazolo[4,3-c]quinolin-2-yl)benzonitrile **[55]** was obtained (67 mg, 0.21 mmol, 71%).

^{1}H NMR (400 MHz, DMSO-d_6) δ 7.61 – 7.71 (m, 2H, H6 and H7), 7.72 – 7.79 (m, 2H, H6' and H9), 8.22 (t, *J* = 1.4 Hz, 1H, H5'), 8.54 – 8.60 (m, 1H, H4'), 8.63 (t, *J* = 1.8 Hz, 1H, H2'), 8.84 (s, 1H, H4), 13.07 (br s, 1H, NH).

^{13}C NMR (101 MHz, DMSO-d_6) δ 105.8 (s, C3a), 111.7 (s, C3'), 118.8 (s, CN), 119.9 (s, C9a), 120.9 (d, C9), 121.4 (d, C6/C7), 122.0 (d, C6/C7), 122.6 (d, C2'), 124.6 (s, C1'), 127.4 (d, C6'), 130.4 (d, C4'/C5'), 130.6 (d, C4'/C5'), 130.9 (s, C8), 134.6 (s, C5a/C9b), 140.5 (d, C4), 143.0 (s, C5a/C9b), 161.9 (s, CO).

HR-MS: Calc.[M+H]: 321.0538

Found [M+H]: 321.0546 (Diff.: -2.54 ppm)

Appearance: Yellow solid

Mp: Decomposes > 300 °C

TLC: R_f = 0.62 (10% MeOH in CH_2Cl_2)

E IV.7.9 2-(4-Aminophenyl)-8-chloro-1,2-dihydro-3H-pyrazolo[4,3-c]quinolin-3-one [50] DCBSLS17

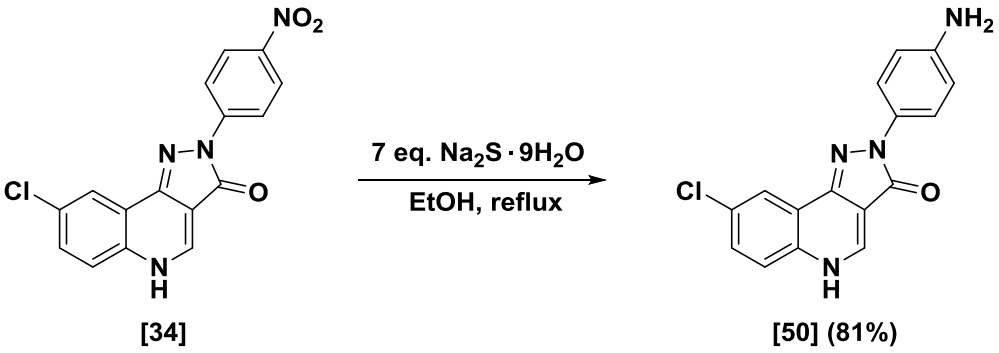

[34]

Chemical Formula: $C_{16}H_9ClN_4O_3$
Molecular Weight: 340.72

[50] (81%)

Chemical Formula: $C_{16}H_{11}ClN_4O$
Molecular Weight: 310.74

The desired compound was synthesized according to general procedure E III.7 using:

Nitro PQ	68 mg	0.20 mmol	1 eq.
$Na_2S{\cdot}9H_2O$	336 mg	1.40 mmol	7 eq.

2-(4-Aminophenyl)-8-chloro-1,2-dihydro-3H-pyrazolo[4,3-c]quinolin-3-one **[50]** was obtained without further purification (50 mg, 0.16 mmol, 81%).

^{1}H NMR (400 MHz, DMSO-d_6) δ 4.93 (bs, 2H, NH_2), 6.60 (d, *J* = 8.8 Hz, 2H, H3' and H5'), 7.51 (dd, *J* = 8.8, 2.5 Hz, 1H, H7), 7.66 (d, *J* = 8.7 Hz, 1H, H6), 7.75 – 7.87 (m, 2H, H2' and H6'), 8.05 (d, *J* = 2.4 Hz, 1H, H9), 8.54 (s, 1H, H4).

^{13}C NMR (151 MHz, DMSO-d_6) δ 106.6 (s, C3a), 113.7 (d, C3' and C5'), 120.1 (s, C9a), 121.0 (d, C2' and C6'), 121.6 (d, C9), 124.2 (s, C8/C1'), 129.6 (s, C8/C1'), 129.8 (d, C6/C7), 130.5 (d, C6/C7), 134.0 (s, C5a/C9b), 139.1 (d, C4), 140.9 (s, C5a/C9b), 145.8 (s, C4'), 160.5 (s, CO).

HPLC-MS: Calc.[M+H]: 311.07

Found [M+H]: 311.96

Appearance: Yellow solid

Mp: Decomposes > 300 °C (Lit.[146]: > 350 °C)

TLC: R_f = 0.41 (10% MeOH in CH_2Cl_2)

E IV.7.10 2-(3-Aminophenyl)-8-chloro-2,5-dihydro-3H-pyrazolo[4,3-c]quinolin-3-one [56] DCBS120

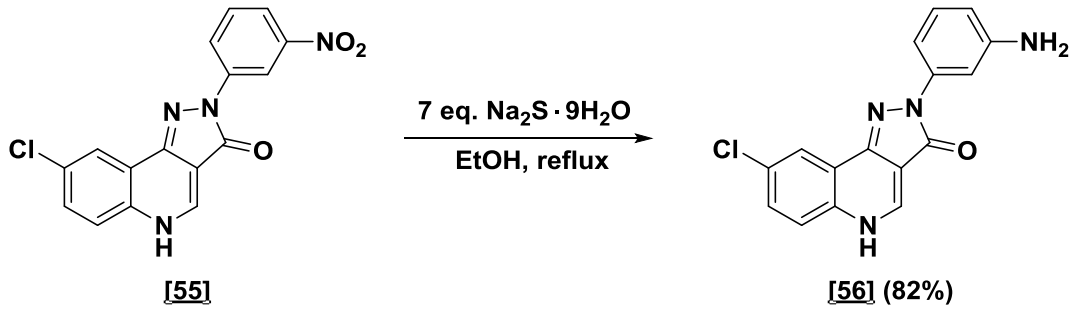

[55] **[56] (82%)**

Chemical Formula: $C_{16}H_9ClN_4O_3$
Molecular Weight: 340.72

Chemical Formula: $C_{16}H_{11}ClN_4O$
Molecular Weight: 310.74

The desired compound was synthesized according to general procedure E III.7 using:

Nitro PQ	100 mg	0.29 mmol	1 eq.
$Na_2S·9H_2O$	488 mg	2.03 mmol	7 eq.

2-(3-Aminophenyl)-8-chloro-1,2-dihydro-3H-pyrazolo[4,3-c]quinolin-3-one **[56]** was obtained without further purification (75 mg, 0.24 mmol, 82%).

^{1}H NMR (600 MHz, DMSO-d_6) δ 5.22 (br s, 2H, NH_2), 6.39 (dd, *J* = 7.9, 2.1 Hz, 1H, H6'), 7.05 (t, *J* = 8.0 Hz, 1H, H5'), 7.39 (dd, *J* = 8.0, 1.9 Hz, 1H, H4'), 7.44 – 7.47 (m, 1H, H2'), 7.68 – 7.74 (m, 2H, H6 and H7), 8.11 (d, *J* = 2.0 Hz, 1H, H9), 8.73 (s, 1H, H4), 12.86 (br s, 1H, NH).

^{13}C NMR (151 MHz, DMSO-d_6) δ 104.6 (d, C9), 106.6 (s, C3), 106.9 (d, C2'), 110.3 (d, C4'), 120.1 (s, C9a), 121.0 (d, C6), 121.7 (d, C6'), 128.9 (d, C5'), 130.1 (d, C7), 130.5 (s, C8), 134.2 (s, C5a/C9b/C1'), 139.4 (d, C4), 140.7 (s, C5a/C9b/C1'), 141.5 (s, C5a/C9b/C1'), 149.0 (s, C3'), 161.3 (s; CO).

HR-MS: Calc.[M+H]: 311.0700

Found [M+H]: 311.0702 (Diff.: -0.62 ppm)

Appearance: Yellow solid

Mp: Decomposes > 300 °C

TLC: R_f = 0.52 (10% MeOH in CH_2Cl_2)

E IV.7.11 4-(8-Chloro-3-oxo-3,5-dihydro-2H-pyrazolo[4,3-c]quinolin-2-yl)benzoic acid [51] DCBS128

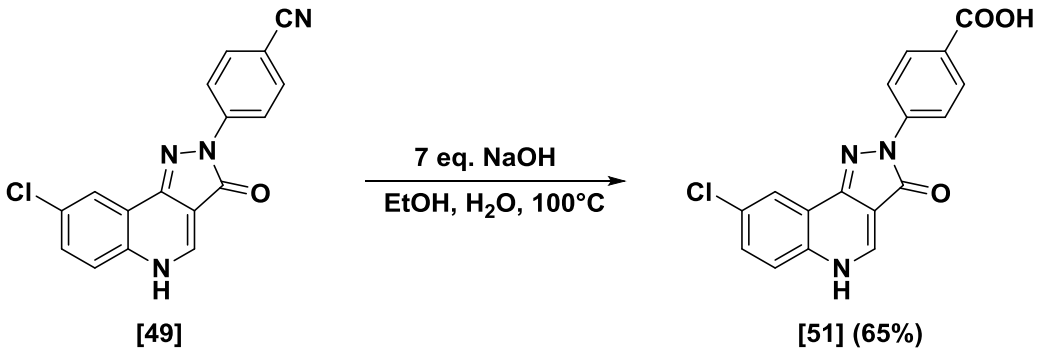

[49] **[51] (65%)**

Chemical Formula: $C_{17}H_9ClN_4O$
Molecular Weight: 320.74

Chemical Formula: $C_{17}H_{10}ClN_3O_3$
Molecular Weight: 339.74

The desired compound was synthesized according to general procedure E III.5 using:

PQ benzonitrile	40 mg	0.13 mmol	1 eq.
NaOH	35 mg	0.89 mmol	7 eq.

After lyophilisation 4-(8-chloro-3-oxo-3,5-dihydro-2H-pyrazolo[4,3-c]quinolin-2-yl)benzoic acid **[51]** was obtained (28 mg, 0.082 mmol, 65%).

^{1}H NMR (400 MHz, DMSO-d_6) δ 7.71 – 7.78 (m, 2H, H6 and H7), 8.03 (d, *J* = 8.8 Hz, 2H, H2' and H6'), 8.18 – 8.21 (m, 1H, H9), 8.38 (d, *J* = 8.9 Hz, 2H, H3' and H5'), 8.83 (d, *J* = 6.3 Hz, 1H, H4), 12.82 (br s, 1H, COOH), 13.07 (br d, *J* = 6.4 Hz, 1H, NH).

^{13}C NMR (101 MHz, DMSO-d_6) δ 106.0 (s, C3a), 117.6 (d, C3' and C5'), 119.9 (s, C9a), 121.3 (d, C6/C7), 121.8 (d, C6/C7), 125.8 (s, C4'), 130.4 (d, C2' and C6'), 130.6 (d, C9), 130.9 (s), 134.4 (s), 140.1 (d, C4), 142.9 (s), 143.4 (s), 162.1 (s, CO), 167.0 (s, COOH).

HPLC-MS: Calc.[M+H]: 340.05

Found [M+H]: 340.06

Appearance: Yellow solid

Mp: Decomposes > 300 °C (Lit.[220]: not reported)

TLC: R_f = 0.59 (20% MeOH in CH_2Cl_2)

E IV.7.12 3-(8-Chloro-3-oxo-3,5-dihydro-2H-pyrazolo[4,3-c]quinolin-2-yl)benzoic acid [57] DCBS152A

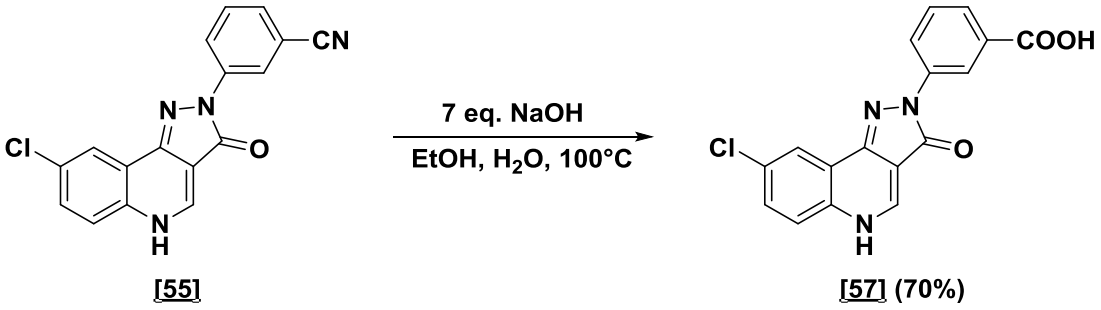

[55] [57] (70%)

Chemical Formula: $C_{17}H_9ClN_4O$
Molecular Weight: 320.74

Chemical Formula: $C_{17}H_{10}ClN_3O_3$
Molecular Weight: 339.74

The desired compound was synthesized according to general procedure E III.5 using:

PQ benzonitrile	20 mg	0.06 mmol	1 eq.
NaOH	18 mg	0.44 mmol	7 eq.

After lyophilisation 3-(8-chloro-3-oxo-3,5-dihydro-2H-pyrazolo[4,3-c]quinolin-2-yl)benzoic acid **[57]** was obtained (15 mg, 0.044 mmol, 70%).

^{1}H NMR (400 MHz, DMSO-d_6) δ 7.56 (t, *J* = 8.0 Hz, 1H, H5'), 7.67 – 7.80 (m, 3H, H6 and H7 and H6'), 8.19 (d, *J* = 2.3 Hz, 1H, H9), 8.49 (d, *J* = 8.4 Hz, 1H, H4'), 8.78 (s, 1H, H4), 8.83 (s, 1H, H2'), 13.02 (br s, 1H, NH/COOH).

^{13}C NMR (151 MHz, DMSO-d_6) δ 106.1 (s, C3a), 119.3 (d, C2'), 120.0, 121.3 (d, C9), 122.0 (d, C6'), 122.6 (d, C4'), 124.9 (d, C6/C7), 129.1 (d, C5'), 130.4 (d, C6/C7), 130.8 (s, C1'/C3'/C8), 131.5 (s, C1'/C3'/C8), 134.7 (s, C1'/C3'/C8), 140.1 (s, C5a/C9b), 140.2 (d, C4), 142.5 (s, C5a/C9b), 161.7 (s, CO), 167.4 (s, CO).

HPLC-MS: Calc.[M+H]: 340.05
Found [M+H]: 340.02

HR-MS: Calc.[M+H]: 340.0483
Found [M+H]: 340.0474
(Diff.: +2.71 ppm)

Appearance: Yellow solid

Mp: Decomposes > 300 °C

TLC: R_f = 0.58 (20% MeOH in CH_2Cl_2)

E IV.7.13 4-(8-Chloro-3-oxo-3,5-dihydro-2H-pyrazolo[4,3-c]quinolin-2-yl)benzamide [52] DCBSLK36

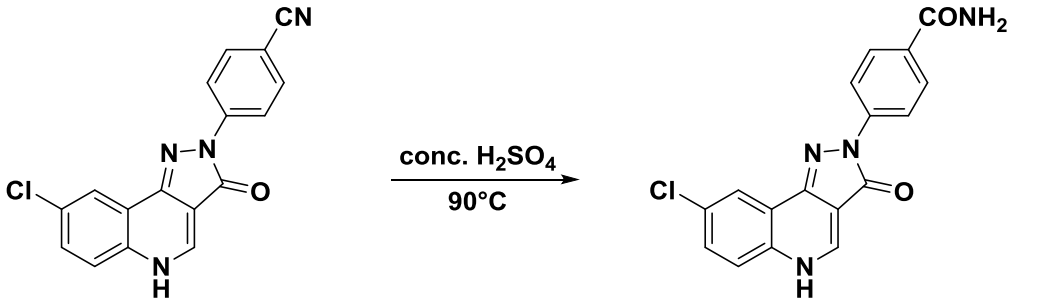

[49]

Chemical Formula: $C_{17}H_9ClN_4O$
Molecular Weight: 320.74

[52] (quant.)

Chemical Formula: $C_{17}H_{11}ClN_4O_2$
Molecular Weight: 338.75

The desired compound was synthesized according to general procedure E III.6 using:

PQ benzonitrile	150 mg	0.47 mmol	1 eq.
Conc. H_2SO_4	0.4 mL	0.8 mL/mmol	

After lyophilisation 4-(8-chloro-3-oxo-3,5-dihydro-2*H*-pyrazolo[4,3-*c*]quinolin-2-yl)benzamide **[52]** was obtained (162 mg, 0.47 mmol, quant.).

^{1}H NMR (600 MHz, DMSO-d_6) δ 7.30 (s, 1H, NH_2), 7.68 (dd, *J* = 8.8, 2.4 Hz, 1H, H7), 7.73 (d, *J* = 8.8 Hz, 1H, H6), 7.91 – 7.99 (m, 3H, H3' and H5' and NH_2), 8.17 (d, *J* = 2.4 Hz, 1H, H9), 8.29 – 8.38 (m, 2H, H2' and H6'), 8.74 (s, 1H, H4).

^{13}C NMR (151 MHz, DMSO-d_6) δ 105.8 (s, C3a), 117.5 (d, C2' and C6'), 120.4, (s, C9a) 121.1 (d, C9), 123.5 (d, C6), 128.3 (d, C3' and C5'), 129.1 (s, C4'), 129.9 (d, C7), 130.2 (s), 136.6 (s), 141.6 (d, C4), 142.5 (s), 143.2 (s), 161.9 (s, CO), 167.5 (s, $CONH_2$).

HR-MS: Calc.[M+H]: 339.0643

Found [M+H]: 339.0649 (Diff.: -1.75 ppm)

Appearance: Yellow solid

Mp: Decomposes > 300 °C

TLC: R_f = 0.23 (10% MeOH in CH_2Cl_2)

E IV.7.14 3-(8-Chloro-3-oxo-3,5-dihydro-2H-pyrazolo[4,3-c]quinolin-2-yl)benzamide [58] DCBS152B

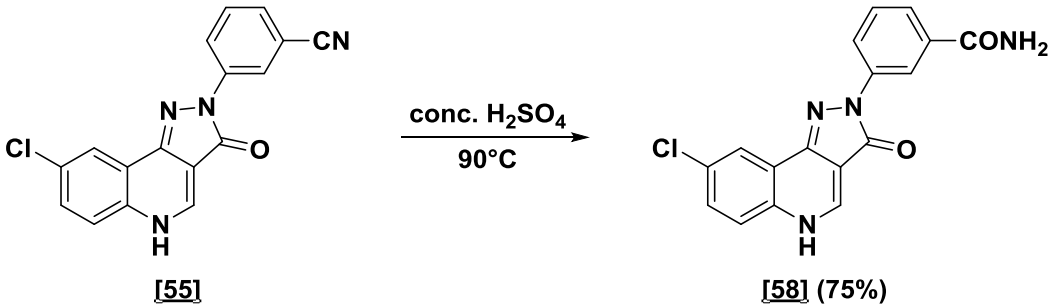

[55] [58] (75%)

Chemical Formula: $C_{17}H_9ClN_4O$
Molecular Weight: 320.74

Chemical Formula: $C_{17}H_{11}ClN_4O_2$
Molecular Weight: 338.75

The desired compound was synthesized according to general procedure E III.6 using:

PQ benzonitrile	20 mg	0.06 mmol	1 eq.
Conc. H_2SO_4	0.1 mL	0.8 mL/mmol	

After lyophilisation 3-(8-chloro-3-oxo-3,5-dihydro-2*H*-pyrazolo[4,3-*c*]quinolin-2-yl)benzamide **[58]** was obtained (16 mg, 0.047 mmol, 75%).

^{1}H NMR (400 MHz, DMSO-d_6) δ 7.43 (br s, 1H, NH_2), 7.51 (t, *J* = 7.9 Hz, 1H, H5'), 7.64 – 7.68 (m, 1H, H6'), 7.69 – 7.77 (m, 2H, H6 and H7), 8.04 (br s, 1H, NH_2), 8.19 (d, *J* = 2.2 Hz, 1H, H9), 8.41 (dd, *J* = 8.1, 2.1 Hz, 1H, H4'), 8.64 (t, *J* = 1.9 Hz, 1H, H2'), 8.78 (s, 1H, H4).

^{13}C NMR (151 MHz, DMSO-d_6) δ 106.0 (s, C3a), 118.2 (d, C2'), 120.3 (s, C9a), 121.1 (d, C6/C7), 121.2 (d, C3'), 122.6 (d, C6/C7), 122.8 (d, C6'), 128.5 (d, C5'), 130.1 (s, C3'/C8), 130.4 (d, C9), 135.1 (s, C1'/C3'/C8), 135.5 (s, C1'/C3'), 140.1 (d, C4), 140.7 (s, C5a/C9b), 142.5 (s, C5a/C9b), 161.6 (s, CO), 167.9 (s, $CONH_2$).

HPLC-MS: Calc.[M+H]: 339.06
Found [M+H]: 339.05

HR-MS: Calc.[M+H]: 339.0643
Found [M+H]: 339.0634
(Diff.: +2.81 ppm)

Appearance: Yellow solid

Mp: Decomposes > 300 °C

TLC: R_f = 0.68 (20% MeOH in CH_2Cl_2)

E IV.8 Pyrazoloquinolinones – R^8 bromo series

E IV.8.1 8-Bromo-2-(p-tolyl)-2,5-dihydro-3H-pyrazolo[4,3-c]quinolin-3-one [60] DCBS148

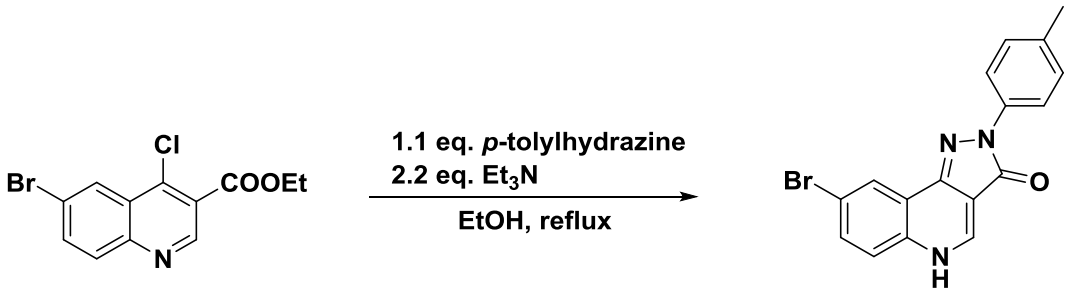

[31]

Chemical Formula: $C_{12}H_9BrClNO_2$
Molecular Weight: 314.56

[60] (64%)

Chemical Formula: $C_{17}H_{12}BrN_3O$
Molecular Weight: 354.21

The desired compound was synthesized according to general procedure E III.4 using:

Chlorinated quinoline	50 mg	0.16 mmol	1 eq.
Arylhydrazine HCl	28 mg	0.17 mmol	1.1 eq.

After filtration 8-bromo-2-(p-tolyl)-2,5-dihydro-3H-pyrazolo[4,3-c]quinolin-3-one **[60]** was obtained (36 mg, 0.10 mmol, 64%).

^{1}H NMR (400 MHz, DMSO-d_6) δ 2.33 (s, 3H, CH_3), 7.26 (d, *J* = 8.3 Hz, 2H, H2' and H6'), 7.68 (d, *J* = 8.8 Hz, 1H, H6), 7.84 (dd, *J* = 8.8, 2.3 Hz, 1H, H7), 8.09 (d, *J* = 8.3 Hz, 2H, H3' and H5'), 8.31 (d, *J* = 2.3 Hz, 1H, H9), 8.77 (d, *J* = 6.1 Hz, 1H, H4), 12.95 (br d, *J* = 6.3 Hz, 1H, NH).

^{13}C NMR (101 MHz, DMSO-d_6) δ 20.6 (q, CH_3), 106.6 (s, C3a), 118.7 (d, C6), 118.8 (s, C3' and C5'), 120.4 (s, C8), 121.8 (d, C9), 124.2 (s, C9a), 129.1 (d, C2' and C6'), 132.9 (d, C7), 133.2 (s, C5a/C9b/C1'), 134.5 (s, C5a/C9b/C1'), 137.6 (s, C4'), 139.6 (d, C4), 141.6 (s, C5a/C9b/C1'), 161.2 (s, CO).

HR-MS: Calc.[M+H]: 354.0237

Found [M+H]: 354.0249 (Diff.: -3.65 ppm)

Appearance: Yellow solid

Mp: Decomposes > 300 °C

TLC: R_f = 0.33 (5% MeOH in CH_2Cl_2)

E IV.8.2 8-Bromo-2-(*m*-tolyl)-2,5-dihydro-3H-pyrazolo[4,3-c]quinolin-3-one [67] DCBS155

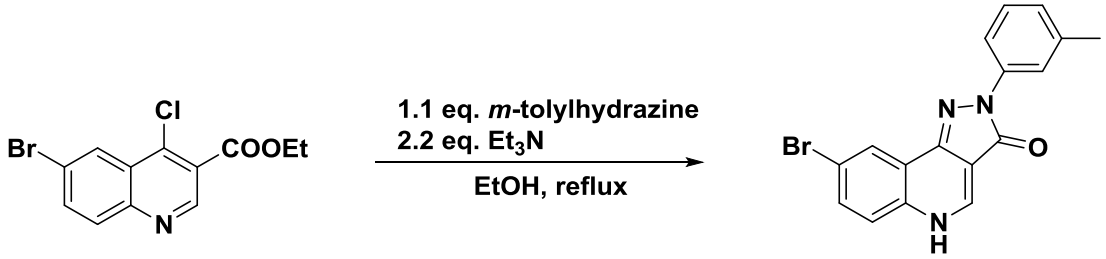

[31]

Chemical Formula: $C_{12}H_9BrClNO_2$
Molecular Weight: 314.56

[67] (52%)

Chemical Formula: $C_{17}H_{12}BrN_3O$
Molecular Weight: 354.21

The desired compound was synthesized according to general procedure E III.4 using:

Chlorinated quinoline	50 mg	0.16 mmol	1 eq.
Arylhydrazine HCl	28 mg	0.17 mmol	1.1 eq.

After filtration 8-bromo-2-(*m*-tolyl)-2,5-dihydro-3H-pyrazolo[4,3-c]quinolin-3-one **[60]** was obtained (29 mg, 0.082 mmol, 52%).

^{1}H NMR (400 MHz, DMSO-d_6) δ 2.37 (s, 3H, CH_3), 7.00 (d, *J* = 7.5 Hz, 1H, H6'), 7.32 (t, *J* = 7.8 Hz, 1H, H5'), 7.66 (d, *J* = 8.8 Hz, 1H, H6), 7.83 (dd, *J* = 8.8, 2.4 Hz, 1H, H7), 7.99 – 8.09 (m, 2H, H2' and H4'), 8.31 (d, *J* = 2.3 Hz, 1H, H9), 8.77 (s, 1H, H4), 12.90 (br s, 1H, NH).

^{13}C NMR (151 MHz, DMSO) δ 21.4 (q, CH_3), 106.5 (s, C3a), 115.9 (d, C2'/C4'), 118.7 (s, C8), 119.2 (d, C2'/C4'), 120.5 (s, C9a), 122.2 (d, C6), 124.2 (d, C9), 124.8 (d, C6'), 128.5 (d, C5'), 132.8 (d, C7), 135.1 (s, C5a/C9b/C1'), 137.9 (s, C3'), 140.0 (d, C4), 140.1 (s, C5a/C9b/C1'), 141.9 (s, C5a/C9b/C1'), 161.5 (s, CO).

HR-MS: Calc.[M+H]: 354.0237

Found [M+H]: 354.0248 (Diff.: -3.25 ppm)

Appearance: Yellow solid

Mp: Decomposes > 300 °C

TLC: R_f = 0.25 (5% MeOH in CH_2Cl_2)

E IV.8.3 8-Bromo-2-(4-methoxyphenyl)-2,5-dihydro-3H-pyrazolo[4,3-c]quinolin-3-one [61] DCBS149

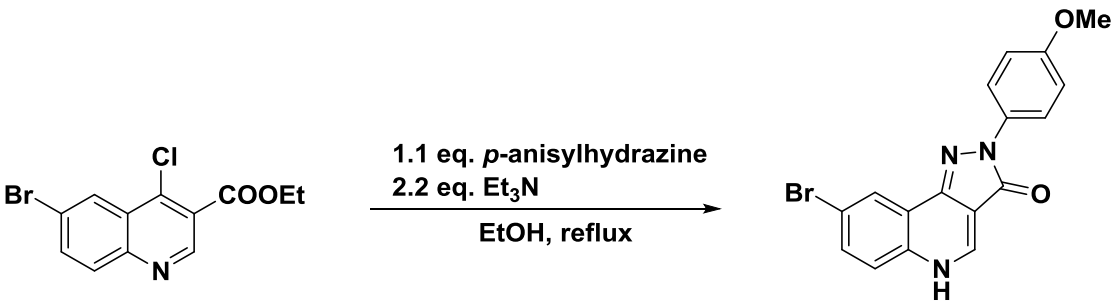

[31]

Chemical Formula: $C_{12}H_9BrClNO_2$
Molecular Weight: 314.56

[61] (63%)

Chemical Formula: $C_{17}H_{12}BrN_3O_2$
Molecular Weight: 370.21

The desired compound was synthesized according to general procedure E III.4 using:

Chlorinated quinoline	50 mg	0.16 mmol	1 eq.
Arylhydrazine HCl	31 mg	0.17 mmol	1.1 eq.

After filtration 8-bromo-2-(4-methoxyphenyl)-2,5-dihydro-3H-pyrazolo[4,3-c]quinolin-3-one **[61]** was obtained (37 mg, 0.10 mmol, 63%).

^{1}H NMR (400 MHz, DMSO-d_6) δ 3.79 (s, 3H, OCH_3), 7.03 (d, *J* = 9.2 Hz, 2H, H2' and H6'), 7.67 (d, *J* = 8.9 Hz, 1H, H6), 7.83 (dd, *J* = 8.8, 2.3 Hz, 1H, H7), 8.09 (d, *J* = 9.1 Hz, 2H, H3' and H5'), 8.30 (d, *J* = 2.3 Hz, 1H, H9), 8.77 (s, 1H, H4), 12.90 (br s, 1H, NH).

^{13}C NMR (101 MHz, DMSO-d_6) δ 55.3 (q, OCH_3), 106.6 (s, C3a), 113.8 (d, C3' and C5'), 118.8 (s, C8), 120.39 (s, C9a), 120.41 (d, C2' and C6'), 121.8 (d, C6), 124.1 (d, C9), 132.8 (d, C7), 133.4 (s, C4a/C9b/C1'), 134.5 (s, C4a/C9b/C1'), 139.5 (d, C4), 141.4 (s, C4a/C9b/C1'), 156.0 (s, C4'), 160.9 (s, CO).

Appearance: Orange solid

Mp: Decomposes > 300 °C (Lit.[221]: 305 °C)

TLC: R_f = 0.41 (5% MeOH in CH_2Cl_2)

E IV.8.4 8-Bromo-2-(3-methoxyphenyl)-2,5-dihydro-3H-pyrazolo[4,3-c]quinolin-3-one [68] DCBS156

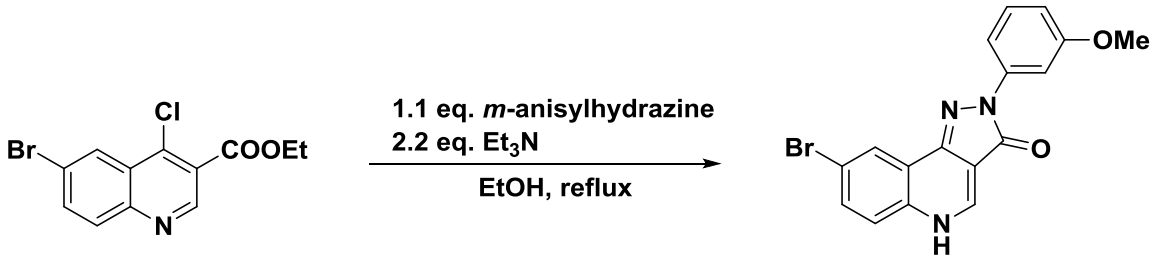

[31]

Chemical Formula: $C_{12}H_9BrClNO_2$
Molecular Weight: 314.56

[68] (63%)

Chemical Formula: $C_{17}H_{12}BrN_3O_2$
Molecular Weight: 370.21

The desired compound was synthesized according to general procedure E III.4 using:

Chlorinated quinoline	50 mg	0.16 mmol	1 eq.
Arylhydrazine HCl	31 mg	0.17 mmol	1.1 eq.

After filtration 8-bromo-2-(3-methoxyphenyl)-2,5-dihydro-3H-pyrazolo[4,3-c]quinolin-3-one **[68]** was obtained (37 mg, 0.10 mmol, 63%).

^{1}H NMR (400 MHz, DMSO-d_6) δ 3.81 (s, 3H, OCH_3), 6.72 – 6.80 (m, 1H, H6'), 7.35 (t, *J* = 8.1 Hz, 1H, H5'), 7.66 (d, *J* = 8.8 Hz, 1H, H6), 7.71 – 7.93 (m, 3H, H2', H4' and H7), 8.32 (d, *J* = 2.2 Hz, 1H, H9), 8.77 (s, 1H, H4), 12.92 (br s, 1H, NH).

^{13}C NMR (151 MHz, DMSO-d_6) δ 55.2 (q, OCH_3), 104.4 (d, C2'), 106.4 (s, C3a), 109.5 (d, C6'), 111.0 (d, C4'), 118.7 (s, C8), 120.5 (s, C9a), 122.3 (d, C6), 124.2 (d, C9), 129.6 (d, C5'), 132.9 (d, C7), 135.2 (s, C5a/C9b/C1'), 140.2 (d, C4), 141.2 (s, C5a/C9b/C1'), 141.9 (s, C5a/C9b/C1'), 159.5 (s, C3'), 161.6 (s, CO).

HR-MS: Calc.[M+H]: 370.0186

Found [M+H]: 370.0204 (Diff.: -4.88 ppm)

Appearance: Yellow solid

Mp: Decomposes > 300 °C

TLC: R_f = 0.25 (5% MeOH in CH_2Cl_2)

E IV.8.5 8-Bromo-2-(4-nitrophenyl)-2,5-dihydro-3H-pyrazolo[4,3-c]quinolin-3-one [62] DCBS147

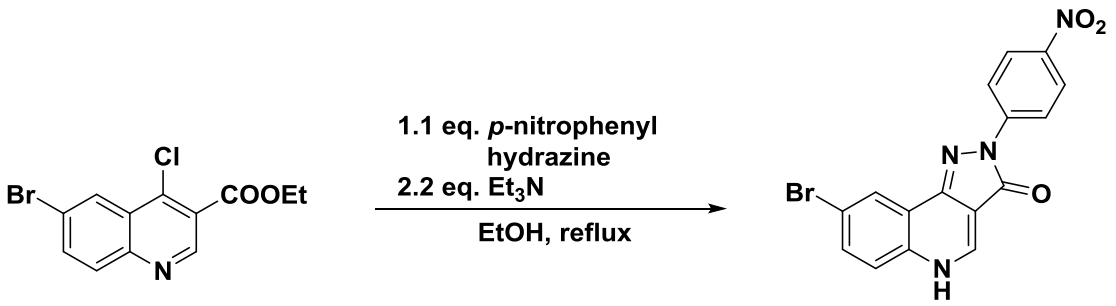

[31]

Chemical Formula: $C_{12}H_9BrClNO_2$
Molecular Weight: 314.56

[62] (55%)

Chemical Formula: $C_{16}H_9BrN_4O_3$
Molecular Weight: 385.18

The desired compound was synthesized according to general procedure E III.4 using:

Chlorinated quinoline	100 mg	0.32 mmol	1 eq.
Arylhydrazine HCl	66 mg	0.35 mmol	1.1 eq.

After filtration 8-bromo-2-(4-nitrophenyl)-2,5-dihydro-3H-pyrazolo[4,3-c]quinolin-3-one **[62]** was obtained (67 mg, 0.17 mmol, 55%).

^{1}H NMR (400 MHz, DMSO-d_6) δ 7.67 (d, *J* = 8.8 Hz, 1H, H6), 7.87 (dd, *J* = 8.8, 2.3 Hz, 1H, H7), 8.30 – 8.37 (m, 3H, H2' and H6' and H9), 8.51 (d, *J* = 9.3 Hz, 2H, H3' and H5'), 8.87 (s, 1H, H4), 13.10 (br s, 1H, NH).

^{13}C NMR (151 MHz, DMSO-d_6) δ 105.0 (s, C3a), 117.7 (d, C3' and C5'), 118.2 (s, C8), 120.9 (d, C6), 122.8 (s, C9a), 124.2 (d, C9), 124.9 (d, C2' and C6'), 132.6 (d, C7), 138.7 (s, C5a/C9b/C1'), 142.2 (d, C4), 143.3 (s, C5a/C9b/C1'), 144.8 (s, C5a/C9b/C1'), 145.6 (s, C4'), 162.6 (s, CO).

HR-MS: Calc.[M+H]: 384.9931

Found [M+H]: 384.9943 (Diff.: -3.16 ppm)

Appearance: Yellow solid

Mp: Decomposes > 300 °C

TLC: R_f = 0.42 (5% MeOH in CH_2Cl_2)

E IV.8.6 8-Bromo-2-(3-nitrophenyl)-2,5-dihydro-3H-pyrazolo[4,3-c]quinolin-3-one [69] DCBS154

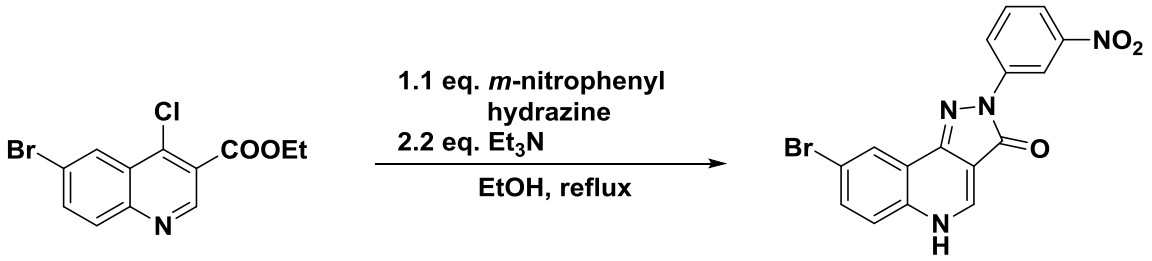

[31] **[69] (62%)**

Chemical Formula: $C_{12}H_9BrClNO_2$
Molecular Weight: 314.56

Chemical Formula: $C_{16}H_9BrN_4O_3$
Molecular Weight: 385.18

The desired compound was synthesized according to general procedure E III.4 using:

Chlorinated quinoline	100 mg	0.32 mmol	1 eq.
Arylhydrazine HCl	66 mg	0.35 mmol	1.1 eq.

After filtration 8-bromo-2-(3-nitrophenyl)-2,5-dihydro-3H-pyrazolo[4,3-c]quinolin-3-one **[69]** was obtained (76 mg, 0.20 mmol, 62%).

^{1}H NMR (400 MHz, DMSO-d_6) δ 7.68 (d, *J* = 8.8 Hz, 1H, H6), 7.75 (t, *J* = 8.2 Hz, 1H, H5'), 7.87 (dd, *J* = 8.8, 2.3 Hz, 1H, H7), 8.03 (dd, *J* = 8.1, 2.3 Hz, 1H, H6'), 8.35 (d, *J* = 2.3 Hz, 1H, H9), 8.66 (dd, *J* = 8.2, 2.0 Hz, 1H, H4'), 8.86 (s, 1H, H4), 9.12 (t, *J* = 2.2 Hz, 1H, H2'), 13.08 (br s, 1H, NH).

^{13}C NMR (151 MHz, DMSO-d_6) δ 105.8 (s, C3a), 112.1 (d, C2'), 118.2 (s, C8), 118.9 (s, C4'), 120.3 (s, C9), 122.7 (d, C6), 124.0 (d, C6'), 124.3 (d, C9), 130.3 (d, C5'), 133.1 (d, C7), 135.7 (s, C5a/C9b/C1'), 140.8 (d, C4), 141.0 (s, C5a/C9b/C1'), 143.1 (s, C5a/C9b/C1'), 148.1 (s, C3'), 162.0 (s, CO).

HR-MS: Calc.[M+H]: 384.9931

Found [M+H]: 384.9931 (Diff.: -0.07 ppm)

Appearance: Yellow solid

Mp: Decomposes > 300 °C

TLC: R_f = 0.31 (5% MeOH in CH_2Cl_2)

E IV.8.7 4-(8-Bromo-3-oxo-3,5-dihydro-2H-pyrazolo[4,3-c]quinolin-2-yl)benzonitrile [63] DCBS150

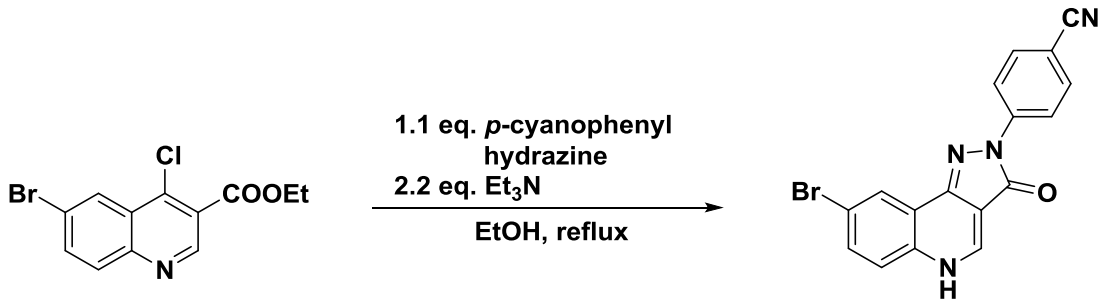

[31]

Chemical Formula: $C_{12}H_9BrClNO_2$
Molecular Weight: 314.56

[63] (77%)

Chemical Formula: $C_{17}H_9BrN_4O$
Molecular Weight: 365.19

The desired compound was synthesized according to general procedure E III.4 using:

Chlorinated quinoline	100 mg	0.32 mmol	1 eq.
Arylhydrazine HCl	59 mg	0.35 mmol	1.1 eq.

After filtration 4-(8-bromo-3-oxo-3,5-dihydro-2H-pyrazolo[4,3-c]quinolin-2-yl)benzonitrile **[63]** was obtained (90 mg, 0.25 mmol, 77%).

^{1}H NMR (400 MHz, DMSO-d_6) δ 7.67 (d, *J* = 8.8 Hz, 1H, H6), 7.80 – 7.97 (m, 3H, H7 and H2' and H6'), 8.27 – 8.36 (m, 1H, H9), 8.44 (d, *J* = 8.5 Hz, 2H, H3' and H5'), 8.84 (s, 1H, H4), 13.06 (br s, 1H, NH).

^{13}C NMR (151 MHz, DMSO-d_6) δ 105.3 (s, C3a/C4'), 105.6 (s, C3a/C4'), 118.1 (d, C3' and C5'), 118.7 (s, C8/CN), 119.2 (s, C8/CN), 120.5 (s, C9a), 123.4 (d, C6), 124.3 (d, C9), 133.0 (d, C7), 133.2 (d, C2' and C6'), 136.6 (s, C5a/C9b/C1'), 141.7 (d, C4), 143.6 (s, C5a/C9b/C1'), 143.7 (s, C5a/C9b/C1'), 162.3 (s, CO).

HR-MS: Calc.[M+H]: 365.0033

Found [M+H]: 365.0043 (Diff.: -2.83 ppm)

Appearance: Yellow solid

Mp: Decomposes > 300 °C

TLC: R_f = 0.43 (5% MeOH in CH_2Cl_2)

E IV.8.8 3-(8-Bromo-3-oxo-3,5-dihydro-2H-pyrazolo[4,3-c]quinolin-2-yl)benzonitrile [70] DCBS157

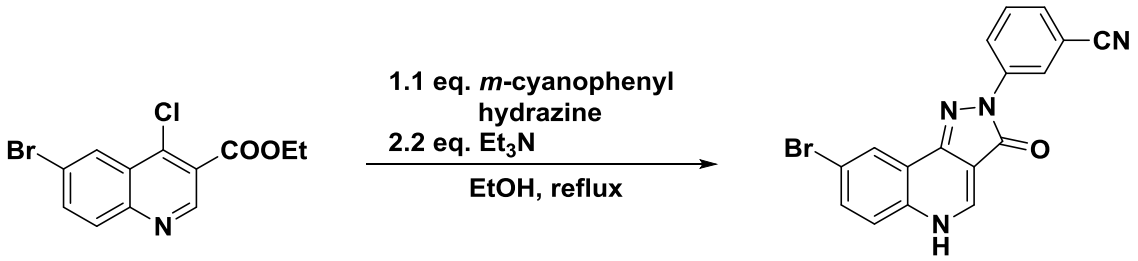

[31]

Chemical Formula: $C_{12}H_9BrClNO_2$
Molecular Weight: 314.56

[70] (86%)

Chemical Formula: $C_{17}H_9BrN_4O$
Molecular Weight: 365.19

The desired compound was synthesized according to general procedure E III.4 using:

Chlorinated quinoline	100 mg	0.32 mmol	1 eq.
Arylhydrazine HCl	59 mg	0.35 mmol	1.1 eq.

After filtration 3-(8-bromo-3-oxo-3,5-dihydro-2H-pyrazolo[4,3-c]quinolin-2-yl)benzonitrile **[70]** was obtained (100 mg, 0.27 mmol, 86%).

^{1}H NMR (400 MHz, DMSO-d_6) δ 7.59 – 7.71 (m, 3H, H5' and H6' and H6), 7.86 (dd, *J* = 8.8, 2.3 Hz, 1H, H7), 8.35 (d, *J* = 2.3 Hz, 1H, H9), 8.54 – 8.65 (m, 2H, H2' and H4'), 8.84 (d, *J* = 6.1 Hz, 1H, H4), 13.08 (br d, *J* = 6.4 Hz, 1H, NH).

^{13}C NMR (151 MHz, DMSO-d_6) δ 105.9 (s, C3a), 111.7 (s, C3'), 118.8 (s, CN), 119.0 (s, C8), 120.3 (s, C9a), 120.9 (d, C2'/C4'), 122.5 (d, C2'/C4'), 122.6 (d, C6), 124.4 (d, C9), 127.3 (d, C5'/C6'), 130.4 (d, C5'/C6'), 133.2 (d, C7), 135.4 (s, C5a/C9b/C1'), 140.5 (s, C4), 140.8 (s, C5a/C9b/C1'), 142.9 (s, C5a/C9b/C1'), 161.9 (s, CO).

HR-MS: Calc.[M+H]: 365.0033

Found [M+H]: 365.0030 (Diff.: +0.69 ppm)

Appearance: Yellow solid

Mp: Decomposes > 300 °C

TLC: R_f = 0.27 (5% MeOH in CH_2Cl_2)

E IV.8.9 2-(4-Aminophenyl)-8-bromo-1,2-dihydro-3H-pyrazolo[4,3-c]quinolin-3-one [64] DCBS164

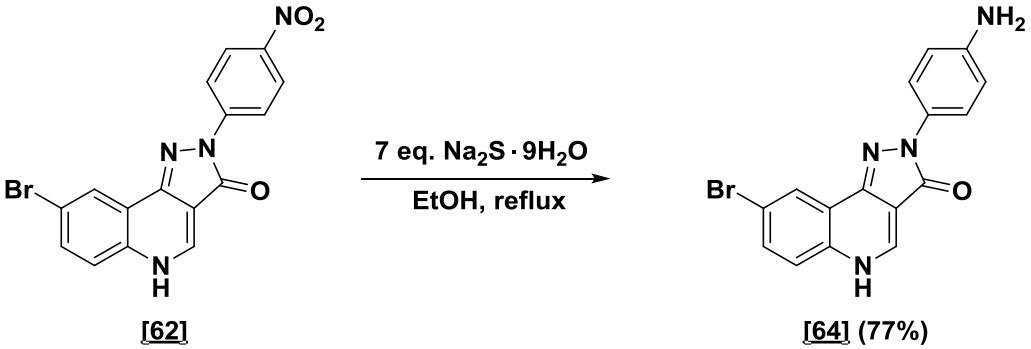

[62] [64] (77%)

Chemical Formula: $C_{16}H_9BrN_4O_3$
Molecular Weight: 385.18

Chemical Formula: $C_{16}H_{11}BrN_4O$
Molecular Weight: 355.20

The desired compound was synthesized according to general procedure E III.7 using:

Nitro PQ	45 mg	0.12 mmol	1 eq.
$Na_2S{\cdot}9H_2O$	201 mg	0.84 mmol	7 eq.

2-(4-Aminophenyl)-8-bromo-1,2-dihydro-3H-pyrazolo[4,3-c]quinolin-3-one **[64]** was obtained without further purification (32 mg, 0.1 mmol, 77%).

^{1}H NMR (600 MHz, DMSO-d_6) δ 5.10 (br s, 2H, NH_2), 6.62 (d, *J* = 8.4 Hz, 2H, H3' and H5'), 7.64 (d, *J* = 8.9 Hz, 1H, H6), 7.75 (d, *J* = 8.3 Hz, 2H, H2' and H6'), 7.78 – 7.82 (m, 1H, H7), 8.21 – 8.33 (m, 1H, H9), 8.71 (s, 1H, H4), 12.80 (br s, 1H, NH).

^{13}C NMR (151 MHz, DMSO-d_6) δ 106.8 (s, C3a), 113.6 (d, C3' and C5'), 118.6 (s, C8), 120.4 (s, C9a), 120.9 (d, C2' and C6'), 121.7 (d, C6), 124.0 (d, C9), 129.5 (s, C1'), 132.5 (d, C7), 134.3 (s, C5a/C9b), 139.1 (d, C4), 140.7 (s, C5a/C9b), 145.8 (s, C4'), 160.5 (s, CO).

HR-MS: Calc.[M+H]: 355.0189

Found [M+H]: 355.0183 (Diff.: +1.55 ppm)

Appearance: Yellow solid

Mp: Decomposes > 300 °C

TLC: R_f = 0.47 (10% MeOH in CH_2Cl_2)

E IV.8.10 2-(3-Aminophenyl)-8-chloro-2,5-dihydro-3H-pyrazolo[4,3-c]quinolin-3-one [71] DCBS163

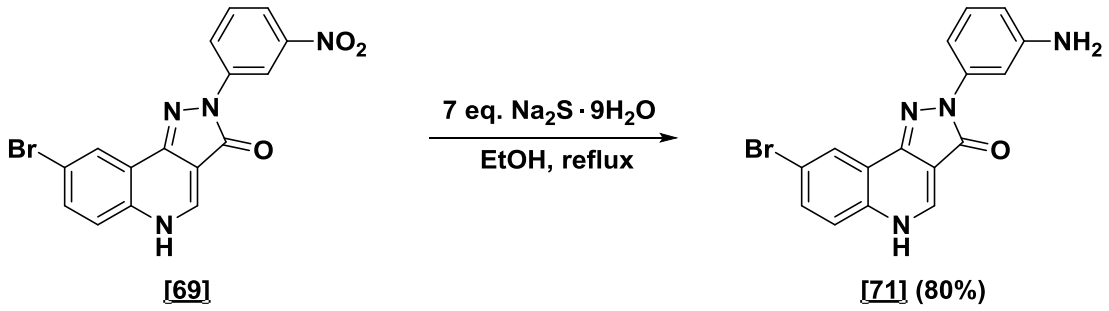

[69] **[71] (80%)**

Chemical Formula: $C_{16}H_9BrN_4O_3$
Molecular Weight: 385.18

Chemical Formula: $C_{16}H_{11}BrN_4O$
Molecular Weight: 355.20

The desired compound was synthesized according to general procedure E III.7 using:

Nitro PQ	50 mg	0.13 mmol	1 eq.
$Na_2S{\cdot}9H_2O$	218 mg	0.91 mmol	7 eq.

2-(3-Aminophenyl)-8-bromo-1,2-dihydro-3H-pyrazolo[4,3-c]quinolin-3-one **[71]** was obtained without further purification (37 mg, 0.104 mmol, 80%).

^{1}H NMR (600 MHz, DMSO-d_6) δ 5.19 (br s, 2H, NH_2), 6.38 (dd, *J* = 7.8, 2.2 Hz, 1H, H6'), 7.05 (t, *J* = 8.0 Hz, 1H, H5'), 7.40 (dd, *J* = 8.0, 1.9 Hz, 1H, H4'), 7.43 – 7.47 (m, 1H, H2'), 7.65 (d, *J* = 8.8 Hz, 1H, H6), 7.82 (dd, *J* = 8.8, 2.4 Hz, 1H, H7), 8.26 (d, *J* = 2.4 Hz, 1H, H9), 8.73 (s, 1H, H4), 12.85 (br s, 1H, NH).

^{13}C NMR (151 MHz, DMSO-d_6**)** δ 104.6 (d, C2'/C4'/C6'), 106.8 (s, C3a), 106.8 (d, C2'/C4'/C6'), 110.3 (d, C2'/C4'/C6'), 118.7 (s, C8), 120.4 (s, C9a), 121.8 (d, C6), 124.1 (d, C9), 128.9 (d, C5'), 132.8 (d, C7), 134.6 (s, C5a/C9b/C1'), 139.5 (d, C4), 140.7 (s, C5a/C9b/C1'), 141.3 (s, C5a/C9b/C1'), 149.0 (s, C3'), 161.3 (s, CO).

HR-MS: Calc.[M+H]: 355.0189

Found [M+H]: 355.0195 (Diff.: -1.59 ppm)

Appearance: Yellow solid

Mp: Decomposes > 300 °C

TLC: R_f = 0.52 (10% MeOH in CH_2Cl_2)

E IV.8.11 4-(8-Bromo-3-oxo-3,5-dihydro-2H-pyrazolo[4,3-c]quinolin-2-yl)benzoic acid [65] DCBS153A

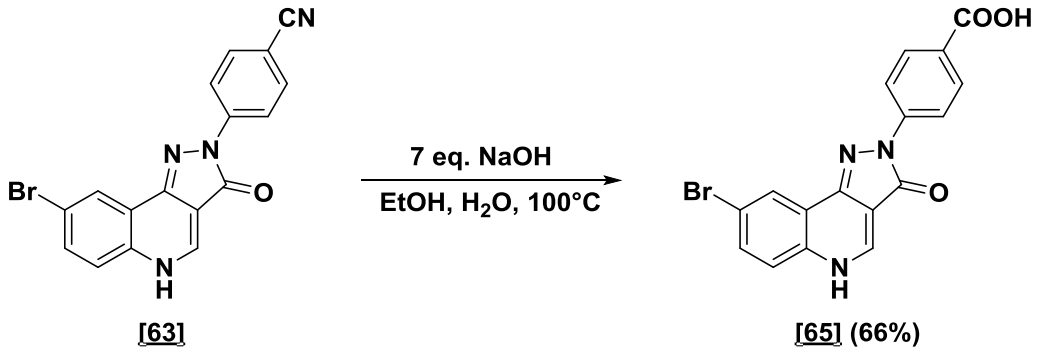

[63] **[65] (66%)**

Chemical Formula: $C_{17}H_9BrN_4O$
Molecular Weight: 365.19

Chemical Formula: $C_{17}H_{10}BrN_3O_3$
Molecular Weight: 384.19

The desired compound was synthesized according to general procedure E III.5 using:

PQ benzonitrile	40 mg	0.13 mmol	1 eq.
NaOH	35 mg	0.89 mmol	7 eq.

After lyophilisation 4-(8-bromo-3-oxo-3,5-dihydro-2H-pyrazolo[4,3-c]quinolin-2-yl)benzoic acid **[65]** was obtained (28 mg, 0.084 mmol, 66%).

^{1}H NMR (400 MHz, DMSO-d_6) δ 7.67 (d, *J* = 8.8 Hz, 1H, H6), 7.82 (dd, *J* = 8.8, 2.3 Hz, 1H, H7), 8.01 (d, *J* = 8.8 Hz, 2H, H2' and H6'), 8.29 – 8.35 (d, *J* = 8.7 Hz, 2H, H3' and H5'), 8.39 (m, 1H, H9), 8.78 (s, 1H, H4), 12.88 (br s, 1 H, NH/COOH).

^{13}C NMR (101 MHz, DMSO-d_6) δ 106.2 (s, C3a), 117.5 (d, C3' and C5'), 118.8 (s, C8), 120.4 (s, C9a), 122.5 (d, C6), 124.3 (d, C9), 128.3 (d, C2' and C6'), 129.4 (s, C4'), 133.0 (d, C7), 135.4 (s, C5a/C9b/C1'), 140.6 (d, C4), 142.3 (s, C5a/C9b/C1'), 142.6 (s, C5a/C9b/C1'), 161.9 (s, CO), 167.4 (s, CO).

HPLC-MS: Calc.[M+H]: 384.00
Found [M+H]: 383.97

HR-MS: Calc.[M+H]: 383.9978
Found [M+H]: 384.0002
(Diff.: -6.26 ppm)

Appearance: Yellow solid

Mp: Decomposes > 300 °C

TLC: R_f = 0.55 (20% MeOH in CH_2Cl_2)

E IV.8.12 3-(8-Bromo-3-oxo-3,5-dihydro-2H-pyrazolo[4,3-c]quinolin-2-yl)benzoic acid [72] DCBS162

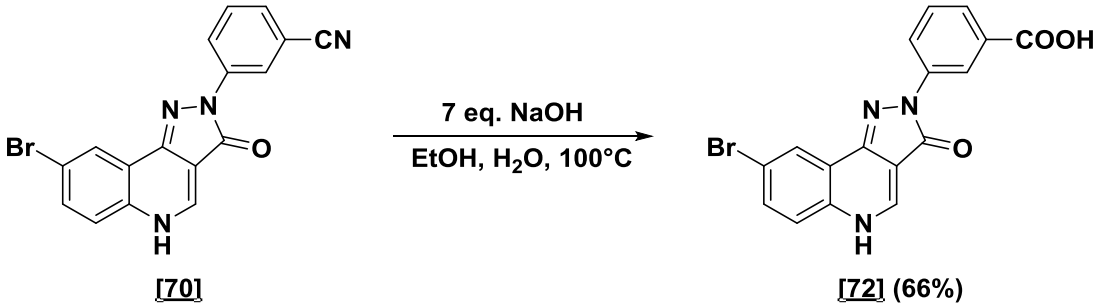

[70] [72] (66%)

Chemical Formula: $C_{17}H_9BrN_4O$
Molecular Weight: 365.19

Chemical Formula: $C_{17}H_{10}BrN_3O_3$
Molecular Weight: 384.19

The desired compound was synthesized according to general procedure E III.5 using:

PQ benzonitrile	20 mg	0.06 mmol	1 eq.
NaOH	17 mg	0.42 mmol	7 eq.

After lyophilisation 3-(8-bromo-3-oxo-3,5-dihydro-2H-pyrazolo[4,3-c]quinolin-2-yl)benzoic acid **[72]** was obtained (14 mg, 0.04 mmol, 66%).

^{1}H NMR (600 MHz, DMSO-d_6) δ 7.57 (t, *J* = 7.9 Hz, 1H, H5'), 7.68 (d, *J* = 8.8 Hz, 1H, H6), 7.75 (dt, *J* = 7.7, 1.4 Hz, 1H, H4'), 7.85 (dd, *J* = 8.8, 2.3 Hz, 1H, H7), 8.33 (d, *J* = 2.3 Hz, 1H, H9), 8.45 – 8.49 (m, 1H, H6'), 8.77 – 8.85 (m, 2H, H4 and H2'), 13.05 (br s, 1H, NH/COOH).

^{13}C NMR (151 MHz, DMSO-d_6) δ 106.2 (s, C3a), 118.9 (s, C8), 119.2 (d, C2'), 120.4 (s, C9a), 122.3 (d, C6), 122.6 (d, C4'), 124.3 (d, C9 and C3'), 124.8 (d, C6'), 129.1 (d, C5'), 133.0 (d, C7) , 135.1 (s, C5a/C9b/C1'), 140.1 (s, C5a/C9b/C1'), 140.4 (d, C4), 142.4 (s, C5a/C9b/C1'), 161.7 (s, CO), 167.4 (s, CO).

HPLC-MS: Calc.[M+H]: 384.00
Found [M+H]: 384.15

HR-MS: Calc.[M+H]: 383.9978
Found [M+H]: 383.9985
(Diff.: -1.77 ppm)

Appearance: Yellow solid

Mp: Decomposes > 300 °C

TLC: R_f = 0.52 (20% MeOH in CH_2Cl_2)

E IV.8.13 4-(8-Bromo-3-oxo-3,5-dihydro-2H-pyrazolo[4,3-c]quinolin-2-yl)benzamid [66] DCBS153B

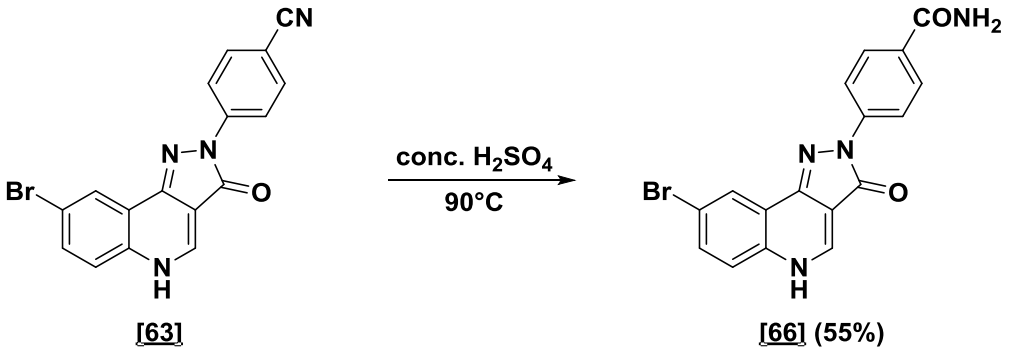

[63] [66] (55%)

Chemical Formula: $C_{17}H_9BrN_4O$
Molecular Weight: 365.19

Chemical Formula: $C_{17}H_{11}BrN_4O_2$
Molecular Weight: 383.21

The desired compound was synthesized according to general procedure E III.6 using:

PQ benzonitrile	100 mg	0.27 mmol	1 eq.
Conc. H_2SO_4	0.2 mL	0.8 mL/mmol	

After lyophilisation 4-(8-bromo-3-oxo-3,5-dihydro-2*H*-pyrazolo[4,3-*c*]quinolin-2-yl)benzamide **[66]** was obtained (61 mg, 0.15 mmol, 55%).

^{1}H NMR (400 MHz, DMSO-d_6) δ 7.31 (s, 1H, NH_2), 7.66 (d, *J* = 8.8 Hz, 1H, H6), 7.83 (dd, *J* = 8.7, 2.3 Hz, 1H, H7), 7.91 – 8.02 (m, 3H, H2' and H6' and NH_2), 8.26 – 8.38 (m, 3H, H3' and H5' and H9), 8.79 (s, 1H, H4).

^{13}C NMR (151 MHz, DMSO-d_6) δ 106.2 (s, C3a), 117.5 (d, C3' and C5'), 118.8 (s, C8), 120.4 (s, C9a), 122.5 (d, C6), 124.3 (d, C9), 128.3 (d, C2' and C6'), 129.4 (s, C4'), 133.0 (d, C7), 135.4 (s, C5a/C9b/C1'), 140.6 (d, C4), 142.3 (s, C5a/C9b/C1'), 142.6 (s, C5a/C9b/C1'), 161.9 (s, CO), 167.4 (s, $CONH_2$).

HPLC-MS: Calc.[M+H]: 383.01
Found [M+H]: 382.93

HR-MS: Calc.[M+H]: 383.0138
Found [M+H]: 383.0109
(Diff.: +7.73 ppm)

Appearance: Yellow solid

Mp: Decomposes > 300 °C

TLC: R_f = 0.70 (20% MeOH in CH_2Cl_2)

E IV.8.14 3-(8-Bromo-3-oxo-3,5-dihydro-2H-pyrazolo[4,3-c]quinolin-2-yl)benzamide [73] DCBSLK58

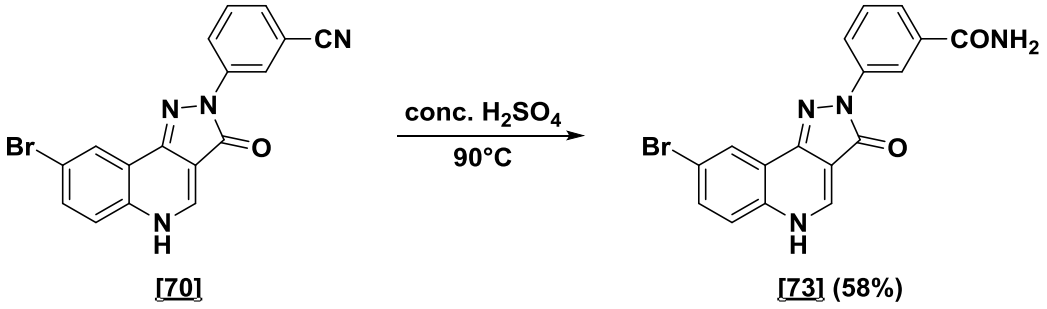

[70] [73] (58%)

Chemical Formula: $C_{17}H_9BrN_4O$
Molecular Weight: 365.19

Chemical Formula: $C_{17}H_{11}BrN_4O_2$
Molecular Weight: 383.21

The desired compound was synthesized according to general procedure E III.6 using:

PQ benzonitrile	100 mg	0.27 mmol	1 eq.
Conc. H_2SO_4	0.2 mL	0.8 mL/mmol	

After lyophilisation 3-(8-bromo-3-oxo-3,5-dihydro-2*H*-pyrazolo[4,3-*c*]quinolin-2-yl)benzamide **[73]** was obtained (61 mg, 0.16 mmol, 58%).

^{1}H NMR (400 MHz, DMSO-d_6) δ 7.42 (s, 1H, NH_2), 7.50 (t, *J* = 7.9 Hz, 1H, H5'), 7.65 (ddd, *J* = 7.7, 3.2, 1.8 Hz, 2H, H4' and H6), 7.80 (dd, *J* = 8.8, 2.3 Hz, 1H, H7), 8.03 (s, 1H, NH_2), 8.32 (d, *J* = 2.3 Hz, 1H, H9), 8.43 (ddd, *J* = 8.2, 2.2, 1.1 Hz, 1H, H6'), 8.64 (t, *J* = 1.9 Hz, 1H, H2'), 8.76 (s, 1H, H4), 12.94 (br s, 1H, NH).

^{13}C NMR (151 MHz, DMSO-d_6) δ 106.3 (s, C3a), 118.2 (d, C2'), 118.9 (s, C8), 120.4 (s, C9a), 121.2 (d, C6'), 122.0 (d, C4'), 123.0 (d, C6), 124.3 (d, C9), 128.6 (d, C5'), 133.0 (d, C7), 134.8 (s), 135.1 (s), 139.9 (s), 140.0 (s), 142.1 (d, C4), 161.6 (s, CO), 167.9 (s, $CONH_2$).

HR-MS: Calc.[M+H]: 383.0138

Found [M+H]: 383.0142 (Diff.: -1.12 ppm)

Appearance: Yellow solid

Mp: Decomposes > 300 °C

TLC: R_f = 0.23 (10% MeOH in CH_2Cl_2)

E IV.9 Pyrazoloquinolinones – R^8 methoxy series

E IV.9.1 8-Methoxy-2-(p-tolyl)-2,5-dihydro-3H-pyrazolo[4,3-c]quinolin-3-one [74] DCBS76

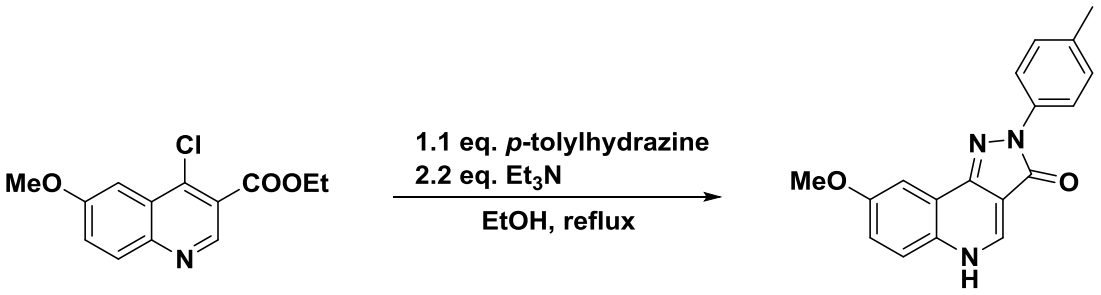

[8]

Chemical Formula: $C_{13}H_{12}ClNO_3$
Molecular Weight: 265.69

[74] (74%)

Chemical Formula: $C_{18}H_{15}N_3O_2$
Molecular Weight: 305.34

The desired compound was synthesized according to general procedure E III.4 using:

Chlorinated quinoline	100 mg	0.38 mmol	1 eq.
Arylhydrazine HCl	66 mg	0.41 mmol	1.1 eq.

After filtration 8-methoxy-2-(p-tolyl)-2,5-dihydro-3H-pyrazolo[4,3-c]quinolin-3-one **[74]** was obtained (85 mg, 0.28 mmol, 74%).

^{1}H NMR (400 MHz, DMSO-d_6) δ 2.32 (s, 3H, CH_3), 3.93 (s, 3H, OCH_3), 7.22 – 7.27 (m, 2H, H2' and H6'), 7.29 (dd, *J* = 9.1, 2.9 Hz, 1H, H7), 7.58 (d, *J* = 2.8 Hz, 1H, H9), 7.67 (d, *J* = 9.0 Hz, 1H, H6), 8.08 – 8.16 (m, 2H, H3' and H5'), 8.65 (s, 1H, H4), 12.79 (br s, 1H, NH).

^{13}C NMR (101 MHz, DMSO-d_6) δ 20.5 (q, CH_3), 55.7 (q, OCH_3), 102.5 (d, C9), 105.3 (s, C3a), 118.7 (d, C3' and C5'), 119.6 (d, C6/C7), 120.0 (s, C9a/C1'), 121.2 (d, C6/C7), 129.0 (d, C2' and C6'), 129.7 (s, C9a/C1'), 132.9 (s, C4'), 137.8 (d, C4), 137.9 (s, C5a/9b), 142.7 (s, C5a/9b), 157.5 (s, C8), 161.4 (s, CO).

HR-MS: Calc.[M+H]: 306.1237

Found [M+H]: 306.1230 (Diff.: +2.31 ppm)

Appearance: Yellow solid

Mp: Decomposes > 300 °C

TLC: R_f = 0.54 (10% MeOH in CH_2Cl_2)

E IV.9.2 8-Methoxy-2-(*m*-tolyl)-2,5-dihydro-3H-pyrazolo[4,3-c]quinolin-3-one [81] DCBS141

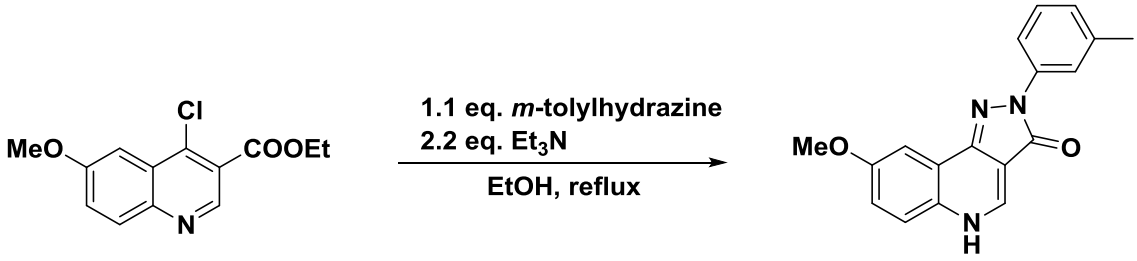

[8]

Chemical Formula: $C_{13}H_{12}ClNO_3$
Molecular Weight: 265.69

[81] (62%)

Chemical Formula: $C_{18}H_{15}N_3O_2$
Molecular Weight: 305.34

The desired compound was synthesized according to general procedure E III.4 using:

Chlorinated quinoline	30 mg	0.11 mmol	1 eq.
Arylhydrazine HCl	20 mg	0.12 mmol	1.1 eq.

After filtration 8-methoxy-2-(*m*-tolyl)-2,5-dihydro-3H-pyrazolo[4,3-c]quinolin-3-one **[81]** was obtained (21 mg, 0.068 mmol, 62%).

^{1}H NMR (400 MHz, DMSO-d_6) δ 2.38 (s, 3H, CH_3), 3.93 (s, 3H, OCH_3), 6.99 (d, *J* = 7.5 Hz, 1H, H6'), 7.25 – 7.37 (m, 2H, H5' and H7), 7.59 (d, *J* = 2.9 Hz, 1H, H9), 7.68 (d, *J* = 9.1 Hz, 1H, H6), 8.02 – 8.11 (m, 2H, H2' and H4'), 8.66 (d, *J* = 6.4 Hz, 1H, H4), 12.80 (br d, *J* = 6.5 Hz, 1H, NH).

^{13}C NMR (101 MHz, DMSO-d_6) δ 21.4 (q, CH_3), 55.7 (q, OCH_3), 102.6 (d, C9), 105.2 (s, C3a), 116.0 (d, C4'/C6'), 119.2 (d, C2'), 119.7 (d, C4'/C6'), 120.0 (s, C9a), 121.3 (d, C6), 124.7 (d, C7), 128.5 (d, C5'), 129.8 (s, C1'/C3'), 137.86 (d, C4), 137.9 (s, C1'/C3'), 140.2 (s, C5a/C9b), 142.9 (s, C5a/C9b), 157.6 (s, C8), 161.7 (s, CO).

HR-MS: Calc.[M+H]: 306.1237

Found [M+H]: 306.1249 (Diff.: -4.07 ppm)

Appearance: Yellow solid

Mp: Decomposes > 300 °C

TLC: R_f = 0.18 (5% MeOH in CH_2Cl_2)

E IV.9.3 8-Methoxy-2-(3-methoxyphenyl)-2,5-dihydro-3H-pyrazolo[4,3-c]quinolin-3-one [82] DCBS135

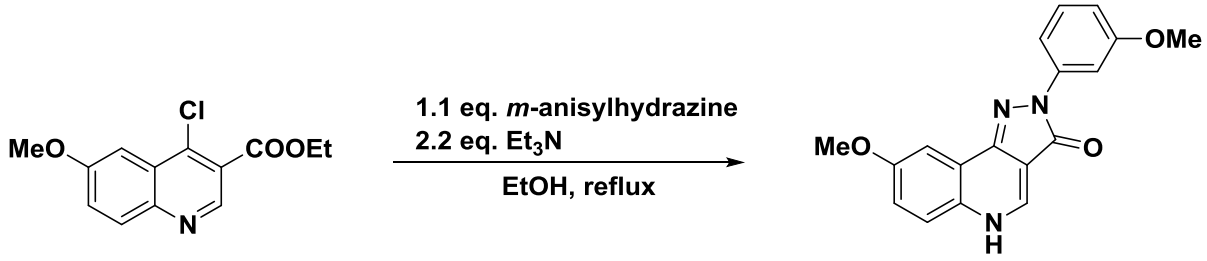

[8]

Chemical Formula: $C_{13}H_{12}ClNO_3$
Molecular Weight: 265.69

[82] (68%)

Chemical Formula: $C_{18}H_{15}N_3O_3$
Molecular Weight: 321.34

The desired compound was synthesized according to general procedure E III.4 using:

Chlorinated quinoline	50 mg	0.19 mmol	1 eq.
Arylhydrazine HCl	36 mg	0.21 mmol	1.1 eq.

After filtration 8-methoxy-2-(3-methoxyphenyl)-2,5-dihydro-3H-pyrazolo[4,3-c]quinolin-3-one **[82]** was obtained (41 mg, 0.13 mmol, 68%).

^{1}H NMR (400 MHz, DMSO-d_6) δ 3.81 (s, 3H, OCH_3), 3.93 (s, 3H, OCH_3), 6.76 (ddd, *J* = 8.3, 2.6, 0.9 Hz, 1H, H6'), 7.30 (dd, *J* = 9.1, 2.9 Hz, 1H, H7), 7.34 (t, *J* = 8.2 Hz, 1H, H5'), 7.60 (d, *J* = 2.8 Hz, 1H, H9), 7.68 (d, *J* = 9.1 Hz, 1H, H6), 7.84 (ddd, *J* = 8.2, 2.0, 0.9 Hz, 1H, H4'), 7.90 (t, *J* = 2.2 Hz, 1H, H2'), 8.65 (s, 1H, H4), 12.80 (br s, 1H, NH).

^{13}C NMR (101 MHz, DMSO-d_6) δ 55.1 (q, OCH_3), 55.7 (q, OCH_3), 102.7 (d, C9/C2'), 104.6 (d, C9/C2'), 105.2 (s, C3a), 109.2 (d, C4'/C6'), 111.1 (d, C4'/C6'), 119.7 (d, C6/C7), 120.0 (s, C9a), 121.3 (d, C6/C7), 129.5 (d, C5'), 129.8 (s, C1'), 138.0 (d, C4), 141.3 (s, C5a/C9b), 142.9 (s, C5a/C9b), 157.6 (s, C8/C3'), 159.5 (s, C8/C3'), 161.8 (s, CO).

HR-MS: Calc.[M+H]: 322.1186

Found [M+H]: 322.1201 (Diff.: -4.69 ppm)

Appearance: Yellow solid

Mp: Decomposes > 300 °C

TLC: R_f = 0.61 (10% MeOH in CH_2Cl_2)

E IV.9.4 8-Methoxy-2-(4-nitrophenyl)-2,5-dihydro-3H-pyrazolo[4,3-c]quinolin-3-one [76] DCBS93

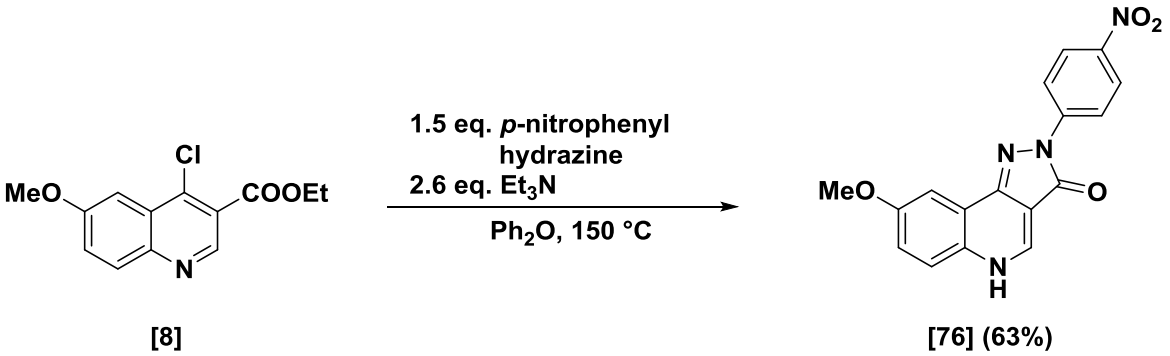

[8]

Chemical Formula: $C_{13}H_{12}ClNO_3$
Molecular Weight: 265.69

[76] (63%)

Chemical Formula: $C_{17}H_{12}N_4O_4$
Molecular Weight: 336.31

The chlorinated quinolinone **[8]** (63 mg, 0.24 mmol, 1 eq.) and the arylhydrazine hydrochloride (67 mg, 0.36 mmol, 1.5 eq.) were dispersed in 3 mL diphenylether, Et_3N (2.6 eq.) was added and the reaction mixture was heated to 150 °C under argon atmosphere. After 20 h the reaction mixture was allowed to cool to room temperature and was rinsed with 3 mL EtOH/EtOAc. The precipitate was collected by filtration and the filtrate was concentrated until EtOH and EtOAc were removed. After a second filtration more precipitate was obtained which was the pure 8-methoxy-2-(4-nitrophenyl)-2,5-dihydro-3H-pyrazolo[4,3-c]quinolin-3-one **[76]** (50 mg, 0.15 mmol, 63%).

^{1}H NMR (600 MHz, DMSO-d_6) δ 3.94 (s, 3H, OCH_3), 7.34 (dd, *J* = 9.0, 2.9 Hz, 1H, H7), 7.60 (d, *J* = 2.8 Hz, 1H, H9), 7.70 (d, *J* = 9.1 Hz, 1H, H6), 8.31 – 8.38 (m, 2H, H2' and H6'), 8.52 – 8.57 (m, 2H, H3' and H5'), 8.77 (d, *J* = 6.6 Hz, 1H, H4), 13.04 (br d, *J* = 6.6 Hz, 1H, NH).

^{13}C NMR (151 MHz, DMSO-d_6) δ 55.8 (q, OCH_3), 102.7 (d, C9), 104.5 (s, C3a), 117.8 (d, C3' and C5'), 119.8 (s, C9a/C1'), 120.4 (d, C7), 121.5 (d, C6), 125.0 (d, C2' and C6'), 130.1 (s, C9a/C1'), 138.8 (d, C4), 142.5 (s, C5a/C9b/C4'), 144.8 (s, C5a/C9b/C4'), 145.2 (s, C5a/C9b/C4'), 157.8 (s, C8), 162.8 (s, CO).

Appearance: Orange solid

Mp: Decomposes > 300 °C (Lit.[222]: not reported)

TLC: R_f = 0.50 (5% MeOH in CH_2Cl_2)

E IV.9.5 8-Methoxy-2-(3-nitrophenyl)-1,2-dihydro-3H-pyrazolo[4,3-c]quinolin-3-one [83] DCBS52

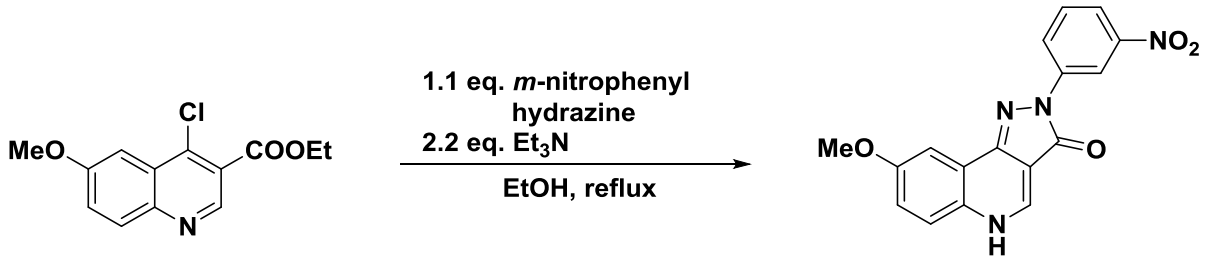

[8]

Chemical Formula: $C_{13}H_{12}ClNO_3$
Molecular Weight: 265.69

[83] (25%)

Chemical Formula: $C_{17}H_{12}N_4O_4$
Molecular Weight: 336.31

The desired compound was synthesized according to general procedure E III.4 using:

Chlorinated quinoline	123 mg	0.46 mmol	1 eq.
Arylhydrazine HCl	97 mg	0.51 mmol	1.1 eq.

After purification by HPLC 8-methoxy-2-(3-nitrophenyl)-1,2-dihydro-3H-pyrazolo[4,3-c]quinolin-3-one **[83]** was obtained (36 mg, 0.11 mmol, 25%).

^{1}H NMR (400 MHz, DMSO-d_6) δ 3.95 (s, 3H, OCH_3), 7.34 (dd, *J* = 9.1, 2.9 Hz, 1H, H7), 7.63 (d, *J* = 2.9 Hz, 1H, H9), 7.68 – 7.82 (m, 2H, H5' and H6), 8.02 (dd, *J* = 8.1, 2.4 Hz, 1H, H6'), 8.71 (d, *J* = 8.3 Hz, 1H, H4'), 8.76 (s, 1H, H4), 9.17 (t, *J* = 2.3 Hz, 1H, H2'), 13.00 (br s, 1H, NH).

^{13}C NMR (151 MHz, DMSO-d_6) δ 56.2 (q, OCH_3), 103.1 (d, C9), 105.1 (s, C3a), 112.7 (d, C2'), 118.7 (d, C6/C7/C4'), 120.3 (d, C9a), 120.7 (d, C6/C7/C4'), 122.0 (d, C6'), 124.5 (d, C6/C7/C4'), 130.5 (d, C1'), 130.8 (d, C5'), 139.2 (d, C4), 141.3 (s, C5a/C9b), 144.5 (s, C5a/C9b), 148.6 (s, C3'), 158.2 (s, C8), 162.7 (s, CO).

HPLC-MS: Calc.[M+H]: 337.09
Found [M+H]: 337.02

HR-MS: Calc.[M+H]: 337.0931
Found [M+H]: 337.0949
(Diff.: -5.38 ppm)

Appearance: Orange solid

Mp: Decomposes > 300 °C

TLC: R_f = 0.53 (10% MeOH in CH_2Cl_2)

E IV.9.6 4-(8-Methoxy-3-oxo-3,5-dihydro-2H-pyrazolo[4,3-c]quinolin-2-yl)benzonitrile [77] DCBS84

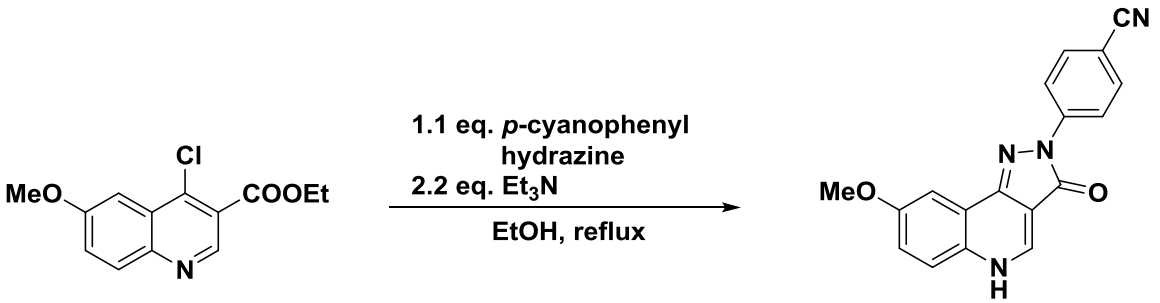

[8]

Chemical Formula: $C_{13}H_{12}ClNO_3$
Molecular Weight: 265.69

[77] (57%)

Chemical Formula: $C_{18}H_{12}N_4O_2$
Molecular Weight: 316.32

The desired compound was synthesized according to general procedure E III.4 using:

Chlorinated quinoline	300 mg	1.13 mmol	1 eq.
Arylhydrazine HCl	211 mg	1.24 mmol	1.1 eq.

After filtration 4-(8-methoxy-3-oxo-3,5-dihydro-2H-pyrazolo[4,3-c]quinolin-2-yl)benzonitrile **[77]** was obtained (202 mg, 0.64 mmol, 57%).

^{1}H NMR (400 MHz, DMSO-d_6) δ 3.93 (s, 3H, OCH_3), 7.33 (dd, *J* = 9.1, 2.9 Hz, 1H, H7), 7.60 (d, *J* = 2.9 Hz, 1H, H9), 7.69 (d, *J* = 9.1 Hz, 1H, H6), 7.87 – 7.95 (m, 2H, H2' and H6'), 8.45 – 8.52 (m, 2H, H3' and H5'), 8.73 (d, *J* = 6.4 Hz, 1H, H4), 12.97 (br d, *J* = 6.2 Hz, 1H, NH).

^{13}C NMR (101 MHz, DMSO-d_6) δ 55.7 (q, OCH_3), 102.7 (d, C9), 104.6 (s, C3a), 105.3 (s, C4'), 118.1 (d, C3' and C5'), 119.2 (s, C9a/CN), 119.8 (d, C7), 120.2 (s, C9a/CN), 121.4 (d, C6), 130.0 (s, C1'), 133.2 (d, C2' and C6'), 138.6 (d, C4), 143.5 (s, C5a/C9b), 144.3 (s, C5a/C9b), 157.7 (s, C8), 162.5 (s, CO).

HR-MS: Calc.[M+H]: 317.1033

Found [M+H]: 317.1038 (Diff.: -1.55 ppm)

Appearance: Yellow solid

Mp: Decomposes > 300 °C (Lit.[146]: Decomposition > 310 °C)

TLC: R_f = 0.50 (10% MeOH in CH_2Cl_2)

E IV.9.7 3-(8-Methoxy-3-oxo-3,5-dihydro-2H-pyrazolo[4,3-c]quinolin-2-yl)benzonitrile [84] DCBS145

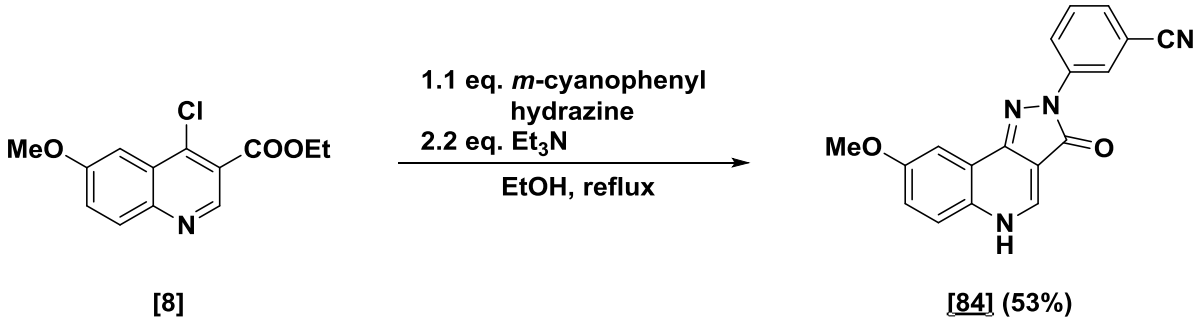

[8]

Chemical Formula: $C_{13}H_{12}ClNO_3$
Molecular Weight: 265.69

[84] (53%)

Chemical Formula: $C_{18}H_{12}N_4O_2$
Molecular Weight: 316.32

The desired compound was synthesized according to general procedure E III.4 using:

Chlorinated quinoline	80 mg	0.30 mmol	1 eq.
Arylhydrazine HCl	56 mg	0.33 mmol	1.1 eq.

After filtration 3-(8-methoxy-3-oxo-3,5-dihydro-2H-pyrazolo[4,3-c]quinolin-2-yl)benzonitrile **[84]** was obtained (50 mg, 0.16 mmol, 53%).

^{1}H NMR (400 MHz, DMSO-d_6) δ 3.93 (s, 3H, OCH_3), 7.32 (dd, *J* = 9.0, 2.9 Hz, 1H, H6'), 7.59 – 7.75 (m, 4H, H6 and H7 and H9 and H5'), 8.56 – 8.63 (m, 1H, H4'), 8.64 – 8.69 (m, 1H, H2'), 8.74 (s, 1H, H4), 12.96 (br s, 1H, NH).

^{13}C NMR (101 MHz, DMSO-d_6) δ 55.8 (q, OCH_3), 102.7 (d, C9), 104.7 (s, C3a), 111.6 (s, C3'), 118.8 (s, CN), 119.9 (s, C9a), 120.1 (d, C6/C7), 120.8 (d, C6/C7), 121.5 (d, C2'/C6'), 122.6 (d, C2'/C6'), 127.1 (d, C5'), 130.0 (s, C1'), 130.3 (d, C4'), 138.6 (d, C4), 140.6 (s, C5a/C9b), 143.9 (s, C5a/C9b), 157.7 (s, C8), 162.2 (s, CO).

HR-MS: Calc.[M+H]: 317.1033

Found [M+H]: 317.1040 (Diff.: -4.41 ppm)

Appearance: Yellow solid

Mp: Decomposes > 300 °C

TLC: R_f = 0.60 (10% MeOH in CH_2Cl_2)

E IV.9.8 2-(4-Aminophenyl)-8-methoxy-2,5-dihydro-3H-pyrazolo[4,3-c]quinolin-3-one [78] DCBS96

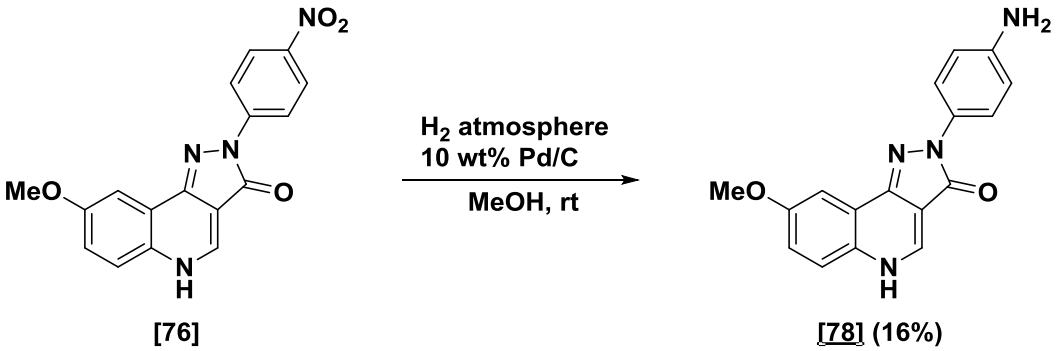

[76] **[78] (16%)**

Chemical Formula: $C_{17}H_{12}N_4O_4$
Molecular Weight: 336.31

Chemical Formula: $C_{17}H_{14}N_4O_2$
Molecular Weight: 306.33

8-Methoxy-2-(4-nitrophenyl)-1,2-dihydro-3H-pyrazolo[4,3-c]quinolin-3-one **[76]** (20 mg, 0.06 mmol) was dissolved in 2.5 mL MeOH, Pd/C (10 wt-%) was added and the reaction mixture was stirred at room temperature under hydrogen atmosphere. After 18 h the reaction mixture was filtrated over celite and the solvent was removed under reduced pressure. The residue was purified by HPLC and the obtained solid was neutralized with 1 mL satd. $NaHCO_3$. The precipitate was washed with water (2 x 2 mL) and dried in *vacuo* to give 2-(4-aminophenyl)-8-methoxy-2,5-dihydro-3H-pyrazolo[4,3-c]quinolin-3-one **[78]** (6 mg, 0.02 mmol, 16%).

^{1}H NMR (600 MHz, DMSO-d_6) δ 3.90 (s, 3H, OCH_3), 4.99 (br s, 2H, NH_2), 6.58 – 6.64 (m, 2H, H2' and H6'), 7.21 (dd, *J* = 9.0, 2.9 Hz, 1H, H7), 7.52 (d, *J* = 2.9 Hz, 1H, H9), 7.63 (d, *J* = 9.0 Hz, 1H, H6), 7.78 – 7.83 (m, 2H, H3' and H5'), 8.54 (s, 1H, H4).

^{13}C NMR (151 MHz, DMSO-d_6) δ 55.6 (q, OCH_3), 102.3 (d, C9), 105.4 (s, C3a), 113.6 (d, C3' and C5'), 119.2 (d, C7), 120.2 (s, C9a/C1'), 120.9 (d, C2' and C6'), 121.5 (d, C6), 129.9 (s, C9a/C1'), 130.0 (s, C5a/C9b), 137.6 (d, C4), 142.0 (s, C5a/C9b), 145.6 (s, C4'), 157.3 (s, C8), 160.6 (s, CO).

HR-MS: Calc.[M+H]: 307.1190

Found [M+H]: 307.1196 (Diff.: -2.21 ppm)

Appearance: Yellow solid

Mp: Decomposes > 300 °C

TLC: R_f = 0.25 (5% MeOH in CH_2Cl_2)

E IV.9.9 2-(3-Aminophenyl)-8-methoxy-2,5-dihydro-3H-pyrazolo[4,3-c]quinolin-3-one [85] DCBSLS24

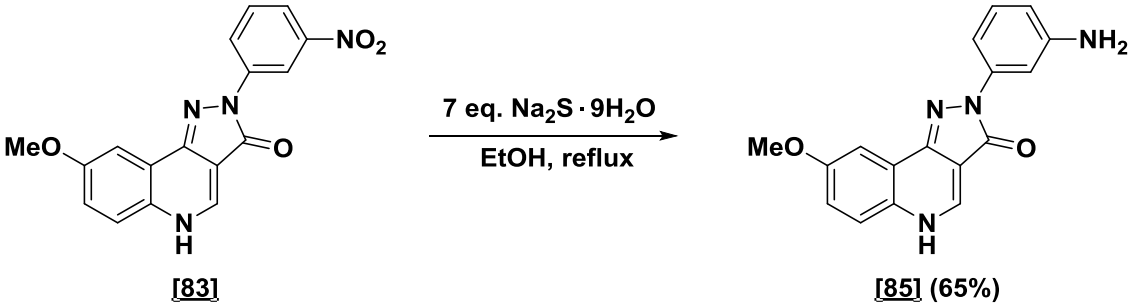

[83] [85] (65%)

Chemical Formula: $C_{17}H_{12}N_4O_4$
Molecular Weight: 336.31

Chemical Formula: $C_{17}H_{14}N_4O_2$
Molecular Weight: 306.33

The desired compound was synthesized according to general procedure E III.7 using:

Nitro PQ	44 mg	0.13 mmol	1 eq.
$Na_2S \cdot 9H_2O$	218 mg	0.91 mmol	7 eq.

2-(3-Aminophenyl)-8-methoxy-1,2-dihydro-3H-pyrazolo[4,3-c]quinolin-3-one **[85]** was obtained without further purification (26 mg, 0.09 mmol, 65%).

^{1}H NMR (400 MHz, DMSO-d_6) δ 3.89 (s, 3H, OCH_3), 5.04 (br s, 2H, NH_2), 6.31 (d, J = 8.0 Hz, 1H, H-Ar), 6.95 – 7.03 (m, 1H, H-Ar), 7.06 – 7.22 (m, 1H, H-Ar), 7.43 – 7.57 (m, 3H, 2 H-Ar and H9), 7.56 – 7.68 (m, 1H, H6), 8.43 (s, 1H, H4).

^{13}C NMR (151 MHz, DMSO-d_6) δ 55.7 (q, OCH_3), 102.4 (d, C9/C2'), 104.8 (s, C3a), 105.5 (d, C9/C2'), 107.3 (s, C1'), 110.3 (d, C4'), 119.6 (s, C9a), 120.1 (d, C6/C6'), 121.3 (d, C6/C6'), 128.9 (d, C7/C5'), 129.8 (d, C7/C5'), 137.7 (d, C4), 140.9 (s, C5a/C9b), 142.5 (s, C5a/C9b), 148.7 (s, C3'), 157.5 (s, C8), 161.5 (s, CO).

HPLC-MS: Calc.[M+H]: 307.12
Found [M+H]: 307.06

HR-MS: Calc.[M+H]: 307.1190
Found [M+H]: 307.1194
(Diff.: -1.57 ppm)

Appearance: Yellow solid

Mp: Decomposes > 300 °C

TLC: R_f = 0.33 (10% MeOH in CH_2Cl_2)

E IV.9.10 4-(8-Methoxy-3-oxo-3,5-dihydro-2H-pyrazolo[4,3-c]quinolin-2-yl)benzoic acid [79] DCBS88

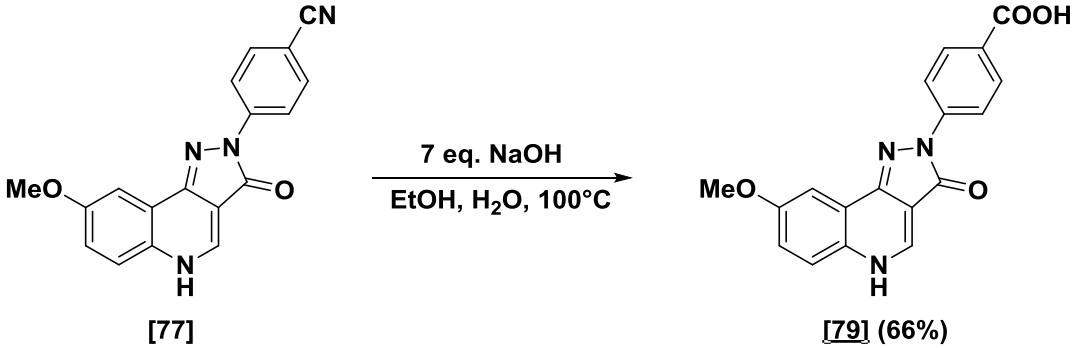

[77] **[79] (66%)**

Chemical Formula: $C_{18}H_{12}N_4O_2$
Molecular Weight: 316.32

Chemical Formula: $C_{18}H_{13}N_3O_4$
Molecular Weight: 335.32

The desired compound was synthesized according to general procedure E III.5 using:

PQ benzonitrile	40 mg	0.13 mmol	1 eq.
NaOH	37 mg	0.91 mmol	7 eq.

After lyophilisation 4-(8-methoxy-3-oxo-3,5-dihydro-2H-pyrazolo[4,3-c]quinolin-2-yl)benzoic acid **[79]** was obtained (28 mg, 0.08 mmol, 66%).

^{1}H NMR (400 MHz, DMSO-d_6) δ 3.95 (s, 3H, OCH_3), 7.33 (dd, *J* = 9.1, 2.9 Hz, 1H, H7), 7.62 (d, *J* = 2.9 Hz, 1H, H9), 7.70 (d, *J* = 9.1 Hz, 1H, H6), 8.04 (d, *J* = 8.5 Hz, 2H, H2' and H6'), 8.42 (d, *J* = 8.5 Hz, 2H, H3' and H5'), 8.73 (d, *J* = 6.6 Hz, 1H, H4), 12.79 (br s, 1H, COOH), 12.92 (br d, *J* = 6.6 Hz, 1H, NH).

^{13}C NMR (151 MHz, DMSO-d_6) δ 55.7 (q, OCH_3), 102.7 (d, C9), 104.9 (s, C3a), 117.6 (d, C3' and C5'), 119.9 (s, C9a/C1'), 120.0 (d, C7), 121.4 (d, C6), 125.5 (s, C4'), 129.9 (s, C9a/C1'), 130.3 (d, C2' and C6'), 138.3 (d, C4), 143.6 (s, C5a/C9b), 143.9 (s, C5a/C9b), 157.7 (s, C8), 162.3 (s, CO), 167.0 (s, COOH).

HR-MS: Calc.[M+H]: 336.0979

Found [M+H]:336.0984 (Diff.: -1.46 ppm)

Appearance: Yellow solid

Mp: Decomposes > 300 °C (Lit.[223]: not reported)

TLC: R_f = 0.57 (20% MeOH in CH_2Cl_2)

E IV.9.11 3-(8-Methoxy-3-oxo-3,5-dihydro-2H-pyrazolo[4,3-c]quinolin-2-yl)benzoic acid [86] DCBS151A

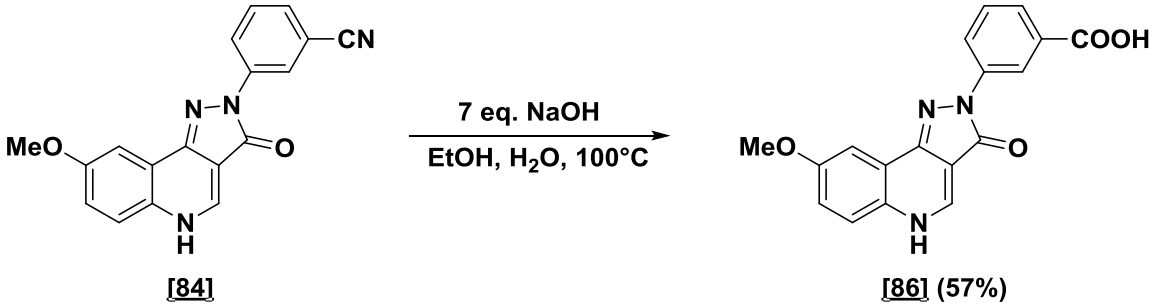

[84] [86] (57%)

Chemical Formula: $C_{18}H_{12}N_4O_2$
Molecular Weight: 316.32

Chemical Formula: $C_{18}H_{13}N_3O_4$
Molecular Weight: 335.32

The desired compound was synthesized according to general procedure E III.5 using:

PQ benzonitrile	40 mg	0.13 mmol	1 eq.
NaOH	37 mg	0.91 mmol	7 eq.

After lyophilisation 3-(8-methoxy-3-oxo-3,5-dihydro-2H-pyrazolo[4,3-c]quinolin-2-yl)benzoic acid **[86]** was obtained (12 mg, 0.04 mmol, 57%).

^{1}H NMR (400 MHz, DMSO-d_6) δ 3.94 (s, 3H, OCH_3), 7.31 (dd, *J* = 9.0, 2.9 Hz, 1H, H7), 7.55 (t, *J* = 7.9 Hz, 1H, H5'), 7.60 (d, *J* = 2.8 Hz, 1H, H9), 7.70 (d, *J* = 9.1 Hz, 1H, H6), 7.74 (d, *J* = 7.7 Hz, 1H, H6'), 8.48 – 8.52 (m, 1H, H4'), 8.70 (s, 1H, H4), 8.79 – 8.85 (m, 1H, H2'), 12.95 (br s, 1H, NH/COOH).

^{13}C NMR (151 MHz, DMSO-d_6) δ 55.7 (q, OCH_3), 102.5 (d, C9), 105.0 (s, C3a), 119.3 (s, C9a), 119.9 (d, C2'), 120.0 (d, C7), 121.6 (d, C6), 122.3 (d, C4'/C6'), 124.7 (d, C4'/C6'), 126.8 (s, C3'), 128.8 (d, C5'), 130.2 (s, C1'), 138.4 (d, C4), 140.3 (s, C5a/9b), 143.5 (s, C5a/9b), 157.6 (s, C8), 161.9 (s, CO), 162.1 (s, CO).

HPLC-MS: Calc.[M+H]: 336.10
Found [M+H]: 336.10

HR-MS: Calc.[M+H]: 336.0979
Found [M+H]: 336.1014
(Diff.: -9.85 ppm)

Appearance: Yellow solid

Mp: Decomposes > 300 °C

TLC: R_f = 0.60 (20% MeOH in CH_2Cl_2)

E IV.9.12 4-(8-Methoxy-3-oxo-3,5-dihydro-2H-pyrazolo[4,3-c]quinolin-2-yl)benzamide [80] DCBSLK60

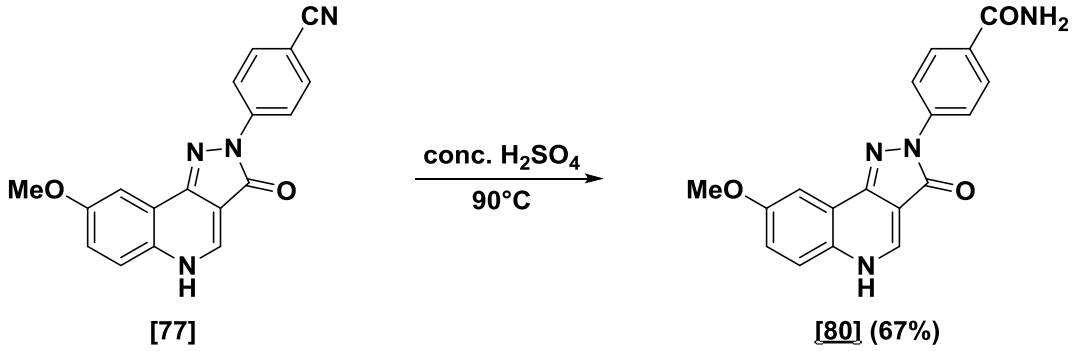

[77] [80] (67%)

Chemical Formula: $C_{18}H_{12}N_4O_2$
Molecular Weight: 316.32

Chemical Formula: $C_{18}H_{14}N_4O_3$
Molecular Weight: 334.34

The desired compound was synthesized according to general procedure E III.6 using:

PQ benzonitrile	20 mg	0.06 mmol	1 eq.
Conc. H_2SO_4	0.2 mL	3 mL/mmol	

After lyophilisation 4-(8-methoxy-3-oxo-3,5-dihydro-2*H*-pyrazolo[4,3-*c*]quinolin-2-yl)benzamide **[80]** was obtained (14 mg, 0.04 mmol, 67%).

^{1}H NMR (400 MHz, DMSO-d_6) δ 3.94 (s, 3H, OCH_3), 7.27 – 7.34 (m, 2H, H7 and NH_2), 7.61 (d, *J* = 2.9 Hz, 1H, H9), 7.69 (d, *J* = 9.1 Hz, 1H, H6), 7.92 – 7.99 (m, 3H, H3' and H5' and NH_2), 8.35 (d, *J* = 8.8 Hz, 2H, H2' and H6'), 8.69 (s, 1H, H4), 12.84 (br s, 1H, NH).

^{13}C NMR (151 MHz, DMSO-d_6) δ 55.7 (q, OCH_3), 102.6 (d, C9), 104.9 (s, 3a), 117.5 (d, C2' and C6'), 119.9 (s, C9a), 120.0 (d, C7), 121.8 (d, C6), 128.3 (d, C3' and C5'), 129.1 (s, C5a/C9b/C1'), 130.5 (s, C5a/C9b/C1'), 138.6 (d, C4), 142.5 (s, C5a/C9b/C1'), 143.8 (s, C4'), 157.6 (s, CO), 162.1 (s, CO), 167.5 (s, C8).

HPLC-MS: Calc.[M+H]: 335.11
Found [M+H]: 335.15

HR-MS: Calc.[M+H]: 335.1139
Found [M+H]: 335.1155
(Diff.: -4.83 ppm)

Appearance: Yellow solid

Mp: Decomposes > 300 °C

TLC: R_f = 0.28 (10% MeOH in CH_2Cl_2)

E IV.9.13 3-(8-Methoxy-3-oxo-3,5-dihydro-2H-pyrazolo[4,3-c]quinolin-2-yl)benzamide [87] DCBS151B

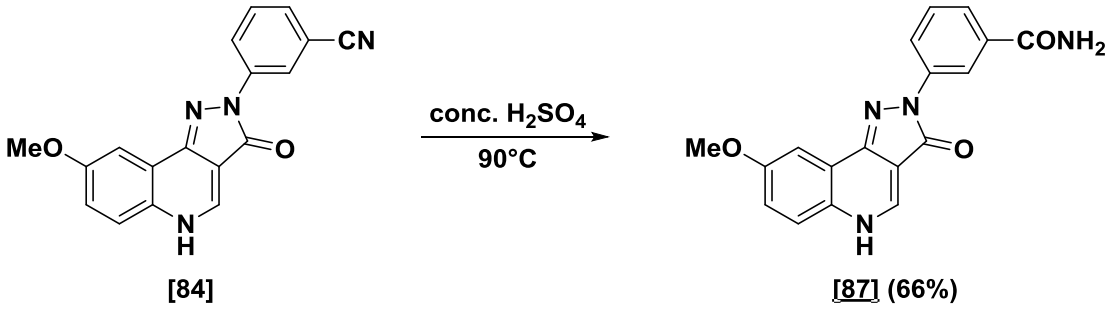

[84] **[87] (66%)**

Chemical Formula: $C_{18}H_{12}N_4O_2$
Molecular Weight: 316.32

Chemical Formula: $C_{18}H_{14}N_4O_3$
Molecular Weight: 334.34

The desired compound was synthesized according to general procedure E III.6 using:

PQ benzonitrile	13 mg	0.04 mmol	1 eq.
Conc. H_2SO_4	0.2 mL	3 mL/mmol	

After lyophilisation 3-(8-methoxy-3-oxo-3,5-dihydro-2*H*-pyrazolo[4,3-*c*]quinolin-2-yl)benzamide **[87]** was obtained (9 mg, 0.03 mmol, 66%).

^{1}H NMR (400 MHz, DMSO-d_6) δ 3.94 (s, 3H, OCH_3), 7.30 (dd, *J* = 9.1, 2.9 Hz, 1H, H7), 7.42 (br s, 1H, NH_2), 7.50 (t, *J* = 7.9 Hz, 1H, H5'), 7.61 (d, *J* = 2.8 Hz, 1H, H9), 7.65 (dt, *J* = 7.7, 1.3 Hz, 1H, H6'), 7.69 (d, *J* = 9.1 Hz, 1H, H6), 8.04 (br s, 1H, NH_2), 8.44 (ddd, *J* = 8.2, 2.2, 1.1 Hz, 1H, H4'), 8.64 (t, *J* = 1.9 Hz, 1H, H2'), 8.69 (s, 1H, H4).

^{13}C NMR (151 MHz, DMSO-d_6) δ 55.7 (q, OCH_3), 102.5 (d, C9), 105.0 (s, C3a), 118.3 (d, C2'), 119.8 (s, C9a), 120.1 (d, C7), 121.3 (d, C4'), 121.8 (d, C6), 122.7 (d, C6'), 128.5 (d, C5'), 130.5 (s, C5a/C9b/C1'/C3'), 135.1 (s, C5a/C9b/C1'/C3'), 138.5 (d, C4), 140.2 (s, C5a/C9b/C1'/C3'), 143.4 (s, C5a/C9b/C1'/C3'), 157.5 (s, CO/C8), 161.8 (s, CO/C8), 168.1 (s, $CONH_2$).

HPLC-MS: Calc.[M+H]: 335.11
Found [M+H]: 335.11

HR-MS: Calc.[M+H]: 335.1139
Found [M+H]: 335.1149
(Diff.: -3.11 ppm)

Appearance: Yellow solid

Mp: Decomposes > 300 °C

TLC: R_f = 0.71 (20% MeOH in CH_2Cl_2)

E IV.10 Pyrazoloquinolinones – R^8 mixed series

E IV.10.1 8-Bromo-2-phenyl-2,5-dihydro-3H-pyrazolo[4,3-c]quinolin-3-one [91] DCBS20

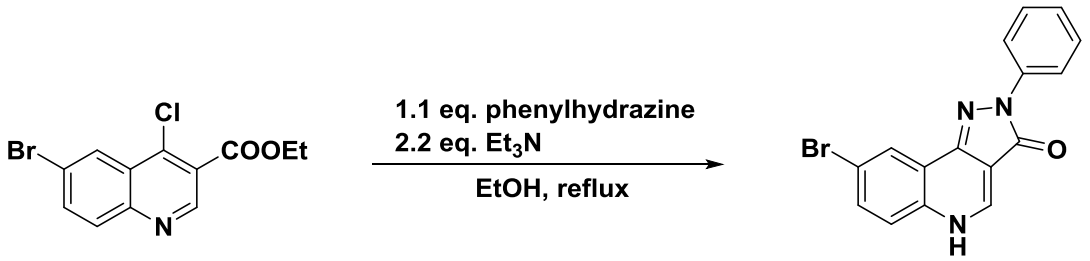

[31]

Chemical Formula: $C_{12}H_9BrClNO_2$
Molecular Weight: 314.56

[91] (41%)

Chemical Formula: $C_{16}H_{10}BrN_3O$
Molecular Weight: 340.18

The desired compound was synthesized according to general procedure E III.4 using:

Chlorinated quinoline	100 mg	0.32 mmol	1 eq.
Arylhydrazine HCl	50 mg	0.35 mmol	1.1 eq.

After purification by HPLC 8-bromo-2-phenyl-2,5-dihydro-3H-pyrazolo[4,3-c]quinolin-3-one **[91]** was obtained (44 mg, 0.13 mmol, 41%).

^{1}H NMR (400 MHz, DMSO-d_6) δ 7.18 (t, *J* = 7.4 Hz, 1H, H4'), 7.45 (t, *J* = 7.9 Hz, 2H, H3' and H5'), 7.67 (d, *J* = 8.8 Hz, 1H, H6), 7.84 (dd, *J* = 8.8, 2.2 Hz, 1H, H7), 8.21 (d, *J* = 7.7 Hz, 2H, H2' and H6'), 8.31 (d, *J* = 2.2 Hz, 1H, H9), 8.78 (s, 1H, H4), 12.91 (br s, 1H, NH).

^{13}C NMR (101 MHz, DMSO-d_6) δ 107.0 (s, C3a), 119.2 (d, C2' and C6'), 119.3 (s, C9a), 122.4 (d, C9), 124.7 (s, C8), 129.2 (d, C3' and C5'), 133.4 (d, C6/C7/C4'), 135.1 (d, C6/C7/C4'), 140.3 (s, C1'), 140.5 (d, C4), 140.8 (d, C6/C7/C4'), 142.3 (s, C5a/C9b), 144.7 (s, C5a/C9b), 162.0 (s, CO).

HPLC-MS: Calc.[M+H]: 340.01

Found [M+H]: 339.92

Appearance: Yellow solid

Mp: Decomposes > 300 °C (Lit.[221]: > 305 °C)

TLC: R_f = 0.52 (10% MeOH in CH_2Cl_2)

E IV.10.2 2,8-Diphenyl-2,5-dihydro-3H-pyrazolo[4,3-c]quinolin-3-one [92] DCBS23

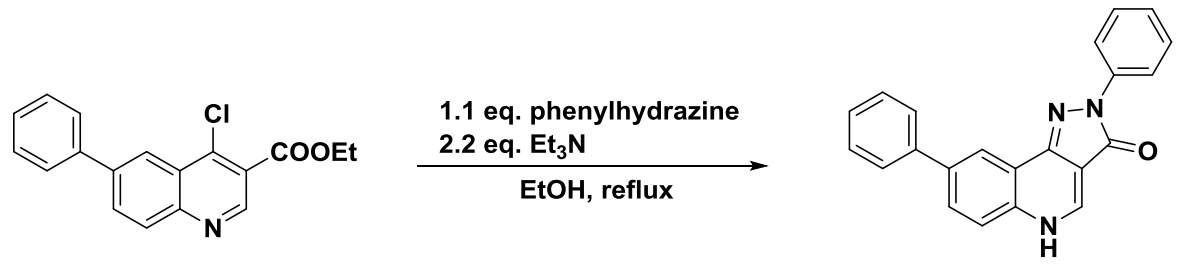

[88d]

Chemical Formula: $C_{18}H_{14}ClNO_2$
Molecular Weight: 311.77

[92] (12%)

Chemical Formula: $C_{22}H_{15}N_3O$
Molecular Weight: 337.38

The desired compound was synthesized according to general procedure E III.4 using:

Chlorinated quinoline	150 mg	0.48 mmol	1 eq.
Arylhydrazine HCl	76 mg	0.53 mmol	1.1 eq.

After purification by HPLC 2,8-diphenyl-2,5-dihydro-3H-pyrazolo[4,3-c]quinolin-3-one **[92]** was obtained (20 mg, 0.06 mmol, 12%).

^{1}H NMR (400 MHz, DMSO-d_6) δ 7.18 (t, *J* = 7.1 Hz, 1H, H4'), 7.39 – 7.51 (m, 3H, H3', H5' and H-Ar), 7.51 – 7.63 (m, 2H, H-Ar), 7.75 – 7.90 (m, 3H, H-Ar), 8.02 (dd, *J* = 8.6, 2.0 Hz, 1H, H7), 8.25 (d, *J* = 7.9 Hz, 2H, H2' and H6'), 8.43 (d, *J* = 2.0 Hz, 1H, H_9), 8.76 (s, 1H, H_4), 12.90 (br s, 1H, NH).

^{13}C NMR (151 MHz, DMSO-d_6) δ 106.3 (s, C3a), 118.8 (d, C2' and C6'), 119.2 (s, C9a), 119.4 (d, C9), 120.4 (d, C6/C7), 124.1 (d, C6/C7), 127.0 (d, C2'' and C6''), 128.1 (d, C4'), 128.8 (s, C4''), 128.9 (d, C3' and C5'), 129.3 (d, C3'' and C5''), 135.0 (s), 138.2 (s), 138.9 (d, C4), 139.3 (s), 140.1 (s), 143.0 (s, C9b), 161.7 (s, CO).

HPLC-MS: Calc.[M+H]: 338.13
Found [M+H]: 338.07

HR-MS: Calc.[M+H]: 338.1288
Found [M+H]: 338.1288
(Diff.: -0.11 ppm)

Appearance: Yellow solid

Mp: Decomposes > 300 °C

TLC: R_f = 0.55 (10% MeOH in CH_2Cl_2)

E IV.10.3 2-(3-Bromophenyl)-8-methoxy-2,5-dihydro-3H-pyrazolo[4,3-c]quinolin-3-one [90] DCBS24

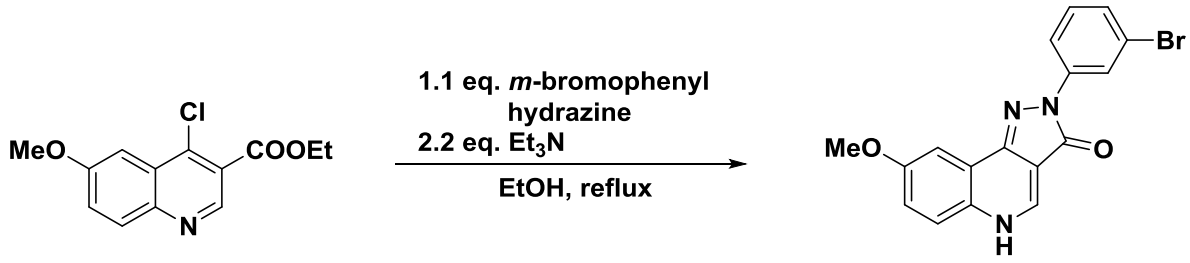

[8]

Chemical Formula: $C_{13}H_{12}ClNO_3$
Molecular Weight: 265.69

[90] (39%)

Chemical Formula: $C_{17}H_{12}BrN_3O_2$
Molecular Weight: 370.21

The desired compound was synthesized according to general procedure E III.4 using:

Chlorinated quinoline	200 mg	0.75 mmol	1 eq.
Arylhydrazine HCl	185 mg	0.83 mmol	1.1 eq.

After purification by HPLC 2-(3-bromophenyl)-8-methoxy-2,5-dihydro-3H-pyrazolo[4,3-c]quinolin-3-one **[90]** was obtained (105 mg, 0.29 mmol, 39%).

^{1}H NMR (600 MHz, DMSO-d_6) δ 3.94 (s, 3H, OCH_3), 7.31 (dd, *J* = 9.1, 2.8 Hz, 1H, H7), 7.35 (ddd, *J* = 7.9, 2.1, 1.1 Hz, 1H, H6'), 7.42 (t, *J* = 8.1 Hz, 1H, H5'), 7.61 (d, *J* = 2.8 Hz, 1H, H9), 7.69 (d, *J* = 9.0 Hz, 1H, H6), 8.29 (ddd, *J* = 8.2, 2.0, 1.0 Hz, 1H, H4'), 8.50 (t, *J* = 2.0 Hz, 1H, H2'), 8.71 (s, 1H, H4), 12.92 (br s, 1H, NH).

^{13}C NMR (151 MHz, DMSO-d_6) δ 55.8 (q, OCH_3), 102.7 (d, C9), 104.9 (C3a), 117.1 (d, C7), 119.9 (s, C9a), 120.1 (d, C4'/C6'), 120.5 (d, C6), 121.4 (s/d, C2'/C3'), 121.7 (s/d, C2'/C3'), 126.4 (d, C4'/C6'), 129.9 (s, C1'), 130.8 (d, C5'), 138.4 (d, C4), 141.5 (s, C5a/C9b), 143.6 (s, C5a/C9b), 157.7 (s, C8), 162.0 (s, CO).

HPLC-MS: Calc.[M+H]: 370.02
Found [M+H]: 370.02

HR-MS: Calc.[M+H]: 370.0186
Found [M+H]: 370.0210
(Diff.: -6.70 ppm)

Appearance: Yellow solid

Mp: Decomposes > 300 °C

TLC: R_f = 0.59 (10% MeOH in CH_2Cl_2)

E IV.10.4 2-(3-Bromophenyl)-8-chloro-2,5-dihydro-3H-pyrazolo[4,3-c]quinolin-3-one [89] DCBS32

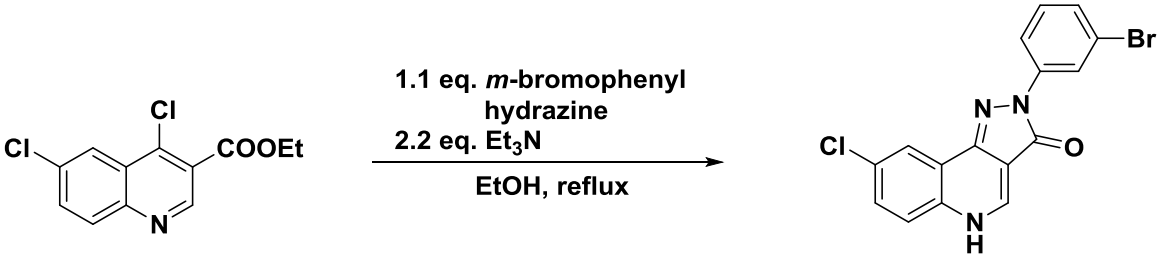

[30]

Chemical Formula: $C_{12}H_9Cl_2NO_2$
Molecular Weight: 270.11

[89] (75%)

Chemical Formula: $C_{16}H_9BrClN_3O$
Molecular Weight: 374.62

The compound was synthesized according to general procedure E III.4 using:

Chlorinated quinoline	100 mg	0.37 mmol	1 eq.
Arylhydrazine HCl	91 mg	0.41 mmol	1.1 eq.

After purification by HPLC 2-(3-bromophenyl)-8-methoxy-2,5-dihydro-3H-pyrazolo[4,3-c]quinolin-3-one **[89]** was obtained (104 mg, 0.28 mmol, 75%).

^{1}H NMR (600 MHz, DMSO-d_6) δ 7.37 (ddd, *J* = 7.9, 2.0, 1.0 Hz, 1H, H6'), 7.43 (t, *J* = 8.0 Hz, 1H, H5'), 7.69 – 7.80 (m, 2H, H6 and H7), 8.21 (t, *J* = 1.4 Hz, 1H, H9), 8.27 (ddd, *J* = 8.2, 2.1, 1.1 Hz, 1H, H4'), 8.47 (t, *J* = 2.0 Hz, 1H, H2'), 8.82 (s, 1H, H4), 13.03 (br s, 1H, NH).

^{13}C NMR (151 MHz, DMSO-d_6) δ 106.0 (s, C3a), 117.1 (d, C9), 119.9 (C9a), 120.5 (d, C7), 121.3 (d, C6/C2'), 121.7 (d, C6/C2'), 121.8 (s, C3'), 126.6 (s, C8), 130.5 (s, C1'), 130.88 (d, C4'), 130.92 (d, C6'), 134.4 (d, C5'), 140.1 (d, C4), 141.2 (s, C5a/C9b), 142.6 (s, C5a/C9b), 161.7 (s, CO).

HPLC-MS: Calc.[M+H]: 373.97
Found [M+H]: 373.92

HR-MS: Calc.[M+H]: 373.9690
Found [M+H]: n.det.

Appearance: Yellow solid

Mp: Decomposes > 300 °C

TLC: R_f = 0.43 (5% MeOH in CH_2Cl_2)

E IV.11 Pyrazoloquinolinones – 2nd generation

E IV.11.1 2-(4-Bromophenyl)-8-chloro-2,5-dihydro-3H-pyrazolo[4,3-c]quinolin-3-one [141] DCBS192

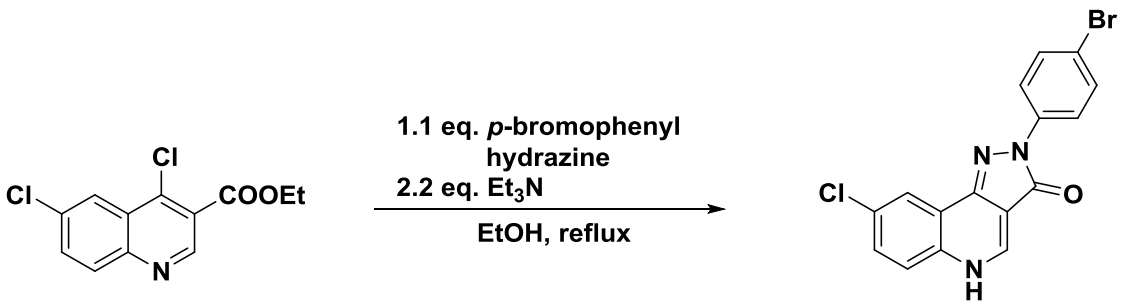

[30]

Chemical Formula: $C_{12}H_9Cl_2NO_2$
Molecular Weight: 270.11

[141] (90%)

Chemical Formula: $C_{16}H_9BrClN_3O$
Molecular Weight: 374.62

The compound was synthesized according to general procedure E III.4 using:

Chlorinated quinoline	800 mg	2.96 mmol	1 eq.
Arylhydrazine HCl	728 mg	3.26 mmol	1.1 eq.

After filtration 2-(4-bromophenyl)-8-methoxy-2,5-dihydro-3H-pyrazolo[4,3-c]quinolin-3-one **[141]** was obtained (1.00 g, 2.67 mmol, 90%).

^{1}H NMR (400 MHz, DMSO-d_6) δ 7.60 – 7.66 (m, 2H, H3' and H5'), 7.71 – 7.76 (m, 2H, H6 and H7), 8.16 – 8.18 (m, 1H, H9), 8.18 – 8.24 (m, 2H, H2' and H6'), 8.80 (d, *J* = 5.5 Hz, 1H, H4), 12.99 (br s, 1H, NH).

^{13}C NMR (151 MHz, DMSO-d_6) δ 106.1 (s, C3a), 116.1 (s, C8/ C9a), 119.9 (s, C8/C9a), 120.3 (d, C2' and C6'), 121.2 (d, C9), 121.8 (d, C6/C7), 130.4 (d, C6/C7), 130.8 (s, C1'), 131.6 (C2' and C6'), 134.3 (s, C4'), 139.2 (s, C5a/C9b), 140.0 (d, C4), 142.4 (s, C5a/C9b), 161.6 (s, CO).

HR-MS: Calc.[M+H]: 373.9690

Found [M+H]: 373.9694 (Diff.: -0.94 ppm)

Appearance: Yellow solid

Mp: Decomposes > 300 °C

TLC: R_f = 0.72 (10% MeOH in CH_2Cl_2)

E IV.11.2 8-Chloro-2-(4-hydroxyphenyl)-2,5-dihydro-3H-pyrazolo[4,3-c]quinolin-3-one [139] DCBS198

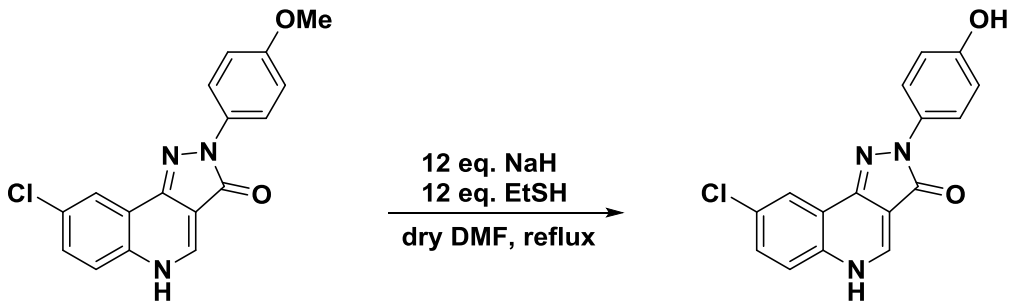

[47] **[139] (73%)**

Chemical Formula: $C_{17}H_{12}ClN_3O_2$
Molecular Weight: 325.75

Chemical Formula: $C_{16}H_{10}ClN_3O_2$
Molecular Weight: 311.73

NaH (18 mg, 0.737 mmol) was dispersed in 1 mL dry DMF and 55 µL (0.737 mmol) EtSH were added at 0 °C under argon atmosphere. After 5 min 8-chloro-2-(4-methoxyphenyl)-2,5-dihydro-3H-pyrazolo[4,3-c]quinolin-3-one **[47]** (20 mg dissolved in 1.5 mL dry DMF) was added via a syringe and the mixture was heated to reflux for 1 h. The reaction was quenched with 1 mL satd. NH_4Cl solution and the solvents were evaporated. The residue was dissolved in DMSO and purified by HPLC to give the desired product **[139]** as yellow solid (14 mg, 0.045 mmol, 73%).

^{1}H NMR (400 MHz, DMSO-d_6) δ 6.73 – 6.82 (m, 2H, H3' and H5'), 7.48 (dd, *J* = 8.8, 2.5 Hz, 1H, H7), 7.65 (d, *J* = 8.8 Hz, 1H, H6), 8.00 – 8.04 (m, 2H, H2' and H6'), 8.04 (d, *J* = 2.5 Hz, 1H, H9), 8.51 (s, 1H, H4), 9.20 (br s, 1H, OH).

^{13}C NMR (151 MHz, DMSO-d_6) δ 105.2 (s, C3a), 114.8 (d, C3' and C5'), 120.4 (d, C9), 120.5 (d, C2' and C6'), 121.7 (s, C9a), 127.1 (s, C8/C1'), 127.9 (d, C6), 128.4 (d, C7), 133.3 (s, C8/C1'), 141.3 (s, C5a/C9b), 143.0 (s, C5a/C9b), 144.9 (d, C4), 153.4 (s, C4'), 160.6 (s, CO).

HPLC-MS: Calc.[M+H]: 312.05
Found [M+H]: 312.05

HR-MS: Calc.[M+H]: 312.0534
Found [M+H]: 312.0539
(Diff.: -1.44 ppm)

Appearance: Yellow solid

Mp: Decomposes > 300 °C

TLC: R_f = 0.33 (10% MeOH in CH_2Cl_2)

E IV.11.3 N-(4-(8-Chloro-3-oxo-3,5-dihydro-2H-pyrazolo[4,3-c]quinolin-2-yl)phenyl)acetamide [140] DCBS199

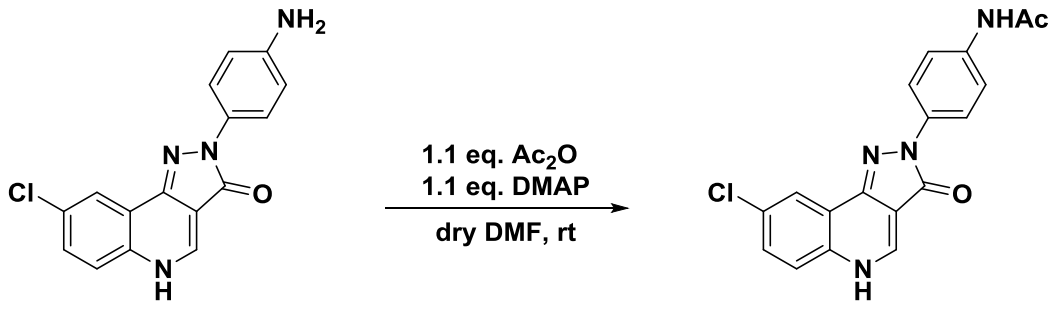

[50]

Chemical Formula: $C_{16}H_{11}ClN_4O$
Molecular Weight: 310.74

[140] (62%)

Chemical Formula: $C_{18}H_{13}ClN_4O_2$
Molecular Weight: 352.78

2-(4-Aminophenyl)-8-chloro-2,5-dihydro-3H-pyrazolo[4,3-c]quinolin-3-one **[50]** (20 mg, 0.064 mmol) and DMAP (8.7 mg, 0.071 mmol) were dissolved in 1 mL dry DMF. After 5 min Ac_2O (7 γL, 0.071 mmol) was added and the reaction mixture was stirred under argon atmosphere. After 18 h the reaction was quenched with 1 mL MeOH and the solvents were evaporated. The residue was purified by FC (3-20% MeOH in CH_2Cl_2) to give the desired product **[140]** (14 mg, 0.04 mmol, 62%).

^{1}H NMR (400 MHz, DMSO-d_6) δ 2.05 (s, 3H, CH_3), 7.61 – 7.67 (m, 2H, H2' and H6'), 7.68 – 7.77 (m, 2H, H6 and H7), 8.08 – 8.12 (m, 2H, H3' and H5'), 8.15 (dd, *J* = 2.1, 0.7 Hz, 1H, H9), 8.75 (s, 1H, H4), 9.97 (s, 1H, NHAc), 12.90 (br s, 1H, NH).

^{13}C NMR (151 MHz, DMSO-d_6) δ 24.0 (q, CH_3), 106.4 (s, C3a), 119.18 (d, C3' and C5'), 119.21 (d, C2' and C6'), 120.0 (s, C9a), 121.1 (d, C9), 121.8 (d, C6/C7), 130.1 (d, C6/C7), 130.6 (s, C8/C1'), 134.3 (s, C4'), 135.3 (s, C8/C1'), 135.8 (s, C5a/C9b), 139.6 (d, C4), 141.8 (s, C5a/C9b), 161.1 (s, CO), 168.1 (s, CO).

HR-MS: Calc.[M+H]: 353.0800

Found [M+H]: 353.0810 (Diff.: -2.83 ppm)

Appearance: Yellow solid

Mp: Decomposes > 300 °C

TLC: R_f = 0.19 (10% MeOH in CH_2Cl_2)

E IV.11.4 8-Chloro-2-(4-((trimethylsilyl)ethynyl)phenyl)-2,5-dihydro-3H-pyrazolo[4,3-c]quinolin-3-one [142] DCBS209

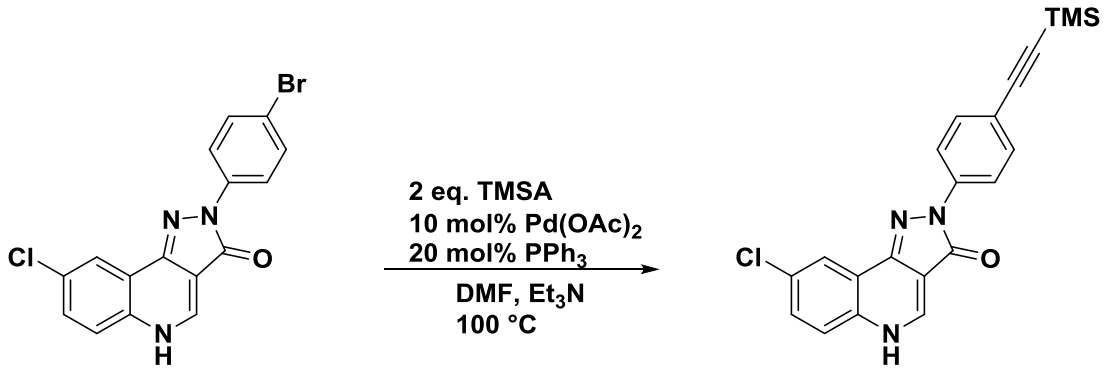

[141]

Chemical Formula: $C_{16}H_9BrClN_3O$
Molecular Weight: 374.62

[142] (37%)

Chemical Formula: $C_{21}H_{18}ClN_3OSi$
Molecular Weight: 391.93

2-(4-Bromophenyl)-8-chloro-2,5-dihydro-3H-pyrazolo[4,3-c]quinolin-3-one **[141]** (300 mg, 0.804 mmol), $Pd(OAc)_2$ (18 mg, 10 mol%) and PPh_3 (42 mg, 20 mol%) were dissolved in Et_3N (10 mL) and DMF (20 mL). After the reaction apparatus was set under argon, TMSA was added and the mixture was heated to 100 °C. After 17 h the reaction mixture was evaporated and the residue was purified by FC (3-10% MeOH in CH_2Cl_2) to give 8-chloro-2-(4-((trimethylsilyl)ethynyl)phenyl)-2,5-dihydro-3H-pyrazolo[4,3-c]quinolin-3-one **[142]** (115 mg, 0.29 mmol, 37%).

^{1}H NMR (400 MHz, DMSO-d_6) δ 0.24 (s, 9H, TMS), 7.51 (d, J = 8.8 Hz, 2H, H3' and H5'), 7.63 (dd, J = 8.7, 2.4 Hz, 1H, H7), 7.71 (d, J = 8.8 Hz, 1H, H6), 8.13 (d, J = 2.4 Hz, 1H, H9), 8.29 – 8.34 (m, 2H, H2' and H6'), 8.68 (s, 1H, H4), 12.98 (br s, 1H, NH).

^{13}C NMR (151 MHz, DMSO-d_6) δ 0.0 (q, TMS), 93.4 (s, $C_{acetylene}$), 105.6 (s, C3a), 116.8 (s), 118.0 (d, C3' and C5'), 120.5 (d, C9), 121.0 (s, C6/C7), 124.0 (s), 124.2 (s), 128.8 (s), 129.66 (s), 129.72 (s, C6/C7), 130.0 (s), 132.3 (d, C2' and C6'), 140.6 (d, C4), 143.4 (s), 161.8 (s, CO).

HPLC-MS: Calc.[M+H]: 392.10
Found [M+H]: 392.18

HR-MS: Calc.[M+H]: 392.0980
Found [M+H]: 392.1005
(Diff.: -6.30 ppm)

Appearance: Yellow solid

Mp: Decomposes > 300 °C

TLC: R_f = 0.80 (10% MeOH in CH_2Cl_2)

E IV.11.5 8-Chloro-2-(4-ethynylphenyl)-2,5-dihydro-3H-pyrazolo[4,3-c]quinolin-3-one [143] DCBS212

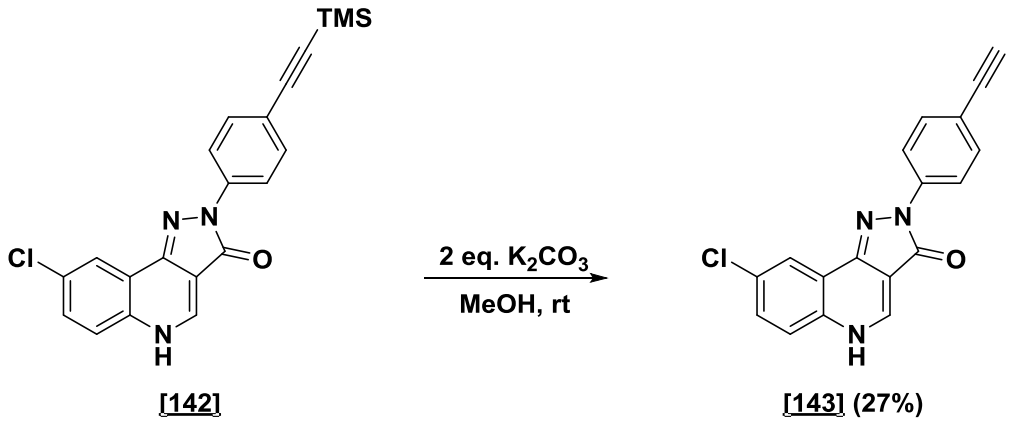

[142] **[143] (27%)**

Chemical Formula: $C_{21}H_{18}ClN_3OSi$
Molecular Weight: 391.93

Chemical Formula: $C_{18}H_{10}ClN_3O$
Molecular Weight: 319.75

8-Chloro-2-(4-((trimethylsilyl)ethynyl)phenyl)-2,5-dihydro-3H-pyrazolo[4,3-c]quin- olin-3-one **[142]** (100 mg, 0.255 mmol) was dissolved in 15 mL MeOH and K_2CO_3 (71 mg, 0.514 mmol) was added. After stirring for 2.5 h at rt the solvent was removed under reduced pressure and the resiude was purified by FC (5-10% MeOH in CH_2Cl_2) to give 8-chloro-2-(4-ethynylphenyl)-2,5-dihydro-3H-pyrazolo[4,3-c]quinolin-3-one **[143]** (20 mg, 0.07 mmol, 27%).

^{1}H NMR (400 MHz, DMSO-d_6) δ 4.16 (s, 1H, $H_{acetylene}$), 7.56 (d, *J* = 8.8 Hz, 2H, H3' and H5'), 7.73 – 7.74 (m, 2H, H6 and H7), 8.16 – 8.18 (m, 1H, H9), 8.27 (d, *J* = 8.8 Hz, 2H, H2' and H6'), 8.80 (s, 1H, H4), 12.98 (br s, 1H, NH).

^{13}C NMR (151 MHz, DMSO-d_6) δ 80.4 (d, $C_{acetylene}$), 83.6 (s, $C_{acetylene}$), 106.1 (s, C3a), 116.9 (s, C4'), 118.2 (d, C3' and C5'), 119.9 (s, C9a), 121.3 (d, C9), 121.8 (d, C6/C7), 130.5 (d, C6/C7), 130.8 (s, C8/C1'), 132.4 (d, C2' and C6'), 134.4 (s, C8/C1'), 140.0 (d, C4), 140.2 (s, C5a/C9b), 142.6 (s, C5a/C9b), 161.8 (s, CO).

HR-MS: Calc.[M+H]: 320.0585

Found [M+H]: 320.0600 (Diff.:-4.61 ppm)

Appearance: Yellow solid

Mp: Decomposes > 300 °C

TLC: R_f = 0.76 (10% MeOH in CH_2Cl_2)

E IV.11.6 2-(4-Acetylphenyl)-8-chloro-2,5-dihydro-3H-pyrazolo[4,3-c]quinolin-3-one [144] DCBSBRP23

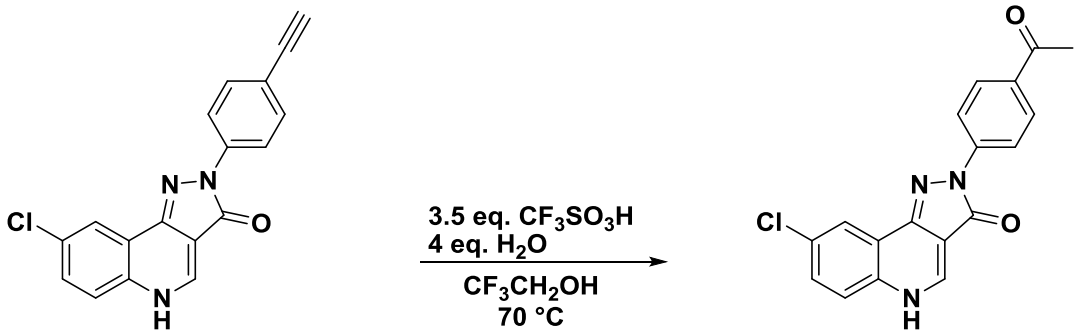

[143] | **[143] (20%)**

Chemical Formula: $C_{18}H_{10}ClN_3O$
Molecular Weight: 319.75

Chemical Formula: $C_{18}H_{12}ClN_3O_2$
Molecular Weight: 337.76

8-Chloro-2-(4-ethynylphenyl)-2,5-dihydro-3H-pyrazolo[4,3-c]quinolin-3-one **[143]** (100 mg, 0.31 mmol) was dissolved in 1.5 mL CF_3CH_2OH. Then H_2O (11.3 µL, 0.63 mmol) and CF_3SO_3H (164 µL, 1.1 mmol) were added and the reaction mixture was heated to 70 °C. After 3 days the solvent was removed under reduced pressure and the resiude was dissolved in DMSO, filtered through a syringe filter (0.2 µm) and purified by HPLC to give 2-(4-acetylphenyl)-8-chloro-2,5-dihydro-3H-pyrazolo[4,3-c]quinolin-3-one **[144]** (20 mg, 0.06 mmol, 20%).

^{1}H NMR (600 MHz, DMSO-d_6) δ 2.58 (s, 3H, $COCH_3$), 7.69 – 7.75 (m, 2H, H6 and H7), 8.05 (d, *J* = 8.8 Hz, 2H, H3' and H5'), 8.17 (d, *J* = 2.2 Hz, 1H, H9), 8.40 (d, *J* = 8.8 Hz, 2H, H2' and H6'), 8.79 (s, 1H, H4).

^{13}C NMR (151 MHz, DMSO-d_6) δ 26.6 (q, $CO\underline{C}H_3$), 105.8 (s, C3a), 117.5 (d, C2' and C6'), 120.1 (s, C9a), 121.3 (d, C9), 122.5 (d, C6/C7), 129.4 (d, C3' and C5'), 130.4 (d, C6/C7), 130.6 (s, C8/C1'/C4'), 132.1 (s, C8/C1'/C4'), 135.3 (s, C8/C1'/C4'), 140.8 (d, C4), 143.3 (s, C5a/C9b), 143.7 (s, C5a/C9b), 162.2 (s, CO), 196.7 (s, $\underline{C}OCH_3$).

HPLC-MS: Calc.[M+H]: 338.07
Found [M+H]: 338.19

HR-MS: Calc.[M+H]: 338.0691
Found [M+H]: 338.0693
(Diff.: -0.51 ppm)

Appearance: Yellow solid

Mp: Decomposes > 300 °C

TLC: R_f = 0.78 (10% MeOH in CH_2Cl_2)

E IV.12 Pyrazoloquinolinones – α+/γ– vs. α+/β–

E IV.12.1 2-(4-Chlorophenyl)-8-methoxy-2,5-dihydro-3H-pyrazolo[4,3-c]quinolin-3-one [222] DCBS122

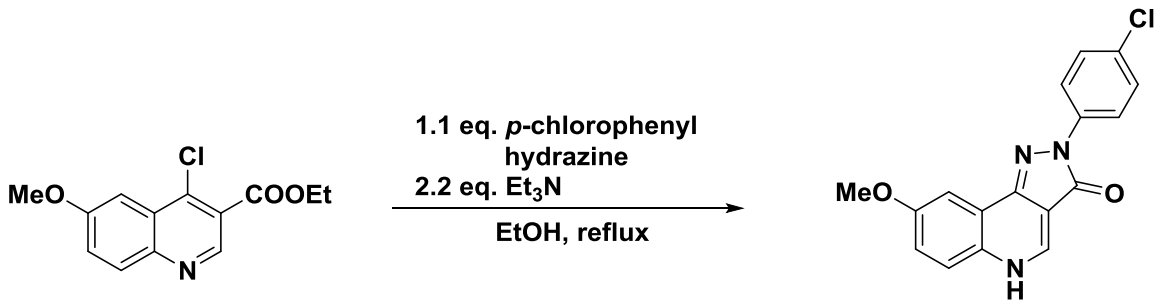

[8]

Chemical Formula: $C_{13}H_{12}ClNO_3$
Molecular Weight: 265.69

[222] (54%)

Chemical Formula: $C_{17}H_{12}ClN_3O_2$
Molecular Weight: 325.75

The desired compound was synthesized according to general procedure E III.4 using:

Chlorinated quinoline	77 mg	0.29 mmol	1 eq.
Arylhydrazine HCl	57 mg	0.32 mmol	1.1 eq.

After filtration 2-(4-chlorophenyl)-8-methoxy-2,5-dihydro-3H-pyrazolo[4,3-c]quinolin-3-one **[222]** was obtained (51 mg, 0.157 mmol, 54%).

^{1}H NMR (400 MHz, DMSO-d_6) δ 3.93 (s, 3H, OCH_3), 7.31 (dd, *J* = 9.1, 2.9 Hz, 1H, H7), 7.50 (d, *J* = 8.6 Hz, 2H, H2' and H6'), 7.59 (d, *J* = 2.9 Hz, 1H, H9), 7.68 (d, *J* = 9.1 Hz, 1H, H6), 8.30 (d, *J* = 8.6 Hz, 2H, H3' and H5'), 8.69 (s, 1H, H4), 12.86 (br s, 1H, NH).

^{13}C NMR (101 MHz, DMSO-d_6) δ 55.7 (q, OCH_3), 102.6 (d, C9), 105.0 (s, C3a), 119.9 (d, C7), 120.0 (d, C2' and C6'), 121.5 (d, C6), 127.6 (s, C4'), 128.6 (d, C3' and C5'), 130.0 (s, C9a), 138.3 (d, C4), 139.1 (s, C5a/C1'), 143.4 (s, C5a/C1'), 157.6 (s, C8), 161.8 (s, CO). Signal of C7 is either overlaid with other signals or not detectable.

HR-MS: Calc.[M+H]: 326.0691

Found [M+H]: 326.0693 (Diff.: -0.57 ppm)

Appearance: Yellow solid

Mp: Decomposes > 300 °C

TLC: R_f = 0.45 (5% MeOH in CH_2Cl_2)

E IV.12.2 2-(5-Chloropyrazin-2-yl)-8-methoxy-2,5-dihydro-3H-pyrazolo[4,3-c]quinolin-3-one [223] DCBS133

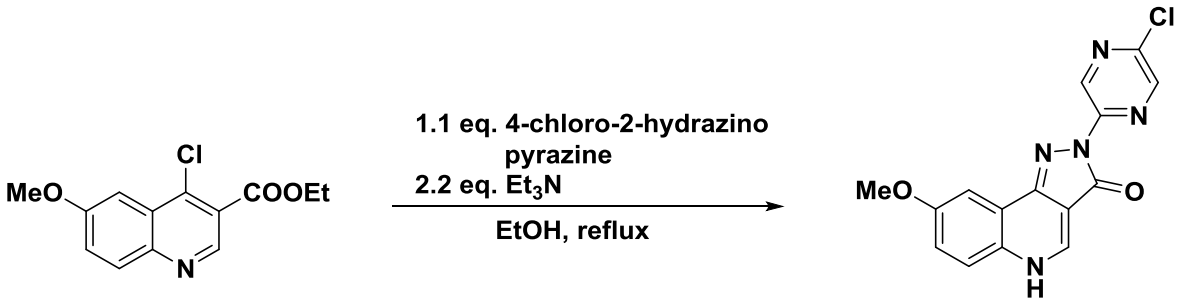

[8]

Chemical Formula: $C_{13}H_{12}ClNO_3$
Molecular Weight: 265.69

[223] (85%)

Chemical Formula: $C_{15}H_{10}ClN_5O_2$
Molecular Weight: 327.73

The desired compound was synthesized according to general procedure E III.4 using:

Chlorinated quinoline	40 mg	0.15 mmol	1 eq.
Arylhydrazine HCl	24 mg	0.17 mmol	1.1 eq.

After filtration and purification by HPLC 2-(5-chloropyrazin-2-yl)-8-methoxy-2,5-dihydro-3H-pyrazolo[4,3-c]quinolin-3-one **[223]** was obtained (42 mg, 0.13 mmol, 85%).

^{1}H NMR (400 MHz, DMSO-d_6) δ 3.93 (s, 3H, OCH_3), 7.33 (dd, *J* = 9.1, 2.9 Hz, 1H, H7), 7.57 (d, *J* = 2.9 Hz, 1H, H-Ar, H9), 7.70 (d, *J* = 9.1 Hz, 1H, H6), 8.70 (d, *J* = 1.4 Hz, 1H, H3'/H6'), 8.75 (d, *J* = 6.4 Hz, 1H, H4), 9.42 (d, *J* = 1.4 Hz, 1H, H3'/H6'), 13.00 (br d, *J* = 6.5 Hz, 1H, NH).

^{13}C NMR (101 MHz, DMSO-d_6) δ 55.8 (q, OCH_3), 102.8 (d, C9), 103.7 (s, C3a), 120.0 (s, C4'), 120.3 (d, C6), 121.5 (d, C7), 130.0 (s, C9a), 135.3 (d, C6'), 138.9 (d, C4), 142.2 (s, C9b), 142.3 (d, C3'), 145.3 (s, C5a/C1'), 146.8 (s, C5a/C1'), 157.8 (s, C7), 162.6 (s, CO).

HPLC-MS: Calc.[M+H]: 328.06
Found [M+H]: 328.03

HR-MS: Calc.[M+H]: 328.0596
Found [M+H]: 328.0616
(Diff.: -6.28 ppm)

Appearance: Brown solid

Mp: Decomposes > 300 °C

TLC: R_f = 0.49 (10% MeOH in CH_2Cl_2)

E IV.12.3 8-Methoxy-2-(pyrazin-2-yl)-2,5-dihydro-3H-pyrazolo[4,3-c]quinolin-3-one [224] DCBS85

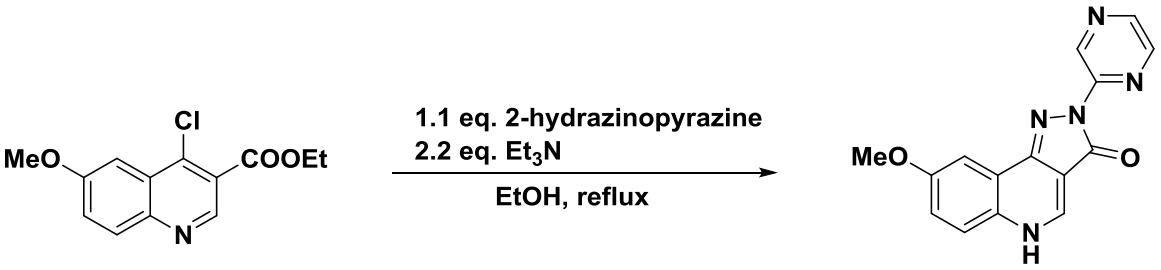

[8]

Chemical Formula: $C_{13}H_{12}ClNO_3$
Molecular Weight: 265.69

[224] (67%)

Chemical Formula: $C_{15}H_{11}N_5O_2$
Molecular Weight: 293.29

The desired compound was synthesized according to general procedure E III.4 using:

Chlorinated quinoline	100 mg	0.38 mmol	1 eq.
Arylhydrazine HCl	45.6 mg	0.41 mmol	1.1 eq.

After filtration 8-methoxy-2-(pyrazin-2-yl)-2,5-dihydro-3H-pyrazolo[4,3-c]quinolin-3-one **[224]** was obtained (74 mg, 0.25 mmol, 67%).

^{1}H NMR (400 MHz, DMSO-d_6) δ 3.93 (s, 3H, OCH_3), 7.32 (dd, *J* = 9.1, 2.9 Hz, 1H, H7), 7.58 (d, *J* = 2.8 Hz, 1H, H9), 7.69 (d, *J* = 9.1 Hz, 1H, H6), 8.46 (d, *J* = 2.5 Hz, 1H, H3'), 8.58 (dd, *J* = 2.6, 1.5 Hz, 1H, H4'), 8.74 (s, 1H, H4), 9.56 (d, *J* = 1.5 Hz, 1H, H6'), 12.92 (br s, 1H, NH).

^{13}C NMR (101 MHz, DMSO-d_6) δ 55.7 (q, OCH_3), 102.7 (d, C9), 103.9 (s, C3a), 120.1 (d, C6), 121.4 (d, C7), 130.0 (s, C9a), 136.7 (d, C4'/C6'), 138.8 (s, C9b), 140.2 (d), 142.88 (d), 142.92 (d) 144.9 (s, C5a/C1'), 148.0 (s, C5a/C1'), 157.7 (s, C8), 162.5 (s, CO).

HR-MS: Calc.[M+H]: 294.0986

Found [M+H]: 294.0994 (Diff.: -2.88 ppm)

Appearance: Yellow solid

Mp: Decomposes > 300 °C

TLC: R_f = 0.46 (10% MeOH in CH_2Cl_2)

E IV.12.4 7-Methoxy-2-(pyrazin-2-yl)-2,5-dihydro-3H-pyrazolo[4,3-c]quinolin-3-one [225] DCBS126

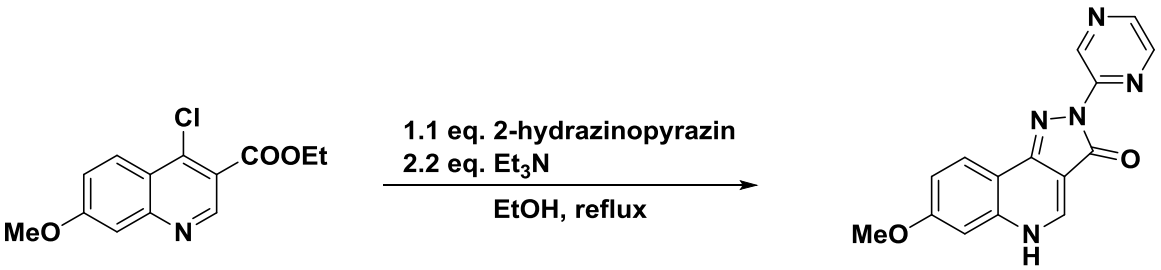

[179]

Chemical Formula: $C_{13}H_{12}ClNO_3$
Molecular Weight: 265.69

[225] (58%)

Chemical Formula: $C_{15}H_{11}N_5O_2$
Molecular Weight: 293.29

The desired compound was synthesized according to general procedure E III.4 using:

Chlorinated quinoline	70 mg	0.26 mmol	1 eq.
Arylhydrazine HCl	32 mg	0.29 mmol	1.1 eq.

After filtration 7-methoxy-2-(pyrazin-2-yl)-2,5-dihydro-3H-pyrazolo[4,3-c]quinolin-3-one **[225]** was obtained (45 mg, 0.15 mmol, 58%).

^{1}H NMR (400 MHz, DMSO-d_6) δ 3.88 (s, 3H, OCH_3), 7.16 – 7.23 (m, 2H, H6 and H9), 8.13 (dd, *J* = 8.5, 0.8 Hz, 1H, H8), 8.44 (d, *J* = 2.5 Hz, 1H, H3'), 8.56 (dd, *J* = 2.5, 1.5 Hz, 1H, H4'), 8.75 (s, 1H, H4), 9.51 (d, *J* = 1.4 Hz, 1H, H6'), 12.74 (br s, 1H, NH).

^{13}C NMR (101 MHz, DMSO-d_6) δ 55.6 (q, OCH_3), 102.1 (d, C8), 105.0 (s, C3a), 112.2 (s, C9a), 115.5 (d, C6), 123.9 (d, C9), 136.6 (d, C4'/C6'), 137.3 (s, C9b), 140.0 (d), 140.1 (d), 142.8 (d), 144.9 (s, C5a/C1'), 148.0 (s, C5a/C1'), 160.8 (s, C7), 162.4 (s, CO).

HR-MS: Calc.[M+H]: 294.0986

Found [M+H]: 294.0992 (Diff.: -2.37 ppm)

Appearance: Yellow solid

Mp: Decomposes > 300 °C

TLC: R_f = 0.38 (10% MeOH in CH_2Cl_2)

E IV.12.5 *N,N'*-(Ethane-1,2-diyl)bis(4-methylbenzenesulfonamide) [236] DCBSBRP01

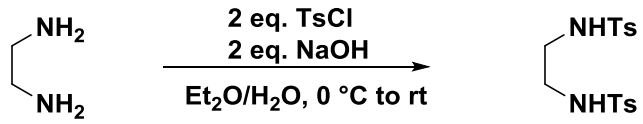

[235] **[236] (66%)**

Chemical Formula: $C_2H_8N_2$
Molecular Weight: 60.10

Chemical Formula: $C_{16}H_{20}N_2O_4S_2$
Molecular Weight: 368.47

Toluene-4-sulfonyl chloride (6.48 g, 34.0 mmol, 2 eq.) was suspended in 13.4 mL diethyl ether at 0 °C and 1.14 mL ethane-1,2-diamine **[235]** (17.0 mmol, 1 eq.) dissolved in 13.4 mL H_2O with NaOH (1.36 g, 0.34 mol, 2 eq.) was added dropwise. The reaction mixture was stirred overnight at room temperature. The colorless precipitate was collected by filtration and recrystallized from MeOH to give the desired product **[236]** (4.13 g, 11.2 mmol, 66%).

^{1}H NMR (400 MHz, $CDCl_3$) δ = 2.36 – 2.40 (s, 6H, 2 CH_3), 2.69 – 2.73 (m, 4H, 2 CH_2), 7.39 – 7.40 (d, *J* = 8.0 Hz, 4H, H_{tosyl}), 7.57 – 7.62 (m, 6H, 4 H_{tosyl} and 2 NH).

^{13}C NMR (101 MHz, $CDCl_3$) δ = 21.0 (q, 2 CH_3), 42.1 (t, 2 CH_2), 126.5 (d, 4 C_{tosyl}), 129.7 (d, 4 C_{tosyl}), 137.3 (s, 2 S-$\underline{C}_{tosyl}$), 142.7 (s, 2 CH_3-$\underline{C}_{tosyl}$).

Appearance: Colorless crystals

Mp: 163-165 °C (Lit.[224]: 164-166 °C)

TLC: R_f = 0.69 (PE/EtOAc = 1/1)

E IV.12.6 1,4-Ditosyl-1,4-diazepan-6-ol [237] DCBSBRP03

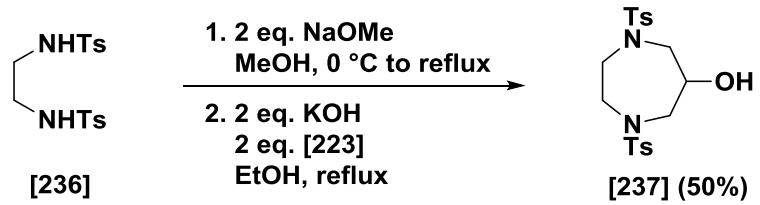

[236] **[237] (50%)**

Chemical Formula: $C_{16}H_{20}N_2O_4S_2$
Molecular Weight: 368.47

Chemical Formula: $C_{19}H_{24}N_2O_5S_2$
Molecular Weight: 424.53

Sodium metal (1.06 g, 46.0 mmol, 2 eq.) was dissolved in 35 mL MeOH at 0 °C. Then *N,N'*-(ethane-1,2-diyl)bis(4-methylbenzenesulfonamide) **[236]** (8.47 g, 22.30 mmol, 1 eq.) was added and the reaction mixture was refluxed. After 30 min the solvent was removed under reduced pressure to give the crude sodium salt. Next, KOH (2.58 g, 46.0 mmol, 2 eq.) was mixed with 1,2-dibromopropan-3-ol **[223]** (2.4 mL, 46.0 mmol, 2 eq.) in 165 mL EtOH and refluxed for 30 min under argon. Then the crude sodium salt (10.3 g, 23 mmol, 1 eq.) was added and the reaction mixture was refluxed for 6 h. The formed precipitate was removed by filtration and washed with hot EtOH. Subsequently, the filtrate was cooled to 4 °C to give the desired product **[237]** as colorless crystals (4.18 g, 9.81 mmol, 50%).

^{1}H NMR (400 MHz, DMSO-d_6) δ 2.39 (s, 6H, 2 CH_3), 2.84 (dd, J = 13.9, 8.1 Hz, 2H, CH_2), 3.05 – 3.13 (m, 2H, CH_2), 3.46 (dt, J = 14.4, 4.1 Hz, 4H, 2 CH_2), 3.69 – 3.77 (m, 1H, C<u>H</u>-OH), 5.27 (s, 1H, OH), 7.41 (d, J = 8.0 Hz, 4H, H_{tosyl}), 7.65 (d, J = 8.2 Hz, 4H, H_{tosyl}).

^{13}C NMR (101 MHz, DMSO-d_6) δ 21.0 (q, 2 CH_3), 49.1 (t, 2 CH_2), 53.1 (t, 2 CH_2), 68.5 (d, C-OH), 126.7 (d, 4 C_{tosyl}), 129.9 (d, 4 C_{tosyl}), 135.6 (s, 2 S-<u>C</u>$_{tosyl}$), 143.3 (s, 2 CH_3-<u>C</u>$_{tosyl}$).

Appearance: Colorless crystals

Mp: 174-176 °C (Lit.[187]: 175-177 °C)

TLC: R_f = 0.29 (PE/EtOAc = 1/1)

E IV.12.7 1,4-Ditosyl-1,4-diazepan-6-yl methanesulfonate [238] DCBSBRP06

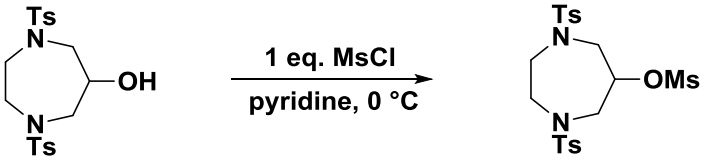

[237]

Chemical Formula: $C_{19}H_{24}N_2O_5S_2$
Molecular Weight: 424.53

[238] (72%)

Chemical Formula: $C_{20}H_{26}N_2O_7S_3$
Molecular Weight: 502.62

1,4-Ditosyl-1,4-diazepan-6-ol **[237]** (100 mg, 0.24 mmol, 1 eq.) was dissolved in 0.5 mL dry pyridine and cooled to 0 °C. Then sulfonyl chloride (182 µL, 0.24 mmol, 1 eq.) was added dropwise and the reaction mixture was stirred for 2 h. Subsequently 0.4 mL 3 M HCl was added and the mixture was stirred for another 2 h at 0 °C. The formed precipitate was collected by filtration, washed with H_2O and boiling EtOH and dried *in vacuo* to give the desired product **[238]** (87 mg, 0.17 mmol, 72%)**.**

^{1}H NMR (400 MHz, DMSO-d_6) δ 2.40 (s, 6H, 2 CH_3), 3.18 – 3.25 (m, 2H, CH_2), 3.26 (s, 3H, SCH_3), 3.34 – 3.43 (m, 2H, CH_2), 3.53 (d, J = 5.2 Hz, 4H, 2 CH_2), 4.86 (p, J = 5.2 Hz, 1H, C<u>H</u>-O), 7.43 (d, J = 8.0 Hz, 4H, H_{tosyl}), 7.69 (d, J = 8.3 Hz, 4H, H_{tosyl}).

^{13}C NMR (101 MHz, DMSO-d_6) δ 21.0 (q, 2 CH_3), 37.8 (q, SCH_3), 50.5 (t, 2 CH_2), 51.2 (t, 2 CH_2), 76.8 (d, C-OH), 126.8 (d, 4 C_{tosyl}), 130.0 (d, 4 C_{tosyl}), 135.4 (s, 2 S-<u>C</u>$_{tosyl}$), 143.6 (s, 2 CH_3-<u>C</u>$_{tosyl}$).

Appearance: Colorless solid

Mp: 209-211 °C (Lit.[187]: not reported)

TLC: R_f = 0.63 (PE/EtOAc = 1/1)

E IV.12.8 1,4-Ditosyl-1,4-diazepan-6-one [241] DCBSJS08

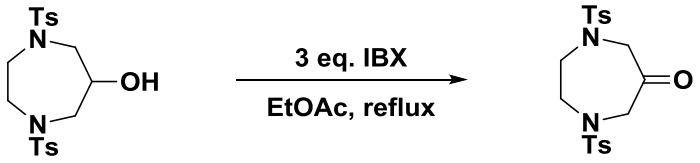

[237] **[241] (64%)**

Chemical Formula: $C_{19}H_{24}N_2O_5S_2$
Molecular Weight: 424.53

Chemical Formula: $C_{19}H_{22}N_2O_5S_2$
Molecular Weight: 422.51

1,4-Ditosyl-1,4-diazepan-6-ol **[237]** (609 mg, 1.43 mmol, 1 eq.) and IBX (1.20 g, 4.29 mmol, 3 eq.) were dissolved in 15 mL dry EtOAc and refluxed. After 3.5 h the solvent was removed under reduced pressure and the residue was purified by FC (25-40% EtOAc in PE) to give the desired product **[241]** (387 mg, 0.92 mmol, 64%)**.**

^{1}H NMR (400 MHz, DMSO-d_6) δ 2.40 (s, 6H, 2 CH_3), 3.56 (s, 4H, 2 CH_2), 3.92 (s, 4H, 2 CH_2), 7.38 – 7.46 (m, 4H, H_{tosyl}), 7.69 (d, J = 8.3 Hz, 4H, H_{tosyl}).

^{13}C NMR (101 MHz, DMSO-d_6) δ 21.0 (q, 2 CH_3), 52.0 (t, 2 CH_2), 57.2 (t, 2 CH_2), 126.7 (d, 4 C_{tosyl}), 130.1 (d, 4 C_{tosyl}), 135.6 (s, 2 S-$\underline{C}_{tosyl}$), 143.9 (s, 2 CH_3-$\underline{C}_{tosyl}$), 204.7 (s, CO).

Appearance: Colorless solid

Mp: 188-190 °C (Lit.[225]: not reported)

TLC: R_f = 0.51 (PE/EtOAc = 2/1)

E IV.12.9 *tert*-Butyl 2-(1,4-ditosyl-1,4-diazepan-6-ylidene)-hydrazine-1-carboxylate [243] DCBSJS11

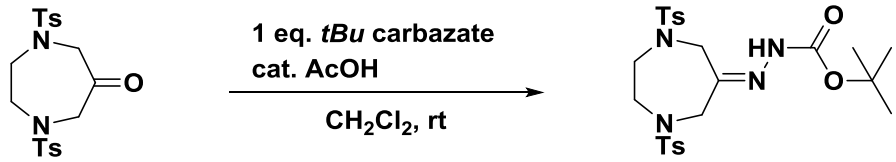

[241]

Chemical Formula: $C_{19}H_{22}N_2O_5S_2$
Molecular Weight: 422.51

[243] (66%)

Chemical Formula: $C_{24}H_{32}N_4O_6S_2$
Molecular Weight: 536.66

1,4-Ditosyl-1,4-diazepan-6-one **[241]** (180 mg, 0.43 mmol, 1 eq.) and *tert*-butyl hydrazine carboxylate (50 mg, 0.43 mmol, 1 eq.) were dissolved in 15 mL dry CH_2Cl_2. 80 µL AcOH were added and the mixture was stirred over night at room temperature. Then 5 mL water was added and the phases were separated. The aqueous layer was extracted with CH_2Cl_2 (3 x 5 mL), the organic phases were combined, dried over Na_2SO_4, filtered and the solvent removed under reduced pressure. The residue was purified by FC (25-45% EtOAc in PE + 1% Et_3N) to give the desired product **[243]** (152 mg, 0.28 mmol, 66%)**.**

^{1}H NMR (400 MHz, DMSO-d_6) δ 1.48 (s, 9H, $C(CH_3)_3$), 2.39 (s, 3H, CH_3), 2.39 (s, 3H, CH_3), 3.25 – 3.39 (m, 4H, 2 CH_2), 3.94 (s, 4H, 2 CH_2), 7.35 – 7.45 (m, 4H, H_{tosyl}), 7.63 – 7.71 (m, 4H, H_{tosyl}), 9.86 (br s, 1H, NH).

^{13}C NMR (101 MHz, DMSO-d_6) δ 21.0 (q, CH_3), 21.0 (q, CH_3), 28.0 (q, $C(\underline{C}H_3)_3$), 49.2 (t, CH_2), 50.9 (t, CH_2), 50.9 (t, CH_2), 53.4 (t, CH_2), 79.8 (s, $\underline{C}(CH_3)_3$), 126.7 (d, 2 C_{tosyl}), 127.1 (d, 2 C_{tosyl}), 129.8 (d, 2 C_{tosyl}), 130.0 (d, 2 C_{tosyl}), 135.3 (s, S-$\underline{C}_{tosyl}$), 135.8 (s, S-$\underline{C}_{tosyl}$), 143.5 (s, CH_3-$\underline{C}_{tosyl}$), 143.6 (s, CH_3-$\underline{C}_{tosyl}$), 147.9 (s, CO), 152.8 (s, C=N).

HR-MS: Calc.[M+H]: 537.1836

Found [M+H]: 537.1820 (Diff.: +2.99 ppm)

Appearance: Colorless solid

Mp: 135-137 °C

TLC: R_f = 0.65 (PE/EtOAc = 2/1)

E IV.12.10 2-(1,4-Ditosyl-1,4-diazepan-6-yl)-8-methoxy-2,5-dihydro-3H-pyrazolo[4,3-c]quinolin-3-one [244] DCBSJS14

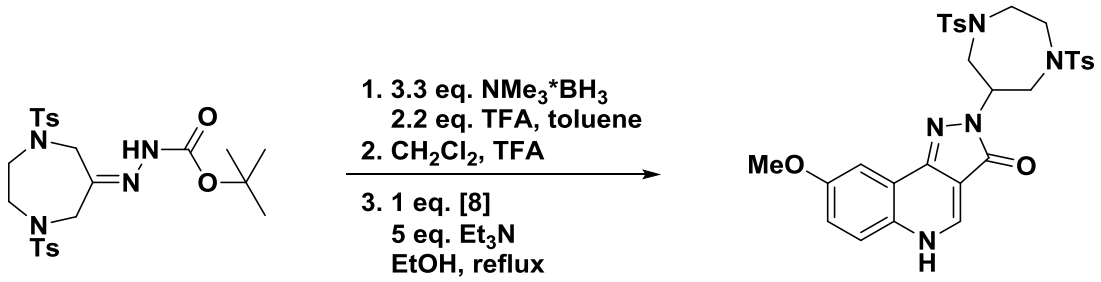

[243] **[244] (15% over 3 steps)**

Chemical Formula: $C_{24}H_{32}N_4O_6S_2$
Molecular Weight: 536.66

Chemical Formula: $C_{30}H_{31}N_5O_6S_2$
Molecular Weight: 621.73

The hydrazone **[243]** (246 mg, 0.46 mmol) was dissolved in 30 mL dry toluene and NMe_3*BH_3 (110 mg, 1.51 mmol) was added. The reaction was stirred for 5 min at room temperature and TFA (78 µL) was added. After 45 min the solvent was evaporated and the residue was redissolved in a mixture of TFA/CH_2Cl_2 (1v/4v). After 15 min the solvents were evaporated and the crude residue was converted according to general procedure E III.4 using **[8]** as chlorinated starting material. After purification by HPLC 2-(1,4-ditosyl-1,4-diazepan-6-yl)-8-methoxy-2,5-dihydro-3H-pyrazolo[4,3-c]quinolin-3-one **[244]** was obtained in 15% yield over 3 steps (41 mg, 0.06 mmol, 15 %)**.**

^{1}H NMR (600 MHz, DMSO-d_6) δ 2.37 (s, 6H, 2 CH_3), 3.10 – 3.19 (m, 2H, CH_2), 3.42 (dd, *J* = 13.8, 9.8 Hz, 2H, CH_2), 3.63 (dd, *J* = 13.7, 4.6 Hz, 2H, CH_2), 3.68 – 3.75 (m, 2H, CH_2), 3.85 (s, 3H, OCH_3), 4.62 – 4.70 (m, 1H, CH), 7.23 (dd, *J* = 9.0, 2.9 Hz, 1H, H7), 7.38 (d, *J* = 2.9 Hz, 1H, H9), 7.39 (d, *J* = 8.1 Hz, 4H, H_{tosyl}), 7.64 (d, *J* = 9.1 Hz, 1H, H6), 7.66 – 7.72 (m, 4H, H_{tosyl}), 8.61 (s, 1H, H4), 12.63 (br s, 1H, NH).

^{13}C NMR (151 MHz, DMSO-d_6) δ 21.0 (q, 2 CH_3), 48.4 (t, 2 CH_2), 50.2 (t, 2 CH_2), 53.1 (d, CH), 55.6 (q, OCH_3), 102.2 (d, C9), 104.0 (s, C3a), 119.2 (d, C7), 120.3 (s, C9a), 121.6 (d, C6), 126.8 (d, 4 C_{tosyl}), 129.8 (d, 4 C_{tosyl}), 130.0 (s, C9b), 135.4 (s, 2 S-$\underline{C}_{tosyl}$), 138.1 (d, C4), 142.2 (s, C5a), 143.4 (s, 2 CH_3-$\underline{C}_{tosyl}$), 157.3 (s, C8), 161.2 (s, CO).

HPLC-MS: Calc.[M+H]: 622.18
Found [M+H]: 622.30

HR-MS: Calc.[M+H]: 622.1789
Found [M+H]: 622.1768
(Diff.: +3.28 ppm)

Appearance: Yellow solid

Mp: 162-165 °C

TLC: R_f = 0.19 (5% MeOH in CH_2Cl_2)

E IV.12.11 *N,N'*-(Ethane-1,2-diyl)bis(4-nitrobenzenesulfonamide) [246] DCBS218

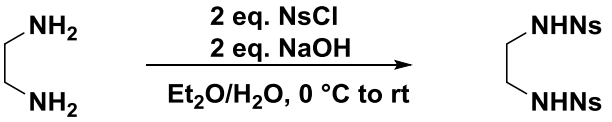

[235] **[246] (88%)**

Chemical Formula: $C_2H_8N_2$
Molecular Weight: 60.10

Chemical Formula: $C_{14}H_{14}N_4O_8S_2$
Molecular Weight: 430.41

2-Nitrobenzenesulfonyl chloride (3.35 g, 15.0 mmol, 2 eq.) was suspended in 10 mL diethyl ether at 0 °C and 0.5 mL ethane-1,2-diamine **[235]** (7.5 mmol, 1 eq.) dissolved in 10 mL H_2O with NaOH (0.6 g, 15 mol, 2 eq.) was added dropwise. The reaction mixture was stirred overnight at room temperature. The colorless precipitate was collected by filtration and recrystallized from MeOH to give the desired product **[246]** (2.88 g, 6.69 mmol, 88%).

^{1}H NMR (400 MHz, DMSO-d_6) δ 2.99 (s, 4H, 2 CH_2), 7.80 – 7.91 (m, 4H, H_{nosyl}), 7.91 – 8.02 (m, 4H, H_{nosyl}), 8.11 – 8.20 (br s, 2H, NH).

^{13}C NMR (101 MHz, DMSO-d_6) δ 42.4 (t, 2 CH_2), 124.6 (d, C_{nosyl}), 129.5 (d, C_{nosyl}), 132.4 (d, C_{nosyl}), 132.8 (d, C_{nosyl}), 134.2 (s, 2 S-$\underline{C}_{nosyl}$), 147.6 (s, 2 NO_2-$\underline{C}_{nosyl}$).

Appearance: Yellowish crystals

Mp: 161-163 °C (Lit.[226]: 163 °C)

TLC: R_f = 0.28 (PE/EtOAc = 1/2)

E IV.12.12 1,4-Bis((4-nitrophenyl)sulfonyl)-1,4-diazepan-6-ol [247] DCBS220

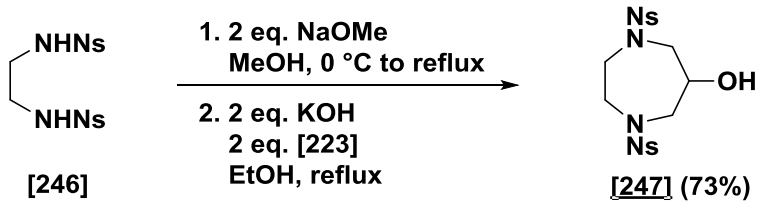

Chemical Formula: $C_{14}H_{14}N_4O_8S_2$
Molecular Weight: 430.41

Chemical Formula: $C_{17}H_{18}N_4O_9S_2$
Molecular Weight: 486.47

Sodium metal (267 mg, 11.6 mmol, 2 eq.) was dissolved in 30 mL MeOH at 0 °C. Then *N,N'*-(ethane-1,2-diyl)bis(4-methylbenzenesulfonamide) **[246]** (2.5 g, 5.8 mmol, 1 eq.) was added and the reaction mixture was refluxed. After 30 min the solvent was removed under reduced pressure to give the crude sodium salt. Next, KOH (978 mg, 17.4 mmol, 3 eq.) was mixed with 1,2-dibrompropan-3-ol **[223]** (1.8 mL, 17.4 mmol, 3 eq.) in 50 mL EtOH and refluxed for 30 min under argon. Then the crude sodium salt was added and the reaction mixture was refluxed for 6 h. The formed precipitate was filtered off and washed with hot EtOH. Subsequently, the filtrate was cooled to 4 °C to give the desired product **[247]** as colorless crystals (2.06 g, 4.21 mmol, 73%).

^{1}H NMR (400 MHz, DMSO-d_6) δ 3.18 (dd, J = 14.5, 8.2 Hz, 2H, CH_2), 3.36 – 3.46 (m, 2H, CH_2), 3.61 – 3.72 (m, 4H, 2 CH_2), 3.77 – 3.88 (m, 1H, C<u>H</u>-OH), 5.43 (d, J = 4.4 Hz, 1H, OH), 7.83 – 7.93 (m, 4H, H_{nosyl}), 7.98 – 8.04 (m, 4H, H_{nosyl}).

^{13}C NMR (101 MHz, DMSO-d_6) δ 49.0 (t, 2 CH_2), 53.1 (t, 2 CH_2), 68.7 (d, CHOH), 124.5 (d, 2 C_{nosyl}), 129.7 (d, 2 C_{nosyl}), 131.2 (s, 2 S-C_{nosyl}), 132.6 (d, 2 C_{nosyl}), 134.6 (d, 2 C_{nosyl}), 147.6 (s, 2 NO_2-<u>C</u>$_{nosyl}$).

HR-MS: Calc.[M+Na]: 509.0407

Found [M+Na]: 509.0416 (Diff.: -1.68 ppm)

Appearance: Yellowish solid

Mp: 167-169 °C

TLC: R_f = 0.52 (PE/EtOAc = 1/2)

E IV.12.13 1,4-Bis((4-nitrophenyl)sulfonyl)-1,4-diazepan-6-one [248] DCBS225

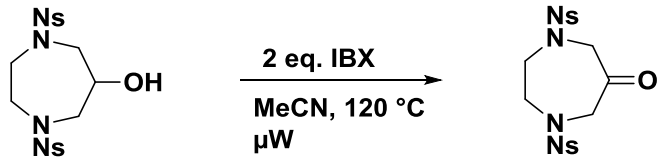

[247]

Chemical Formula: $C_{17}H_{18}N_4O_9S_2$
Molecular Weight: 486.47

[248] (97%)

Chemical Formula: $C_{17}H_{16}N_4O_9S_2$
Molecular Weight: 484.45

1,4-Bis((4-nitrophenyl)sulfonyl)-1,4-diazepan-6-ol **[247]** (620 mg, 1.27 mmol, 1 eq.) and IBX (713 mg, 2.55 mmol, 2 eq.) were dissolved in 14 mL MeCN and heated to 120 °C in the microwave for 10 min. The reaction mixture was filtered over celite using MeCN as eluent and the filtrate was evaporated to give the desired product **[248]** (595 mg, 1.23 mmol, 97%)**.**

^{1}H NMR (400 MHz, DMSO-d_6) δ 3.81 (s, 4H, 2 CH_2), 4.19 (s, 4H, 2 CH_2), 7.85 – 7.97 (m, 4H, H_{nosyl}), 8.04 – 8.09 (m, 4H, H_{nosyl}).

^{13}C NMR (101 MHz, DMSO-d_6) δ 52.7 (t, 2 CH_2), 57.1 (t, 2 CH_2), 124.9 (d, 2 C_{nosyl}), 129.8 (d, 2 C_{nosyl}), 131.0 (s, 2 S-C_{nosyl}), 133.1 (d, 2 C_{nosyl}), 135.0 (d, 2 C_{nosyl}), 147.3 (s, 2 NO_2-C_{nosyl}), 204.3 (s, CO).

HR-MS: Calc.[M+H]: 485.0431

Found [M+H]: n.det.

Appearance: Colorless crystals

Mp: 185-187 °C

TLC: R_f = 0.87 (PE/EtOAc = 1/2)

E IV.12.14 *tert-Butyl* 2-(1,4-bis((4-nitrophenyl)sulfonyl)-1,4-diazepan-6-ylidene)hydrazine-1-carboxylate [249] DCBS227

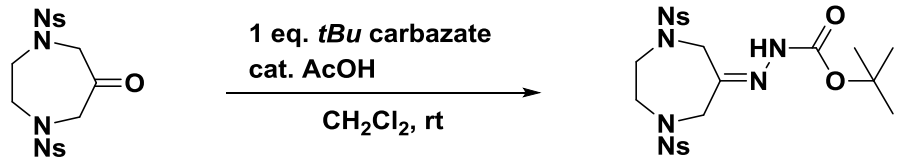

[248] [249] (quant.)

Chemical Formula: $C_{17}H_{16}N_4O_9S_2$
Molecular Weight: 484.45

Chemical Formula: $C_{22}H_{26}N_6O_{10}S_2$
Molecular Weight: 598.60

1,4-Bis((4-nitrophenyl)sulfonyl)-1,4-diazepan-6-one **[248]** (590 mg, 1.22 mmol, 1 eq.) and *tert*-butyl hydrazine carboxylate (214 mg, 1.83 mmol, 1.5 eq.) were dissolved in 40 mL dry CH_2Cl_2. 244 µL AcOH were added and the mixture was stirred over night at room temperature. Then 20 mL water were added and the phases were separated. The aqueous layer was extracted with CH_2Cl_2 (3 x 20 mL), the organic phases were combined, dried over Na_2SO_4, filtered and the solvent removed under reduced pressure. The residue was purified by FC (30-80% EtOAc in PE + 1% Et_3N) to give the desired product **[249]** (720 mg, 1.20 mmol, quantitative)**.**

^{1}H NMR (400 MHz, DMSO-d_6) δ 1.46 (s, 9H, $C(CH_3)_3$), 3.52 – 3.59 (m, 2H, CH_2), 3.65 – 3.72 (m, 2H, CH_2), 4.21 (s, 2H, CH_2), 4.28 (s, 2H, CH_2), 7.78 – 7.97 (m, 4H, H_{nosyl}), 7.99 – 8.08 (m, 4H, H_{nosyl}), 9.94 (br s, 1H, NH).

^{13}C NMR (101 MHz, DMSO-d_6) δ 28.0 (q, $C(\underline{C}H_3)_3$), 48.9 (t, CH_2), 51.1 (t, CH_2), 52.3 (t, CH_2), 53.8 (t, CH_2), 79.9 (s, $\underline{C}(CH_3)_3$), 124.6 (d, C_{nosyl}), 124.9 (d, C_{nosyl}), 129.2 (d, C_{nosyl}), 130.0 (d, C_{nosyl}), 131.1 (s, S-$\underline{C}_{nosyl}$), 131.5 (s, S-$\underline{C}_{nosyl}$), 132.6 (d, C_{nosyl}), 133.0 (d, C_{nosyl}), 134.8 (d, C_{nosyl}), 134.8 (d, C_{nosyl}), 147.5 (s, 2 NO_2-C_{nosyl}), 148.2 (s, CO), 152.7 (s, C=N).

HR-MS: Calc.[M+Na]: 621.1044

Found [M+Na]: 621.1046 (Diff.: -0.29 ppm)

Appearance: Colorless crystals

Mp: 130-132 °C

TLC: R_f = 0.29 (PE/EtOAc = 1/1)

E IV.12.15 2-(1,4-Bis((4-nitrophenyl)sulfonyl)-1,4-diazepan-6-yl)-8-chloro-2,5-dihydro-3H-pyrazolo[4,3-c]quinolin-3-one [250] DCBS229

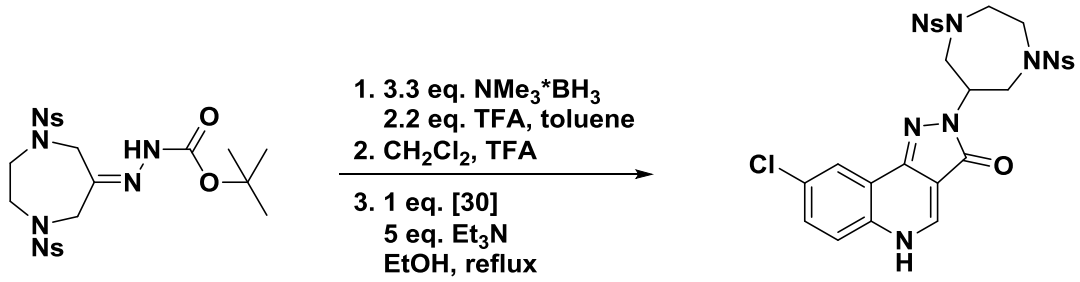

[249] [250] (25% over 3 steps)

Chemical Formula: $C_{22}H_{26}N_6O_{10}S_2$
Molecular Weight: 598.60

Chemical Formula: $C_{27}H_{22}ClN_7O_9S_2$
Molecular Weight: 688.08

The hydrazone **[249]** was dissolved in 30 mL dry toluene and NMe_3*BH_3 (286 mg, 3.92 mmol, 3.3 eq.) was added. The reaction was stirred for 5 min at room temperature and TFA (200 µL) was added. After 45 min the solvent was evaporated and the residue was redissolved in a mixture of 10 mL TFA/CH_2Cl_2 (1v/4v). After 15 min the solvents were evaporated and the crude residue was converted according to general procedure E III.4 using precursor **[30]** as starting material. After purification by HPLC 2-(1,4-bis((4-nitrophenyl)sulfonyl)-1,4-diazepan-6-yl)-8-chloro-2,5-dihydro-3H-pyrazolo[4,3-c]quinolin-3-one **[250]** was obtained in 25% yield over 3 steps (201 mg, 0.29 mmol, 25 % over 3 steps)**.**

^{1}H NMR (400 MHz, DMSO-d_6) δ 3.48 – 3.58 (m, 2H, CH_2), 3.73 – 3.89 (m, 6H, 3 CH_2), 4.69 – 4.80 (m, 1H, CH), 7.64 – 7.73 (m, 2H, H6 and H7), 7.81 – 7.91 (m, 4H, H_{nosyl}), 7.96 – 8.01 (m, 3H, 2 H_{nosyl} and H9), 8.06 (dd, J = 7.7, 1.6 Hz, 2H, H_{nosyl}), 8.71 (s, 1H, H4), 12.83 (br s, 1H, NH).

^{13}C NMR (151 MHz, DMSO-d_6) δ 48.8 (t, 2 CH_2), 50.4 (t, 2 CH_2), 53.3 (d, CH), 105.2 (s, C3a), 120.2 (d, C9), 120.8 (s, C8), 121.6 (d, C6), 124.6 (d, 2 C_{nosyl}), 129.7 (d, 2 C_{nosyl}), 129.8 (d, C7), 130.4 (s, C9a), 131.2 (s, 2 S-C_{nosyl}), 132.8 (d, 2 C_{nosyl}), 133.8 (s, C5a/C9b), 134.6 (d, 2 C_{nosyl}), 139.5 (d, C4), 141.0 (s, C5a/C9b), 147.6 (s, 2 NO_2-C_{nosyl}), 161.3 (s, CO).

HR-MS: Calc.[M+H]: 688.0682

Found [M+H]: 688.0680 (Diff.: +0.23 ppm)

Appearance: Yellow solid

Mp: 120-122 °C

TLC: R_f = 0.22 (5% MeOH in CH_2Cl_2)

E IV.12.16 6-(8-Chloro-3-oxo-3,5-dihydro-2H-pyrazolo[4,3-c]quinolin-2-yl)-1,4-diazepane-1,4-diium chloride [251] DCBS231

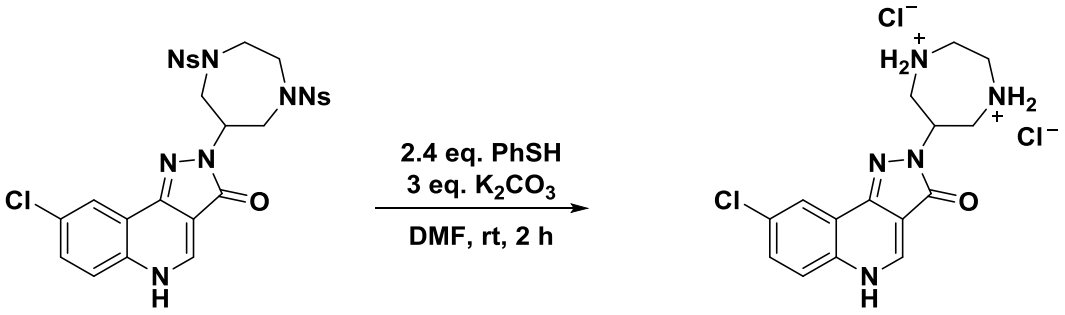

[250] **[251] (30%)**

Chemical Formula: $C_{27}H_{22}ClN_7O_9S_2$
Molecular Weight: 688.08

Chemical Formula: $C_{15}H_{18}Cl_3N_5O$
Molecular Weight: 390.69

2-(1,4-Bis((4-nitrophenyl)sulfonyl)-1,4-diazepan-6-yl)-8-chloro-2,5-dihydro-3H-pyrazolo[4,-3-c]quinolin-3-one **[250]** (156 mg, 0.227 mmol, 1 eq) and K_2CO_3 (94 mg, 0.68 mmol, 3 eq) were dissolved in DMF and thiophenol (56 µL, 0.54 mmol, 2.4 eq) was added. The reaction mixture was stirred for 2 h. Then 20 mL H_2O were added and the solution was neutralized. The aqueous layer was washed with EtOAc (3 x 30 mL) and subsequently a precipitate was formed in the aqueous layer. The precipitate was collected by centrifugation. Next, it was redissolved in MeOH and 2 M HCl in Et_2O was added to precipitate the hydrochloride salt which was collected by centrifugation. The supernatant was removed and the salt was dissolved in H_2O and transferred into a flask to dry the salt at the lyophilizer. After the salt was dried *in vacuo* 6-(8-chloro-3-oxo-3,5-dihydro-2H-pyrazolo[4,3-c]quinolin-2-yl)-1,4-diazepane-1,4-diium chloride **[251]** was obtained (26 mg, 0.067 mmol, 30 %)**.**

^{1}H NMR (400 MHz, DMSO-d_6) δ 3.52 – 3.75 (m, 8H, 4 CH_2), 5.13 – 5.23 (m, 1H, CH), 7.72 (dd, *J* = 8.9, 2.4 Hz, 1H, H7), 7.84 (d, *J* = 8.9 Hz, 1H, H6), 8.32 (d, *J* = 2.4 Hz, 1H, H9), 8.77 (d, *J* = 5.9 Hz, 1H, H4), 9.47 (br s, 2H, NH_2^+), 10.22 (br s, 2H, NH_2^+), 13.37 (br d, *J* = 6.6 Hz, 1H, NH).

^{13}C NMR (151 MHz, DMSO-d_6) δ 42.5 (t, 2 CH_2), 47.2 (d, CH), 47.3 (t, 2 CH_2), 104.9 (s, C3a), 120.1 (s, C8), 121.6 (d, C9), 121.7 (d, C6), 130.1 (d, C7), 130.7 (s, C9a), 133.9 (s, C5a/C9b), C, 139.7 (d, C4), 142.0 (s, C5a/C9b), 161.2 (s, CO).

HPLC-MS: Calc.[M+H]: 318.11
Found [M+H]: 318.06

HR-MS: Calc.[M+H]: 318.1116
Found [M+H]: 318.1119
(Diff.: -0.81 ppm)

Appearance: Yellow solid

Mp: Decomposes at 255 °C

TLC: Salt

E IV.13 Triazoloquinazolinediones

E IV.13.1 5-Chloro-2-(3-(ethoxycarbonyl)thioureido)benzoic acid [103] DCBSBJ03

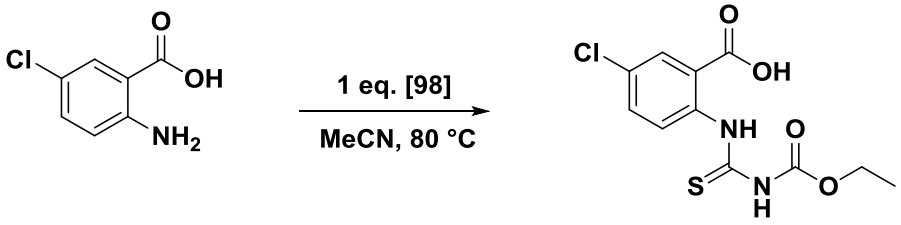

[101] [103] (82%)

Chemical Formula: $C_7H_6ClNO_2$
Molecular Weight: 171.58

Chemical Formula: $C_{11}H_{11}ClN_2O_4S$
Molecular Weight: 302.73

2-Amino-5-chlorobenzoic acid **[101]** (0.92 g, 5.3 mmol) was dissolved in 8.5 mL MeCN and ethoxycarbonyl isothiocyanate **[98]** (0.63 mL, 5.3 mmol) was added dropwise to the solution. The mixture was stirred at reflux for 2 h and allowed to cool to room temperature. After stirring for additional 15 h at room temperature a colourless precipitate was collected by filtration to give the desired product **[103]** (1.33 g, 4.40 mmol, 82%).

^{1}H-NMR (400 MHz, DMSO-d_6) δ 1.25 (t, *J* = 7.1 Hz, 3H, CH_3), 4.21 (q, *J* = 7.1 Hz, 2H, CH_2), 7.66 (dd, *J* = 2.64, 8.8 Hz, 1H, H4), 7.86 (d, *J* = 8.8 Hz, 1H, H3), 8.13 (d, *J* = 2.6 Hz, 1H, H6), 11.38 (br s, 1H, NH), 12.26 (br s, 1H, NH), 13.74 (br s, 1H, COOH).

^{13}C-NMR (101 MHz, DMSO-d_6) δ 14.1 (q, CH_2-$\underline{C}H_3$), 62.0 (t, $\underline{C}H_2$-CH_3), 126.2 (d, C3), 129.3 (d, C4/C6), 129.6 (d, C4/C6), 129.8 (s, C1/C2), 131.6 (s, C1/C2) 137.3 (s, C5), 152.9 (s, $\underline{C}$OOEt), 166.0 (s, COOH), 179.3 (s, CS).

HR-MS: Calc.[M+H]: 303.0201

Found [M+H]: 303.0206 (Diff.: -1.64 ppm)

Appearance: Colorless solid

Mp: 164 – 166 °C

TLC: R_f = 0.20 (PE/EtOAc = 3/1)

E IV.13.2 2-(3-(Ethoxycarbonyl)thioureido)-5-methoxybenzoic acid [104] DCBSBJ12

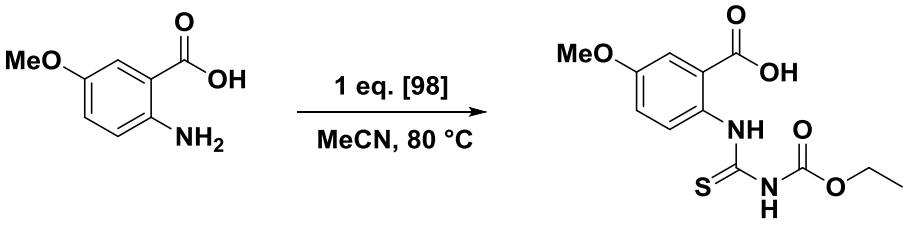

[102] **[104] (67%)**

Chemical Formula: $C_8H_9NO_3$
Molecular Weight: 167.16

Chemical Formula: $C_{12}H_{14}N_2O_5S$
Molecular Weight: 298.31

2-Amino-5-methoxybenzoic acid **[102]** (0.700 g, 4.19 mmol) was dissolved in 8.6 mL MeCN and ethoxycarbonyl isothiocyanate **[98]** (0.50 mL, 4.19 mmol) was added dropwise to the solution. The mixture was stirred at reflux for 5 h and allowed to cool to room temperature. A beige precipitate was collected by filtration to give the desired product **[104]** (0.84 g, 2.8 mmol, 67%).

^{1}H-NMR (400 MHz, DMSO-d_6) δ 1.25 (t, J = 7.1 Hz, 3H, CH_2-C$\underline{H}_3$), 3.81 (s, 3H, OCH_3)**,** 4.20 (q, J = 7.1 Hz, 2H, C$\underline{H}_2$-CH_3), 7.17 (dd, J = 3.1, 8.9 Hz, 2H, H3 and H4), 7.36 (d, J = 3.1 Hz, 1H, H6), 11.22 (br s, 1H, NH), 12.01 (br s, 1H, NH), 13.39 (br s, 1H, COOH).

^{13}C-NMR (101 MHz, DMSO-d_6) δ 14.2 (q, CH_2-$\underline{C}H_3$), 55.5 (q, OCH_3), 61.9 (t, $\underline{C}H_2$-CH_3), 114.2 (d, C6), 117.8 (d, C4), 126.1 (s, C1), 129.3 (d, C3), 131.1 (s, C2), 152.0 (s, $\underline{C}$OOEt), 156.8 (s, C5), 166.8 (s, COOH), 179.1 (s, CS).

HR-MS: Calc.[M+H]: 299.0696

Found [M+H]: 299.0704 (Diff.: -2.74 ppm)

Appearance: Beige solid

Mp: 154.5 – 155.2 °C

TLC: R_f = 0.45 (PE/EtOAc = 3/1)

E IV.13.3 Ethyl 6-chloro-4-oxo-2-thioxo-1,4-dihydroquinazoline-3(2H)-carboxylate [105] DCBSBJ04

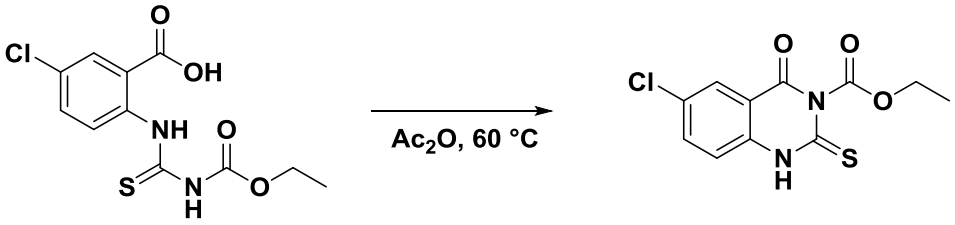

[103] **[105] (76%)**

Chemical Formula: $C_{11}H_{11}ClN_2O_4S$
Molecular Weight: 302.73

Chemical Formula: $C_{11}H_9ClN_2O_3S$
Molecular Weight: 284.71

Compound **[103]** (1.02 g, 2.4 mmol) was dissolved in 14 mL of acetic anhydride and stirred at 60 °C. After 3 h the mixture was allowed to cool to rt and stirred for additional 15 h. The suspension was cooled to 5 °C, the colorless solid was collected by filtration, washed with 5 mL cold acetic anhydride and dried under vacuum to give the desired product **[105]** (0.73 g, 2.6 mmol, 76%).

^{1}H-NMR (400 MHz, DMSO-d_6) δ 1.25 (t, J = 7.1 Hz, 3H, CH_2-C$\underline{H}_3$), 4.19 (q, J = 7.1 Hz, 2H, C$\underline{H}_2$-CH_3), 7.55 (d, J = 8.7 Hz, 1H, H8), 7.87 (dd, J = 2,63, 8.75 Hz, 1H, H7), 7.94 (d, J = 2.54 Hz, 1H, H5) 11.87 (br s, 1H, NH).

^{13}C-NMR (101 MHz, DMSO-d_6) δ 14.2 (q, CH_2-$\underline{C}H_3$), 61.9 (t, $\underline{C}H_2$-CH_3), 119.5 (d, C7/C8), 123.3 (d, C7/C8), 130.8 (s, C5), 130.9 (d, C4a/C8a), 136.0 (d, C4a/C8a), 146.6 (s, $\underline{C}$OOEt), 153.4 (s, C6), 154.1 (s, CO), 183.6 (s, CS).

HR-MS: Calc.[M+H]: 285.0095

Found [M+H]: n.det.

Appearance: Colorless solid

Mp: 160.1 – 161.5 °C

TLC: R_f = 0.55 (PE/EtOAc = 3/1)

E IV.13.4 Ethyl 6-methoxy-4-oxo-2-thioxo-1,4-dihydroquinazoline-3(2H)-carboxylate [106] DCBSBJ15

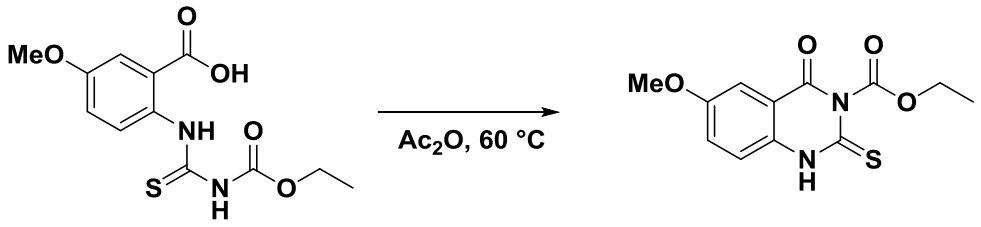

[104] **[106] (84%)**

Chemical Formula: $C_{12}H_{14}N_2O_5S$
Molecular Weight: 298.31

Chemical Formula: $C_{12}H_{12}N_2O_4S$
Molecular Weight: 280.30

Compound **[104]** (0.840 g, 2.82 mmol) was dissolved in 12 mL of acetic anhydride and stirred at 60 °C. After 4 h the mixture was allowed to cool to r.t. and was stirred for additional 16 h. The dispersion was cooled to 5 °C, the colorless solid was collected by filtration, washed with 5 mL cold acetic anhydride and dried under vacuum to give the desired product **[106]** (0.66 g, 2.4 mmol, 84%).

^{1}H-NMR (400 MHz, DMSO-d_6) δ 1.24 (t, *J* = 7.1 Hz, 3H, CH_2-C<u>H</u>$_3$), 3.86 (s, 3H, OCH_3), 4.18 (q, *J* = 7.08, 2H, C<u>H</u>$_2$-CH_3), 7.42 (d, *J* = 2.93, 1H, H5), 7.46 (dd, *J* = 3.0 Hz, 8.9 Hz,1H, H7), 7.51 (d, *J* = 8.9 Hz, 1H, H8), 11.60 (br s, 1H, NH).

^{13}C-NMR (101 MHz, DMSO-d_6) δ 14.2 (q, CH_2-<u>C</u>H_3), 55.7 (q, OCH_3), 61.7 (t, <u>C</u>H_2-CH_3), 104.9 (d, C5), 119.3 (d, C7/C8), 125.1 (d, C7/C8), 130.6 (s, C4a/C8a), 142.6 (s, C4a/C8a), 150.7 (s, <u>C</u>OOEt), 153.4 (s,C6), 157,7 (s, CO), 184,1 (s, CS).

HR-MS: Calc.[M+H]: 281.0591

Found [M+H]: 281.0599 (Diff.: -3.09 ppm)

Appearance: Colorless solid

Mp: 273 – 274 °C

TLC: R_f = 0.63 (PE/EtOAc = 3/1)

E IV.13.5 6-Chloro-2-thioxo-2,3-dihydroquinazolin-4(1H)-one [107] DCBSBJ05

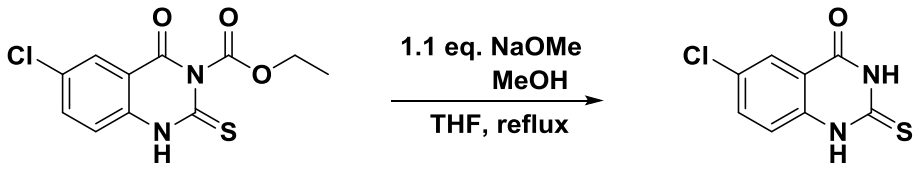

[105] **[107] (73%)**

Chemical Formula: $C_{11}H_9ClN_2O_3S$
Molecular Weight: 284.71

Chemical Formula: $C_8H_5ClN_2OS$
Molecular Weight: 212.65

A solution of sodium methoxide (0.5 M, 2.8 mmol) in methanol (5.6 mL) was added to a solution of **[105]** (0.73 g, 2.55 mmol) in 12 mL THF and the mixture was heated at reflux for 2 h. The solution was allowed to cool to rt, stirred for additional 15 h and quenched by addition of acetic acid (0.16 mL, 2.8 mmol). The solvent was evaporated and a mixture of 8 mL H_2O and 16 mL of EtOH was added. The slurry was heated to reflux for 30 min, cooled to room temperature and the solid was collected by filtration to give the desired product **[107]** (0.40 g, 1.9 mmol, 73%).

^{1}H-NMR (400 MHz, DMSO-d_6) δ 7.36 (d, *J* = 8.73, 1H, H8), 7.77 (dd, *J* = 2.5 Hz, 8.8 Hz, 1H, H7), 7.85 (d, *J* = 2.41, 1H, H5), 12.61 (br s, 1H, Ar-NH), 12.79 (br s, 1H, CONH).

^{13}C-NMR (101 MHz, DMSO-d_6) δ 117.7 (s, C4a/C8a), 118.1 (d, C5/C7/C8), 125.7 (d, C5/C7/C8), 128.3 (d, C5/C7/C8), 135.3 (s, C4a/C8a), 139.3 (s, C6), 158.7 (s, CO), 174.3 (s, CS).

HR-MS: Calc.[M+H]: 212.9884

Found [M+H]: n.det.

Appearance: Colorless solid

Mp: 289.9 – 290.2 °C

TLC: R_f = 0.36 (1% MeOH in CH_2Cl_2)

E IV.13.6 6-Methoxy-2-thioxo-2,3-dihydroquinazolin-4(1H)-one [108] DCBSBJ17

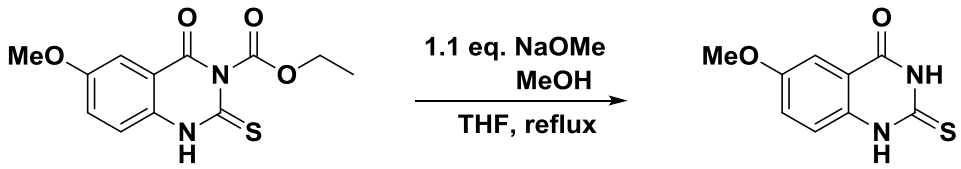

[106] **[108] (75%)**

Chemical Formula: $C_{12}H_{12}N_2O_4S$
Molecular Weight: 280.30

Chemical Formula: $C_9H_8N_2O_2S$
Molecular Weight: 208.24

A solution of sodium methoxide (0.5 M, 2.67 mmol) in methanol (5.2 mL) was added to a solution of **[106]** (0.73 g, 2.36 mmol) in 11 mL THF and the mixture was heated to reflux for 3 h. The mixture was allowed to cool to r.t., stirred for additional 15 h and quenched by addition of acetic acid (0.16 mL, 2.8 mmol). After the solvent was evaporated a mixture of 7 mL H_2O and 14 mL EtOH was added. The slurry was heated to reflux for 30 min and cooled to room temperature. The solid was collected by filtration to give the desired product **[108]** (0.37 g, 1.8 mmol, 75%).

^{1}H-NMR (400 MHz, DMSO-d_6) δ 3.81 (s, 3H, OCH_3), 7.29 – 7.38 (m, 3H, H5 and H7 and H8), 12.42 (br s, 1H, NH), 12.65 (br s, 1H, NH).

^{13}C-NMR (101 MHz, DMSO-d_6) δ 55.7 (q, OCH_3), 107.5 (d, C5), 117.1 (s, C4a/C8a), 117.7 (d, C7/C8), 124.3 (d, C7/C8), 134.8 (s, C4a/C8a) 156.0 (s, C6), 159.6 (s, CO), 172,8 (s, CS).

HR-MS: Calc.[M+H]: 209.0379

Found [M+H]: n. det.

Appearance: Colorless solid

Mp: Decomposes > 300 °C

TLC: R_f = 0.35 (PE/EtOAc = 3/1)

E IV.13.7 6-Chloro-2-(methylthio)quinazolin-4(3H)-one [109] DCBSBJ23

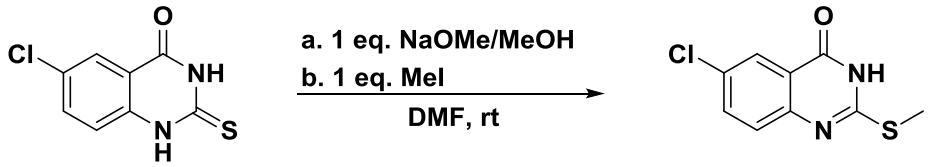

[107] **[109] (78%)**

Chemical Formula: $C_8H_5ClN_2OS$
Molecular Weight: 212.65

Chemical Formula: $C_9H_7ClN_2OS$
Molecular Weight: 226.68

Compound **[107]** (0.127 g, 0.6 mmol) was dissolved in 2.4 mL DMF and a mixture of sodium methoxide (0.5 M, 0.6 mmol) in methanol (1.2 mL) was added. The solution was stirred at room temperature for 20 min. After addition of iodomethane (0.085 g, 0.6 mmol) the reaction mixture was stirred for 26 h at rt. The solvents were evaporated and the residue was redissolved in 25 mL EtOAc. The organic layer was washed with satd. $NaHCO_3$ (4 x 25 mL), dried over Na_2SO_4, filtered and the solvent was removed under reduced pressure to give the desired product **[109] (**0.11 g, 0.5 mmol, 78%).

^{1}H-NMR (400 MHz, DMSO-d_6) δ 2.56 (s, 3H, SCH_3), 7.55 (d, J = 8.7 Hz, 1H, H8), 7.77 (dd, J = 2.6, 8.7 Hz, 1H, H7), 7.95 (d, J = 2.5 Hz, 1H, H5), 12.76 (br s, 1H, NH).

^{13}C-NMR (101 MHz, DMSO-d_6) δ 12.8 (q, SCH_3), 121.2 (s, C4a/C8a), 125.0 (d, C5/C7/C8), 128.2 (d, C5/C7/C8), 129.6 (d, C5/C7/C8), 134.6 (s, C4a/C8a), 147.2 (s, C6), 157.2 (s, CS), 160.3 (s, CO).

HR-MS: Calc.[M+H]: 227.0040

Found [M+H]: 227.0050 (Diff.: -4.14 ppm)

Appearance: Colorless solid

Mp: 231.4 – 232.0 °C

TLC: R_f = 0.32 (2% MeOH in CH_2Cl_2)

E IV.13.8 6-Methoxy-2-(methylthio)quinazolin-4(3H)-one [110] DCBSBJ22

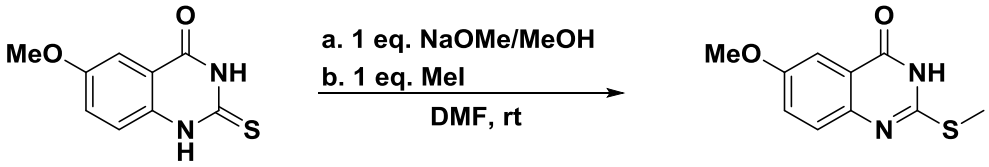

[108] **[110] (69%)**

Chemical Formula: $C_9H_8N_2O_2S$
Molecular Weight: 208.24

Chemical Formula: $C_{10}H_{10}N_2O_2S$
Molecular Weight: 222.26

Compound **[108]** (0.22 g, 1.05 mmol) was dissolved in 2.9 mL DMF and a mixture of sodium methoxide (0.5 M, 1.05 mmol) in methanol (2.1 mL) was added. The solution was stirred at room temperature for 15 min. After addition of iodomethane (0.15 g, 1.05 mmol) the reaction mixture was stirred for 22 h at rt. The solvents were evaporated and the residue was redissolved in 30 mL EtOAc. The organic layer was washed with satd. $NaHCO_3$ (4 x 25 mL), dried over Na_2SO_4, filtered and the solvent was removed under reduced pressure to give the desired product **[110]** (0.16 g, 0.70 mmol, 69%).

^{1}H-NMR (400 MHz, DMSO-d_6) δ 2.55 (s, 3H, SCH_3), 3.80 (s, 3H, OCH_3), 7.30 (dd, *J* = 3.0, 8.8 Hz, 1H, H7), 7.38 (d, *J* = 3.0, 1H, H5), 7.45 (d, *J* = 8.8, 1H, H8), 12.48 (br s, 1H, NH).

^{13}C-NMR (101 MHz, DMSO-d_6) δ 12.7 (q, SCH_3), 55.6 (q, OCH_3), 106.2 (d, C5), 120.6 (s, C4a/C8a), 123.8 (d, C7/C8), 127.7 (d, C7/C8), 143.1 (s, C4a/C8a), 153.5 (s, CS), 156.9 (s, C6), 161.1 (s, CO).

HR-MS: Calc.[M+H]: 223.0536

Found [M+H]: 223.0543 (Diff.: -3.33 ppm)

Appearance: Colorless solid

Mp: 241.0 – 241.3 °C

TLC: R_f = 0.40 (PE/EtOAc = 3/1)

E IV.13.9 4,6-Dichloro-2-(methylthio)quinazoline [111] DCBSBJ26

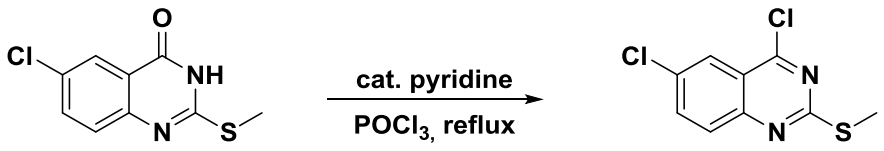

[109] **[111] (90%)**

Chemical Formula: $C_9H_7ClN_2OS$
Molecular Weight: 226.68

Chemical Formula: $C_9H_6Cl_2N_2S$
Molecular Weight: 245.12

10 µL Pyridine were added to compound **[109]** (0.15 g, 0.66 mmol) in 1.8 mL $POCl_3$ and the mixture was heated at 110 °C for 15 h. The reaction mixture was allowed to cool to rt and quenched with 150 mL of aqueous $NaHCO_3$. The aqueous layer was extracted with EtOAc (4 x 20 mL), dried over Na_2SO_4, filtered and the solvent was removed under reduced pressure. The residue was purified by FC (PE/EtOAc = 19/1) to give **[111]** as a colourless solid (0.15 g, 0.6 mmol, 90%).

^{1}H-NMR (200 MHz, $CDCl_3$) δ 2.66 (s, 3H, SCH_3), 7.76 – 7.83 (m, 2H, H7 and H8), 8.09 - 8.16 (m, 1H, H5).

^{13}C-NMR (101 MHz, $CDCl_3$) δ 14.6 (q, SCH_3), 121.8 (d, C5), 125.1 (s, C4a/C8a), 129.0 (d, C7/C8), 132.8 (d, C7/C8), 136.2 (s, C4a/C8a), 150.4 (s, Cl-C-Ar), 160.8 (s, Cl-C-Ar), 168.4 (s, CS).

HR-MS: Calc.[M+H]: 244.9702

Found [M+H]: n.det.

Appearance: Colorless solid

Mp: 124.5 – 124.8 °C

TLC: Rf = 0.88 (1% MeOH in CH_2Cl_2)

E IV.13.10 4-Chloro-6-methoxy-2-(methylthio)quinazoline [112] DCBSBJ25

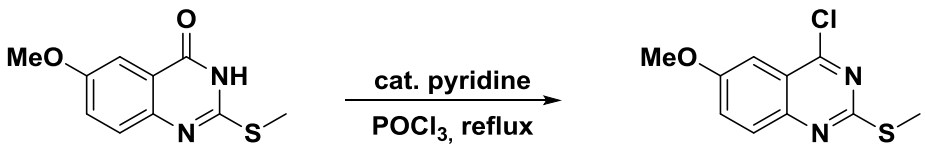

[110] **[112] (86%)**

Chemical Formula: $C_{10}H_{10}N_2O_2S$
Molecular Weight: 222.26

Chemical Formula: $C_{10}H_9ClN_2OS$
Molecular Weight: 240.71

10 µL Pyridine were added to compound **[110]** (0.180 g, 0.79 mmol) in 2.0 mL $POCl_3$ and the mixture was heated at 110 °C for 15 h. The reaction mixture was allowed to cool to r.t. and quenched with 150 mL of aqueous $NaHCO_3$. The aqueous layer was extracted with EtOAc (4 x 20 mL), dried over Na_2SO_4, filtered and the solvent was removed under reduced pressure. The residue was purified by FC (PE/EtOAc = 9/1) to give the desired compound **[112]** (0.16 g, 0.6 mmol, 86%).

^{1}H-NMR (400 MHz, DMSO-d_6) δ 2.66 (s, 3H, SCH_3), 3.96 (s, 3H, OCH_3), 7.34 (d, *J* = 2.78, 1H, H5), 7.50 (dd, *J* = 2.8, 9.2 Hz, 1H, H7), 7.78 (d, *J* = 9.2 Hz, 1H, H8).

^{13}C-NMR (101 MHz, $CDCl_3$) δ 14.5 (q, SCH_3), 56.0 (q, OCH_3), 103.4 (d, C5), 122.0 (s, C4a/C8a), 128.1 (d, C7/C8), 128.9 (d, C7/C8), 148.3 (s, C4a/C8a), 158.3 (s, C6), 160.3 (s, Cl-C-Ar), 165.2 (s, CS).

HR-MS: Calc.[M+H]: 241.0197

Found [M+H]: 241.0201 (Diff.: -1.69 ppm)

Appearance: Pale yellow solid

Mp: 278.6 – 278.7 °C

TLC: Rf = 0.85 (1% MeOH in CH_2Cl_2)

E IV.13.11 Ethyl 1-(p-tolyl)hydrazine-1-carboxylate [118] DCBSBJ02

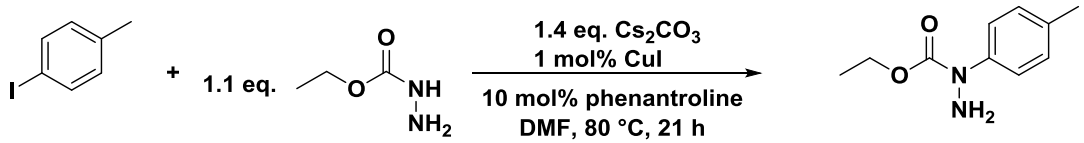

[114] **[99]** **[118] (58%)**

Chemical Formula: C_7H_7I
Molecular Weight: 218.04

Chemical Formula: $C_{10}H_{14}N_2O_2$
Molecular Weight: 194.23

DMF (3.3 mL) was added to 4-iodotoluene **[114]** (501 mg, 2.3 mmol), ethyl carbazate (285 mg, 2.7 mmol), 1,10-phenanthroline (83 mg, 0.46 mmol), CuI (218 mg, 0,11 mmol), and Cs_2CO_3 (1.05 g, 3.21mmol). The mixture was stirred at 80 °C for 20 h under argon atmosphere. The solvent was removed under reduced pressure and the residue was purified by FC (N-heptane/EtOAc = 4/1) to give **[118]** as tan oil (26 mg, 1.3 mmol, 58%).

^{1}H-NMR (400 MHz, $CDCl_3$) δ 1.29 (t, *J* = 7.1, 3H, $CH_2C\underline{H}_3$), 2.33 (s, 3H, Ar-CH_3), 4.23 (q, *J* = 7.1, 2H, $C\underline{H}_2CH_3$), 4.49 (br s, 2H, NH_2), 7.14 (d, 2H, H2 and H6), 7.31 (d, 2H, H3 and H5).

^{13}C-NMR (101 MHz, $CDCl_3$) δ 14.8 (q, $CH_2\underline{C}H_3$), 21.0 (q, Ar-CH_3), 62.6 (t, $\underline{C}H_2CH_3$), 123.9 (d, C3 and C5), 129.2 (d, C2 and C6), 135.2 (s, C1), 140.4 (s, C4), 156.5 (s, CO).

HR-MS: Calc.[M+H]: 195.1028

Found [M+H]: 195.1139 (Diff.: -5.68 ppm)

Appearance: Tan oil

TLC: R_f = 0.68 (10 % MeOH in CH_2Cl_2)

E IV.13.12 Ethyl 1-(4-methoxyphenyl)hydrazine-1-carboxylate [120] DCBSBJ13

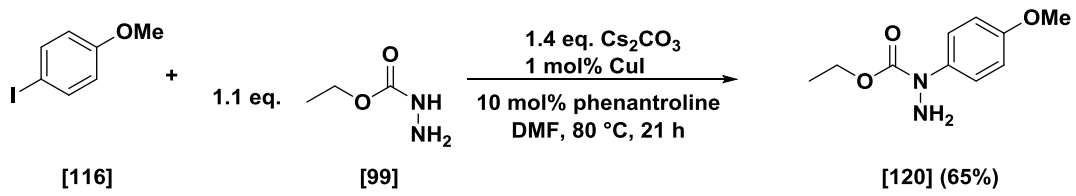

[116] **[99]** **[120] (65%)**

Chemical Formula: C_7H_7IO
Molecular Weight: 234.0365

Chemical Formula: $C_{10}H_{14}N_2O_3$
Molecular Weight: 210.2330

DMF (3.2 mL) was added to a mixture of 4-iodoanisol **[116]** (502 mg, 2.1 mmol), ethyl carbazate (266 mg, 2.6 mmol), 1,10-phenanthroline (739 mg, 0.21 mmol), CuI (21 mg, 0.11 mmol), and Cs_2CO_3 (994 mg, 3.05 mmol). The mixture was stirred at 80 °C for 20 h under argon atmosphere, the solvent was removed under reduced pressure and the residue purified by FC (PE/EtOAc = 3/1) to give **[120]** as brown oil (287 mg, 1.37 mmol, 65%).

^{1}H-NMR (400 MHz, DMSO-d_6) δ 1.19 (t, J = 7.1, 3H, $CH_2C\underline{H}_3$), 3.73 (s, 3H, OCH_3), 4.09 (q, J = 7.0, 2H, $C\underline{H}_2CH_3$), 5.08 (br s, 2H, NH_2), 6.87 (d, J = 9.1Hz, 2H, H3 and H5), 7.32 (m, 2H, H2 and H6).

^{13}C-NMR (101 MHz, DMSO-d_6) δ 14.5 (q, $CH_2\underline{C}H_3$), 55.2 (q, OCH_3), 61.3 (t, $\underline{C}H_2CH_3$), 113.2 (d, C3 and C5), 125.1 (d, C2 and C6), 136.9 (s, C1), 155.8 (s, C4), 156.2 (s, CO).

HR-MS: Calc.[M+H]: 211.1077

Found [M+H]: 211.1084 (Diff.: -3.44 ppm)

Appearance: Brown oil

TLC: R_f = 0.54 (PE/EtOAc = 1/1)

E IV.13.13 Ethyl 1-(4-aminophenyl)hydrazine-1-carboxylate [119] DCBSLA1

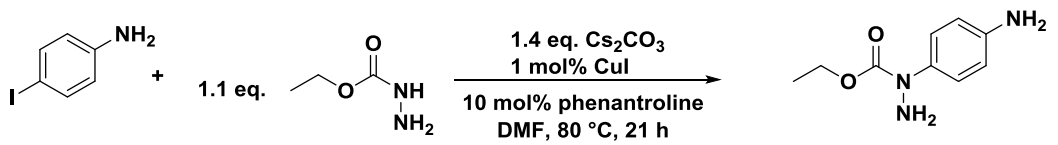

[115] **[99]** **[119] (69%)**

Chemical Formula: C_6H_6IN
Molecular Weight: 219.03

Chemical Formula: $C_9H_{13}N_3O_2$
Molecular Weight: 195.22

DMF (0.5 mL) was added to a mixture of 4-iodoaniline **[115]** (110 mg, 0.50 mmol), ethyl carbazate (62.6 mg, 0.60 mmol), 1,10-phenanthroline (9 mg, 0.05 mmol), CuI (0.9 mg, 0,005 mmol), and Cs_2CO_3 (229 mg, 0.70 mmol). The mixture was stirred at 80 °C for 21 h under argon atmosphere. The solvent was removed under reduced pressure and the residue was purified by FC (PE/EtOAc = 1/1) to give ethyl 1-(4-aminophenyl)hydrazine-1-carboxylate **[119]** (68 mg, 0.35 mmol, 69%).

^{1}H NMR (400 MHz, DMSO-d_6) δ 1.16 (t, *J* = 7.1 Hz, 3H, $CH_2C\underline{H}_3$), 4.04 (q, *J* = 7.1 Hz, 2H, $C\underline{H}_2CH_3$), 4.94 (br s, 2H, NH_2), 4.98 (br s, 2H, NH_2), 6.47 (d, *J* = 8.7 Hz, 2H, H3 and H5), 6.97 (d, *J* = 8.7 Hz, 2H, H2 and H6).

^{13}C NMR (101 MHz, DMSO-d_6) δ 14.6 (q, $CH_2\underline{C}H_3$), 61.0 (t, $C\underline{H}_2CH_3$), 113.2 (d, C3 and C5), 125.5 (d, C2 and C6), 132.7 (s, C1), 146.2 (s, C4), 155.9 (s, CO).

Appearance: Light brown oil

TLC: R_f = 0.41 (PE/EtOAc = 1/2)

E IV.13.14 Ethyl 1-(4-cyanophenyl)hydrazine-1-carboxylate [117] DCBSLA9

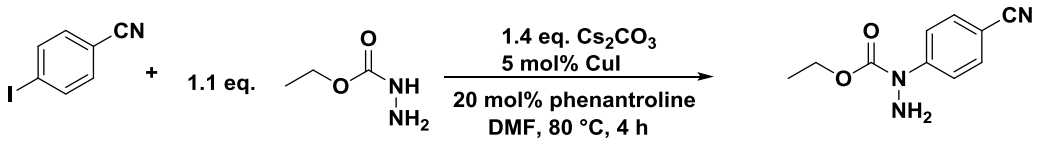

[113] [99] [117] (72%)

Chemical Formula: C_7H_4IN
Molecular Weight: 229.02

Chemical Formula: $C_{10}H_{11}N_3O_2$
Molecular Weight: 205.22

To a mixture of 4-cyanoaniline **[113]** (110 mg, 0.50 mmol), ethyl carbazate (62.6 mg, 0.60 mmol), 1,10-phenanthroline (18 mg, 0.10 mmol), CuI (4.5 mg, 0,025 mmol), and Cs_2CO_3 (229 mg, 0.70 mmol) was added 0.5 mL DMF and the mixture was stirred at 80 °C for 4 h under argon atmosphere. The solvent was removed under reduced pressure and the residue was purified by FC (PE/EtOAc = 5/1) to give ethyl 1-(4-cyanophenyl)hydrazine-1-carboxylate **[117]** (74 mg, 0.36 mmol, 72%).

^{1}H NMR (400 MHz, DMSO-d_6) δ 1.27 (t, J = 7.1 Hz, 3H, $CH_2C\underline{H}_3$), 4.19 (q, J = 7.1 Hz, 2H, $C\underline{H}_2CH_3$), 5.27 (br s, 2H, NH_2), 7.73 – 7.78 (m, 2H, H2 and H6), 7.79 – 7.85 (m, 2H, H3 and H5).

^{13}C NMR (101 MHz, DMSO-d_6) δ 14.3 (q, $CH_2\underline{C}H_3$), 62.2 (t, $C\underline{H}_2CH_3$), 105.0 (s, C4), 119.1 (s, CN), 121.6 (d, C2 and C6), 132.3 (d, C3 and C5), 147.8 (s, C1), 155.1 (s, CO).

HR-MS: Calc.[M+H]: 206.0924

Found [M+H]: 206.0927 (Diff.: -1.49 ppm)

Appearance: Yellow solid

Mp: 99 – 101 °C

TLC: R_f = 0.78 (PE/EtOAc = 1/2)

E IV.13.15 *tert*-Butyl (4-iodophenyl)carbamate [121] DCBS99

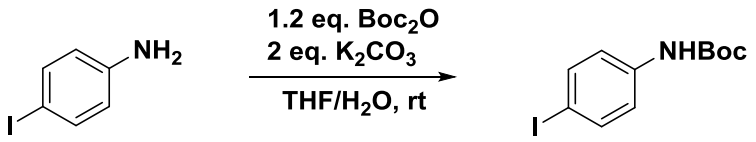

[115] **[121] (86%)**

Chemical Formula: C_6H_6IN
Molecular Weight: 219.03

Chemical Formula: $C_{11}H_{14}INO_2$
Molecular Weight: 319.14

4-Iodaniline **[115]** was dissolved in 2 mL THF/H_2O (v/v) and K_2CO_3 was added. After 5 min Boc_2O was added and the mixture was stirred at room temperature. After 24 h the organic and the aqueous phases were separated and the aqueous layer was extracted with EtOAc (3 x 3 mL). The combined organic layer was dried over Na_2SO_4, filtered and evaporated. The residue was purified by FC (5% - 15% EtOAc in PE) to give *tert*-butyl (4-iodophenyl)carbamate **[121]** (630 mg, 1.97 mmol, 86%).

^{1}H NMR (400 MHz, $CDCl_3$) δ 1.51 (s, 9H, 3 CH_3), 6.45 (s, 1H, NH), 7.09 – 7.19 (m, 2H, H3 and H5), 7.53 – 7.62 (m, 2H, H2 and H6).

^{13}C NMR (101 MHz, $CDCl_3$) δ 28.4 (q, 3 CH_3), 81.1 (s, $\underline{C}(CH_3)_3$), 85.8 (s, C4), 120.5 (d, C3 and C5), 138.0 (d, C2 and C6), 138.3 (s, C1), 152.6 (s, CO).

Appearance: Colorless solid

Mp: 133-135 °C (Lit.[227]: 134-136 °C)

TLC: R_f = 0.58 (PE/EtOAc = 10/1)

E IV.13.16 Ethyl 1-(4-((*tert*-butoxycarbonyl)amino)phenyl)hydrazine -1-carboxylate [122] DCBS100

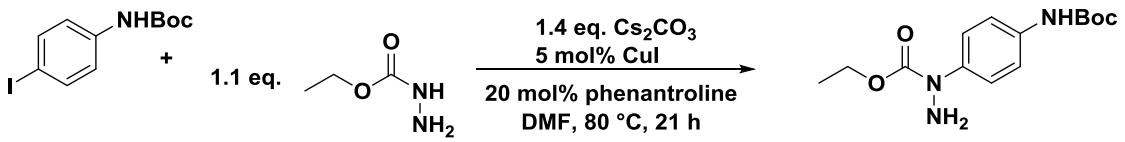

[121] [99] [121] (31%)

Chemical Formula: $C_{11}H_{14}INO_2$
Molecular Weight: 319.14

Chemical Formula: $C_{14}H_{21}N_3O_4$
Molecular Weight: 295.34

To a mixture of **[121]** (500 mg, 1.57 mmol), ethyl carbazate (196 mg, 1.88 mmol), 1,10-phenanthroline (57 mg, 0.31 mmol), CuI (15 mg, 0,078 mmol), and Cs_2CO_3 (732 mg, 2.25 mmol) was added 3.5 mL DMF and the mixture was stirred at 80 °C for 20 h under argon atmosphere. The solvent was removed under reduced pressure and the residue was purified by FC (20% EtOAc in n-heptane) to give ethyl 1-(4-((*tert*-butoxycarbonyl)amino)phenyl)hydrazine-1-carboxylate **[122]** (102 mg, 0.345 mmol, 31%).

^{1}H NMR (400 MHz, DMSO-d_6) δ 1.19 (t, *J* = 7.1 Hz, 3H, $CH_2C\underline{H}_3$), 1.47 (s, 9H, 3 CH_3), 4.09 (q, *J* = 7.1 Hz, 2H, $C\underline{H}_2CH_3$), 5.07 (br s, 2H, NH_2), 7.30 (d, *J* = 9.1 Hz, 2H, H3 and H5), 7.36 (d, *J* = 9.1 Hz, 2H, H2 and H6), 9.28 (br s, 1H, NH).

^{13}C NMR (101 MHz, DMSO-d_6) δ 14.5 (q, $CH_2\underline{C}H_3$), 28.1 (q, $C(\underline{C}H_3)_3$), 61.3 (t, $C\underline{H}_2CH_3$), 78.9 (s, $\underline{C}(CH_3)_3$), 117.7 (d, C3 and C5), 123.8 (d, C2 and C6), 136.0 (s, C1/C4), 138.1 (s, C1/C4), 152.8 (s, CO), 155.6 (s, CO).

HR-MS: Calc.[M+H]: 296.1605

Found [M+H]: 296.1597 (Diff.: +2.58 ppm)

Appearance: Yellow oil

TLC: R_f = 0.17 (PE/EtOAc = 3/1)

E IV.13.17 9-Chloro-5-(methylthio)-2-(p-tolyl)-[1,2,4]triazolo[4,3-c]quinazolin-3(2H)-one [124] DCBSBJ27

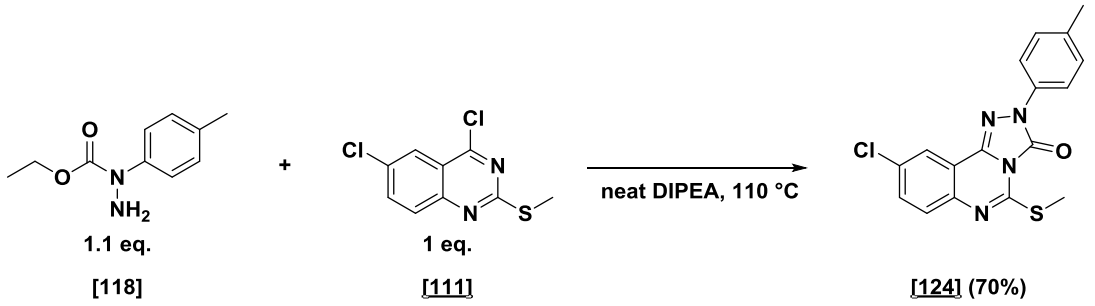

Chemical Formula: $C_{10}H_{14}N_2O_2$
Molecular Weight: 194.23

Chemical Formula: $C_9H_6Cl_2N_2S$
Molecular Weight: 245.12

Chemical Formula: $C_{17}H_{13}ClN_4OS$
Molecular Weight: 356.83

N,N-Diisopropylethylamine (38 mg, 0.29 mmol) was added to compound **[111]** (40 mg, 0.16 mmol) and **[118]** (35 mg, 0.18 mmol) and the reaction mixture was stirred at 110 °C for 18 h. The mixture was cooled to room temperature and the solvent was removed under reduced pressure. The crude solid was recrystallized from EtOH to give **[124]** as a pale grey solid (40 mg, 0.11 mmol, 70%).

^{1}H-NMR (400 MHz, DMSO-d_6) δ 2.38 (s, 3H, Ar-CH_3), 2.64 (s, 3H, SCH_3), 7.25 - 7.28 (m, 2H, H7 and H8), 7.55 (m, 2H, H3' and H5'), 7.93 (m, 2H, H2' and H6'), 8.05 – 8.13 (m, 1H, H10).

^{13}C-NMR (101 MHz, $CDCl_3$) δ 13.6 (q, SCH_3), 21.2 (q, Ar-CH_3), 115.6 (s), 119.5 (d, C2' and C6'), 122.1 (d, C10), 128.6 (d, C7/C8), 129.8 (d, C3' and C5'), 132.8 (d, C7/C8), 132.9 (s), 134.9 (s), 136.4 (s), 138.6 (s), 141.3 (s), 146.3 (s, CO) 150.7 (s, CS).

HR-MS: Calc.[M+H]: 357.0571

Found [M+H]: 357.0584 (Diff.: -3.64 ppm)

Appearance: Pale grey solid

Mp: 189.6 – 190.6 °C

TLC: R_f = 0.69 (PE/EtOAc = 7/1)

E IV.13.18 9-Chloro-2-(4-methoxyphenyl)-5-(methylthio)-[1,2,4]triazolo-[4,3-c]quinazolin-3(2H)-one [125] DCBSBJ52

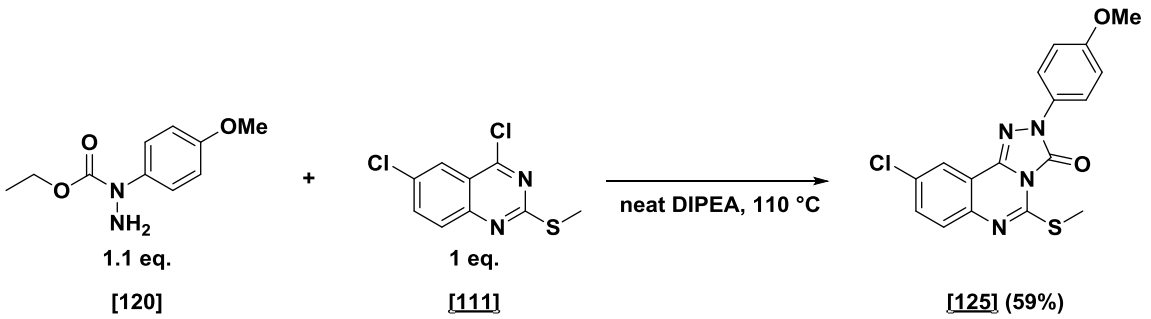

Chemical Formula: $C_{10}H_{14}N_2O_3$ Molecular Weight: 210.23

Chemical Formula: $C_9H_6Cl_2N_2S$ Molecular Weight: 245.12

Chemical Formula: $C_{17}H_{13}ClN_4O_2S$ Molecular Weight: 372.83

N,N-Diisopropylethylamine (62 mg, 0.48 mmol) was added to compound **[111]** (40 mg, 0.16 mmol) and **[120]** (44 mg, 0.21 mmol) and the reaction mixture was stirred at 110 °C for 18 h. The mixture was cooled to room temperature and the solvent was removed under reduced pressure. The crude solid was recrystallized from EtOH to give **[125]** as a pale grey solid (40 mg, 0.09 mmol, 59%).

^{1}H-NMR (400 MHz, DMSO-d_6) δ 2.59 (s, 3H, SCH_3), 3.81 (s, 3H, OCH_3), 7.09 (d, *J* = 9.2 Hz, 2H, H3 and H5), 7.62 (d, *J* = 8.7 Hz, 1H, H7), 7.71 (dd, *J* = 8.7, 2.4 Hz, 1H, H8), 7.85 (d, *J* = 9.1 Hz, 2H, H2 and H6), 8.03 (d, *J* = 2.3 Hz, 1H, H10).

^{13}C-NMR (101 MHz, $CDCl_3$) δ 13.6 (q, SCH_3), 55.7 (q, OCH_3), 114.4 (d, C3' and C5'), 115.7 (s), 121.4 (d, C2' and C6'), 122.1 (d, C10), 128.6 (s), 130.5 (d, C7/C8), 132.8 (d, C7/C8), 132.9 (s), 138.5 (s), 141.3 (s), 146.9 (s, CO), 150.7 (s, CS), 158.2 (s, C4').

HR-MS: Calc.[M+H]: 373.0521

Found [M+H]: 373.0524 (Diff.: -0.99 ppm)

Appearance: Pale grey solid

Mp: 239.5 – 240.6 °C

TLC: R_f = 0.90 (PE/EtOAc = 3/1)

E IV.13.19 9-Methoxy-5-(methylthio)-2-(p-tolyl)-[1,2,4]triazolo[4,3-c]quinazolin-3(2H)-one [127] DCBSBJ43

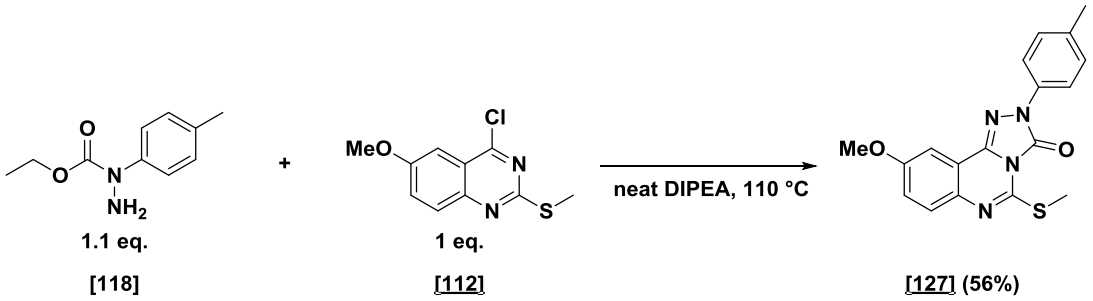

Chemical Formula: $C_{10}H_{14}N_2O_2$
Molecular Weight: 194.23

Chemical Formula: $C_{10}H_9ClN_2OS$
Molecular Weight: 240.71

Chemical Formula: $C_{18}H_{16}N_4O_2S$
Molecular Weight: 352.41

N,N-Diisopropylethylamine (51 mg, 0.40 mmol) was added to compound **[112]** (38 mg, 0.16 mmol) and **[118]** (37 mg, 0.19 mmol) and the reaction mixture was stirred at 110 °C for 18 h. The mixture was cooled to room temperature and the solvent was removed under reduced pressure. The crude solid was recrystallized from EtOH to give **[127]** as a pale grey soid (31 mg, 0.09 mmol, 56%).

^{1}H-NMR (400 MHz, $CDCl_3$) δ 2.39 (s, 3H, Ar-CH_3), 2.63 (s, 3H, SCH_3), 3.93 (s, 3H, OCH_3), 7.18 (dd, *J* = 8.9 and 2.9 Hz, 1H, H8), 7.22 – 7.32 (m, 2H, H3' and H5'), 7.51 (d, *J* = 2.9 Hz, 1H, H10), 7.56 (d, *J* = 8.9 Hz, 1H, H7), 7.96 (d, *J* = 8.5 Hz, 2H, H2' and H6').

^{13}C-NMR (101 MHz, $CDCl_3$) δ 13.2 (q, SCH_3), 20.9 (q, Ar-CH_3), 55.7 (q, OCH_3), 103.2 (d, C10), 114.8 (s), 119.3 (d, C2' and C6'), 121.3 (d, C7/C8), 128.4 (d, C7/C8), 129.4 (s), 134.7 (d, C3' and C5'), 135.9 (s), 137.2 (s), 139.5 (s), 147.0 (s, CO/CS), 147.1 (s, CO/CS), 158.2 (s, C9).

HR-MS: Calc.[M+H]: 353.1067

Found [M+H]: 353.1067 (Diff.: +0.06 ppm)

Appearance: Pale grey solid

Mp: 177.5 – 180.0 °C

TLC: R_f = 0.84 (PE/EtOAc = 3/1)

E IV.13.20 9-Methoxy-2-(4-methoxyphenyl)-5-(methylthio)-[1,2,4]triazolo-[4,3-c]quinazolin-3(2H)-one [128] DCBSBJ34

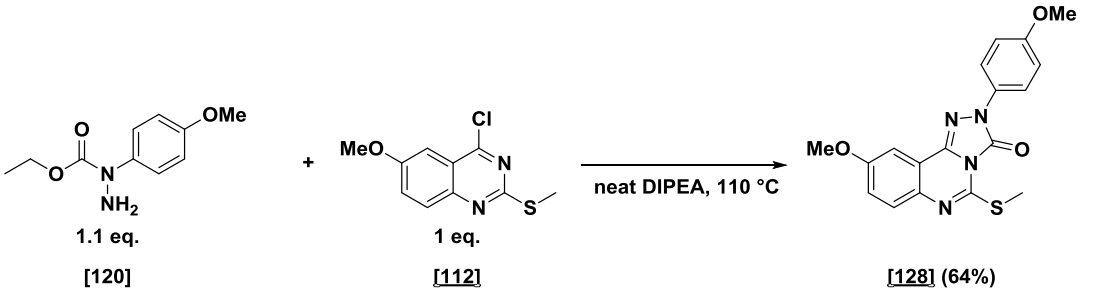

Chemical Formula: $C_{10}H_{14}N_2O_3$ **Molecular Weight: 210.23**

Chemical Formula: $C_{10}H_9ClN_2OS$ **Molecular Weight: 240.71**

Chemical Formula: $C_{18}H_{16}N_4O_3S$ **Molecular Weight: 368.41**

N,N-Diisopropylethylamine (31 mg, 0.29 mmol) was added to compound **[112]** (20 mg, 0.08 mmol) and **[120]** (51 mg, 0.23 mmol) and the reaction mixture was stirred at 110 °C for 18 h. The mixture was cooled to room temperature and the solvent was removed under reduced pressure. The crude solid was recrystallized from EtOH to give **[128]** as a pale grey solid (20 mg, 0.05 mmol, 64%).

^{1}H-NMR (400 MHz, $CDCl_3$) δ 2.63 (s, 3H, SCH_3), 3.85 (s, 3H, OCH_3), 3.93 (s, 3H, OCH_3), 6.92 – 7.04 (m, 2H, H3' and H5'), 7.19 (dd, *J* = 2.9 Hz, 8.9 Hz, 1H, H8), 7.50 (d, *J* = 2.9 Hz, 1H, H10), 7.56 (d, *J* = 8.9 Hz 1H, H7), 7.86 – 8.10 (m, 2H, H2' and H6').

^{13}C-NMR (101 MHz, $CDCl_3$) δ 13.5 (q, SCH_3), 55.7 (q, OCH_3), 56.0 (q, OCH_3), 103.5 (d, C10), 114.4 (d, C3' and C5'), 115.1 (s), 121.4 (d, C2' and C6'), 121.6 (d, C7/C8), 128.7 (d, C7/C8), 130.7 (s), 137.5 (s), 139.7 (s), 147.2 (s, CO/CS), 147.4 (s, CO/CS), 158.1 (s, C9/C4'), 158.6 (s, C9/C4').

HR-MS: Calc.[M+H]: 369.1016

Found [M+H]: 369.1010 (Diff.: +1.71 ppm)

Appearance: Pale grey solid

Mp: 204 – 207 °C

TLC: R_f = 0.59 (PE/EtOAc = 3/1)

E IV.13.21 4-(9-Chloro-5-(methylthio)-3-oxo-[1,2,4]triazolo[4,3-c]quinazolin-2(3H)-yl)benzonitrile [123] DCBSLA20

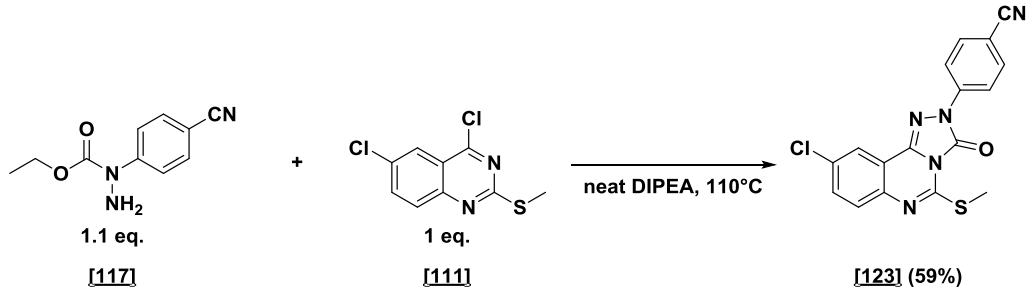

Chemical Formula: $C_{10}H_{11}N_3O_2$
Molecular Weight: 205.22

Chemical Formula: $C_9H_6Cl_2N_2S$
Molecular Weight: 245.12

Chemical Formula: $C_{17}H_{10}ClN_5OS$
Molecular Weight: 367.81

N,N-Diisopropylethylamine (222 mg, 1.72 mmol) was added to compound **[111]** (30 mg, 0.13 mmol) and **[117]** (28 mg, 0.15 mmol) and the reaction mixture was stirred at 110 °C for 22 h. The mixture was cooled to room temperature and the solvent was removed under reduced pressure. The crude solid was recrystallized from EtOH to give **[123]** as a colorless solid (26 mg, 0.077 mmol, 59%).

^{1}H-NMR (400 MHz, $CDCl_3$) δ 2.66 (s, 3H, SCH_3), 7.59 – 7.61 (m, 2H, H7 and H8), 7.75 – 7.80 (m, 2H, H2' and H6j'), 8.11 – 8.13 (m, 1H, H10), 8.27 – 8.32 (m, 2H, H3' and H5').

^{13}C-NMR (101 MHz, $CDCl_3$) δ 13.7 (q, CH_3), 109.6 (s, C4), 115.1 (s), 118.6 (s, CN), 119.1 (d, C3' and C5'), 122.4 (s), 128.8 (d, C7/C8), 133.2 (s), 133.5 (d, C2' and C6'), 133.6 (d, C7/C8), 139.8 (s), 140.7 (s), 141.5 (s), 147.1 (s, CO/CS), 150.4 (s, CO/CS).

HR-MS: Calc.[M+H]: 368.0367

Found [M+H]: n.det.

Appearance: Colorless solid

Mp: 210 – 212 °C

TLC: R_f = 0.46 (PE/EtOAc = 20/1)

E IV.13.22 *tert*-Butyl (4-(9-chloro-5-(methylthio)-3-oxo-[1,2,4]triazolo[4,3-c]quinazolin-2(3H)-yl)phenyl)carbamate [126] DCBS101

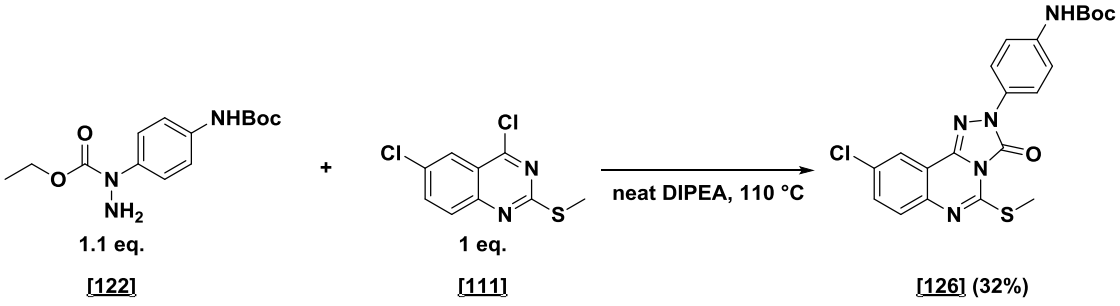

Chemical Formula: $C_{14}H_{21}N_3O_4$
Molecular Weight: 295.34

Chemical Formula: $C_9H_6Cl_2N_2S$
Molecular Weight: 245.12

Chemical Formula: $C_{21}H_{20}ClN_5O_3S$
Molecular Weight: 457.93

Compound **[122]** (40 mg, 0.135 mmol) and the chlorinated compound **[111]** (30 mg, 0.122 mmol) were dispersed in N,N-diisopropylethylamine and heated to 110 °C. After 72 h the solvent was evaporated and the residue was recrystallized from EtOH (2.5 mL). The precipitate was collected by filtration and washed with cold EtOH (4 mL) to give the desired product **[126]** (20 mg, 0.044 mmol, 32%).

^{1}H NMR (400 MHz, DMSO-d_6) δ 1.49 (s, 9H, 3 CH_3), 2.59 (s, 3H, SCH_3), 7.56 – 7.62 (m, 2H, H2' and H6'), 7.63 (d, *J* = 8.7 Hz, 1H, H7), 7.72 (dd, *J* = 8.7, 2.5 Hz, 1H, H8), 7.81 – 7.88 (m, 2H, H3' and H5'), 8.05 (d, *J* = 2.4 Hz, 1H, H10), 9.53 (br s, 1H, NH).

^{13}C NMR (101 MHz, DMSO-d_6) δ 12.9 (q, SCH_3), 28.1 (q, 3 CH_3), 79.2 (s, $\underline{C}(CH_3)_3$), 115.7 (s), 118.4 (d, C7), 119.9 (d, C2' and C6'/C3' and C5'), 121.2 (d, C10), 128.6 (d, C8), 131.2 (s), 131.2 (s), 132.5 (d, C2' and C6'/C3' and C5'), 137.8 (s), 138.2 (s), 140.9 (s), 146.4 (s), 150.7 (s, CO), 152.7 (s, CO).

HR-MS: Calc.[M+H]: 458.1054

Found [M+H]: n.det.

Appearance: Colorless solid

Mp: 185-187 °C

TLC: R_f = 0.48 (PE/EtOAc = 4/1)

E IV.13.23 9-Chloro-2-(p-tolyl)-2,6-dihydro-[1,2,4]triazolo[4,3-c]quinazoline-3,5-dione [130] DCBSBJ28

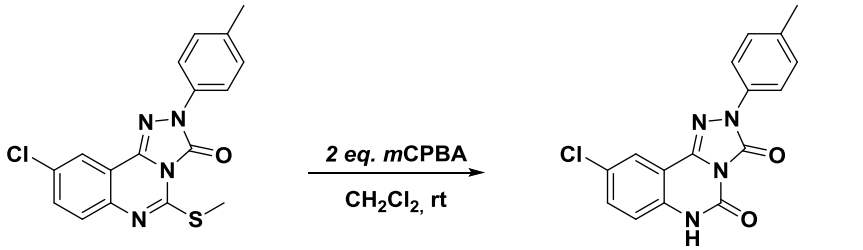

[124] [130] (71%)

Chemical Formula: $C_{17}H_{13}ClN_4OS$
Molecular Weight: 356.83

Chemical Formula: $C_{16}H_{11}ClN_4O_2$
Molecular Weight: 326.74

Substrate **[124]** (20 mg, 0.06 mmol) was dissolved in 2.5 mL CH_2Cl_2, (77 %) *m*CPBA (20 mg, 0.11 mmol) was added and the mixture was stirred at rt for 60 h. A colorless precipitate was slowly formed. To the mixture were added saturated solutions of aqueous $Na_2S_2O_3$ (1 mL) and $NaHCO_3$ (1 mL) and the suspension was stirred for 3 h. The precipitate was collected by filtration and washed with 20 mL of H_2O. The residue was dispersed in 1.5 mL EtOH and 1.5 mL H_2O and the dispersion was stirred at reflux for 1 h. The mixture was cooled to rt and the precipitate was collected by filtration to give **[130]** as a colorless solid (10 mg, 0.04 mmol, 71%).

^{1}H-NMR (400 MHz, DMSO-d_6) δ 2.34 (s, 3H, Ar-CH_3), 7.19 (d, *J* = 8.7 Hz, 1H, H7), 7.31 (d, *J* = 8.2 Hz, 2H, H3' and H5'), 7.51 – 7.73 (m, 1H, H8), 7.84 (d, *J* = 8.2, 2H, H2' and H6'), 7.89 – 7.97 (m, 1H, H10), 11.53 (br s, 1H, NH).

^{13}C-NMR (101 MHz, DMSO-d_6) δ 20.5 (q, Ar-CH_3), 110.8 (s), 117.7 (d, C2' and C6'), 118.8 (s), 121.6 (d, C10), 127.3 (d, C3' and C5'), 129.5 (d, C7/C8), 132.3 (d, C7/C8), 134.7 (s), 135.2 (s), 136.2 (s), 139.5 (s), 143.6 (s, CO), 146.5 (s, CO).

HR-MS: Calc. [M+H]: 327.0650

Found [M+H]: 327.0644 (Diff.: -2.53 ppm)

Appearance: Colorless solid

Mp: Decomposes > 300 °C

TLC: R_f = 0.10 (PE/EtOAc = 3/1)

E IV.13.24 9-Chloro-2-(4-methoxyphenyl)-2,6-dihydro-[1,2,4]triazolo[4,3-c]quinazoline-3,5-dione [131] DCBSBJ55

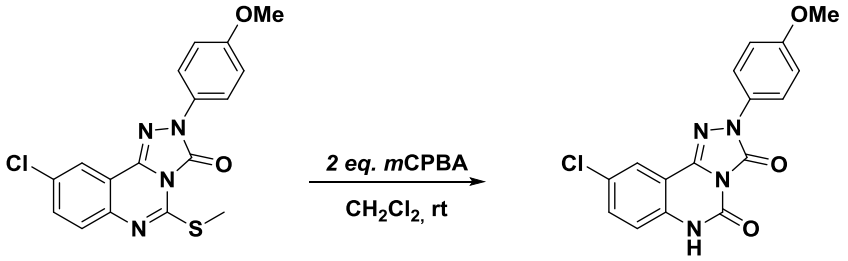

[124]

Chemical Formula: $C_{17}H_{13}ClN_4OS$
Molecular Weight: 372.83

[130] (71%)

Chemical Formula: $C_{16}H_{11}ClN_4O_4$
Molecular Weight: 342.74

Substrate **[125]** (31 mg, 0.08 mmol) was dissolved in 2.5 mL CH_2Cl_2, (77 %) *m*CPBA (29 mg, 0.17 mmol) was added and the mixture was stirred at rt for 60 h. A colorless precipitate was slowly formed. To the mixture were added saturated solutions of aqueous $Na_2S_2O_3$ (1 mL) and $NaHCO_3$ (1 mL) and the suspension was stirred for 3 h. The precipitate was collected by filtration and washed with 20 mL of H_2O. The residue was dispersed in 1.5 mL EtOH and 1.5 mL H_2O and the dispersion was added to the solid and was stirred at reflux for 1 h. The mixture was cooled to rt and the precipitate was collected by filtration to give **[131]** as a tan solid (20 mg, 0.05 mmol, 62%).

^{1}H-NMR (400 MHz, DMSO-d_6) δ 3.80 (s, 3H, OCH_3), 7.08 (d, *J* = 9.1 Hz, 2H, H3' and H5'), 7.19 (d, *J* = 8.8 Hz, 1H, H7), 7.61 (dd, *J* = 8.7, 2.4, 1H, H8), 7.79 – 7.87 (m, 2H, H2' and H6'), 7.92 (s, *J* = 2.3, 1H, H10), 11.53 (br s, 1H, NH).

^{13}C-NMR (101 MHz, DMSO-d_6) δ 55.4 (q, OCH_3), 110.9 (s), 114.3 (d, C3' and C5'), 117.7 (d, C10), 121.0 (d, C7/C8), 121.6 (d, C2' and C6'), 127.6 (s), 130.1 (s), 132.2 (d, C7/C8), 136.1 (s), 139.3 (s), 143.7 (s, CO), 146.6 (s, CO), 157.3 (s, C4').

HR-MS: Calc. [M+H]: 343.0599

Found [M+H]: 343.0590 (Diff.: -3.41 ppm)

Appearance: Tan solid

Mp: Decomposes > 300 °C

TLC: R_f = 0.15 (PE/EtOAc = 3/1)

E IV.13.25 9-Methoxy-2-(p-tolyl)-2,6-dihydro-[1,2,4]triazolo[4,3-c]quinazoline-3,5-dione [133] DCBSBJ48

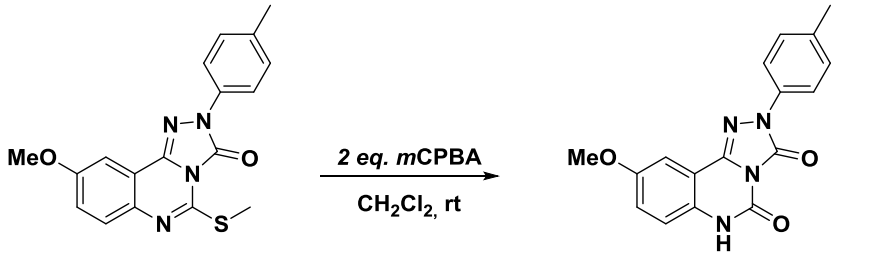

[127] [133] (50%)

Chemical Formula: $C_{18}H_{16}N_4O_2S$
Molecular Weight: 352.41

Chemical Formula: $C_{17}H_{14}N_4O_3$
Molecular Weight: 322.32

Substrate **[127]** (20 mg, 0.06 mmol) was dissolved in 2.5 mL CH_2Cl_2, (77 %) *m*CPBA (20 mg, 0.11 mmol) was added and the mixture was stirred at rt for 60 h. A colorless precipitate was slowly formed. To the mixture were added saturated solutions of aqueous $Na_2S_2O_3$ (1 mL) and $NaHCO_3$ (1 mL) and the suspesion was stirred for 3 h. The precipitate was collected by filtration and washed with 20 mL of H_2O. The residue was dispersed in 1.5 mL EtOH and 1.5 mL of H_2O and the dispersion was stirred at reflux for 1 h. The mixture was allowed to cool to rt and the solid was collected by filtration to give **[133]** (10 mg, 0.03 mmol, 50%).

^{1}H-NMR (400 MHz, DMSO-d_6) δ 2.34 (s, 3H, Ar-CH_3), 3.83 (s, 3H, OCH_3), 7.13 (d, *J* = 9.0 Hz, 1H, H7), 7.18 (dd, *J* = 2.8, 9.0 Hz, 1H, H8), 7.31 (d, *J* = 8.2, 2H, H3' and H5'), 7.37 (d, *J* = 2.8 Hz, 1H, H10) 7.85 (d, *J* = 8.5 Hz, 2H, H2' and H6'), 11.28 (br s, 1H, NH).

^{13}C-NMR (101 MHz, DMSO-d_6) δ 20.5 (q, Ar-CH_3), 55.7 (q, OCH_3), 104.5 (s, C-Ar), 109.9 (d, C10), 117.3 (d, C7/C8), 118.9 (d, C2' and C6'), 120.9 (d, C7/C8), 129.9 (d, C3' and C5'), 131.2 (s), 134.8 (s), 135.0 (s), 140.3 (s), 143.7 (s, CO), 146.7 (s, CO), 155.2 (s, C9).

HR-MS: Calc.[M+H]: 323.1145

Found [M+H]: 323.1150 (Diff.: -1.45 ppm)

Appearance: Colorless solid

Mp: Decomposes > 300 °C

TLC: R_f = 0.70 (10% MeOH in CH_2Cl_2)

E IV.13.26 9-Methoxy-2-(4-methoxyphenyl)-2,6-dihydro-[1,2,4]triazolo-[4,3-c]quinazoline-3,5-dione [134] DCBSBJ30

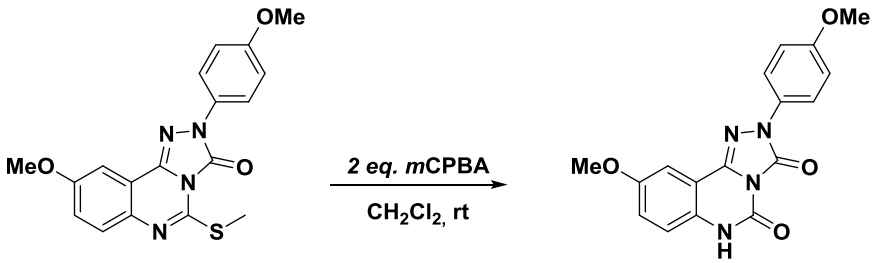

[128] [134] (71%)

Chemical Formula: $C_{18}H_{16}N_4O_3S$
Molecular Weight: 368.41

Chemical Formula: $C_{17}H_{14}N_4O_4$
Molecular Weight: 338.32

Substrate **[128]** (25 mg, 0,07 mmol) was dissolved in 1.4 mL CH_2Cl_2, (77%) *m*CPBA (23 mg, 0.14 mmol) was added and the mixture was stirred at rt for 18 h. A colorless precipitate was slowly formed. To the mixture were added saturated solutions of aqueous $Na_2S_2O_3$ (1 mL) and $NaHCO_3$ (1 mL) and the suspension was stirred for 3 h. The precipitate was collected by filtration and washed with 20 mL of H_2O. The residue was dispersed in 1.5 mL EtOH and 1.5 mL of H_2O and the dispersion was stirred at reflux for 1 h. The mixture was allowed to cool to rt and the precipitate was collected by filtration to give **[134]** (20 mg, 0.05 mmol, 71%).

^{1}H-NMR (400 MHz, DMSO-*d_6*) δ 3.81, (s, 6H, 2 OCH_3), 6.25 - 7.24 (m, 4H, H7 and H8 and H3' and H5'), 7.24 – 7.43 (m, 1H, H10), 7.78 – 8.08 (m, 2H, H2' and H6'), 11.28 (br s, 1H, NH).

^{13}C-NMR (101 MHz, DMSO-*d_6*) δ 55.4 (q, OCH_3), 55.7 (q, OCH_3), 104.4 (s), 109.7 (d, C10), 114.2 (d, C3' and C5'), 117.3 (d, C7/C8), 120.8 (d, C7/C8), 121.1 (d, C2' and C6'), 130.3 (s), 131.1 (s), 140.2 (s), 143.7 (s, CO), 146.7 (s, CO), 155.2 (s, C9/C4'), 157.2 (s, C9/C4').

HR-MS: Calc.[M+H]: 339.1094

Found [M+H]: 339.1101 (Diff.: -1.98 ppm)

Appearance: Colorless solid

Mp: Decomposes > 300 °C

TLC: R_f = 0.36 (PE/EtOAc = 3/1)

E IV.13.27 4-(9-Chloro-3,5-dioxo-5,6-dihydro-[1,2,4]triazolo[4,3-c]quinazolin-2(3H)-yl)benzonitrile [129] DCBS136

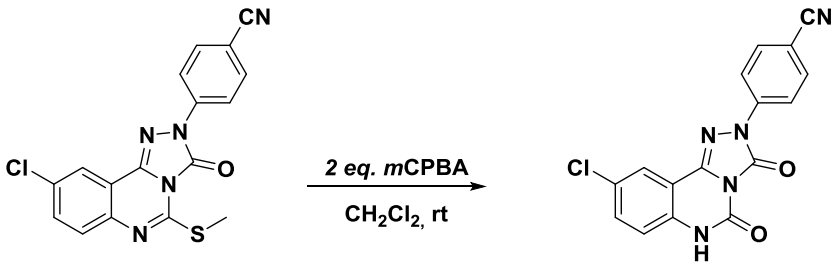

[123]

Chemical Formula: $C_{17}H_{10}ClN_5OS$
Molecular Weight: 367.81

[129] (17%)

Chemical Formula: $C_{16}H_8ClN_5O_2$
Molecular Weight: 337.72

Substrate **[123]** (23 mg, 0.06 mmol) was dissolved in 2.5 mL CH_2Cl_2, (77 %) *m*CPBA (1.8 mg, 0.1 mmol) was added and the mixture was stirred at rt for 60 h. A colorless precipitate was slowly formed. To the mixture were added saturated solutions of aqueous $Na_2S_2O_3$ (1 mL) and $NaHCO_3$ (1 mL) and the suspension was stirred for 3 h. The precipitate was collected by filtration and washed with 20 mL of H_2O. The residue was dispersed in 1.5 mL EtOH and 1.5 mL H_2O and the dispersion was stirred at reflux for 1 h. The mixture was cooled to rt and the precipitate was collected by filtration to give **[129]** as a colorless solid (3.6 mg, 0.01 mmol, 17%).

^{1}H-NMR (400 MHz, DMSO-d_6) 7.21 (d, *J* = 8.8 Hz, 1H, H7), 7.65 (dd, *J* = 8.8, 2.5 Hz, 1H, H8), 7.94 – 8.07 (m, 3H, H10 and H2' and H6'), 8.22 (d, *J* = 8.5 Hz, 2H, H3' and H5'), 11.64 (br s, 1H, NH).

^{13}C-NMR (151 MHz, DMSO-d_6) δ 107.6 (s), 110.5 (s), 117.8 (d, C7), 118.4 (d, C3' and C5'), 118.6 (s, CN), 122.0 (d, C10), 127.4 (s), 132.9 (d, C8), 133.7 (d, C2' and C6'), 136.5 (s), 140.6 (s), 140.7 (s), 143.5 (s, CO), 146.8 (s, CO).

HR-MS: Calc.[M+H]: 338.0439

Found [M+H]: 338.0446 (Diff.: -2.10 ppm)

Appearance: Colorless solid

Mp: Decomposes > 300 °C

TLC: R_f = 0.17 (PE/EtOAc = 3/1)

E IV.13.28 *tert*-Butyl (4-(9-chloro-3,5-dioxo-5,6-dihydro-[1,2,4]triazolo-[4,3-c]quinazolin-2(3H)-yl)phenyl)carbamate [132] DCBS104

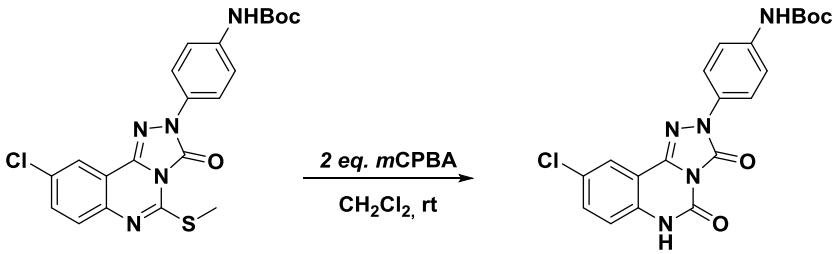

[126] [132] (40%)

Chemical Formula: $C_{21}H_{20}ClN_5O_3S$
Molecular Weight: 457.93

Chemical Formula: $C_{20}H_{18}ClN_5O_4$
Molecular Weight: 427.85

Substrate **[126]** (15 mg, 0,033 mmol) was dissolved in 2 mL CH_2Cl_2, (77 %) *m*CPBA (11 mg, 0.07 mmol) was added and the mixture was stirred at room temperature for 60 h. A colorless precipitate was formed slowly. Saturated $Na_2S_2O_3$ (1 mL) and $NaHCO_3$ (1 mL) solutions were added to the mixture and the dispersion was stirred for 3 h. The precipitate was collected by filtration and washed with 20 mL water. The residue was dissolved in 1.5 mL EtOH and 1.5 mL H_2O and stirred at reflux for 1 h. The mixture was cooled to room temperature and the precipitate was collected by filtration to give the desired product **[132]** (5 mg, 0.012 mmol, 40%).

^{1}H NMR (400 MHz, DMSO-d_6) δ 1.49 (s, 9H, 3 CH_3), 7.20 (d, *J* = 8.8 Hz, 1H, H7), 7.54 – 7.65 (m, 3H, H6 and H2' and H6'), 7.81 (d, *J* = 9.1 Hz, 2H, H3' and H5'), 7.93 (d, *J* = 2.4 Hz, 1H, H10), 9.50 (br s, 1H, NH), 11.52 (br s, 1H, NHBoc).

^{13}C NMR (101 MHz, DMSO-d_6) δ 28.1 (q, 3 CH_3), 79.2 (s, $\underline{C}(CH_3)_3$), 110.9 (s), 117.7 (d, C7), 118.4 (d, C10), 119.8 (d, C2' and C6'/C3' and C5'), 121.6 (d, C8), 127.2 (s), 131.3 (s), 132.3 (d, C2' and C6'/C3' and C5'), 136.1 (s), 137.5 (s), 139.4 (s), 143.6 (s, CO), 146.5 (s, CO), 152.7 (s, CO).

HR-MS: Calc.[M+H]: 428.1120

Found [M+H]: 428.1120 (Diff.: +0.05 ppm)

Appearance: Colorless solid

Mp: Decomposes > 300 °C

TLC: R_f = 0.55 (5% MeOH in CH_2Cl_2)

E IV.13.29 2-(4-Aminophenyl)-9-chloro-2,6-dihydro-[1,2,4]triazolo[4,3-c]quinazoline-3,5-dione [135] DCBS117

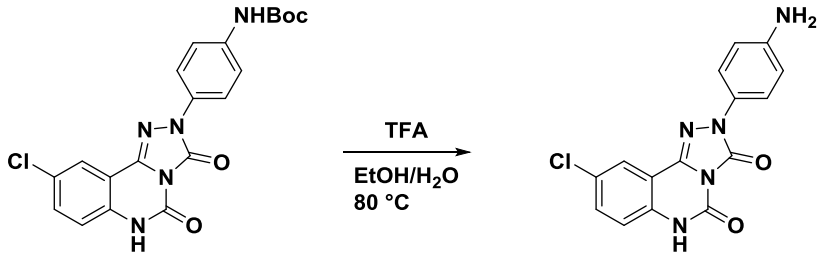

[132] [135] (quant.)

Chemical Formula: $C_{20}H_{18}ClN_5O_4$
Molecular Weight: 427.85

Chemical Formula: $C_{15}H_{10}ClN_5O_2$
Molecular Weight: 327.73

tert-Butyl (4-(9-chloro-3,5-dioxo-5,6-dihydro-[1,2,4]triazolo[4,3-c]quinazolin-2(3H)-yl)-phenyl)carbamate **[132]** (5 mg, 0.0117 mmol) was dissolved in 1 mL EtOH/water (1/1), TFA (9 µL, 0.117 mmol) was added and the reaction mixture was heated to 80 °C. After 17 h the solvent was removed under reduced pressure and the residue was washed with satd. $NaHCO_3$ (1 x 1 mL) and water (3 x 1 mL). After lyophilization the desired product **[135]** was obtained (3.8 mg, 0.0117 mmol, quantitative).

^{1}H NMR (400 MHz, DMSO-d_6) δ 5.28 (br s, 2H, NH_2), 6.62 – 6.70 (m, 2H, H3' and H5'), 7.18 (d, *J* = 8.8 Hz, 1H, H7), 7.48 (d, *J* = 8.8 Hz, 2H, H2' and H6'), 7.54 (dd, *J* = 8.7, 2.5 Hz, 1H, H8), 7.85 (d, *J* = 2.5 Hz, 1H, H10), 11.50 (br s, 1H, NH).

^{13}C NMR (151 MHz, DMSO-d_6) δ 111.0 (s), 114.2 (d, C3' and C5'), 117.7 (d, C7), 121.5 (d, C10), 121.7 (d, C2' and C6'), 127.2 (s), 132.1 (d, C8), 136.0 (s), 138.8 (s), 143.8 (s), 146.6 (s), 157.6 (s, CO), 157.8 (s,CO).

HR-MS: Calc.[M+H]: 328.0606

Found [M+H]: 328.0601 (Diff.: -2.57 ppm)

Appearance: Colorless solid

Mp: Decomposes > 300 °C

TLC: R_f = 0.35 (10% MeOH in CH_2Cl_2)

F Appendix

F I Publications resulting from this thesis

Journal articles

1. **David Chan Bodin Siebert**[§], Konstantina Bampali[§], Bernhard Jandl, Petra Scholze, Miroslav Savic, Marko D. Mihovilovic, Michael Schnürch, Margot Ernst; *Triazoloquinazolinediones as potential benzodiazepine site antagonists*, **MS in preparation**.
2. **David Chan Bodin Siebert**[§], Marcus Wieder[§], Lydia Schlener, Margot Ernst, Thierry Langer, Gerhard Ecker, Petra Scholze, Marko D. Mihovilovic, Michael Schnürch, Lars Richter; *Ranking of docking poses with Structure Activity Data: benzodiazepine site ligands revisited*; *J. Med Chem.*, **to be submitted 2018**.
3. Alshaimaa A. Elgarf, **David Chan Bodin Siebert**, Friederike Steudle, Roman Furtmüller, Zdravko Varagic, Roshan Puthenkalam, Angelika Draxler, Guanguan Li, Michael M. Poe, James Cook, Margot Ernst and Petra Scholze; *Different benzodiazepines bind with distinct binding modes to $GABA_A$ receptors; ACS Chem. Biol.*,**submitted**.
4. **David Chan Bodin Siebert**[§], Konstantina Bampali[§], Roshan Puthenkalam, Zdravko Varagic, Isabella Sarto-Jackson, Petra Scholze, Werner Sieghart, Marko D. Mihovilovic, Michael Schnürch, Margot Ernst; *Engineered benzodiazepine binding site reveals functional conservation of allosteric $GABA_A$ receptor binding sites; ACS Chem. Biol.,* **submitted**.
5. Marco Treven[§], **David Chan Bodin Siebert**[§], Raphael Holzinger, Konstantina Bampali, Jure Fabjan, Zdravko Varagic, Laurin Wimmer, Michael Schnürch, Marko D. Mihovilovic and Margot Ernst; *Towards Functional Selectivity for $\alpha 6\beta 3\gamma 2$ $GABA_A$ Receptors: A Series of Novel Pyrazoloquinolinones; Br. J. Pharmacol.*, **2017**.
6. Patent:"*Utilization of 8-chloro-2-(3-methoxyphenyl)-2H-pyrazolo[4,3-c]quinolin-3(5H)-one for the treatment of neuropsychiatric disorders with sensorimotor gating deficit and to influence pain processing in peripheral sensory ganglia*", **submitted**.
7. Xenia Simeone[§], **David Chan Bodin Siebert**[§], Konstantina Bampali, Zdravko Varagic, Marco Treven, Sabah Rehman, Jakob Pyszkowski, Raphael Holzinger, Friederike Steudle, Petra Scholze, Marko D. Mihovilovic, Michael Schnürch, Margot Ernst; *Molecular tools for $GABA_A$ receptors: High affinity ligands for β1- containing subtypes; Sci. Rep.,* **2017**.

8. Matthias Weil, **David Chan Bodin Siebert** and Michael Schnürch; *(Z)-4,6-Dichloro-N-(4-chlorophenyl)quinoline-3-carbimidoyl chloride*; *IUCrData 2*, **2017**, x170274.

Conference talks

1. *Pyrazoloquinolinones, revisited $GABA_A$ receptor tool compounds*, 27th European Heterocyclic Colloquium on Chemistry, Amsterdam, The Netherlands, **07/2016**.
2. *Post-Docking Derivatization reveals pyrazoloquinolinone binding mode at the $\alpha+/\gamma2-$ $GABA_A$ receptor interface*, 3rd Vienna Young Scientist Symposium, TU Wien, Vienna, Austira, **06/2017**.
3. *Pyrazoloquinolinones, revisited $GABA_A$ receptor tool compounds*, 10th Joint Meeting on Medicinal Chemistry, Dubrovnik, Croatia, **06/2017**.
4. *Pyrazoloquinolinones, revisited $GABA_A$ receptor tool compounds* (Flashtalk), 17th Blue Danube Symposium on Heterocyclic Chemistry, Linz, Autria, **09/2017**.

Poster Presentations

1. **David C. B. Siebert**, Xenia Simeone, Konstantina Bampali, Zdravko Varagic, Marco Treven, Sabah Rehman, Jakob Pyszkowski, Raphael Holzinger, Friederike Steudle, Petra Scholze, Michael Schnürch, Marko D. Mihovilovic & Margot Ernst, *Molecular mechanism of selective $GABA_A$ receptor modulation with pyrazoloquinolinones*, 3rd Summer School “Advances in Drug Discovery”, Prague, Czech Republic, **09/2016**.
2. **David C. B. Siebert**, Xenia Simeone, Konstantina Bampali, Zdravko Varagic, Marco Treven, Sabah Rehman, Jakob Pyszkowski, Raphael Holzinger, Friederike Steudle, Petra Scholze, Michael Schnürch, Marko D. Mihovilovic & Margot Ernst, *Molecular mechanism of selective $GABA_A$ receptor modulation with pyrazoloquinolinones*, 2nd MolTag Science Day, Vienna, Austria, **11/2016**.
3. **David C. B. Siebert**, Xenia Simeone, Konstantina Bampali, Zdravko Varagic, Marco Treven, Sabah Rehman, Jakob Pyszkowski, Raphael Holzinger, Friederike Steudle, Petra Scholze, Michael Schnürch, Marko D. Mihovilovic & Margot Ernst, *Pyrazoloquinolinones, revisited $GABA_A$ receptor tool compounds*, 17th Blue Danube Symposium on Heterocyclic Chemistry, Linz, Austria, **09/2017**.

F II Curriculum vitae

Education

10/2017- 02/2018 **Medical Science Liaison Management**
- Basic knowledge concerning public health and the pharmaceutical sector
- Effective communication, KOL and project management

09/2012- 09/2014 **MSc. Chemistry**, University of Konstanz
- Focus: organic synthesis and medicinal chemistry

09/2009- 08/2014 **BSc. Chemistry**, University of Konstanz
- Focus: biochemistry

08/1999- 07/2008 **Uhland Gymnasium**, Tübingen

2006- 2007 **Language school**, Nice, France
School exchange, Ann Arbor, US

Work Experience

03/2015- 02/2018 **PhD student at TU Wien**
- Drug development and optimization for CNS active compounds
- Synthetic chemistry and computational analysis
- Supervision of undergrads

03/2016- 05/2016 **Visiting Researcher** at Medical University of Vienna
- Department of Molecular Neuroscience, Center for Brain Research
- Investigation of allosteric modulators for $GABA_A$ receptors

09/2015- 11/2015 **Visiting Researcher** at University of Vienna
- Department of Pharmaceutical Chemistry
- Improving ligand design using docking and pharmacophore modelling

03/2014-08/2014 **Visiting Researcher** at Helmholtz-Institute for Pharmaceutical Research
- Department of Chemical Biology of Carbohydrates
- Synthesis of novel antibiotic drug candidates

05/2008-09/2008 **Emergency Medical Technician** at Red Cross
- Emergency medicine services

Extracurricular Engagement

Since 2016 **Volunteer at Roland McDonald House,** Vienna
- Supporting families of children with severe diseases

07/2015-03/2017 **Student representative** in the doctoral program MolTag
- Actively contributing to the educational concept of the program
- Organisation of small scientific conferences (“MolTag Sience Day”)

Additional Skills

Languages

- German – mother tongue
- English – fluent in speech and writing
- French – B1
- Latin proficiency certificate

Computing

- Windows – MS office (Word, Excel, PPT)
- Linux and IOS – Basics

Other Matters

Workshops
- Organization, Human Resource and Project Management, GDCh, 11/2016
- MOE Training, Chemical Computing Group, 04/2016
- MuTaLig COST Action Training, 02/2017

Summer Schools
- Novel Approaches in Drug Design and Development, Prague, 09/2016
- Drug Design - Computational Chemistry, Vienna, 09/2015
- Novel Approaches in Drug Design and Development, Prague, 09/2015

Driving license B

Interests: Sports, Sailing, Travelling, Cooking

F III List of abbreviations

AcOH	acetic acid
Ac_2O	acetic anhydride
aq.	aqueous
Boc	*tert*-butoxycarbonyl
Calc.	calculated
cat.	catalytic
CH_2Cl_2	dichloromethane
CSA	camphorsulfonic acid
COSY	correlated spectroscopy
DEMM	diethoxymethylene malonate
Diff.	difference
DIPEA	*N,N*-diisopropylethylamine
DMAP	4-dimethylaminopyridine
DMF	dimethylformamide
eq.	molar equivalents
EtOAc	ethyl acetate
EtOH	ethanol
EtSH	ethyl mercaptan
Et_2O	diethyl ether
Et_3N	triethylamine
GABA	*gamma* aminobutyric acid
$GABA_AR$	$GABA_A$ receptor
HPLC	high-performance liquid chromatography
HR-MS	high resolution mass spectrometry
HSQC	heteronuclear single quantum coherence
IBX	2-iodobenzoic acid
*m*CPAB	*meta*-chloroperoxybenzoic acid
MeOH	methanol
MeCN	acetonitrile
Mp	melting point
MsCl	methanesulfonyl chloride
µW	microwave irradiation
NaH	sodium hydride
NAM	negative allosteric modulator
NaOH	sodium hydroxide
NCS	N-chloro-succinimide
NMR	nuclear magnetic resonance
NOESY	nuclear overhauser enhancement spectroscopy
NsCl	2-nitrobenzenesulfonyl chloride
n.d.	not determined
n.det.	not detactable
no conv.	no conversion
OAc	acetyl
OMe	methoxy
PAM	positive allosteric modulator
PE	petroleum ether
PhSH	thiophenol
$POCl_3$	phosphoryl chloride
PPh_3	triphenylphosphine
ppm	parts per million
PQ	pyrazoloquinolinone
quant.	Quantitative
Red-Al	sodium bis(2-methoxyethoxy)aluminum hydride
RMSD	root-mean-square deviation
rt	room temperature
SAM	silent allosteric modulator
satd.	saturated
TEV	two-electrode voltage clamp method
TFA	trifluoroacetic acid
THF	tetrahydrofuran
TLC	thin layer chromatography
TMSA	trimethylsilylacetylene
TsCl	*p*-toluenesulfonyl chloride
wt%	weight percent

F IV List of laboratory journal codes

1. DCBS David Chan Bodin Siebert
2. DCBSBRP Benjamin Regen-Preziger
3. DCBSBJ Bernhard Jandl
4. DCBSJS Josefine Sprachmann
5. DCBSLA Leila Ayatollahi
6. DCBSLG Lukas Gaggl
7. DCBSLK Lukas Kalchgruber
8. DCBSLS Lisa Sinawehl
9. DCBSPU Patricia Ulrich

	1.
[6]	DCBS10
[7]	DCBS50
[8]	DCBS19
[9]	DCBS45B
[10]	DCBS45A
[12]	DCBS40B
[13]	DCBS40A
[14]	DCBS105
[15]	DCBS63B
[16]	DCBS63A
[17]	DCBS66B
[18]	DCBS53
[19]	DCBS38
[24	DCBS21]
[25]	DCBS01
[27]	DCBS25
[28]	DCBS08
[30]	DCBS30
[31]	DCBS16
[36]	DCBS193
[46]	DCBS54
[47]	DCBS138
[49]	DCBS139
[51]	DCBS128
[52]	DCBS142
[53]	DCBS137
[54]	DCBS119
[55]	DCBS146
[56]	DCBS120
[57]	DCBS152A
[58]	DCBS152B
[60]	DCBS148
[61]	DCBS149
[62]	DCBS147
[63]	DCBS150
[64]	DCBS164
[65]	DCBS153A
[66]	DCBS153B
[67]	DCBS155
[68]	DCBS156
[69]	DCBS154
[70]	DCBS157
[71]	DCBS163
[72]	DCBS162
[74]	DCBS76
[76]	DCBS93
[77]	DCBS84
[78]	DCBS96
[79]	DCBS88
[81]	DCBS141
[82]	DCBS135
[83]	DCBS52
[84]	DCBS145
[86]	DCBS151A
[87]	DCBS151B
[88b]	DCBS02
[88c]	DCBS07
[88d]	DCBS15
[89]	DCBS32
[90]	DCBS24
[91]	DCBS20
[92]	DCBS23

[121] DCBS99
[122] DCBS100
[126] DCBS101
[129] DCBS136
[132] DCBS132
[135] DCBS135
[140] DCBS199
[141] DCBS192
[142] DCBS209
[143] DCBS212
[155] DCBS172
[156] DCBS176
[157] DCBS177
[158] DCBS183
[180] DCBS165
[222] DCBS122
[223] DCBS133
[224] DCBS85
[225] DCBS126
[246] DCBS218
[247] DCBS220
[248] DCBS225
[249] DCBS227
[250] DCBS229
[251] DCBS231

2.

[144] DCBSBRP23
[236] DCBSBRP01
[237] DCBSBRP03
[238] DCBSBRP06

3.

[103] DCBSBJ03
[104] DCBSBJ12
[105] DCBSBJ14
[106] DCBSBJ15
[107] DCBSBJ05
[108] DCBSBJ17
[109] DCBSBJ23
[110] DCBSBJ22
[111] DCBSBJ26
[112] DCBSBJ25
[118] DCBSBJ02
[120] DCBSBJ13
[124] DCBSBJ27
[125] DCBSBJ52
[127] DCBSBJ43
[128] DCBSBJ34
[130] DCBSBJ28
[131] DCBSBJ55
[133] DCBSBJ48
[134] DCBSBJ30

4.

[241] DCBSJS08
[243] DCBSJS11
[244] DCBSJS14

5.

[117] DCBSLA09
[119] DCBSLA01
[123] DCBSLA20
[177] DCBSLA08
[178] DCBSLA11
[179] DCBSLA13

6.

[160] DCBSLG01
[161] DCBSLG02
[162] DCBSLG03
[163] DCBSLG04

7.

[23] DCBSLK01
[26] DCBSLK05
[29] DCBSLK08
[32] DCBSLK32
[33] DCBSLK12
[34] DCBSLK59
[35] DCBSLK15
[37] DCBSLK38
[38] DCBSLK32
[39] DCBSLK17

[40] DCBSLK29
[41] DCBSLK23
[42] DCBSLK40
[43] DCBSLK55
[44] DCBSLK39
[45] DCBSLK33
[52] DCBSLK36
[73] DCBSLK58
[80] DCBSLK60

8.

[11] DCBSLS25
[48] DCBSLS02
[50] DCBSLS17
[85] DCBSLS24

9.

[183] DCBSPU28
[184] DCBSPU29
[186] DCBSPU41
[187] DCBSPU43
[188] DCBSPU44
[194] DCBSPU07
[195] DCBSPU18
[196] DCBSPU05
[197] DCBSPU06
[198] DCBSPU17
[199] DCBSPU47
[200] DCBSPU46
[201] DCBSPU13
[202] DCBSPU23
[203] DCBSPU11
[204] DCBSPU12
[205] DCBSPU22
[206] DCBSPU50
[207] DCBSPU48
[208] DCBSPU16
[209] DCBSPU25
[210] DCBSPU14
[211] DCBSPU15
[212] DCBSPU24
[213] DCBSPU52
[214] DCBSPU49
[215] DCBSPU21
[216] DCBSPU27
[217] DCBSPU19
[218] DCBSPU42
[219] DCBSPU26
[220] DCBSPU53
[221] DCBSPU51

F V References

1 Wu, Z. S., Cheng, H., Jiang, Y., Melcher, K. & Xu, H. E. Ion channels gated by acetylcholine and serotonin: structures, biology, and drug discovery. *Acta Pharmacol Sin* **36**, 895-907, (2015).

2 Du, J., Lu, W., Wu, S. P., Cheng, Y. F. & Gouaux, E. Glycine receptor mechanism elucidated by electron cryo-microscopy. *Nature* **526**, 224-+, (2015).

3 Huang, X., Chen, H., Michelsen, K., Schneider, S. & Shaffer, P. L. Crystal structure of human glycine receptor-alpha 3 bound to antagonist strychnine. *Nature* **526**, 277-+, (2015).

4 Krankenkasse, T. Entspann dich, Deutschland - TK-Stressstudie 2016. 56 (2016).

5 Draskovits, M. *Synthesis of Pyrazoloquinolinones and Imidazoquinolines as potential $GABA_A$ receptor ligands* Diplom thesis, TU Wien, (2016).

6 Puthenkalam, R. *et al.* Structural Studies of $GABA_A$ Receptor Binding Sites: Which Experimental Structure Tells us What? *Frontiers in molecular neuroscience* **9**, 44, (2016).

7 Whiting, P. J. $GABA_A$ receptors: a viable target for novel anxiolytics? *Current opinion in pharmacology* **6**, 24-29, (2006).

8 Ferguson, J. M. SSRI Antidepressant Medications: Adverse Effects and Tolerability. *Primary care companion to the Journal of clinical psychiatry* **3**, 22-27 (2001).

9 Baldwin, D. S. *et al.* Evidence-based guidelines for the pharmacological treatment of anxiety disorders: recommendations from the British Association for Psychopharmacology. *Journal of psychopharmacology* **19**, 567-596, (2005).

10 Sieghart, W. Allosteric modulation of GABAA receptors via multiple drug-binding sites. *Advances in pharmacology* **72**, 53-96, (2015).

11 Sauguet, L. *et al.* Crystal structures of a pentameric ligand-gated ion channel provide a mechanism for activation. *Proceedings of the National Academy of Sciences of the United States of America* **111**, 966-971, (2014).

12 Sigel, E. & Steinmann, M. E. Structure, function, and modulation of $GABA_A$ receptors. *The Journal of biological chemistry* **287**, 40224-40231, (2012).

13 Lynagh, T. & Pless, S. A. Principles of agonist recognition in Cys-loop receptors. *Frontiers in physiology* **5**, 160, (2014).

14 Unwin, N. Refined structure of the nicotinic acetylcholine receptor at 4A resolution. *Journal of molecular biology* **346**, 967-989, (2005).

15 Tretter, V., Ehya, N., Fuchs, K. & Sieghart, W. Stoichiometry and assembly of a recombinant $GABA_A$ receptor subtype. *The Journal of neuroscience : the official journal of the Society for Neuroscience* **17**, 2728-2737 (1997).

16 Smit, A. B., Brejc, K., Syed, N. & Sixma, T. K. Structure and function of AChBP, homologue of the ligand-binding domain of the nicotinic acetylcholine receptor. *Annals of the New York Academy of Sciences* **998**, 81-92 (2003).

17 Ernst, M., Brauchart, D., Boresch, S. & Sieghart, W. Comparative modeling of $GABA_A$ receptors: Limits, insights, future developments. *Neuroscience* **119**, 933-943, (2003).

18 Olsen, R. W. & Sieghart, W. International Union of Pharmacology. LXX. Subtypes of gamma-aminobutyric acid(A) receptors: classification on the basis of subunit composition, pharmacology, and function. Update. *Pharmacological reviews* **60**, 243-260, (2008).

19 Verdoorn, T. A. Formation of heteromeric gamma-aminobutyric acid type A receptors containing two different alpha subunits. *Molecular pharmacology* **45**, 475-480 (1994).

20 Ralvenius, W. T., Benke, D., Acuna, M. A., Rudolph, U. & Zeilhofer, H. U. Analgesia and unwanted benzodiazepine effects in point-mutated mice expressing only one benzodiazepine-sensitive $GABA_A$ receptor subtype. *Nature communications* **6**, 6803, (2015).

21 Araujo, F., Ruano, D. & Vitorica, J. Native gamma-aminobutyric acid type A receptors from rat hippocampus, containing both alpha 1 and alpha 5 subunits, exhibit a single benzodiazepine binding site with alpha 5 pharmacological properties. *The Journal of pharmacology and experimental therapeutics* **290**, 989-997 (1999).

22 Moraga-Cid, G., Yevenes, G. E., Schmalzing, G., Peoples, R. W. & Aguayo, L. G. A Single phenylalanine residue in the main intracellular loop of alpha1 gamma-aminobutyric acid type A and glycine receptors influences their sensitivity to propofol. *Anesthesiology* **115**, 464-473, (2011).

23 Sigel, E. & Luscher, B. P. A closer look at the high affinity benzodiazepine binding site on $GABA_A$ receptors. *Current topics in medicinal chemistry* **11**, 241-246 (2011).

24 Smith, G. B. & Olsen, R. W. Identification of a [3H]muscimol photoaffinity substrate in the bovine gamma-aminobutyric acidA receptor alpha subunit. *The Journal of biological chemistry* **269**, 20380-20387 (1994).

25 Sieghart, W., Ramerstorfer, J., Sarto-Jackson, I., Varagic, Z. & Ernst, M. A novel $GABA_A$ receptor pharmacology: drugs interacting with the alpha(+) beta(-) interface. *British journal of pharmacology* **166**, 476-485, (2012).

26 Rudolph, U. & Knoflach, F. Beyond classical benzodiazepines: novel therapeutic potential of $GABA_A$ receptor subtypes. *Nature reviews. Drug discovery* **10**, 685-697, (2011).

27 Ernst, M., Bruckner, S., Boresch, S. & Sieghart, W. Comparative models of $GABA_A$ receptor extracellular and transmembrane domains: important insights in pharmacology and function. *Molecular pharmacology* **68**, 1291-1300, (2005).

28 Belelli, D. & Lambert, J. J. Neurosteroids: endogenous regulators of the $GABA_A$ receptor. *Nature reviews. Neuroscience* **6**, 565-575, (2005).

29 Saras, A. *et al.* Histamine action on vertebrate $GABA_A$ receptors: direct channel gating and potentiation of GABA responses. *The Journal of biological chemistry* **283**, 10470-10475, (2008).

30 Hoerbelt, P., Lindsley, T. A. & Fleck, M. W. Dopamine directly modulates $GABA_A$ receptors. *The Journal of neuroscience : the official journal of the Society for Neuroscience* **35**, 3525-3536, (2015).

31 Sigel, E. *et al.* The major central endocannabinoid directly acts at $GABA_A$ receptors. *Proceedings of the National Academy of Sciences of the United States of America* **108**, 18150-18155, (2011).

32 Reddy, D. S. Pharmacology of endogenous neuroactive steroids. *Critical reviews in neurobiology* **15**, 197-234 (2003).

33 Lambert, J. J., Belelli, D., Peden, D. R., Vardy, A. W. & Peters, J. A. Neurosteroid modulation of $GABA_A$ receptors. *Progress in neurobiology* **71**, 67-80, (2003).

34 Laverty, D. *et al.* Crystal structures of a $GABA_A$-receptor chimera reveal new endogenous neurosteroid-binding sites. *Nature structural & molecular biology*, (2017).

35 Bateson, A. N. The benzodiazepine site of the $GABA_A$ receptor: an old target with new potential? *Sleep medicine* **5 Suppl 1**, S9-15 (2004).

36 Savic, M. M. *et al.* Are $GABA_A$ receptors containing alpha5 subunits contributing to the sedative properties of benzodiazepine site agonists? *Neuropsychopharmacology : official publication of the American College of Neuropsychopharmacology* **33**, 332-339, (2008).
37 Sigel, E. & Buhr, A. The benzodiazepine binding site of $GABA_A$ receptors. *Trends in pharmacological sciences* **18**, 425-429 (1997).
38 Vinkers, C. H. & Olivier, B. Mechanisms Underlying Tolerance after Long-Term Benzodiazepine Use: A Future for Subtype-Selective $GABA_A$ Receptor Modulators? *Advances in pharmacological sciences* **2012**, 416864, (2012).
39 Lopez-Munoz, F., Ucha-Udabe, R. & Alamo, C. The history of barbiturates a century after their clinical introduction. *Neuropsychiatric disease and treatment* **1**, 329-343 (2005).
40 Marszalec, W. & Narahashi, T. Use-dependent pentobarbital block of kainate and quisqualate currents. *Brain research* **608**, 7-15 (1993).
41 Werz, M. A. & Macdonald, R. L. Barbiturates decrease voltage-dependent calcium conductance of mouse neurons in dissociated cell culture. *Molecular pharmacology* **28**, 269-277 (1985).
42 Yang, J. S. & Olsen, R. W. gamma-Aminobutyric acid receptor binding in fresh mouse brain membranes at 22 degrees C: ligand-induced changes in affinity. *Molecular pharmacology* **32**, 266-277 (1987).
43 Drafts, B. C. & Fisher, J. L. Identification of structures within $GABA_A$ receptor alpha subunits that regulate the agonist action of pentobarbital. *The Journal of pharmacology and experimental therapeutics* **318**, 1094-1101, (2006).
44 Mehta, A. K. & Ticku, M. K. An investigation on the role of nitric oxide in the modulation of the binding characteristics of various radioligands of $GABA_A$ receptors by 5alpha-pregnan-3alpha-ol-20-one in the rat brain regions. *Brain research* **832**, 164-167 (1999).
45 Jayakar, S. S. *et al.* Multiple propofol-binding sites in a gamma-aminobutyric acid type A receptor ($GABA_AR$) identified using a photoreactive propofol analog. *The Journal of biological chemistry* **289**, 27456-27468, (2014).
46 Chiara, D. C. *et al.* General Anesthetic Binding Sites in Human alpha4beta3delta gamma-Aminobutyric Acid Type A Receptors ($GABA_ARs$). *The Journal of biological chemistry* **291**, 26529-26539, (2016).
47 Garcia, P. S., Kolesky, S. E. & Jenkins, A. General anesthetic actions on $GABA_A$ receptors. *Current neuropharmacology* **8**, 2-9, (2010).
48 Alkire, M. T., Hudetz, A. G. & Tononi, G. Consciousness and anesthesia. *Science* **322**, 876-880, (2008).
49 Franks, N. P. & Lieb, W. R. Molecular and cellular mechanisms of general anaesthesia. *Nature* **367**, 607-614, (1994).
50 Belelli, D., Pistis, M., Peters, J. A. & Lambert, J. J. General anaesthetic action at transmitter-gated inhibitory amino acid receptors. *Trends in pharmacological sciences* **20**, 496-502 (1999).
51 Orser, B. A., Wang, L. Y., Pennefather, P. S. & MacDonald, J. F. Propofol modulates activation and desensitization of $GABA_A$ receptors in cultured murine hippocampal neurons. *The Journal of neuroscience : the official journal of the Society for Neuroscience* **14**, 7747-7760 (1994).
52 Hemmings, H. C., Jr. *et al.* Emerging molecular mechanisms of general anesthetic action. *Trends in pharmacological sciences* **26**, 503-510, (2005).
53 Newman, D. J. & Cragg, G. M. Natural products as sources of new drugs over the last 25 years. *Journal of natural products* **70**, 461-477, (2007).
54 Rosen, J., Gottfries, J., Muresan, S., Backlund, A. & Oprea, T. I. Novel chemical space exploration via natural products. *Journal of medicinal chemistry* **52**, 1953-1962, (2009).
55 Harvey, A. L., Edrada-Ebel, R. & Quinn, R. J. The re-emergence of natural products for drug discovery in the genomics era. *Nature reviews. Drug discovery* **14**, 111-129, (2015).
56 Johnston, G. A., Hanrahan, J. R., Chebib, M., Duke, R. K. & Mewett, K. N. Modulation of ionotropic GABA receptors by natural products of plant origin. *Advances in pharmacology* **54**, 285-316 (2006).
57 Yin, H., Cho, D. H., Park, S. J. & Han, S. K. GABA-mimetic actions of Withania somnifera on substantia gelatinosa neurons of the trigeminal subnucleus caudalis in mice. *The American journal of Chinese medicine* **41**, 1043-1051, (2013).
58 Elsas, S. M. *et al.* Passiflora incarnata L. (Passionflower) extracts elicit GABA currents in hippocampal neurons in vitro, and show anxiogenic and anticonvulsant effects in vivo, varying with extraction method. *Phytomedicine : international journal of phytotherapy and phytopharmacology* **17**, 940-949, (2010).
59 Santos, M. S. *et al.* Synaptosomal GABA release as influenced by valerian root extract--involvement of the GABA carrier. *Archives internationales de pharmacodynamie et de therapie* **327**, 220-231 (1994).
60 Huang, W. J. *et al.* Hispidulin, a constituent of Clerodendrum inerme that remitted motor tics, alleviated methamphetamine-induced hyperlocomotion without motor impairment in mice. *Journal of ethnopharmacology* **166**, 18-22, (2015).
61 Kavvadias, D. *et al.* The flavone hispidulin, a benzodiazepine receptor ligand with positive allosteric properties, traverses the blood-brain barrier and exhibits anticonvulsive effects. *British journal of pharmacology* **142**, 811-820, (2004).
62 Ishola, I. O. *et al.* Antidepressant and anxiolytic effects of amentoflavone isolated from Cnestis ferruginea in mice. *Pharmacology, biochemistry, and behavior* **103**, 322-331, (2012).
63 Fernandez, S. P., Wasowski, C., Paladini, A. C. & Marder, M. Synergistic interaction between hesperidin, a natural flavonoid, and diazepam. *European journal of pharmacology* **512**, 189-198, (2005).
64 Kumar, A., Lalitha, S. & Mishra, J. Hesperidin potentiates the neuroprotective effects of diazepam and gabapentin against pentylenetetrazole-induced convulsions in mice: Possible behavioral, biochemical and mitochondrial alterations. *Indian journal of pharmacology* **46**, 309-315, (2014).
65 Hansen, R. S., Paulsen, I. & Davies, M. Determinants of amentoflavone interaction at the $GABA_A$ receptor. *European journal of pharmacology* **519**, 199-207, (2005).
66 Marder, M. *et al.* 6,3'-Dinitroflavone, a Novel High-Affinity Ligand for the Benzodiazepine Receptor with Potent Anxiolytic Properties. *Bioorganic & medicinal chemistry letters* **5**, 2717-2720, (1995).
67 Marder, M. *et al.* Detection of benzodiazepine receptor ligands in small libraries of flavone derivatives synthesized by solution phase combinatorial chemistry. *Biochemical and biophysical research communications* **249**, 481-485, (1998).
68 Sultana, N. & Saify, Z. S. Naturally occurring and synthetic agents as potential anti-inflammatory and immunomodulants. *Anti-inflammatory & anti-allergy agents in medicinal chemistry* **11**, 3-19 (2012).
69 Priestley, C. M., Williamson, E. M., Wafford, K. A. & Sattelle, D. B. Thymol, a constituent of thyme essential oil, is a positive allosteric modulator of human $GABA_A$ receptors and a homo-oligomeric GABA receptor from Drosophila melanogaster. *British journal of pharmacology* **140**, 1363-1372, (2003).
70 Mohammadi, B. *et al.* Structural requirements of phenol derivatives for direct activation of chloride currents via $GABA_A$ receptors. *European journal of pharmacology* **421**, 85-91 (2001).
71 Houghton, P. J. The scientific basis for the reputed activity of Valerian. *The Journal of pharmacy and pharmacology* **51**, 505-512 (1999).

72 Khom, S. *et al.* Valerenic acid derivatives as novel subunit-selective $GABA_A$ receptor ligands - in vitro and in vivo characterization. *British journal of pharmacology* **161**, 65-78, (2010).
73 Khom, S. *et al.* Valerenic acid potentiates and inhibits $GABA_A$ receptors: molecular mechanism and subunit specificity. *Neuropharmacology* **53**, 178-187, (2007).
74 Johnston, G. A. Muscimol as an ionotropic GABA receptor agonist. *Neurochemical research* **39**, 1942-1947, (2014).
75 Curtis, D. R., Duggan, A. W., Felix, D. & Johnston, G. A. GABA, bicuculline and central inhibition. *Nature* **226**, 1222-1224 (1970).
76 Krishek, B. J., Moss, S. J. & Smart, T. G. A functional comparison of the antagonists bicuculline and picrotoxin at recombinant GABAA receptors. *Neuropharmacology* **35**, 1289-1298 (1996).
77 Clark, J. B. Effect of a polyacetylenic fish poison on the oxidative phosphorylation of rat liver mitochondria. *Biochemical pharmacology* **18**, 73-83 (1969).
78 Quilliam, J. P. & Stables, R. Action of cunaniol on goldfish. *British journal of pharmacology* **35**, 382P (1969).
79 Uwai, K. *et al.* Exploring the structural basis of neurotoxicity in C(17)-polyacetylenes isolated from water hemlock. *Journal of medicinal chemistry* **43**, 4508-4515 (2000).
80 Uwai, K. *et al.* Virol A, a toxic trans-polyacetylenic alcohol of Cicuta virosa, selectively inhibits the GABA-induced Cl(-) current in acutely dissociated rat hippocampal CA1 neurons. *Brain research* **889**, 174-180 (2001).
81 Mayer, M. & Meyer, B. Characterization of ligand binding by saturation transfer difference NMR spectroscopy. *Angew Chem Int Edit* **38**, 1784-1788, (1999).
82 Ruoho, A. E., Kiefer, H., Roeder, P. E. & Singer, S. J. Mechanism of Photoaffinity Labeling. *Proceedings of the National Academy of Sciences of the United States of America* **70**, 2567-2571, (1973).
83 Ramerstorfer, J. *et al.* The $GABA_A$ receptor alpha+beta- interface: a novel target for subtype selective drugs. *The Journal of neuroscience : the official journal of the Society for Neuroscience* **31**, 870-877, (2011).
84 Baur, R. *et al.* Covalent modification of $GABA_A$ receptor isoforms by a diazepam analogue provides evidence for a novel benzodiazepine binding site that prevents modulation by these drugs. *Journal of neurochemistry* **106**, 2353-2363, (2008).
85 Bill, R. M. *et al.* Overcoming barriers to membrane protein structure determination. *Nat Biotechnol* **29**, 335-340, (2011).
86 Chothia, C. & Lesk, A. M. The Relation between the Divergence of Sequence and Structure in Proteins. *Embo J* **5**, 823-826 (1986).
87 Kaczanowski, S. & Zielenkiewicz, P. Why similar protein sequences encode similar three-dimensional structures? *Theor Chem Acc* **125**, 643-650, (2010).
88 Marti-Renom, M. A. *et al.* Comparative protein structure modeling of genes and genomes. *Annu Rev Bioph Biom* **29**, 291-325, (2000).
89 Cromer, B. A., Morton, C. J. & Parker, M. W. Anxiety over $GABA_A$ receptor structure relieved by AChBP (vol 27, pg 280, 2002). *Trends Biochem Sci* **27**, 380-380, (2002).
90 Miller, P. S. & Aricescu, A. R. Crystal structure of a human $GABA_A$ receptor. *Nature* **512**, 270-275, (2014).
91 Huang, S. Y. & Zou, X. Advances and challenges in protein-ligand docking. *International journal of molecular sciences* **11**, 3016-3034, (2010).
92 Kuntz, I. D., Blaney, J. M., Oatley, S. J., Langridge, R. & Ferrin, T. E. A geometric approach to macromolecule-ligand interactions. *Journal of molecular biology* **161**, 269-288 (1982).
93 McGann, M. R., Almond, H. R., Nicholls, A., Grant, J. A. & Brown, F. K. Gaussian docking functions. *Biopolymers* **68**, 76-90, (2003).
94 Venkatachalam, C. M., Jiang, X., Oldfield, T. & Waldman, M. LigandFit: a novel method for the shape-directed rapid docking of ligands to protein active sites. *Journal of molecular graphics & modelling* **21**, 289-307 (2003).
95 Huang, S. Y. & Zou, X. Ensemble docking of multiple protein structures: considering protein structural variations in molecular docking. *Proteins* **66**, 399-421, (2007).
96 Huang, S. Y. & Zou, X. Efficient molecular docking of NMR structures: application to HIV-1 protease. *Protein science : a publication of the Protein Society* **16**, 43-51, (2007).
97 Jones, G., Willett, P. & Glen, R. C. Molecular recognition of receptor sites using a genetic algorithm with a description of desolvation. *Journal of molecular biology* **245**, 43-53 (1995).
98 Jones, G., Willett, P., Glen, R. C., Leach, A. R. & Taylor, R. Development and validation of a genetic algorithm for flexible docking. *Journal of molecular biology* **267**, 727-748, (1997).
99 Morris, G. M. *et al.* Automated docking using a Lamarckian genetic algorithm and an empirical binding free energy function. *J Comput Chem* **19**, 1639-1662, (1998).
100 Thomsen, R. & Christensen, M. H. MolDock: a new technique for high-accuracy molecular docking. *Journal of medicinal chemistry* **49**, 3315-3321, (2006).
101 Grosdidier, A., Zoete, V. & Michielin, O. EADock: docking of small molecules into protein active sites with a multiobjective evolutionary optimization. *Proteins* **67**, 1010-1025, (2007).
102 Jiang, F. & Kim, S. H. "Soft docking": matching of molecular surface cubes. *Journal of molecular biology* **219**, 79-102 (1991).
103 Ferrari, A. M., Wei, B. Q., Costantino, L. & Shoichet, B. K. Soft docking and multiple receptor conformations in virtual screening. *Journal of medicinal chemistry* **47**, 5076-5084, (2004).
104 Leach, A. R. Ligand docking to proteins with discrete side-chain flexibility. *Journal of molecular biology* **235**, 345-356 (1994).
105 Gohlke, H. & Klebe, G. Statistical potentials and scoring functions applied to protein-ligand binding. *Curr Opin Struc Biol* **11**, 231-235, (2001).
106 Schulz-Gasch, T. & Stahl, M. Scoring functions for protein-ligand interactions: a critical perspective. *Drug discovery today. Technologies* **1**, 231-239, (2004).
107 Jain, A. N. Scoring functions for protein-ligand docking. *Current protein & peptide science* **7**, 407-420 (2006).
108 Rajamani, R. & Good, A. C. Ranking poses in structure-based lead discovery and optimization: current trends in scoring function development. *Current opinion in drug discovery & development* **10**, 308-315 (2007).
109 Gilson, M. K. & Zhou, H. X. Calculation of protein-ligand binding affinities. *Annu Rev Biophys Biomol Struct* **36**, 21-42, (2007).
110 Weiner, P. K. & Kollman, P. A. Amber - Assisted Model-Building with Energy Refinement - a General Program for Modeling Molecules and Their Interactions. *J Comput Chem* **2**, 287-303, (1981).
111 Nilsson, L. & Karplus, M. Empirical Energy Functions for Energy Minimization and Dynamics of Nucleic-Acids. *J Comput Chem* **7**, 591-616, (1986).
112 Brooks, B. R. *et al.* Charmm - a Program for Macromolecular Energy, Minimization, and Dynamics Calculations. *J Comput Chem* **4**, 187-217, (1983).
113 Huang, N., Kalyanaraman, C., Bernacki, K. & Jacobson, M. P. Molecular mechanics methods for predicting protein-ligand binding. *Physical Chemistry Chemical Physics* **8**, 5166-5177, (2006).

114 Meng, E. C., Shoichet, B. K. & Kuntz, I. D. Automated Docking with Grid-Based Energy Evaluation. *J Comput Chem* **13**, 505-524, (1992).
115 Eldridge, M. D., Murray, C. W., Auton, T. R., Paolini, G. V. & Mee, R. P. Empirical scoring functions: I. The development of a fast empirical scoring function to estimate the binding affinity of ligands in receptor complexes. *Journal of computer-aided molecular design* **11**, 425-445 (1997).
116 Bohm, H. J. The development of a simple empirical scoring function to estimate the binding constant for a protein-ligand complex of known three-dimensional structure. *Journal of computer-aided molecular design* **8**, 243-256 (1994).
117 Wang, R. X., Liu, L., Lai, L. H. & Tang, Y. Q. SCORE: A new empirical method for estimating the binding affinity of a protein-ligand complex. *Journal of molecular modeling* **4**, 379-394, (1998).
118 Krammer, A., Kirchhoff, P. D., Jiang, X., Venkatachalam, C. M. & Waldman, M. LigScore: a novel scoring function for predicting binding affinities. *Journal of molecular graphics & modelling* **23**, 395-407, (2005).
119 Halgren, T. A. *et al.* Glide: a new approach for rapid, accurate docking and scoring. 2. Enrichment factors in database screening. *Journal of medicinal chemistry* **47**, 1750-1759, (2004).
120 Muegge, I. & Martin, Y. C. A general and fast scoring function for protein-ligand interactions: A simplified potential approach. *Journal of medicinal chemistry* **42**, 791-804, (1999).
121 Huang, S. Y. & Zou, X. Q. An iterative knowledge-based scoring function to predict protein-ligand interactions: I. Derivation of interaction potentials. *J Comput Chem* **27**, 1866-1875, (2006).
122 Huang, S. Y. & Zou, X. Q. An iterative knowledge-based scoring function to predict protein-ligand interactions: II. Validation of the scoring function. *J Comput Chem* **27**, 1876-1882, (2006).
123 Tanaka, S. & Scheraga, H. A. Medium- and long-range interaction parameters between amino acids for predicting three-dimensional structures of proteins. *Macromolecules* **9**, 945-950, (1976).
124 Miyazawa, S. & Jernigan, R. L. Estimation of Effective Interresidue Contact Energies from Protein Crystal-Structures - Quasi-Chemical Approximation. *Macromolecules* **18**, 534-552, (1985).
125 Sippl, M. J. Calculation of Conformational Ensembles from Potentials of Mean Force - an Approach to the Knowledge-Based Prediction of Local Structures in Globular-Proteins. *Journal of molecular biology* **213**, 859-883, (1990).
126 Verkhivker, G., Appelt, K., Freer, S. T. & Villafranca, J. E. Empirical Free-Energy Calculations of Ligand-Protein Crystallographic Complexes .1. Knowledge-Based Ligand-Protein Interaction Potentials Applied to the Prediction of Human-Immunodeficiency-Virus-1 Protease Binding-Affinity. *Protein Eng* **8**, 677-691, (1995).
127 Perret, P. *et al.* Interaction of non-competitive blockers within the gamma-aminobutyric acid type A chloride channel using chemically reactive probes as chemical sensors for cysteine mutants. *The Journal of biological chemistry* **274**, 25350-25354 (1999).
128 Foucaud, B., Perret, P., Grutter, T. & Goeldner, M. Cysteine mutants as chemical sensors for ligand-receptor interactions. *Trends in pharmacological sciences* **22**, 170-173 (2001).
129 Ruoho, A. E., Kiefer, H., Roeder, P. E. & Singer, S. J. The mechanism of photoaffinity labeling. *Proceedings of the National Academy of Sciences of the United States of America* **70**, 2567-2571 (1973).
130 Middendorp, S. J., Puthenkalam, R., Baur, R., Ernst, M. & Sigel, E. Accelerated discovery of novel benzodiazepine ligands by experiment-guided virtual screening. *ACS chemical biology* **9**, 1854-1859, (2014).
131 Richter, L. *et al.* Diazepam-bound $GABA_A$ receptor models identify new benzodiazepine binding-site ligands. *Nature chemical biology* **8**, 455-464, (2012).
132 Yokoyama, N., Ritter, B. & Neubert, A. D. 2-Arylpyrazolo[4,3-c]quinolin-3-ones: novel agonist, partial agonist, and antagonist of benzodiazepines. *Journal of medicinal chemistry* **25**, 337-339 (1982).
133 Czernik, A. J. *et al.* CGS 8216: receptor binding characteristics of a potent benzodiazepine antagonist. *Life sciences* **30**, 363-372 (1982).
134 Schwarz, M., Turski, L. & Sontag, K. H. CGS 8216, Ro 15-1788 and methyl-beta-carboline-3-carboxylate, but not EMD 41717 antagonize the muscle relaxant effect of diazepam in genetically spastic rats. *Life sciences* **35**, 1445-1451 (1984).
135 Santi, M. *et al.* Evidence that 2-phenylpyrazolo[4,3-c]-quinolin-3(5H)-one antagonises pharmacological, electrophysiological and biochemical effects of diazepam in rats. *Neuropharmacology* **24**, 99-105 (1985).
136 File, S. E., Pellow, S. & Wilks, L. The sedative effects of CL 218,872, like those of chlordiazepoxide, are reversed by benzodiazepine antagonists. *Psychopharmacology* **85**, 295-300 (1985).
137 File, S. E. & Pellow, S. The anxiogenic action of FG 7142 in the social interaction test is reversed by chlordiazepoxide and Ro 15-1788 but not by CGS 8216. *Archives internationales de pharmacodynamie et de therapie* **271**, 198-205 (1984).
138 File, S. E. & Lister, R. G. Interactions of ethyl-beta-carboline-3-carboxylate and Ro 15-1788 with CGS 8216 in an animal model of anxiety. *Neuroscience letters* **39**, 91-94 (1983).
139 Treit, D. Ro 15-1788, CGS 8216, picrotoxin, and pentylenetetrazol: do they antagonize anxiolytic drug effects through an anxiogenic action? *Brain research bulletin* **19**, 401-405 (1987).
140 Maldifassi, M. C., Baur, R. & Sigel, E. Molecular mode of action of CGS 9895 at alpha1 beta2 gamma2 $GABA_A$ receptors. *Journal of neurochemistry* **138**, 722-730, (2016).
141 Simeone, X. *et al.* Molecular tools for $GABA_A$ receptors: High affinity ligands for beta1-containing subtypes. *Scientific reports* **7**, 5674, (2017).
142 Ali, N. J. & Olsen, R. W. Chronic benzodiazepine treatment of cells expressing recombinant $GABA_A$ receptors uncouples allosteric binding: studies on possible mechanisms. *Journal of neurochemistry* **79**, 1100-1108 (2001).
143 Savini, L. *et al.* High affinity central benzodiazepine receptor ligands: synthesis and structure-activity relationship studies of a new series of pyrazolo[4,3-c]quinolin-3-ones. *Bioorganic & medicinal chemistry* **6**, 389-399 (1998).
144 Savini, L. *et al.* High affinity central benzodiazepine receptor ligands. Part 2: quantitative structure-activity relationships and comparative molecular field analysis of pyrazolo[4,3-c]quinolin-3-ones. *Bioorganic & medicinal chemistry* **9**, 431-444 (2001).
145 Huang, Q. *et al.* Pharmacophore/receptor models for $GABA_A$/BzR subtypes (alpha1beta3gamma2, alpha5beta3gamma2, and alpha6beta3gamma2) via a comprehensive ligand-mapping approach. *Journal of medicinal chemistry* **43**, 71-95 (2000).
146 Varagic, Z. *et al.* Identification of novel positive allosteric modulators and null modulators at the $GABA_A$ receptor alpha+beta-interface. *British journal of pharmacology* **169**, 371-383, (2013).
147 Rivilli, M. J. L., Moyano, E. L. & Yranzo, G. I. An alternative approach toward 2-aryl-2H-pyrazolo[4,3-c]-quinolin-3-ones by a multistep synthesis (vol 51, pg 478, 2010). *Tetrahedron letters* **51**, 1444-1444, (2010).
148 Nilsson, J. *et al.* Triazoloquinazolinediones as novel high affinity ligands for the benzodiazepine site of $GABA_A$ receptors. *Bioorganic & medicinal chemistry* **19**, 111-121, (2011).

149 Wolter, M., Klapars, A. & Buchwald, S. L. Synthesis of N-aryl hydrazides by copper-catalyzed coupling of hydrazides with aryl iodides. *Organic letters* **3**, 3803-3805 (2001).
150 Olsen, R. W. & Tobin, A. J. Molecular biology of GABAA receptors. *FASEB journal : official publication of the Federation of American Societies for Experimental Biology* **4**, 1469-1480 (1990).
151 Wu, C. & Nebert, D. W. Update on genome completion and annotations: Protein Information Resource. *Human genomics* **1**, 229-233 (2004).
152 Varagic, Z. *et al.* Subtype selectivity of alpha+beta- site ligands of $GABA_A$ receptors: identification of the first highly specific positive modulators at alpha6beta2/3gamma2 receptors. *British journal of pharmacology* **169**, 384-399, (2013).
153 Friesner, R. A., Abel, R., Goldfeld, D. A., Miller, E. B. & Murrett, C. S. Computational methods for high resolution prediction and refinement of protein structures. *Curr Opin Struct Biol* **23**, 177-184, (2013).
154 Fiser, A., Do, R. K. & Sali, A. Modeling of loops in protein structures. *Protein science : a publication of the Protein Society* **9**, 1753-1773 (2000).
155 Sergeeva, O. A. *et al.* Fragrant dioxane derivatives identify beta1-subunit-containing $GABA_A$ receptors. *The Journal of biological chemistry* **285**, 23985-23993, (2010).
156 Thompson, S. A. *et al.* Salicylidene salicylhydrazide, a selective inhibitor of beta 1-containing $GABA_A$ receptors. *British journal of pharmacology* **142**, 97-106, (2004).
157 Carotti, A. *et al.* High affinity central benzodiazepine receptor ligands. Part 3: insights into the pharmacophore and pattern recognition study of intrinsic activities of pyrazolo[4,3-c]quinolin-3-ones. *Bioorganic & medicinal chemistry* **11**, 5259-5272 (2003).
158 Dillon, G. H. *et al.* U-93631 causes rapid decay of gamma-aminobutyric acid-induced chloride currents in recombinant rat gamma-aminobutyric acid type A receptors. *Molecular pharmacology* **44**, 860-865 (1993).
159 Anstee, Q. M. *et al.* Mutations in the Gabrb1 gene promote alcohol consumption through increased tonic inhibition. *Nature communications* **4**, 2816, (2013).
160 Ueno, S., Wick, M. J., Ye, Q., Harrison, N. L. & Harris, R. A. Subunit mutations affect ethanol actions on $GABA_A$ receptors expressed in Xenopus oocytes. *British journal of pharmacology* **127**, 377-382, (1999).
161 Groll, B., Schnurch, M. & Mihovilovic, M. D. Selective Ru(0)-catalyzed deuteration of electron-rich and electron-poor nitrogen-containing heterocycles. *The Journal of organic chemistry* **77**, 4432-4437, (2012).
162 Kelley, M. H. *et al.* Alterations in Purkinje cell $GABA_A$ receptor pharmacology following oxygen and glucose deprivation and cerebral ischemia reveal novel contribution of beta1 -subunit-containing receptors. *The European journal of neuroscience* **37**, 555-563, (2013).
163 Hirschberg, Y., Oberle, R. L., Ortiz, M., Lau, H. & Markowska, M. Oral absorption of CGS-20625, an insoluble drug, in dogs and man. *Journal of pharmacokinetics and biopharmaceutics* **23**, 11-23 (1995).
164 Das, A. K., Park, S., Muthaiah, S. & Hong, S. H. Ligand- and Acid-Free Gold(I) Chloride Catalyzed Hydration of Terminal Alkynes. *Synlett* **26**, 2517-2520, (2015).
165 Liu, W., Wang, H. & Li, C. J. Metal-Free Markovnikov-Type Alkyne Hydration under Mild Conditions. *Organic letters* **18**, 2184-2187, (2016).
166 Jechlinger, M., Pelz, R., Tretter, V., Klausberger, T. & Sieghart, W. Subunit composition and quantitative importance of hetero-oligomeric receptors: $GABA_A$ receptors containing alpha6 subunits. *The Journal of neuroscience : the official journal of the Society for Neuroscience* **18**, 2449-2457 (1998).
167 Liao, Y. H., Lee, H. J., Huang, W. J., Fan, P. C. & Chiou, L. C. Hispidulin alleviated methamphetamine-induced hyperlocomotion by acting at alpha6 subunit-containing $GABA_A$ receptors in the cerebellum. *Psychopharmacology* **233**, 3187-3199, (2016).
168 Yang, L. *et al.* The essential role of hippocampal alpha6 subunit-containing $GABA_A$ receptors in maternal separation stress-induced adolescent depressive behaviors. *Behavioural brain research* **313**, 135-143, (2016).
169 Puri, J. *et al.* Reduced $GABA_A$ receptor alpha6 expression in the trigeminal ganglion alters inflammatory TMJ hypersensitivity. *Neuroscience* **213**, 179-190, (2012).
170 Kramer, P. R. & Bellinger, L. L. Reduced $GABA_A$ receptor alpha6 expression in the trigeminal ganglion enhanced myofascial nociceptive response. *Neuroscience* **245**, 1-11, (2013).
171 Gutierrez, A., Khan, Z. U. & De Blas, A. L. Immunocytochemical localization of the alpha 6 subunit of the gamma-aminobutyric acid A receptor in the rat nervous system. *The Journal of comparative neurology* **365**, 504-510, (1996).
172 Hortnagl, H. *et al.* Patterns of mRNA and protein expression for 12 $GABA_A$ receptor subunits in the mouse brain. *Neuroscience* **236**, 345-372, (2013).
173 Kucken, A. M., Teissere, J. A., Seffinga-Clark, J., Wagner, D. A. & Czajkowski, C. Structural requirements for imidazobenzodiazepine binding to $GABA_A$ receptors. *Molecular pharmacology* **63**, 289-296 (2003).
174 Sigel, E., Schaerer, M. T., Buhr, A. & Baur, R. The benzodiazepine binding pocket of recombinant alpha1beta2gamma2 gamma-aminobutyric acid A receptors: relative orientation of ligands and amino acid side chains. *Molecular pharmacology* **54**, 1097-1105 (1998).
175 Mihic, S. J., Whiting, P. J., Klein, R. L., Wafford, K. A. & Harris, R. A. A single amino acid of the human gamma-aminobutyric acid type A receptor gamma 2 subunit determines benzodiazepine efficacy. *The Journal of biological chemistry* **269**, 32768-32773 (1994).
176 Sancar, F., Ericksen, S. S., Kucken, A. M., Teissere, J. A. & Czajkowski, C. Structural determinants for high-affinity zolpidem binding to $GABA_A$ receptors. *Molecular pharmacology* **71**, 38-46, (2007).
177 Zhang, P. *et al.* Synthesis of novel imidazobenzodiazepines as probes of the pharmacophore for "diazepam-insensitive" $GABA_A$ receptors. *Journal of medicinal chemistry* **38**, 1679-1688 (1995).
178 He, X. *et al.* Studies of molecular pharmacophore/receptor models for $GABA_A$/BzR subtypes: binding affinities of symmetrically substituted pyrazolo[4,3-c]quinolin-3-ones at recombinant alpha x beta 3 gamma 2 subtypes and quantitative structure-activity relationship studies via a comparative molecular field analysis. *Drug design and discovery* **16**, 77-91 (1999).
179 Kruskal, J. B. Nonmetric multidimensional scaling: A numerical method. *Psychometrika* **29**, 115-129, (1964).
180 Kruskal, J. B. Multidimensional scaling by optimizing goodness of fit to a nonmetric hypothesis. *Psychometrika* **29**, 1-27, (1964).
181 Sakano, T., Mahamood, M. I., Yamashita, T. & Fujitani, H. Molecular dynamics analysis to evaluate docking pose prediction. *Biophysics and physicobiology* **13**, 181-194, (2016).
182 Liu, K., Watanabe, E. & Kokubo, H. Exploring the stability of ligand binding modes to proteins by molecular dynamics simulations. *Journal of computer-aided molecular design* **31**, 201-211, (2017).
183 Takada, S. *et al.* Synthesis and structure-activity relationships of fused imidazopyridines: a new series of benzodiazepine receptor ligands. *Journal of medicinal chemistry* **39**, 2844-2851, (1996).

184 Ritchie, T. J., Macdonald, S. J. F., Peace, S., Pickett, S. D. & Luscombe, C. N. The developability of heteroaromatic and heteroaliphatic rings - do some have a better pedigree as potential drug molecules than others? *Medchemcomm* **3**, 1062-1069, (2012).
185 Narender, N., Srinivasu, P., Kulkarni, S. J. & Raghavan, K. V. Highly efficient, para-selective oxychlorination of aromatic compounds using potassium chloride and Oxone (R). *Synthetic communications* **32**, 279-286, (2002).
186 Chen, J., Xiong, X. Y., Chen, Z. H. & Huang, J. H. Imidazolium Salt Catalyzed para-Selective Halogenation of Electron-Rich Arenes. *Synlett* **26**, 2831-2834, (2015).
187 Romba, J. *et al.* Facially coordinating cyclic triamines, 3. The coordination chemistry of 1,4-diazepan-6-amine. *Eur J Inorg Chem*, 314-328, (2006).
188 Perdicchia, D., Licandro, E., Maiorana, S., Baldoli, C. & Giannini, C. A new 'one-pot' synthesis of hydrazides by reduction of hydrazones. *Tetrahedron* **59**, 7733-7742, (2003).
189 Wolber, G. & Langer, T. LigandScout: 3-D pharmacophores derived from protein-bound ligands and their use as virtual screening filters. *Journal of chemical information and modeling* **45**, 160-169, (2005).
190 Lipinski, C. A. Lead- and drug-like compounds: the rule-of-five revolution. *Drug discovery today. Technologies* **1**, 337-341, (2004).
191 Sieghart, W. Structure and pharmacology of gamma-aminobutyric acid A receptor subtypes. *Pharmacological reviews* **47**, 181-234 (1995).
192 Treven, M. *et al.* Towards Functional Selectivity for α6β3γ2 $GABA_A$ Receptors: A Series of Novel Pyrazoloquinolinones. *British journal of pharmacology* ***175***, 419-428, (2017).
193 Sali, A. & Blundell, T. L. Comparative protein modelling by satisfaction of spatial restraints. *Journal of molecular biology* **234**, 779-815, (1993).
194 Thompson, J. D., Higgins, D. G. & Gibson, T. J. CLUSTAL W: improving the sensitivity of progressive multiple sequence alignment through sequence weighting, position-specific gap penalties and weight matrix choice. *Nucleic acids research* **22**, 4673-4680 (1994).
195 Fors, B. P., Dooleweerdt, K., Zeng, Q. & Buchwald, S. L. An Efficient System For the Pd-Catalyzed Cross-Coupling of Amides and Aryl Chlorides. *Tetrahedron* **65**, 6576-6583, (2009).
196 Long, J. *et al.* Intramolecular, Site-Selective, Iodine-Mediated, Amination of Unactivated (sp(3))C-H Bonds for the Synthesis of Indoline Derivatives. *Organic letters* **19**, 2793-2796, (2017).
197 Altau, K. *et al.* Some Derivatives of Ethylbenzene. *Journal of Chemical & Engineering Data* **8**, 122-130, (1963).
198 Podanyi, B., Kereszturi, G., Vasvari-Debreczy, L., Hermecz, I. & Toth, G. An NMR study of halogenated 1,4-dihydro-1-ethyl-4-oxoquinoline-3-carboxylates. *Magn Reson Chem* **34**, 972-978, (1996).
199 Tong, Y. C. Chlorination of Quinoline. *Journal of Heterocyclic Chemistry* **7**, 171-& (1970).
200 Forezi Lda, S. *et al.* Synthesis, cytotoxicity and mechanistic evaluation of 4-oxoquinoline-3-carboxamide derivatives: finding new potential anticancer drugs. *Molecules* **19**, 6651-6670, (2014).
201 Ohnmacht, C. J., Davis, F. & Lutz, R. E. Antimalarials .5. Alpha-Dibutylaminomethyl-3-Quinolinemethanols and Alpha-(2-Piperidyl)-3-Quinolinemethanols. *Journal of medicinal chemistry* **14**, 17-+, (1971).
202 Kang, T., Kim, Y., Lee, D., Wang, Z. & Chang, S. Iridium-Catalyzed Intermolecular Amidation of sp(3) C-H Bonds: Late-Stage Functionalization of an Unactivated Methyl Group. *Journal of the American Chemical Society* **136**, 4141-4144, (2014).
203 Medapi, B. *et al.* 4-Aminoquinoline derivatives as novel Mycobacterium tuberculosis GyrB inhibitors: Structural optimization, synthesis and biological evaluation. *European journal of medicinal chemistry* **103**, 1-16, (2015).
204 Liu, P. *et al.* 4-Oxo-1,4-dihydro-quinoline-3-carboxamides as BACE-1 inhibitors: synthesis, biological evaluation and docking studies. *European journal of medicinal chemistry* **79**, 413-421, (2014).
205 Chen, Y. L., Zacharias, J., Vince, R., Geraghty, R. J. & Wang, Z. C-6 aryl substituted 4-quinolone-3-carboxylic acids as inhibitors of hepatitis C virus. *Bioorganic & medicinal chemistry* **20**, 4790-4800, (2012).
206 Heikkila, T. *et al.* Design and synthesis of potent inhibitors of the malaria parasite dihydroorotate dehydrogenase. *Journal of medicinal chemistry* **50**, 186-191, (2007).
207 Nsumiwa, S., Kuter, D., Wittlin, S., Chibale, K. & Egan, T. J. Structure-activity relationships for ferriprotoporphyrin IX association and beta-hematin inhibition by 4-aminoquinolines using experimental and ab initio methods. *Bioorganic & medicinal chemistry* **21**, 3738-3748, (2013).
208 Niedermeier, S. *et al.* A small-molecule inhibitor of Nipah virus envelope protein-mediated membrane fusion. *Journal of medicinal chemistry* **52**, 4257-4265, (2009).
209 Lager, E. *et al.* 4-quinolone derivatives: high-affinity ligands at the benzodiazepine site of brain $GABA_A$ receptors. synthesis, pharmacology, and pharmacophore modeling. *Journal of medicinal chemistry* **49**, 2526-2533, (2006).
210 Huang, L. J., Hsieh, M. C., Teng, C. M., Lee, K. H. & Kuo, S. C. Synthesis and antiplatelet activity of phenyl quinolones. *Bioorganic & medicinal chemistry* **6**, 1657-1662 (1998).
211 Hanburys, A. Chinolin-3-carboxamidotetrazolderivate, Verfahren zu ihrer Herstellung und diese Verbindungen enthaltenden Mittel (1974).
212 HENNEQUIN, L. F. A., Mckerrecher, D., Ple, P. & Stokes, E. S. E. (Google Patents, 2005).
213 Takada, S. *et al.* Thienylpyrazoloquinolines - Potent Agonists and Inverse Agonists to Benzodiazepine Receptors. *Journal of medicinal chemistry* **31**, 1738-1745, (1988).
214 Takada, S. *et al.* Thienylpyrazoloquinolines: potent agonists and inverse agonists to benzodiazepine receptors. *Journal of medicinal chemistry* **31**, 1738-1745 (1988).
215 Aicher, T. D., Taylor, C. B. & Vanhuis, C. A. (Google Patents, 2015).
216 Heindel, N. D. & Fine, S. A. Synthesis and antimalarial activity of 4-aminobenzo[g-1,5]naphthyridines. *Journal of medicinal chemistry* **13**, 760-762, (1970).
217 Karolak-Wojciechowska, J., Lange, J., Ksiazek, W., Gniewosz, M. & Rump, S. Structure-activity relationship investigations of the modulating effect of core substituents on the affinity of pyrazoloquinolinone congeners for the benzodiazepine receptor. *Farmaco* **53**, 579-585 (1998).
218 Wimmer, L. *Synthesis of bioactive molecules for the investigation of ion channels and transporters,* PhD thesis, TU Wien, (2016).
219 Draskovits, M. *Synthesis of Pyrazoloquinolinones and Imidazoquinolinones as potential $GABA_A$ receptor ligands,* MSc. thesis, TU Wien, (2016).
220 Uzgiris, E. E. (Google Patents, 2004).
221 López Rivilli, M. J., Moyano, E. L. & Yranzo, G. I. An alternative approach toward 2-aryl-2H-pyrazolo[4,3-c]-quinolin-3-ones by a multistep synthesis. *Tetrahedron letters* **51**, 478-481, (2010).

222 Yokoyama, N. (Google Patents, 1982).
223 Bjork, P., Fex, T., Pettersson, L., Sorensen, P. & Da Graca Thrige, D. (Google Patents, 2003).
224 Venkatesan Balaji, P. & Chandrasekaran, S. Reagent-switch controlled metal-free intermolecular geminal diamination and aminooxygenation of vinylarenes. *Tetrahedron* **72**, 1095-1104, (2016).
225 Wellner, E., Sandin, H. & Paakkonen, L. Synthesis of 6,6-difluorohomopiperazines via microwave-assisted detosylation. *Synthesis-Stuttgart*, 223-226, (2003).
226 Aucagne, V., Leigh, D. A., Lock, J. S. & Thomson, A. R. Rotaxanes of cyclic peptides. *Journal of the American Chemical Society* **128**, 1784-1785, (2006).
227 Ferreira, I. M., Casagrande, G. A., Pizzuti, L. & Raminelli, C. Ultrasound-Promoted Rapid and Efficient Iodination of Aromatic and Heteroaromatic Compounds in the Presence of Iodine and Hydrogen Peroxide in Water. *Synthetic communications* **44**, 2094-2102, (2014).